MATHEMATICS AND NATURAL SCIENCE

Proceedings of the Fourth International Scientific Conference – FMNS2011
8 – 11 June 2011
Faculty of Mathematics and Natural Science

VOLUME 1

South-West University “Neofit Rilski”
Blagoevgrad

Fourth International Scientific Conference – FMNS2011
South-West University,
Faculty of Mathematics and Natural Science
8 – 11 June 2011

ORGANIZING COMMITTEE:
Honorary Chairman:
Prof. Ivan Mircev, PhD, Rector of the SOUTH-WEST UNIVERSITY "NEOFIT RILSKI"
Chairman: *Assoc. Prof. Borislav Yurukov, PhD, Dean of the Faculty of Mathematics&Natural Sciences*

Members:
Prof. Ilia Giudjenov, PhD
Assoc. Prof. Stanko Shtrakov, PhD
Assoc. Prof. Mitko Stoev, PhD
Assoc. Prof. Luben Mihov, PhD
Assoc. Prof. Stefan Manev, PhD
Assoc. Prof. Mihail Mihailov, PhD
Assoc. Prof. Valentin Hristov, PhD
Assoc. Prof. Stefan Stefanov, PhD
Assist. Prof. Ivan Trenchev, PhD
Assist. Prof. Grigor Iliev

PROGRAM COMMITTEE:

Chairman: Prof. Kiril Chimev, DrSc
Members:
Acad. P. Bonchev (Bulgaria)
Acad. K. Boyanov (Bulgaria)
Acad. Evg. Golovinski (Bulgaria)
Acad. T. Nikolov (Bulgaria)
Acad. St. Dodunekov (Bulgaria)
Acad. Al. Popov (Bulgaria)
Corr. Member of BAS J. Stamenov
Prof. A. Antonov (Bulgaria)
Prof. P. Argyrakis (Greece)
Prof. P. Frangos (Greece)
Prof. A. Borisov (Bulgaria)
Prof. C. Cankov (Bulgaria)
Prof. Iv. Ganchev (Bulgaria)
Prof. S. Grozdev (Bulgaria)
Prof. D. Havlichek (Czech republic)
Prof. Ken Y. Hsu (Taiwan)
Prof. G.-J. Krauss (Germany)
Prof. C. Milkova (Bulgaria)
Prof. T. Pavlovich (Serbia)
Prof. D. Tsipas (Greece)
Dr. eng. A. Majchrzycka (Poland)

Revewers:

Assoc. Prof. Stefan Stefanov
Assoc. Prof. Penka Bozarova
Assoc. Prof. Stanko Shtrakov
Assoc. Prof.Valentin Hristov
Assoc. Prof. Luben Mihov
Assoc. Prof. Slavcho Shtrakov
Assoc. Prof. Krasimir Yordzev
Assoc. Prof.Ivan Drenovski
Assoc. Prof.Michail Michailov
Assoc. Prof.Plamen Gramatikov
Assoc. Prof.Boyko Kolev
Assoc. Prof.Atanas Chapkanov
Assoc. Prof. Krasimir Stoyanov

ISSN 1314-0272

Minimization of a strictly convex separable function subject to a convex inequality constraint or linear equality constraints and bounds on the variables

Stefan M. Stefanov
Department of Informatics, Neofit Rilski South-West University,
Blagoevgrad, BULGARIA

Abstract. *In this paper, we consider the problem of minimizing a strictly convex separable function over a feasible region defined by a convex inequality constraint and two-sided bounds on the variables (box constraints). Also, the convex separable program with a strictly convex objective function subject to linear equality constraints and bounded variables is considered. These problems are interesting from both theoretical and practical point of view because they arise in some mathematical programming problems and in various practical problems. Characterization theorems (necessary and sufficient conditions) for the optimal solution to the considered problems are proved. Simple illustrative examples are also presented.*

Key words. *Convex programming, separable programming, algorithms.*
2010 Mathematics Subject Classification. 90C30, 90C25.

1 Introduction

Consider the following strictly convex separable program with strictly convex inequality constraint and bounded variables

(SCS)

$$\min\{c(x) \equiv \sum_{j\in J} c_j(x_j)\} \tag{1.1}$$

subject to

$$\sum_{j\in J} d_j(x_j) \equiv \sum_{j\in J} d_j x_j^p \le \alpha \tag{1.2}$$

$$a_j \le x_j \le b_j, j \in J, \tag{1.3}$$

where $c_j(x_j)$ are strictly convex differentiable functions, $c'_j(x_j) > 0, d_j > 0$, $x_j > 0$ for every $j \in J$, $p > 1$, $x = (x_j)_{j \in J}$, and $J \overset{def}{=} \{1, \ldots, n\}$.

Functions $d_j(x_j), j \in J$, are also stricly convex because $d''_j(x_j) \equiv p(p-1)x_j^{p-2} > 0, j \in J$, under the assumptions. In particular, since $x_j > 0, j \in J$, then $a_j > 0, b_j > 0, j \in J$.

Feasible region X defined by (1.2) -- (1.3) is intersection of the half-space (1.2) and the $n-$dimensional box (1.3). Therefore X is a convex set.

One of the most important problems of the form (SCS) is the program with $c_j(x_j) = c_j x_j^q, j \in J$. Functions $c_j(x_j) = c_j x_j^q$ are strictly convex for $c_j > 0, x_j > 0, j \in J, q > 1$, and the assumption $c'_j(x_j) \equiv q c_j x_j^{q-1} > 0, j \in J$, is also satisfied for $c_j > 0, x_j > 0, j \in J, q > 1$ in this case.

Problem (SCS) is a convex separable programming problem because the objective function and constraint function are convex (moreover, strictly convex) and separable (that is, these functions can be expressed as the sums of single-variable functions). Because of the strict convexity, if problem (SCS) is solvable, its solution is unique.

Also, consider the following convex separable program with strictly convex objective function subject to linear equality constraints and bounded variables

$(C_m^=)$

$$\min\{c(x) = \sum_{j \in J} c_j(x_j)\} \tag{1.4}$$

subject to

$$Dx = \alpha \tag{1.5}$$

$$a \le x \le b, \tag{1.6}$$

where $c_j(x_j)$ are strictly convex differentiable functions, $j \in J$, $D = (d_{ij}) \in R^{m \times n}$, $\alpha \in R^m, a = (a_1, \ldots, a_n), b = (b_1, \ldots, b_n) \in R^n$.

The feasible region $X^=$ defined by (1.5) -- (1.6) is an intersection of m hyperplanes (1.5) and the box (1.6). Therefore $X^=$ is a convex set.

Problem $(C_m^=)$ is also a convex separable programming problem because the objective function and constraint functions are convex and

separable. Because of the strict convexity of objective function, if problem $(C_m^=)$ is solvable, its solution is unique.

Problems (SCS) and $(C_m^=)$, defined by (1.1) -- (1.3) and (1.4) -- (1.6), respectively, and related to them, arise in production planning and scheduling [18], in allocation of resources [1, 4, 5, 18, 20], in decision making [1, 5, 6, 20], in the theory of search, in facility location [6, 8, 20], etc.

Problems like (SCS) and $C_m^=)$ are subject of intensive study. Related problems and methods for them are considered in [1 -- 20]. Algorithms for resource allocation problems are proposed in [1, 4, 5, 20], and algorithms for facility location problems are suggested in [6], etc. Singly constrained quadratic programs with bounded variables are considered in [2, 3], and some separable programs are considered and methods for solving them are suggested in [2, 8 -- 19], etc.

This paper is devoted to solution of problems (SCS) and $(C_m^=)$. The paper is organized as follows. In Section 2, characterization theorems (necessary and sufficient conditions) for the optimal solution to problems (SCS) and $(C_m^=)$ are proved. Due to the specific form of the optimal solution to problem (SCS), this solution can be obtained directly and it is not necessary to develop iterative algorithms for solving problem (SCS). In Section 3 we present results of two simple illustrative examples for both problem (SCS) and problem $(C_m^=)$.

2 Characterization theorems

2.1 Problem (SCS)

Consider problem (SCS) defined by (1.1) -- (1.3).

Suppose that following assumptions are satisfied.

(A1) $a_j \le b_j$ for all $j \in J$. If $a_k = b_k$ for some $k \in J$, then the value $x_k := a_k = b_k$ is determined in advance.

(A2) $\sum_{j \in J} d_j a_j^p \le \alpha$. Otherwise the constraints (1.2) -- (1.3) are inconsistent and $X = \varnothing$, where the feasible region X is defined by (1.2) -- (1.3).

The Lagrangian for problem (SCS) is

$$L(x,u,v,\lambda) = \sum_{j \in J} c_j(x_j) + \lambda(\sum_{j \in J} d_j x_j^p - \alpha) + \sum_{j \in J} u_j(a_j - x_j) + \sum_{j \in J} v_j(x_j - b_j), \quad (2.1)$$

where $\lambda \in R_+^1; u, v \in R_+^n$, and R_+^n consists of all vectors with n real nonnegative components.

The Karush-Kuhn-Tucker (KKT) necessary and sufficient optimality conditions for the minimum solution $x^* = (x_j^*)_{j \in J}$ to problem (SCS) are

$$c'_j(x_j^*) + \lambda p d_j . (x_j^*)^{p-1} - u_j + v_j = 0, \quad j \in J \tag{2.2}$$

$$u_j (a_j - x_j^*) = 0, \quad j \in J \tag{2.3}$$

$$v_j (x_j^* - b_j) = 0, \quad j \in J \tag{2.4}$$

$$\lambda (\sum_{j \in J} d_j . (x_j^*)^p - \alpha) = 0, \quad \lambda \in R_+^1 \tag{2.5}$$

$$\sum_{j \in J} d_j . (x_j^*)^p \le \alpha \tag{2.6}$$

$$a_j \le x_j^* \le b_j, \quad j \in J \tag{2.7}$$

$$u_j \in R_+^1, v_j \in R_+^1, \quad j \in J, \tag{2.8}$$

where $\lambda, u_j, v_j, j \in J$, are the Lagrange multipliers associated with the constraints (1.2), $a_j \le x_j, x_j \le b_j, j \in J$, respectively. If $a_j = -\infty$ or $b_j = +\infty$ for some j, we do not consider the corresponding condition (2.3) ((2.4), respectively) and Lagrange multiplier u_j (v_j, respectively).

According to conditions (2.2) -- (2.8), $\lambda \ge 0, u_j \ge 0, v_j \ge 0, j \in J$, and complementary conditions (2.3), (2.4), (2.5) must be satisfied. In order to find $x_j^*, j \in J$, from system (2.2) -- (2.8), we have to consider all possible cases for λ, u_j, v_j: all λ, u_j, v_j equal to 0; all λ, u_j, v_j different from 0; some of them equal to 0 and some of them different from 0. The number of these cases is 2^{2n+1}, where $2n+1$ is the number of all $\lambda, u_j, v_j, j \in J, |J| = n$. This is an enormous number of cases, especially for large-scale problems. Moreover, in each case we have to solve a large-scale system of nonlinear equations in $x_j^*, \lambda, u_j, v_j, j \in J$. Therefore the *direct* application of the KKT theorem, using explicit enumeration of all possible cases, for solving large-scale problems of the considered form

would not be effective. That is why, we need efficient methods for solving the considered problem.

Theorem 2.1 gives a characterization of the optimal solution to problem (SCS). Its proof is based on the KKT theorem.

Theorem 2.1 (Characterization of the optimal solution to problem (SCS)) *The point* $x^* = (x_j^*)_{j\in J}$ *is the optimal solution to problem* (SCS) *if and only if* $x^* = (a_1, \ldots, a_n)$.

Proof. *Necessity.* Let $x^* = (x_j^*)_{j\in J}$ be the optimal solution to (SCS). Then there exist constants $\lambda, u_j, v_j, j \in J$, such that KKT conditions (2.2) -- (2.8) are satisfied. Consider both possible cases for λ.

(1) Let $\lambda > 0$. Then system (2.2) -- (2.8) becomes (2.2), (2.3), (2.4), (2.7), (2.8) and

$$\sum_{j\in J} d_j.(x_j^*)^p = \alpha, \qquad (2.10)$$

that is, the inequality constraint (1.2) is satisfied with an equality for $x_j^*, j \in J$, in this case.

(a) If $x_j^* = a_j$, then $u_j \geq 0$, and $v_j = 0$ according to (2.4). Therefore (2.2) implies $c'_j(x_j^*) = u_j - \lambda p d_j.(x_j^*)^{p-1} \geq -\lambda p d_j.(x_j^*)^{p-1}$. Since $d_j > 0, x_j^* > 0, j \in J, p > 1$, then

$$\lambda \geq -c'_j(x_j^*) / p d_j.(x_j^*)^{p-1} \equiv -c'_j(a_j) / p d_j a_j^{p-1}. \qquad (2.11)$$

Because $c'_j(.) > 0, d_j > 0, a_j > 0, j \in J, p > 1 (> 0)$, and $\lambda \geq 0$, the inequality (2.11) is always satisfied.

(b) If $x_j^* = b_j$, then $u_j = 0$ according to (2.3), and $v_j \geq 0$. Therefore (2.2) implies $c'_j(x_j^*) = -v_j - \lambda p d_j.(x_j^*)^{p-1} \leq -\lambda p d_j.(x_j^*)^{p-1}$. Hence

$$\lambda \leq -c'_j(x_j^*) / p d_j.(x_j^*)^{p-1} \equiv -c'_j(b_j) / p d_j b_j^{p-1}. \qquad (2.12)$$

Since $c'_j(.) > 0, d_j > 0, b_j > 0, j \in J, p > 1 (> 0)$, then

$$-c'_j(b_j) / p d_j b_j^{p-1} < 0, \qquad (2.13)$$

and since λ must be nonnegative, from (2.12) and (2.13) it is obvious that this case *is impossible*.

(c) If $a_j < x_j^* < b_j$, then $u_j = v_j = 0$ according to (2.3) and (2.4). Therefore (2.2) implies

$$-c'_j(x_j^*) = \lambda p d_j.(x_j^*)^{p-1}. \qquad (2.14)$$

Since $c_j'(.) > 0, d_j > 0$, $x_j^* > 0, j \in J$, $p > 1$ by the assumption, and $\lambda \geq 0$, from (2.14) it follows that this case *is impossible*.

(2) Let $\lambda = 0$. Then system (2.2) -- (2.8) becomes

$$c_j'(x_j^*) - u_j + v_j = 0, j \in J, \tag{2.15}$$

and (2.3), (2.4), (2.6), (2.7), (2.8).

(a) If $x_j^* = a_j$, then $u_j \geq 0, v_j = 0$. Therefore

$$c_j'(a_j) \equiv c_j'(x_j^*) = u_j \geq 0. \tag{2.16}$$

Since $c_j'(.) > 0$ by the assumption, then (2.16) is always satisfied.

(b) If $x_j^* = b_j$, then $u_j = 0, v_j \geq 0$. Therefore

$$c_j'(b_j) \equiv c_j'(x_j^*) = -v_j \leq 0. \tag{2.17}$$

Since $c_j'(.) > 0$, this case *is impossible*.

(c) If $a_j < x_j^* < b_j$, then $u_j = v_j = 0$. Therefore $c_j'(x_j^*) = 0$, and since $c_j'(.) > 0$, this case *is impossible*.

As we have proved, in both cases (1) and (2), only subcases (a) are possible, that is, $x^* = (a_1, \ldots, a_n)$.

The ``necessity'' part is proved.

Sufficiency. Conversely, let $x^* = (a_1, \ldots, a_n)$. Obviously $x^* \in X$, where X is defined by (1.2) -- (1.3).

Set

$$u_j = c_j'(a_j) + \lambda p d_j a_j^{p-1} \quad (\geq 0 \text{ under the assumptions}), \quad v_j = 0. \tag{2.18}$$

By using these expressions, it is easy to check that $x_j^*, \lambda, u_j, v_j, j \in J$, satisfy conditions (2.2), (2.3), (2.4), (2.5), (2.8); conditions (2.6) and (2.7) are also satisfied because $x^* = (a_1, \ldots, a_n) \in X$.

Since (2.2) -- (2.8) are necessary and sufficient conditions for an optimal solution to the convex minimization problem (SCS), then x^* is an optimal solution to this problem, and since $c(x)$ is a strictly convex function as the sum of strictly convex functions, this optimal solution is unique. □

2.2 Problem $(C_m^=)$

Denote by $P_c(D, \alpha, a, b)$ the solution to problem $(C_m^=)$. Since $c(x)$ is strictly convex as a sum of strictly convex functions, then $P_c(D, \alpha, a, b)$ is

uniquely defined, that is, there is at most one minimum which is both local and global.

Denote $y = [x]_a^b$ where $y_j = \min\{\max\{x_j, a_j\}, b_j\}$ for each $j \in J$.

The KKT conditions for $x^* \in R^n$ to be minimum solution to problem $(C_m^=)$ are

$$Dx^* = \alpha \tag{2.19}$$

$$a \le x^* \tag{2.20}$$

$$x^* \le b \tag{2.21}$$

$$c'(x^*) + D^T \lambda - u + v = 0 \tag{2.22}$$

$$u_j(a_j - x_j^*) = 0, \quad j \in J \tag{2.23}$$

$$v_j(x_j^* - b_j) = 0, \quad j \in J \tag{2.24}$$

$$u \ge 0 \tag{2.25}$$

$$v \ge 0, \tag{2.26}$$

where $\lambda \in R^m, u, v \in R_+^n$ are the Lagrange multipliers associated with (1.5) and the two inequalities of (1.6), respectively.

The map $c' \equiv \nabla c : R^n \to R^n$ is strict monotone increasing since c is a strictly convex function. Therefore $(\nabla c)^{-1} : R^n \to R^n$ is well-defined.

Theorem 2.2 *Let $c : R^n \to R$ be separable, differentiable and strictly convex. Then*

$$\{P_c(D, \alpha, a, b)\} = \left\{(c')^{-1}[-D^T t]_{c'(a)}^{c'(b)} : t \in R^m\right\}, \tag{2.27}$$

where D, α, a, b are defined above.

Proof. Relation (2.27) is proved by two-way inclusion.

i) Let $x^* = P_c(D, \alpha, a, b)$ for some $\alpha \in R^m$. Then there exist $\lambda \in R^m$, $u, v \in R_+^n$ satisfying the KKT conditions (2.19) -- (2.26) together with this x^*.

From (2.22) it follows that

$$D^T \lambda = -c'(x^*) + u - v, \tag{2.28}$$

that is,

$$\langle D_j,\ \lambda\rangle = -c'_j(x_j^*) + u_j - v_j \tag{2.29}$$

for each $j \in J$.

If $\langle D_j,\ \lambda\rangle > -c'_j(x_j^*)$, then $u_j > v_j \geq 0$, so $x_j^* = a_j$ according to (2.23), that is,

$$\langle D_j,\ \lambda\rangle > -c'_j(x_j^*) \quad \text{i}mplies \quad x_j^* = a_j. \tag{2.30}$$

Similarly, if $\langle D_j,\ \lambda\rangle < -c'_j(x_j^*)$, then $v_j > u_j \geq 0$, so $x_j^* = b_j$ according to (2.24), that is,

$$\langle D_j,\ \lambda\rangle < -c'_j(x_j^*) \quad \text{i}mplies \quad x_j^* = b_j. \tag{2.31}$$

Since $a_j \leq b_j, j \in J$, by assumption, we have three cases to consider.

Case 1. $\langle D_j,\ \lambda\rangle > -c'_j(a_j)$.

Then $\langle D_j,\ \lambda\rangle > -c'_j(x_j^*)$ according to (2.20) and the monotonicity of c'_j . Hence $x_j^* = a_j$ in accordance with (2.30).

Case 2. $\langle D_j,\ \lambda\rangle < -c'_j(b_j)$.

Then $\langle D_j,\ \lambda\rangle < -c'_j(x_j^*)$ according to (2.21) and the monotonicity of c'_j . Hence $x_j^* = b_j$ in accordance with (2.31).

Case 3. $-c'_j(b_j) \leq \langle D_j,\ \lambda\rangle \leq -c'_j(a_j)$.

If $\langle D_j,\ \lambda\rangle < -c'_j(x_j^*)$, then $x_j^* = b_j$ according to (2.31). Therefore $\langle D_j,\ \lambda\rangle \geq -c'_j(x_j^*)$ because $\langle D_j,\ \lambda\rangle \geq -c'_j(b_j)$ by the assumption of Case 3, a contradiction. Similarly, if we assume that $\langle D_j,\ \lambda\rangle > -c'_j(x_j^*)$ strictly, this would imply $x_j^* = a_j$ according to (2.30) and $\langle D_j,\ \lambda\rangle \leq -c'_j(x_j^*)$, a contradiction.

Then $\langle D_j,\ \lambda\rangle = -c'_j(x_j^*)$, so it follows that $x_j^* = (c'_j)^{-1}(-\langle D_j,\ \lambda\rangle)$.

In the three cases considered, we have

$$x_j^* = (c'_j)^{-1}[-\langle D_j,\ \lambda\rangle]_{c'_j(a_j)}^{c'_j(b_j)}. \tag{2.32}$$

Hence $x^* = (c')^{-1}[-D^T\ \lambda]_{c'(a)}^{c'(b)}$, that is,

$$\{P_c(D,\ \alpha, a, b)\} \subseteq \left\{(c')^{-1}[-D^T t]_{c'(a)}^{c'(b)} : t \in R^m\right\}. \tag{2.33}$$

ii) Conversely, suppose that $x^* \in R^n$ and $x^* = (c')^{-1}[-D^T t]_{c'(a)}^{c'(b)}$ for some $t \in R^m$. Set:

$$\alpha = D(c')^{-1}[-D^T t]_{c'(a)}^{c'(b)}$$
$$\lambda = t$$
$$u = c'(a) + D^T t$$
$$v = -c'(b) - D^T t.$$

We have to prove that x^*, α, λ, u, v satisfy the KKT conditions (2.19) -- (2.26).

Obviously x^* and α satisfy (2.19), x^* satisfies (2.20) and (2.21) (these are (1.6)) according to definition of $[x]_a^b$ and monotonicity of c'.

In order to verify (2.22) -- (2.26), we consider each $j \in J$. There are three possible cases.

Case 1. $\langle D_j, t\rangle > -c'_j(a_j)$.

Then $c'_j(a_j) + \langle D_j, t\rangle > 0$, and since $a_j \le b_j$, then $-c'_j(b_j) - \langle D_j, t\rangle < 0$. Therefore $x_j^* = a_j$, $\lambda = t, u_j = c'_j(a_j) + \langle D_j, t\rangle, v_j = 0$.

Case 2. $\langle D_j, t\rangle < -c'_j(b_j)$.

Then $-c'_j(b_j) - \langle D_j, t\rangle > 0$, and since $a_j \le b_j$, then $c'_j(a_j) + \langle D_j, t\rangle < 0$. Therefore $x_j^* = b_j$, $\lambda = t, u_j = 0, v_j = -c'_j(b_j) - \langle D_j, t\rangle$.

Case 3. $-c'_j(b_j) \le \langle D_j, t\rangle \le -c'_j(a_j)$.

Then $-c'_j(b_j) - \langle D_j, t\rangle \le 0$, $\langle D_j, t\rangle + c'_j(a_j) \le 0$. Therefore $x_j^* = (c')_j^{-1}(-\langle D_j, t\rangle)$, $\lambda = t, u_j = v_j = 0$.

Obviously in each of the three cases, $x_j^*, u_j, v_j (j \in J)$, λ satisfy (2.22) -- (2.26) as well.

Therefore x^*, α, λ, u, v satisfy the KKT conditions (2.19) -- (2.26), so $x^* \in P_c(D, \alpha, a, b)$ according to definition of $P_c(D, \alpha, a, b)$.

The two-way inclusion implies (2.27). □

Define the functions $x: R^m \to R^n$, $\alpha: R^m \to R^m$ by

$$x(t) = (c')^{-1}[-D^T t]_{c'(a)}^{c'(b)} \tag{2.34}$$

$$\alpha(t) = D(c')^{-1}[-D^T t]_{c'(a)}^{c'(b)} \tag{2.35}$$

Then the following Corollary holds.

Corollary 2.1 *Vectors* $x^* \in R^n$, $\alpha^* \in R^m$ *satisfy* $x^* = P_c(D, \alpha^*, a, b)$ *if and only if there exists* $t^* \in R^m$ *such that*

$$x(t^*) = x^* \tag{2.36}$$

$$\alpha(t^*) = \alpha^*. \tag{2.37}$$

Proof of Corollary 2.1 follows from the statement of problem $(C_m^=)$ and (2.27).

From Corollary 2.1 it follows that $x^* = P_c(D, \alpha^*, a, b)$ can be solved with respect to x^* for given α^* by first solving (2.37) for t^* and then calculating x^* by using (2.36).

Let S be the set of solutions to (2.37) for a particular value of α^*:

$$S = \{t \in R^m : \alpha(t) = \alpha^*\}. \tag{2.38}$$

According to (2.35), each component of $\alpha(t)$ is a linear combination of the same set of terms. Each term $(c')^{-1}[-D^T t]_{c_j(a_j)}^{c_j(b_j)}$ is a smooth function of t except on the pair of break hyperplanes

$$A_j = \{t \in R^m : \langle D_j, t\rangle = -c_j(a_j)\}, \tag{2.39}$$

$$B_j = \{t \in R^m : \langle D_j, t\rangle = -c_j(b_j)\}. \tag{2.40}$$

In the case when $m = 1$, that is, there is a single linear equality constraint of the form (1.5), the break hyperplanes are reduced to break points.

3 Illustrative examples

In this section, we illustrate application of Theorem 2.1 and Theorem 2.2 to simple particular problems.

Example 1.

$$\min\{c(x) = x_1^3 + x_2^3\}$$

subject to

$$x_1^2 + 2x_2^2 \le 10$$

$$1 \le x_1 \le 3$$

$$1 \le x_2 \le 5.$$

This problem is of the form (SCS) with

$c_j(x_j) = c_j x_j^q, q = 3, c_1 = 1, c_2 = 1, p = 2, d_1 = 1, d_2 = 2, \alpha = 10, a_1 = 1, b_1 = 3, a_2 = 1, b_2 = 5$

.

The optimal solution, obtained by Theorem 2.1, is

$$x^* = (x_1^*, x_2^*) = (1,1),$$

and

$$c_{\min} = c(x^*) = 2.$$

Example 2.

$$\min\{c(x) = 4x_1^2 + 10x_2^2 + 4x_3^2 + 3x_4^2 + 7x_5^2 + 3x_6^2 + x_7^2\}$$

subject to

$$\sum_{j=1}^{7} x_j = 72$$

$$4 \le x_1 \le 7$$

$$4.5 \le x_2 \le 10$$

$$8 \le x_3 \le 13$$

$$5 \le x_4 \le 8$$

$$4 \le x_5 \le 7$$

$$30 \le x_6 \le 40$$

$$4 \le x_7 \le 7.$$

This problem is of the form $(C_m^=)$ with $m = 1$, $n = 7$; $c_j(x_j) = c_j x_j^q, q = 2; \alpha = 72; d_j = 1,\ j = 1,\ldots,7; c = (c_j)_{j=1}^7 = (4,10,4,3,7,3,1),$

$$a = (a_j)_{j=1}^7 = (4,4.5,8,5,4,30,4), \quad b = (b_j)_{j=1}^7 = (7,10,13,8,7,40,7).$$

The optimal solution is

$$x^* = (7,4.5,9.8636,8,5.6363,30,7),$$

and

$$c_{\min} = c(x^*) = 3951.0454$$

References

[1] G.R. Bitran and A.C. Hax, Disaggregation and resource allocation using convex knapsack problems with bounded variables, *Management Science* **27** (1981), No. 4, 431 - 441.

[2] K. Dahiya, S.K. Suneja, and V. Verma, Convex programming with single separable constraint and bounded variables, *Computational Optimization and Applications* **36** (2007), No. 1, 67 - 82.

[3] J.-P. Dussault, J. Ferland, and B. Lemaire, Convex quadratic programming with one constraint and bounded variables, *Mathematical Programming* **36** (1986), No. 1, 90 - 104.

[4] R. Helgason, J. Kennington, and H. Lall, A polynomially bounded algorithm for a singly constrained quadratic program, *Mathematical Programming* **18** (1980), No. 3, 338 - 343.

[5] N. Katoh, T. Ibaraki, and H. Mine, A polynomial time algorithm for the resource allocation problem with a convex objective function, *Journal of the Operations Research Society* **30** (1979), No. 5, 449 - 455.

[6] H. Luss and S.K. Gupta, Allocation of effort resources among competing activities, *Operations Research* **23** (1975), No. 2, 360 - 366.

[7] S.M. Stefanov, On the implementation of stochastic quasigradient methods to some facility location problems, *Yugoslav Journal of Operations Research* **10** (2000), No. 2, 235 - 256.

[8] S.M. Stefanov, Convex separable minimization subject to bounded variables, *Computational Optimization and Applications. An International Journal* **18** (2001), No. 1, 27 - 48.

[9] S.M. Stefanov, Convex separable minimization problems with linear constraint and bounds on the variables, in *Applications of Mathematics in Engineering and Economics*, Sofia, 2002, pp. 392 - 402.

[10] S.M. Stefanov, Method for solving a convex integer programming problem, *International Journal of Mathematics and Mathematical Sciences*, vol. **2003**, No. 44, 2829 - 2834.

[11] S.M. Stefanov, Convex quadratic minimization subject to a linear constraint and box constraints, *Applied Mathematics Research Express*, vol. **2004**, No. 1, 17 - 42.

[12] S.M. Stefanov, Polynomial algorithms for projecting a point onto a region defined by a linear constraint and box constraints in R^n, *Journal of Applied Mathematics*, vol. **2004**, No. 5, 409 - 431.

[13] S.M. Stefanov, Convex separable minimization problems with a linear constraint and bounded variables, *International Journal of Mathematics and Mathematical Sciences*, vol. **2005**, No. 9, 1339 - 1363.

[14] S.M. Stefanov, An efficient method for minimizing a convex separable logarithmic function subject to a convex inequality constraint or linear equality constraint, *Journal of Applied Mathematics and Decision Sciences*, vol. **2006**, 1 - 19, article ID 89307.

[15] S.M. Stefanov, Minimizing a convex separable exponential function subject to linear inequality or equality constraint and bounds on the variables, *Journal of Interdisciplinary Mathematics* **9** (2006), No. 1, 207 - 226.

[16] S.M. Stefanov, Minimization of a convex linear-fractional separable function subject to a convex inequality constraint or linear inequality constraint and bounds on the variables, *Applied Mathematics Research Express*, vol. **2006**, 1 - 24, article ID 36581.

[17] S.M. Stefanov, Applications of convex separable unconstrained nonsmooth optimization to numerical approximation with respect to l_1- and l_∞-norms, *Journal of Interdisciplinary Mathematics*, **10** (2007), No. 6, 767 - 788.

[18] S.M. Stefanov, Solution of some convex separable resource allocation and production planning problems with bounds on the variables, *Journal of Interdisciplinary Mathematics*, vol. **13** (2010) No. 5, 541 - 569.

[19] T.V. Tchemisova, On the constructive solution of convex programming problems in separable form, *Journal of Mathematical Sciences* **120** (2004), No. 1, 1016 - 1031.

[20] P.H. Zipkin, Simple ranking methods for allocation of one resource, *Management Science* **26** (1980), No. 1, 34 - 43.

Lorentz Link Problem and Solutions

Emilija Celakoska, Dushan Chakmakov
Department of Mathematics & Informatics, Faculty of Mech. Engineering, Ss. Cyril and Methodius University, Skopje, Republic of Macedonia

***Abstract**: Lorentz transformations between given pair of 4-vectors with an equal Minkowski norm are usually referenced as Lorentz links. We present two equivalent formulas which generally solve the problem of finding Lorentz boost links. The first one is an algebraically derived formula in a rather compound form. In this paper, we are focused on the second one, derived in a more geometrical manner using reflections. This approach results in a more insightful and elegant solution of the Lorentz link problem.*

***Keywords:** transformation, boost, reflection*

1. INTRODUCTION

The Lorentz group together with translations (Poincare group) is the group of symmetries of the metric tensor of the empty space-time. It is the linear group (subgroup of GL(4,**R**)) of orthogonal transformations of Minkowski space, also called O(1,3), which preserves distances. Hence, $L \in$ O(1,3) iff

$$\eta(L(x), L(y)) = \eta(x, y)\,.$$

For the sake of brevity we shall further denote scalar product simply by $x \cdot y \equiv \eta(x,y) \equiv \eta_{ij}x^i y^j$. We work with $\eta = \mathrm{diag}(1, -1, -1, -1)$.

Geometrically, Lorentz transformations are usually classified as rotations, boosts and reflections. We discussed this classification in [2], together with some facts concerning the connected components of the Lorentz group O(1,3) related to the algebraic structure of the space of 4-vectors of velocity. Here, we consider a space of 4-vectors whose equal Minkowski norm does not necessarily refer to a physical quantity, such as the speed of light. However, we will need the concept of timelike vector X, i.e. a 4-vector for which $\eta(X,X) > 0$.

In Lorentz link problem, of particular interest are Lorentz boosts, because only boosts act nontrivially representing relative 4-velocity between different frames. Boosts, are proper and orthochronous transformations, i.e. they belong to, and together with rotations, generate the restricted Lorentz

group. Thus, a boost is a Lorentz transformation without spatial rotation, which justifies its other name of "pure" Lorentz transformation. While the composition of rotations is always a rotation, the composition of boosts in general case is not a boost.

Lorentz links are Lorentz transformations between given pair of 4-vectors. The problem of determining the Lorentz transformations that link 4-vectors with an equal norm has been addressed by several authors [1], [3], [4], [5], [6], [7], [8] using different approaches. In the recent article [2], we gave an overview on the seemingly different solutions of the Lorentz link problem in the coplanar case and we obtained that they are equivalent.

Regarding the Lorentz links, it is sufficient to restrict the problem to determination of boosts. Lorentz links by rotations are not interesting since they are reduced to trivial solutions. However, as we shall see, the Lorentz boost links can be obtained by using composition of reflections [6].

Definition 1. Parameterized by 4-vector U, an orthogonal reflection at the non-null hyperplane with normal U is given by the tensor

$$S_U = \delta - 2\frac{U \otimes \eta U}{U^2}.$$

Lorentz link by reflection has a simple solution. Namely, for two vectors U and V with an equal Minkowski norm one can straightforwardly obtain that $S_{U-V}U = V$ and it is the unique reflection that links U to V, that is to say, if $S_X U = V$ and $S_Y V = U$ hold simultaneously, it immediately follows that X and Y are proportional to $U-V$ and hence are linearly dependent, so $S_X = S_Y$. Thus, Lorentz link by a reflection between U and V is given by

$$S_{U,V} = \delta - 2\frac{(U-V) \otimes \eta (U-V)}{(U-V)^2}, \quad (U-V)^2 \neq 0. \tag{1}$$

Note that Lorentz link by reflections is undefined for $U = V$. It is not a boost since it does not satisfy the criteria for boost given below, as one can easily verify subsequently.

2. ON LORENTZ BOOST LINKS

In a set of 4-vectors with an equal Minkowski norm there exists a Lorentz link that transforms one 4-vector into another. Let U and V be 4-vectors with $U^2 = V^2$. Each Lorentz link $L_{U,V}$ between U and V defines a set of Lorentz transformations parameterized by 6 independent components. Note that in case of Lorentz boost links, the first components of U and V ("time" components) must have the same sign to make the problem well defined.

It is easy to see that if $L_{U,V}$ transforms U into V, i.e. $L_{U,V}U = V$, then it is always possible to obtain additional Lorentz links by

$$(Id_V \cdot L_{U,V} \cdot Id_U)U = V$$

for any two orthogonal transformations Id_U and Id_V such that $Id_U U = U$ and $Id_V V = V$. For example, simple transformations of that kind are

$$Id_U = \frac{U \otimes \eta U}{U^2} \quad \text{and} \quad Id_V = \frac{V \otimes \eta V}{V^2}.$$

All the elements Id_V of the Lorentz group that fix the 4-vector V, form a subgroup called little (or stability) Lorentz group at V, [9].

It has been shown that every little Lorentz group is isomorphic with the proper rotation group SO(3). If we put an additional requirement on L in form $L_{U,U} = \delta$, we ensure that L is in the restricted Lorentz group (the connected component with the identity δ) and we eliminate the rotations from L providing L to be a pure Lorentz transformation, i.e. a boost. Conversely, let $L_{U,V}$ be a Lorentz boost which links two 4-vectors U and V, $L_{U,V}U = V$. Replacing V by U we obtain $L_{U,U}U = U$, where $L_{U,U}$ is a boost, implying that it must be $L_{U,U} = \delta$. This criteria enables an easy check whether a given Lorentz link is a boost. It can be summarized as follows.

Theorem 1. If $L_{U,V}$ is a Lorentz transformation which links two 4-vectors U and V, then $L_{U,V}$ is a boost iff $L_{U,U} = \delta$.

The following theorem [3], which gives one solution to Lorentz link problem, is formulated independently by more authors .

Theorem 2. Lorentz boost link, parameterized only by the initial 4-vector U and the resulting 4-vector V is given by

$$(2) \qquad B_{U,V} = \delta \; - \; 2\frac{(U+V)\otimes\eta(U+V)}{(U+V)^2} \; + \; 2\frac{V\otimes\eta U}{V^2}, \quad (U+V)^2 \neq 0 .$$

It is easy to see that $(B_{U,V})^{-1} = \eta\cdot(B_{U,V})^{\mathrm{T}}\cdot\eta = B_{V,U}$. The proofs that the tensor $B_{U,V}$ is an orthogonal transformation, $B_{U,V}B_{V,U} = \delta$ and that $B_{U,V}U = V$ are straightforward. It is obvious that $B_{U,U} = \delta$, implying that Lorentz transformation given by (2) is a boost.

However, it is known that there is a continuum of boosts that link two given 4-vectors U and V. The obvious one which rotates in $U \wedge V$ plane is given by (2). However, it is interesting that there are other boosts that link U and V which rotate in different planes.

Oziewicz [4] has given a generalized solution to the problem of finding Lorentz boosts between given 4-vectors. His solution is additionally parameterized by an arbitrary timelike 4-vector X.

Theorem 3. The Lorentz boost links parameterized by the initial 4-vector U, the resulting 4-vector V and an arbitrary timelike 4-vector X are given by

$$B_{U,V,X} = \delta - \frac{2X \otimes \left\{ (U-V)^2 \eta X - (X \cdot U)\eta(U-V) \right\}}{X^2(U-V)^2 + 4(X \cdot U)(X \cdot V)} - \frac{(U-V) \otimes \left\{ 2X^2 \eta(U-V) + 4(X \cdot V)\eta X \right\}}{X^2(U-V)^2 + 4(X \cdot U)(X \cdot V)} \tag{3}$$

$$X^2(U-V)^2 + 4(X \cdot U)(X \cdot V) \neq 0, \quad (U-V)^2 \neq 0,$$
$$X(U+V) \neq 0, \quad X \wedge (U-V) \neq 0.$$

From the constraints accompanying (3), only the first one is related to the existence of the corresponding boost link. The rest of the constraints simply exclude singular solutions and impose constraints on X. One can straightforwardly prove that the tensor $B_{U,V,X}$ is an orthogonal transformation and $B_{U,V,X}U = V$.

The solution (2) can be obtained from (3) when the 4-vectors U, V and X are coplanar. When the parameterization is made only by linear combination of the initial and the final vector, the vector X is in $U \wedge V$ plane and then the Lorentz link becomes unique, given by (2). However, by choice of a preferred 4-vector X to be non-coplanar relative to the $U \wedge V$ plane, one can obtain a continuum of Lorentz boost links.

3. LORENTZ BOOST LINKS OBTAINED BY REFLECTIONS

The Lorentz boost links can be derived in a more insightful and pedagogically more appealing way using reflections. In particular, any boost in a plane containing the timelike vector X is of the form $S_Y S_X$ for some timelike 4-vector Y, and hence S_Y is uniquely determined [6]. So, we can look for all boosts $B_{U,V,X}$ in a plane containing X that map U to V. Since it should be $B_{U,V,X}U = V$, it follows $S_Y(S_X U) = V$ and now according to (1) we obtain the solution $Y = V - S_X U$ which is timelike. Note that this is the unique solution for S_Y up to a scalar.

Theorem 4. All Lorentz boosts between the initial U and the resulting V additionally parameterized by an arbitrary timelike 4-vector X, are given by a family of boosts

$$B_{U,V,X} = S_{V - S_X U} S_X, \quad (V - S_X U)^2 \neq 0. \tag{4}$$

Note that the constraint $(V - S_X U)^2 \neq 0$ is equal to the first constraint given in (3). The formula (4) has more general interpretation than the similar formula for Lorentz boost that links space-time events [6].

By simple calculation we obtain

$$B_{U,U,X} = S_{U-S_X U} S_X = S_{\lambda X} S_X = \delta$$

where λ is a scalar, proving that $B_{U,V,X}$ is a boost. For X coplanar to U and V this reduces to the "standard" Lorentz boost link given by (2). One can also straightforwardly prove that (4) is equal to (3).

The issue of uniqueness of the Lorentz links was discussed in [2] on the formulae (2) and (3). It seems that (4) offers a much simpler and geometrically clearer picture of the non-uniqueness of the Lorentz boost linking given 4-vectors. Actually, the formula (3) relies entirely on the extensive algebraic operations whose complicated structure hides its simple geometrical meaning. Note that existence and uniqueness of the required Lorentz boosts are easily obtained in this "geometric" approach.

4. CONCLUSION

In this paper, we presented two formulas to obtain all Lorentz boosts that link two given 4-vectors. The first one is the known formula (3) which is derived by tedious algebraic calculations. The second formula (4) is a result of more elegant geometrical observations. This geometric approach is based on reflections and gives simpler and conceptually clearer solution.

5. REFERENCES

[1] Bolós, V.J., (2006) Lightlike simultaneity, comoving observers and distances in general relativity, *Journal of Geometrical Physics* 56, 813-829

[2] Celakoska, E. (2008) On Isometry Links between 4-Vectors of Velocity, *Novi Sad Journal of Mathematics* 38 (3), 165-172.

[3] Fahnline D.E. (1982) A covariant four-dimensional expression for Lorentz transformation, *American Journal of Physics* 50 (9), 818–821.

[4] Oziewicz, Z. (2006) The Lorentz boost-link is not unique. Relative velocity as a morphism in a connected groupoid category of null objects, Paper presented at the *5th International Workshop Applied Category Theory, Graph-Operad-Logic, UADY, CINVESTAV, Merida, 15-19 May 2006*. Cited 30 August 2006, http://arxiv.org/abs/math-ph/0608062.

[5] Ungar, A.A. (2001) *Beyond the Einstein addition law and its gyroscopic Thomas precession, the theory of gyrogroups and gyrovector spaces*, Boston, Kluwer Academic.
[6] Urbantke, H.K. (2003) Lorentz transformations from reflections, *Foundations of Physics Letters* 16 (2), 111–117.
[7] van Wyk, C.B. (1986) Lorentz transformastions in terms of initial and final vectors, *Journal of Mathematical Physics* 27 (5) 1306–1314.
[8] van Wyk, C.B. (1991) The Lorentz operator revisited, *Journal of Mathematical Physics* 32 (2), 425–430.
[9] Wigner, E.P. (1939) On unitary representations of the inhomogeneous Lorentz group, *Annals of Mathematics* 40 (1), 149-204.

On free medial semigroups

Vesna Celakoska-Jordanova
Faculty of Natural Sciences and Mathematics,
Ss. Cyril and Methodius University, Skopje
Republic of Macedonia

Abstract. *Descriptions of free objects in the variety of medial semigroups are obtained.*

Key words: *medial semigroup, free semigroup, quotient semigroup, V-canonical semigroup.*

A semigroup ***S*** is said to be ***medial*** if $abcd = acbd$, for every a, b, c, d in S. The class of all medial semigroups is a variety of semigroups defined by the identity $xyuv \approx xuyv$. We denote this variety by *Med*. If ***S*** is a medial semigroup, then the following equalities hold in ***S***:

$$px_1x_2x_3q = py_1y_2y_3q,$$

for any $p, x_1, x_2, x_3, q \in S$ and any permutation $y_1y_2y_3$ of $x_1x_2x_3$.

A free medial semigroup as a quotient structure of the free semigroup over an alphabet is constructed below. Recall that the free semigroup over a nonempty set A, is the set A^+ of all finite sequences $(a_1,a_2,\ldots,a_n)$ of elements of A endowed by the operation concatenation of sequences:

$$(a_1,a_2,\ldots,a_n)(b_1,b_2,\ldots,b_m) = (a_1,a_2,\ldots,a_n,b_1,b_2,\ldots,b_m).$$

Identifying each sequence of the form (a) with $a \in A$, we have $(a_1,a_2,\ldots,a_n) = a_1a_2\ldots a_n$. The elements of A are ***letters*** and elements of A^+ are ***words*** on A. Two words $u = a_1a_2\ldots a_n$ and $v = b_1b_2\ldots b_n$ are ***equal*** if and

only if $n = m$ and $a_i = b_i$, for $i = 1,2,\ldots,n$. The number n is called the ***length*** of the word $w = a_1a_2\ldots a_n$ and it is denoted by $|w|$. For any word w we define the ***content*** cnt(w) inductively by:

$$a \in A \Rightarrow \text{cnt}(w) = \{a\},\ \ w = uv \Rightarrow \text{cnt}(uv) = \text{cnt}(u) \cup \text{cnt}(v).$$

We introduce the notion of "elementary medial transformation" of a word in A^+ analogously as for the left commutative groupoids ([1]).

Definition 1. Let $w \in A^+$, $w = a_1a_2\ldots a_n$ where $a_1,a_2,\ldots,a_n \in A$. A ***segment*** of w is called any expression of the form $a_ia_{i+1}\ldots a_{i+j}$, where $i+j \leq n$, i runs in $\{1,2,\ldots, n\}$ and j runs in $\{0,1,\ldots, n-1\}$. ***The set of segments*** of w is denoted by seg(w). Thus:

$$\text{seg}(w) = \{a_ia_{i+1}\ldots a_{i+j} \mid i+j \leq n,\ i \in \{1,2,\ldots, n\},\ j \in \{0,1,\ldots, n-1\}\}.$$

Proposition 1. If $w = a_1a_2\ldots a_n$, then $n \leq |\text{seg}(w)| \leq (n(n-1))/2$. □

Definition 2. Let $w \in A^+$, $|w| \geq 4$ and $txyz$ be a segment of w. If one occurrence of $txyz$ in w is replaced by $tyxz$, an element $u \in A^+$ is obtained that is different from w only in the replaced segment $txyz$ by $tyxz$. In that case we say that an ***elementary medial transformation*** is performed on w and write $w \rightharpoonup u$. In the cases when $w = a$ or $w = ab$ or $w = abc$, where a, b, $c \in A$, we put by definition $w \rightharpoonup w$. Thus, $w = \alpha txyz\beta \rightharpoonup \alpha tyxz\beta = u$, where $\alpha, \beta \in A^+$ or, α or β is the empty symbol.

We can "go back" from u to w performing the elementary medial transformation $u = \alpha tyxz\beta \rightharpoonup \alpha txyz\beta = w$ in the same place. We call this transformation an ***inverse return*** from u to w. Thus, $w \rightharpoonup u \rightharpoonup w$.

Note that an elementary medial transformation of an arbitrary word w does not lead to a transformation on A^+, because the "image" of w is not uniquely determined. For instance, the word $w = abcde$, where a, b, c, d, $e \in A$, with one elementary medial transformation can be transformed in $acbde$, but also in $w = abdce$.

Definition 3. Define a relation ~ on A^+ by:

$$w \sim u \Leftrightarrow (\exists w_0, w_1,\ldots,w_k \in A^+)\ w = w_0 \rightharpoonup w_1 \rightharpoonup \ldots \rightharpoonup w_{k-1} \rightharpoonup w_k = u.$$

Proposition 2. $w \sim u$, where $w = a_1a_2\ldots a_n$, $u = b_1b_2\ldots b_m$ if and only if $n = m$, $a_1 = b_1$, $a_n = b_n$ and $b_2\ldots b_{n-1}$ is a permutation of $a_2\ldots a_{n-1}$.

Proof. If $w \sim u$, then $|w|=|u|$, cnt(w) = cnt(u), left and right ends of w and u are equal and the appearance of any $a \in A$ in w is equal to the appearance of a in u. Therefore, $n = m$, $a_1 = b_1$, $a_n = b_n$ and $b_2\ldots b_{m-1}$ is a permutation of $a_2\ldots a_{n-1}$. Conversely, for $n = 1$, $n = 2$ and $n = 3$, $w \sim u$ is trivially fulfilled. Suppose that $w \sim u$, for $n \leq k$ and $k \geq 4$. If $n = k+1$, then

$m = k+1$, $a_1 = b_1$, $a_{k+1} = b_{k+1}$ and so $u = a_1b_2\ldots b_ka_{k+1}$. By the inductive supposition we obtain that $b_2\ldots b_k \sim a_2\ldots a_k$, and thus $a_1a_2\ldots a_{k+1} \rightharpoonup a_1b_2\ldots b_ka_{k+1}$, i.e. $w \sim u$. □

Directly from the definition of ~ it follows that ~ is an equivalence relation. If $w \sim u$ and $v \in A^+$, then $wv \sim uv$ and $vw \sim vu$, i.e. ~ is a congruence relation in A^+.

Define an operation $\cdot$ on $A^+/\sim = \{w^\sim \mid w \in A^+\}$ by:

$$w^\sim, u^\sim \in A^+/\sim \;\Rightarrow\; w^\sim \cdot u^\sim = (wu)^\sim .$$

It is clear that $(A^+/\sim,\cdot)$ is a semigroup. Further on we write $A^+/\sim$ instead of $(A^+/\sim,\cdot)$. Since $w_1^\sim \cdot w_2^\sim \cdot w_3^\sim \cdot w_4^\sim = (w_1w_2)^\sim \cdot (w_3w_4)^\sim = (w_1w_2w_3w_4)^\sim = (w_1w_3w_2w_4)^\sim = (w_1w_3)^\sim \cdot (w_2w_4)^\sim = w_1^\sim \cdot w_3^\sim \cdot w_2^\sim \cdot w_4^\sim$, for any $w_1^\sim$, $w_2^\sim$, $w_3^\sim$, $w_4^\sim \in A^+/\sim$, the semigroup $(A^+/\sim,\cdot)$ is medial. Note that $a^\sim = \{a\}$, for any $a \in A$.

If $w^\sim \in A^+/\sim$, then $w^\sim = (a_1a_2\ldots a_n)^\sim = a_1^\sim \cdot a_2^\sim \cdot \ldots \cdot a_n^\sim$. Thus, $w^\sim$ is presented as a product of elements of $A/\sim$ and therefore $A/\sim$ is a generating set for $A^+/\sim$. Moreover, $A/\sim$ is a set of prime elements in $A^+/\sim$. Namely, if $a^\sim \in A/\sim$, then $a^\sim \neq w^\sim u^\sim$, for any $w^\sim, u^\sim \in A^+/\sim$, since a is not a product of elements of A^+. There are no other prime elements in $A^+/\sim$ except those of $A/\sim$. Namely, if $w^\sim \in (A^+/\sim)\setminus(A/\sim)$, then $w^\sim \notin (A/\sim)$, i.e. $w \notin A$. Thus, there are $u, v \in A^+$ such that $w = uv$. In that case, $w^\sim = (uv)^\sim = u^\sim \cdot v^\sim$, i.e. $w^\sim$ is not prime in $A^+/\sim$.

$A^+/\sim$ has the universal mapping property for Med over $A/\sim$, i.e. if $\boldsymbol{S} \in Med$ and $\lambda : A/\sim \to S$, then there is a homomorphism ψ from $A^+/\sim$ into $\boldsymbol{S}$ that is an extension of λ. Define the mapping $\psi : A^+/\sim \to S$ by $\psi(w^\sim) = \varphi(w)$, where φ is the homomorphism from A^+ in $\boldsymbol{S}$ that is an extension of λ.

The mapping ψ is well defined, that follows by the implication $w \sim u \Rightarrow \varphi(w) = \varphi(u)$. Namely, let $w \sim u$, i.e. $w_0, w_1, \ldots, w_k \in A^+$ are such that $w = w_0 \rightharpoonup w_1 \rightharpoonup \ldots \rightharpoonup w_{k-1} \rightharpoonup w_k = u$ and let $w_i = \alpha txyz\beta$, where $\alpha, \beta \in A^+$ or, α or β is the empty symbol. Since φ is a homomorphism it follows that:

$$\varphi(w_i) = \varphi(\alpha txyz\beta) = \varphi(\alpha)\varphi(t)\varphi(x)\varphi(y)\varphi(z)\varphi(\beta) = [S \in Med] =$$
$$= \varphi(\alpha)\varphi(t)\varphi(y)\varphi(x)\varphi(z)\varphi(\beta) = \varphi(\alpha tyxz\beta) = \varphi(w_{i+1}),$$

for $i \in \{0,...,k-1\}$. Hence, $\varphi(w) = \varphi(w_0) = \varphi(w_1) = ... = \varphi(w_k) = \varphi(u)$. The mapping ψ is a homomorphism from $A^+/\sim$ into $\boldsymbol{S}$, since

$$\psi(w^{\sim} \cdot u^{\sim}) = \psi((wu)^{\sim}) = \varphi(wu) = \varphi(w)\varphi(u) = \psi(w^{\sim})\psi(u^{\sim}).$$

By the above discussion we obtain that the following theorem holds.

Theorem 1. The quotient semigroup $(A^+/\sim,\cdot)$ is a free medial semigroup over $A^+/\sim$. □

Below we give a canonical description of a free medial semigroup.

Definition 4. Let V be a variety of semigroups. A semigroup $\boldsymbol{R} = (R,*)$ is said to be ***canonical*** in V, i.e. V-***canonical***, over A if the following conditions are satisfied:

(c_0) $A \subseteq R \subseteq A^+$ and $w \in R \Rightarrow \mathrm{seg}(w) \subseteq R$;

(c_1) $wu \in R \Rightarrow w * u = wu$;

(c_2) $\boldsymbol{R}$ is a free semigroup in V over A.

Definition 5. Let the alphabet A be linearly ordered by $\leq$. A word $a_1a_2\ldots a_n \in A^+$ is said to be ***monotonic***, i.e. it has ***a natural order*** if and only if $a_1 \leq a_2 \leq \ldots \leq a_n$.

As a candidate for the carrier of a free medial semigroup we choose the subset R of A^+ defined in the following way:

(i) $A \cup A^2 \cup A^3 \subseteq R$;

(ii) $(\forall w = a_1...a_n \in A^+, n \geq 4)(w \in R \Rightarrow a_2...a_{n-1}$ is monotonic$)$.

By the definition of R and by induction on length of a word, one can obtain that the condition (c_0) is fulfilled. Note that among all the words of letters $a_1, a_2, ..., a_n$, only one is monotonic, i.e. only one has the natural order. We denote by $(a_1a_2...a_n)'$ the permutation of $a_1, a_2, ..., a_n$ that gives their natural order.

Define an operation $*$ on R by:

$$w = a_1a_2...a_n,\ u = b_1b_2...b_m \in R \ \Rightarrow\ w * u = a_1(a_2...a_nb_1...b_{m-1})'b_m.$$

Theorem 2. $\boldsymbol{R} = (R,*)$ is a Med-canonical semigroup over A. □

Proof. The permutation $(a_2...a_nb_1...b_{m-1})'$ gives the natural order of the elements $a_2, ..., a_n, b_1, ..., b_{m-1}$ and therefore $w * u$ is a uniquely determined word in $\boldsymbol{R}$, i.e. $*$ is a well-defined operation. Since $w * u = wu$, the condition (c_1) is fulfilled.

Let $w_1 = a_1a_2...a_n$, $w_2 = b_1b_2...b_m$, $w_3 = c_1c_2...c_k$, $w_4 = d_1d_2...d_p$.

Verifying the condition (c_2), we obtain:

$$(w_1 * w_2) * w_3 = a_1(a_2...a_nb_1b_2...b_{m-1})'b_m * c_1c_2...c_k =$$

$$= a_1(a_2...a_nb_1...b_{m-1}b_mc_1...c_{k-1})'c_k =$$

$$a_1...a_n * b_1(b_2...b_{m-1}b_mc_1...c_{k-1})'c_k =$$

$= w_1 * (w_2 * w_3)$. Therefore, $\boldsymbol{R} = (R, *)$ is a semigroup.

$\boldsymbol{R} = (R, *)$ is medial. Namely,

$$w_1 * w_2 * w_3 * w_4 = a_1a_2...a_nb_1b_2...b_mc_1c_2...c_kd_1d_2...d_{p-1}d_p =$$

$$= a_1(a_2...a_nb_1b_2...b_mc_1c_2...c_kd_1d_2...d_{p-1})'d_p =$$

$$= a_1(a_2...a_nc_1c_2...c_kb_1b_2...b_md_1d_2...d_{p-1})'d_p =$$

$$= a_1a_2...a_nc_1c_2...c_kb_1b_2...b_md_1d_2...d_{p-1}d_p = w_1 * w_3 * w_2 * w_4$$

If $w = a_1a_2...a_n \in R$, then $w = a_1 * a_2 * ... * a_n$ and thus, A is a generating set for $\boldsymbol{R}$. Moreover, A is the set of prime elements in $\boldsymbol{R}$. Namely, if $a \in A$, then $a \neq w * u$, for any $w, u \in R$, i.e. every element of A is prime in $\boldsymbol{R}$. If $w = a_1a_2...a_n \in R \setminus A$, then $n \geq 2$ and $a_1a_2...a_n = a_1 * a_2 * ... * a_n$, which means that w is a product in $\boldsymbol{R}$. There are no other prime elements in $\boldsymbol{R}$ except those in A.

$\boldsymbol{R}$ has the universal mapping property for Med over A, i.e. if $\boldsymbol{S} \in Med$ and $\lambda : A \to S$ is a mapping, then there is a homomorphism ψ from $\boldsymbol{R}$ into $\boldsymbol{S}$ such that ψ is an extension of λ. Define the mapping ψ from $\boldsymbol{R}$ into $\boldsymbol{S}$ by $\psi(w) = \varphi(w)$, for any $w \in R$, where φ is the homomorphism from A^+ in $\boldsymbol{S}$ that is an extension of λ. It is sufficient to show that $\psi(w * u) = \varphi(w)\varphi(u)$, for any $w = a_1a_2...a_n$, $u = b_1b_2...b_m$ in $\boldsymbol{R}$. Namely,

$$\psi(w * u) = \varphi(a_1(a_2...a_nb_1b_2...b_{m-1})'b_m) = \varphi(a_1c_2...c_nc_{n+1}...c_{n+m-1}b_m) =$$

$$= \varphi(a_1)\varphi(c_2)...\varphi(c_n)\varphi(c_{n+1})...\varphi(c_{n+m-1})\varphi(b_m) =$$

$$= [S \in Med] = \varphi(a_1)\varphi(a_2)...\varphi(a_n)\varphi(b_1)...\varphi(b_{m-1})\varphi(b_m) =$$

$$= \varphi(a_1...a_n)\varphi(b_1...b_m) = \varphi(w)\varphi(u).$$

The conditions (c_0), (c_1) and (c_2) are satisfied. Hence, $\boldsymbol{R} = (R, *)$ is a Med-canonical semigroup over A. □

REFERENCES

[1] Celakoska-Jordanova V., Janeva B. (2009) Free left commutative groupoids, Annual Review of the European University, Skopje, Republic of Macedonia, 687 – 694.

[2] Markovski S., Sokolova A., Goracinova-Ilieva L. (2001) Approaches to the Problem of Constructing Free Algebras, Proc. Sixth Int. Conf. On Discrete Math 2001, Bansko Bulgaria, 109 – 117.

[3] McKenzie R. N., McNulty G. F., Taylor W. F. (1987) *Algebras, Latices, Varieties*, Wadsworth & Brooks/Cole.

Intuitionistic fuzzy preopen (preclosed) mappings

Biljana Krsteska
Faculty of Mathematics and Natural Sciences, Skopje, Macedonia

***Abstract**: In this paper, we will introduce and characterize intuitionistic fuzzy preopen and intuitionistic fuzzy preclosed mappings between intuitionistic fuzzy topological spaces. Their properties and relationships with early defined classes of intuitionistic fuzzy mappings have been investigated.*

***Keywords**: Intuitionistic fuzzy topology, Intuitionistic fuzzy preopen mapping, Intuitionistic fuzzy preclosed mapping*.

1. Introduction

The concept of fuzzy set was introduced by Zadeh in his classic paper [6]. Using the concept of fuzzy sets Chang [2] introduced the fuzzy topological spaces. Since Atanassov [1] introduced the notion of intuitionistic fuzzy sets, Coker [3] defined the intuitionistic fuzzy topological spaces. This approach provided a wide field for investigation in the area of fuzzy topology and its applications. One of directions is related to the intuitionistic fuzzy generalized set introduced by Coker (Gurcay and Coker [4]). Following this work, Jeon et al. [5] get some deeper results about the intuitionistic fuzzy generalized sets, intuitionistic $\alpha-$continuity and the intuitionistic fuzzy precontinuity.

In this paper we will introduce intuitionistic fuzzy preopen (preclosed) mappings and we will study some of their properties. We will establish their relationships with other forms of intuitionistic fuzzy continuous mappings.

2. Preliminaries

We introduce some notions and results that are used in the sequel.

Definition 2.1. [1] Let X be a nonempty fixed set and I the closed interval [0,1]. An intuitionistic fuzzy set (IFS) A is an object of the following form

$$A = \{< x, \mu_A(x), \gamma_A(x) >| x \in X\}$$

where the mapping $\mu_A : X \to I$ and $\gamma_A : X \to I$ denote the degree of membership (namely $\mu_A(x)$) and the degree of nonmembership

(namely $\gamma_A(x)$) for each element $x \in X$ to the set A, respectively, and $0 \le \mu_A(x) + \gamma_A(x) \le 1$ for each $x \in X$.

Obviously, every fuzzy set A on a nonempty set X is an IFS of the form

$$A = \{< x, \mu_A(x), 1 - \mu_A(x) > | \, x \in X\}.$$

Definition 2.2. [1] Let A and B be IFS's of the form $A = \{< x, \mu_A(x), \gamma_A(x) > | \, x \in X\}$ and $B = \{< x, \mu_B(x), \gamma_B(x) > | \, x \in X\}$. Then

(i) $A \subseteq B$ if and only if $\mu_A(x) \le \mu_B(x)$ and $\gamma_A(x) \ge \gamma_B(x)$;

(ii) $\overline{A} = \{< x, \gamma_A(x), \mu_A(x) > | \, x \in X\}$;

(iii) $A \cap B = \{< x, \mu_A(x) \wedge \mu_B(x), \gamma_A(x) \vee \gamma_B(x) > | \, x \in X\}$;

(iv) $A \cup B = \{< x, \mu_A(x) \vee \mu_B(x), \gamma_A(x) \wedge \gamma_B(x) > | \, x \in X\}$. .

We will use the notation $A =< x, \mu_A, \gamma_A >$ instead of $A = \{< x, \mu_A(x), \gamma_A(x) > | \, x \in X\}$. A constant fuzzy set α taking value $\alpha \in [0,1]$ will be denoted by $\underline{\alpha}$. The IFS's $0_\sim$ and $1_\sim$ are defined by

$$0_\sim = \{< x, \underline{0}, \underline{1} > | \, x \in X\} \text{ and } 1_\sim = \{< x, \underline{1}, \underline{0} > | \, x \in X\}.$$

Let f be a mapping from an ordinary set X into an ordinary set Y. If

$$B = \{< y, \mu_B(y), \gamma_B(y) > | \, y \in Y\}$$

is an IFS in Y, then the inverse image of B under f is IFS defined by

$$f^{-1}(B) = \{< x, f^{-1}(\mu_B)(x), f^{-1}(\gamma_B)(x) > | \, x \in X\}.$$

The image of IFS $A = \{< x, \mu_A(x), \gamma_A(x) > | \, x \in X\}$ under f is IFS defined by $f(A) = \{< y, f(\mu_A)(y), f(\gamma_A)(y) > | \, y \in Y\}$ where

$$f(\mu_A)(y) = \begin{cases} \sup\limits_{x \in f^{-1}(y)} \mu_A(x) & f^{-1}(y) \neq 0 \\ 0 & \text{otherwise} \end{cases}$$

and

$$f(\mu_A)(y) = \begin{cases} \inf\limits_{x \in f^{-1}(y)} \gamma_A(x) & f^{-1}(y) \neq 0 \\ 1 & \text{otherwise,} \end{cases}$$

for each $y \in Y$.

Definition 2.3. [3] An intuitionistic fuzzy topology (IFT) in Coker's sense on a nonempty set X is a family τ of IFSs in X satisfying the following:

(T_1) $0_\sim, 1_\sim \in \tau$;

(T_2) $G_1 \cap G_2 \in \tau$ for any $G_1, G_2 \in \tau$;

(T_2) $\cup G_i \in \tau$ for arbitrary family $\{G_i \mid i \in I\} \subseteq \tau$.

In this paper by (X, τ) or simply by X we will denote the Coker's intuitionistic fuzzy topological space (IFTS). Each IFS in τ is called intuitionistic fuzzy open set (IFOS) in X. The complement $\overline{A}$ of an IFOS in X is called an intuitionistic fuzzy closed set (IFCS) in X.

Definition 2.4.[3] Let $A = < x, \mu_A, \gamma_A >$ be an IFS in IFTS X. The intuitionistic fuzzy interior and intuitionistic fuzzy closure of A are defined by

$\text{int}A = \cup\{G \mid G \text{ is an IFOS in X and } G \subseteq A\}$ is called an intuitionistic fuzzy interior of A;

$\text{cl}A = \cap\{G \mid G \text{ is an IFCS in X and } G \supseteq A\}$ is called an intuitionistic fuzzy closure of A.

Definition 2.5. [5] An IFS A in an IFTS X is called an intuitionistic fuzzy preopen set (IFPOS) if $A \subseteq \text{int}(\text{cl}A)$.

The complement $\overline{A}$ of an IFPOS in X is called an intuitionistic fuzzy preclosed set (IFPCS) in X.

Definition 2.6.[5] Let $A = < x, \mu_A, \gamma_A >$ be an IFS in IFTS X. The intuitionistic fuzzy preinterior and intuitionistic fuzzy preclosure of A are defined by

$\text{pint}A = \cup\{G \mid G \text{ is an IFPOS in X and } G \subseteq A\}$

is called an intuitionistic fuzzy preinterior of A;

$\text{pcl}A = \cap\{G \mid G \text{ is an IFPCS in X and } G \supseteq A\}$ is called an intuitionistic fuzzy preclosure of A.

Definition 2.7. [5] Let f be a mapping from an IFTS X into an IFTS Y. The mapping f is called

(i) an intuitionistic fuzzy continuous if $f^{-1}(B)$ is an IFOS in X, for each IFOS B in Y.

(ii) an intuitionistic fuzzy $\alpha-$continuous if $f^{-1}(B)$ is an IFαOS in X, for each IFOS B in Y;

Definition 2.8. [5] Let f be a mapping from an IFTS X into an IFTS Y. The mapping f is called

(i) an intuitionistic fuzzy open (closed) if f(A) is IFOS of Y, for each IFOS (IFCS) A of X.

(ii) an intuitionistic fuzzy $\alpha-$open ($\alpha-$closed) if f(A) is IFαOS (IFαCS) of Y, for each IFOS (IFCS) A of X.

3. Inuitionistic fuzzy preopen (preclosed) mappings

Definition 3.1. A mapping $f : X \to Y$ from an IFTS X into an IFTS Y is called intuitionistic fuzzy preopen (preclosed) if f(A) is IFPOS (IFPCS) of Y, for each IFOS (IFCS) A of X.

Remark 3.1. The following diagram of implications is true.

intuitionistic fuzzy open (closed) $\Rightarrow$ intuitionistic fuzzy $\alpha-$open (closed)

$\Downarrow$ $\Downarrow$

intuitionistic fuzzy preopen (preclosed)

With the following example we can show that the reverse may not be true.

Example 3.1. Let $X = \{a,b,c\}$ and A, B and C are IFSs defined by

$$A = \left\langle x, \left(\frac{a}{0,3}, \frac{b}{0,1}, \frac{c}{0,7}\right), \left(\frac{a}{0,6}, \frac{b}{0,8}, \frac{c}{0,3}\right), \right\rangle$$

$$B = \left\langle x, \left(\frac{a}{0,8}, \frac{b}{0,8}, \frac{c}{0,4}\right), \left(\frac{a}{0,1}, \frac{b}{0,2}, \frac{c}{0,6}\right), \right\rangle$$

$$C = \left\langle x, \left(\frac{a}{0,8}, \frac{b}{0,7}, \frac{c}{0,6}\right), \left(\frac{a}{0,1}, \frac{b}{0,3}, \frac{c}{0,4}\right), \right\rangle$$

Let $\tau_1 = \{0_{\sim}, C, 1_{\sim}\}$, $\tau_2 = \{0_{\sim}, A, B, A \cap B, A \cup B, 1_{\sim}\}$. Then the mapping $f = id : (X, \tau_1) \to (X, \tau_2)$ is intuitionistic fuzzy preopen (preclosed) but it is not intuitionistic fuzzy $\alpha-$open ($\alpha-$closed). Also, f is not intuitionistic fuzzy open (closed).

Theorem 3.1. Let $f : X \to Y$ be a bijective mapping from an IFTS X into an IFTS Y. Then f is an intuitionistic fuzzy preopen (preclosed) mapping if and only if it is an intuitionistic fuzzy preclosed (preopen) mapping.

Proof. It can be proved by using the complement.

Theorem 3.2. Let $f : X \to Y$ be a bijective mapping from an IFTS X into an IFTS Y. Then f is an intuitionistic fuzzy preopen (preclosed) mapping if and only if f^{-1} is intuitionistic fuzzy precontinuous mapping.

Proof. It follows from the relation $(f^{-1})^{-1}(A) = f(A)$, for each IFOS (IFCS) set A of X.

Theorem 3.3. Let $f : X \to Y$ be a mapping from an IFTS X into an IFTS Y. Then f is an intuitionistic fuzzy preopen mapping if and only if $f(\text{int}\, A) \subseteq \text{pint}\, f(A)$, for each IFS A of X.

Proof. Let f be an intuitionistic fuzzy preopen mapping and let A be any IFS of X. Then $f(\text{int}\, A) = \text{pint}\, f(\text{int}\, A) \subseteq \text{pint}\, f(A)$.

Conversely, let A be any IFOS of X. According to the assumption we have $f(A) = f(\text{int}\, A) \subseteq \text{pint}\, f(A)$. Thus f(A) is an IFPOS of X, so f is an intuitionistic fuzzy preopen mapping.

Theorem 3.4. Let $f : X \to Y$ be a mapping from an IFTS X into an IFTS Y. Then f is an intuitionistic fuzzy preclosed mapping if and only if $\text{pclf}(A) \subseteq f(\text{cl}A)$, for each IFS A of X.

Proof. It can be proved in a similar manner as Theorem 3.3.

Theorem 3.5. Let $f : X \to Y$ be a bijective mapping from an IFTS X into an IFTS Y. Then the following statements are equivalent:

(i) f is an intuitionistic fuzzy preopen (preclosed) mapping;

(ii) $f(\text{int}\, A) \subseteq \text{pint}\, f(A)$, for each IFS A of X;

(iii) $\text{pclf}(A) \subseteq f(\text{cl}A)$, for each IFS A of X.

Proof. It follows from the Theorem 3.1, Theorem 3.3 and Theorem 3.4.

Theorem 3.6. Let $f : X \to Y$ be a mapping from an IFTS X into an IFTS Y. Then the following statements hold:

(1) f is an intuitionistic fuzzy preopen mapping if and only if $f(\text{int}\, A) \subseteq \text{int}(\text{pclf}(A))$, for each IFS A of X.

(2) f is an intuitionistic fuzzy preclosed mapping if and only if $\text{cl}(\text{pint}\, f(A) \subseteq f(\text{cl}A)$, for each IFS A of X.

Proof. We will prove the statement (1) only. Let f be intuitionistic fuzzy preopen mapping. Then, $f(\text{int}\, A)$ is an IFPOS of Y. Therefore

$$f(\text{int}\, A) \subseteq \text{int}(\text{pcl}(\text{int}\, A)) \subseteq \text{int}(\text{pcl}A).$$

Conversely, let A be any IFOS of X. From $f(A) = f(\text{int}\, A) \subseteq \text{int}(\text{pclf}(A))$, it follows that f(A) is an IFPOS, so f is an intuitionistic fuzzy preopen mapping.

Theorem 3.7. Let $f : X \to Y$ be a mapping from an IFTS X into an IFTS Y. Then f is intuitionistic fuzzy preopen if and only if for each IFS B of Y and each IFCS A of X, where $f^{-1}(B) \subseteq A$, there exists an IFPCS C of Y such that $B \subseteq C$ and $f^{-1}(C) \subseteq A$.

Proof. Let B be any IFS of Y and let A be an IFCS of X such that $f^{-1}(B) \subseteq A$. Then $\overline{A} \subseteq f^{-1}(\overline{B})$, so $f(\overline{A}) \subseteq ff^{-1}(\overline{B}) \subseteq \overline{B}$. Since $\overline{A}$ is an IFOS, $f(\overline{A})$ is an IFPOS, so $f(\overline{A}) \subseteq \text{pint}\, \overline{B}$. Hence $\overline{A} \subseteq f^{-1}f(\overline{A}) \subseteq f^{-1}(\text{pint}\, \overline{B})$. Therefore $A \supseteq \overline{f^{-1}(\text{pint}\, \overline{B})} = f^{-1}(\text{pcl}B)$. The result follows for $C = \text{pcl}B$.

Conversely, let U be any IFOS of X. We will show that f(U) is an IFPOS of Y. From $U \subseteq f^{-1}f(U)$ it follows that $\overline{U} \supseteq \overline{f^{-1}f(U)} \supseteq f^{-1}\overline{f(U)}$ where $\overline{U}$ is an IFCS of X. Hence there is an IFPCS B of Y such that $B \supseteq \overline{f(U)}$ and $f^{-1}(B) \subseteq \overline{U}$. From $B \supseteq \overline{f(U)}$ it follows that $B \supseteq \text{pclf}(U)$, so we have that

$\overline{B} \subseteq \overline{\text{pclf}(U))} \subseteq \text{pint}\, f(U)$. From $f^{-1}(B) \subseteq \overline{U}$ we have $B \supseteq f^{-1}(\overline{B}) \supseteq U$, so $\overline{B} \supseteq ff^{-1}(\overline{B}) \supseteq f(U)$. Hence $f(U) = \text{pint}\, f(U)$. Thus f(U) is an IFPOS, so f is an intuitionistic fuzzy preopen mapping.

Theorem 3.8. Let $f : X \to Y$ be a mapping from an IFTS X into an IFTS Y. Then f is an intuitionistic fuzzy preclosed mapping if and only if for each IFS set B of Y and each IFOS A of X, where $f^{-1}(B) \subseteq A$, there exists an IFPOS C of Y such that $B \subseteq C$ and $f^{-1}(C) \subseteq A$.

Proof. It can be proved in a similar manner as Theorem 3.7.

Theorem 3.9. Let $f : X \to Y$ and $g : Y \to Z$ be mappings, where X, Y and Z are IFTS. If g is intuitionistic fuzzy preopen (preclosed) and f is intuitionistic fuzzy open (closed), then gf is intuitionistic fuzzy preopen (preclosed).

Proof. For any IFOS (IFCS) A of X we have $(gf)(A) = g(f(A)$. Since f is intuitionistic fuzzy open (closed) and g is intuitionistic fuzzy preopen (preclosed), we obtain that $(gf)(A)$ is an IFPOS (IFPCS) of Z.

REFERENCES

[1] Atanassov, K. (1986) Intuitionistic fuzzy sets. *Fuzzy Sets and Systems* 20, 87-96.

[2] Chang, C. (1986) Fuzzy topological spaces. *J. Math. Anal. Appl.* 24 182-190.

[3] Coker, D. (1997) An introduction to intuitionistic fuzzy topological spaces. *Fuzzy Sets and Systems* 88, 81-89.

[4] Gurcay, H., Coker D. (1997) On fuzzy continuity in intuitionistic fuzzy topological spaces. *J. Fuzzy Math.* 5, 365-378.

[5] Joen, J., Jun, Y., Park, J. Intuitionistic fuzzy alpha-continuity and intuitionistic fuzzy precontinuity, *IJMMS*, 19 (2005) 3091–3101.

[6] Zadeh L. (1965) Fuzzy sets. *Information and control* 8, 338-353.

Free generalized $(2m,m)$ – rectangular bands of type $(3,2)$

Valentina Miovska, Donco Dimovski
Faculty of Natural Sciences and Mathematics, Ss. Cyril and Methodius University, Skopje, Republic of Macedonia

Abstract: *A characterization of generalized $(2m,m)$ – rectangular bands of type $(3,2)$, using the generalized rectangular bands of type $(3,2)$ is given in [3]. This result is used to obtain a free generalized $(2m,m)$ – rectangular band of type $(3,2)$.*

Keywords: *generalized rectangular band of type $(3,2)$, generalized $(2m,m)$ – rectangular band of type $(3,2)$, free generalized $(2m,m)$ – rectangular band of type $(3,2)$*

1. Introduction

First, we will introduce some notations which will be used further on:

1) The elements of Q^s, where Q^s denotes the s – th Cartesian power of Q, will be denoted by x_1^s.
2) The symbol x_i^j will denote the sequence $x_i x_{i+1} ... x_j$ when $i \le j$, and the empty sequence when $i > j$.
3) If $x_1 = x_2 = ... = x_s = x$, then x_1^s is denoted by the symbol $\overset{s}{x}$.
4) The set $\{1,2,...,s\}$ will be denoted by $\mathbf{N_s}$.

Let $Q \neq \varnothing$ and n,m be positive integers. If $[\ ]$ is a map from Q^n into Q^m, then $[\ ]$ is called an (n,m) – operation. A pair $(Q;[\ ])$ where $[\ ]$ is an (n,m) – operation is said to be an (n,m) – groupoid. Every (n,m) – operation on Q induces a sequence $[\ ]_1,[\ ]_2,...,[\ ]_m$ of n – ary operations on the set Q, such that

$$((\forall i \in \mathbf{N_m})\ \left[x_1^n\right]_i = y_i) \Leftrightarrow \left[x_1^n\right] = y_1^m .$$

Let $m \geq 2, k \geq 1$. An $(m+k, m)-$groupoid $(Q;[\ ])$ is called an $(m+k, m)-$semigroup if for each $i \in \{0,1,2,...,k\}$

$$\left[x_1^i \left[x_{i+1}^{i+m+k}\right] x_{i+m+k+1}^{m+2k}\right] = \left[\left[x_1^{m+k}\right] x_{m+k+1}^{m+2k}\right].$$

Let $(L;[\ ])$ be an $(m+k, m)-$groupoid, where $[\ ]$ is an $(m+k, m)-$operation defined by $[x_1^{m+k}] = x_1^m$. Then $(A;[\ ])$ is an $(m+k, m)-$semigroup and it is called a left-zero $(m+k, m)-$semigroup.

Dually, a right-zero $(m+k, m)-$semigroup $(R;[\ ])$ is defined by the operation $[x_1^{m+k}] = x_{k+1}^{m+k}$.

The pair $(L \times R;[\ ])$, where $[\ ]$ is an $(m+k, m)-$operation on $L \times R$ defined by

$$[x_1^{m+k}] = y_1^m \ \Leftrightarrow\ (x_i = (a_i, b_i), y_j = (a_j, b_{j+k}), i \in \mathbf{N_m},\ j \in \mathbf{N_m})$$

is an $(m+k, m)-$semigroup and it is a direct product of a left-zero and a right-zero $(m+k, m)-$semigroup on L and R, respectively. Such an $(m+k, m)-$semigroup is called $(m+k, m)-$rectangular band.

The notions of generalized left-zero $(2m, m)-$semigroups of type $(3, 2)$ and generalized right-zero $(2m, m)-$semigroups of type $(3, 2)$ are given in [3]. Let $(L;[\ ])$ be a $(2m, m)-$semigroup in which the identities:

(GLZ I) $\left[x_1^{2m}\right]_j = \left[y_1^{j-1} x_i y_{j+1}^{j+m-1} x_{i+m} y_{j+m+1}^{2m}\right]_j$, $i, j \in \mathbf{N_m}$ and

(GLZ II) $\left[x_1^{3m}\right] = \left[x_1^{2m}\right]$

hold. Then $(L;[\ ])$ is a generalized left-zero $(2m, m)-$semigroup of type $(3, 2)$.

Dually, a generalized right-zero $(2m, m)-$semigroup of type $(3, 2)$ is a $(2m, m)-$semigroup $(R;[\ ])$ in which the identities:

(GRZ I) $\left[x_1^{2m}\right]_j = \left[y_1^{j-1} x_i y_{j+1}^{j+m-1} x_{i+m} y_{j+m+1}^{2m}\right]_j$, $i, j \in \mathbf{N_m}$ and

(GRZ II) $\left[x_1^{3m}\right] = \left[x_{m+1}^{3m}\right]$

hold.

Also, in [3] is introduced the notion of a generalized $(2m, m)-$rectangular band of type $(3, 2)$. Namely, the $(2m, m)-$semigroup $(Q;[\ ])$ in which the identities:

(G I) $\left[x_1^{2m}\right]_j = \left[y_1^{j-1} x_i y_{j+1}^{j+m-1} x_{i+m} y_{j+m+1}^{2m}\right]_j$, $i, j \in \mathbf{N_m}$;

(G II) $\left[x_1^{5m}\right] = \left[x_1^{2m} x_{3m+1}^{5m}\right]$ and

(G III) $\left[\left[x_1^{2m}\right]_j\right] = \left[x_1^{m}\right]_j$, $i \in \mathbf{N_m}$

hold, is called generalized $(2m,m)$ – rectangular band of type $(3,2)$.

The following propositions are true:

Propositon 1.1. ([3, Proposition 3.2]) Let $(L;[\ ])$ be a generalized left-zero and $(R;[\ ])$ a generalized right-zero $(2m,m)$ – semigroup of type $(3,2)$. Then, $(Q;[\ ])$, where $Q = L \times R$, is a generalized $(2m,m)$ – rectangular band of type $(3,2)$.

Theorem 1.2. ([3, Theorem 3.3]) $\mathbf{Q} = (Q;[\ ])$ is a generalized $(2m,m)$ – rectangular band of type $(3,2)$ if and only if there is a generalized rectangular band $(Q;*)$ of type $(3,2)$, such that $\left[x_1^{2m}\right]_i = x_i * x_{i+m}$, $x_1^{2m} \in Q^{2m}$, $i \in \mathbf{N_m}$.

Theorem 1.2 gives a characterization of $(2m,m)$ – rectangular bands of type $(3,2)$ using the generalized rectangular bands of type $(3,2)$. Generalized rectangular band of type $(3,2)$ is a semigroup $(Q;*)$ that satisfies the following two identities

$x * y * z * u * v = x * y * u * v$ and

$x * y * x * y = x * y$,

for each $x,y,z,u,v \in Q$.

This result of Theorem 1.2 is used to obtain a free generalized $(2m,m)$ – rectangular band of type $(3,2)$.

2. Free generalized $(2m,m)$ – rectangular bands of type $(3,2)$

Let $(Q;*)$ be a free generalized rectangular band of type $(3,2)$ with a basis B.

Let $[\ ]$ be the $(2m,m)$ – operation on Q defined by

$$\left[x_1^{2m}\right]_j = x_i * x_{i+m},\ x_1^{2m} \in Q^{2m},\ i \in \mathbf{N_m}.$$

Then:

Theorem 2. $(Q;[\ ])$ is a free generalized $(2m,m)$ – rectangular band of type $(3,2)$ with a basis B.

Proof. First, we will prove that $\left[\left[x_1^{2m}\right]x_{2m+1}^{3m}\right]_j = x_i * x_{i+m} * x_{i+2m}$. We have:

$\left[\left[x_1^{2m}\right]x_{2m+1}^{3m}\right]_j$

$= \left[x_1^{2m}\right]_i * x_{2m+i}$

$= \left(x_i * x_{i+m}\right) * x_{i+2m}$

$= x_i * x_{i+m} * x_{i+2m}$

Further on, we will prove that $\left[x_1^j \left[x_{j+1}^{j+2m}\right] x_{j+2m+1}^{3m}\right]_i = x_i * x_{i+m} * x_{i+2m}$.

a) Let $i \le j$. Then $i+m \le j+m$. Let $i+m = j+\lambda$, $\lambda \in \mathbf{N_m}$.

Then:

$\left[x_1^j \left[x_{j+1}^{j+2m}\right] x_{j+2m+1}^{3m}\right]_i$

$= \left[x_1^i x_{i+1}^j \left[x_{j+1}^{j+2m}\right]_1 \ldots \left[x_{j+1}^{j+2m}\right]_\lambda \left[x_{j+1}^{j+2m}\right]_{\lambda+1} \ldots \left[x_{j+1}^{j+2m}\right]_m x_{j+2m+1}^{3m}\right]_i$

$= x_i * \left[x_{j+1}^{j+2m}\right]_\lambda$

$= x_i * \left(x_{j+\lambda} * x_{j+\lambda+m}\right)$

$= x_i * x_{i+m} * x_{i+2m}$.

b) Let $j < i$. Then $j < m$. Let $j + r = m$, $j + \lambda = i$, where $\lambda \in N_r$ and $i + m > j + m$.

Then:

$\left[x_1^j \left[x_{j+1}^{j+2m}\right] x_{j+2m+1}^{3m}\right]_i$

$= \left[x_{j+1}^{j+2m}\right]_\lambda * x_{j+2m+\lambda}$

$= \left(x_{j+\lambda} * x_{j+\lambda+m}\right) * x_{j+2m+\lambda}$

$= x_i * x_{i+m} * x_{i+2m}$.

Then $\left[\left[x_1^{2m}\right] x_{2m+1}^{3m}\right]_j = \left[x_1^j \left[x_{j+1}^{j+2m}\right] x_{j+2m+1}^{3m}\right]_i$, for all $i \in \mathbf{N_m}$, $0 \le j \le m$. So, $(Q;[\ ])$ is an $(2m,m)-$semigroup.

According to Thorem 1.2 $(Q;[\ ])$ is a generalized $(2m,m)-$rectangular band of type $(3,2)$.

It is clear that $B \subseteq Q$. Let $u \in Q$ and let $[B]$ be an $(2m,m)-$subsemigroup of $(Q;[\ ])$ generated by B. Then, for $c \in B$ we have $u = a * b = \left[\begin{matrix} i-1 & m-1 & m-i \\ c\ a\ c\ b\ c \end{matrix}\right]_i \in [B]$, i.e. $Q \subseteq [B]$. So, $(Q;[\ ])$ is generated by B.

Let $(S;[\ ]')$ be a generalized $(2m,m)-$rectangular band of type $(3,2)$ and let $f : B \to S$ be a map. By Theorem 1.2, there is a generalized rectangular band $(S;\circ)$ of type $(3,2)$ such that $\left[x_1^{2m}\right]_i' = x_i \circ x_{i+m}$, $x_1^{2m} \in S^{2m}$, $i \in \mathbf{N_m}$. Since $(Q;*)$ is a free generalized rectangular band of

type $(3,2)$ with a basis B, there is a homomorphism $g: Q \to S$, such that $g(b) = f(b), b \in B$.

Let $x_1^{2m} \in Q^{2m}$. Then

$$g\left(\left[x_1^{2m}\right]_i\right) = g(x_i * x_{i+m}) = g(x_i) \circ g(x_{i+m}) = [g(x_1)g(x_2)...g(x_{2m})]_i'.$$

So, g as an extension of the map f, is $(2m,m)-$homomorphism from $(Q;[\ ])$ into $(S;[\ ]')$. Hence, $(Q;[\ ])$ is a free generalized $(2m,m)-$rectangular band of type $(3,2)$ with a basis B. ■

References

[1] Čupona G. (1983) Vector valued semigroups, Semigroup forum, Vol 26, 65-74.

[2] Čupona G., Celakoski N., Markovski S., Dimovski D. (1988) Vector valued groupoids, semigroups and groups, "Vector valued semigroups and groups", Maced. Acad. of Sci. and Arts, 1-79.

[3] Miovska V., Dimovski D. Generalized $(2m,m)-$rectangular band of type $(3,2)$, submitted

Conceptual model of business analysis domain

Irena Atanasova
SWU "N. Rilski", Blagoevgrad, Bulgaria

***Abstract**: This paper proposes the building of the knowledge model, inspired by Knowledge Engineering. The methodology is used to engineer a model of an ontology Onto-BAn of business analysis domain in order to develop an easy and correct way to find the needed information in a knowledge base. We will represent a conceptual model of business analysis domain.*

***Keywords:** ontology, Protégé, business analysis.*

1. INTRODUCTION

Ontology represents common semantics of the domain. Since the nineties, ontologies have become one of the hottest issues of research among different communities - Artificial Intelligence, Databases, Knowledge bases, etc. Nowadays, ontologies have become the backbone of many enterprises and governmental institutions. Research in ontologies has been conducted in many different areas.

Several methodologies and frameworks (CommonKADS, MIKE, MOKA, and Protégé) have been developed. They all lay emphasis on modeling. Models capture the essential features of a real system by breaking them down into smaller components to be better understood. They are used in system development to facilitate communication between different people.

To understand the working mechanisms within a knowledge-based system we use models [2]. Models and modeling contribute to the understanding of the source of knowledge [1]. Thus knowledge modeling is the important key component for the construction of knowledge bases. One of the modeling paradigms for knowledge engineering methodologies is ontology. The ontology provides a way of representing domain knowledge. It consists of concepts, relations and constraints on the relations

The domain knowledge consists of the domain schema and the knowledge base.

The research into ontologies is widespread in research fields as knowledge representation, knowledge engineering, database, information system, knowledge management and organization. Ontology can be seen as meta data that explicitly represents the semantics of data in a machine processable way. Ontologies could help people and computers to access

the information they need by making the link between the information form and content explicit. Moreover, ontology is now recognized as powerful tool that enables sharing knowledge.

Our work is motivated to exploit repositories of information in a specific domain - business analysis.

In our area of interest, domain and its applications appear to be an area of challenge in constructing ontology.

Objective: Our domain of interest for this study is business analysis. We build and engine an ontology representing business analysis domain – Onto-BAn.

Onto-BAn is an ontology that has been under development at the South West University of Blagoevgrad since 2009. Its objective is to conceptualize the business analysis objects. The underlying data model for Onto-BAn is a frame-based structure implemented with Protégé 3.4.4.

2. KNOWLEDGE MODEL CONSTRUCTION OF BUSINESS ANALYSIS DOMAIN

The most important task in the methodology is the definition of a Domain Conceptual Model. Then, it is important to assign all the necessary time to carry out a good conceptual analysis. The conceptual model resumes the knowledge adquired during the specification phase and it is the basis of conceptualization. This conceptualization has to be agreed on by domain experts.

We are going to follow the three of six phases (specification, conceptualization, and implementation) for the construction of the knowledge model of business analysis domain.

Specification*:* This section describes the process of developing an Onto-BAn ontology for business analysis domain. This ontology considers the needs for creating the investment decisions, statistics, planning and control, marketing, and est. It includes general concepts for the investment, different kind of reports, forecasting, methods, and activities. There are two situations where the availability of semantic information associated to business analysis is critical: information and approval tasks. In the first case, only leadership staff with specific knowledge can be involved, concentrating a great responsibility on a few people. In the second case, semantics information is necessary for analyzing data and then having the law passed. This is more complex because all legislators must vote and most of them have no specific knowledge. According to the level of conceptualization and granularity, the ontology proposed here is domain ontology. Domain ontology describes the vocabulary related to a specific domain. In this case study, the ontology describes the business analysis domain . The ontology objective is to facilitate communication among the

members of the central administration staff that must deal with the budget, bringing adequate terminology to non-expert users.

***Conceptualization**:* In this step, a list of the most important terms was elaborated. The core of basic terms is identified first and then they are specified. Then with these concepts, the key term list was defined. The list shown in table 1 includes concepts and relations.

Tab 1. Key Terms in business analysis ontology

Concepts	Relations
Business_analysis	about
Investment_decisions	base_on
Planning_and_control	based_on
Report	basedon
Sales_and_marketing	by
Investirane	for
Forecast_evaluat	of
Plan_fin_dejnost	per
Kapital_zakup_oborud	perr
Naemane_novi_sluj	realize
Okepl	chrez
Pazarno_prouchvane	za
Kontrol	_za_
Cenoobraz	bazirase_na
Predel_prihodi	byy
Realiz_prihod	influence
Regist_prihod	kontrolira
Balan_otchet	to
Schet_otchet	v

Implementation: In order to implement the ontology, we chose Protégé 3.4.4 because of the fact that it is extensible and provides a plug-and-play environment that makes it a flexible base for rapid prototyping and application development. Protégé ontologies can be exported into different formats including RDF Schema and Web Ontology Language.

Protégé is a popular open source ontology editor and knowledge base framework [5].

Protégé supports the export to standard ontology languages as OWL and RDF schema, but it is easily extensible through its plug-in interface. This makes it a flexible base for a rapid prototyping and application development. Protégé has several built-in advantageous features. These include GUI – a standardized graphical user interface, and flexible platform for knowledge-based domain modeling.

We are going to describe the Protégé features in detail, and demonstrate how we used them for ontology of business analysis development.

Protégé is an ontology development environment with a large community of active users. The representation mechanism for ontologies and knowledge bases (Protégé’s model) is based on a flexible metamodel which is comparable to object-orientated and frame-based systems. It basically can represent ontologies consisting of classes, properties (slots), property characteristics (facets and constraints), and instances. Recently Protégé has been extended with support for OWL, and has become one of the leading OWL tools. Protégé provides functionality for editing classes, properties, and instances.

In this paper we propose domain ontology for business analysis. In order to elaborate an ontology for that domain we have used terms proposed in [3] and [4] for the business analysis of a company.

As shown in figure 1 the company has various departments such as legal, marketing, sales, financial accounting, planning, human resources.

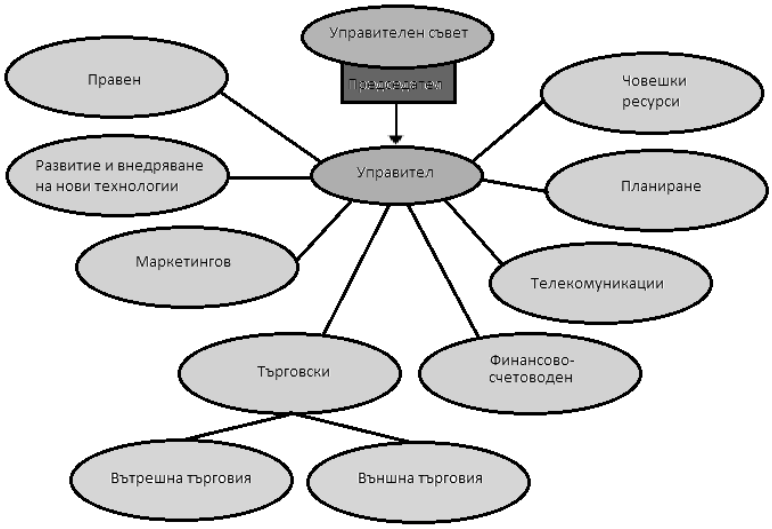

Fig. 1. Sscenario of Business Analysis domain

These departments share the company's computer network with a central database and knowledge base. These databases are permanently updated with different types of data and information. Due to the large amount of data, many business analysts are embarrassed in making the correct and exact decisions, the necessary forecasting and evaluations and trends. Therefore, such a developed ontology will monitor the data, identify different models for analysis and forecasts, it will provide appropriate education and qualifications and will generate suggestions for future development. To implement these requirements it must be based on knowledge that formally describe and present the ontology and what is her purpose. This set of knowledge will be called a model of knowledge.

For example: a simple model of knowledge for business analysis must include information about types of reports, capital movements, the statistical methods for forecasting and assessments, the basic concepts in decision making , marginal revenue.

Ontology Onto-BAn uses a dictionary of about 160 atomic terms and concepts. The top level of ontology contains four terms with definitions and hierarchical relationships between them. These are the most common concepts. They describe the main objects of business analysis domain - Report, Planning and control, Investment decisions, Sales and marketing.

Basic features of the ontology Onto-BAn

Objective: Systematization of basic knowledge about the business analysis domain.

Scope: Ontology of a sector of Finance - Business analysis - the pattern of human knowledge of this sector of economy. The aim of the developers is companies with more specific activity to be able to use the upper model of ontology by attaching branches that describe their subdomain.

Content: All concepts are in taxonomy. In ontology Onto-BAn there are properties and roles, and links that connect concepts.

Practical application: the ontology Onto-BAn will be used in the field of analysis in a company to help business analysts. It can be used in the simulations and modeling.

The main component of the ontology Onto-BAn is the knowledge base, which formally presents much of the basic human knowledge of business analysis domain, including facts and rules to facilitate making of conclusions about objects and events in the economy.

Onto-BAn ontology

The main terms are organized in:

- Report;
- Planning and control;
- Investment decisions;
- Sales and marketing.

Each term is defined in properties and relations, generating a complex network of classes, subclasses, instance and slots. The ontology Onto-BAn is designed as a reflection of the views of specialists in the areas of business analysis, statistics, and knowledge engineering.

Investigation of business situations is the one of the most important activity, which the financial department can do to contribute the leadership (managers) to make decisions. The business situation has different form according to submitted question for discussion and the decision which can be made. She should confirm the logical assumptions, reporting the results of sensitivity analysis to changes in similar data. Business risk is the uncertainty that exists in every business activity.

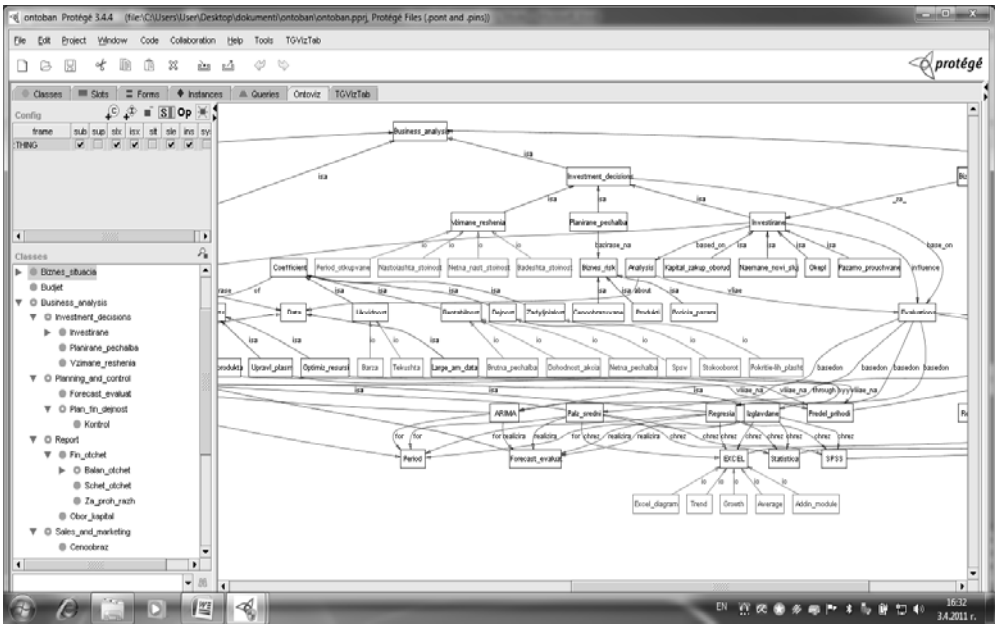

Fig. 2 Implementation of the ontology Onto-BAn in Protégé

3. RESULTS, DISCUSSIONS, CONCLUSIONS

Building domain ontologies is not a simple task when domain experts have no background knowledge on engineering techniques and/or they have not much time to invest in domain conceptualization.

Ontology building process is characterized by its very high cost and elaborate overlapping activities of development.

4. REFERENCES

[1] Abdullah, M. S., Evants, A., Benest, I., Paige, R., Kimble, C., (2004) Modelling Knowledge Based Systems Using the eXecutable Modelling Framework (XMF), Proceeding of the 2004 IEEE, *Conference on Cybernetics and Intelligent Systems*, Singapore.

[2] Booch,G., Rumbaugh, J. E., Jacobson, I., (1999) *The Unified Modelling Language User Guide*, Addison-Wesley, Reading, MA.

[3] Karlberg, K. (2003) *Business analysis with Microsoft Excel*, SoftPress Ltd.

[4] Newbold, P. (1984) *Statistics for business and economics*, Prentice-Hall, New Jersey.

[5] Protégé (2008) *Protégé* Available online at http://protege.stanford.edu (Accessed January 2010).

On Some Algebraic Structures

DIMITER STOICHKOV KOVACHEV, SLAVCHO SHTRAKOV
Department of Computer Science,
South-West University, 2700 Blagoevgrad, Bulgaria,
Email: dkovach@abv.bg and shtrakov@swu.bg

Abstract: *H-functions and some their generalizations are investigated in the paper. The matrix presentation of a H-function and the matrix presentation of a function corresponding to an n-ary quasigroup of order k is a Latin hypercube. Several applications of H-functions in coding theory concerning MDS (Maximum Distance Separable) are described in the works of D. S. Krotov, Steven Dougherty, M.M. Skriganov, Jon-Lark Kim, Hamid Kulosman, Sunghyu Han, T.L. Alderson and others.*

Keywords: *H-functions, H[1;q]– functions, Latin hypercubes, spectrum.*

1. INTRODUCTION

Let $E_k = \{0, 1, \ldots k\text{-}1\}$, $k \geq 1$, and $P_n^k = \{f : E_k^n \to E_k \,/\, k \geq 2\}$ be the set of all functions of *n* variables of *k*-valued logic.

Definition 1.1 [3] *The number Rng (f) of different values of the function f is called range of f .*

The set of functions from P_n^k which assume exactly *q* different values, that is, which have range equal to *q,* is denoted by $P_n^{k,q}$.

We denote the set of variables of the function $f(x_1,\ldots,x_n)$ by X_f .

Definition 1.2 *Every function obtained from f by replacing the variables of M, $M \subseteq X_f$, $0 \leq |M| \leq n$, with constants is called a subfunction of $f(x_1,\ldots,x_n)$ with respect to M.*

The notation $g \overset{M}{\prec\!\!\!-} f$ ($g \overset{M}{\prec\!\!\!-} f$) means that g is a subfunction of f (with respect to M).

Definition 1.3 *[3] If M is a set of variables of the function f and $G=\{g: g \overset{X_f \setminus M}{\prec\!\!\!-} f\}$ is a set of all subfunctions of f with respect to $X_f \setminus M$, then the set* ***Spr****(M, f)=* $\bigcup_{g \in G} \{$ ***Rng****(g)****}*** *is called spectrum of the set M for the*

function f.

If $M=X_f$ then $Spr(X_f, f) = \{ Rng(f) \}$. For every function of one variable $g(x) \in P_1^k$, since $\{x\}=X_g$, we have $Spr(\{x\}, g)=Spr(x, g)=\{Rng(g)\}$.

In [2], the class of $H[1;q]$ functions of P_n^k is investigated.

Definition 1.4 *[2] We say that the function $f(x_1, x_2, ..., x_n) \in P_n^k$ is an $H[1;q]$–function, $1 \le q \le k$, if for every variable x_i, $i=1,\ldots, n$ of the function f, we have* ***Spr***$(x_i, f)=\{q\}$.

When $q=k$, the set of $H[1; k]$–functions of P_n^k is equal to the set of H–functions of P_n^k, which are studied by many authors [1, 2, 5].

Matrix with m rows and m columns will be denoted by $|| a_{ij} ||_0^{m-1}$, $i,j \in \{0, 1,\ldots,m\text{-}1\}$ and it will be called 2–dimensional matrix of order m. By $|| b_{i_1 i_2 \ldots i_n} ||_0^{k-1}$, $i_1, i_2, ..., i_n \in \{0, 1,\ldots,k\text{-}1\}$ we denote n–dimensional matrix of order k.

Each function $f(x_1, x_2, ..., x_n) \in P_n^k$ via the equality $a_{i_1 i_2 \ldots i_n} = f(x_1 = i_1, x_2 = i_2, ..., x_n = i_n)$, can be presented in matrix form $|| a_{i_1 i_2 \ldots i_n} ||_0^{k-1}$, as an n–dimensional hypercube of order k, based on the set E_k.

Matrix expression of $H[1;q]$–function of P_n^k is called n-dimensional $H[1;q]$-hypercube of order k, induced by the set E_k, and this is each ***n***–dimensional matrix $\boldsymbol{A}=|| a_{i_1 i_2 \ldots i_n} ||_0^{k-1}$ of order $\boldsymbol{k}$, if for each s, $s=1, 2,..., n$ we have

$$|\{a_{i_1 \ldots i_{s-1}\, 0\, i_{s+1} \ldots i_n}\} \cup \{a_{i_1 \ldots i_{s-1}\, 1\, i_{s+1} \ldots i_n}\} \cup \ldots \cup \{a_{i_1 \ldots i_{s-1}\, (k-1)\, i_{s+1} \ldots i_n}\}| =$$

$$|\bigcup_{j=0}^{k-1} \{a_{i_1 \ldots i_{s-1}\, j\, i_{s+1} \ldots i_n}\}| = q.$$

When fixing arbitrary n-1 indices of the matrix of n-dimensional $H[1;q]$-hypercube of order k, we get 1-dimensional matrix of order k, in which there are exactly q different elements.

It is proved [2] that matrix representation of every H–function of P_n^k is a Latin hypercube and that each n-dimensional $H[1;k]$-hypercube of order k, induced by the set E_k, is n-dimensional Latin hypercube of order k, induced

by the set E_k.

In [2], the "construction" of $H[1;q]$-hypercubes is also presented.

2. MAIN RESULTS.

Let a, b, c_i, i=1, 2,…, q, be elements of the set E_k.

Lemma 2.1 If function $f(x_1,...,x_n)=(a.g + b) \bmod k$, where $(a, k)=1$, that is, a and k are mutually prime numbers and $g(x_1,x_2,...,x_n) \in P_n^{k,q}$, $1 \le q \le k$, then $Rng(f)=Rng(g)=q$.

Proof: From $g \in P_n^{k,q}$ it follows that $Rng(g)=q$ and function g assumes q different values. Let these values be c_1, c_2,..., c_q, where $c_i \neq c_j$ for $i \neq j$, i, j = 1, 2,…, q. Then function $f(x_1,...,x_n)$ will assume the values $< ac_1+b, ac_2+b,..., ac_q+b > \bmod k$. If these values, taken by $\bmod k$, are different, it will follow that $Rng(g)=Rng(f)$. Assume that there exist $i \neq j$, such that $ac_i+b=ac_j+b \bmod k$. After simplification we get that $a(c_i-c_j)=0 \bmod k$ and since $(a, k)=1$, it follows that $c_i = c_j$, which contradicts the assumption that $c_i \neq c_j$. The contradiction we have obtained is due to the assumption that among the values ac_1+b, ac_2+b,..., ac_q+b there are equal values taken by $\bmod k$. It follows that $f(x_1,...,x_n)$ also assumes q different values, like $g(x_1,x_2,...,x_n)$. Therefore $Rng(f)=Rng(g)=q$.

Theorem 2.1 If functions $g(x_1,...,x_r)$ and $h(y_1,...,y_l)$ are k-valued and $H[1;q]$–functions, and $X_g \bigcap X_h = \phi$, then function

$$f(x_1,...,x_r,y_1,...,y_l)=[g(x_1,...,x_r) + h(y_1,...,y_l)] \bmod k,$$

is also $H[1;q]$–function.

Proof: Rename the variables as follows

$$z_1 = x_1,...,z_r = x_r,\ z_{r+1} = y_1,...,\ z_{r+l} = y_l$$

Function $f(z_1,...,z_{r+l})=[g(z_1,...,z_r) + h(z_{r+1},...,z_{r+l})] \bmod k$ is $H[1;q]$–function if for each variable z_i, i=1, 2,…, $r+l$, we have

$$\mathbf{Spr}(z_i, f)=\{q\}.$$

Let f_i, $f_i(z_i) \xrightarrow{X_f \setminus z_i} f(z_1,...,z_{r+l})$ be an arbitrary subfunction of f. If $i \le r$, then $f_i(z_i)=(g_i(z_i)+c)$, where $g_i(z_i) \xrightarrow{X_g \setminus z_i} g$, and c is the value of function h,

obtained by replacing its variables by constants. Since g is $H[1;q]$–function, then $Rng(g_i(z_i))=q$. From Lemma 2.1 it follows that $Rng(f_i(z_i))=q$. Since $f_i(z_i)$ is arbitrary, it follows that each subfunction of f with respect to $X_f \setminus z_i$ has the range equal to q. Similarly, it can be proved that for $i>r$ each subfunction of f with respect to $X_f \setminus z_i$ has also range equal to q. Since z_i was chosen arbitrarily, it follows that $\boldsymbol{Spr}(z_i, f)=\{q\}$ for each $i=1, 2,\ldots, r+l$ and f is $H[1;q]$–function.

Corollary 2.1 If $f_1, f_2,\ldots,f_n$ are k-valued, $H[1;q]$–functions and **no** two of them have (depend on) common variables, then function $f=(f_1+f_2+\ldots+f_n) \bmod k$, is also $H[1;q]$–function.

When $q=k$, we have:

Corollary 2.2 If $f_1, f_2,\ldots,f_n$ are k-valued, H–functions and **no** two of them have (depend on) common variables, then function $f=(f_1+f_2+\ldots+f_n) \bmod k$, is also H–function.

For example, Corollary 2.2 gives us the opportunity from r-dimensional and l-dimensional Latin hypercubes of order k to construct $(r+l)$-dimensional Latin hypercube of order k.

Corollary 2.3 If functions $g_i(x_i) \in P_1^{k,q}$, $i=1, 2,\ldots, n$, then function $f(x_1, x_2,..., x_n)=[\sum_{i=1}^{n} g_i(x_i)]$ mod k, is $H[1;q]$–function, and matrix

$$\boldsymbol{B}=\| b_{j_1 j_2 \ldots j_n} \|_0^{k-1}=f(j_1, j_2,..., j_n)=[\sum_{r=1}^{n} g_r(j_r)] \bmod k$$

is n-dimensional $H[1;q]$-hypercube of order k.

When $q=k$ and **Corollary 2.3**, we have:

Corollary 2.4 [2] If functions $g_i(x_i)$, $i=1, 2,\ldots, n$ are bijective, that is, if they belong to the set $P_1^{k,k}$, then function $f(x_1, x_2,..., x_n)=[\sum_{i=1}^{n} g_i(x_i)]$ mod k, is H–function, and matrix

$$\boldsymbol{B}=\| b_{j_1 j_2 \ldots j_n} \|_0^{k-1}=f(j_1, j_2,..., j_n)=[\sum_{r=1}^{n} g_r(j_r)] \bmod k$$

is n-dimensional Latin hypercube of order k.

Since a function from $P_1^{k,q}$ can be chosen [3] in

$$|P_1^{k,q}| = C_k^q \cdot \sum_{\substack{r_1+r_2+\ldots+r_q=k \\ r_i \geq 1,\ i=1,2,\ldots,q}} \frac{k!}{r_1!\,r_2!\ldots r_q!} = C_k^q \cdot \sum_{s=0}^{q-1} (-1)^s C_q^s (q-s)^k$$

ways, then according to Corollary 2.3, $|P_1^{k,q}|^n$ $H[1;q]$–functions of P_n^k can be generated. The "defect" of this corollary is that among the generated functions there will be many identical functions.

Indeed, let g_i, i=1, 2,…, n be arbitrary, fixed functions from $P_1^{k,q}$. According to Lemma, functions $(g_i + c_i)$ mod k, $c_i \in E_\kappa$, i=1, 2,…, n, also belong to $P_1^{k,q}$. Each constant c_i, i=1, 2,…, n, can be chosen in k ways and, therefore, k^n functions of the following form will be generated

$$f=[(g_1+c_1)+(g_2+c_2)+\ldots.+(g_n+c_n)] \text{ mod } k.$$

After simplification we obtain that

$f=(g_1+g_2+\ldots+g_n+c_1+c_2+\ldots.+c_n)$ mod $k=(g_1+g_2+\ldots+g_n+c_0)$ mod k,

where $c_0=(c_1+c_2+\ldots.+c_n)$ mod k. Since c_0 can assume exactly k different values, then the number of generated non-identical functions f will be equal to k, not equal to k^n.

Let $\tilde{P}_1^{k,q}$ be a set of k-valued functions of one variable, such that

1, $\tilde{P}_1^{k,q} \subset P_1^{k,q}$.

2. If f_1, $f_2 \in \tilde{P}_1^{k,q}$ and $f_1 \neq f_2$, then $f_1 \neq (f_2 + c)$ mod k, for each $c \in E_k$.

The set $\tilde{P}_1^{k,q}$ is not uniquely determined but its cardinality is fixed.

In order to optimize generation of $H[1;q]$–functions, we have:

Corollary 2.5 If functions $g_i(x_i) \in \tilde{P}_1^{k,q}$, i=1, 2,…, n, then function

$$f(x_1, x_2, \ldots, x_n) = [\sum_{i=1}^{n} g_i(x_i) + c] \text{ mod k}, \ c \in E_k,$$

is $H[1;q]$–function, and matrix

$$\boldsymbol{B} = \| b_{j_1 j_2 \ldots j_n} \|_0^{k-1} = f(j_1, j_2, \ldots, j_n) = [\sum_{r=1}^{n} g_r(j_r) + c] \text{ mod k}$$

is n-dimensional $H[1;q]$-hypercube of order k.

Each function $h \in P_1^{k,k}$ is of the form $h=\begin{pmatrix} 0 & 1 & \ldots & k-1 \\ b_1 & b_2 & \ldots & b_k \end{pmatrix}$, where $b_1\ b_2\ \ldots b_k$ is a permutation of numbers 0 1 ... κ-1. Generation of the

functions of $P_1^{k,k}$ is connected with generation of permutations of the elements of E_k.

A set of permutations, connected with generation of the functions of $\tilde{P}_1^{k,k}$, can be obtained in the following way: to each permutation, generated by elements of E_{k-1}={0,…, *k*-2), we add the element (*k*-1). The number of these permutations is $(k-1)!$, and therefore $|P_1^{k,k}|=k!$, whereas $|\tilde{P}_1^{k,k}|=(k-1)!$,

Using Corollary 2.5, we will generate $k[(k-1)!]^n$ *H*–functions (*n*-dimensional Latin hypercubes of order *k*, respectively). The number of generated via Corollary 2.4 *H*–functions of P_n^k will be $[k!]^n$, that is, k^{n-1} more times, because there are identical among them.

Matrix representation of *H*–functions, namely Latin squares and hypercubes have their applications [4] in coding theory, error correcting codes, information security, decision making, statistics, cryptography, conflict-free access to parallel memory systems, experiment planning, tournament design, etc.

3. REFERENCES

[1] Chimev K. N., (1967), *On a way some functions of P_k depend on their arguments*, Annuaire Des Ecoles Techniques Superieures, Mathematique, vol. IV, livre. 1, pp. 5-12.

[2] Kovachev D. St., (2006), *On a Class of Discrete Functions*, Acta Cybernetica, volume17, number 3, Szeged, pp. 513-519. (MR 2237557).

[3] Kovachev D. St., (2000), *On the Number of Discrete Functions with a Given Range*, General Algebra and Applications, Proceedings of the “59th Workshop on General Algebra“, Potsdam 2000, edited by K. Denecke and H.-J. Vogel, pp.125-134.

[4] Laywine Ch. F., Mullen G. L., (1998), *Discrete Mathematics Using Latin Squares*, John Wiley & Sons, New York.

[5] Mirchev I. A., Yurukov B. P., (1995), *Some Properties of H–functions*, Acta Cybernetica, 12, pp. 137-143.

Chain recurrence and topological transitivity in the plane

Martin Shoptrajanov, Nikita Shekutkovski
Faculty of Natural sciences and Mathematics, Skopje, Macedonia

***Abstract**: We shall investigate the connection between the chain recurrent set and the notion of topological transitivity in the plane. Example of topologically transitive set will be given and the property of the corresponding limit set will be discussed.*

***Keywords**: limit sets, topological transitivity, chain recurrence*

1. INTRODUCTION

The interesting problems in the study of dynamical systems are to understand the structure of various invariant sets of a given system and to explain how these sets varies as the given system changes. One of these sets is the chain recurrent set introduced by C.Conley in his fundamental theorem of dynamical systems which states that any flow on a compact metric space decomposes into chain recurrent part and the rest, so called gradient-like part. In this paper we investigate the connections with the notion of topological transitivity in the plane. The concept and problems involving characterization of topologically transitive sets for example were raised in the paper [1].

Definition**.** Let (X,d) be a given metric space. We say that a continuous map $\varphi : X \times R \to X$ is a flow in X if it satisfies the following two conditions:

$$\varphi(x,0) = x, \forall x \in X \quad , \quad \varphi(\varphi(x,t),s) = \varphi(x,t+s) \; \forall x \in X, \forall s,t \in R$$

Definition**.** We say that a given set $M \subseteq X$ is invariant under the flow if $\varphi(M,t) \subseteq M$, $\forall t \in R$.

Definition. The set $\gamma(x) = \{\varphi(x,t) \mid t \in R\}$ is called orbit through x.

2. TOPOLOGICALLY TRANSITIVE SETS OF PLANAR FLOWS

One of the important problems in dynamical system theory concerns the asymptotic behavior of orbits as time goes to plus or minus infinity. In the study of asymptotic behavior the so called limit sets play an important role. We will start with some basic notions from dynamical system theory.

Definition**.** Positive*(* Negative*)* limit sets of a given subset $M \subseteq X$ are the following sets:

$$\omega(M) = \{x \mid \exists x_n \in M, \exists t_n \to +\infty,\ \varphi(x_n, t_n) \to x\}$$

$$\alpha(M) = \{x \mid \exists x_n \in M, \exists t_n \to -\infty,\ \varphi(x_n, t_n) \to x\}$$

Theorem1.1[2].The limit sets are closed and invariant.

Definition**.** We say that a set A is topologically transitive (TT) if it admits a point $x \in A$ such that $\overline{\gamma(x)} = A$.

Definition. A point x is said to be periodic if $T \neq 0$ exists such that $\varphi(x, T) = x$. A point x is said to be critical if $\varphi(x, t) = x$, $\forall t \in R$. If a point x is periodic but not critical, then the smallest positive period of x is called its fundamental period.

We now state the following easy proposition:

Proposition1.1.[2]. Every non critical periodic point has orbit which is homeomorphic to S^1.

The following two lemmas are from Poincare-Bendixson theory of C^1 planar flows.

Lemma1.1 [2] In a planar flow, every ω limit point of an ω limit point lies on a periodic orbit.

Lemma1.2 [2] In a planar flow, if an ω limit set $\omega(x)$ contains a non critical periodic orbit P, then $\omega(x) = P$.

Now we are ready to state:

Theorem1.2 Let A be a topologically transitive set of a plane flow. Then $\operatorname{int} A = \varnothing$.

Proof: Let A be a topologically transitive set, i.e. $\exists x \in R^2$ such that $\overline{\gamma(x)} = A$. Let us suppose the opposite, namely let $\operatorname{int} A \neq \varnothing$ .We will discuss two cases.

In the first case we shall assume that there exists a point $p \in \operatorname{int} A$ such that it admits a compact neighborhood (we choose it as a compact disc) U_p such that

$$U_p \cap (\omega(x) \cup \alpha(x)) = \varnothing \tag{1}$$

Let us note that the orbit through x should cross every point from this neighborhood exactly ones which means that there exists a subset $W \subseteq R$ such that the map $g : W \to U_p$, $g(t) = \varphi(x, t)$ is a bijection. In the contrary, if g is not surjective a point $q \in U_p$ will exists such that it admits a sequence

(τ_n) such that $\varphi(x,\tau_n)\to q$, but $q\notin\gamma(x)$. The sequence (τ_n) must be bounded because of (1). So, the sequence (τ_n) is bounded and passing to a subsequence we could assume that the sequence is convergent, i.e. $\tau_n\to\tau_0$. Then by the continuity of the phase map we have $\varphi(x,\tau_n)\to\varphi(x,\tau_0)=q$, i.e. $q\in\gamma(x)$, which is a contradiction. So the map is surjective. Now, let us suppose that the map is not injective. But the possibility $\varphi(x,\tau_1)=\varphi(x,\tau_0)\ \tau_1\neq\tau_0$ would imply that the point x is periodic and hence has orbit homeomorphic to S^1 according to proposition 1.1 which is contradiction with the assumption $\operatorname{int}A=\operatorname{int}\overline{\gamma(x)}\neq\varnothing$. So the map g is bijective. We will show that the set W is compact. First, if we suppose that the set W is unbounded a sequence $\tau_n\to\pm\infty$ would exists such that $\tau_n\in W$, but then we will have that $g(\tau_n)=\varphi(x,\tau_n)\in U_p$ which by compactness of U_p means that $\varphi(x,\tau_n)\to z\in U_p$. From the other hand we would have that $z\in\alpha(x)\cup\omega(x)$ which is a contradiction. Second, let us pick arbitrary convergent sequence $\tau_n\in W$, $\tau_n\to\tau_0$ .We now have from $g(\tau_n)=\varphi(x,\tau_n)\in U_p$, and from the continuity of the phase map that $g(\tau_n)\to\varphi(x,\tau_0)$. By the fact that U_p is closed, we have that $\varphi(x,\tau_0)\in U_p$. As we saw the map g is a bijection which means that $\tau_0\in W$ .We proved that W is compact, and consequently that the continuous bijection $g:W\to U_p$ is a homeomorphism. Since U_p is connected it follows that W is connected as well, which implies that W is an interval. This is a contradiction.

So let us discuss the second case. Namely, this means that for arbitrary point $p\in\operatorname{int}A$ and every neighborhood U_p of this point the following holds:

$$U_p\cap(\omega(x)\cup\alpha(x))\neq\varnothing \tag{2}$$

But this would imply that $\overline{\omega(x)\cup\alpha(x)}=\omega(x)\cup\alpha(x)=A$ according to theorem 1.1. Let us assume that $x\in\omega(x)$. From the invariance of the limit set according to theorem 1.1 we have the following inclusion $\gamma(x)\subseteq\omega(x)$,and from the same theorem we get the relations $\overline{\gamma(x)}=A=\omega(x)\cup\alpha(x)\subseteq\omega(x)$,which means that $\alpha(x)\subseteq\omega(x)$,and hence $A=\omega(x)$. Now for arbitrary movable point (noncritical) such that $z\in A=\omega(x)$, we have from $x\in\omega(x)$ that z is an ω limit point of a ω limit point which from lemma 1.1 implies that z is a periodic point. Now

from lemma 1.2 because $\omega(x)$ contains a noncritical periodic orbit we conclude that $A = \omega(x)$ is periodic orbit which according to proposition 1.1 implies that A is homeomorphic to S^1 which is a contradiction with $\operatorname{int} A \neq \emptyset$. The second possibility $x \in \alpha(x)$ is similar, once we use the inverse flow trick (i.e. instead of $\varphi(x,t)$ we can work with $\varphi(x,-t)$).

3. CHAIN RECURRENCE AND TOPOLOGICALLY TRANSITIVITY

We will need the definitions of Lyapunov function and the chain recurrent set for continuous flows.

Definition. Let $K = \{K_j \mid j \in J\}$ be a family of disjoint compact invariant subsets of the phase space X. A Lyapunov function for K is a continuous function $G : X \to R$ such that:

- $G(\varphi(x,t)) < G(x), \forall t > 0, \forall x \in X \setminus \bigcup_{j \in J} K_j$
- $G(K_j) = c_j, \forall j \in J, c_i \neq c_j \text{ for } i \neq j$

Proposition2.1[3]. Suppose that $K = \{K_j \mid j \in J\}$ admits a Lyapunov function G and $W = \bigcup_{j \in J} K_j$ is compact. Then:

- $(\forall x \in X), \exists K_s, K_r$ in K such that $\alpha(x) \subseteq K_s$ and $\omega(x) \subseteq K_r$.
- If $x \notin W$ then $\alpha(x)$ and $\omega(x)$ are nonempty sets and the following inequalities hold $G_{|\alpha(x)} > G(x) > G_{|\omega(x)}$.

Theorem2.1 [3] Let the phase space X be compact. Then there exists a unique family $K = \{K_j \mid j \in J\}$ of disjoint compact invariant sets which admits a Lyapunov function and is maximal with respect to this property. The set $CR(\varphi) = \bigcup_{j \in J} K_j$ is closed and K_j's are its components.

The set $CR(\varphi)$ is called the chain recurrent set for the flow φ.

Theorem2.2: Let X be a compact subset of the plane in which a C^1 flow is defined. If the chain recurrent set $CR(\varphi)$ is topologically transitive then $\operatorname{int}_{R^2} X = \emptyset$.

Proof: We shall prove that topological transitivity of the chain recurrent set implies topological transitivity of the whole space. Then the claim follows directly from theorem 1.2. First from topological transitivity of $CR(\varphi)$ a point $x \in X$ exists such that $\overline{\gamma(x)} = CR(\varphi)$. This implies that $CR(\varphi)$ is connected set. Now from theorem 2.1 the family $\{CR(\varphi)\}$ with only one

element admits a Lyapunov function G. If we suppose that a point $x \in X \setminus CR(\varphi)$ exists then from proposition 2.1 we have that $\alpha(x)$ and $\omega(x)$ are nonempty limit sets and $G_{|\alpha(x)} > G(x) > G_{|\omega(x)}$. Then from the same proposition we have that $\alpha(x)\omega(x) \subseteq CR(\varphi)$ because we have family with only one element. This implies that $G_{|\alpha(x)} = G_{|\omega(x)}$, surely a contradiction.

Example: Let us discuss the flow defined on the Polish circle such that the points on the line segment L connecting the points $(0,-1)$, $(0,1)$ are critical points. The other points are regular. Each noncritical point has the line segment L as it's α and ω limit set. Each noncritical point is chain recurrent. Hence the chain recurrent set is TT. Since critical points are trivially chain recurrent it follows that $X = CR(\varphi)$. Let us also note that $\operatorname{int}_{R^2} X = \varnothing$.

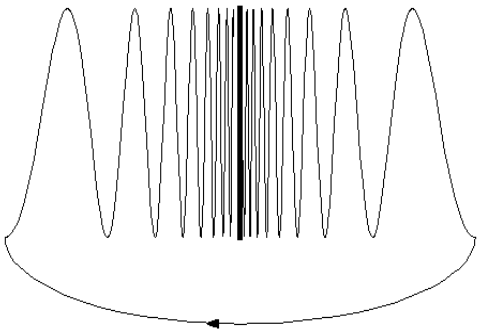

Fig 1: Polish circle with two $\sin\frac{1}{x}$ curves

4. REFERENCES

[1] Gunther, B. ,Segal,J. (1993) Every attractor of a flow on a manifold has the shape of a finite polyhedron, Proceedings of the American Mathematical Society, Volume 119, Number 1.

[2] Lawrence, P. (2001) Differential Equations and Dynamical Systems, New York, Springer.

[3] Sancez,G.(2008) Revista de la Real Academia de Ciencias Exactas, Físicas y Naturales. Serie A, Matemáticas, Vol. 102 (1), pp. 127–159.

Optimality Concept in Multi-criteria Optimization with Infinite Many Criteria

Zdravko Slavov[1], Christina Evans[2]

[1] Varna Free University, Varna, Bulgaria

[2] The George Washington University, USA

Abstract: *This article presents the optimality concept in multi-criteria optimization with infinite many criteria and a compact metric space of alternatives. It is examined a number of characteristics of the Pareto-optimal sets of the alternatives.*

Keywords: *multi-criteria optimization, Pareto-optimal, infinite, binary relation, metric, distance.*

1. Introduction

Consider a compact metric space of alternatives (X,d), d is Euclidean distance. Let this decision space have infinite many alternatives. Denote by $Rl(X)$ a set of all binary relation on X, from X to itself, such that each relation $R \subset X \times X$ satisfies the following conditions:

(A1) If $x \in X$, then $(x,x) \in R$ (reflexive).

(A2) If $x,y,z \in X$, $(x,y) \in R$ and $(y,z) \in R$, then $(x,z) \in R$ (transitive).

(A3) If $x,y \in X$, then $(x,y) \in R$ holds or $(y,x) \in R$ holds (complete).

(A4) If $x \in X$, then $\{y \in X \mid (x,y) \in R\}$ is closed (upper closed).

This shows that any relation $R \in Rl(X)$ is a preorder (reflexive and transitive).

In the metric space (X,d), let τ be the topology induced by d.

Now, for $R \in Rl(X)$ we will denote two new relations as follows:

(1) Denote the asymmetric part of relation R *by relation* $P \subset X \times X$ *(for* $x, y \in X$ *there is* $(x, y) \in P$ *if and only if* $(x, y) \in R$ *holds and* $(y, x) \in R$ *does not hold). The relation* P *is irreflexive and transitive.*

(2) Denote the symmetric part of relation R *by relation* $I \subset X \times X$ *(for* $x, y \in X$ *there is* $(x, y) \in I$ *if and only if* $(x, y) \in R$ *and* $(y, x) \in R$ *hold). The relation* I *is reflexive, symmetric and transitive.*

Let $RI_0(X) \subset RI(X)$ be an infinite set of binary relation and let $R \in RI_0(X)$ be a relation representing "more preferred than" or "dominant" with respect. Therefore, for $x, y \in X$ the following statement is true: $(y, x) \in R$ is equivalent to an alternative x dominates an alternative y (or preferences x by y). The relations of $RI_0(X)$ are the mathematical description of the optimization criteria in decision making, which are often in conflict with each other [2] [3]. Thus, for $RI_0(X)$ definitions of the Pareto-optimal alternatives can be formally stated as follows:

Definition 1. (a) An alternative $x \in X$ is called a ideal Pareto-optimal alternative if and only if $(y, x) \in R$ for all $R \in RI_0(X)$ and for all $y \in X$. The set of the ideal Pareto-optimal alternatives of X is denoted by $IPO(X, RI_0(X))$ and is called a ideal Pareto-optimal set.

(b) An alternative $x \in X$ is called a Pareto-optimal alternative if and only if there does not exist an alternative $y \in X$ such that $(x, y) \in R$ for all $R \in RI_0(X)$ and $(x, y) \in P$ for some $R \in RI_0(X)$. The set of the Pareto-optimal alternatives of X is denoted by $PO(X, RI_0(X))$ and is called a Pareto-optimal set.

(c) An alternative $x \in X$ is called a weakly Pareto-optimal alternative if and only if there does not exist an alternative $y \in X$ such that $(x, y) \in P$ for all $R \in RI_0(X)$. The set of the weakly Pareto-optimal alternatives of X is denoted by $WPO(X, RI_0(X))$ and is called a weakly Pareto-optimal set.

(d) An alternative $x \in X$ is called a strictly Pareto-optimal alternative if and only if there does not exist an alternative $y \in X$ such that $(x,y) \in R$ for all $R \in RI_0(X)$ and $x \neq y$. The set of the strictly Pareto-optimal alternatives of X is denoted by $SPO(X, RI_0(X))$ and is called a strictly Pareto-optimal set. □

If the ideal Pareto-optimal set $IPO(X, RI_0(X))$ is empty, then we will accept the elements into the Pareto-optimal and weakly Pareto-optimal sets as two different solutions of the given multi-criteria decision making problem [5] [12].

Remark 1. From definition it is obvious that:

(1) $SPO(X, RI_0(X)) \subset PO(X, RI_0(X)) \subset WPO(X, RI_0(X))$.

(2) If $IPO(X, RI_0(X)) \neq \varnothing$, then $IPO(X, RI_0(X)) = PO(X, RI_0(X))$. □

Example 1. Let us consider an exchange economics. This system consists of many agents, but we may assume that they are infinite, i.e. the economics model is “large”, see [6], [7] and [8]. If the exchange goods are perfecting divisible, then the set of alternatives is infinite. □

Example 2. Let us consider a game model. It consists of many players. They form a society and let assume that this society is “large”, i.e. it has infinite elements [9] [11]. □

2. Hausdorff metric

In this section we will study a set $Cl(X)$ of all nonempty closed subset of X. It is well-known that $Cl(X)$ is compact [1]. For each $A \in Cl(X)$ and $r > 0$ we consider closed neighborhood $N_r(A)$ of A defined by $N_r(A) = \{x \in R^m \mid d(x,A) \leq r\}$.

The upper semi-metric on X is defined as follows: $\delta_u(A,B) = \inf\{r > 0 \mid B \subset N_r(A)\}$ for $A, B \in Cl(X)$. The following properties follow straight the definition:

(1) $\delta_u(A,B) \geq 0$;

(2) $\delta_u(A,B) = 0$ if and only if $B \subset A$;

(3) $\delta_u(A,C) \leq \delta_u(A,B) + \delta_u(B,C)$.

Similarly, the lower semi-metric on X is defined as follows: $\delta_l(A,B) = \inf\{r > 0 \mid A \subset N_r(B)\}$. Here, we have the following properties:

(1) $\delta_l(A,B) \geq 0$;

(2) $\delta_l(A,B) = 0$ if and only if $A \subset B$;

(3) $\delta_l(A,C) \leq \delta_l(A,B) + \delta_l(B,C)$.

As a result we obtain:

(1) $\delta_u(A,B) = \delta_l(B,A)$;

(2) $\delta_u(A,B) = \delta_l(A,B) = 0$ if and only if $A = B$.

Finally, the Hausdorff metric is defined by $\delta(A,B) = \max\{\delta_l(A,B), \delta_u(A,B)\}$ [4].

Remark 2. We can consider the metric hyperspace $(Cl(X), \delta)$ with the Hausdorff metric $\delta(A,B) = \max\{\max_{x\in A}\min_{y\in B} d(x,y), \max_{x\in B}\min_{y\in A} d(x,y)\}$ for $A,B \in Cl(X)$. In this space a sequence of sets $\{A_k\}_{k=1}^{\infty} \subset Cl(X)$ is called to be Hausdorff convergence to $A \in Cl(X)$ if and only if $\lim_{k\to\infty} \delta(A_k, A) = 0$ [1]. □

Remark 3. Let denote the distance between $x \in X$ and $A \subset X$ by $d(x,A) = \inf\{d(x,y) \mid y \in A\}$. A sequence of sets $\{A_k\}_{k=1}^{\infty} \subset Cl(X)$ is called to be Wijsman convergence to $A \in Cl(X)$ if and only if for each $x \in X$, $\lim_{k\to\infty} d(x,A_k) = d(x,A)$. □

Remark 4. It is important to note that the Hausdorff and Wijsman topologies on $Cl(X)$ coincide if and only if (X,d) is a totally bounded space [1]. Hence, in our case these two topologies coincide. □

For fixed $x \in X$ and $R \in Rl_0(X)$, $\{y \in X \mid (x,y) \in R\}$ is nonempty compact. This allows us to define a multifunction $\rho : X \Rightarrow X$ by $\rho(x) = \bigcap_{R\in Rl_0(X)} \{y \in X \mid (x,y) \in R\}$ and a binary relation $S \subset X \times X$ by $(y,x) \in S \Leftrightarrow \rho(x) \subset \rho(y)$.

3. Some characteristics of the optimality sets

Consider the metric space $(Ps(X),\delta)$. Based on the definitions of the Pareto-optimal alternatives we introduce new equivalent form of these definitions, for $x \in X$:

(1) $x \in IPO(X, RI_0(X))$ if and only if $\rho(x) \subset \rho(y)$ for all $y \in X$.

(2) $x \in PO(X, RI_0(X))$ if and only if for $y \in X$ and $\rho(y) \subset \rho(x) \Rightarrow \rho(y) = \rho(x)$.

(3) $x \in WPO(X, RI_0(X))$ if and only if $\text{int}(\rho(x)) = \varnothing$.

(4) $x \in SPO(X, RI_0(X))$ if and only if $\{x\} = \rho(x)$.

Additionally, let us also assume the following conditions:

(A5) $\left| \bigcap_{R \in RI_0(X)} \{y \in X \mid (x,y) \in I\} \right| = 1$ for all $x \in X$.

(A6) The multifunction ρ is continuous on X.

Remark 5. We get that ρ' is bijective function on compact space X. As a result we obtain that ρ' is homeomorphism between the topological spaces (X,τ) and $(Ps(X),T')$. Clearly, it is also uniformly continuous. This means that ρ' is uniform homeomorphism [14]. □

Remark 6. It is important to note that $(Ps(X),\delta)$ is compact metric spaces, see Remark 5. □

Remark 7. It can be shown that:

(1) The space (X,S) is partially ordered (the relation S is reflexive, antisymmetric and transitive).

(2) The space $(Ps(X),\subset)$ is partially ordered (the relation $\subset$ is reflexive, antisymmetric and transitive).

(3) The spaces (X,S) and $(Ps,\subset)$ are order isomorphic. □

Remark 8. Based on the assumptions it can be shown that if a sequence $\{x_k\}_{k=1}^{\infty} \subset X$ is convergence to $x_0 \in X$, then following are equivalent:

(1) The sequence of sets $\{\rho(x_k)\}_{k=1}^{\infty} \subset Ps(X)$ is Hausdorff convergence to $\rho(x_0) \in Ps(X)$.

(2) The sequence of sets $\{\rho(x_k)\}_{k=1}^{\infty} \subset Ps(X)$ is Wijsman convergence to $\rho(x_0) \in Ps(X)$. □

Remark 9. From the assumptions it is obvious that $SPO(X, RI_0(X)) = PO(X, RI_0(X))$ [5]. The strictly Pareto-optimal alternatives are the multi-criteria analogue of unique optimal solutions in scalar optimization. □

Theorem 1. If $x \in X$, then there exists $y \in SPO(X, RI_0(X))$ such that $(x, y) \in R$ for all $R \in RI_0(X)$.

Proof. If $x \in SPO(X, RI_0(X))$, then $y = x$. If $x \notin SPO(X, RI_0(X))$, then set $S = \{A \in Ps(X) \mid A \subseteq \rho(x))\}$. Define a function $f : S \to R$ by $f(A) = \delta(A, \rho(x))$. From S is compact and f is continuous it follows that there exists $B \in S$ such that $f(B) = \max\{f(A) \mid A \in S\}$ and $f(B) > 0$. Clearly, $x \notin B$ and there exists $y \in \rho(x)$ such that $B = \rho(y)$.

Now we will prove $y \in SPO(X, RI_0(X))$. First, we will prove $y \in PO(X, RI_0(X))$. Let assume $y \in PO(X, RI_0(X))$. This means that there exists $z \in PO(X, RI_0(X))$ such that $\rho(z) \subset \rho(y)$ and $\rho(z) \neq \rho(y)$. In this case we have $f(\rho(z)) > f(\rho(y))$. This contradicts the condition $f(\rho(y)) = \max\{f(A) \mid A \in S\}$. As a result we obtain $y \in PO(X, RI_0(X))$. Next, according to Remark 9 we deduct $y \in SPO(X, RI_0(X))$. The theorem is proven.

Corollary 1. If $x \in X$, then there exists $y \in PO(X, RI_0(X))$ such that $(x, y) \in R$ for all $R \in RI_0(X)$.

Corollary 2. If $x \in X$, then there exists $y \in WPO(X, RI_0(X))$ such that $(x, y) \in R$ for all $R \in RI_0(X)$.

Corollary 3. The sets $SPO(X, RI_0(X))$, $PO(X, RI_0(X))$ and $WPO(X, RI_0(X))$ are nonempty.

Corollary 4. If $IPO(X, RI_0(X))$ is nonempty and $x \in X$, then there exists $y \in IPO(X, RI_0(X))$ such that $(x, y) \in R$ for all $R \in RI_0(X)$.

Theorem 2. If $X \subset R^n$, then $SPO(X, RI_0(X))$ is compact.

Lemma 1 [13, Theorem 9.14 – The Maximum Theorem]. Let $S \subset R^n$, $\Theta \subset R^m$, $g : S \times \Theta \to R$ a continuous function, and $D : \Theta \Rightarrow S$ be a compact-valued and continuous multifunction. Then, the function $g^* : \Theta \to R$ defined by $g^*(\theta) = \max\{g(x,\theta) \mid x \in D(\theta)\}$ is continuous on Θ, and the multifunction $D^* : \Theta \Rightarrow S$ defined by $D^*(\theta) = \{x \in D(\theta) \mid g(x,\theta) = g^*(\theta)\}$ is compact-valued and upper semi-continuous on Θ.

Lemma 2 [10]. Let $\Theta \subset R^m$ be compact and $D : \Theta \Rightarrow \Theta$ be an upper semi-continuous multifunction. If $D(x) \neq \varnothing$ is compact for all $x \in \Theta$, then $D(\Theta)$ is compact.

Proof of Theorem 2. Define a function $b : X \to R$ by $b(x) = \max\{\delta(A, \rho(x)) \mid A \in Ps(X)\}$. It is clear to show that b is continuous on the compact set X. Applying Lemma 1 for $S = \Theta = X$, $D = \rho$ and $g = b$ we deduce that there exist a function $b^*(x) = \max\{b(y) \mid y \in \rho(x)\}$ and a multifunction $\pi : X \Rightarrow X$ such that $\pi(x) = \{y \in \rho(x) \mid b(y) = b^*(x)\}$. We have known that π is compact-valued and upper semi-continuous on X.

Of course, $\pi(x) \in SPO(X, RI_0(X))$, see the proof of Theorem 1.

For definition of π we see that $x \in \pi(x)$ for $x \in SPO(X, RI_0(X))$. Therefore we have $\pi(X) = SPO(X, RI_0(X))$. According to Lemma 2 we obtain that $\pi(X) = SPO(X, RI_0(X))$ is compact. The theorem is proven.

REFERENCES

[1] Beer G., (1993) Topologies on Closed and Closed Convex Sets. Kluwer.
[2] Chankong V., Haimes Y., (1983) Multiobjectite Decision Making. North-Holland.
[3] Ching-Lai H., Masud A., (1978) Multiple Objective Decision Making – Methods and Applications, Springer.
[4] Edgar G., (1990) Measure, Topology and Fractal Geometric. Springer.
[5] Ehrgott M., (2005) Multi-criteria Optimization. Springer.
[6] Hildenbrand W., (1974) Core and equilibria of a large economy. Princeton University Press.

[7] Hildenbrand W., (1982) Core of an economy. K. Arrow, M. Intriligator, Handbook of Mathematical Economics. North-Holland, vol 2.
[8] Klein E., (1973) Mathematical methods in theoretical economics. Academic Press.
[9] Luce R., Rajffa H., (1989) Games and Decisions. Dover Publications.
[10] Mukherjea A., Pothoven K., (1978) Real and Functional Analysis. Plenum Press.
[11] Slavov Z., (2002) The Optimality Alternatives at Decision-Making. Mathematics and Education in Mathematics 31, 181-186.
[12] Slavov Z., (2004) On the optimality concept in decision-making system with finitely many criteria. RaDMI 2004, 31 August - 04 September 2004, Zlatibor, Serbia and Montenegro, 529-537.
[13] Sundaran R., (1996) A First Course in Optimization Theory. Cambridge University Press.
[14] Wilansky A., (2008) Topology for Analysis. Dover Publications.

Contractibility of the Pareto Optimality Set in Mathematical Model of Pure Exchange Economics

Zdravko Slavov[1], Desislava Slavova[2]

[1] Varna Free University, Varna, Bulgaria, slavovibz@yahoo.com

[2] Virginia Tech, Blacksburg, USA, slavova_desi@yahoo.com

Abstract. *In this paper we consider a mathematical model in pure exchange economics with finite number of agents and goods. It is proved that a Pareto optimality set and Pareto frontier set are homeomorphic and contractible.*

Keywords: *exchange economy, mathematical model, retraction, homeomorphism, contractible.*

1. Introduction

Consider a pure exchange economy $\varepsilon(A,G,\{e^i\}_{i=1}^n,\{X_i\}_{i=1}^n,\{\succeq\}_{i=1}^n)$ with finite numbers of agents and goods. This economy is defined by a set A of economic agents, $|A|=n\geq 2$, $J_A=\{1,2,...,n\}$, and a set G of exchange goods, $|G|=m\geq 2$, $J_G=\{1,2,...,m\}$. Let each agent $a_i\in A$ have an endowment $e^i\in R_+^m$ and a consumption closed set $X_i\in R_+^m$, $e^i\in X_i$. A set $\Sigma=\{x(x^1,x^2,...,x^n)\in X_1\times X_2\times...\times X_n \mid \sum_{i=1}^n x^i=\sum_{i=1}^n e^i\}$ is called a space of individual rational allocations (rational space) at endowment $e(e^1,e^2,...,e^n)$, where agent $a_i\in A$ owns of $x^i(x_1^i,x_2^i,...,x_m^i)\in R_+^m$, a number $x_j^i\geq 0$ shows the quantity of $g_j\in G$ property of this agent [10].

In addition, let each agent $a_i\in A$ have a binary weak preference relation $\succeq_i$ defined on X_i, $\succeq_i\subset X_i\times X_i$. A strict preference relation $\succ_i$ is associated with $\succeq_i$ as usual: $y\succ_i x$ is equivalent to $y\succeq_i x$ and not $x\succeq_i y$ for $x,y\in X_i$.

2. Definitions and notations

Let d be Euclidean metric in R^{mn}. In a metric space (Σ, d), let τ be a topology induced by d. In a topological space (Σ, τ), for set $X \subset \Sigma$ we recall some definitions:

(a) The set X is called connected if and only if it is not the union of a pair of nonempty sets of τ, which are disjoint.

(b) The set X is called pathwise connected if and only if for every $x, y \in X$ there exists a continuous function $p : [0;1] \to X$ such that $p(0) = x$ and $p(1) = y$.

(c) The set X is a retract of Σ if and only if there exists a continuous function $r : \Sigma \to X$ such that $r(\Sigma) = X$ and $r(x) = x$ for all $x \in X$.

(d) The set X is contractible if and only if there exist a continuous function $h : X \times [0;1] \to X$ and $a \in X$ such that $h(x,0) = a$ and $h(x,1) = x$ for all $x \in X$.

It is well known that: from convexity implies contractibility; from contractibility implies pathwise connectedness; from pathwise connectedness implies connectedness. Note that the reverse implications are not true in general, see [4] and [7].

As usually, we assume that every relation $\succeq_i$ of $\{\succeq\}_{i=1}^{n}$ is reflexive, transitive, complete and continuous on X_i. Thus each binary relation $\succeq_i$ can be represented by a continuous utility function $u_i : X_i \to R$ such that for every $x, y \in X_i$, $x \succeq_i y$ is equivalent to $u_i(x) \geq u_i(y)$ [2] [5]. It is well known that a relation $\succeq_i$ can be represented by different utility functions. Let denote a set of these utility functions by $\tilde{U}(\succeq_i, X_i)$; therefore, $\left|\tilde{U}(\succeq_i, X_i)\right| > 1$. Let each agent $a_i \in A$ have a utility function u_i of $\tilde{U}(\succeq_i, X_i)$ and define a function $U : \Sigma \to R^n$ such that $U(x) = (u_1(x^1), u_2(x^2), ..., u_n(x^n))$ for all $x(x^1, x^2, ..., x^n) \in \Sigma$.

Now, we are ready to introduce the definition of Pareto optimality allocation: an allocation $x \in \Sigma$ is called Pareto optimality if and only if there does not exists $y \in \Sigma$ such that $y \succeq_i x$ (or $u_i(y) \geq u_i(x)$) for all $i \in J_A$ and $y \succ_k x$ (or $u_k(y) > u_k(x)$) for some $i \in J_A$. We denote the set of the Pareto optimality allocations on Σ by P and it is called a

Pareto optimality set. The set $U(P)$ is called a Pareto optimality frontier [8] [9].

Of course, it can also be shown that the Pareto optimality allocations are only depended on the preference relations $\{\succeq_i\}_{i=1}^n$ and not depended on choice of utility functions $\{u_i\}_{i=1}^n$. Therefore, without loss of generality we can use the utility functions in our optimization problem.

3. Main result

Our aim is to obtain a collection of conditions which guarantee the contractibility of the sets P and $U(P)$. From mathematical point of view, the Pareto optimality allocations are solutions of a multi-objective optimization problem written as: Maximize $U(x)$ subject to $x \in \Sigma$.

The utility maximization is a basic optimization problem in exchange economic theory. For this optimization problem it is known that the set P is nonempty compact and $U(P) \subset \partial U(\Sigma)$ [1] [6].

To get the retraction, we must also make some assumptions:

Assumption 1. The sets $\{X_i\}_{i=1}^n$ are convex.

Assumption 2. $|\Sigma| > 1$.

Assumption 3. The weak preference relations $\{\succeq_i\}_{i=1}^n$ are monotone and convex.

The weak preference relation $\succeq_i$ is called monotone on X_i if and only if for every $x, y \in X_i$ such that $x \neq y$ and $x \geq y$ imply that $x \succ_i y$ (or $u_i(x) > u_i(y)$). Therefore the utility function u_i is monotone on X_i.

The weak preference relation $\succeq_i$ is called convex on X_i if and only if for every $x, y \in X_i$ such that $y \succ_i x$ and $t \in (0;1]$ imply that $ty + (1-t)x \succ_i x$. For utility function u_i we find that for every $x, y \in X_i$ such that $x \neq y$ and $t \in (0;1)$ imply that $u_i(tx + (1-t)y) > \min(u_i(x), u_i(y))$. In the other words, the utility function u_i is strictly quasi-concave on X_i.

Let define a multifunction $\rho : \Sigma \Rightarrow \Sigma$ such that $\rho(x) = \{y \in \Sigma : u_i(y^i) \geq u_i(x^i), i \in J_A\}$ for $x \in \Sigma$. We can easily check that the set $\rho(x)$ is a nonempty, convex and compact set for all $x \in \Sigma$ and there

is $x \in \rho(x)$. In the other words, the multifunction ρ is convex-valued and compact-valued.

Theorem 1. If ρ is lower semi-continuous on Σ, then:

(a) The Pareto optimality set P is a retract of Σ.

(b) The sets P and $U(P)$ are homeomorphic and contractible.

For proving Theorem 1 we need several lemmas.

Lemma 1. ρ is upper semi-continuous on Σ.

Proof. If $\{x_k\}_{k=1}^{\infty} \subset \Sigma$ and $\{y_k\}_{k=1}^{\infty} \subset \Sigma$ are a pair of sequences such that $\lim\limits_{k\to\infty} x_k = x_0 \in \Sigma$ and $y_k \in \rho(x_k)$ for all $k \in N$, then there exists a convergent subsequence of $\{y_k\}_{k=1}^{\infty}$ whose limit belongs to $\rho(x_0)$.

Since the assumption $y_k \in \rho(x_k)$ for all $k \in N$ implies that $u_i(y_k) \geq u_i(x_k)$ for all $k \in N$ and all $i \in J_A$. From the condition $\{y_k\}_{k=1}^{\infty} \subset \Sigma$ it follows that there exists a convergent sequence $\{y'_k\}_{k=1}^{\infty} \subset \{y_k\}_{k=1}^{\infty}$ such that $\lim\limits_{k\to\infty} y'_k = y_0 \in \Sigma$, $\{x'_k\}_{k=1}^{\infty} \subset \{x_k\}_{k=1}^{\infty}$, $\lim\limits_{k\to\infty} x'_k = x_0$ and $y'_k \in \rho(x'_k)$. So, we can deduce that $u_i(y'_k) \geq u_i(x'_k)$ for all $k \in N$ and all $i \in J_A$. Taking the limit as $k \to \infty$ we get $u_i(y_0) \geq u_i(x_0)$ for all $i \in J_A$. As a result we obtain $y_o \in \rho(x_0)$. This means that ρ is upper semi-continuous on Σ. The lemma is proven.

Lemma 2. ρ is continuous on Σ.

Proof. From Lemma 1 it follows that the multifunction ρ is upper semi-continuous on Σ. We have known that ρ is lower semi-continuous on Σ. See also [3] and [7]. Finally, we obtain the multifunction ρ is continuous on Σ.

The lemma is proven.

Lemma 3. If $x \in \Sigma$, then $x \in P$ is equivalent to $|\rho(x)| = 1$.

Proof. Let $x \in P$ and assume that $|\rho(x)| > 1$. From both conditions $x \in \rho(x)$ and $\{x\} \neq \rho(x)$ it follows that there exists $y \in \rho(x) \setminus \{x\}$ such that $u_i(y^i) \geq u_i(x^i)$ for all $i \in J_A$.

Let $t \in (0;1)$ and $z = tx + (1-t)y$, therefore $z \in \rho(x)$. Fix a number $i \in J_A$. There are two cases as follows: $x^i = y^i$ and $x^i \neq y^i$. First, if $x^i = y^i$, then $u_i(z^i) = u_i(y^i) = u_i(x^i)$. Second, if $x^i \neq y^i$, that $u_i(z^i) > \min(u_i(y^i), u_i(x^i) = u_i(x^i)$. Then, since $x \neq y$ implies that $x^k \neq y^k$

for some $k \in J_A$. This allows us to conclude that $u_i(z^i) \geq u_i(x^i)$ for all $i \in J_A$ and $u_k(z^k) > u_k(x^k)$ for some $k \in J_A$, which contradicts the assumption $x \in P$. Therefore we obtain $|\rho(x)| = 1$.

Conversely, let $|\rho(x)| = 1$ and assume that $x \notin P$. From $x \notin P$ it follows that there exists $y \in \Sigma$ such that $u_i(y^i) \geq u_i(x^i)$ for all $i \in J_A$ and $u_k(y^k) > u_k(x^k)$ for some $k \in J_A$. Obviously, we have that $y \in \rho(x)$ and $x \neq y$, which contradicts the assumption $|\rho(x)| = 1$. Therefore we obtain $x \in P$.

The lemma is proven.

Choose $a_i \in A$ and $x \in \Sigma$. Now we will consider an optimization problem with single objective function written as: Maximize $u_1(y^1)$ subject to $y \in \rho(x)$.

We will prove that for every $x \in \Sigma$ this problem has a unique solution $\overline{x} \in P$. In [1], we can see a similar idea in economics without consumption sets.

This note allows introducing the following lemma.

Lemma 4. If $x \in \Sigma$, then $|Arg\max(u_1, \rho(x))| = 1$.

Proof. Clearly, there is $|Arg\max(u_1, \rho(x))| \geq 1$. Let assume that $|Arg\max(u_1, \rho(x))| > 1$ and $y_1, y_2 \in Arg\max(u_1, \rho(x))$, $y_1 \neq y_2$, $t \in (0;1)$ and $z = ty_1 + (1-t)y_2$. It is not hart to see that the set $Arg\max(u_1, \rho(x))$ is convex, therefore we have that $z \in Arg\max(f, \rho(x))$. Hence, we derive $u_1(z^1) = u_1(y_1^1) = u_1(y_2^1)$.

From the assumption $y_1 \neq y_2$ it follows that there exists $k \in J_A$ such that $y_1^k \neq y_2^k$. It is obvious that there are two cases as follows: $k = 1$ and $k \neq 1$. First, if $k = 1$, then $u_1(z^1) > \min(u_1(y_1^1), u_1(y_2^1)) = u_1(y_1^1)$. But, we have shown that $u_1(z^1) = u_1(y_1^1) = u_1(y_2^1)$. This leads to a contradiction. Second, if $k \neq 1$, then $u_k(z^k) > \min(u_k(y_1^k), u_k(y_2^k))$. In this case there exists $y \in \rho(x)$ such that $u_k(z^k) > u_k(y^k) > \min(u_k(y_1^k), u_k(y_2^k))$, $u_1(y^1) > u_1(z^1)$ and $y^j = z^j$ for all $j \in J_A \setminus \{1, k\}$. But, we have shown that $z \in Arg\max(f, \rho(x))$. So again, this leads to a contradiction.

Finally, we obtain $|Arg\max(u_1, \rho(x))| = 1$. The lemma is proven.

Lemma 5. If $x \in \Sigma$, then $Arg\max(u_1, \rho(x)) \subset P$.

Proof. Let $y \in Arg\max(u_1, \rho(x))$ and assume that $y \notin P$. From the assumption $y \notin P$ it follows that there exists $z \in \Sigma$ such that $u_i(z^i) \geq u_i(y^i)$ for all $i \in J_A$ and $u_k(z^k) > u_k(y^k)$ for some $k \in J_A$. As a result we have that $z \in \rho(x)$.

On one hand, since the condition $u_i(z^i) \geq u_i(y^i)$ for all $i \in J_A$ implies that $z \in Arg\max(u_1, \rho(x))$. On the other hand, since the condition $u_k(z^k) > u_k(y^k)$ for some $k \in J_A$ implies that $z \neq y$. But, in Lemma 4 we have proved that $|Arg\max(u_1, \rho(x))| = 1$. This leads to a contradiction, therefore we obtain $y \in P$.

The lemma is proven.

Using the results of Lemmas 4 and 5 we are in position to construct a function $r : \Sigma \to P$ such that $r(x) \in Arg\max(u_1, \rho(x))$ for all $x \in \Sigma$. Now, our attention will be focused on the function r.

Lemma 6. $r(P) = P$ and $r(\Sigma) = P$.

Proof. Applying now Lemmas 3, 4 and 5 we get $r(P) = P$. According to Lemma 5, from the fact that $P \subset \Sigma$, we obtain $r(\Sigma) = P$. The lemma is proven.

Lemma 7. [3] [5] Let X be a topological space. If $F : X \to R$ is continuous function and $B : X \Rightarrow X$ is a continuous compact-valued multifunction, then the multifunction $\gamma : X \Rightarrow X$ defined by $\gamma(y) = \{x \in B(y) \mid F(x) \geq F(x'), x' \in B(y)\}$ is upper semi-continuous and compact-valued, and the function $f : X \to R$ defined by $f(y) = F(\gamma(y))$ is continuous.

Lemma 8. The function r is continuous on Σ.

Proof. By the previous lemma, let $X = \Sigma$, $F(x) = u_1(x^1)$ for all $x(x^1, x^2, ..., x^n) \in \Sigma$ and $B = \rho$. Applying now Lemma 5 we derive $|\gamma(y)| = 1$ for all $y \in \Sigma$. This means that γ is function and $\gamma = r$. As a result we obtain the function r is continuous on Σ. The lemma is proven.

Lemma 9. P is homeomorphic to $U(P)$

Proof. Since the function $U:\Sigma \to R^n$ is continuous it follows that the restriction $h:P \to U(P)$ of U is continuous too. Applying Lemma 3 we deduce that if $x,y \in P$ and $x \neq y$, then $h(x) \neq h(y)$. We derive the function h is bijective. Consider the inverse function $h^{-1}:U(P) \to P$ of h. As mentioned before, the set P is compact; therefore, h^{-1} is continuous too. Finally, we obtain the function h is homeomorphism. The lemma is proven.

Proof of Theorem 1. (a) This follows from applications of Lemmas 6 and 8.

(b) This follows from applications of Theorem 1(a), and Lemma 9.

This completes the proof of our theorem.

Remark 1. In [9], it is proved that the Pareto optimality set is compact and pathwise connected in exchange economics with fixed total resources and consumption sets.

REFERENCES

[1] Balasko Y., (1988) Foundations of the Theory of General Equilibrium, Academic Press.
[2] Barten A., Bohm V., (1982) Consumer Theory, Handbook of Mathematical Economics vol. II, North-Holland Publishing Co, 381-429.
[3] Green J., Heller W., (1981) Mathematical Analysis and Convexity with Applications to Economics, Handbook of Mathematical Economics vol. I, North-Holland Publishing Co, 15-52.
[4] Hatcher A., (2002) Algebraic Topology, Cambridge University Press.
[5] Klein E., (1973) Mathematical Methods in Theoretical Economics, Academic Press.
[6] Luc D., (1989) Theory of Vector Optimization, Springer.
[7] Mukherjea A., Pothoven K., (1978) Real and Functional Analysis, Plenum Press.
[8] Slavov Z., (2003) Weak and strong optimality and increasing concave functions, Applied Mathematics and Computation 135, 517-529.
[9] Slavov Z., (2004) Structure of the Pareto optimality set with fixed total resources and consumption sets, Applied Mathematics and Computation 154, 75-81.

[10] Slavov Z., (2006) Scalarization techniques or relationship between a social welfare function and a Pareto optimally concept, Applied Mathematics and Computation 172, 464-471.

Reductions for a class of presentations of *(n,m)* - semigroups

Irena Stojmenovska, Dončo Dimovski*
**Faculty of Natural Sciences and Mathematics, Ss. Cyril and Methodius University, Skopje, Macedonia*

Abstract: *We give a contribution to the combinatorial theory of (n,m)-semigroups, by constructing good reductions for a sequence of (n,m)-presentations of (n,m)-semigroups. As a consequence, we obtain good descriptions for the corresponding (n,m)-semigroups.*

Keywords: *(n,m)-semigroup, (n,m)-presentation, (n,m)-reduction.*

1. INTRODUCTION

We will use the following notations: N for the set of positive integers and N_r, N_r^0 for the sets $\{1,2,...,r\}$ and $\{0,1,2,...,r\}$ respectively, $(r \in N)$; Q^+ for the set of all finite (nonempty) sequences of the elements of a set Q and Q^* for the set $Q^+ \cup \{1\}$, where 1 is a notation for the empty sequence; a_1^r for the elements of Q^r, where Q^r denotes the r-th Cartesian power of Q. When $a_1 = ... = a_r = a$ we use the notation $\overset{r}{a}$. Also, a_i^j will denote the sequence $a_i a_{i+1} ... a_j$ when $i \le j$, or the empty sequence when $i > j$.

Let $Q \neq \varnothing$ and n, m are positive integers.

A mapping $f : Q^n \to Q^m$ is called an (n,m)-operation and the pair $\boldsymbol{Q} = (Q; f)$ is called an (n,m)-groupoid. A mapping $f : \bigcup_{s \ge 1} Q^{m+sk} \to Q^m$ is called a poly-(n,m)-operation and the pair $\boldsymbol{Q} = (Q; f)$ is said to be a poly-(n,m)-groupoid.

Let $m \ge 2$, $k = n - m$ and let $k \ge 1$.

An (n,m)-groupoid $\boldsymbol{Q}=(Q;f)$ is an (n,m)-semigroup if $f(f(x_1^n)x_{n+1}^{n+k})=f(x_1^i f(x_{i+1}^{i+n})x_{i+n+1}^{n+k})$ for all $x_\upsilon \in Q$, $i \in N_k$.

For more details on (n,m)-semigroups see [4] - \$5, \$6.

The notions of (n,m)-operations (and poly-(n,m)-operations) are easily thought of as algebras with m n-ary (poly n-ary) operations (see [4]-\$1).

Let $\boldsymbol{F(B)}=(F(B);f)$ be a free poly-(n,m)-groupoid with a basis B, $B\neq\varnothing$. We recall its construction: $B_{-1}=\varnothing$, $B_0=B$,

$$B_{p+1}=B_p\cup(N_m\times\bigcup_{s\geq 1}B_p^{m+sk}),\qquad F(B)=\bigcup_{p\geq 0}B_p;$$

$f(u_1^{m+sk})=v_1^m \Leftrightarrow v_i=(i,u_1^{m+sk})$, $i\in N_m$. (See [4]-\$6).

Hierarchy of the elements of $F(B)$ is a mapping $\chi: F(B)\to N\cup\{0\}$ defined by $\chi(u)=\min\left\{p\middle|u\in B_p\right\}$. Clearly, $\chi(u)=p\Leftrightarrow u\in B_p\setminus B_{p-1}$. Length on $F(B)$ is a mapping $|\ |: F(B)\to N$ defined by induction on χ as follows: $|u|=1$, $u\in B_0$; $\left|(i,u_1^{m+sk})\right|=|u_1|+\ldots+\left|u_{m+sk}\right|$, $(i,u_1^{m+sk})\in B_{p+1}\setminus B_p$.

Let $\Delta\subseteq F(B)\times F(B)$. Δ is called a set of (n,m)-defining relations on B and the pair $\langle B,\Delta\rangle$ is an (n,m)-presentation of an (n,m)-semigroup. It presents the factor (n,m)-semigroup $\boldsymbol{F(B)}/\overline{\Delta}$ where $\overline{\Delta}$ is the least congruence on $\boldsymbol{F(B)}$ such that $\Delta\subseteq\overline{\Delta}$ and $\boldsymbol{F(B)}/\overline{\Delta}$ is an (n,m)-semigroup. We use the notation $\langle B;\Delta\rangle=\boldsymbol{F(B)}/\overline{\Delta}$. (See [3]-\$1).

The structure of the (n,m)-semigroup $\boldsymbol{F(B)}/\overline{\Delta}$ might be found by defining a reduction for the given (n,m)-presentation $\langle B,\Delta\rangle$.

Reduction for $\langle B,\Delta\rangle$ is a mapping $\psi: F(B)\to F(B)$ satisfying:

(i) $(u,v)\in\Delta\Rightarrow\psi(u)=\psi(v)$;

(ii) $\psi(i,x'(1,y)(2,y)\ldots(m,y)x'')=\psi(i,x'yx'')$;

(iii) $\psi(i,x'wx'')=\psi(i,x'\psi(w)x'')$; (iv) $u\overline{\Delta}\psi(u)$; (v) $\psi(\psi(u))=\psi(u)$,

for all $u,v,w,(i,x'wx''),(i,x'(1,y)(2,y)\ldots(m,y)x'')\in F(B)$, $x',x''\in F(B)^*$.

If ψ is a reduction for $\langle B;\Delta\rangle$ such that $\psi(u)$ can be determined in a finite number of steps for a given $u\in F(B)$, then ψ is said to be a good

(effective) reduction for $\langle B;\Delta\rangle$ and it provides a good description for the corresponding (n,m)-semigroup $\langle B;\Delta\rangle$. (See [2], [3]-\$2).

In the case when $\Delta=\varnothing$, $\langle B;\varnothing\rangle$ presents the free (n,m)-semigroup with a basis B. Let $\psi_0 : F(B)\to F(B)$ be the good reduction for $\langle B;\varnothing\rangle$ defined in [2]. (Recall that ψ_0 is defined by reducing the length, i.e. $\psi_0(u)\neq u$ implies $|\psi_0(u)|<|u|$). The mapping ψ_0 provides a good combinatorial description of the free (n,m)-semigroup with a basis B. ($\langle B;\varnothing\rangle=(\psi_0(F(B));g)$ where … - see [2]). For deeper reading, overview the definiton and the properties of ψ_0 given in [2]. See also [3] - \$1, \$2.

The question of finding a good combinatorial description of an (n,m)-semigroup given with its (n,m)-presentation $\langle B;\Delta\rangle$ is quite complicated to solve. Some examples and results on the issue are given in [3], [5], [6], [7]. Here, we give example of a sequence of (n,m)-presentations of (n,m)-semigroups $\langle B;\Delta\rangle$ such that good reductions for $\langle B;\Delta\rangle$ can be defined, and we give the construction of such reductions. Consequently, good descriptions of these (n,m)-semigroups can be obtained.

2. A SEQUENCE OF (n,m)- PRESENTATIONS $\langle B,\Delta_p\rangle$ WITH GOOD REDUCTIONS ψ^p, $p=0,1,...$

Let $B\neq\varnothing$, $p=0,1,...$

Define a sequence of (n,m)-defining relations $\Delta_p\subseteq F(B)\times F(B)$ by:

$$\begin{aligned}
&\big[\ u\ \Delta_p v\ \big]\Leftrightarrow\big[\ u=(i,u_1^{m+sk}),\ v=(i,v_1^{m+sk}),\\
&\qquad(\exists\lambda)(1\le\lambda<m)(\exists h)(1\le h\le m+sk-\lambda-1)\\
&\qquad(\forall j\in N_\lambda,\ u_{h+j},v_{h+j}\in(B_{p+1}\setminus B_p)\cap\psi_0(F(B)),\\
&\qquad u_h,v_h,u_{h+\lambda+1},v_{h+\lambda+1}\in B_p,\\
&\qquad\quad u_\eta=v_\eta,\eta\in\{1,...,h\}\cup\{h+\lambda+1,...,m+sk\}),\ i\in N_m,\ s\ge1\ \big]
\end{aligned}$$

We want to construct good reductions for the (n,m)-presentations $\langle B,\Delta_p\rangle$ $(p=0,1,...)$. In that purpose, we will use the reduction $\psi_0 : F(B)\to F(B)$ for $\langle B;\varnothing\rangle$. We will also define an invariant

$m_p : F(B) \to N$ and an auxiliary mapping $\overline{\psi}^p : \psi_0(F(B)) \to \psi_0(F(B))$ which will reduce the invariant m_p. Bellow we introduce those definitions as well as some properties of m_p, ψ_0 and $\overline{\psi}^p$, which will be given in 5 auxiliary lemmas. Using this results and the properties of the reduction ψ_0 ([2]), we will define an appropriate mapping $\psi^p : F(B) \to F(B)$ which will be a good reduction for $\langle B, \Delta_p \rangle$.

Lemma 2.1. If $(u,v) \in \Delta_p$ then $(\psi_0(u), \psi_0(v)) \in \Delta_p$.

Proof. The proof is by induction on the length, applying the definition of ψ_0 (see the proofs in [2]). Also, note that ψ_0 does not increase the hierarchy. □

Choose an element $a \in B$ and construct a sequence of elements $z_{p+1} \in (B_{p+1} \setminus B_p) \cap \psi_0(F(B)),\ p = 0,1,...$ as given:

$$z_1 = (1, \overset{m+k}{a}),\ z_2 = (1, \overset{m+k-1}{a}\ z_1),\ \ldots,\ z_{p+1} = (1, \overset{m+k-1}{a}\ z_p),\ \ldots$$

Define a mapping (invariant) $m_p : F(B) \to N$ by

$$m_p(u) = |u|,\ u \in B_p;\quad m_p(u) = \begin{cases} |u|, & u \in B_{p+1} \setminus B_p,\ u = z_{p+1} \\ |u| + 1, & u \in B_{p+1} \setminus B_p,\ u \neq z_{p+1} \end{cases};$$

Assume that $m_p(v)$ is well defined for all $v \in B_{p+j}$ $(j \geq 1)$ (induction on χ); Then, $m_p(i, u_1^{m+sk}) = \sum_{r=1}^{m+sk} m_p(u_r)$ for $(i, u_1^{m+sk}) \in B_{p+j+1} \setminus B_{p+j}$.

Lemma 2.2. 1) $|z_{p+1}| \leq |u|$ for all $u \in B_{p+1} \setminus B_p$.

2) $m_p(z_{p+1}) < m_p(u)$ for all $u \in B_{p+1} \setminus B_p$, $u \neq z_{p+1}$.

Proof. 1). By induction on p; 2). Direct consequence of 1). □

Next, we define a mapping $\overline{\psi}^p : \psi_0(F(B)) \to \psi_0(F(B))$ as follows:

$\overline{\psi}^p(u) = u,\ u \in \psi_0(F(B)) \cap B_{p+1}$.

Let $u = (i, u_1^{m+sk}) \in \psi_0(F(B)) \setminus B_{p+1}$ and assume that $\overline{\psi}^p(v)$ is well defined for all $v \in \psi_0(F(B))$ such that $m_p(v) < m_p(u)$. Moreover, assume that

$\overline{\psi}^p(v) \neq v$ implies $m_p(\overline{\psi}^p(v)) < m_p(v)$.

(I) Let exist $1 \le \lambda < m$ and $1 \le h \le m + sk - \lambda - 1$ such that: $u_h, u_{h+\lambda+1} \in B_p$, $u_{h+j} \in B_{p+1} \setminus B_p$ for all $j \in N_\lambda$ and $u_{h+j'} \neq z_{p+1}$ for some $j' \in N_\lambda$. Let also, h be the smallest such index. Since Lemma 2.2 implies that $m_p(i, u_1^h \overset{\lambda}{z}_{p+1} u_{h+\lambda+1}^{m+sk}) < m_p(u)$, we consequently define

$$\overline{\psi}^p(i, u_1^{m+sk}) = \overline{\psi}^p(i, u_1^h \overset{\lambda}{z}_{p+1} u_{h+\lambda+1}^{m+sk}).$$

Note that $m_p(\overline{\psi}^p(i, u_1^h \overset{\lambda}{z}_{p+1} u_{h+\lambda+1}^{m+sk})) \le m_p(i, u_1^h \overset{\lambda}{z}_{p+1} u_{h+\lambda+1}^{m+sk}) < m_p(i, u_1^{m+sk})$.

(II) If u doesn't satisfy the condition in (I), we put $\overline{\psi}^p(u) = u$.

Lemma 2.3. 1) $\overline{\psi}^p(u) \neq u$ implies $m_p(\overline{\psi}^p(u)) < m_p(u)$.

2) Let $(i, u_1^{m+sk}) \in \psi_0(F(B))$ where
$\chi(u_h), \chi(u_{h+\lambda+1}) \le p$ $\chi(u_{h+j}) = p+1, j \in N_\lambda$, $1 \le \lambda < m$,
$1 \le h \le m + sk - \lambda - 1$. Then
$$\overline{\psi}^p(i, u_1^{m+sk}) = \overline{\psi}^p(i, u_1^h \overset{\lambda}{z}_{p+1} u_{h+\lambda+1}^{m+sk}).$$

Proof. 1). Shown above, while defining $\overline{\psi}^p$; 2). By induction on m_p. □

Lemma 2.4. 1) If $(u, v) \in \Delta_p \cap \psi_0(F(B))$ then $\overline{\psi}^p(u) = \overline{\psi}^p(v)$.

2) If $\overline{\psi}^p(i, u_1^{m+sk}) \neq (i, u_1^{m+sk})$ then exists a sequence of elements $(i, x_0), (i, x_1), \ldots, (i, x_t) \in \psi_0(F(B))$ $(t \ge 1)$ such that

$$(i, u_1^{m+sk}) = (i, x_0)\Delta_p(i, x_1)\Delta_p \ldots \Delta_p(i, x_t) = \overline{\psi}^p(i, u_1^{m+sk}).$$

3) $\overline{\psi}^p(\overline{\psi}^p(u)) = \overline{\psi}^p(u)$ and $\psi_0(\overline{\psi}^p(u)) = \overline{\psi}^p(u)$ for all $u \in \psi_0(F(B))$.

Proof. 1). Follows from the definition of Δ_p, applying 2) from Lemma 2.3;

2). Straightforward, by induction on m_p and applying the definition of $\overline{\psi}^p$; 3). The proof of the first equality is by induction on m_p. The second equality follows immediately, since $\psi_0\psi_0 = \psi_0$ ([2]). □

Lemma 2.5. $\psi_0(u) \neq u$ implies $m_p(\psi_0(u)) < m_p(u)$.

Proof. By induction on $|\ |$. (See [2] and apply the same techniques). □

Now, we define a mapping $\psi^p : F(B) \to F(B)$ as follows:

$\psi^p(u) = \psi_0(u)$ $(\forall u \in B_{p+1})$;

Let $u = (i, u_1^{m+sk}) \in F(B) \setminus B_{p+1}$ and assume that $\psi^p(v)$ is well defined for all $v \in F(B)$ such that $\chi(v) < \chi(u)$. Thus, $\psi^p(u_\mu)$ is well defined for all u_μ, $\mu \in N_{m+sk}$ and consequently define $\psi^p(u)$ by

$\psi^p(u) = \overline{\psi}^p \psi_0(i, \psi^p(u_1)...\psi^p(u_{m+sk}))$.

Lemma 2.6. 1) $\psi^p(u) \neq u$ implies $m_p(\psi^p(u)) < m_p(u)$.

2) $\overline{\psi}^p(\psi^p(u)) = \psi^p(u)$ and $\psi_0(\psi^p(u)) = \psi^p(u)$, $u \in F(B)$.

Proof. 1). By induction on m_p and applying Lemma 2.3-1) and Lemma 2.5.

2). Direct consequences from the statements 3) in Lemma 2.4. □

Proposition 2.7. The mapping ψ^p is a good reduction for the (n,m)-presentation $\langle B; \Delta_p \rangle$, $p = 0,1,...$

Proof. ψ^p satisfies (i)-(v). Using similar discussions as in [2], in this case we have: (i) follows from the properties of ψ_0, Lemma 2.1 and Lemma 2.4-1); (ii) follows by using Lemma 2.4-2), Lemma 2.1, Lemma 2.4-1) and applying the properties of ψ_0; (iii) partially follows by induction on m_p, and the other part follows from the definitions of ψ_0, $\overline{\psi}^p$, ψ^p, and by Lemma 2.6-2); (iv) follows by induction on χ, and from Lemma 2.4-2); (v) is a consequence from (i) to (iv) (see [3]-$2). Thus, ψ^p is a reduction for $\langle B; \Delta_p \rangle$. Also, $\psi^p(u)$ $u \in F(B)$, can be determined in a finite number of steps, according to Lemma 2.6-1). Hence, the mapping ψ^p is a good reduction for the (n,m)-presentation $\langle B; \Delta_p \rangle$ $(p = 0,1,...)$. □

As a consequence, we get good descriptions of the corresponding (n,m)-semigroups $\langle B; \Delta_p \rangle$, $p = 0,1,...$ (For more details, see [3]-$2).

REFERENCES

[1] Čupona G. (1983) Vector valued semigroups, *Semigroup forum, Vol 26,* 65-74.

[2] Dimovski, D. (1985) Free vector valued semigroups, *Proc. Conf. Algebra & Logic (Cetinje, Montenegro),* 55-62.

[3] Čupona G., Markovski S., Dimovski D., Janeva B. (1988) Introduction to the combinatorial theory of vector valued semigroups, *Vector valued semigroups and groups,* Skopje, Maced. Acad. of Sci. and Arts, 141-184.
[4] Čupona G., Celakoski N., Markovski S., Dimovski D. (1988) Vector valued groupoids, semigroups and groups, *Vect. valued semigroups and groups*, Maced. Acad. of Sci. and Arts, 1-79.
[5] Dimovski D., Čupona G. (1999) Injective vector valued semigroups, *Novi Sad J. Math, Vol. 29, No. 3,* 151-163.
[6] Miovska V. (2008) *Vector valued bands,* PhD thesis - Ss. Cyril and Methodius University, Skopje, Macedonia.
[7] Stojmenovska I. (2007) *Combinatorial theory of vector valued algebraic structures*, MSc thesis - Ss. Cyril and Methodius University, Skopje, Macedonia.

Intrinsic shape based on ε - continuity and on continuity up to a covering are equivalent

Zoran Misajleski[1], Nikita Shekutkovski[2]
[1]*Department of mathematics, Faculty of Civil Engineering,*
Sts. Cyril and Methodius University, Skopje, Republic of Macedonia
[2]*Faculty of natural sciences and mathematics,*
Sts. Cyril and Methodius University, Skopje, Republic of Macedonia

Mathematics Subject Classification 2000: Primary 54C56

Abstract: *The first intrinsic definition of shape morphism is presented in [3], without complete definition of a category. In the paper [1] is shown that the definitions of shape morphism in [1] and [3] coincide.*

In this paper we show that shape categories constructed by intrinsic approaches in [1] and [2] are isomorphic.

Keywords*: intrinsic definition of shape, proximate sequence, proximate nets, isomorphism.*

1. INTRODUCTION

Let X and Y be compact metric spaces. We repeat the intrinsic approaches to shape from articles [1] and [2] respectively. According to [2], we have:

Definition 1: ([1]) A function $f : X \to Y$ is ε-continuous, if for every $x \in X$ there is a neighborhood of x whose image lies in the ε-neighbourhood of the image of x.

Definition 2: The functions $f, g : X \to Y$ are ε-homotopic, if there exists a ε-continuous function $F : X \times I \to Y$ such that for every $x \in X$, $F(x,0) = f(x)$ and $F(x,1) = g(x)$.

The relation of ε-homotopy is an equivalence relation on the set of ε-continuous functions.

Definition 3: A proximate net, from X to Y, is a sequence of (not necessarily continuous) functions $f_n : X \to Y$ such that for every $\varepsilon > 0$ there is an index n_0 such that f_n is ε-homotopic to f_{n+1} for every $n \geq n_0$. We denote proximate nets with $(f_n) : X \to Y$, or just with (f_n).

Definition 4: Two proximate nets (f_n) and (f'_n) are homotopic if for every $\varepsilon > 0$, f_n is ε-homotopic to f'_n for almost every n.

We use symbol [ ] to denote homotopy classes.

Definition 5: A null sequence $\varepsilon_1 \geq \varepsilon_2 \geq \text{K} \geq \varepsilon_n \geq \text{K}$ of positive numbers is sequence of positive numbers such that $\varepsilon_n \to 0$ when $n \to \infty$.

Let $[(f_n)] : X \to Y$ and $[(g_n)] : Y \to Z$ be classes of proximate nets, and $(f_n) : X \to Y$ and $(g_n) : Y \to Z$ be their representatives. We choose a null sequence of positive numbers $\varepsilon_1 \geq \varepsilon_2 \geq \text{K} \geq \varepsilon_n \geq \text{K}$ such that g_n is $\frac{\varepsilon_{n_0}}{2}$ homotopic to g_{n_0} for every $n \geq n_0$, null sequence $\delta_1 \geq \delta_2 \geq \text{K}\ \delta_n \geq \text{K}$ such that $d(g_n(y), g_n(y')) < \varepsilon_n$ for every δ_n-close points y и y' in Y, and sequence of indices $k_1 < k_2 < \text{K}\ k_n < \text{K}$ such that f_k is $\frac{\delta_n}{2}$-homotopic to f_{k_n} for every $k \geq k_n$. We define $[(f_n)][(g_n)] = [(f_n g_{k_n})]$. In [2] is proven that on this way, we get a category.

According to [1] we have:

Definition 6: A function $f : X \to Y$ is $\mathcal{V}$-continuous, where $\mathcal{V}$ is finite covering of Y, if for every point $x \in X$ there exists a neighborhood U_x of x, and $V \in \mathcal{V}$, such that $f(U_x) \subseteq V$.

Definition 7: The functions $f, g : X \to Y$ are $\mathcal{V}$-homotopic, if there exists a continuous function $F : X \times I \to Y$ such that for every $x \in X$, $F(x,0) = f(x)$ and $F(x,1) = g(x)$, F is $st(\mathcal{V})$-continuous and $F|_{N \times X}$ is $\mathcal{V}$–continuous for some neighbourhood $N = [0, \varepsilon) \cup (1 - \varepsilon, 1]$ of ∂I.

Definition 8: A cofinal sequence of finite covering $\mathcal{V}_1$ f $\mathcal{V}_2$ f K $\mathcal{V}_n$ f K is a sequence of finite covering of spaces, such that for any covering $\mathcal{V}$, there exists n, such that $\mathcal{V}_n$ p $\mathcal{V}$

Definition 9: The sequence (f_n) of functions $f_n : X \to Y$ is a proximate sequence from X to Y, if there exists a cofinal sequence of finite coverings of Y, $\mathcal{V}_1$ f $\mathcal{V}_2$ f K $\mathcal{V}_n$ f K, and for all indices $m \geq n$, f_n and f_m are $\mathcal{V}_n$-homotopic.

Definition 10: Two proximate sequences (f_n) and (f'_n) are homotopic if there exists a cofinal sequence of finite coverings of Y,

$\mathcal{V}_1$ f $\mathcal{V}_2$ f K $\mathcal{V}_n$ f K , such that (f_n) and (f_n') are $\mathcal{V}_n$–homotopic for all integers n.

Let $(f_n): X \to Y$ be a proximate sequence over $(\mathcal{V}_n)$ and $(g_k): Y \to Z$ be a proximate sequence over $(\mathcal{W}_k)$. For a covering $\mathcal{W}_k$ of Z, there exists a covering $\mathcal{V}_{n_k}$ of Y such that $g(\mathcal{V}_{n_k})$ p $\mathcal{W}_k$. Then, the composition is the proximate sequence $(h_k) = (g_k f_{n_k}): X \to Z$. In [1] is proven that compact metric spaces and homotopy classes of proximate sequences $[(f_n)]$ form the shape category.

2. REQUIRED PROPERTIES

Definition 11: ([4]) Function $f: X \to Y$ is ε- continuous in the sense of Klee, if there exists $\delta > 0$ such that for every $x, x' \in X$ for which $d(x, x') < \delta$, follows $d(f(x), f(x')) < \varepsilon$.

Proposition 1: Let X and Y be compact metric spaces. If $f: X \to Y$ is ε-continuous function, then f is 2ε-continuous in the sense of Klee.

Proposition 2: Let X and Y be compact metric spaces. If $f: X \to Y$ is ε-continuous in the sense of Klee then f is ε-continuous function.

Proposition 3: Let X and Y be compact metric spaces. $f: X \to Y$ is ε-continuous function in the sense of Klee for some $\varepsilon > 0$, if and only if it is $\mathcal{V}$-continuous for some finite cover $\mathcal{V}$ consisting of open balls of radius ε.

Proposition 4: Let (f_n) be proximate seguence from X to Y over $(\mathcal{V}_n)$. Then for arbitrary null sequence of positive numbers $\varepsilon_1 \geq \varepsilon_2 \geq \text{K} \geq \varepsilon_n \geq \text{K}$. there exists:

1) Cofinal sequence of finite coverings $(\mathcal{W}_n)$, such that for all n greater than or equal to some natural number n_0, $\mathcal{W}_n$ is consisting of open balls and for every ε from the null sequence there exists s covering $W \in \mathcal{W}$ which is consisting of ε balls.

2) (f_n) be proximate seguence over $(\mathcal{W}_n)$.

Proposition 5: (Lebesque number) If the metric space X is compact, and $\mathcal{V}$ is covering of X, then there exists a number $\delta > 0$ such that, every subset of X having diameter less than δ, is contained in some

member of the covering. The number δ is called a Lebesque number of this covering.

3. EQUIVALENCE OF THE CATEGORIES *InSh* AND *NH*

Let (f_n) be proximate net from X to Y.

Choose arbitrarily $\varepsilon_1 > 0$. There is a natural number n_1 such that for all $n \geq n_1$ the function f_n is ε_1 homotopic to f_{n_1}. So there is ε_1-homotopy $F_{n,n_1} : X \times I \to Y$, which connects f_n and f_{n_1}. Then F_{n,n_1} is ε_1- continuous function and according to proposition 1 and proposition 3, F_{n,n_1} is $\mathcal{V}_{2\varepsilon_1}$- continuous function for some finite covering $\mathcal{V}_{2\varepsilon_1}$ on Y, which consists of open balls with radius $2\varepsilon_1$ (Specially f_n are $\mathcal{V}_{n_1}$- continuous functions for each $n \geq n_1$). Hence f_n is $\mathcal{V}_{2\varepsilon_1}$-homotopic with f_{n_1} for all $n \geq n_1$. We put $\mathcal{W}_n = \{Y\}$ for all $n < n_1$. It is clear that f_m is $\{Y\}$ homotopic to f_n for all natural numbers m and n.

From the Lebesques number lemma, there exists a number $\varepsilon_2 > 0$, $\varepsilon_2 \leq \varepsilon_1$, such that each open ball with radius $2\varepsilon_2$, is contained in a set from covering $\mathcal{V}_{2\varepsilon_1}$. There is a natural number $n_2 > n_1$ such that for all $n \geq n_2$ the function f_n is ε_2-homotopic to f_{n_2}. Hence f_n is $\mathcal{V}_{2\varepsilon_2}$- homotopic to f_{n_2} for some finite covering $\mathcal{V}_{2\varepsilon_2}$ of Y, which consists of open balls with radius $2\varepsilon_2$. At the same time covering $\mathcal{V}_{2\varepsilon_2}$ is containing in the covering $\mathcal{V}_{2\varepsilon_1}$. We put $\mathcal{W}_n = \mathcal{V}_{2\varepsilon_1}$ for all natural numbers $n = n_1, n_1 + 1, \mathrm{K}\ n_2 - 1$.

In the k-th step we get from Lebesques number lemma, that there exists number $\varepsilon_k > 0$, $\varepsilon_k \leq \varepsilon_{k-1}$, such that each open ball with radius $2\varepsilon_k$, is contained in some set of covering $\mathcal{V}_{2\varepsilon_k - 1}$. There is a natural number $n_k > n_{k-1}$ such that for all $n \geq n_k$ the function f_n is ε_k - homotopic with f_{n_k}. Therefore f_n is $\mathcal{V}_{2\varepsilon_k}$ - homotopic to f_{n_k} for some finite covering $\mathcal{V}_{2\varepsilon_k}$ of Y, which consists of open balls with radius $2\varepsilon_k$. In the same time the covering $\mathcal{V}_{2\varepsilon_k}$ is contained in the covering $\mathcal{V}_{2\varepsilon_k - 1}$. We put $\mathcal{W}_n = \mathcal{V}_{2\varepsilon_k - 1}$ for all natural numbers $n = n_{k-1}, n_{k-1} + 1, \mathrm{K}\ n_k - 1$.

Continuing the procedure we get proximate sequence of $\mathcal{W}_n$-continuous functions $f_n : X \to Y$ over cofinal sequence of finite coverings $(\mathcal{W}_n)$. It follows that $(f_n): X \to Y$ is a proximate sequence over $(\mathcal{W}_n)$.

Definition 12: We say that (f_n) is proximate sequence obtained from proximate net (f_n) and we denote it by $\Omega_{X,Y}((f_n))$.

If two proximate nets are homotopic, then proximate sequences obtained from them also are homotopic. That allows us to define function $\Omega_{X,Y}$, from the set of all classes of proximate nets, to the set of all classes of proximate sequences from X to Y, defined by $\Omega_{X,Y}([(f_n)]) = [(f_n)]$.

We will show that the mapping $\Omega_{X,Y}$ is surjection. Let (f_n) be proximate sequence over $(\mathcal{V}_n)$. From proposition 4, there exists a proximate sequence (f_n') over $(\mathcal{V}_{\varepsilon_n})$, where $\mathcal{V}_{\varepsilon_n}$ consists of open balls with radius ε_n for all n greater or equal to some number n_0 where $\varepsilon_1 \geq \varepsilon_2 \geq \mathrm{K} \geq \varepsilon_n \geq \mathrm{K}$ is null sequence. Let's look coverings $\mathcal{V}_{\varepsilon_n}$. f_m is $\mathcal{V}_{\varepsilon_n}$-homotopic to f_n for every $m \geq n$, or there exists a homotopy $F_{m,n} : X \times I \to Y$ such that, $F_{m,n}$ is $st(\mathcal{V}_{\varepsilon_n})$-continuous and $F_{m,n}|_{N \times X}$ is $\mathcal{V}_{\varepsilon_n}$–continuous on some neighborhood N of ∂I. Then F is $\mathcal{V}_{3\varepsilon_n}$ continuous. From proposition 1 and proposition 2 we have that F is $3\varepsilon_n$- continuous. Clearly, specially f_m and f_n are $3\varepsilon_n$-continuous. Also $3\varepsilon_1 \geq 3\varepsilon_2 \geq \mathrm{K} \geq 3\varepsilon_n \geq \mathrm{K}$ is null sequence. It follows that (f_n) is proximate net and class of proximate net (f_n) is mapping to class of proximate sequence (f_n).

We will show that the mapping $\Omega_{X,Y}$ is injection. Let (f_n') and (f_n'') be proximate sequences over $(\mathcal{V}_n')$ obtained from proximate nets (f_n') и (f_n'') and let (f_n') and (f_n'') be homotopic. It follows that there exists a cofinal sequence of finite coverings over Y, $(\mathcal{V}_n)$, such that (f_n') and (f_n'') are $\mathcal{V}_n$ –homotopic for all natural numbers n. Starting from some number n, $\mathcal{V}_n$ can be chosen such that to consist of open balls ε_n, where (ε_n) is null sequence. Then f_n' is $3\varepsilon_n$ homotopic to f_n'', from where it follows that (f_n') and (f_n'') are homotopic.

Now we will describe functor $\Omega : HN \to InSh$, which consists of:

1) Mapping $\Omega : Cpt(X) \to Cpt(X)$ defined by $\Omega(X) = X$ for every compact metric space X.

2) Mapping $\Omega : Mor_{HN}(X,Y) \to Mor_{InSh}(X,Y)$ for every compact metric spaces X and Y, defined by $\Omega([(f_n)]) = \Omega_{X,Y}[(f_n)]$ for each class of proximate nets $[(f_n)]$ from X to Y.

Because of the bijection $\Omega_{X,Y} : Mor_{HN}(X,Y) \to Mor_{InSh}(X,Y)$, to be Ω functor should apply equalities

$$\Omega([(1_X)]) = 1_{\Omega(X)} \text{ and } \Omega([(g_k f_{n_k})]) = \Omega([(g_n)])\Omega([(f_n)]).$$

Representation of the class of proximate nets $[(1_X)]$ from X to X, is proximate net $(Id) : X \to X$, which consists of sequence identical functions $Id : X \to X$. From the construction of the previous bijection, it follows that we accompany it to represent the identical element of the category $InSh$.

Second equality is also a consequence of previous bijection. Namely to consider proximate nets $(g_k f_{n_k})$ from X to Z, (g_n) from Y to Z and (f_n) from X to Y, which are representatives of classes $[(g_k f_{n_k})], [(g_n)]$ and $[(f_n)]$ appropriate. From the way of constructions of composition, it follows that functions $g_k f_{n_k} : X \to Z$ from the represent $(g_k f_{n_k})$ of the class $[(g_k f_{n_k})]$, can be choosen, such that to match with functions $g_k f_{n_k} : X \to Z$ from the represent $\Omega_{X,Y}(g_n)\Omega_{X,Y}(f_n)$ of the class $[(g_n)][(f_n)]$.

REFERENCES

[1] Shekutkovski, Nikita, (2012), *Intrinsic definition of strong shape for compact metric spaces*, Topology Proceedings, Volume 39, 27-39.

[2] Jose M. R. Sanjurjo**,** (1989), *A non continuous description of the shape*, Quart. J. Math. Oxford Ser. 40, 351-359.

[3] James Felt, (December 1974), *ε-continuity and shape*, Proceedings of the American Mathematical society, 46 No. 3, 426-430.

[4] V.L.Klee and A.Yandy, (1974), Some proximate concept in topology, Simposia Math. Publ. Inst. Naz. di Alta Matematica, Academic Press 16, 21-39.

FUNCTOR BETWEEN CATEGORIES OF PROPER PROXIMATE NETS

Gjorgji Markoski[1]

Abstract: *It is proved that there exists a functor between the category with objects locally compact paracompact spaces and morphisms classes of proper proximate nets defined over arbitrary directed sets ([2], [3]), and the second category from [1], with the same objects and with morphisms classes of proper proximate nets defined over coverings of a space consisting of open sets with compact closures.*

Keywords: *continuity up to a covering, proper proximate net, category, functor.*

1 Proper ν-continuous functions

In [1] are defined proper proximate nets over arbitrary directed set, and are proved some properties. Also, proper proximate nets are defined, indexed by the set of all coverings of a space consisting of open set with compact closures.

In the paper the spaces will be localy compact and paracompact. Also all coverings will be open. By a function $f : X \to Y$ we mean a maping which is not necessarily continuous.

The set $(A,\leq)$ is *directed* if A is ordered set and for every $a,b \in A$ there exists $c \in A$ such that $a,b \leq c$. Let A and B be two collections of subsets of X. If for every $A \in \mathcal{A}$ there exists $B \in \mathcal{B}$ such that $A \subseteq B$ then we say that $\mathcal{A}$ *refines* $\mathcal{B}$ and we denote by $\mathcal{A} \prec \mathcal{B}$. By $\mathrm{cov}X$ is denoted the set of all star-finite coverings of X consisting of open sets with compact closures. It is known that if X is locally compact and paracompact space, then for every covering $\mathcal{A}$ of X there exists $\mathcal{B} \in covX$ such that $\mathcal{B} \prec \mathcal{A}$. It is easy to prove that $\mathrm{cov}\,X$ is directed set with relation $\geq$, where $\mathcal{A} \geq \mathcal{B} \Leftrightarrow \mathcal{A} \prec \mathcal{B}$. For $\mathcal{U} \in \mathrm{cov}\,X$ and $A \subseteq X$ let $\mathrm{st}(A,\mathcal{U}) = \bigcup \{U \,|\, U \in \mathcal{U}, A \cap U \neq \varnothing\}$, and $\mathrm{st}\,U = \{\mathrm{st}(U,\mathcal{U}) \,|\, U \in \mathcal{U}\}$.

Definition. Function $f : X \to Y$ is *proper* if for every compact set D in Y there exists a compact set C in X such that $f(X \setminus C) \subseteq Y \setminus D$.

Clearly, the composition of two proper functions is proper and restriction of proper function on closed subset is proper.

Definition. Let X, Y, be spaces, and $\mathcal{V} \in \operatorname{cov} Y$. The proper function $f : X \to Y$ is $\mathcal{V}$- *continuous*, if for any $x \in X$, there exists a neighborhood U of x, such that $f(U) \subseteq V$, for some member $V \in \mathcal{V}$.

(The family of all U, form a covering $\mathcal{U}$ of X. Shortly, we say that $f : X \to Y$ is $\mathcal{V}$-continuous, if there exists $\mathcal{U} \in \operatorname{cov} X$ such that $f(\mathcal{U}) \prec \mathcal{V}$.)

It is clear that if $f : X \to Y$ is $\mathcal{V}$-continuous, then f is $\mathcal{V}_1$-continuous, for every $\mathcal{V} \prec \mathcal{V}_1$.

With I we denote the unit interval $[0,1]$.

Definition. Two proper $\mathcal{V}$ - continuous functions $f, g : X \to Y$ are properly $\mathcal{V}$- *homotopic*, if there exists a proper function $F : X \times I \to Y$ such that:

1) $F : X \times I \to Y$ is $\operatorname{st}\mathcal{V}$-continuous;

2) There exists a neighborhood $N = [0, \varepsilon) \cup (1-\varepsilon, 1]$ of $\{0,1\}$ in I such that $F|_{X \times N}$ is $\mathcal{V}$-continuous, and

3) $F(x,0) = f(x)$, $F(x,1) = g(x)$.

We denote $f \overset{\mathcal{V}}{\sim}_p g$, and we call F a *proper $\mathcal{V}$-continuous homotopy* from f to g.

Remark. As is shown in simple example in [1], page 302, the function F is not always $\mathcal{V}$-continuous, if we define homotopy in a usual way. Because of this, the function F is defined as a $\operatorname{st}\mathcal{V}$-continuous. In [4] there is mistake about this definition.

The next proposition is easy to prove:

Proposition 1.1 *The relation "$\overset{\mathcal{V}}{\sim}_p$" is an equivalence relation.*

The next two lemmas will be used later. First of them is easy to prove, and the second is proved in [1], lemma 3.4.

Lemma 1.2 *Let $h : Y \to Z$ be a proper function such that $h(\mathcal{V}) \prec \mathcal{W}$, where $\mathcal{V} \in \operatorname{cov} Y$ and $\mathcal{W} \in \operatorname{cov} Z$. Then from $f \overset{\mathcal{V}}{\sim}_p g$ it follows that $hf \overset{\mathcal{W}}{\sim}_p hg$, for any two proper $\mathcal{V}$-continuous functions $f, g : X \to Y$.*

Lemma 1.3 *Let $\mathcal{V} \in \operatorname{cov} Y$ and $f, g : X \to Y$ be proper $\mathcal{V}$-continuous functions such that $f \overset{\mathcal{V}}{\sim}_p g$. Then there exists $\mathcal{U} \in \operatorname{cov} X$ such*

that $f(\mathcal{U}), g(\mathcal{U}) \prec \mathcal{V}$ *and* $fh \overset{\mathcal{V}}{\sim}_p gh$ *for any proper* $\mathcal{U}$*-continuous function* $h: Z \to X$ *of an arbitrary space* Z*.*

Lemma 1.4 *Let* $g_0, g_1 : Y \to Z$ *be proper* $\mathcal{W}$*-continuous functions such that* $g_0 \overset{\mathcal{W}}{\sim}_p g_1$*, where* $\mathcal{W} \in \operatorname{cov} Z$*. Then*

1. There exists $\mathcal{V} \in \operatorname{cov} Y$ such that $g_0(\mathcal{V}), g_1(\mathcal{V}) \prec \mathcal{W}$;

2. If $f_0, f_1 : X \to Y$ are proper $\mathcal{V}$-continuous functions such that $f_0 \overset{\mathcal{V}}{\sim}_p f_1$, then $g_0 f_0 \overset{\mathcal{W}}{\sim}_p g_1 f_1$.

Proof. From the Lemma 1.3 it follows that there exists $\mathcal{V} \in \operatorname{cov} Y$ such that $g_0(\mathcal{V}), g_1(\mathcal{V}) \prec \mathcal{W}$ and $g_0 f \overset{\mathcal{W}}{\sim}_p g_1 f$ for every V-continuous function $f: X \to Y$.

Let $f_0, f_1 : X \to Y$ be proper $\mathcal{V}$-continuous functions such that $f_0 \overset{\mathcal{V}}{\sim}_p f_1$. The function f_1 is $\mathcal{V}$-continuous, it follows $g_0 f_1 \overset{\mathcal{W}}{\sim}_p g_1 f_1$. Because of $g_0(\mathcal{V}) \prec \mathcal{W}$ and $f_0 \overset{\mathcal{V}}{\sim}_p f_1$ we obtain that $g_0 f_0 \overset{\mathcal{W}}{\sim}_p g_0 f_1$. Finally, $g_0 f_0 \overset{\mathcal{W}}{\sim}_p g_0 f_1 \overset{\mathcal{W}}{\sim}_p g_1 f_1$. ♦

2 Proper proximate nets. Proper proximate Čech nets

Definition. A *proper proximate net* $(f_\lambda) = (f_\lambda | \lambda \in \Lambda) : X \to Y$ is a net of proper functions $f_\lambda : X \to Y$ indexed by directed set $\Lambda = (\Lambda, \leq)$ such that, for each $\mathcal{V} \in \operatorname{cov} Y$, there exists $\lambda_0 \in \Lambda$ such that $f_{\lambda_0} \overset{\mathcal{V}}{\sim}_p f_\lambda$ for all $\lambda \geq \lambda_0$.

From the definition it follows that f_λ is $\mathcal{V}$-continuous for all $\lambda \geq \lambda_0$.

Definition. Proper proximate net $(f_\lambda) : X \to Y$ is *properly homotopic* to a proper proximate net $(g_\delta) : X \to Y$ (indexed by a directed set Δ) if for each $\mathcal{V} \in \operatorname{cov} Y$, there exist $\lambda_0 \in \Lambda$ and $\delta_0 \in \Delta$ such that $f_\lambda \overset{\mathcal{V}}{\sim}_p g_\delta$ for all $\lambda \geq \lambda_0$ and $\delta \geq \delta_0$.

We denote this relation by $(f_\lambda) \simeq_p (g_\delta)$.

It is clear that $\simeq_p$ is an equivalence relation. The equivalence class of a proper proximate net (f_λ) is denoted by $[(f_\lambda)]_p$ and called the *proper homotopy class* of (f_λ). The collection of all proper homotopy classes of proper proximate nets from X to Y is denoted by $[X,Y]_{ppn}$.

Clearly, every continuous function $f: X \to Y$ can be considered a proper proximate net as the net consisting of function f indexed by one-element set. Obviously, if $\Lambda_1 \subseteq \Lambda$ is cofinal in Λ, then $\left(f_\lambda \middle| \lambda \in \Lambda_1\right) \simeq_p \left(f_\lambda \middle| \lambda \in \Lambda\right)$.

The composition of proper proximate nets $(f_\lambda): X \to Y$ and $(g_\delta): Y \to Z$ is defined by $(g_\delta)(f_\lambda) = \left(g_\delta f_\lambda \middle| (\lambda,\delta) \in \Lambda \times \Delta\right): X \to Z$. It is indexed by the directed set $\Lambda \times \Delta$ (directed by the relation $(\lambda,\delta) \le (\lambda',\delta') \Leftrightarrow \lambda \le \lambda', \delta \le \delta'$).

Lemma 2.1 *If* $\left(f_\lambda\right) = \left(f_\lambda \middle| \lambda \in \Lambda\right): X \to Y$ *and* $\left(g_\delta\right) = \left(g_\delta \middle| \delta \in \Delta\right): Y \to Z$, *then* $\left(g_\delta\right)\left(f_\lambda\right) = \left(g_\delta f_\lambda \middle| (\lambda,\delta) \in \Lambda \times \Delta\right): X \to Z$ *is proper proximate net.*

Proof. The function $g_\delta f_\lambda$ is proper for all $(\lambda,\delta) \in \Lambda \times \Delta$. Let $\mathcal{W} \in \operatorname{cov} Z$. The net $\left(g_\delta\right): Y \to Z$ is proper proximate net, it follows that there exists $\delta_0 \in \Delta$ such that $g_\delta \overset{\mathcal{W}}{\sim}_p g_{\delta_0}$, for all $\delta \ge \delta_0$. There exists $\mathcal{V} \in \operatorname{cov} Y$ such that $g_{\delta_0}\left(\mathcal{V}\right) \prec \mathcal{W}$. Since $\left(f_\lambda\right): X \to Y$ is proper proximate net, it follows that there exists $\lambda_0 \in \Lambda$ such that $f_\lambda \overset{\mathcal{V}}{\sim}_p f_{\lambda_0}$ for all $\lambda \ge \lambda_0$. From the Lemma 1.2 we obtain that $g_{\delta_0} f_\lambda \overset{\mathcal{W}}{\sim}_p g_{\delta_0} f_{\lambda_0}$. From the Lemma 1.3 it follows that there exists $\mathcal{V}_1 \in \operatorname{cov} Y$ such that $g_\delta\left(\mathcal{V}_1\right), g_{\delta_0}\left(\mathcal{V}_1\right) \prec \mathcal{W}$ and $g_\delta f \overset{\mathcal{W}}{\sim}_p g_{\delta_0} f$ for every proper $\mathcal{V}_1$-continuous function $f: X \to Y$. We may choose $\mathcal{V}_1 \prec \mathcal{V}$.

Because $\left(f_\lambda\right): X \to Y$ is proper proximate net it follows that there exists $\lambda_1 \in \Lambda, \lambda_1 \ge \lambda_0$ such that $f_\lambda \overset{\mathcal{V}_1}{\sim}_p f_{\lambda_1}$ for every $\lambda \ge \lambda_1$.

Let $\lambda \ge \lambda_1, \delta \ge \delta_0$. Then we have $g_\delta f_\lambda \overset{\mathcal{W}}{\sim}_p g_{\delta_0} f_\lambda$. It follows that

$$g_\delta f_\lambda \overset{\mathcal{W}}{\sim}_p g_{\delta_0} f_\lambda \overset{\mathcal{W}}{\sim}_p g_{\delta_0} f_{\lambda_0}. \blacklozenge$$

Theorem 2.2 *Let* $\left(f_\lambda^0\right)=\left(f_\lambda^0 \middle| \lambda\in\Lambda\right),\left(f_{\lambda'}^1\right)=\left(f_{\lambda'}^1 \middle| \lambda'\in\Lambda_1\right): X\to Y$ *and* $\left(g_\delta^0\right)=\left(g_\delta^0 \middle| \delta\in\Delta\right),\left(g_{\delta'}^1\right)=\left(g_{\delta'}^1 \middle| \delta'\in\Delta_1\right): Y\to Z$ *be proper proximate nets such that* $\left(f_\lambda^0\right)\simeq_p\left(f_{\lambda'}^1\right)$ *and* $\left(g_\delta^0\right)\simeq_p\left(g_{\delta'}^1\right)$. *Then* $\left(g_\delta^0 f_\lambda^0\right)\simeq_p\left(g_{\delta'}^1 f_{\lambda'}^1\right)$.

Proof. Let $\mathcal{W}\in\operatorname{cov} Z$. From $\left(g_\delta^0\right)\simeq_p\left(g_{\delta'}^1\right)$ if follows that there exist $\delta_0\in\Delta$ and $\delta_0'\in\Delta_1$ such that $g_\delta^0 \overset{\mathcal{W}}{\sim}_p g_{\delta'}^1$ for every $\delta\in\Delta,\ \delta\geq\delta_0$ and $\delta'\in\Delta_1,\ \delta'\geq\delta_0'$. There exists $\mathcal{V}\in\operatorname{cov} Y$ such that $g_\delta^0(\mathcal{V}), g_{\delta'}^1(\mathcal{V})\prec\mathcal{W}$. If $f_0, f_1: X\to Y$ are proper $\mathcal{V}$-continuous functions such that $f_0\overset{\mathcal{V}}{\sim}_p f_1$, then from Lemma 1.4 it follows

$$g_\delta^0 f_0 \overset{\mathcal{W}}{\sim}_p g_{\delta'}^1 f_1.$$

Because of $\left(f_\lambda^0\right)\simeq_p\left(f_{\lambda'}^1\right)$ it folows that there exist $\lambda_0\in\Lambda$ and $\lambda_0'\in\Lambda_1$ such that $f_\lambda^0 \overset{\mathcal{V}}{\sim}_p f_{\lambda'}^1$ for all $\lambda\in\Lambda,\ \lambda\geq\lambda_0$ and $\lambda'\in\Lambda_1,\ \lambda'\geq\lambda_0'$. We may choose f_λ^0 and $f_{\lambda'}^1$ to be $\mathcal{V}$-continuous for all $\lambda\in\Lambda,\ \lambda\geq\lambda_0$ and $\lambda'\in\Lambda_1,\ \lambda'\geq\lambda_0'$.

Let $\lambda\geq\lambda_0,\ \lambda'\geq\lambda_0',\ \delta\geq\delta_0$ and $\delta'\geq\delta_0'$.

Then for functions f_λ^0 and $f_{\lambda'}^1$ holds (1) (instead of f_0 and f_1), it follows $g_\delta^0 f_\lambda^0 \overset{\mathcal{W}}{\sim}_p g_{\delta'}^1 f_{\lambda'}^1$. We obtain that $\left(g_\delta^0 f_\lambda^0\right)\simeq_p\left(g_{\delta'}^1 f_{\lambda'}^1\right)$. ♦

In a similar way one may show that composition is associative.

The identity $[(1_\Lambda)]_p: X\to X$ is the proper proximate net consisting of identity function $\mathrm{id}_X: X\to X$ (defined by $\mathrm{id}_X(x)=x$ for all $x\in X$) indexed by one-element set.

We obtain the category $\mathcal{P}_{ppn}$ of locally compact and paracompact spaces and proper homotopy classes of proper proximate nets.

Definition. A *proper proximate Čech net* $\left(f_\mathcal{V}\right)=\left(f_\mathcal{V} \middle| \mathcal{V}\in\operatorname{cov} Y\right): X\to Y$ is a net of proper $\mathcal{V}$-continuous functions

$f_{\mathcal{V}} : X \to Y$ indexed by the directed set $\operatorname{cov} Y$, such that $f_{\mathcal{V}} \overset{\mathcal{V}}{\sim}_p f_{\mathcal{V}'}$, for every $\mathcal{V}' \in \operatorname{cov} Y$, $\mathcal{V}' \prec \mathcal{V}$.

It is clear that every proper proximate Čech net is a proper proximate net.

Lemma 2.3 *Every proper proximate net is properly homotopic to a proper proximate Čech net.*

Proof. [1], Lemma 4.1. ♦

Lemma 2.4 *For any two proper proximate Čech nets* $(f_{\mathcal{V}}),(g_{\mathcal{V}}) : X \to Y$ *holds* $(f_V) \simeq_p (g_V)$ *if and only if* $f_{\mathcal{V}} \overset{\mathcal{V}}{\sim}_p g_{\mathcal{V}}$ *for each* $\mathcal{V} \in \operatorname{cov} Y$.

Proof. [1], lemma 4.2. ♦

The composition of two proper proximate Čech nets is defined in the following way: Let $(f_{\mathcal{V}}) : X \to Y$ and $(g_{\mathcal{W}}) : Y \to Z$ be two proper proximate nets and $\mathcal{W} \in \operatorname{cov} Z$. Then there exists $\mathcal{V} \in \operatorname{cov} Y$ such that $g_{\mathcal{W}}(\mathcal{V}) \prec \mathcal{W}$. Then $(h_{\mathcal{W}}) = \left(h_{\mathcal{W}} \middle| \mathcal{W} \in \operatorname{cov} Z\right) : X \to Z$ is the composition of $(f_{\mathcal{V}})$ and $(g_{\mathcal{W}})$, where $h_{\mathcal{W}} = g_{\mathcal{W}} f_{\mathcal{V}}$. The composition is well defined ([4] Lemma 2.4 and Theorem 2.5; [1] Lemma 4.3). The class of $(f_{\mathcal{V}})$ we denote by $\left[(f_{\mathcal{V}})\right]_{pc}$. The identity $\left[(1_{\mathcal{U}})\right]_{pc} : X \to X$ is the proper proximate Čech net consisting of identity function $\mathrm{id}_X : X \to X$, i.e. $(1_{\mathcal{U}}) = \left(f_{\mathcal{U}} \middle| \mathcal{U} \in \operatorname{cov} X\right)$ such that $f_{\mathcal{U}} = \mathrm{id}_X$ for all $\mathcal{U} \in \operatorname{cov} X$. In this way category $\mathcal{P}_{ppcn}$ of localy compact paracompact spaces and classes of proper proximate Čech nets is obtained.

Lemma 2.5 *Let* $\left(g_{\mathcal{W}} f_{\mathcal{V}} \middle| \mathcal{W} \in \operatorname{cov} Z\right) : X \to Z$ *be the composition of proper proximate Čech nets* $\left(f_{\mathcal{V}} \middle| \mathcal{V} \in \operatorname{cov} Y\right) : X \to Y$ *and* $\left(g_{\mathcal{W}} \middle| \mathcal{W} \in \operatorname{cov} Z\right) : Y \to Z$. *Then* $\left(g_{\mathcal{W}} f_{\mathcal{V}} \middle| \mathcal{W} \in \operatorname{cov} Z\right) \simeq_p \left(g_{\mathcal{W}'} f_{\mathcal{V}'} \middle| (\mathcal{V}', \mathcal{W}') \in \operatorname{cov} Y \times \operatorname{cov} Z\right)$.

Proof. Let $(\mathcal{V}', \mathcal{W}') \in \operatorname{cov} Y \times \operatorname{cov} Z$ be arbitrary element of $\operatorname{cov} Y \times \operatorname{cov} Z$. There exists $\mathcal{V}_1 \in \operatorname{cov} Y$ such that $g_{\mathcal{W}}(\mathcal{V}_1) \prec \mathcal{W}'$. The set $\operatorname{cov} Y$ is directed, it follows that there exists $\mathcal{V}_2 \in \operatorname{cov} Y$ such that $\mathcal{V}_2 \prec \mathcal{V}_1$ and $\mathcal{V}_2 \prec \mathcal{V}'$. It follows that $g_{\mathcal{W}}(\mathcal{V}_2) \prec \mathcal{W}'$. We obtain that $g_{\mathcal{W}}(\mathcal{V}_2) \prec \mathcal{W}'$. The definition of composition of proper proximate Čech nets does not

depend on the choice of $\mathcal{V}$ ([4] and [1]). We choose one $\mathcal{V}$ for every $\mathcal{W}$ such that $g_{\mathcal{W}}(\mathcal{V}) \prec \mathcal{W}$

It follows that $\left\{(\mathcal{V},\mathcal{W}) \middle| (\mathcal{V},\mathcal{W}) \in \operatorname{cov} Y \times \operatorname{cov} Z,\, g_{\mathcal{W}}(\mathcal{V}) \prec \mathcal{W}\right\}$ is cofinal in $\operatorname{cov} Y \times \operatorname{cov} Z$. ♦

3 The Functor

Let $[(f_\lambda)]_p$ be morphism in $\mathcal{P}_{ppn}$, i.e., $(f_\lambda): X \to Y$ is proper proximate net. From Lemma 2.3 it follows that there exists proper proximate Čech net $(f_{\mathcal{V}}): X \to Y$ such that $(f_\lambda) \simeq_p (f_{\mathcal{V}})$. We define $\Phi: \mathcal{P}_{ppn} \to \mathcal{P}_{ppcn}$ with $\Phi(X) = X$ and $\Phi([(f_\lambda)]_p) = [(f_V)]_{pc}$.

Let $(f_\lambda): X \to Y$ and $(g_\delta): Y \to Z$ be proper proximate nets. If $(f_\lambda) \simeq_p (f_{\mathcal{V}})$ and $(g_\delta) \simeq_p (g_{\mathcal{W}})$, then from Lemma 2.5 and Theorem 2.2 it follows that

$$(g_\delta)(f_\lambda) \simeq_p (g_{\mathcal{W}})(f_{\mathcal{V}}).$$

We obtain that

$$\Phi\left(\left[(g_\delta)\right]_p\left[(f_\lambda)\right]_p\right) = \Phi\left(\left[(g_\delta)(f_\lambda)\right]_p\right) = \Phi\left(\left[(g_\delta f_\lambda)\right]_p\right) = \left[(g_{\mathcal{W}} f_{\mathcal{V}})\right]_{pc} =$$

$$= \left[(g_{\mathcal{W}})\right]_{pc}\left[(f_{\mathcal{V}})\right]_{pc} = \Phi\left(\left[(g_\delta)\right]_p\right)\Phi\left(\left[(f_\lambda)\right]_p\right).$$

If $[(1_\Lambda)]_p$ is the class of identity proper proximate net, then $(1_\Lambda) \simeq_p (1_{\mathcal{U}})$. It follows that $\Phi\left([(1_\Lambda)]_p\right) = [(1_{\mathcal{U}})]_{pc}$, i.e. $\Phi([(1_\Lambda)]_p)$ is the class of identity proper proximate Čech net $(1_{\mathcal{U}}): \Phi(X) \to \Phi(X)$. We obtain that Φ is functor.

References

[1] Y. Akaike, K. Sakai, *Describing the proper n-shape category by using non-continuous functions*, Glasnik matematicki, Vol. 33 **(53)**, 1998, 299-321.

[2] N. Shekutkovski, G. Markoski, *Equivalence of the inverse system approach and the intrinsic approach to proper shape*, God. Zb. Inst. Mat. **(41)**, 2008, 43-56.

[3] Gj. Markoski, N. Shekutkovski, *Intrinsic definition of proper shape and spaces with compact components*, Proceedings of IV congress of mathematicians of Republic of Macedonia, Struga, Macedonia, 19-22.10.2008, 2010, Pages 272-286.

[4] R. W. Kieboom, *An intrinsic characterization of the shape of paracompacta by menas of non-continuous single-valued maps*, Bull. Belg. Math. Soc. **1**, 1994, 701-711.

[5] R. Engelking, *General Topology*, Monografie Matematiczne, Warszawa, 1977.

[6] N. Shekutkovski, *Intrinsic definition of strong shape for compact metric spaces*, Topology Proceedings **(39)**, 2012, 27-39.

[1] Institute of Mathematics,
Faculty of Natural Sciences and Mathematics
Sts. Cyril and Methodius University,
1000 Skopje, Macedonia
e-mail:gorgim@pmf.ukim.mk

On separable sets in finite functions with non-trivial arity gap

Slavcho Shtrakov
Department of Computer Science,
South-West University, 2700 Blagoevgrad, Bulgaria,
Email: shtrakov@swu.bg,

Jörg Koppitz
Institute of Mathematics, University of Potsdam,
14415 Potsdam, Germany,
Email: koppitz@rz.uni-potsdam.de,

Dimiter Kovachev
Department of Computer Science,
South-West University, 2700 Blagoevgrad, Bulgaria,
Email: dkovach@swu.bg

Abstract: *Given an n-ary $k-$valued function f, $gap(f)$ denotes the minimal number of essential variables in f which become fictive when identifying any two distinct essential variables in f.*

We particularly solve a problem concerning the description of separable sets in n-ary $k-$valued functions f with $2 \le gap(f) \le n \le k$.

Keywords: *essential variable, identification minor, essential arity gap.*

1 Introduction

Let $k > 2$ be a natural number. Denote by $K = \{0,1,\ldots,k-1\}$ the set (ring) of remainders modulo k. A function (operation) on K is a mapping $f : K^n \to K$ where n is a natural number, called *the arity* of f. The set of the all such functions is denoted by P_k^n. Operations from P_2^n are called *Boolean functions*.

Let $X_n = \{x_1,\ldots,x_n\}$ be the set of n variables and $f \in P_k^n$ be a k-valued function.

Definition 1.1 *A variable* x_i *is called essential in* f*, or* f *essentially depends on* x_i*, if there exist values* $a_1,\ldots,a_n,b \in K$*, such that*

$$f(a_1,\ldots,a_{i-1},a_i,a_{i+1},\ldots,a_n) \neq f(a_1,\ldots,a_{i-1},b,a_{i+1},\ldots,a_n).$$

The set of all essential variables in a function f is denoted by $Ess(f)$ and the number of its essential variables is denoted by $ess(f) = |Ess(f)|$.

Let x_i and x_j be two distinct essential variables in f. We say that the function g is obtained from $f \in P_k^n$ by *the identification of the variable* x_i *with* x_j, if

$$g(a_1,\ldots,a_{i-1},a_i,a_{i+1},\ldots,a_n) = f(a_1,\ldots,a_{i-1},a_j,a_{i+1},\ldots,a_n),$$

for all $(a_1,\ldots,a_n) \in K^n$.

Briefly, when g is obtained from f, by identification of the variable x_i with x_j, we will write $g = f_{i\leftarrow j}$ and g is called *the identification minor of* f and $Min(f)$ denotes the set of all identification minors of f.

Definition 1.2 *Let* $f \in P_k^n$ *be an* n*-ary* k*-valued function. Then the essential arity gap (briefly arity gap or gap) of* f *is defined as follows*

$$gap(f) := ess(f) - \max_{g \in Min(f)} ess(g).$$

We say that the function f has non-trivial arity gap if $gap(f) \geq 2$.

We let $G_{p,k}^m$ denote the set of all functions in P_k^n which essentially depend on m variables whose arity gap is equal to p i.e. $G_{p,k}^m = \{f \in P_k^n \mid ess(f) = m \ \& \ gap(f) = p\}$, with $m \leq n$.

2 Essential arity gap of k-valued functions

Given two natural numbers $k, n \geq 2$, Eq_k^n denotes the set of all strings over $K = \{0,1,\ldots,k-1\}$ with length n which have at least two equal letters i.e.

$$Eq_k^n := \{\alpha_1\ldots\alpha_n \in K^n \mid \alpha_i = \alpha_j, \text{ for some } i,j \leq n, i \neq j\},$$

where K^n denotes the set of all strings over K with length n.

In this section we shall present some preliminary results from [3, 5] which treat the representation of the functions with non-trivial arity gap.

Theorem 2.1 *[3] Let f be a k-valued function which depends essentially on the all of its n variables and $2 < p < n \le k$. Then $f \in G_{p,k}^n$ if and only if*

$$f = h \oplus g,$$

where $ess(h) = n - p$ and $g \in G_{n,k}^n$. Moreover, $g_{i \leftarrow j} = 0$ for all $1 \le i, j \le n$ with $i \ne j$.

There are two subclasses of the class $G_{2,k}^n$ with $4 \le n \le k$. First one, consists of functions satisfying conditions similar as the conditions in Theorem 2.1 for $p = 2$. The second subclass consists of functions whose behavior is similar to the functions from $G_{2,k}^n$ with $n > k$ (Theorem 2.1 in [6]).

Lemma 2.1 *[3] Let f be a k-valued function which depends essentially on all of its n, $n > 3$ variables and $gap(f) = 2$. Then there exist two distinct essential variables x_u, x_v such that $ess(f_{u \leftarrow v}) = n - 2$, and $x_v \notin Ess(f_{u \leftarrow v})$. Moreover, $ess(f_{u \leftarrow m}) = ess(f_{v \leftarrow m}) = n - 2$ for all m, $1 \le m \le n$ with $m \notin \{u, v\}$.*

Let us denote by $G_{p,k}^{n,+}$ the set of all functions $f \in G_{p,k}^n$ for which there exist i and j with $1 \le i, j \le n$ such that $i \ne j$, $x_j \in Ess(f_{i \leftarrow j})$ and $ess(f_{i \leftarrow j}) = n - p$.

$G_{p,k}^{n,-}$ denotes the set of all functions $f \in G_{p,k}^n$ for which $x_v \notin Ess(f_{u \leftarrow v})$ for all $1 \le u, v \le n$ with $u \ne v$.

Proposition 2.1 *[3] If $3 < n \le k$ then $G_{2,k}^n = G_{2,k}^{n,+} \cup G_{2,k}^{n,-}$.*

Proposition 2.2 *[3]*

$$G_{p,k}^{n} = \begin{cases} G_{p,k}^{n,+} & if \quad 2 < p < n \le k \\ G_{p,k}^{n,-} & if \quad (2 \le n \le k \ \& \ p = n) \quad or \ (n > k) \\ G_{p,k}^{n,+} \cup G_{p,k}^{n,-} & if \quad 3 < n \le k \ \& \ p = 2. \end{cases}$$

Theorem 2.2 *[3] Let* $4 \le n \le k$ *and* $f \in P_k^n$. *Then the following statements are equivalent:*

(i) $f \in G_{2,k}^{n,+}$;

(ii) There is a function $h \in P_k^n$ with $ess(h) = n-2$ and $f_{r \leftarrow s} = h$ for all $1 \le r, s \le n$ with $r \ne s$ and $x_r \notin Ess(h)$.

Theorem 2.3 *[3] Let* f *be a* k*-valued function which depends essentially on the all of its* n *variables ,* $n > 3$. *Then* $f \in G_{2,k}^{n,+}$ *if and only if*

$$f = h \oplus g,$$

where $ess(h) = n-2$ and $g \in G_{n,k}^{n}$. Moreover $g_{i \leftarrow j} = 0$ for all $1 \le i, j \le n$ with $i \ne j$.

The next theorem in the case of $n > k$ is proved by R. Willard in [6].

Theorem 2.4 *[3, 6] Let* f *be a* k*-valued function which depends essentially on all of its* n*,* $n > 3$ *variables. If* $f \in G_{2,k}^{n,-}$ *then each identification minor of* f *is a symmetric function with respect to its essential variables.*

We can now give a representation of the functions in $G_{2,k}^{n,-}$.

Theorem 2.5 *[3] Let* f *be an* n*-ary* k*-valued function with* $3 < n \le k$. *Then the following sentences are equivalent:*

(i) $f \in G_{2,k}^{n,-}$;

(ii) $f = t \oplus g$ where $g \in G_{n,k}^{n}$ and t is an n-ary totally symmetric function with $Ess(t_{i \leftarrow j}) = X_n \setminus \{x_i, x_j\}$ for all $i, j \in \{1, \ldots, n\}$, $i \ne j$. Moreover $g_{i \leftarrow j} = 0$ for all $1 \le i, j \le n$ with $i \ne j$.

Let us note that the class $G_{2,k}^2$ is described in Theorem 2.1 [5] and the class $G_{2,3}^3$ in Example 2.1 [5].

Separable set of functions with non-trivial arity gap

Let $f \in P_k^n$ be an n-ary k-valued function. Then *the subfunctions* of f are all n-ary k-valued functions which are obtained from f after replacing of some its variables with constants from K. If g is a subfunction of f we shall write $g \prec f$. Clearly, $\prec$ is a partial order relation in the set P_k^n. A set M of essential variables in f is called *separable in* f if there is a subfunction g of f such that $M = Ess(g)$.

Theorem 2.6 *If* $f \in G_{n,k}^n$, $n \le k$, *then each set of essential variables in* f *is separable in* f.

Proof. Let $Ess(f) := \{x_1, \ldots, x_n\}$ and without loss of generality let us prove that $M = \{x_1, \ldots, x_m\}$, $m < n$ is a separable set in f. According to Theorem 2.1 [5] there are n constants $c_1, \ldots, c_n \in K$ such that

$$f(c_1, \ldots, c_n) \neq a_0,$$

where $a_0 = f(d_1, \ldots, d_n)$ for all $d_1, \ldots, d_n \in Eq_k^n$. We have to prove that $M = Ess(f_1)$ where $f_1 = f(x_{m+1} = c_{m+1}, \ldots, x_n = c_n)$. Let $x_t \in M$ be an arbitrary variable from M i.e. $1 \le t \le m$. Again from Theorem 2.1 [5] it follows that

$$f(c_1, \ldots, c_{t-1}, c_n, c_{t+1}, \ldots, c_m, \ldots, c_n) = a_0.$$

Hence $x_t \in Ess(f_1)$ which implies $M = Ess(f_1)$. ■

Theorem 2.7 *If* $f \in G_{2,k}^{n,-}$, *then each set of essential variables in* f *is separable in* f.

Proof. According to Theorem 2.5 f is a symmetric function. Without loss of generality let us assume that $M = \{x_1, \ldots, x_m\}$, $m < n$ be a set of essential variables in f. We have to prove that M is a separable set in f. Since $x_1 \in Ess(f)$ by Theorem 1.2 [1] it follows that there is a chain of subfunctions

$$f_1 \prec f_2 \prec \ldots \prec f_n = f$$

such that $Ess(f_1) = \{x_1\}$ and $Ess(f_j) = \{x_1, x_{i_1}, \ldots, x_{i_j}\}$ for $j = 2,3,\ldots,n$. Since f is a symmetric function, then there are constants $c_{m+1},\ldots,c_n$ for the variables in $Ess(f) \setminus Ess(f_m)$ such that

$$f(x_{i_{m+1}} = c_{m+1}, x_{i_{m+2}} = c_{m+2}, \ldots, x_{i_n} = c_n) =$$

$$= f_m = f(x_{m+1} = c_{m+1}, x_{m+2} = c_{m+2}, \ldots, x_n = c_n).$$

Consequently, $f(x_{m+1} = c_{m+1}, x_{m+2} = c_{m+2}, \ldots, x_n = c_n)$ is a function which depends essentially on the variables $x_1,\ldots,x_m$, i.e. M is a separable set in f.

References

[1] K. Chimev, Separable sets of arguments of functions, MTA SzTAKI Tanulmanyok, 180, (1986), 173 p.

[2] M. Couceiro, E. Lehtonen, Generalizations of Swierczkowski's lemma and the arity gap of finite functions, Discrete Mathematics, (2009), doi:10.1016/j.disc.2009.04.009.

[3] Sl. Shtrakov, J. Koppitz, On finite functions with non-trivial arity gap, Discussiones Mathematicae, General Algebra and Applications, vol.30, (2010), pp. 217-245.

[4] Sl. Shtrakov, Essential arity gap of Boolean functions, Serdica Journal of Computing, vol.2, No. 3, (2008), pp. 249-266.

[5] Sl. Shtrakov, On the number of functions in a class of k-valued logic, Proc. of III-rd International Conference, South-West University, Faculty of Mathematics and Natural Sciences, Blagoevgrad, Bulgaria, 3 - 7 June, 2009, pp. 22-26.

[6] R. Willard, Essential arities of term operations in finite algebras, Discrete Mathematics, 149 (1996), pp. 239-259.

The maximal subsemigroups of the semigroup of all orientation-preserving partial injections

Ilinka Dimitrova

Faculty of Mathematics and Natural Science
South-West University "Neofit Rilski"
Blagoevgrad, 2700, Bulgaria
ilinka_dimitrova@yahoo.com

Abstract: *We study the structure of the semigroup $POPI_n$ of all orientation-preserving partial injections on an n-element set. The main result is the characterization of the maximal subsemigroups of $POPI_n$.*

Keywords: *finite transformation semigroup, orientation-preserving partial injections, maximal subsemigroups.*

2000 Mathematics Subject Classification: 20M20

1 Introduction

For $n \in \mathbb{N}$, let $X_n = \{1 < 2 < \cdots < n\}$ be a finite chain with n elements. As usual, we denote by PT_n the monoid (under composition) of all partial transformations of X_n. The (inverse) submonoid of PT_n of all injective partial transformations of X_n is denoted by I_n.

Let $a = (a_1, a_2, \ldots, a_t)$ be a sequence of t $(t \geq 1)$ elements from the chain X_n. We say that a is *cyclic* if there exists no more than one index $i \in \{1, \ldots, t\}$ such that $a_i > a_{i+1}$, where a_{t+1} denotes a_1. We say that a transformation $\alpha \in PT_n$ is *orientation-preserving* if the sequence of its images is cyclic. The notion of an orientation-preserving transformation was introduced by McAlister in [6] and also by Catarino and Higgins in [2]. We denote by $POPI_n$ the submonoid of I_n whose elements are all orientation-preserving partial injections. A presentation for the inverse monoid I_n was given by Popova in [8]. For the monoid $POPI_n$, a presentation was

exhibited by Fernandes in [4]. Also in [4], the Green's relations, the ideals, the size and rank of $POPI_n$ were determined.

Interest in maximal subsemigroups of the symmetric semigroup and the analogous question of maximal subgroups of the symmetric group was stimulated in large measure by the corresponding question for Post algebras, which has important applications to mathematical many-valued logic, abstract automata, formal languages and combinatorics in general. In group theory describing the maximal subgroups of the symmetric groups has long been an interesting problem. In recent years maximal subsemigroups of the transformation semigroups have also aroused interest.

In [1], Bayramov has presented a complete description of the maximal subsemigroups of the semigroup T_n. Nichols ([7]) as well as Reilly ([9]) have studied the maximal inverse subsemigroups of T_n. Yang Xiuliang ([10]) has determined the maximal inverse subsemigroups of I_n. The maximal subsemigroups of the monoid of all order-preserving partial injections were described by Ganyushkin and Mazorchuk in [5]. Recently, Dimitrova and Koppitz ([3]) characterized the maximal subsemigroups of the monoid of all order-preserving or order-reversing partial injections. In [11], Zhao, Bo and Mei characterized the locally maximal idempotent-generated subsemigroups of $POPI_n$ (excluding the permutations).

In this paper, we aim to give more insight into the subsemigroup structure of the monoid $POPI_n$ by characterizing its maximal subsemigroups.

We will try to keep the standard notation. For every transformation $\alpha \in PT_n$, we denote by $\mathrm{d}om\,\alpha$ and $\mathrm{i}m\,\alpha$ the domain and the image of α, respectively. The number $\mathrm{r}ank\,\alpha = |\,\mathrm{d}om\,\alpha\,| = |\,\mathrm{i}m\,\alpha\,|$ is called the rank of α. Given a subset U of PT_n, we denote by $E(U)$ its set of idempotents.

Since $POPI_n$ is an inverse submonoid of I_n, the definition of the Green's relations $\mathcal{L}$, $\mathcal{R}$ and $\mathcal{H}$ on $POPI_n$ follow immediately from well known results on inverse semigroups. In [4] was given a description for the Green's relation $\mathfrak{I}$. We have

$$\alpha \mathcal{L} \beta \Leftrightarrow \mathrm{i}m\ \alpha = \mathrm{i}m\ \beta$$

$$\alpha \mathcal{R} \beta \Leftrightarrow \mathrm{d}om\ \alpha = \mathrm{d}om\ \beta$$

$$\alpha \mathfrak{J} \beta \Leftrightarrow \mathrm{r}ank\ \alpha = \mathrm{r}ank\ \beta$$

$$\mathcal{H} = \mathcal{L} \cap \mathcal{R}.$$

2 Maximal subsemigroups of the semigroup $POPI_n$

Let $n \in \mathbb{N}$. The semigroup $POPI_n$ is the union of its $\mathfrak{J}$-classes $J_1, J_2, \ldots, J_n$, where

$$J_k = \{\alpha \in POPI_n \mid \mathrm{r}ank\ \alpha = k\},$$

for $k = 1, \ldots, n$. It is well known that the ideals of the semigroup $POPI_n$ are the unions of the $\mathfrak{J}$-classes $J_1, J_2, \ldots, J_k$, i.e. the sets

$$I_k = \{\alpha \in POPI_n \mid \mathrm{r}ank\ \alpha \leq k\},$$

with $k = 1, \ldots, n$. Every principal factor on $POPI_n$ is a Rees quotient I_k / I_{k-1} ($2 \leq k \leq n$) of which we may think as $J_k \cup \{0\}$, where the product of two elements of J_k is taken to be zero if it falls into I_{k-1}.

Denote by L_α, R_α and H_α the $\mathcal{L}$-class, $\mathcal{R}$-class and $\mathcal{H}$-class, respectively, of an element $\alpha \in POPI_n$. Since the product $\alpha\beta$, for $\alpha, \beta \in J_k$, belongs to the class J_k (if and only if $\alpha\beta \in R_\alpha \cap L_\beta$) if and only if $\mathrm{i}m\ \alpha = \mathrm{d}om\ \beta$, it is easy to show:

Lemma 1 *Let $\alpha, \beta \in J_k$, with $k = 1, 2, \ldots, n$. Then*

1. $\alpha R_\beta = \begin{cases} R_{\alpha\beta} = R_\alpha & \text{if } \mathrm{i}m\ \alpha = \mathrm{d}om\ \beta, \\ 0 & \text{otherwise,} \end{cases}$

2. $L_\alpha\beta = \begin{cases} L_{\alpha\beta} = L_\beta & if \ \text{im}\,\alpha = \text{dom}\,\beta, \\ 0 & otherwise, \end{cases}$

3. $L_\alpha R_\beta = \begin{cases} J_k & if \ \text{im}\,\alpha = \text{dom}\,\beta, \\ 0 & otherwise \end{cases}$

4. $\alpha H_\beta = H_\alpha\beta = \begin{cases} H_{\alpha\beta} & if \ \text{im}\,\alpha = \text{dom}\,\beta, \\ 0 & otherwise. \end{cases}$

Let us recall some results on the monoid $POPI_n$, proved by Fernandes in [4]:

Proposition 1 ([4]) *Let $\alpha \in POPI_n$ and let $|\text{im}\,\alpha| = k$, for $k = 1, 2, \ldots, n$. Then $|H_\alpha| = k$. Moreover, if α is an idempotent, then H_α is a cyclic group of order k.*

Let G be a cyclic group of order k, with $k \in \mathbb{N}$. It is well known that there exists an one-to-one correspondence between the subgroups of G and the (positive) divisors of k. Moreover, if r is a divisor of k then there exits a (cyclic) subgroup G_r of G such that $|G_r| = r$. On the other hand, being $x \in G$, there exists a (positive) divisor r of k such that x^r is the identity of G.

Let us consider the following elements:

$$g := \begin{pmatrix} 1 & 2 & \ldots & n-1 & n \\ 2 & 3 & \ldots & n & 1 \end{pmatrix} \in J_n,$$

$$g_1 := \begin{pmatrix} 1 & 2 & \ldots & n-2 & n-1 \\ 1 & 2 & \ldots & n-2 & n \end{pmatrix} \in J_{n-1},$$

$$\varepsilon_i := \begin{pmatrix} 1 & 2 & \ldots & i-1 & i+1 & \ldots & n \\ 1 & 2 & \ldots & i-1 & i+1 & \ldots & n \end{pmatrix} \in J_{n-1}, \ for \ i = 1, 2, \ldots, n.$$

Notice that $J_n = H_g$, whence J_n is a cyclic group of order n and H_{ε_i} $(i = 1, 2, \ldots, n)$ is a cyclic group of order $n-1$.

Proposition 2 ([4]) *Let* $n \geq 2$ *and* $G = \{g, g_1\}$. *Then* $POPI_n = \langle G \rangle$.

Proposition 3 *Let* $\alpha \in J_n$ *be a permutation of order* n *and let* $\delta \in H_{\varepsilon_i}$ *for some* $i \in \{1, 2, \ldots, n\}$ *be a transformation of order* $n-1$. *Then* $POPI_n = \langle \alpha, \delta \rangle$.

Proof: Since $\alpha \in J_n$ has order n, we have $\langle \alpha \rangle = J_n$ and so $g \in \langle \alpha \rangle$. Moreover, $\delta \in H_{\varepsilon_i}$ has order $n-1$ and thus we obtain $\langle \delta \rangle = H_{\varepsilon_i}$. Let

$$\gamma_i := \begin{pmatrix} 1 & 2 & \ldots & i-2 & i-1 & i+1 & \ldots & n-1 & n \\ 2 & 3 & \ldots & i-1 & i+1 & i+2 & \ldots & n & 1 \end{pmatrix} \in H_{\varepsilon_i}.$$

For $i = 1$ we take $i - 1 = n$ and for $i = n$ we take $i + 1 = 1$. Then, it is a routine matter to show that $g_1 = g^i \gamma_i g^{n-i-1}$. Thus by Proposition 2, we deduce that $POPI_n = \langle \alpha, \delta \rangle$. ■

Remark 1 *Let* $\beta \in J_{n-1}$ *with* $\mathrm{dom}\, \beta = X_n \setminus \{i\}$ *and* $\mathrm{im}\, \beta = X_n \setminus \{j\}$. *Then* $H_\beta g^{i-j} = H_{\varepsilon_i}$, *for* $i > j$ *and* $H_\beta g^{n+i-j} = H_{\varepsilon_i}$, *for* $i \leq j$. *Therefore,* $POPI_n = \langle g, H_\beta \rangle$ *for any* $\beta \in J_{n-1}$.

For a prime divisor p of n, we put $W_p = \langle g^p \rangle = \{1, g^p, g^{2p}, \ldots, g^{n-p}\}$, which is, clearly, a cyclic group of order $\frac{n}{p}$. Analogously, for a prime divisor q of $n-1$, we put $U_q(\varepsilon_i) = \langle \gamma_i^q \rangle = \{1, \gamma_i^q, \gamma_i^{2q}, \ldots, \gamma_i^{n-1-q}\}$, which is, clearly, a cyclic group of order $\frac{n-1}{q}$. Furthermore, from well known results regarding finite cyclic groups, we have:

Lemma 2 *The groups* W_p, *with* p *a prime divisor of* n, *are the maximal subgroups of* J_n.

Lemma 3 *For $1 \le i \le n$, the groups $U_q(\varepsilon_i)$, with q a prime divisor of $n-1$, are the maximal subgroups of H_{ε_i}.*

Remark 2 *Let $1 \le i < j \le n$ and let q be a prime divisor of $n-1$. Then it is a routine matter to show that $H_{\varepsilon_i} = g^{j-i} H_{\varepsilon_j} g^{n-j+i}$, $H_{\varepsilon_j} = g^{n-j+i} H_{\varepsilon_i} g^{j-i}$ and $U_q(\varepsilon_i) = g^{j-i} U_q(\varepsilon_j) g^{n-j+i}$, $U_q(\varepsilon_j) = g^{n-j+i} U_q(\varepsilon_i) g^{j-i}$. Therefore, we have*

$$\bigcup_{l,m} g^l U_q(\varepsilon_i) g^m = \bigcup_{l,m} g^l U_q(\varepsilon_j) g^m.$$

Let us put $U_q := U_q(\varepsilon_n)$.

Now, we can describe the maximal subsemigroups of $POPI_n$.

Theorem 1 *A subsemigroup S of the semigroup $POPI_n$ is maximal if and only if it belongs to one of the following two types:*

1) $S'_p = I_{n-1} \cup W_p$, for a prime divisor p of n;
2) $S''_q = I_{n-2} \cup J_n \cup \bigcup_{l,m} g^l U_q g^m$, for a prime divisor q of $n-1$.

Proof: 1) From Lemma 2, we have that $S'_p = I_{n-1} \cup W_p$, for a prime divisor p of n is a maximal subsemigroup of $POPI_n$.

2) From Remark 2, it follows that $U_q(\varepsilon_i) \in S''_q$ for all $i = 1, 2, \ldots, n$. Let $\alpha \in J_{n-1} \setminus S''_q$. If $\alpha \in H_{\varepsilon_i}$ for some $i \in \{1, 2, \ldots, n\}$ then $\langle \alpha, U_q(\varepsilon_i) \rangle = H_{\varepsilon_i}$, since $U_q(\varepsilon_i)$ is a maximal subgroup of H_{ε_i}. Therefore, from Proposition 3, we obtain $\langle S''_q, \alpha \rangle = POPI_n$. Now let $\alpha \notin H_{\varepsilon_i}$ for any $i \in \{1, 2, \ldots, n\}$, i.e. $\mathrm{dom}\,\alpha = X_n \setminus \{i\}$ and $\mathrm{im}\,\alpha = X_n \setminus \{j\}$, for some $i \ne j \in \{1, 2, \ldots, n\}$. Then $\alpha g^{i-j} \in H_{\varepsilon_i}$, for $j < i$ and $\alpha g^{n+i-j} \in H_{\varepsilon_i}$, for $i < j$. Thus, by the previous case, we have $\langle S''_q, \alpha \rangle = POPI_n$, i.e. S''_q is a maximal subsemigroup of $POPI_n$.

For the converse part let S be a maximal subsemigroup of $POPI_n$. Then, it is clear that $I_{n-2} \subseteq S$ and thus $S = I_{n-2} \cup T$, for some subset T of

$J_{n-1} \cup J_n$. From Proposition 3, we have T does not contain any element of J_n of order n or T does not contain any element of J_{n-1} of order $n-1$. In the first case, we must have $J_{n-1} \subseteq T$, by the maximality of S. This shows that $S = I_{n-1} \cup T'$, for some subset T' of J_n, whence T' must be a maximal subgroup of J_n. Thus, by Lemma 2, we have $T' = W_p$, for some prime divisor p of n, i.e. $S = S'_p$. In the second case, we must have $J_n \subseteq T$, otherwise $S \subset S'_p$ for a some prime divisor p of n, which contradicts the maximality of S. This shows that $S = I_{n-2} \cup J_n \cup T'$, for some subset T' of J_{n-1}. If $H_{\varepsilon_i} \subseteq T'$ for some $i \in \{1,2,\ldots,n\}$ then $S = POPI_n$, by Proposition 3. If $H_{\varepsilon_i} \cap T' = \varnothing$ for some $i \in \{1,2,\ldots,n\}$ then by Remark 1 and Remark 2, we obtain that $T' = \varnothing$, i.e. S is a proper subset of S''_q. In both cases, we obtain a contradiction to the maximality of S. Therefore, T' contains $U_q(\varepsilon_i)$ for all $i = 1,2,\ldots,n$ and thus $I_{n-2} \cup J_n \cup \bigcup_{l,m} g^l U_q g^m = S''_q \subseteq S$. Since S''_q is a maximal subsemigroup of $POPI_n$, we deduce that $S = S''_q$.

■

References

[1] Bayramov, P.A., On the Problem of Completeness in a Symmetric Semigroup of Finite Degree, Diskret Analiz, (Russian) 8(1966), 3-27.

[2] Catarino, P.M., P.M. Higgins, The monoid of orientation-preserving mappings on a chain, Semigroup Forum 58(1999), 190-206.

[3] Dimitrova, I., J. Koppitz, The Maximal Subsemigroups of the Ideals of Some Semi-groups of Partial Injections, Discussiones Mathematicae General Algebra and Applications, 29(2009) 153-167.

[4] Fernandes, V.H., The Monoid of All Injective Orientation-preserving Partial Trans-formations on a Finite Chain, Communications in Algebra, 28(2000), 3401-3426.

[5] Ganyushkin O., V. Mazorchuk, On the Structure of IO_n, Semigroup Forum, 66(2003), 455-483.

[6] McAlister, D., Semigroups generated by a group and an idempotent, Communica-tions in Algebra 26(1998), 515-547.

[7] Nichols, J.W., A Class of Maximal Inverse Subsemigroups of T_X, Semigroup Forum, 13(1976), 187-188.

[8] Popova, L.M., Defining Relations in Some Semigroups of Partial Transformations of a Finite Set, Uč en. Zap. Leningrad Gos. Ped. Inst., (Russian) 218(1961), 191-212.

[9] Reilly, N.R., Maximal Inverse Subsemigroups of T_X, Semigroup Forum, 15(1978), 319-326.

[10] Yang, X., A Classification of Maximal Inverse Subsemigroups of Finite Symmetric Inverse Semigroups, Communications in Algebra, 27(1999), 4089-4096.

[11] P. Zhao, X. Bo, and Y. Mei, Locally Maximal Idempotent-Generated Subsemigroups of Singular Orientation-preserving Transformation Semigroups, Semigroup Forum 77(2008), 187-195.

An Actor-Network Perspective of QR Utilization

Malinka Ivanova[1], Javed Alam[2]
[1]*Technical University-Sofia, College of Energetics and Electronics, Sofia, Bulgaria*
[2]*Youngstown State University, College of Engineering & Technology, Youngstown, Ohio, USA*

***Abstract**: In the paper the software solutions that automate the authoring of QR-code generation are explored and those appropriate for educational purposes are marked. Good practices with learning strategies of QR-code utilization are examined and discussed with aim several of them to be selected as candidates for adoption in an engineering learning process. A reference model presenting relationships among participants, resources and concepts is created and it is analyzed with the support of the Actor-Network theory. The model is prototyped and pilot tested in a given educational context.*

***Keywords:** QR code, experimentation, actor-network theory, automation, mLearning, reference model*

1. INTRODUCTION

Mobile learning (mLearning) in its variety of forms and scenarios is increasingly recognized and adopted by universities and training organizations [2]. Recent research indicates a growing interest and acceptance of the utilization of mobile technologies for teaching and learning [5], [6], [10]. Also, all of the emerging trends in the 2010 Horizon report (a joint report by The New Media Consortium and Educause) have a relationship to mobility and augmented reality [8]. Among the key advantages of mobile technologies are considered: no time constraints, no location border, easier access to (multimedia) content, knowledge and people, giving opportunities for just in time learning, for location based learning, community based learning, personal learning. However, implemented mLearning methods for access to stored information and services through the limited input functionalities of mobile phones are time-consuming and sometimes frustrating. This is the reason for looking of different ways for effective deployment of mobile technologies and their increased impact among a wide range of audiences. Quick Response (QR) codes are considered as promising technology providing learners with speedy and ready access to multimedia learning resources, information and

services [4]. The recent challenges are related to organization of technology enhanced learning environments embedding QR codes with aim to enable learners to be more effective and productive in their learning when they move from one place to other, using widely distributed handheld computing devices and communication technology. Such environment needs to be monitored and continuously improved with instruction and scenarios, according to changing student's learning requirements and needs. Actor Network Theory (ANT) is utilized as an analytical framework to understand the taxonomy and working flows in an information system and to describe the role of technology in relationship technology-educators-students.

2. QR CODE SPECIFICATION

A QR code is a two-dimensional code readable by mobile phones. The code consists of black modules (or colored) arranged in a square pattern on a white background (or colored). The information encoded can be text, URL, SMS, email, vCard, video, spreadsheet or other data. So, if the device has QR code decoding software installed on it, it will open up its browser and go straight to that URL or open up the correct application to handle the encoded data appropriately according to the FNC1 Application Identifiers that are embedded in the encoded data [3]. The QR code also contains control information to ensure the good picture identification at different conditions. The error correction capability allows data to be restored even if the symbol is partially dirty or damaged. Several editors for QR code that can automate learning assets and information presentation in form of QR code are presented in Table 1.

Tab. 1: Functional characteristics of QR editors

QR Editor	Content type	Output formats	Store code	Features	QR code
Kaywa http://qrcode.kaywa.com/	URL, text, phone, SMS, RSS feed	Embed code Manual pics	no	data matrix generation	
ZXing Project http://zxing.appspot.com/generator/	event, contact info, Email, geolocation,phone, SMStext, URLwifi network	Embed code, png manual	no		
Delivr http://delivr.com/qr-code-generator	URL, Google places/map,contact info, Email, phone, SMS, text, RSS feed	png, eps	yes	API, QR code tracking, analytics	

Mobile barcodes http://www.mobile-barcodes.com/qr-code-generator/	URL, text, phone, SMS, email	png, embed code	no		
GOQR http://goqr.me/	text, URL,call, SMS, vcard	png, embed code	no	library (php, C++)	
QR stuff http://www.qrstuff.com/	text, URL,phone, SMS, Email, vcard, event, Google maps, location, Wifi Login, Paypal Buy, social media, iTunes, YouTube video	png	no		
Maestro http://www.sparqcode.com/static/maestro	phone, SMS, map, URL, contact, raw, vcard	gif, svg, embed code, URL	yes	error correction	
Be QRious http://www.beqrious.com/generato	URL, map, Email, text, YouTube video, vcard, contacts	pdf, gif, URL	yes	picture including	

3. GOOD PRACTICES

Created QR codes with content of text/news/images/audio/video materials/web pages can be placed onto the worksheet, textbook or integrated into web pages. With just a quick scanning action and a click, the students can see/listen the needed learning material or instruction (Figure 1). By linking the QR codes on a paper-based task to the multimedia resources published on the Web or offline information reading is possible with just two simple operations provide a very efficient and flexible way for the students to obtain the resources ubiquitously.

Rivers describes three specific examples of basic QR code-driven activities performed into a Japanese university in English as a Foreign Language classroom: through QR code activity the students create opinion paragraphs based on their interactions with other people and materials, through an activity “collaborative mobile tagging” wth purpose to promote communicative interaction outside of the traditional classroom environment, and through an activity related to team working on a given problem [12]. Ramsden experimented with QR codes as a learning technology in University of Bath in several cases: for printed handbooks with links to online resources, lectures content with links to online presentations, for classroom formative feedback, video user guides, campus/library induction, Moodle print materials. [11]. A student of Computer Science in Universite of Bologne, Italy designed in form of QR codes a complete periodic table of elements with characteristics of every element [13]. A wide range of QR usage in classroom is given in [1] and that includes: (1) QR codes utilization for voting, (2) QR codes for information enhancement in books and printed

materials, (3) for access to mobile site with important information, (4) for sharing of students resources among them, (5) QR codes as link to polls and surveys. Other suggestions for QR adoption are related to: QR code of the blog URL, QR code designed to present the homework for students and also as a link to students' homework products, QR code as reminder for class events.

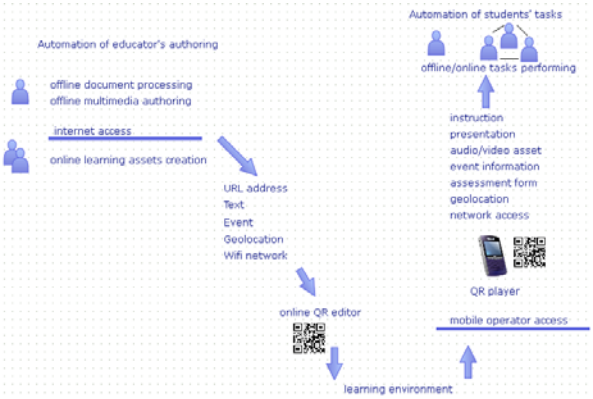

Fig. 1: The workflow of QR code authoring process and QR code utilization by students

4. ACTOR NETWOR THEORY

Actor-Network theory (ANT) explores how relations between objects, artifacts, people and concepts are formed, mapped and re-maked. The main concepts behind ANT are: (1) *Actors* could be humans, collectivities of humans, texts, graphical representations, and technical artifacts. Actors with aligned interests could be organized a *heterogeneous actor-network*. (2) *Translation* is the process of an actor-network with three major stages: problematization, interessmant, and enrolment. (3) *Problematization* is the first stage of translation during which a focal actor defines identities and interests of other actors and establishes itself as an obligatory passage point (OPP). (4) *OPP* is related to a situation when all the actors are satisfied according to their interests (5) *Interessement* as a second stage of translation includes a process of convincing other actors to accept definition of the focal actor. (6) *Enrollment* is the stage when another actor accepts the interests defined by the focal actor. (7) *Inscription* is defined as a process of creating technical artifacts that would ensure the protection of an actor's interests. (8) *Irreversibility* is the degree to which it is subsequently impossible to return to a point where alternative possibilities exist [14].

Its perspective is applied in the researching of QR and marker Augmented Reality technologies implementation in a learning process.

5. A REFERENCE MODEL FOR QR CODES IMPLEMENTATION

After a survey about mobile devices usage in everyday life of our students in USA (62 students from Youngstown State University) and Bulgaria (45 students from South-West University “N. Rilski”) it is found that 100% of students possess mobile devices with camera. 91% of students in Bulgaria and 97% of students in USA exploited devices for texting; about 75% of Bulgarian and 90% of American students use phones for pictures taking and 68% of Bulgarian and 47% of American students for music playing. 48% of Bulgarian and 68% of American students have internet access through their phones, 26% of Bulgarian and 56% of American students perform email checking, 40% of Bulgarian and 61% of American students use phones for web browsing, about 35% of Bulgarian and 53% of American students utilized phones for access to social networks like Facebook. The results show that students are equipped with needed mobile devices and many of them have internet access. Anyway, only several of them know the purposes of QR codes and AR markers. In the other hand the literature review presents a wide range of scenarios for QR code adoption in engaging and motivating learning tasks. Based on this research and with support of ANT, a reference model for QR and AR technology implementation in an engineering learning process is created and it is presented on Figure 2.

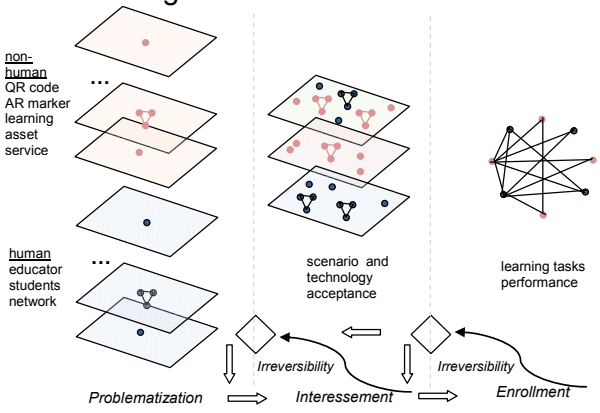

Fig. 2: A reference model in three stages

Fig.3. Experimentation

6. RESULTS

The first pilot experimentation of QR codes utilization in online and offline variants is done with students from South-West University “N. Rilski”, Faculty of Mathematics and Natural Sciences, Department of Computer Systems and Technology during the course Applied Electronics (Figure 3). The advantages of mobile technologies and QR codes related to: (1)

students learning support with annotations, text messages, URLs, multimedia assets in-time and in different locations; (2) proposition of attractive and engaging learning activities; (3) increased attention to the technologies and curriculum material are ascertained. The future work will be oriented to examination of effective implementations of scenarios according to the concrete students' audience and according their personal requirements.

7. REFERENCES

[1] *40 Interesting Ways to Use QR Codes in the Classroom.* Retrieved April 21, 2011, from https://docs.google.com/present/view?id=dhn2vcv5_765hsdw5xcr&revision=_latest&start=0&theme=blank&authkey=COX05IsF&cwj=true

[2] Alexander, B. (2004) *Going Nomadic: Mobile Learning in Higher Education*, September/October EDUCAUSE review. http://net.educause.edu/ir/library/pdf/ERM0451.pdf

[3] Denso. (2010) QR Code Standardization. Retrieved April 21, 2011, from http://www.denso-wave.com/qrcode/qrstandard-e.html

[4] Elena. (2009) *Educational Qrcodes*. Retrieved April 21, 2011, from http://www.qrcode.es /?p=350&language=en

[5] Herrington, A., Herrington, J. (2007) *Authentic mobile learning in higher education*, Proceedings of the AARE 2007 International Educational Research Conference. http://www.aare.edu.au/07pap/her07131.pdf

[6] Järvelä, S., Näykki, P., Laru, J., Luokkanen., T. (2007) *Structuring and Regulating Collaborative Learning in Higher Education with Wireless Networks and Mobile Tools*, Educational Technology and Society, 10 (4), 71-79.

[7] JISC (2005) *Innovative Practice with e-Learning: a good practice guide to embedding mobile and wireless technologies into everyday practice*, Bristol: Joint Information Services Committee.

[8] Johnson, L., Levine, A., Smith, R., Stone, S. (2010) *The 2010 Horizon Report,* Austin, Texas: The New Media Consortium

[9] Kerry. (2010) *10 ways to use QR Codes in a History classroom*. Retrieved April 21, 2011, from http://www.kerryjturner.com/?p=365

[10] Lee, Y., Lee, S. (2008) *Situated Mobile Learning in Higher Education*, Proceedings of World Conference on E-Learning in Corporate, Government, Healthcare, and Higher Education, 1745-1750, Chesapeake, VA: AACE.

[11] Ramsden, A. (2009) *Exploring the use of QR Codes as a Learning Technology*, In: Mobile Learning: Telling Tales, 9th July, University of Westminster. Retrieved April 21, 2011, from

http://opus.bath.ac.uk/14790/1/QR_Codes_in_education_mimas_july_09.pdf
[12] Rivers, D. (2009) *Utilizing the quick response (QR) code within a Japanese EFL environment*, JaltcallJournal 5(2),15-28.
[13] Rizzo, S. (2009) *QR-code Periodic Table of Elements*. Retrieved April 21, 2011, from http://www.nerdnews.it/2009/03/17/qr-code-periodic-table-of-elements/
[14] *Actor-Network Theory*, Wikipedia. Retrieved April 21, 2011, from http://en.wikipedia.org/wiki/Actor-network_theory

Class Library for Boolean Function Manipulation

Mila Sukalinska, Ivo Damyanov
South-West University, Blagoevgrad, Bulgaria

***Abstract**: In this paper we present a .NET Framework class library for Boolean functions manipulation. The class library is designed as educational and research tool for studying structural properties of Boolean functions and performing symbolic manipulations. Several basic internal representations of Boolean functions are implemented as independent classes inheriting common interface. Conversion between different representations is performed automatically by helper classes.*

***Keywords:** Boolean function, class library, .NET Framework, symbolic manipulation*

1. INTRODUCTION

Boolean functions are a part of the foundation of computer science. In theoretical computer science various representations of Boolean function are developed and used such as truth-tables, formulae, binary decision trees, decision diagrams, etc. For n variables there are 2^{2^n} Boolean functions.

There are many software packages for Boolean functions [4, 5, 7] but most of them use only one internal implementation which means that for students studying discrete mathematics they need to use different packages in their coursework. The goal of this paper is to present a new developed class library for symbolic manipulation of Boolean functions that provide various internal representations. The library can be easily used with languages from .NET Framework family as education and research tool. It also provides us with options to extend this library in future to accommodate other types of internal representations and more implementation independent symbolic manipulations. We propose robust, flexible and compact syntax for performing different tasks (some shown by examples).

A *symbolic manipulation* over Boolean functions is execution of a sequence of commands that build up representations of functions and determine various properties about them. In the table below we summarize main symbolic manipulations procedures that are implemented in our library.

Procedure	Description

Reduce	Simplification of the internal representation is performed
Apply	Obtain new function applying some operation ∇ between existing two other functions $f = f_1 \nabla f_2$
Restrict	Replace variable with a constant $f\|_{x_i=b}$
Compose	Replace variable with a function $f_1\|_{x_i=f_2}$

2. BOOLEAN FUNCTIONS CLASS LIBRARY

The .NET framework is a programming model for developing and deploying open applications [1]. Every .NET-aware language is compiled to intermediate language code which is executed in Common Language Runtime (CLR). This provides us easy to use code sharing through class hierarchy and libraries.

Overall structure of the library

Our class library developed in C# can be divided into three main parts:

- *Internal Implementations of Boolean Functions* – This is a set of Interface restricted implementations.
- *Implementation Independent Functionality* – Wrapper class for implementation independent methods. Available implementations are interchangeable using dependency injection pattern.
- *Algorithms* – Set of helper classes that provide us functionality like conversion between different implementations, minimization and combinatory set manipulations.

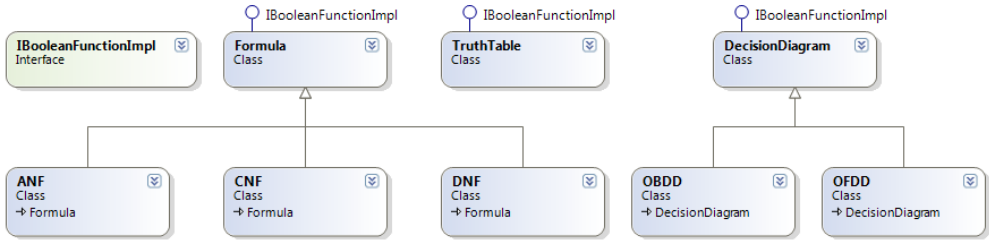

Fig. 1: Implementations sharing common interface

Internal Implementations

The different implementations of Boolean function inherit common interface – *IBooleanFunctionImpl*.

The interface cover all the main functionality for symbolic manipulation of Boolean functions: Restrict, Reduce, Apply, Compose and some other like function evaluation, variable swapping, checks for essentiality [2] and separability [3].

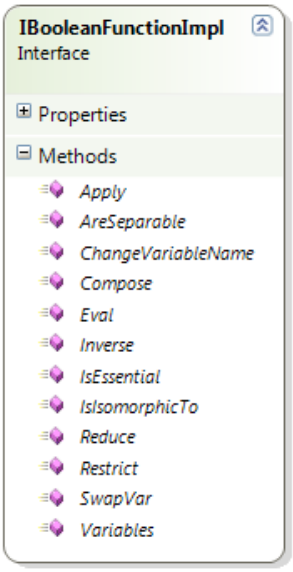

Since different implementations exploit different internal data structures (arrays, trees, etc.) we have two-side views for Boolean function variables:

Internal – each variable has its index

External – each variable has its name.

The interface forces us to use variable names rather their indexes. For simplicity we have only one letter variable names allowed.

Because of limitations and exponential blowup each implementation has its own check rule for maximum number of variables which can be reasonably handled.

As semantically simplest implementation in the class library we have ***TruthTable*** implementation. Truth tables are commonly used in various packages for Boolean function minimization and manipulation such as ESPRESSO[6].

Another very common syntactical representation of Boolean functions is Boolean expressions or Formulae. That's why we have implemented a ***Formula*** class to represent Boolean expressions.

As a state of the art data structure for symbolic manipulation of Boolean functions in recent decades ***DecisionDiagram*** also could take place in this library.

Implementation Independent Functionality, Convertors and Helpers

Using different implementations we can manipulate Boolean functions to observe their properties. There are some classical and non-classical properties which are independent from Boolean function representation. Following .NET Framework template we have implemented separate class for converting Boolean function represented in one way into another. In other words we have class ***ImplConverter*** which allow us to change internal implementation of the given Boolean function. Some classical algorithms are exploited. Since most of the tasks are performed on the search space we have implemented also a helper class.

Usage of the Class Library

With the class library many standard operations can be performed by the students in solving different tasks connected with the studying of Boolean functions.

Task 1: Enumerating variables

The basic operation that can be involved in any other task for studying Boolean function is enumeration of function arguments.

```
IBooleanFunctionImpl f=new IBooleanFunctionImpl();
foreach (char varName in f.Variables())
{
   Console.Write(varName);
}
```

Task 2: Get all subfunctions of the given function f

Many operations are based on combinations of arguments assignments for the Boolean functions. Exploiting ***CombinatoricsHelper*** class a following construction can help us to obtain all subfunctions of the given function:

```
IBooleanFunctionImpl f=new IBooleanFunctionImpl ();
CombinatoricsHelper helper = new CombinatoricsHelper
                                  (f.NumberOfVariables);
foreach (Tuple t in helper.Tuples())
{
   IBooleanFunctionImpl SubFunction =
   f.Restrict (variableNamesCombination,
               helper.CurrentCombination);
}
```

Task 3: Building graph of separable pairs

This is a graph with vertices - essential variables and branches – separable pairs.

```
IBooleanFunctionImpl f=new IBooleanFunctionImpl ();
CombinatoricsHelper helper = new CombinatoricsHelper
                                        (f.Variables());
foreach (var pair in helper.PairsOfVariables
                                        (f.Variables()))
{
     if (f.AreSeparable(pair))
   {
        Console.Write(pair);
   }
}
```

Task 4: Find all quasi-fictive variables of the given Boolean function f

```
IBooleanFunctionImpl f=new IBooleanFunctionImpl ();
foreach (char varName in f.Variables())
{
```

```
    BooleanFunction subfunction0;
    BooleanFunction subfunction1;
    f.PositiveDavio(varName, out subfunction0,
                             out subfunction1)
    if (subfunction0 == subfunction1)
    {
         Console.Write(varName);
    }
}
```

Task 5: Finding distributors of the given Boolean function f

```
IBooleanFunctionImpl f=new IBooleanFunctionImpl ();
foreach(char  varName  in f.Variables())
{
      char[] RestVarialbes =
                      new char[f.NumberOfVariables()-1];
      int br=0;
      foreach (char currName in f.Variable())
      {
         if (varName!=currName)
         {
            RestVarialbes[br] = currName;
            br++;
          }
      }
  if (!f.AreSeparable(RestVarialbes))
    {
        Console.WriteLine("Variable {0} is distributor",
                          varName);
    }
}
```

Task 6: Comparing graphs of separable pairs of the subfunctions and given function f

```
IBooleanFunctionImpl f=new IBooleanFunctionImpl ();
IBooleanFunctionImpl subfunction1;
IBooleanFunctionImpl subfunction2;
int count=0;
subfunction1=f.Restrict(new char[] {varName},
                        new bool[] {true});
subfunction2=f.Restrict(new char[] {varName},
                        new bool[] {false});
List<KeyValuePair<char, char>> FunctionGraph(f);
List<KeyValuePair<char,char>> SubFunctionGraph1(
                                    subfunction1);
List<KeyValuePair<char,char>> SubFunctionGraph2(
                                    subfunction2);
foreach(KeyValuePair<char,char> pair in FunctionGraph)
```

```
{
   if (!SubFunctionGraph1.Contains(pair))
   {
      count++;
      Console.Write(“Different pair:{0}”,pair.Key);
   }
}
Console.Write(“Different pairs count:{0}”,count);
Count=0;
foreach(KeyValuePair<char,char> pair in FunctionGraph)
{
   if (!SubFunctionGraph2.Contains(pair))
   {
      count++;
      Console.Write(“Different pair:{0}”,pair.Key);
   }
}
Console.Write(“Different pairs count:{0}”,count);
```

3. CONCLUSION AND FUTURE WORK

The presented initial implementation of the class library provides us optimal C# syntax, easy to use by students and researchers. The library is able to efficiently perform basic Boolean operations upon Boolean functions. Shown by example are some tasks that can be solved. Further work is to optimize the internal implementation and expand the functionality of the library. The BFL binaries are available at: *http://dispatcher.swu.bg/BCL*

4. REFERENCES

[1] *An Introduction to Microsoft .NET.* White Paper, Microsoft Corporation, 2001.

[2] Брейтбарт, Ю., *О существенных переменных фунцкции алгебры логики*, Доклады АНСССР, 172, (1967), 9-10

[3] Chimev, K., *Separable sets of arguments of functions*, MTA SzTAKI, Budapest, 180, (1986), 1-173

[4] Fiser, P., D. Toman, *BoolTool: A Tool for Manipulation of Boolean Functions (2008)*, 8th International Workshop on Boolean Problems (IWSBP'08), Freiberg, Germany

[5] Jensen, R.M., *A Comparison Study Between the CUDD and BuDDy OBDD Package Applied to AI-Planning problems*, Technical Report CMU-CS-02-173, Computer Science Department, Carnegie Mellon University, 2002

[6] Rudell, R., *Multiple-Valued Logic Minimization for PLA Synthesis*, Memorandum No. UCB/ERL M86-65, 1986
[7] Tomaszewski, S., I. Celik, G. Antoniou, *WWW-Based Boolean function minimization, International Journal of Applied Mathematics and Computer Science*, 2003, Vol. 13, No. 4, 577–583

An adaptive mechanism with aggregation and fragment retransmission for 802.11 wireless networks

Valentin Hristov, Oleg Panagiev
South- West University- Blagoevgrad,
Technical university - Sofia,
Bulgaria

***Abstract**: In present paper an analytic model is developed to calculated optimal fragment size which to use in this adaptive mechanism with aggregation and fragment retransmission. Throughput is maximized by using proposed here mechanism where only lost fragments of frame are retransmitted immediately once the error occur in wireless link.*
***Keywords:** high-speed wireless networks, adaptive aggregating mechanism, and Throughput.*

1. INTRODUCTION

In upcoming very high-speed wireless LANs (WLANs), the physical (PHY) layer rate may reach 600 Mbps. As the PHY rate increases, for a fixed packet size, the time to transmit the packet payload decreases, but the PHY header overhead and the MAC header overhead are left untouched. Hence, MAC efficiency rapidly decreases, and efforts to increase the system capacity purely by increasing the data rate are thus of limited effectiveness.

To achieve high MAC efficiency at the medium access control (MAC) layer, different aggregation schemes were proposed in the literature [3 - 7], e. g. Burst ACK, Block ACK, Aggregation and Fragment Retransmission (AFR), Packet Concatenation (PAC), and Aggregation. These schemes can

be classified into two categories. The schemes in the first category are Burst ACK and Block ACK, which transmit multiple frames at each transmission opportunity. The schemes in the second category as PAC, Aggregation, and AFR transmit only one frame and use packet aggregation.

In the Burst ACK and Block ACK schemes, collisions lead to the whole Burst/Block being lost while errors lead to retransmission only of the corrupted packet.

AFR is the only scheme to use both fragmentation and aggregation. The PAC scheme is similar to AFR scheme, except that before each packet in a frame there is a subphysical header. The scheme which is called Aggregation uses a special delimiter before each packet in a frame.

In other work [8] we propose a modification of AFR scheme called Adaptive with Aggregation and Fragment Retransmission (A-AFR) scheme that can achieve optimal throughput/minimum delays.

The present paper aims at optimizing size of fragments used in this adaptive mechanism with aggregation and fragment retransmission./The present paper aims at determining optimal number of packets, which will be able to aggregate in this adaptive mechanism with aggregation and fragment retransmission.

2. A-AFR SCHEME

As mentioned above for the AFR scheme, multiple packets are aggregated into and transmitted in a single large frame. If errors happen during the transmission, only the corrupted fragments of the large frame are retransmitted. The AFR scheme was developed as part of the IEEE 802.11n working group work.

The A-AFR scheme [8] is a modification of AFR scheme that can achieve optimal throughput/minimum delays. Thus, the streamed audio and video traffic, e. g. VoIP and HDTV, will be able to benefit from the aggregation of packets. This adaptive scheme determines a certain threshold of utilization, over that threshold is used AFR aggregation, as transmission delays will be the same as without aggregation. More precisely, the threshold [2] is:

(1) $$\rho^* = \frac{1}{4}(7 - 3\sqrt{1+8h}),$$

where *h* is a ratio of time for transmission of headers toward time for transmission of frames.

Unlike wired networks, wireless transmissions are inherently broadcast in nature, which leads to the packet service times at different stations in a WLAN being strongly coupled. For example, the basic 802.11 backoff mechanism ensures that the wireless stations in a WLAN win a roughly

equal number of transmission opportunities [6], hence the mean packet service time at a station is longer when the number of other active stations in the WLAN increase. In addition to variations in the mean service time, the distribution of packet service times is also strongly dependent on the WLAN offered load, because this directly affects the burstiness of transmissions.

Note that a wireless station can measure its own utilization ρ and parameter h by direct observation. Thus, when the utilization is over the threshold of utilization, AFR aggregation is realized.

In A-AFR scheme, a MAC frame consists of a frame header and a frame body (Fig.1). In the new MAC header, all the fields of MAC header remain unchanged. There are three additional fields—fragment size, fragment number, and a spare field. The fragment size represents the size of fragment used in the MAC frames. The fragment number represents the number of fragments in the current MAC frame. The spare field is left for future extension and maintaining alignment. The frame body consists of fragment headers, fragment bodies and the corresponding frame check sequences (FCS).

The fragment header section of the frame body has a variable size (Fig.1). It includes up to 256 fragment headers, each of which is protected by a FCS. The length of each fragment header is constant and known to both the sender and the receiver. For the receiver, it knows from where the first fragment header starts and what the fragment header size is, thus it can locate all the fragments in the frame even if some of them are corrupted during the transmission.

Each fragment header is composed of six fields: packet ID (pID), packet length (pLEN), start position (startPos), offset, spare, and FCS. The fields pID and pLEN represent the corresponding ID and length of the packet P to which this fragment belongs. The field startPos is used to indicate the position of the fragment body in this frame, and offset is used to record the position of this fragment in packet.

The ACK frame format includes a bit map in the legacy ACK format. Each bit of the bitmap (32B) is used to indicate the correctness of a fragment.

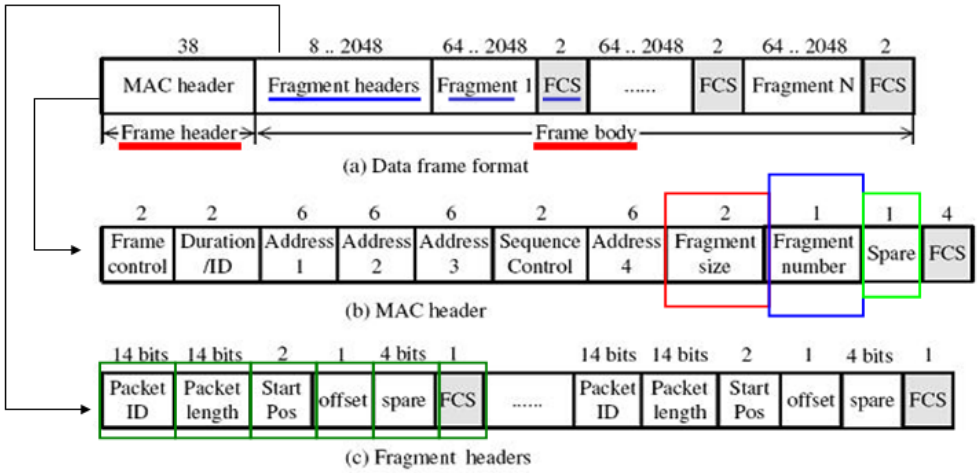

Fig.1.A- AFR frame formats.

Wireless stations dynamically adjust the physical transmission rate/modulation used in order to regulate noncongestive channel losses. This rate adaptation, whereby the transmit rate may change by a factor of 50 or more (e.g. from 1 to 54 Mb/s in 802.11a/g).

3. OPTIMAL FRAGMENT SIZE

Fragmentation plays a central role in aggregation schemes, with fragments being the unit used for retransmission. When a very small fragment size is used, only corrupted bits are retransmitted, but since each fragment has a fixed size header, the overhead is relatively large. When a large fragment size is used, the overhead created by the fragment header is small, but many bits will be unnecessarily retransmitted since a single damaged bit in a fragment will lead to the entire fragment being retransmitted.

For a given BER, an optimal fragment size exists, i. e. maximizes efficiency coefficient- *Ke* , and balances the tradeoff between the fragment header overhead and excessive retransmissions.

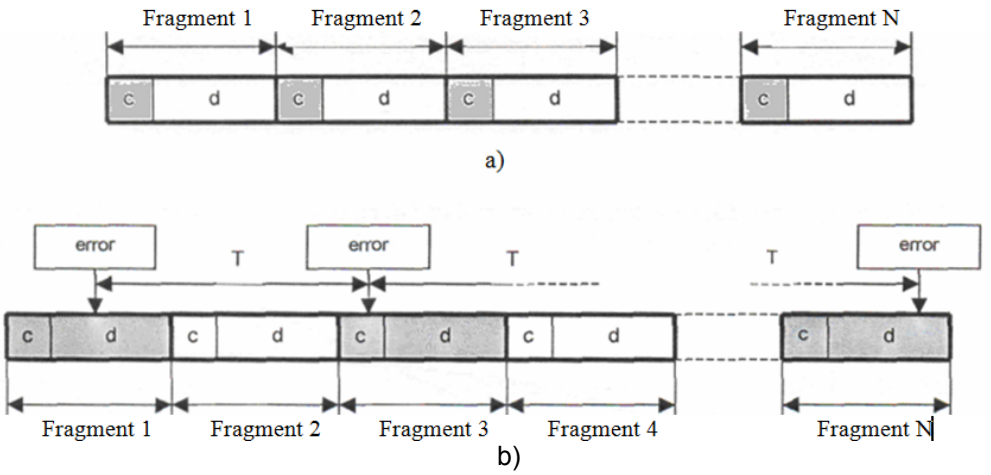

Fig.2. Coefficient of efficiency

In case of error free communication channel the efficiency coefficient can be expressed by the ratio of total quantity of correctly received data to the total quantity of transmitted data (fig. 2a).

For real communication channel (error prone) this coefficient- *Ke* can be reduced by the quantity of rejected data (fig. 2b). The efficiency coefficient decreases with the increase of the user data in fragments as well as decrease of the communication error period- *T* (T=1/BER), i. e:

$$(2) \qquad K_e = \frac{d}{c+d} - \frac{d}{T},$$

where *d* is user data in a fragment, c is control information and *T* is the communication error period

To find the maximum of *Ke*, (2) is differentiated and made equal to zero, and then the got equation is solved for *d*:

$$(3) \qquad d = -c + \sqrt{cT},$$

Fig.3 plots coefficient of efficiency versus Bit Error Rate (BER) from which the existence of an optimal fragment size that maximizes efficiency is evident. Observe that the optimal fragment size depends on the BER, as expected. In practice, e. g. implementation [1] of A-AFR on FPGA, we are interested in determining a simple scheme that approximates the optimal fragment sizes' performance. In [6] can be seen that the throughput peak is relatively flat and broad, and thus we expect that the throughput reduction resulting from an approximate scheme can be kept relatively small. In the reduction in throughput is compared to that achieved with the optimal fragment sizes, of using a suboptimal fragment size. Ibid, throughput is lost

of up to 10%, across a wide range of BERs when fragment sizes are near-optimal (128 and 256 B).

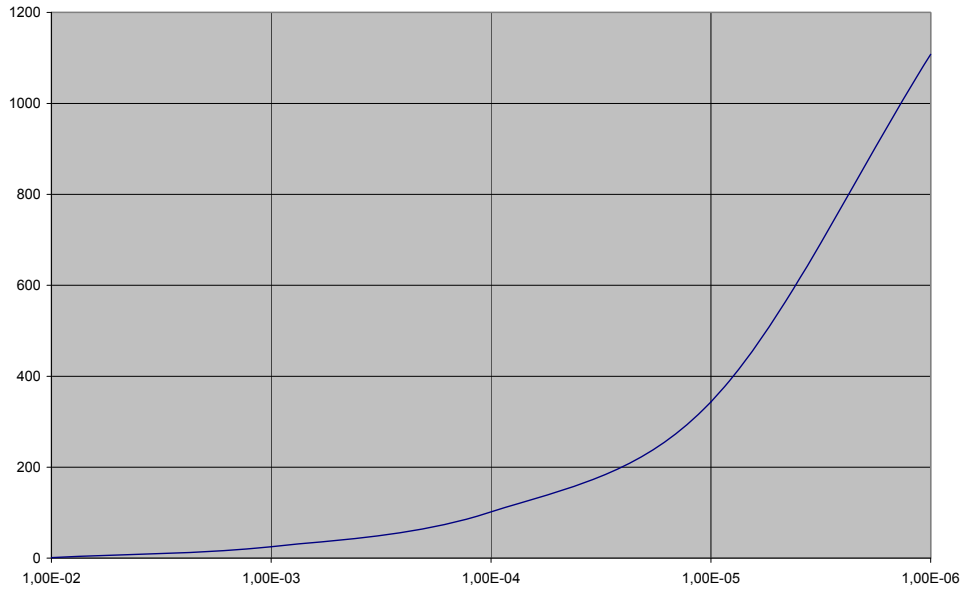

Fig.3. Optimal coefficient of efficiency

4. CONCLUSION AND FUTURE WORK

In present paper, a novel scheme called adaptive aggregation with fragment retransmission (A AFR) that exhibits optimal transmission delays is enhanced.

To achieve high efficiency for next-generation very high-speed WLANs, we develop a modified aggregation scheme called AFR, in which multiple packets are aggregated into and transmitted in a single large frame. Only the corrupted fragments are retransmitted instead of retransmitting the whole frame in case of errors. Analytical model is developed to find optimal fragment size of A-AFR over a noisy channel.

My future work is going to create simulation model and to evaluate the throughput and delay performance of A-AFR over a noisy channel, as well as to compare these throughput and delay with AFR and similar schemes in the literature

5. REFERENCES

[1] Chen W. and all Synchronous fine- adjustable rate control circuit for Ethernet congestion management, Electronics Letters, febr. 2008, vol.44, no. 4,pp.325- 326.

[2] Hong J. and K. Sohraby "On Modeling, Analysis, and Optimization of Packet Aggregation Systems", IEEE Transactions On Communications, vol. 58, no. 2, February 2010, pp 660-668.

[3] Olteanu A. and Yang Xiao Security overhead and performance for aggregation with fragment retransmission (AFR) in very high-speed wireless 802.11 LANs IEEE Transactions on Wireless Communications, Volume: 9, Issue: 1 ,2010,.pp. 218 – 226.

[4] Mujtaba S. A. et al., "TGn sync proposal technical specification," 2005 [Online]. Available: www.tgnsync.org

[5] R. Jain, C. So-In and A. Tamimi "Level Modeling Of IEEE 802.16e Mobile Wimax Networks: Key Issues", IEEE Wireless Communications, October 2008, pp 73-79.

[6] Tianji Li and all Aggregation with fragment retransmission for Very High-Speed WLANs , IEEE/ACM Transactions on Networking,Volume: 17 , Issue: 2 2009 , pp. 591 – 604.

[7] Li et al.: Buffer Sizing for 802.11-Based Networks IEEE/ACM Transactions on Networking, Vol. 19, No. 1, February 2011, pp.156-169.

[8] V. Hristov, Implementation of Adaptive Mechanism with Aggregation and Fragment Retransmission for 802.11 Wireless Networks, International Conference on Information Technologies (InfoTech-2011), September 2011,Varna, Bulgaria, submitted

COMPUTER PROGRAMS AND THEIR INTELLECTUAL PROPERTY PROTECTION IN BULGARIA

Tereza Trencheva
State University of Library Studies and Information Technology, Sofia, Bulgaria, e-mail: tereza_trencheva@abv.bg

***Abstract**: Problems associated with the operation of computer crimes and the legislation become more valid in Bulgaria. As a member of the European Union, there are high requirement for us about combating piracy and counterfeiting. Overcoming those problems will enhance our reputation in the field of information technology. The paper aims to analyze computer programs as an object of copyright in on one hand and the subject of industrial property on the other. It is an assessment of advantages and disadvantages of different methods of protection for purpose of the Act are considered copyright and related rights, The Patent Law and the registration of utility models and 2009/24/EO Directive of the European Parliament and the Council for the legal protection of computer programs from 23 April 2009.*

Keywords: *computer programs, intellectual property, legislation, piracy, counterfeiting, copyright, patent law*

1. PROTECTION OF COMPUTER PROGRAMS THROUGH THE SYSTEM OF COPYRIGHT

The rapid development of digital infosfera by applying new information and communication technologies causes the appearance of new objects of intellectual property, like databases in all fields of knowledge and computer programs. [1]

In Bulgaria computer programs are object of copyright since the early nineties. In accordance with the Copyright and Related Rights Law (CRRL) Article 3, paragraph 1 " Object of copyright shall be work in the field of science, literature and art, which is a result of creative activity and is expressed by any ways or in any objective form, such as: literary works, including works of scientific and technical literature, political journalism and computer programs ". [2] At first glance this may seem odd, but this method of protection has serious advantages.

In order to unify the legal regulation of computer programs in Europe, The European Council voted Directive 91/250/EC for protection of computer programs on 14th May 1991, which was replaced by Directive 2009 / 24 / EC of the European Parliament and the Council from April 23, 2009 for the legal protection of computer programs. The repeal of the old directive and its replacement by a new one was provoked by multitude of amendments to the Directive 91/250/ESS during the years from its induction till the moment. Therefore imposed all new elements to be integrated with the new Directive 2009/24/EO which also preserves and updates the texts of old Directive.

Lack of adequate protection of computer programs in the laws of Member countries, the investment of considerable human, technical and financial resources in developing of computer programs that can be easily and qualitatively reproduced and used illegally, the increasing role of computer programs in developing European market, the differences in the mode and resources of protection for computer programs and etc. leads to the necessity for European countries to update their laws related to copyright, taking into account the recommendations of the Directive. According to Art. 1, item 1 of the Directive 'computer programs are protected by copyright as literary works according to the Berne Convention. [3] Art. 1 also specifies that the ideas and principles underlying in the computer program or in some of its elements are not protected by copyright, and that protection extends only to those programs which are genuine, and are result of the author's intellectual creation.

Bulgarian legislation has adopted the argument of the European Directive and its text is taken in determining the system of legal protection of computer programs.

In accordance with Article 3 of the aforementioned CRRL we have three main criteria which have to fulfill t a work to enjoy the provided legal protection:

- to be a work of literature, art and science - this is the criterion on which computer programs are absolutely responsible.

Here, however, the dispute arises, whether the software is inherently much more a product of science rather than literature. Namely this formulation is faced with the legal fiction of Art. 1 of the Directive and Art. 3, par. 1, item 1 of the CRRL, according to which a computer program is treated as a literary work. This compromise is necessary in order that one of the new objects of copyright can be used with an already developed system of principles applicable to one of the oldest objects of protection - literary works, rather than having to develop new rules.

The second criteria which must fulfill a work is:

• to be a result of creative activity - and on this criterion, there are many disputes that are not focused on how the computer program fulfills this requirement, but rather the correctness of the wording of this principle.

According some authors, the term "creativity" or "creative activity" is incorrect and it’s more literary than legal content, and that its interpretation in the absence of legal definition, can lead to misjudgment about which objects to be protected and which - no. [4] But other authors argue that the term "result of creative activity" contains within itself implicitly the criteria of novelty and originality work and danger lies not in determining the objects of copyright protection. [5] In support of this assertion is art. 1, par. 3 of the Directive, which says, "The computer program is protected if it is original in the sense that it is their own intellectual work of the author." [3]

Despite different opinions, it is undisputed that it is a distinction between a new and original work, the result of intellectual creativity of the author, from literal copying or reproduction of an existing product.

The last of the three criteria that need to fullfill a work is:

• to be expressed in any way and in any objective form

Our legislation follows the European legal conception under which a work is sufficient to be embodied in a form that is or can be objectively perceived, for it to be the subject of protection of copyright. The way of expression and the form in which the work is objectified are not important. Computer programs fulfill this criteria admittedly too.

However, computer programs that fully fulfill those criteria and there can be no doubt to them if they are objects of copyright or not, our legislature has considered it necessary to explicitly indicate them in the non-exhaustive list of protected object of art. 3, par. 1, item 1 of the CRRL.

2. PROTECTION OF COMPUTER PROGRAMS BY PATENT LAW

In the patenting of computer programs appear two main problems:

• The majority of industrial property laws in the world specifically exclude computer programs as such from the circle of innovation.

• Another issue is whether the patenting of computer programs are technical in nature and represent a technical solution to a problem such inventions.

In the Republic of Bulgaria computer programs are specifically excluded from protection in the Law of Patents and Registration of Utility Models (LPRUM), they are not considered as inventions to some extent. [6] But the exclusion applies only to cases in which protection is sought for them as such. Which means that a computer program can be protected as an invention by the Bulgarian legislation, if it fulfills certain conditions. These conditions are:

• Program is not applied to itself;

• The program is part of or be incorporated in the invention (technical device, method) in order to proof of a technical nature);

• Invention, which is incorporated into the program to fulfill the criteria for patentability.

3. ADVANTAGES AND DISADVANTAGES OF VARIOUS MEANS OF PROTECTION

Advantages and disadvantages of the two main mechanisms of protection of computer programs need to be addressed in the following aspects:

• procedure for protection;
• scope of exclusive rights;
• duration of protection;
• the opportunity to prosecute offenders.

Procedure for protection

In terms of procedure for protection of computer programs more beneficial to the creators of the software is a copyright protection mechanism. It is automatically provided at the time of the creation of the program and her expression. While protection of computer programs by patent law is necessary to go "heavy" process expertise, in addition to the presence of the criteria for patentability of computer program will need to demonstrate a technical nature and find ways for incorporating the program in technical device, method or system.

However there are some drawbacks from protection through CRRL, because it's more difficult to prove the moment of the creation to the program if there is a dispute on its authorship. While the patent protection beginning is evidenced by the date of the patent document.

Scope of exclusive right

Rights of authors of computer programs under CRRL are:

• moral;
• property.

According to Article 15 par. 1 of the CRRL, the moral rights of authors of computer programs are as follows:

- The author has the right to decide whether it created programming to be disclosed and to determine the time, place and manner in which to do so;

- The author has the right to seek recognition of his authorship in the program;

- The author has the right to decide whether its program to be disclosed under a pseudonym or anonymously;

- The author has the right to ask his name, his pseudonym or other identifying copyright mark it to be labeled appropriately with any use of the computer program;

- The author has the right to ask for preserving the integrity of the work and to oppose any changes to it

- The author has the right to change the program if this does not infringe the rights acquired by others;

- The author has a right of access to the original computer program, where she is in possession of another person

- The author has the right to suspend the use of the program due to changes in their beliefs as to compensate victims who have legally acquired the right to use the program.

According to Article 18 paragraph 1 of the CRRL property rights associated with the use of the computer program and authorization of use by other persons to whom the author is entitled to seek and obtain compensation. For acts of exploitation shall be considered: the reproduction of computer programs, broadcasting of the program, the computer program broadcast by wireless means, the processing of the computer program, computer program for translating into another language (from one computer language to another would be a translation of the program); demand in the wireless router, cable or other technical means of access to an unlimited number of persons to the computer program.

The holder of a patent for an invention in which the incorporation is a computer program, according to Art. 19 of LPRUM acquires exclusive rights, including the following powers: the right to use the invention, the ban others from using it without the consent of the patentee the right to dispose of the patent.

In terms of scope of protection can be said that both options provide significant protection to holders of rights to commercial use of computer programs and make a profit from such use. Copyright protection measures in use are detailed, unless expressly included and rights of users of computer programs. And although the approach of determining the scope of exclusive rights in patent law is different, it was clearly demonstrated what can make the owner of an exclusive right protected by the computer program.

Term of protection

The term of copyright in a computer program has a duration of life of the author plus 70 years after his death. For computer programs created within the employment relationship, the period is 70 years after their disclosure. The term of protection of the invention, which is incorporated in the computer program is 20 years from the date of filing.

There is no question what kind of protection is more appropriate from the viewpoint of the criterion duration of protection - copyright. But in view of

the high speed at which computer technology is evolving and changes in the incidence of end products, which is within months, the period of protection of computer program patent also is not small at all.

Opportunity to prosecute offenders

In the CRRL and in LPRUM, offenders are considered for those who perform actions with the object of protection without the author's consent or in violation of the provisions of law. In CRRL said that "who violate copyright or related right, due to the rightholder or the person to whom it is granted to the exclusive right to use damages. While in LPRUM "any use of the invention which comes within the scope of patent protection and is made without the consent of the patentee is a patent violation. Although the texts are different in itself is a meaning to them.

There are two main issues in prosecuting violators of the rights to computer programs and CRRL, and LPRUM:

• Which individuals will be considered for offenders in respect of acts committed without the consent of the author, or which are inconsistent with the statutory provisions to the protected site;

• Which individuals will be considered as such in respect of acts done without the author's consent or in violation of the law, in view of the scope of exclusive rights.

Copyright does not protect ideas, but the shape of the object, how the external expression of the idea in the case of computer program code, which is painted. The exclusive right of the author of computer program results in a prohibition on copying and commercialization of this code. Copyright protects computer programs as such and such violators will be pursued those who just play the protected computer program and / or take action without the consent of the author (in violation of law) with this computer program.

But copyright does not protect the idea embodied in software, and how the machine works with this software. Ideas, practical knowledge embodied in the facility can be protected only by patent law. In patent law the scope of legal protection is defined by the claims. A claims cover not only as expressed, but their equivalents. Which means that the scope of protection of the computer program under patent law is not only the exact copy and use the computer program without the consent of the patentee, but also on the equivalent of the attributes of a computer program expressed in the patent claims.

An element is considered equivalent to an element as expressed in the claims where:

• perform essentially the same function in the same manner and gives essentially the same result;

• a specialist in the field is obvious that the priority date of the result obtained by the element, expressed in the claims can be obtained by the equivalent.

From this perspective, patent law provides better opportunities for the prosecution of offenders compared with the system of copyright.

In view of the scope of the exclusive right, even though both laws provide a wide range of rights for creators of computer programs, opportunities to prosecute violators differ. In the copyright protection measures of use are detailed and comprehensive. Which means that if possible other action against the protected computer program falling under the scope of the actions described in the law, the person performing the action, will hardly be considered in default. While patent law in action within the scope of use of the computer program are not exhaustive and is listed as a possible violators must be prosecuted and persons engaged in acts contrary to laws which are not specifically mentioned in the law, but are using computer program.

The issue of protection of computer programs is still controversial and internationally and nationally. The choice of method of protection for computer programs is a matter of discretion on the part of their creators and goals to pursue. Bulgarian legislation allows the accumulation of protection that allows the creators of computer programs to take advantage of all the advantages of both types of protection and eliminating their disadvantages.

References

[1] Гълъбова, С. Интегративност на източниците на научна информация и интелектуалната собственост, стандартизацията и управлението на качеството. С., WINI-1837, 2009, 411 с.

[2] Закон за авторсктото право и сродните му права. // Държ. вестник, бр. 56, 1993; изм. Държ. вестник, бр. 32 от 28.04.2009.

[3] Directive 2009/24/EC of the European Parliament and of the council of 23 April 2009 on the legal protection of computer programs

[4] Лозев, Е. Актуални проблеми на авторсктото право и сродните му права. С. Сиела, 2007, 203 с.

[5] Саракинов, Г. Авторско право и сродните му права в Република България, С. Сиби, 2005г., 311с.

[6] Закон за патентите и регистрацията на полезните модели. // Загл. Изм. Държ. вестник, бр. 64, 2006; изм. Държ. вестник, бр. 36 от 04.04.2008.

BIOINFROMATICS AND INTELLECTUAL PROPERTY

Tereza Trencheva[1], Ivan Trenchev[2], Peter Milanov[2], Ivan Mirchev[2]
State University of Library Studies and Information Technologies[1],
Sofia, Bulgaria, e-mail: e-mail: tereza_trencheva@abv.bg
South-West University "Neofit Rilski"[2], Blagoevgrad, Bulgaria

***Abstract**: The article aims to describe the nature of bioinformatics and its relation to intellectual property. Bioinformatics is presented by its three main categories: first of all biological sequences such as DNA, RNA and protein sequences; second of all databases in which these sequences are organized; and third of all software and hardware designed to access, organize and analyze information contained within this sequences and databases. The article analyzes how these three categories of bioinformatics are related to Patent law, Copyright law and where protection may be available and practical.*

***Keywords:** bioinformatics, DNA, RNA, intellectual property, copyright, patents, databases*

1. INTRODUCTION

Bioinformatics is a relatively new discipline which has gained much recognition in the last decade. In fact Bioinformatics is a quite new interdisciplinary scientific area, which operates at the intersection of Biology (Molecular Biology, Biotechnology, Genetic Engineering), Chemistry (Biochemistry), Mathematics, Engineering, Computer Systems and Computational Biology. It can be defined in simple terms as the use of **informatics** for the investigation of **biological databases.**

It can be hard to describe what bioinformatics *is*, it is somewhat easy to explain what bioinformatics is *not* -- it is not just using computers to look at biological sequence data.

Bioinformatics has very fast become established as a main branch of modern bioscience, with a assortment of sophisticated tools for analyzing proteins and genes, ***in silico, in vitro***, and ***in vivo***.

In common, we can say that bioinformatics is concerned, but not limited to:

- modeling of biological systems and functions;
- analysis of laboratory data;
- generation models based on accumulated data from experiments;
- study of new data using mathematical models;

- recognition motifs in the experimental data;
- predicting functions of genes and proteins.
- in silico experiments.

Using a computer in bioinformatics is ideal for the job of analysing biological complex data sets, such as sequence data for proteins and nucleic acids. This often involves a series of computing procedures, each of which may be comparatively simple in isolation. The calculation may need to be repeated millions of times; therefore, it is momentous that this is achieved quickly and exactly.

Before one can understand intellectual property protection for bioinformatics, it’s necessary to understand the nature of the various components that comprise the field of bioinformatics.

For the purpose of this article, in general bioinformatics is presented by its three main categories: first of all biological sequences such as DNA, RNA and protein sequences; second of all databases in which these sequences are organized; and third of all software and hardware designed to access, organize and analyze the information contained within this sequences and databases.

2. BIOLOGICAL SEQUENCES - DNA, RNA AND PROTEIN SEQUENCES

A biological sequence is a single, continuous molecule of nucleic acid or protein.

Biological sequences can be presented as follows:

- DNA (nucleotides, 4 types): storage of the genetic information;
- RNA (nucleotides, 4 types): bridge from DNA to protein;
- Protein (amino acids, 20 types): active molecules.
- Genetic code: deciphering genetic information.

The main role of DNA molecules is the long-term storage of genetic information. The four bases found in DNA are adenine (abbreviated A), cytosine (C), guanine (G) and thymine (T)[1]. These four bases are attached to the sugar/phosphate to form the complete nucleotide *(O’Neil, 2000).*

Like DNA, RNA is made up of a long chain of components called nucleotides. Each nucleotide consists of a nucleobase, a ribose sugar, and a phosphate group. The sequence of nucleotides allows RNA to encode genetic information[2]. The chemical structure of RNA is very similar to that of DNA, with two differences-(a) RNA contains the **sugar ribose** while DNA contains the slightly different sugar deoxyribose, and (b) RNA has the

[1] Definition of DNA according Wikipedia: http://en.wikipedia.org/wiki/DNA
[2] Definition of RNA according Wikipedia: http://en.wikipedia.org/wiki/RNA

nucleobase **uracil** while DNA contains thymine. The protein is a sequence of 20 standard amino acids.

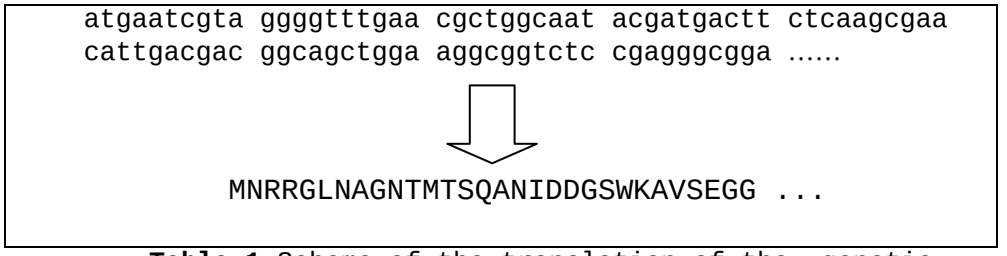

Table 1 Scheme of the translation of the genetic information from DNA to protein

3. BIOINFORMATICS DATABASES.

Bioinformatics Databases play a key role in bioinformatics for the collection, storage and maintenance of biological data *(D'Souza, 2004 : 35).* To search for information on biological, physicochemical, biochemical and others. characteristics of different nucleotide sequences and amino acids and the sites on which they are obtained it using biological databases.

Bioinformatics database is a combined product of biotechnology and information technology and plays a vital role in accelerating modern life science research *(Chang, Zhu, 2010 : 447-454)*

Basics elements of these databases are:

- sequence - a key element showing the sequence of nucleotides or amino acids, it is continuous, as found in nature, if the sequence has not been investigated fully, then each fragment is a separate record, nucleotides are marked with four Latin letters A, G, T, C, amino acids with a three-letter code, for example, amino acid series are marked by Ser, amino acid meteonin - Met; nucleotides in the database is marked with four small Latin letters a, c, g and t, and AK with a big Latin letter as serine is denoted with S;
- Length - the number of nucleotides or the number of amino acids involved in sequencing sequence;
- The type of nucleic acid - DNA, mRNA, tRNK, rRNA;
- Location - Defines the position of the 5 'end of the nucleotide chain or the location of the genetic map;
- Segment - defines the relationship between adjacent, disjoint sections of the sequences if the distance between two or more sequences known to be marked and the number of amino acids or nucleotide. *(McBride, 2002 : 13)*

Some of the most popular database in the field of bioinformatics are ExPASy, KEGG and NCBY. They are freely available, as the oldest of them is ExPASy, established in 1993 in Geneve.

4. SOFTWARE FOR BIOLOGICAL DATABASES

Software for access, organization and analyses of biological sequence and databases can be freely available or commercial. Here are some examples for commercial software.

Matlab is a software package, built on a modular principle which has its own language, called the M language, which is similar to the language C + +. The advantage of Matlab is the ability to visualize data in 3D graphics.

CIPLEX is an optimization package to IBM, which can perform both integer optimization, and continuous. This package solves very successfully problems which examine HPfolding.

Tomlab is a software package for optimization that runs in the middle of Matlab, but is installed separately. It has more options than optimization program Matlab.

Hyperchem is a software product that provides good opportunities for establishing a chemical molecular models, spatial monitoring of the established models and tools to optimize them. During the creation of models can be set and changed certain lengths of chemical bonds, valent and torsion angles and atomic charges. Moreover, the program has databases of amino acids and nucleosides, which makes it easy to be modeled natural polymers - protein and nucleic acids.

5. MAIN TYPES OF INTELLECTUAL PROPERTY IN BIOINFORMATICS

Intellectual property protection in bioinformatics is a really important process. As it not only afford the owner, the right to exclude others from using the protected technology, but can also potentially provide he owner a monopoly right for manufacture and sale the technology *(Muralidharan, 2005 : 43).*

Intellectual property protection for bioinformatics is a largely untested area in Bulgarian legislation. However, it’s clear that ability to obtain intellectual property protection in any given area of bioinformatics depends on the type of bioinformatic tool involved.

In Bulgaria Copyright can be used to protect bioinformatics-related materials such as scientific articles, books, software, compilation of facts (databases), manuals and etc.

According to the Law of patents and registration of utility models by a patent can be protected, "an element isolated from the human body or

otherwise obtained through the technical process, including the sequence or partial sequence of the gene may constitute a patentable invention, even if the structure of this element is identical to that of a natural element".

Trade secrets can be used to protect Bioinformatics-related intellectual Property such as software code, manuals, databases, formulas and processes.

Trademarks can be used to protect trade names, product names, domain names, and service marks/slogans for bioinformatics companies.

6. CONCLUSION

Bioinformatics comprises a wide array of components, and it follows that a wide array of protection might be available, depending on the particular nature of the bioinformatic component and its intended use. In Bulgaria the IP protection of bioinformatics is still in the begging and there will be a lot of discussions on this hot point of innovation. The article just aimed to outline the framework of main types intellectual property forms of bioinformatics according the Bulgarian laws.

7. ACKNOWLEDGEMENTS

This study was supported by Grant DVU 01/0197 of Ministry of Education and Science.

REFERENCE

1. ***Chang**,J., Zhu,X., Bioinformatics Databases: Intellectual Property Protection Strategy, 2010, Journal of Intellectual property rights, Vol.15, p. 447-454*
2. ***D'Souza**, S. Gene meets machine: Intellectual Property issues in Bioinformatics, 2004, Health Law Review,Volume 12, Number 2, p. 34 – 43*
3. ***McBride**, M. Bioinformatics and Intellectual property protection, 2002, Berkley technology law journal, Vol 17:1, p.33*
4. ***Muralidharan**, R. Intellectual property rights in bioinformatics and biotechnology, 2005, Krishna & Saurastri Assosiates, p. 43-49*
5. ***O'Neil**, S.A., 2000. Mapping the human genome. Hillards Lyons Equity Research.*
6. ***Закон** за авторското право и сродните му права. // Държ. вестник, бр. 56, 1993; изм. Държ. вестник, бр. 32 от 28.04.2009.*

7. ***Закон*** *за патентите и регистрацията на полезните модели. // Загл. Изм. Държ. вестник, бр. 64, 2006; изм. Държ. вестник, бр. 36 от 04.04.2008.*

Bioinformatics research of 3D structure of the proteins

Radoslav Stoev, Kiril Gashteovski, Ivan Todorin, Ivan Trenchev[1], Nadezhda Borisova, Metodi Traykov
South-West University "Neofit Rilski", Blagoevgrad, Bulgaria

***Abstract**: In this article we will represent a HP model for protein folding using their properties in water environment. This model is based on combinatorial algorithms. Some of the examples will be solved by Branch and Bound. The calculations will be performed via CLPEX and MATLAB. Graphical software for presentation of the results will be demonstrated.*
***Keywords:** Bioinformatics, 3D structure, HP folding.*

1. INTRODUCTION

The HP folding in lattice models, which are used for prediction of the 3D structure of proteins, are based on the fact, that in the cell environment, peptides fold in a way, in which more hydrophobic amino-acids are closed together in a kernel, in contact between them, and more polar amino-acids are oriented outside in contact with the water in the cell environment [5]. The first HP model of this kind has been presented by Ken Dill in 1985. Such a form of the folded peptide is with minimum of the potential energy, because of the hydrogen bonds between water molecules and polar amino-acids and it is more stable, so we can expect that a 3D structure, which is folded like this, will be the real case. In this way we can predict the 3D structure of a protein from its primary structure [3]. Today many primary structures of proteins are known and less their 3D structures, which determine the properties of the proteins. Databases with 3D structures are used in Drug Design, for simulation of ligand-target interactions, for pocket detection of targets, for virtual screening, etc. Enlarging such databases is in great interest of pharmacology, as it helps for cheaper and faster Drug discovery [1, 2, 4].

These models use combinatorial algorithms to find out a conformation of the folded protein, which has so many contacts between hydrophobic amino-acids, as possible. These contacts have to be counted for many possible conformations, which is very hard computational problem, because the number of possible folds is extremely large. The problem to be found out the structure with most contacts, which seems to be with minimum of the potential energy, is NP-complete [6, 7]. We have a possibility to obtain a

fold, which is close to the optimal, but we might miss to check the best one. Also we assume that the amino-acids are only two types – hydrophobic (H) and polar or hydrophilic (P), with equal size and ordered in cubic lattice of two types – face-to-face cubic lattice (FFC) and face-to-center cubic lattice (FCC) [8]. Last is necessary to improve the time for solving the problem by the contemporary computational resources. Different models may be improved for accuracy or for speed by choosing the lattice – FCC is more accurate, using backbone chain [9], including only the carbon atoms of the peptide connection or using side-chain structure, in which the other part of the amino-acid is oriented in one of the possible sides in its own position in the lattice, etc.

2. METHODOLOGY

In the following model, an input sequence of numbered amino-acids is used, in which every member is defined as H – in case of a hydrophobic amino-acid, and as P – in case of a hydrophilic (polar) amino-acid [6]:

INPUT PPHP...H

All amino-acids have to be put in a cubic lattice with m rows and m columns, which lattice is transformed in a row:

m x m – lattice (i,j) i,j $\xrightarrow{(i-1)m+j}$ i

Every position in the lattice and its occupation of any member of the input sequence is assigned as a point, so if member k is put in the position i – this variable has value 1, otherwise it has value 0:

m^2n – points $x_{ik}\{1,0\}$

Every member k has to be put just in one position:

$$\sum_{i=1}^{N} x_{ik} = 1 \text{, for every k}$$

Every position i might be occupied only by one member or it might be free:

$$\sum_{k=1}^{N} x_{ik} = 1 \text{, for every i}$$

If a position is occupied by a member, we must have at least one occupied position neighbor to it, or if it is free, we might have zero or more occupied neighbor positions:

$$x_{ik} \leq \sum_{j \in G(i)} x_{jk+1} \text{ , G(i) is a set of all neighbors of } x_{ik}$$

We define additional variable y, which has value 0 or 1 if two neighbor cells in the lattice are occupied by hydrophobic amino-acids:

$$x_{ik} \leq \sum_{j \in G(i)} y_{ikjl}$$

where G= {l-k>2∩Sk=H∩Sl=H}

$$x_{jl} \leq \sum_{i \in G(j)} y_{ikjl}$$

G(j) – set of points, neighbor to j

The final goal is the maximum number of contacts between hydrophobic amino-acids, which is represented by our variable y:

$$\max \sum y_{ikjl}$$

We will present a table with classification of amino-acids according to their hydrophobic properties [9].

Name	Symbol	Classification	Name	Symbol	Classification
Alanine	A	Hydrophobic	Leucine	L	Hydrophobic
Arginine	R	Polar	Lysine	K	Polar
Asparagine	N	Polar	Methionine	M	Hydrophobic
Aspartic Acid	D	Polar	Phenylalanine	F	Hydrophobic
Cysteine	C	Polar	Proline	P	Hydrophobic
Glutamic Acid	E	Polar	Serine	S	Polar
Glutamine	Q	Polar	Threonine	T	Polar
Glycine	G	Polar	Tryptophan	W	Hydrophobic
Histidine	H	Polar	Tyrosine	Y	Polar
Isoleucine	I	Hydrophobic	Valine	V	Hydrophobic

TABLE 1: Hydrophobic / Polar classification of the 20 a-amino-acids.

We have developed a software, written on C++, which transform protein sequence in FASTA format into a sequence of 0 and 1, where 0 is for a polar amino-acid and 1 is for a hydrophobic amino-acid.

3. RESULTS

We will present three examples. The first and the third example are calculated on a 3D lattice and the second example on a 2D lattice [5, 7, 8].

All calculations will be done by using the software package CPLEX, for which we have a license for academic use from the IBM [8]. The package has been installed on an IBM server.

For every example we have developed a software, which calculates an input LP file for CPLEX. The time for calculation of the three examples is generally 36,5 hours.

We have also developed a software for visualization in 3Ds Max.
The following calculations are done for the protein 1101010101.

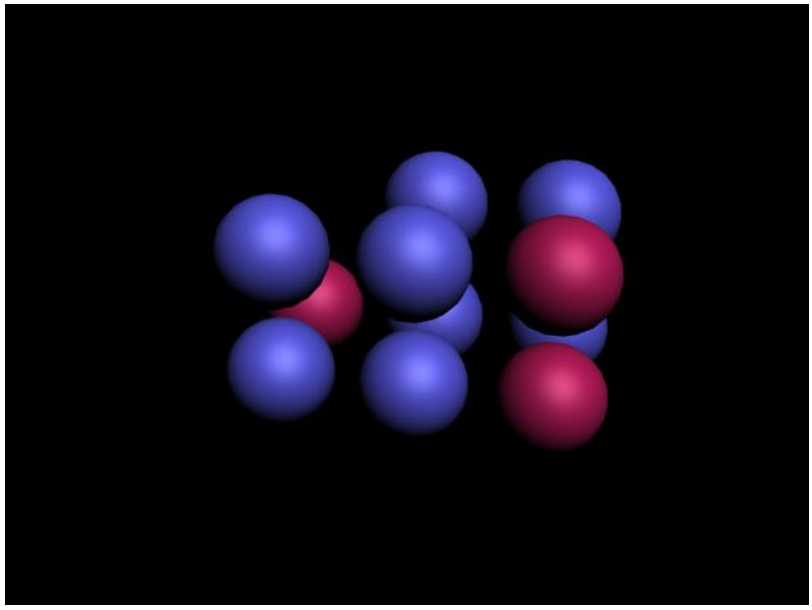

Fig. 1: Solution of the protein 1101010101.

The next figure represents the result for the described protein in 2D lattice.

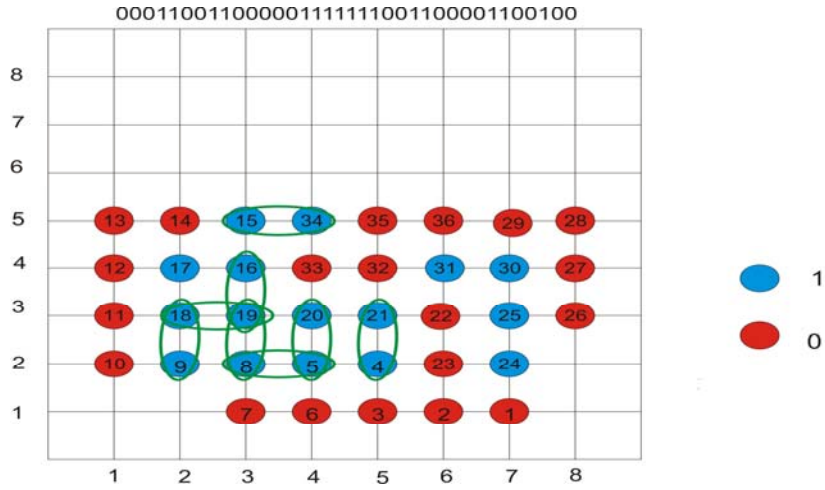

Fig. 2: Solution of the protein 0001100110000011111111001100001100100.

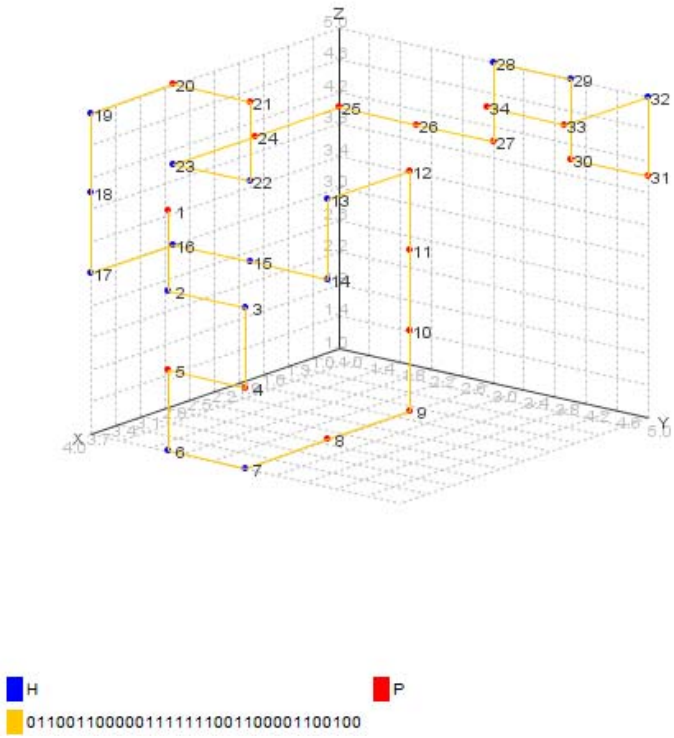

Fig. 3: Solution of the protein 10100110100101100101

4. CONCLUSIONS

Our mathematical model can be used in the gene engineering for modelling of the 3D structure of the RNA. RNA has enzyme activity and we can predict some structures and properties of it.

5. ACKNOWLEDGEMENTS

This study was supported by Grant DVU 01/0197 of Ministry of Education and Science.

6. REFERENCES

[1] Duan Y., Kollman P. A. (2001) Computational protein folding: From lattice to all-atom. IBM Systems Journal, 40, 297–309.
[2] Dyson F.. (2008) Birds and frogs. Notics of the American Mathematical Society, 56:212–223 .
[3] Guo Y.Z., Feng E., Wang Y. (2007) Optimal HP configurations of proteins by combining local search with elastic net algorithm. J. Biochem. Biophys. Methods 70, 335–340
[4] Hengyun L., Yang G. (2009) Extremal Optimization for protein folding simulations on the lattice Computers and Mathematics with Applications 57 1855-1861
[5] Istrail S., Hurd A., Lippert R., Walenz B., Batzoglou S., Conway J. H., Peyerl F. W. (2000). Prediction of self-assembly of energetic tiles and dominoes: Experiments, mathematics, and software. Sandia National Labs Technical Report, April.
[6] Jiang M., Zhu B. (2005) Protein folding in the hexagonal lattice in the hp model. J. of Bioinformatics and Computational Biology, 3 19–34.
[7] Namsu A. Park S., (2010) Finding an Upper Bound for the Number of Contacts in Hydrophobic-Hydrophilic Protein Structure Prediction Model Journal Of Computational Biology 17(4), 647–656
[8] Neumann J. V. (1947) The mathematician. in ”The Works of the Mind”, University of Chicago Press, 180–196
[9] Shakhnovich E. (1996) Modeling protein folding: the beauty and power of simplicity. Folding and Design, 1, 50–54.

Matrix representation of a solution of a combinatorial problem of the groups theory

Krasimir Yordzhev, Lilyana Totina
Faculty of Mathematics and Natural Sciences
South-West University
66 Ivan Mihailov Str, 2700 Blagoevgrad, Bulgaria
E-mail: yordzhev@swu.bg , liliana_totina@abv.bg

***Abstract**: An equivalence relation in the symmetric group S_n, where $n \geq 2$ is a positive integer has been considered. An algorithm for calculation of the number of the equivalence classes by this relation for arbitrary integer n has been described.*

***Keywords:** Symmetric Group, Equivalence Relation, Equivalence Classes, Directed Graph, Euler Function, C++ Programming Language*

1. INTRODUCTION

The object of the present study is to be received an algorithm for computer calculation of some combinatorial characteristics of the symmetric group. This algorithm has been based on the theoretical elaborations described closely in [3] and [4].

In our study with $\mathbb{N}$ we denote the set of the positive integers. Let $n \in \mathbb{N}$. Then with $\mathbb{Z}_n$ we denote the set

$$\mathbb{Z}_n = \{1, 2, \ldots, n\}.$$

With

$$S_n = \left\{ \begin{pmatrix} 1 & 2 & \cdots & n \\ i_1 & i_2 & \cdots & i_n \end{pmatrix} \middle| \, i_s \in \mathbb{Z}_n, s = 1, 2, \ldots, n, i_s \neq i_t \text{ for s} \neq \text{t} \right\}$$

we denote the symmetric group on the set $\mathbb{Z}_n$, i. e. the group of all one-to-one mappings $\alpha : \mathbb{Z}_n \to \mathbb{Z}_n$ of the set $\mathbb{Z}_n$ in oneself.

If $k, m \in \mathbb{N}$ then with $GCD(k, m)$ we denote the greatest common divisor of integers k and m. Then k and m are relatively primes if and only if when $GCD(k, m) = 1$.

With $\varphi(n)$ we denote the Euler function, i. e. the number of elements of $\mathbb{Z}_n$ that are relatively primes with n (see more for example in [1] or [5]). By definition $\varphi(1)=1$.

2. PRIOR INFORMATION

Let n be a positive integer. We consider an element

$$\sigma=\begin{pmatrix}1 & 2 & \dots & n-1 & n\\ 2 & 3 & \dots & n & 1\end{pmatrix}\in S_n.$$

In [3] the following equivalence relation had been introduced in S_n: we say that $\alpha,\beta\in S_n$ are σ - equivalent if the integers k and l exist such that $\alpha=\sigma^k\beta\sigma^l$, that is equivalent to condition that integers k_1 and l_1 exist such that $\sigma^{k_1}\alpha=\beta\sigma^{l_1}$. The following task has been put: To find the number of the equivalence classes by so defined equivalence relation, with another words the cardinality of the factor set $Q_n=S_{n/\sigma}$.

To be solved so putting task a directed graph Γ_n with the set of vertices

$$V_n\subset\mathbb{Z}_n^2=\left\{\langle a,b\rangle \mid a,b\in\mathbb{Z}_n\right\},$$

has been constructed, formed by the next mean:

1. For every integer $m\in\mathbb{Z}_n$ such that $GSD(n,m)=1$ a vertex $\langle 1,m\rangle\in V_n$ exists, as in this vertex arcs do not enter.
2. If $\langle k,l\rangle\in V_n$, then k divides n.
3. Let $\langle k,l\rangle\in V_n$ and let p is a prime divisor of $\frac{n}{k}$. Then we receive the number r that is equal to the remainder after the multiplication pl is divided into n. We construct a vertex $\langle pk,r\rangle\in V_n$ and an arc with begin the vertex $\langle k,l\rangle$ and end the vertex $\langle pk,r\rangle$.
4. Another vertex and another arc in the graph Γ_n accepting received by the mean described above do not exist.

For example at $n=12$ the graph Γ_{12} is shown on figure 1:

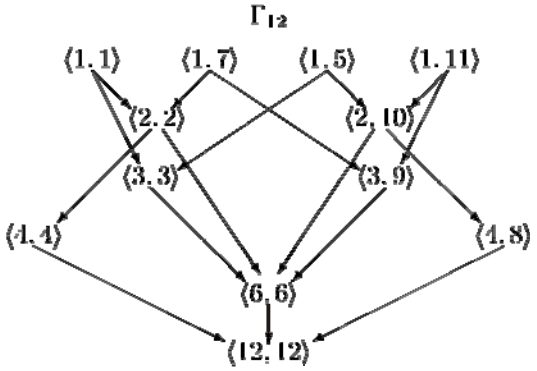

Fig. 1: The graph Γ_{12}.

We introduce the following partial order in the vertices set V_n of the graph Γ_n: If $v_1, v_2 \in V_n$, then $v_1 < v_2$ if and only if when a directed path with begin vertex v_1 and end vertex v_2 exists. It is easily to see that by so introduced order V_n is semilattice with the unique maximal element $\langle n, n \rangle \in V_n$ and $\varphi(n)$ in number minimal elements, each of kind $\langle 1, m \rangle \in V_n$, where $\varphi(n)$ is the Euler function.

For more details of the graph theory see for example in [6].

For each vertex $\langle k, l \rangle \in V_n$ we define the function $h(n,k)$ that depends on n and k, but does not depend on l.

$$h(n,k) = \frac{1}{k}\left((k-1)! \left(\frac{n}{k}\right)^{k-1} - \sum_{\langle r,t\rangle < \langle k,l\rangle} r\, h(n,r) \right) \tag{1}$$

The following assertion had been demonstrated in [3]:

Theorem 1 [3] *The number of the equivalence classes by the σ-equivalence is equal to*

$$|Q_n| = \sum_{\langle k,l\rangle \in V_n} h(n,k) \tag{2}$$

Theorem 1 gives us an effective algorithm for the manual calculation of $|Q_n|$. Construction of the graph Γ_n is necessary for this object. This approach gives relatively good results at relatively small values of n as the experience of authors has been shown. With

increase of n probability of errors increases repeatedly, because of the number of classes increases exponentially, according to formulas (1) and (2).

It had been demonstrate in [4] that all assertions considered in [3] are valid for an arbitrary element $\sigma \in S_n$, on condition that σ is a cycle with length n.

It is easy to see that we can reorganize the formula (1) in the following recursive kind:

$$h(n,k) = \frac{1}{k}\left((k-1)!\left(\frac{n}{k}\right)^{k-1} - \sum_{\substack{r|k \\ r<k}} r\,\tau(n,k,r)\,h(n,r) \right) \quad \text{for} \quad k>1 \tag{3}$$

and

$$h(n,1) = 1, \tag{4}$$

where the function $\tau(n,k,r)$ gives as the number of vertices $\langle r,s\rangle \in V_n$, such that $\langle r,s\rangle < \langle k,k\rangle \in V_n$.

The following assertion had been demonstrated in [4]:

Theorem 2 [4] *The number of the vertices of kind* $\langle k,l\rangle \in V_n$ *is equal to* $\varphi\left(\frac{n}{k}\right)$, *where* $\varphi(m)$ *is the Euler function.*

As a consequence of theorem 2 the formula (2) has been reorganized in the following kind:

$$|Q_n| = \sum_{k|n} h(n,k)\,\varphi\left(\frac{n}{k}\right) \tag{5}$$

3. MATRIX REPRESENTATION AND PROGRAM REALIZATION

In this section we use program language C++ for description of algorithms considered in the present study. The program was been tested in a programming environment Borland C++ Builder.

At the examples we consider that n is a global constant integer parameter, equal to the order of the group S_n and may be used without explicit declaration.

For using theorem 1 as we avail ourselves of formulas (3) and (4) it is convenient to fill the elements of the matrix $M = \left(m_{ij}\right)$, consisting of 4 rows and q columns, where q is equal to the number of all positive divisors of the integer n (including 1 and n). Never the less the integer will be written down in M, in our program realization we declare M as two-dimensional array of type double because of fact that we expect to receive too large values at calculation of the function $h(n,k)$ according to formula (3).

In the first row we write down all integers dividing without remainder the parameter n. That can be realized with the help of the following procedure, for example:

```
void Divisors(int n, int FirstRow[], int& q)
{
 q = 1;
 FirstRow[0] = 1;
 for (int t = 2 ; t <= n; t++) {
    if (n%t == 0) {
       FirstRow[q] = t;
       q++;
    }
 }
}
```

As additional effect of the work of the function Divisors we receive the number q of all divisors of the global parameter n. It the end the procedure receives an integer array FirstRow, correctly filled with the divisors of n. We copy the values of the array FirstRow to first row of the array M.

We fill the second row of M with the values of the Euler function $\varphi\left(\frac{n}{k}\right)$, where k has been taken from the corresponding component of the first row of M. The function $\varphi(m)$ can be realized as we use a variety of the algorithm, known as “the Sieve of Eratosthenes” [2,5]

```
int EulerFunction(int m) {
 int t =1;
 int b[100];
 for (int i=1; i <= m; i++) {
    b[i] = i;
```

```
 }
 for (int i=2; i <= m; i++) {
    if (b[i] == 0) {
       continue;
    }
    if (m%b[i] == 0) {
       for (int j=1; i*j<=m; j++) {
          b[i*j] = 0;
       }
    }
    else t++;
 }
 return t;
}
```

We fill the third row of M with the values of the function $h(n,k)$, according to formulas (3) and (4), where k has been taken from the corresponding component of the first row of M. Here we consider again that n is a global constant parameter, i.e. it is not necessary n to be present in the list of formal parameters of the function described below. For simplicity of the exposition we will not verify correctness of the data, i.e. whether k divides n. This condition has been ensured by the fact that k has been taken from the first row of the matrix M, where on condition only divisors of n has been written down. We declare the type of the function h(int), as well as some working variables, which values are integers with the type long double because of expectation to receive to large values according to formula (3).

For the calculation of the function $h(n,k)$, must first be calculated the function $\tau(n,k,r)$. This can be done using the following algorithm:

// Euclidean algorithm for finding the greatest common divisor of integers a and b:

```
int GCD(int a, int b) {
 while (a != b)
    if (a > b) {
       a = a-b;
    }
    else b = b-a;
 return a;
}
```

```
//------------------------------------------------------------------------

// Function examined whether ⟨k,l⟩ is the vertex of V_n

bool Vertex(int k, int l, int n) {
 if ((k<=0) || (k>n) || (l>n) || (n%k != 0)) {
    return false;
 }
 else {
   if ((k == n)) {
      if (l == n) return true;
   }
   else
     for (int m=1; m<=n; m++) {
        if ((GCD(m,n) == 1) && (m*k%n == l)) return true;
     }
 }
 return false;
}

//------------------------------------------------------------------------

// The function τ(n,k,r):

int tau(int n, int k, int r) {
 int t=0;
 int p = k/r;
 for (int s=1; s<n; s++) {
    if (Vertex(r,s,n) && (s*p%n == k%n)) {
       t++;
    }
 }
 return t;
}
```

Then an algorithm for obtaining $h(n,k)$ according to formulas (3) and (4) can be realized using the following C++ function:

```
long double h(int n, int k) {
 long double t;
 if (k == 1) {
    t=1;
 }
```

```
    else {
       long double fact = 1;
       for (int i=2; i <= k-1; i++) {
          fact = fact*i;
       }
       long double pow = 1;
       int p = n/k;
       for (int i=1; i<=k-1; i++) {
          pow = pow*p ;
       }
       long double sum = 0;
       for (int r=1; r<=k-1; r++) {
          if (k%r == 0) {
             sum = sum+r*tau(n,k,r)*h(n,r);
          }
       }
       t = (fact*pow-sum)/k;
    }
    return t;
   }
```

We receive the fourth row of M as multiply component by component the second with the third rom.

Here we will skip the description of the main function and the input and output operations as they are specific to different programming environments.

At $n=12$ the filled matrix M is shown in table 1:

Tab. 1: Matrix M at $n=12$.

$k \mid n$	1	2	3	4	6	12
$\varphi\left(n/k\right)$	4	2	2	2	1	1
$h\left(n,k\right)$	1	2	10	39	628	3326054
$m_{3j} * m_{4j}$	4	4	20	78	628	3326054

We receive the final result for the number $\left|Q_n\right|$ of the equivalence classes of S_n by the considered equivalence relation as we add the elements of the last row of the matrix M according to formula (5)

We calculate from table 1:

$$\left|Q_{12}\right| = 4+4+20+78+628+3326054 = 3326788$$

We show in table 2 the values of $|Q_n|$ at $n \leq 30$ calculated by the algorithm described above:

Tab. 1: The number of the equivalence classes in S_n concerning to equivalence at $n \leq 19$.

n	2	3	4	5	6	7	8	9	10
$\|Q_n\|$	1	2	3	8	24	108	640	4492	36336

n	11	12	13	14	15
$\|Q_n\|$	329900	3326788	36846288	444790512	5811886656

n	16	17	18	19
$\|Q_n\|$	81729688428	1230752346368	19760413251956	336967037143596

REFERENCES

[1] Andreescu, T., Andrica, D., Feng, Z. (2007) 104 Number Theory Problems. Boston: Birkhauser.

[2] Reingold E. W. (1977) Combinatorial Algorithms. Theory and Practice. New Jersey, Prentice-Hall.

[3] Yordzhev, K. (2004) On an equivalence relation in the set of the permutation matrices, in Discrete Mathematics and Applications, Blagoevgrad, SWU "N. Rilski", 77-87.

[4] Yordzhev, K. (to appear) On a Combinatorial Problem in the Symmetric Group.

[5] Мирчев, И., (1995) Теория на числата, Благоевград, ЮЗУ „Н. Рилски".

[6] Мирчев И., (2001) Графи. Оптимизационни алгоритми в мрежи, Благоевград, ЮЗУ „Н. Рилски".

Testing in the electronics manufacturing

Liudmila Taneva[1], Roumen Bagalev[2]
[1]South-West University, Blagoevgrad, Bulgaria, [2]Technical University, Sofia, Bulgaria

***Abstract**: Testing of the printed circuit boards and final products is vital part of the electronics manufacturing process. In this paper we will overview some of the most widely used tests in electronics manufacturing, their purpose and specifics and will outline the most important elements of the test strategy. There are two main test groups – structural tests and functional tests. The structural tests check the structure of the PCB/PCBA for open or short circuits; the quality of the solder joints; component presence and orientation etc. The functional tests validate the functionality of the devices and their performance. The paper describes CPU tests routines for testing MSP430 memory.*

***Keywords:** test strategy, PCB, structural tests, functional tests*

1. INTRODUCTION

The costs of the test could be one of the major costs of manufacturing a product and at high volume production it will have a huge impact. For this reason the test strategy must be chosen very carefully. The test strategy determines what tests and where in the manufacturing process to be used. The type of tests and the respective test equipment depend on many factors and the majority of them are directly related to the manufactured pro-duct itself. The technique of product design that adds certain testability features is known as Design For Test (DFT). Sometimes DFT stands for Design For Testability [3], which is the same. Well designed, with testability in mind products, provide easy and convenient access to the circuits and the test points and allow the use of the most efficient for this particular board test methodologies. Decisions about the way the sub-assemblies are tested must be taken as early as at the design stage to ensure that the optimum fault coverage is achieved for the lowest cost [5].

In this paper we will overview some of the most widely used tests in electronics manufacturing, their purpose and specifics and will outline the most important elements of the test strategy. Here are presented some fast algorithms for memory test, developed for MSP430 devices.

2. TYPES OF TEST

There are two main test groups – Structural tests and Functional tests. The structural tests check the structure of the PCB/PCBA for open or short circuits; the quality of the solder joints; component presence and orientation etc. The functional tests validate the functionality of the devices and their performance (fig. 1).

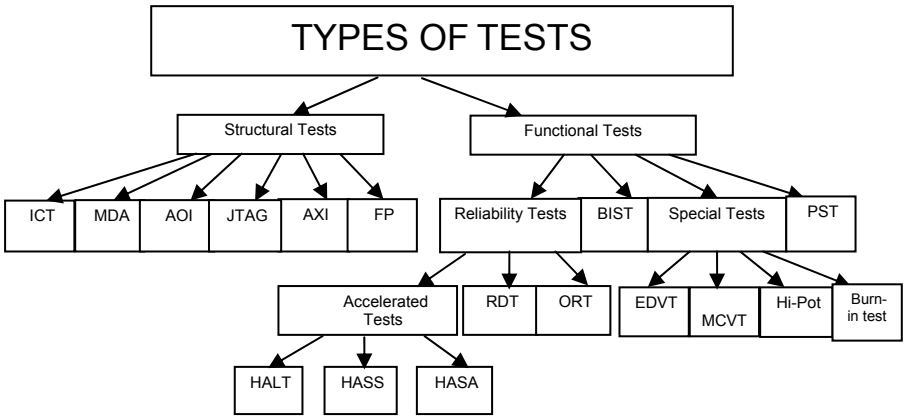

Fig.1. Classification of the tests in the electronics manufacturing

2.1. Structural Tests

2.1.1. In Circuit Test (ICT)

In Circuit Test (ICT) provides convenient and efficient way for testing boards circuits for opens and shorts as well as the components placement, orientation and value [1]. It is common during ICT some components, like CPLD or FPGA to be programmed or specific board information known as cookies to be written to an onboard EEPROM.

2.1.2. Manufacturing Defect Analyzer (MDA)

MDA is a simplified variant of ICT. It is used mainly for testing PCBs for opens, shorts and values of some components. Its coverage is limited compared to ICT, but its advantage is the significantly lower cost.

2.1.3. JTAG Boundary scan testing

JTAG test (Boundary scan logic) uses special integrated circuits with built-in shift registers on their outputs [2]. All JTAG compatible components are connected serially forming a loop. During the test the channel is enabled and test patterns are sent through it. At the output the test information is retrieved and analyzed.

2.1.4. Flying probe (FP)

FP testers are used mainly for testing of prototypes and production boards with limited access to the tested components. These testers use electro-mechanically controlled probes to access the assembled PCB.

2.1.5. Automated optical inspection (AOI)

AOI is a form of automated control and is widely used in many manufacturing areas. AOI provides very high level of discovering various solder defects, misplaced components, wrong parts or parts with wrong orientation and other visible defects.

2.1.6. Automated X-Ray inspection (AXI)

AXI is very similar to AOI, but works in the invisible spectrum using X-rays. The introduction of the BGA packaging called for finding a way to control optically inaccessible objects and AXI provides it.

2. 2. Functional tests (FT)

FT are usually performed after the product is fully assembled. Typically they emulate or simulate the real work of the device at various environment conditions. The purpose is to verify the functionality of the final product.

2.2.1. Reliability tests

- *Accelerated Test.* The purpose of this test is to artificially induce defects in lab environment by testing the product at stress conditions at the edge or slightly over the normal work parameters.

a) Highly Accelerated Life Testing (HALT) has four variations. Initially the tests are performed with temperature and step vibration load. The purpose of these tests is to find work tolerance (limits). They reveal the qualities of the product as a cyclic step change of environment variables such as temperature, shock and vibration.

b) Highly Accelerated Stress Screening (HASS) is another form of HALT. HASS is a constant product screening of the regular production. At this test the product is not tested to fail but rather for proper working at successively changing environment parameters.

c) Highly Accelerated Test Auditing (HASA). For high volume production where with volume increase the number of defects decrease is used HASS audit. The key parameters are monitored constantly on product samples and this way provide information on the process quality and stability.

- *Reliability Demonstration Test (RDT).*RDT is a process for product reli-

ability demonstration. It is used for determining the product readiness to be released to the market as well as its life span without work defects.

- *On-Going Reliability Testing)* (*ORT)* is ongoing test on samples of regular production units used for monitoring for tendencies of reliability change during the manufacturing process.

2.2.2. Special tests

- *Electrical Design Verification Test (EDVT)* is a test performed on the products prior their entering in the production phase. Its main purpose is to validate the electrical design of the product as well as the used materials and components for proper working at environmental stress conditions.

- *Material Change Verification Test (MCVT)* is a test performed for qualifying new parts or new vendors during the sustained phase of the production. The qualified parts and vendors are included in AVL. MCVT is very similar to EDVT in terms of the tests and the way they are performed.

- *High Potential Test (Hi-Pot)* is performed with high voltage, usually over 1000V and its purpose is to certify the product insulation is in compliance with the respective regulatory documents.

- *Burn-in test* is a test process designed for inducing the initial higher number of defects to appear during the manufacturing rather than at the field. For this purpose the product is tested at stress environmental conditions such as increased temperature, and increased voltage.

2.2.3. Product Specific Tests (PST) are real functional tests and they are specific for each particular product.

2.2.4. Built-in Self Test (BIST) is a conception for creating hardware and software structures inside a component allowing for it to self test.

3. BASIC STEPS IN TEST STRATEGY CREATION.

Developing a test strategy for electronic products [4] is as important as developing the product itself. This is a complex task that must take into account all aspects of product, including its design, complexity and type of board, the purpose of the device. It is necessary developing a test strategy to start at the outset to design the product and be done in parallel with it.

Here are the essential elements of a test strategy and they include the following phases: Phase 1: Technical and financial analysis of the assembled PCB. Phase 2: Selection of proper tests equipment. Phase 3: Creation of the test strategy. In order to achieve the goals the test strategy must provide optimum coverage with minimal overlapping of the tests at minimal cost. Phase 4: Test strategy realization. Phase 5: Test metrics

analysis. Phase 6: Change and improvement of the test strategy if necessary.

4. DEVELOPING FAST MEMORY TEST

The memory is one of the most critical resources in any computer system. During product manufacturing there is a need for memory testing. One type of memory problem usually is caused by physical or electrical damage to the memory chip during manufacture. Another type of problem is the circuit board. Typical circuit board problems are problems with the wiring between the processor and memory device, missing memory chips, and improperly installed memory components. Three individual memory tests are able to detect these kind of problems: a data bus test, an address bus test, and a device test. The device test has to be run after successful completion of data and address bus tests.

For testing RAM (MSP430x family) here are used the industry recognised March C and March X algorithms [6]. These tests consist of a finite sequence of March elements, while a March element is a finite sequence of operations applied to every cell in the memory array before proceeding to the next cell. In general the more March elements the algorithm consists of the better will be its fault coverage but at the expense of a slower execution time.

Tab 1. Source code test description.

Declaration	
SetMemory((unsigned char*)&RAMField[0], 1024, 0x55); Counter1 = 0; CompareMemory((unsigned char*)&RAMField[0], 1024, 0x55) SetMemory((unsigned char*)&RAMField[0], 1024, 0xAA); Counter2 = 0; CompareMemory((unsigned char*)&RAMField[0], 1024, 0xAA)	
Description	
RAM memory test using upgraded March X algorithm	
Input Parameters	
RAMField[0[	Block size of the array of bytes of RAM to be tested
Const	Fill constant set to memory for test
Output Parameters	
Counter1	Counter of h’55s
Counter2	Counter of h’AAs

The proposed algorithm has been created from a standard March X algorithm and it is byte oriented memory version. The developed algorithm uses four elements:

- Starting at the lowest address, write h'55s, increment up array byte by byte.
- Read all h'55s from array and write the value in int Counter1.
- Starting at highest address, write h'AAs, decrement down byte by byte.
- Read all h'AAs from array and write the value in int Counter2.

The source code TestRAM.c is written in ANSI C and compiled with IDE IAR EW 5.20 for MCU MSP430x family (table 1). This algorithm is faster than March C and March X algorithms and could be used for testing Flash memory also. The period of testing is eight times less than the standard March C and March X algorithms and two times faster than byte oriented memory version of March X algorithm.

5. CONCLUSIONS

There is a wide variety automated methods and tools for testing the electronics products. Their integration into the manufacturing process is a complex task and requires careful technical evaluation of the effectiveness of each of the tests and financial analysis of alternative tests and equipment.

The MCU must be tested with specific tests to ensure correct operation These tests include ALU and CPU tests, RAM tests, ROM/flash tests, clock tests, and peripheral tests. The routines are made available as source code and can be quickly integrated into existing software. They can be called easy when necessary during the operation.

6. REFERENCES

[1] http://www.radio-electronics.com/info/t_and_m/ate/ict-in-circuit-test
[2]http://www.corelis.com/education/Boundary_ Scan_Tutorial.htm
[3] http://www.radio-electronics.com/info/t_and_m/design-for-testability-dft/basics-guidelines.php
[4]http://www.radio-electronics.com/info/t_and_m/ate/developing-testing-automation-strategy.php
[5] http://www.teradyne.com/atd/resource/docs/testStation/SMT7060
[6] Application Note 223/3.0 (2008) Self Test Sample Code for Renesas Microcontroller Families, App 223/3.0 (2).

An Entertaining Example for the Usage of Bitwise Operations in Programming

Hristina Kostadinova, Krasimir Yordzhev
South-West University "Neofit Rilski"

***Abstract**: The present study is meant to fill in some information gaps occurring in the most widespread and well-known educational and reference literature about programming. The stress is laid on a very useful instrument - the bitwise operations, topic which is, unfortunately, seldom dealt with in most of the well-known books on programming. In addition, the research is very useful as regards the topic of overloading operators in any Object-oriented programming course. Given some appropriate examples, with the emphasis being laid on some particular and data structures language constructions, the results are quite interesting. The algorithm of solving the popular Sudoku puzzle is one such entertaining example.*

***Keywords:** Object-oriented programming, bitwise operation, class, set, overloading operators, Sudoku matrix, Sudoku puzzle*

1. INTRODUCTION

The use of bitwise operations is a popular and well-working method, used in C/C++ and Java programming languages. Unfortunately, in many widespread books on this topic there is only scarce or incomplete information as to how exactly bitwise operators function [4,14,15,16,20]. The aim of this article is to bridge this information gap to a certain extent and present a meaningful example of a programming task, where the use of bitwise operators is appropriate, in so far as to facilitate the work and increase the efficiency of the respective algorithm. Thus, we shall help the programming teachers in their work by presenting a good programming example, which demonstrates the use of bitwise operations in C/C++.

Some applications of the bitwise operations in the realization of algorithms designed to determine quantitative evaluations in the textile industry, as shown in [7,11,12].

Let $M = \{\mu_0, \mu_1, \ldots, \mu_{m-1}\}$, $|M| = m$ be a finite and discrete set. By the rule of thumb [17], each subset could be denoted by means of a Boolean vector $b(A) = \langle b_0, b_1, \ldots, b_{m-1} \rangle$, where $b_i = 1 \Leftrightarrow \mu_i \in A$ and $b_i = 0 \Leftrightarrow \mu_i \notin A$, $i = 1,2,...,m-1$. A great memory economy could be achieved, if natural

numbers are presented in a binary number system, where the number "zero" corresponds to null set, while the number 2^m-1, which in a binary number system is written by means of m "ones", corresponds to the basic set M. Thus, a natural one to one correspondence between the integers of the closed interval $\left[0,2^m-1\right]$ and the set of all subsets of M is achieved. The integer $a\in\left[0,2^m-1\right]$ corresponds to the set $A\subseteq M$, if for every $i=1,2,...,m-1$ the i-bit of the binary representation of a equals one, and if and only if $\mu_i\in A$. The need of the use of bitwise operations naturally arises in cases involving the computer realization of various operations with different sets of numbers.

Such an approach is also comfortable and quite efficient, given a relatively small cardinal number $m=|M|$ of the basic set M, and it also has a significant importance, in relation to the operating system and programming environment that is used. This is so, because m bits are necessary to encode in the abovementioned method a set, which a subset of M, where $|M|=m$. And if k-bits are given for the type integer in the programming environment dealing with data, then $\left[\frac{m}{k}\right]+1$ variables of that certain kind will be necessary, so as to put the abovementioned ideas into practice, where $[x]$ denotes the function "the whole part of x". Four bytes (thirty-two bits) are necessary to write a program that can solve a Sudoku puzzle in the size of $n^2\times n^2$ if we use the set theory method at $n\le 5$. In this case, every set of the kind $A=\{\alpha_1,\alpha_2,...,\alpha_s\}$, where $1\le\alpha_i\le n^2$, $i=1,2,...,s$, $0\le s\le n^2$, or the null set, could be simply encoded with an integer.

The programming realization of the problem of finding prime numbers using the method Sieve of Eratosthenes [1,5,8,19] has become a classical example for the use of sets in programming. Here we have to emphasize that a mistake has been made in [19], concerning this method's realization, and namely the number 1 has been reckoned among the set of the prime numbers. Such a mistake is inadmissible if the method is applied at schools, as the users may be confused.

How to construct a faster algorithm, solving the problem for receiving all $n\times n$ binary matrices, which contain exactly k ones in each row and each column, with the help of the set theory and the operations over sets, is shown in [13].

Unfortunately the programming languages C/C++ and Java do not support a standard type “set”, whereas the Pascal language does [1,5,8,19]. For this reason, if there should be a need to use the language of sets in the realization of some of our algorithms, and if there should be a need to write a program in some of these languages, we have to look for additional instruments to work with sets, such as, for example, the associative containers set and multiset, realized in Standard Template Library (STL) [15]**.** The template class set of the system of computer algebra “Symbolic C++” can also be used. The programming code is given in details in [9]. Of course, another class set can also be built, and specific methods of this class can be described, as a means of training. This is a good exercise, having in mind the fact that the cardinal number of the basic (“universal”) set is not very big. For example the “standard” Sudoku puzzle has basic set the set of the integers from 1 to 9 plus the empty set.

We shall examine the entertaining problem with Sudoku solving algorithms, which is very interesting to many students. Sudoku is popular puzzle nowadays, populating the recreation pages of many newspapers and magazines, and it could also be found on many websites. Sudoku, or Su Doku, is a Japanese word (or phrase) meaning something like Number Place.

On the other hand, Sudoku matrices find an interesting combinatorial application. The connection between the set of all $m \times m$ permutation matrices (i.e. binary matrices which contain just one 1 in every row and every column) and the set of all $m \times m$ Sudoku matrices, is shown in [2].

2. TASK LAYOUT AND DESCRIPTION OF THE ALGORITHM USING THEORETIC SET OPERATIONS

Let n be random positive integer and let $m = n^2$. Let $S = \left(s_{ij}\right)$ be a square $m \times m$ matrix (square table), all elements in this table are integers, belonging to the closed interval $[1, m]$. The matrix S is divided to n^2, $n \times n$ square submatrices, which are not intersected and will be called blocks, with the help of $n-1$ horizontal and $n-1$ vertical lines (the matrix S, when $n = 3$**,** is shown on fig.1).

S_{11}	S_{12}	S_{13}	S_{14}	S_{15}	S_{16}	S_{17}	S_{18}	S_{19}
S_{21}	S_{22}	S_{23}	S_{24}	S_{25}	S_{26}	S_{27}	S_{28}	S_{29}
S_{31}	S_{32}	S_{33}	S_{34}	S_{35}	S_{36}	S_{37}	S_{38}	S_{39}
S_{41}	S_{42}	S_{43}	S_{44}	S_{45}	S_{46}	S_{47}	S_{48}	S_{49}
S_{51}	S_{52}	S_{53}	S_{54}	S_{55}	S_{56}	S_{57}	S_{58}	S_{59}
S_{61}	S_{62}	S_{63}	S_{64}	S_{65}	S_{66}	S_{67}	S_{68}	S_{69}
S_{71}	S_{72}	S_{73}	S_{74}	S_{75}	S_{76}	S_{77}	S_{78}	S_{79}
S_{81}	S_{82}	S_{83}	S_{84}	S_{85}	S_{86}	S_{87}	S_{88}	S_{89}
S_{91}	S_{82}	S_{93}	S_{94}	S_{95}	S_{96}	S_{97}	S_{98}	S_{99}

Fig. 1:

Let denote by $A_{kl}, 1 \le k, l \le n$ the blocks in the above described *matrix* $S = (s_{ij})$. Then by definition if $s_{ij} \in A_{kl}$, then

$$(k-1)n < i \le kn$$

and

$$(l-1) < j \le (l-1).$$

Let s_{ij} belong to the block A_{kl} and let i and j be known. Then it is easy to guess that k and l can be calculated with the help of the formulas

$$k = \left[\frac{i-1}{n}\right] + 1$$

and

$$l = \left[\frac{j-1}{n}\right] + 1,$$

where, as usual, we denote by $[x]$ the function: whole part of the real number x.

We say that $S = (s_{ij})$, $1 \le i, j \le m = n^2$ is a *Sudoku matrix* if there is just one number of the set $Z_m = \{1,2,\ldots,m = n^2\}$ in every row, every column and every block.

The Sudoku puzzle is quite popular these days. The user is given a Sudoku matrix, in which some of the elements have been erased. The missing elements could be equal to 0. The user's task is to restore the missing elements of the Sudoku matrix. It is supposed that the authors of the particular puzzle have chosen the missing elements in such a way that the problem has only one solution. This condition will be ignored. In this study we will build our programming product so that it can show the number of every possible solution. If the task has no solution this number will be zero.

The most popular Sudoku puzzles are with $n=3$, i.e. $m=9$.

We are going to describe an algorithm for creating a computer program, which can find all solutions (if there are any) of random Sudoku puzzle. For this purpose, we will use the knowledge of the set theory.

We examine the sets R_i, C_j and B_{kl}, where $1\le i,j\le m=n^2$, $1\le k,l\le n$. For every $i=1,2,\ldots,m$, the set R_j consists of all missing numbers in the i-th row of the matrix. Analogously we define the sets C_j, $j=1,2,\ldots,m$ correspondingly for the missing numbers in the j-th column and B_{kl}, $k,l=1,2,\ldots,n$ correspondingly for the missing numbers in the blocks A_{kl} of S.

Whenever the algorithm comes into operation it traverses many times all of the elements $s_{ij}\in S$, such that $s_{ij}=0$, i.e. these are the elements, which real values we have to find.

Let $s_{ij}=0$ and let $s_{ij}\in A_{kl}$. We assume

$$P=R_i\cap C_j\cap B_{kl}.$$

Then the following three cases are possible:

i) $P=\phi$ (empty set). The task has no solution in this case;

ii) $P=\{d\}$, $d\in Z_m=\{1,2,\ldots,m\}$, i.e. $|P|$: the number of the elements of P is equal to 1 (P is a set containing one element). Then the only one possibility for s_{ij} is $s_{ij}=d$, i.e. we have found the unknown value of s_{ij} in this case. After this we remove the common element d from the sets R_i, C_j and B_{kl}, and then we continue to the next zero element of the matrix S (if there is such an element);

iii) $|P|\ge 2$. Then, we cannot say anything about the unknown value of s_{ij} and we move on the next missing (zero) element of the matrix S.

We traverse all zero elements of the matrix S, until one the following events occur:

e1) For some $i,j\in\{1,2,\ldots,m\}$ is true $s_{ij}=0$, but $P=R_i\cap C_j\cap B_{kl}=\phi$;

e2) All elements in S become positive;

e3) All zero elements of S are traversed, but neither event e1, nor event e2 occur. In other words, for all the remaining zero elements in S, the above described case iii is always true.

In case any of the events e1 or e2 occurs, then the procedure is brought to a halt and the result visualizes on the screen.

In case event e3 occurs, then the algorithm has to continue operating by using other methods such as, for example, applying the "trial and error" method. In this particular case, the method would consist of the following steps:

We choose random $s_{ij} \in S$, such that $s_{ij} = 0$ and let $k = \left[\frac{i-1}{n}\right] + 1$, $l = \left[\frac{j-1}{n}\right] + 1$. Let $P = R_i \cap C_j \cap B_{kl} = \{d_1, d_2, \ldots, d_t\}$. Then for every $d_r \in P$, $r = 1,2,\ldots,t$ we assume $s_{ij} = d_r$. Such an assumption is called a *random trial*. We count the number of all random trials, until the solution is found in the programming realization of the algorithm. Then, we solve the problem for finding the unknown elements of the Sudoku matrix, which contain one element less than the previous matrix. It is convenient to use a recursion here. The procedure is halted if event e1 or e2 occurs. It is absolutely certain to occur (i.e. there will not be "an infinite cycle"), because whenever we perform random trials, we reduce the number of the zero elements by 1.

3. BITWISE OPERATORS IN C/C++

Bitwise operations can be applied for integer data type only, i.e. they cannot be used for float and double types. For the definition of the bitwise operators in C/C++ and some of their elementary applications could be seen, for example in [3,6,10,18].

We assume as usual that bits numbering in variables starts from right to left, and that the number of the very right one is 0.

Let x, y and z are integer variables of one type, for which w bits are needed. Let x and y are initialized and let the $z = x \alpha y$ assignment is made, where α is one of the operators & (bitwise AND), | (bitwise inclusive OR) or ^ (bitwise exclusive OR). For each $i = 0,1,\ldots,w-1$ the new contents of the i bit in z will be as it is presented in the following table:

The i bit of x	The i bit of y	The i bit of $x \& y$	The i bit of $x \mid y$	The i bit of $x \wedge y$
0	0	0	0	0
0	1	0	1	1
1	0	0	1	1
1	1	1	1	0

In case $z = \sim x$, if the i bit of x is 0, then the i bit of z becomes 1, and if the i bit of x is 1, then the i bit of z becomes 0, $i = 0,1,\ldots,w-1$

In case k is a nonnegative integer, then the statement $z = x << k$; (bitwise shift left) will write in the $(i+k)$ bit of z the value of the k bit of x, where $i = 0,1,\ldots,w-k-1$, and the very right k bits of z will be filled by zeroes. This operation is equivalent to a multiplication of x by 2^k. The statement $z = x >> k$ functions similarly (bitwise shift right). But we must be careful here, as in various programming environments this operator has different interpretations – somewhere k bits of z from the very right place are compulsory filled by 0 (logical displacement), and elsewhere the very right k bits of z are filled with the value from the very left (sign) bit; i.e. if the number is negative, then the filling will be with 1 (arithmetic displacement). Therefore it is recommended that we use unsigned type of variables (if the opposite is not necessary) whenever we work with bitwise operations.

The effectiveness of the function computing 2^k is the direct result of the definition of the operator bitwise shift left, where k is a nonnegative integer:

```
unsigned int Power2(unsigned int k) {
 return 1<<k;
}
```

To compute the value of the i bit of an integer variable x we can use the function:

```
int BitValue(int x, unsigned int i) {
 if ( (x & (1<<i) ) == 0 ) return 0;
    else return 1;
}
```

Bitwise operators are left associative.

The priority of operators in descending order is as follows: *bitwise complement* ~; *arithmetic operators* * (multiply), / (divide), % (remainder or

modulus); *arithmetic operators* + (binary plus or add) - (binary minus or subtract); the *bitwise operators* << and >>; *relational operators* <, >, <=, >=, ==, !=; *bitwise operators* &,^ and |; *logical operators* && and ||.

4. DESCRIPTION OF THE CLASS SET BY MEANS OF OVERLOADING OPERATORS AND USING BITWISE OPERATIONS

```
class Set_N {
int n;
public:
 /*Constructor without parameter – creates empty set*/
 Set_N();
 /*Constructor with parameter – creates the set, corresponding to every bit position of the parameter*/
 Set_N(int k);
/*Returns the integer encoding of the set*/
 int get_n() const;
/*Overloading operators *, +, -, ==, <=*/
 Set_N operator * (Set_N const &);
 Set_N operator + (Set_N const &);
 Set_N operator + (int k);
 Set_N operator - (Set_N const &);
 Set_N operator - (int k);
 bool operator == (Set_N const &);
 bool operator <= (Set_N const &);
/*Checks if the first parameter belongs to the given set*/
 bool in(int k);
/*Destructor*/
 ~Set_N();
};
```

The realization of the Set_N methods is described below:

```
Set_N::Set_N() {n = 0;}
Set_N::Set_N(int k) {n = k;}
int Set_N::get_n() const {
 return n;
}
Set_N Set_N::operator * (Set_N const & s) {
 return (this->n) & s.get_n();
}
Set_N Set_N::operator + (Set_N const & s) {
 return (this->n) | s.get_n();
}
Set_N Set_N::operator + (int k) {
```

```
 return (this->n) | (1<<(k-1));
}
Set_N Set_N::operator - (Set_N const & s) {
 int temp = 0;
 temp = this->n ^ s.get_n();
 return (this->n) & temp;
}
Set_N Set_N::operator - (int k) {
 return (this->n) ^ (1<<(k-1));
}
bool Set_N::operator == (Set_N const & s) {
 return ((this->n ^ s.get_n()) == 0);
}
bool Set_N::operator <= (Set_N const & s) {
 return ((this->n & s.get_n()) == n);
}
bool Set_N::in(int k, Set_N const & s) {
 return this->n & (1<<(k-1));
}
```

5. REFERENCES

[1] Dahl, D. J., Dijkstra, E. W., Hoare, C. A. R. (1972) *Structured Programming.* Academic Press Inc.

[2] Dahl, G. (2009) Permutation matrices related to Sudoku. *Linear Algebra and its Applications* 430, 2457–2463.

[3] Davis, S. R. (2000) *C++ for dummies.* IDG Books Worldwide.

[4] Horstmann, C. S. (1999) *Computing concepts with C++ essentials*. John Wiley & Sons.

[5] Jensen, K., Wirth, N. (1985) *Pascal User Manual and Report*. 3rd ed., Springer-Verlag.

[6] Kernigan, B. W., Ritchie D. M. (1998) *The C programming Language*. AT&T Bell Laboratories.

[7] Kostadinova, H., Yordzhev, K. (2010) A Representation of Binary Matrices. *Mathematics and education in mathematics,* v. 39, 198-206.

[8] Price, D. (1983) *UCSD Pascal A Considerate Approach*. Prentice-Hall.

[9] Shi, T. K., Steeb, W.-H., Hardy, Y. (2000)*Symbolic C++: An Introduction to Computer Algebra using Object-Oriented Programming*. Springer.

[10] Schildt, H. *Java 2 A Beginner’s Guide.* (2001) McGraw-Hill.

[11] Yordzhev, K. (2009) An example for the use of bitwise operations in programming. *Mathematics and education in mathematics,* v. 38, 196-202
[12] Yordzhev, K., Kostadinova, H. (*2010)* Mathematcal Modeling of the Weaving Structure Design *Mathematics and education in mathematics,* v. 39, 212-220.
[13] Yordzhev, K., Stefanov, S. (2003) On Some Applications of the Consept of Set in Computer Science Course. *Mathematics and Educations in Mathematics*, v.32, 249-252.
[14] Азълов П. (2005) *Информатика Езикът C++ в примери и задачи за 9-10 клас.* София, Просвета.
[15] Азълов П. (2008) *Обектно-ориентирано програмиране – Структури от данни и STL*. София, Сиела.
[16] Крушков, Х. (2006) *Практическо ръководство по програмиране на C++.* Пловдив, Макрос.
[17] Наков, П., Добриков П. (2005) Програмиране =++ Алгоритми, Трето издание, София, ISBN 954-8905-16-X.
[18] Романов, Е. Л. (2004) *Практикум по программированию на C++*. Петербург, БХВ.
[19] Стоянова, Р., Гочев, Г. (1994) *Програмиране на Pascal с 99 примерни програми*. София, Paraflow.
[20] Тодорова М. (2002) Програмиране на C++. Част I, Част II, София, Сиела.

Investigation of Internet Delays

Valentin Hristov, Stanko Shtrakov, Ljudmila Taneva
South- West University- Blagoevgrad, Bulgaria

Abstract*: The purpose of present paper is to investigate the RTT delays in Internet, to create a program which describes the observed RTTs with Weibull distribution as well as to present some results got with this program.*

Keywords: *Round Trip Time, Internet delays, Weibull distribution*

1. INTRODUCTION

Our main focus in this paper is on Round-Trip Times because this parameter as well as packet loss probability gives the TCP throughput. It is well known fact that TCP traffic continues to constitute the bulk of traffic in modern networks, e.g. 80%–90% of current Internet traffic is TCP traffic.

The Round Trip Time (RTT) is the length of time it takes for a data packet to be sent plus the length of time it takes for an acknowledgment of that packet to be received. An internet user can determine the RTT by using the ping command.

Using the algorithm proposed in this paper, the observed RTTs are described with the Weibull distribution [6]. The presented results in this paper could be used in order to investigate the delay, the throughput for Internet applications and services as well as to set buffer sizes and etc.

The throughput of TCP is limited by two windows: the congestion window and the receive window. The first one tries not to exceed the capacity of the network (congestion control) and the second one tries not to exceed the capacity of the receiver to process data (flow control). The receiver may be overwhelmed by data if for example it is very busy (such as a Web server). Each TCP segment contains the current value of the receive window. If for example a sender receives an ACK which acknowledges byte 4000 and specifies a receive window of 10000 (bytes), the sender will not send packets after byte 14000, even if the congestion window allows it.

The classical rule of thumb for sizing buffers is to set buffer sizes to be the product of the bandwidth and the average delay of the flows utilizing this link, namely the Bandwidth-Delay Product (BDP) rule [1-4].

In fact, network links with both a high bandwidth and a high RTT can have a very large amount of data (the bandwidth-delay product) "in flight" at

any given time. Such "long fat pipes" require a special protocol design (One example is the TCP window scale option).

The probability distribution tools can be used in the investigations and project calculations for RTT. Their mathematical functions propose a wide range of techniques utilized to identify the parameters of the distribution functions [5].

The purpose of present paper is to investigate the RTT delays in Internet, to create a program which describes the observed RTTs with Weibull distribution as well as to present some results got with this program.

2. INVESTIGATION OF ROUND TRIP TIME

The Round Trip Time is the length of time it takes for a data packet to be sent plus the length of time it takes for an acknowledgment of that packet to be received (Fig. 1).

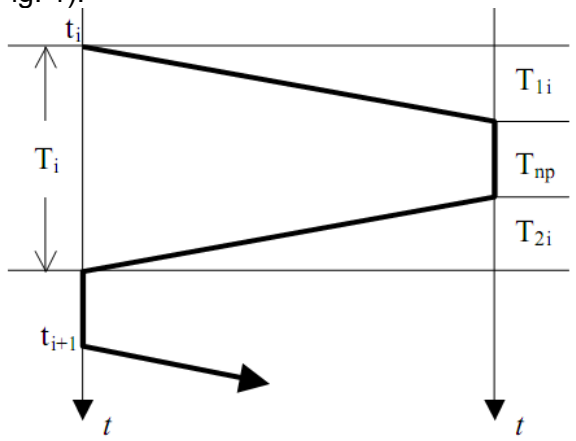

Fig. 1: RTT-delay

All the intervals T_i form the discrete sequence of RTT-delays. The intervals T_{1i} and T_{2i} represent the delay in processing and transmitting of the information as well as the queue time in the respective nodes of the web. For preset packet routes it is possible to split the delay in two with a constant representing the minimal delay without queue in the nodes and a variable representing the random delay representing the delay due the queue and the random nature of the Internet traffic.

In this paper, we recorded Round-Trip Times (RTTs) over the Internet as we ping the www.canada.com from a desktop computer from domain swu.bg every five seconds, each time sending 100 ping packets. The remote test receiver is chosen by the following criteria:

- The receiver must be distant enough to allow random traffic fluctuations to be noticed.

- The communication channels to the receiver should not be overloaded, but still loaded at the level of a regular Internet traffic.
- During the experiment all packets to the receiver must travel trough same route.
- The packet loss should be minimal in order to avoid significant distortions in the test results.
- The receiver should not reject Internet Control Message Protokol-ICMP packets.

The RTT-delay values were determined using a modified program Ping which according its algorithm each 5 seconds sends test packets to remote computer-receiver and receives confirmation packets from it. During the experiment all packets to the receiver travel through following routers: core-swu.lines.acad.bg, bren.rt1.sof.bg.geant2.net, so-2-3-0.bud.hu.geant2.net, so-6-1-0.vie.at.geant2.net, tenGigabitEthernet.1-3.ar2.vie1.gblx.net, and three core routers in North America. The RTT-delay is calculated with error < 1 ms as a difference between the time-marks of the moments of sending the test packet and receiving of the confirmation one. The RTTs reported by this ping program were between 2 –230 ms, and were written in txt file. During the experiment, normal services such as Web browsing experienced obvious pauses.

Let’s first proceed to the definition of interval statistics of second-order RTT-delay – correlation coefficient and dispersion.

On fig. 2 is shown the RTT- delay histogram, based on 66410 attempts for time interval for the selected receiver (www.canada.com). On X-axis are set time intervals and on Y-axis are the numbers of RTT events, for each interval.

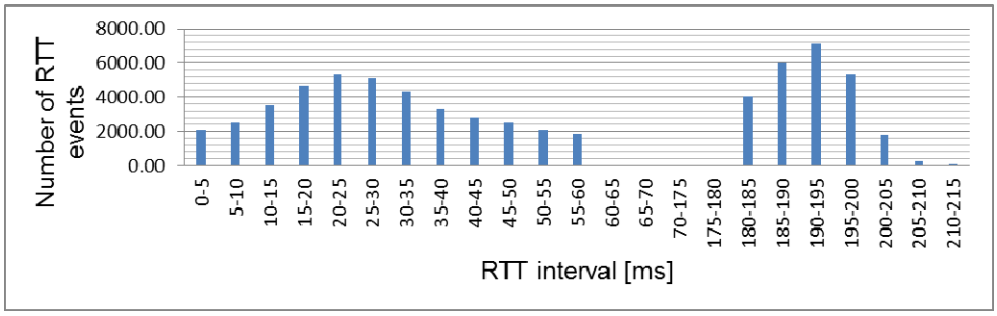

Fig. 2: RTT-events for time intervals in the test

The determination of the selective correlation coefficient of the number of reports at intervals with preset duration is done by our program using the formula:

$$\tilde{r}(k) = \frac{N}{N-k} \sum_{j=1}^{N-k} \frac{\left[X_j - \tilde{M}\{X_j\}\right]\left[X_{j,k} - \tilde{M}\{X_j\}\right]}{\sum_{j=1}^{N}\left[X_j - \tilde{M}\{X_j\}\right]^2} \quad (1)$$

where Xj is the recorded value (number packets) In the intervals with duration 0.1s ; N=10Te is the size of the reading, k=0,1,… - shift parameter, multiple of the number of intervals:

$$\tilde{M}\{X_j\} = \frac{1}{N}\sum_{j=1}^{N} X_j \quad (2)$$

The value of the fractal parameter can be calculated using the correlation coefficient in function of the shift parameter and approximation done according expression (3):

$$r_H(k;T) \approx \frac{1}{2}\alpha(\alpha+1)k^{\alpha-1} \quad (3)$$

Thus, based on correlation coefficient in function of the shift parameter the value of the fractal parameter is determined, i.e. $\tilde{\alpha}$ = 0.752.

The RTT can be modeled, applying the Weibull distribution [6]. This statistical tool tells us how often time of different attempts will be happened at a location with a certain average (mean) RTT. The distribution mentioned is widely used in reliability and life data analysis, due to its versatility. Depending on the values of the parameters, it can be harnessed to model also a variety of life behaviors.

Advantage can be taken of the two-parameter Weibull probability model, the lognormal, gamma and Rayleigh ones [5, 6]. The practice and investigations show, that the Weibull probability distribution function should be found to fit the frequency distribution of RTT measurements very accurately. This means that, the most of the RTT distribution characteristics at any situation can be described by two parameters: the shape parameter K and the scale one C. The fraction of time duration in which the time access T, is thus determined therefore by (4):

$$f(V) = \frac{K}{C}\cdot\left[\frac{T}{C}\right]^{K-1}\exp\left(-\left[\frac{T}{C}\right]^{K}\right) \quad (4)$$

This expression is valid for $K > 1$, $T \geq 0$, and $C > 0$. The shape factor typically ranges from 1 to 3. For a given average time access, the smaller shape factor indicates a relatively wide distribution of the RTTs around its

average value, while the larger one points out a relatively narrow distribution of the RTTs around the latter. C is the scale factor which is calculated from the following equation:

(5) $$C = \frac{\overline{T}}{\Gamma\left(1+\frac{1}{K}\right)},$$

where $\overline{T}$ is the average RTT value and Γ is the gamma function.

The duration curve may be found from the total probability function, i.e.

(6) $$F(T \le T_0) = 1 - \exp\left[-\frac{T_0^k}{C}\right]$$

Here ‘‘F’’ represents the probability for the RTT ‘‘T’’ to be lower than a certain value ‘‘T0’’.

A key problem for the time access analysis is the estimation of the Weibul parameters K and C. They depend on type of time access data, collected for a given situarion. Numerous methods have been proposed over the last few years for the Weibul parameter estimation [6,8]. In this study, the two parameters of the Weibull distribution are determined by using the mean time access-standard deviation method and an approach, based on the data of the time access duration in time intervals. The first of them uses the mean time access and standard deviations, calculated for the available time-series data.

The value that fits best for K is found to be:

(7) $$K = \left(\frac{\sigma}{\overline{T}}\right)^{-1.086}$$

where, $\overline{T}$ is the mean RTT and σ is the standard deviation.

The second method employs the data of the observations for RTT in intervals with preliminary defined boundaries. The same can be utilized to construct a rough approximation to the duration curve. The latter represents the probability of the RTT T to be lower than a certain value T_0.

These results can be used to create the duration curve for the RTT distribution and by means of equation (4) – to find the parameters K and C. The equation referred to can be written also as follows:

(8) $$\ln(-\ln(1 - F(T \le T_0))) = K \ln\left(\frac{T_b}{C}\right) = K \ln(T_b) - K \ln(C)$$

The values of the quantities K and C can be calculated through the least squares fitting of the duration curve that describes the above data.

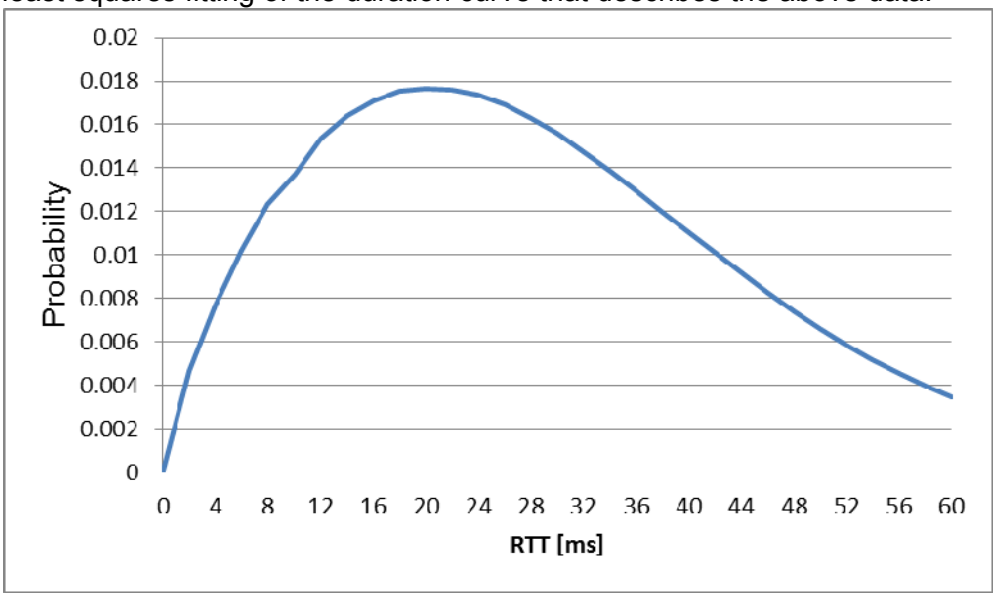

Fig. 3: Probability distribution (0 – 65 ms) – K=1.76; C=32.8

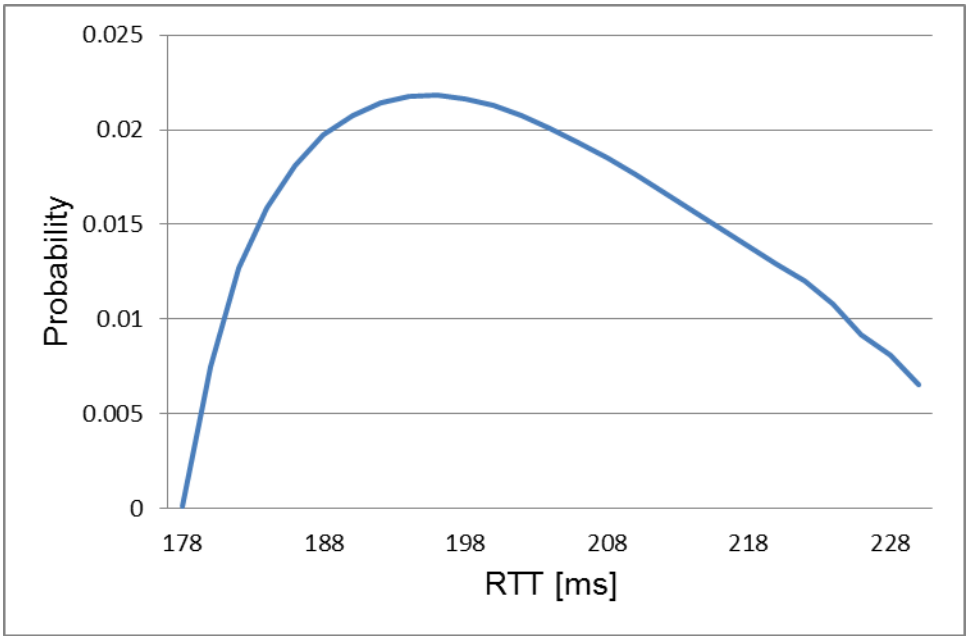

Fig. 4: Probability distribution (180 – 230 ms) – K=1.51; C=34.15

The calculations made, using the two methods, give different results for the available data. The probability curves of the RTT, calculated through the least squares fitting of the duration curve represent the source data more accurately. Because of that, these calculations were used to receive the probability distribution of RTT.

Data analysis shows, that entire time interval for RTT is divided in two main intervals: 0 – 60 ms and 180 – 230 ms. Interval between these subintervals is empty. Because of that, a two probability distribution curves were calculated. The curves are shown in fig. 3 and fig. 4.

These results can be explained with the fluctuations in Internet traffic and the routes delays. It is possible to split the delay in two- with a constant representing the minimal delay without queue in the routers, and a variable representing the random delay representing the delay due the queue and the random nature of the Internet traffic. The increase in measured RTT could be almost entirely attributed to the resulting queuing delay at the routers.

3. CONCLUSIONS

Using the approah proposed in this paper, the observed RTTs are described with the Weibull distribution. The presented results in this paper could be used in order to investigate the throughput for Internet applications and services as well as to set buffer sizes of internet nodes and so on.

4. REFERENCES

[1] Villamizar C., Song C. (1994) High performance TCP in ANSNET, *Comput. Commun*, 24 (5), 45–60.

[2] Vu-Brugier G., Stanojevic R., Leith D., Shorten R. (2007) A critique of recently proposed buffer-sizing strategies, *Comput. Commun*., 37(1), 43–48.

[3] Wischik D., McKeown N. (2005) Part I: Buffer sizes for core router, *Comput. Commun*. 35 (3), 75–78.

[4] Zhang Y., Loguinov D. (2008) ABS: Adaptive buffer sizing for heterogeneous networks, *Proc. IWQos*, 90–99.

[5] Sfetsos A. (2000) Comparison of various forecasting techniques applied to mean hourly wind speed time series, *Renewable Energy*, 21, 23–35.

[6] Carta J., Ramır'rez P. (2007) Analysis of two-component mixture Weibull statistics for estimation of wind speed distributions, *Renewable Energy*, 32, 518–531.

Building Steps for the Enterprise Cloud

Plamena Zlateva[1], Vladimir Velev[2], Dimiter Velev[3]
[1]*Institute of System Engineering and Robotics - BAS, Sofia, Bulgaria*
[2]*Independent Software Developer, Sofia, Bulgaria*
[3]*University of National and World Economy, Sofia, Bulgaria*

***Abstract**: The paper gives with a short overview of cloud computing and the IT architecture of the traditional enterprise. The need for migration of existing structures to the enterprise cloud is explained. The main emphasis of the article is to outline and define the necessary steps that should be followed for establishing an enterprise cloud. The Enterprise Cloud will provide powerful resources that can be used to rapidly develop and deploy applications and provide on-demand resources.*

***Keywords:** Enterprise, Cloud Computing, Software Applications, Networking, Data Storage.*

1. INTRODUCTION

The enterprise is in transition to a new operating model that uses and offers capabilities as a service to achieve significant improvement in efficiency. In era of cloud computing there is a need for the enterprise companies to work together in order to ensure an optimal, flexible and efficient ecosystem of suppliers and services.

Cost savings represent a significant driver to enterprise cloud computing. Nevertheless far more important are the changes going on in the larger world outside of the business world in ITC-based global society. With the advent of simplified software or Web 2.0 usage of the Internet, Social Networks are changing the ways users live, learn, collaborate and work. Such significant changes in society also change the manner of design and management of current organizations and the value delivered to customers.

2. CLOUD COMPUTING ESSENCE

Cloud computing refers to the provision of computational resources on demand via a computer network. In the traditional model of computing, both data and software are fully contained on the user's computer whereas in cloud computing, the user's computer may contain almost no software or data, or just an operating system and web browser only.

The cloud is a metaphor for the Internet and is an abstraction for the complex infrastructure it conceals. It is a style of computing in which users access technology-enabled services from the Internet without knowledge of, expertise with, or control over the technology infrastructure that supports them. Cloud computing incorporates software as a service (SaaS), infrastructure as a service (IaaS), platform as a service (PaaS), Web 2.0, virtualization, multi-tenancy and other recent technology trends in which the common theme is reliance on the Internet for satisfying the computing needs of the users [1, 5].

Cloud computing is often associated with new Web 2.0 start-up companies. The best known Cloud application is the Google search engine that, while consuming huge amounts of processing power, never needs to rely on database. Amazon’s Elastic Compute Cloud hosts start-up companies that provide photo sharing, phone text message collection and redistribution services, and social networking and collaboration [12].

The U.S. National Institute of Standards and Technology provides the most neutral definition of cloud computing. “Cloud computing is a model for enabling convenient, on-demand network access to a 18 Enterprise Cloud Computing shared pool of configurable computing resources (e.g., networks, servers, storage, applications and services) that can be rapidly provisioned and released with minimal management effort or service provider interaction. This cloud model promotes availability and is composed of five essential characteristics, three delivery models, and four deployment models.”

3. ENTERPRISE CLOUD COMPUTING

Enterprise cloud computing is a behind-the-firewalls use of commercial, Internet-based cloud technologies specifically focused on the computing needs of a certain company or one business environment. Enterprise cloud computing is a controlled, internal place that offers the rapid and flexible provisioning of compute power, storage, software and security services to meet the specific requirements. The main reason behind the Enterprise Cloud is often to avoid any transitional costs of redesigning the existing architecture and Enterprise Clouds are used to minimise disruptional risks. However they will be subjected to a transition to the new architecture because of high operational costs [3, 6, 10, 12].

In order to achieve a simple advantage in Enterprise Cloud Computing, at least a storage cloud and a compute/processing cloud will be needed placed on top of the company’s network cloud. However, this demands each cloud user to bring database, application, web services and security services with them [11].

A full-fledged Enterprise Cloud Computing environment will have storage, computing utilities, databases, applications and additional layers. It will support rapid stand-up of development and test environments to reduce time to market by applications developers. It will include standard data management approaches and flexible storage schemes to allow broad re-use of corporate data without storing the data in multiple locations. It should have security as a service that dictates a common, consistent approach to assuring the identity, access, and audit of individuals and systems. Such an Enterprise Cloud will be built on a solid foundation of common processes, management, and governance principles to keep the cloud optimized [11].

Enterprise Cloud Computing helps IT deliver a safer environment [7]. The standards of the cloud reduces the complexity and variety of the infrastructure allowing deploying patches more rapidly across the enterprise. By keeping the cloud inside company's firewalls, one can focus his strongest intrusion detection and prevention sensors on his perimeter. By virtualizing storage protection is obtained against a physical intruder. Putting the cloud to the desktop and delivering office automation through a virtual desktop, a reduction of workstation security anomalies is achieved. The transition to security services in the cloud, provides for a multi-dimensional safety model that extends beyond people and their accesses. The multiple dimensions allows to make security decisions based on the user identity, his current location, the required types of data or applications and the used devices.

Conventional cloud hosting plans usually utilize a plethora of virtual private servers (VPS) that evenly distribute traffic within an infinitely expandable server network [13]. In the case of enterprise cloud hosting, instead of utilizing VPS servers within the network, all of the servers are dedicated servers, which are significantly more powerful. Each dedicated server is capable of handling dozens or even thousands of websites by itself, hence the reason why dedicated hosting is an enterprise-level solution that is often utilized by large corporations and online entrepreneurs. An enterprise cloud hosting plan gives an unlimited access to an entire network of dedicated servers that websites can utilize at any time. Thus, enterprise cloud hosting provides the same versatility as conventional cloud hosting, yet with the additional power of dedicated servers.

Many enterprise-computing resources remain significantly underutilized, even with first generation server virtualization [4]. In general, in-house IT operations retain substantial cost structures and are only just starting to capitalize on the opportunity to consume infrastructure, platforms and services on-demand.

4. BUILDING STEPS FOR THE ENTERPRISE CLOUD

Just bringing commercial Cloud computing environments to the Enterprise is not enough. Cloud computing generally means rewriting or authoring new applications in Python, Ruby or other languages. The ability to seamlessly layer Web Service protocols such as HTTP, HTTPS, SOAP, XML or AJAX is a need [7].

The necessary steps that should be followed for establishing an efficient enterprise cloud should include management of the ICT environment, cloud networking, cloud storage, deploying applications in the cloud [2].

4.1. Management of the ICT environment

One of the advantages of enterprise cloud computing is the management of the infrastructure – including the servers, network devices and storage systems. One of the costs of offloading this infrastructure is that the cloud becomes something different and separate from the data center [2].

4.2. Enterprise Cloud Networking

Every enterprise has a unique network infrastructure for accessing servers and allowing applications to communicate between components. Various layers support the management of network addressing, deliver critical services, and ensure security. The infrastructure includes specific addressing, services like DHCP/DNS, identity and directory services like LDAP, and firewalls and routing rules – all reflecting the specific requirements and evolution of the given enterprise [2].

The next major issue with networking in the cloud is data protection [5]. In the data center, there is a secure perimeter defined and developed by the IT organization that is comprised of firewalls, rules, and systems to create a protected environment for internal applications. This is important because most applications need to communicate over ports and services that are not well protected and certainly not safe for general internet access. Since applications are developed for the protected environment of the data center, it can be dangerous to move them unmodified into the cloud. Under normal circumstances, the application owner or developer has to build protection on a per-server basis and enact corporate protection policies [2].

4.3. Cloud Storage

The problems in storage and data management in the cloud result from the diverse and often unfamiliar processes and infrastructures offered by the cloud providers, including: new provisioning methods, storage

properties, data population and transfer, and systems for data management. The cloud providers define the relationship between servers and storage and often impose constraints on everything from allocation size limits to the ways in which storage is managed. These are just some of the things that should be taken into account when start to integrate cloud computing into the existing IT environments [2].

Cloud storage can be simultaneously simple and complex – just like cloud computing in general. It's simple to use if users just want to try something new; complex if users want to integrate cloud storage into their existing processes and infrastructures.

4.4. Enterprise Cloud applications

There are three major cases emerging in the enterprise cloud, reflecting the ways in which specific web apps are architected and the appropriate levels of the customer in exposing their applications in the cloud [9] :

1. Build the entire web application to run in the cloud - Many new companies and start-ups already also use this approach since they don't have any legacy infrastructure to integrate.
2. Move parts of the application to the cloud. Keep some of the app components internal and move others to the cloud. The key considerations are what kind of data the application needs to access, how much data is required.
3. Use the cloud for peak-period scaling - This approach involves scaling portions of the web application into the cloud during peak periods. The cloud becomes an extension of company's data center for on-demand scenarios.

5. CONCLUSIONS

The most important feature of Cloud Computing is the ability to deliver services faster. The storage, computational power and infrastructure layers of Enterprise Cloud Computing allow to rapidly increase capacity to respond to usage peaks. There is no need anymore for long times to preprovision service and a minimal amount of excess capacity to expand rapidly exists. More capacity is achieved without lengthy acquisition cycles [8].

The adoption of true on-demand computing and enterprises buying into the platform and infrastructure-as-a-service models will change the services demanded of the large technology vendors. As those vendors adapt to their customers' wants, it is expected from them to continue buying cloud startups to meet this demand. The best positioned will have something easy to deploy and will also recognize that enterprises need products that can

work for the hybrid environments enterprise customers will likely have for years to come.

6. REFERENCES

[1] Cloud computing (2011) http://en.wikipedia.org/wiki/Cloud_computing.

[2] Considine, J., (2009) Moving to the Cloud: 5-Part Series, http://www.cloudswitch.com.

[3] Mulholland, A., Pyke J., Fingar P. (2010) Enterprise Cloud Computing FAQ, http://whatis.techtarget.com/definition/enterprise-cloud-computing-faq.html.

[4] Enterprise Cloud Leadership Council (2011) http://www.tmforum.org/EnterpriseCloudLeadership/8009/.

[5] Enterprise Cloud Services, (2011) http://cloudservices.microfocus.com/main/Namespaces/MFECS/doc/MFECS-WP-deriving-business-value.pdf.

[6] Higginbotham, S. (2010) Enterprise Cloud Adoption Is Changing the Playing Field, http://gigaom.com/author/shigginbotham/.

[7] Jenkins, J. (2010) *Managing Content in the Cloud, Open Text Corporation*, Open Text Corporation.

[8] Ravi Mhatre, R. (2010) Top 5 trends for enterprise cloud computing in 2010, http://lsvp.wordpress.com/2010/01/05/top-5-trends-for-enterprise-cloud-computing-in-2010/.

[9] Rubin, E., (2010) Three Ways to Do Web Apps in the Cloud, http://www.cloudswitch.com.

[10] Singer, J. (2009) What is Enterprise Cloud Computing, http://soa.sys-con.com/node/1017378.

[11] Shroff, G., (2011) *Enterprise Cloud Computing: Technology, Architecture, Applications*. Cambridge University Press, UK.

[12] Wardle, S., (2011) Private vs Enterprise Clouds, http://blog.gardeviance.org/2011/02/.

[13] What is Enterprise Cloud Hosting? (2011) http://www.webhostingfan.com/2011/03/what-is-enterprise-cloud-hosting.

Neural networks – basic principles for construction, their application in drug design and genetic algorithms

Kiril Gashteovski, Ivan Trenchev[1], Nadezhda Borisova, Ivan Todorin, Grigor Iliev
South-West University "Neofit Rilski", Blagoevgrad, Bulgaria

***Abstract**: In this article we will introduce the basic principles for constructing a neural network. Here will be shown some basic architectures and examples for using the neural networks in chemo-informatics and predicting the properties of biologically active substances. We will discuss some classes of genetic algorithms-training techniques that attempts to emulate the natural process of evolution.*

***Keywords:** neural networks, chemoinformatics, algorithm, genetic algorithm.*

1. NEURAL NETWORKS – BASIC PRINCIPLES FOR CONSTRUCTING A NEURAL NETWORK

First of all – we will make clear the term "neural network". The term "neural network" by itself traditionally means "biological neural network", or more precisely - a network or circuit of biological neurons [1, 2]. Computers today attempt to simulate this networks by the use of the "artificial neural networks", which actually are mathematical or computational models of the biological neuron networks. From this point forward, when we say "neural network" we actually mean "artificial neural network", and if we want to talk about biological neural networks, we will explicitly call them "biological neural networks" [1, 3].

1.1. Biological neural networks

If we want to talk about the mathematical or computational models of the biological neural networks, we must discuss about the biological neural networks first.

The human nerve system consists of about 10^{10} neural cells, also called neurons. The neurons are the basic unit of the human neural system and brain. Neural networks actually are trying to simulate these cells. On the following figure, we can see a biological neural cell [3,5.6]:

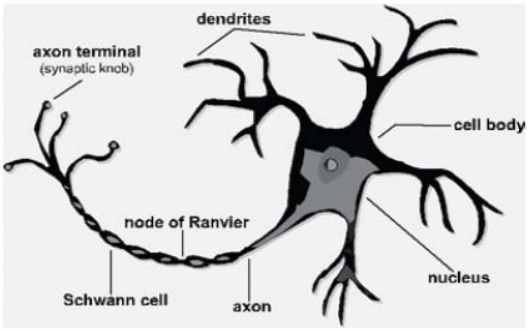

Fig. 1: A neural cell

First, the neural cell accepts signals from the dendrites and afterward when the signal or signals are accepted – that neuron may fire. If the neuron fires – a signal is transmitted over its axon, and through the axon terminals it will leave the neuron and will enter to another neuron through its dendrites, and so on. So, all these neurons that interact with each other with these signals, form a network – biological neuron network [4, 8] .

These kind of signals are analog signals, but most of the modern computers are digital, so simulating biological neural network which works with analog signals on a digital computer can be quite challengeable.

An important part of the neurons is the synapse. It is the area of contact between two neurons. They do not physically touch because they are separated by a cleft [7].

1.2. Neural networks

Now that we have seen the biological neurons, we can talk about the artificial models of them.

First, the synapses that we talked about before, are modelled as *weights.* For an artificial neuron, these weights are in fact numbers. From before, we acknowledged that the neuron can have only one output: either it fires – either not. But, also, the neuron can have one or more inputs, so from this is clear that we actually are talking about a mathematical function, which is called *activation function.* Also, there is another very important attribute in every neuron – *the threshold.* If the weight of the input exceeds the threshold - the neuron fires [4].

To be this process clearer, we will present the following figure:

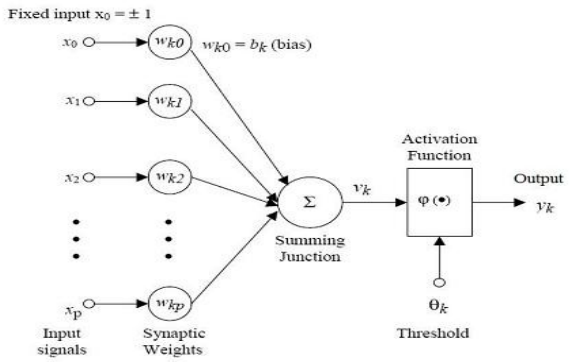

Fig. 2: Mathematical model of neural network

From Fig. 2 it is clear that the internal activity of the neuron is:

$$v_k = \sum_{j=1}^{p} w_{kj} x_j \quad (1)$$

The output of the neuron, y_k, would therefore be the outcome of some activation function on the value of v_k.

There are a lot of neural network architectures and so called “learning methods” with which the neural network learns.

2. TWO LAYER AND ONE-HIDDEN-LAYER NEURAL NETWORK

2.1. Two layer neural network

We will now present one classical example from the mathematical logics – the operator OR. As we all know for the OR logical operator with two input parameters, the statement has value of 0 (false) if and only if the both input parameters have values of 0 (false) – the statement has value of 1 (true) otherwise [3, 8. This is how a simple neuron network that recognizes the OR logical operator looks like:

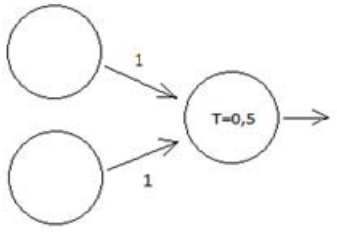

Fig. 3: A neural network that recognizes the OR logical operator

From Fig. 3 is clear the solution of the problem using a simple neural network: there are 2 inputs to the network, the weights of each neurons are 1 and the threshold is 0,5 – hence: the neuron will not fire if and only if the both inputs are 0, but it will fire in all other cases.

This neural network *has only two layers* – an input and an output layer.

2.2. One-hidden-layer neural network

Now we will talk about the XOR operator, which is more complex than the OR operator, and the neural network that recognizes it requires more than two layers – it requires a hidden layer. More complex problems require one or more hidden layers to be solved. The following figure shows how this problem can be solved with *one-hidden-layer neural network:*

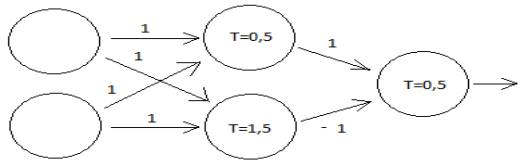

Fig. 4: A neural network that recognizes the XOR logical operator

3. BACK-PROPAGATION LEARNING STRATEGY

One of the most commonly used training method for multi-layered neural network is the *back-propagation learning method (or back-propagation learning strategy).* It is a *supervised-learning* method, and it's a generalization of the *delta rule.*

Supervised-learning method is a training method that provides a neural network with expected outputs, so the neural network is trained in a way that can produce these desired outputs.

The delta rule is also known as the *least mean squared* error rule (LMS). With this rule, the actual output of a neural network is compared against the expected output. This rule is used in supervised training (because the expected output is specified). This is the equation of the delta rule:

$$\Delta w_{kl} = 2\mu\, x_k (ideal - actual)_l \qquad (2)$$

This equation calculates the needed change *(delta)* in the weights from neuron *k* to neuron *l*, μ is the learning rate, and *ideal* is the desired output for the *l* neuron and *actual* is the actual output of the *l* neuron, which means that *(ideal – actual)* is the error.

The basic idea of the back-propagation learning strategies is this: backpropagation works by analyzing the output layer and evaluating the

contribution to the error of each of the previous layer's neurons. The previous layer is adjusted to attempt to minimize its contribution to the error. This process continues until the program has worked its way back to the input layer.

We will now explain the back-propagation learning algorithm through two phases. The first phase is *propagation,* and the second phase is *weight update [4,7].*

Phase 1: Each propagation has this two steps:

1. *Feed-forward propagation* – so, each propagation has forward propagation of a training pattern's input through the NN, so it can generate the propagation's output activations.
2. *Back propagation* of the propagation's output activations through the NN, using the training pattern's target, so it can generate the deltas of all output and hidden neurons.

Phase 2: For each weight of each synapse, we have:

1. Multiply weight-synapse's input activation and its output delta, in order to get the weight-gradient.
2. Bring the weight in the opposite direction of the gradient, by subtracting a ratio of it from the weight. This ratio is the so-called learning rate.

Now, the 2 mentioned phases need to be repeated until the performance of the NN is good enough [3].

4. APPLICATION OF THE NEURAL NETWORKS IN CHEMOINFORMATICS

First, we will make this "chemoinformatics" term clear. Cheminformatics (also known as chemoinformatics and chemical informatics) is the use of computer and informational techniques, applied to a range of problems in the field of chemistry.

The number of applications of the neural networks in chemoinformatics increases every day. In general, different types of problems require different neural network architectures and different learning strategies. An interesting fact though, is that about 90% of the problems described until now in the chemical literature have used one-hidden-layer neural networks and the back-propagation learning strategy [7, 8]. Here are some examples where can we use the neural networks in chemistry: analytical chemistry, organic chemistry, pharmaceutical and biochemistry, chemical engineering and chemical industry etc.

5. GENETIC ALGORITHMS

Basically, “the genetic algorithms” are algorithms that are trying to imitate the biological evolution, based on the principles of the Darvin's theory of evolution. These algorithms are part of a bigger category of algorithms – *the evolutionary algorithms.* The genetic algorithms can be applied to solve search and optimization problems [3, 6].

The natural selection is the main characteristic of the evolution in nature. The organisms that are better suited in their environment have bigger chances of survival and reproduction, while the organisms that are not so well suited in their environment have smaller chances of survival and reproduction [3]. The same principle is used in the genetic algorithms.

6. ACKNOWLEDGEMENTS

This study was supported by Grant DVU 01/0197 of Ministry of Education and Science.

7. PREFERENCES

[1] Blake J. F. (2000) Chemoinformaticsv – predicting the physicochemical properties of ‘drug-like’ molecules *Current Opinion in Biotechnology*, *(11) 1 , 104-107;*

[2] Da Costa F. B., Terfloth L., Gasteiger J. (2005) Sesquiterpene lactone-based classification of three Asteraceae tribes: a study based on self-organizing neural networks applied to chemosystematics Phytochemistry, (66) 3, 345-353

[3] Heaton, J. (2010) *Introduction to neural networks with Java,* Heaton Research, *ISBN: 1604390085*

[4] Jure Zupan J., Gasteiger J. (1999) *Neural Networks in Chemistry and Drug Design;* Weinheim, New-York, Chichester, Brisbane, Singapore, Toronto; WILEY-VCH

[5] Paul J. Werbos (1994). The Roots of Backpropagation. From Ordered Derivatives to Neural Networks and Political Forecasting. New York, NY: John Wiley & Sons, Inc.

[6] Rojas R. (1996), *Neural Networks - A Systematic Introduction*, Berlin, New York, Springer-Verlag

[7] Russell S.,N. (2003) P. Artificial Intelligence A Modern Approach. 578.

[8] Tohru N. (2003) Solving the XOR problem and the detection of symmetry using a single complex-valued neuron Neural Networks, (16), 8, 1101-1105

Creation of Soil Water and Physical data base and its inclusion in a new version of GIS of Soil Resources Attributive Table

Boyko Kolev
SWU "N. Rilski", Blagoevgrad, Bulgaria

Abstract: *For better using of GIS of Soil Resources a new version of the attributive table formation was created. This gives the possibility soil physical and water properties to be included into the table. The simulation procedure for soil hydro-physical properties determination was realized by using soil particle size distribution data only. This develops a calculation algorithm for soil water content dynamic monitoring, which was realized for some of Bulgarian soils by [2], with developed in his Ph.D. thesis simulation model.*

The main aims of the study are:

To demonstrate how useful is the new version of the attributive table formation.

To show how could be applied the simulation model for environment conditions monitoring and agricultural production management.

Keywords: *environment conditions, simulation model, soil moisture at field capacity, wilting point, effective soil water content, particle size distribution.*

1. INTRODUCTION

Sustainable agriculture means to create rules and mechanisms, which are created from last reaching of soil science and information about plant science for effective management of productive resources of agricultural lands and protect their ecological functions.

For operative of legal information about soil resources the Soil Resources Agency developed Geographic Information System (GIS) that is based of soil survey in scale 1:10000 and together with constant land use and separation. In GIS input an information as follow: soil cover, soil type, particle size distribution, depth of hard roc, salt and carbonate content, mean soil bonitet and soil category for non irrigated areas and bonitet for 22 agricultural crops, slope and exposition of the areas, type and quantity of pollution est.

The aim of this article is to estimate a method suggested by [2] for conversion soil particle size distribution as determined according to the soil standards in Bulgaria according to Kachinsky to the FAO and USDA classification scheme for a given soil. This method gives a lot of possibilities for calculating some physical and hydro-physical properties for the given soil. Including of these soil parameters in GIS of Soil Resources (GISoSR) attributive table give better possibilities for monitoring and management of crop production and realization of sustainable development in agriculture.

The aims of this study are:

To demonstrate a simulation procedure for soil hydro-physical properties determination by using the created soil particle size distribution database only.

To demonstrate how useful could be the developed model for agricultural production management.

2. OBJECT AND METHODS

2.1. Geographical characteristics

Yakoruda Municipality [7] is located in the northeastern part of Blagoevgrad an area of 339.3 sq. km. It borders the municipalities of Samokov and Kostenets at Sofia and Velingrad, Belitsa and Belovo from Pazardzhik district. The municipality is composed of eight villages - the municipal center of Yakoruda seven villages which are located in the southeastern part of the municipality., single line spacing, 24 pt spacing before and 6 pt spacing after the capital letters.

Relief is mountainous and hilly, covered parts of the Rila and the Rhodope Mountains and narrow valley in the upper course of Mesta. The average altitude is 1603 m and average slope is 11.1%, which adversely affect general economic and infrastructural development of the municipality and the development of the urban network.

The climate is temperate continental with very low Mediterranean influence, penetrating the valley of the Mesta River, the average annual temperature is 8^0C. Winters are cold, with average January temperature is - 2^0C - snow 150 days a year. Summer is short and cool with average temperatures in July 18^0C.

2.2. Soil resources

The general view of the object is presented in Fig. 1.

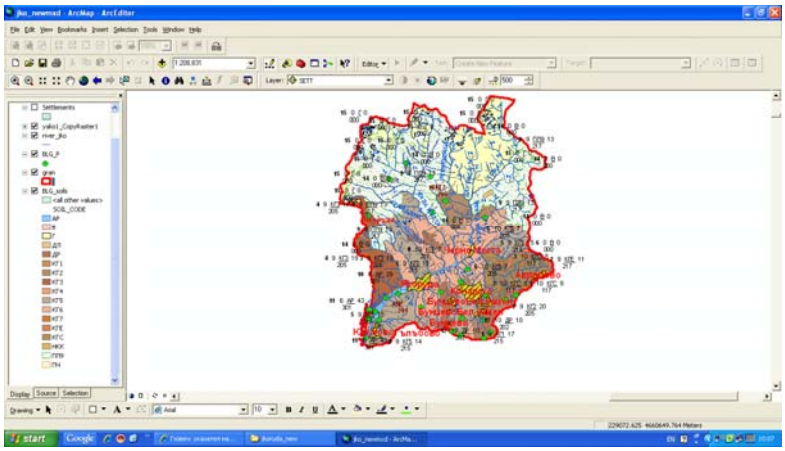

Fig. 1: General view of the object.

Brown forest soils predominate (1-7 KG) - Fig. 1 and found more brown, shallow, middle eroding (KGE) and brown, shallow, high eroded (KGC). They are the most widespread soils in mountain areas and represent 1.7 million ha or 15%. These soils are rich in humus, but the average stock to absorb nitrogen and phosphorus. They need a combination of fertilization. In the high mountains brown forest soils pass into dark colored forest and mountain-meadow soils.

In river beds are found alluvial (AP - alluvial, medium strong) and on the slopes - delluvial (SF - (delluvial, slightly strong) and delluvial (RD - deluvial, medium strong) soils. In the high parts of the municipality the mountain-meadow, shallow, weak and middle eroded soils (PL9) dominated. Cinnamonic soils - Fig. 1 are represented by cinnamonic and immature, shallow, highly eroded and rocks (NCC). Rocks (D), sand and gravel (PM) and gorges and gullies (B) complete the soil resources of the municipality.

2.3. Methods

The survey instruments used ArcGIS 9.3 - ArcMap for objects, Visual Basic and Access to realize the determination of hydro-physical and hydrological properties of studied soils [3, 4].

3. RESULTS AND DISCUSSIONS

The simulation procedure for soil hydro-physical properties derivation was realized by using soil particle size distribution data only [5]. This develops a calculation algorithm for the soil water content dynamic monitoring. The general database use for the calculation is presented in Fig. 2 and chemical properties in Fig. 3.

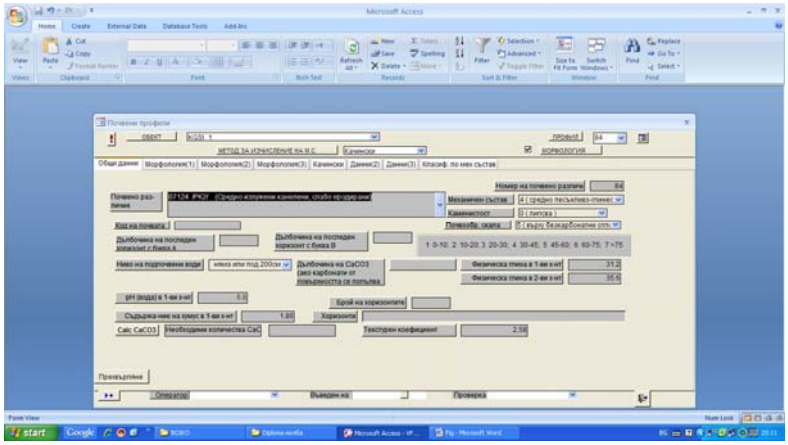

Fig. 2: The general database table (6).

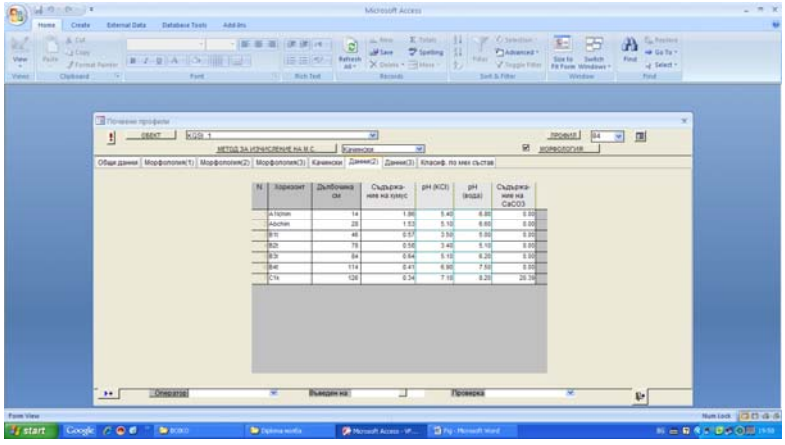

Fig. 3: Chemical properties (6).

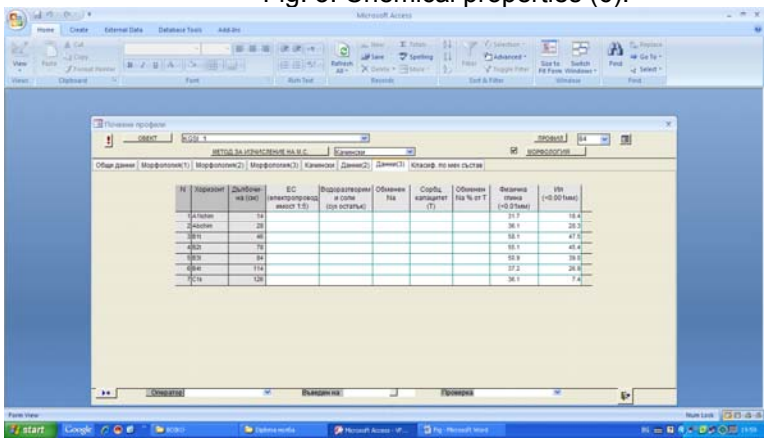

Fig. 4: Content of physical clay and il in soil horizons.

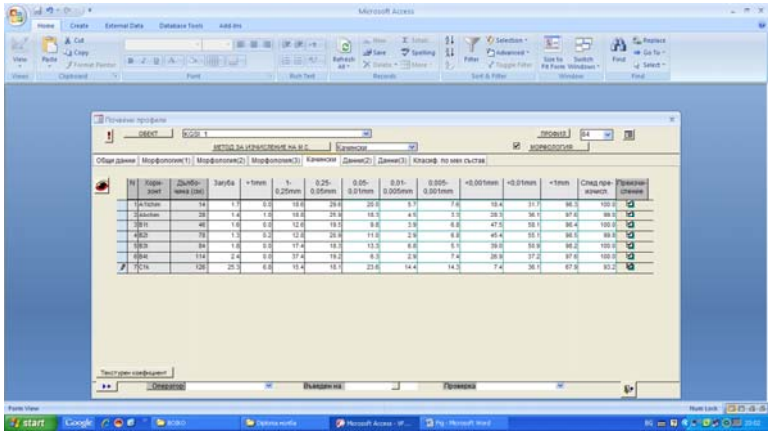

Fig. 5: Particle size distributions table.

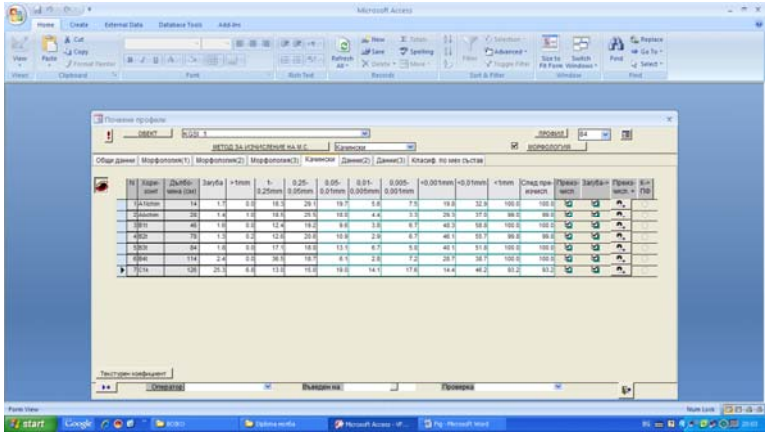

Fig. 6: Particle size distributions (after adjustment for losses after HCl treatment).

Fig. 4, 5 and 6 show content of physical clay and il in soil horizons, particle size distributions and particle size distributions (after adjustment for losses after HCl treatment) respectively.

To perform the classification of the soil mechanical composition is necessary to pass from Kachinsky classification scheme [1], which is mainly used in Bulgaria to the USDA classification scheme developed in [5].

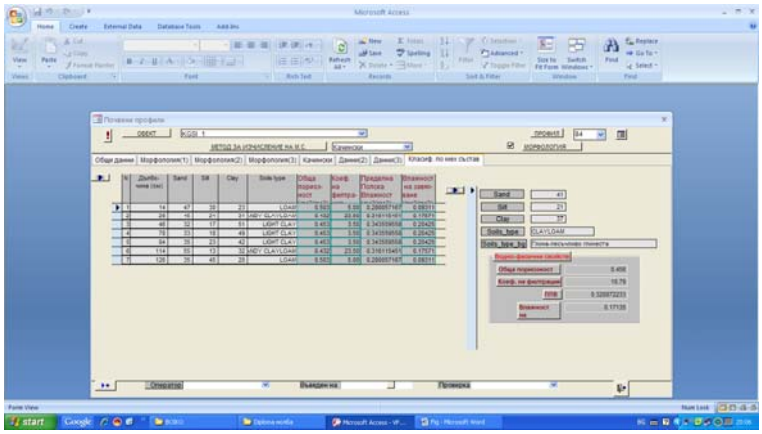

Fig. 7: Soil classification according to soil texture information and derivation of some water physical and hydrological properties of a given soil.

The derivation of soil moisture at field capacity (SMfc), soil moisture at wilting point (SMwp) hydraulic conductivity at full saturation (K0), effective water content (Tpwc), total porosity (SM0) from standard soil texture information, percent of sand, silt, clay according to the USDA classification scheme and soil texture classification for a given soil, are presented in Fig. 7. These data could be added in the GIS of soil resources attributive table.

4. CONCLUSIONS

The approach suggested by [2, 5] for derivation SMfc, SMwp, K0, SM0 and Tpwc and include them in GISoSR attributive table, gives more quality and quantity information of the studied soils.

Recommendations have been made to minimize negative impacts on environmental components.

The derived monitoring information system could be used for effective monitoring and strict control of air, soil and water resources of the municipality.

5. ACKNOWLEDGEMENTS

Author thanks to Mr. Damian Mihalev - Executive Director of the Soil Resources Agency - Sofia for his assistance during this paper realization. Thanks also to the staff of General Direction of Agriculture and Forestry in Yakoruda municipality for the information that allowed the elaboration of the study.

6. REFERENCES

[1] Gurov G., Artinova N. 2001. Soil Science, Makros, Plovdiv.
[2] Kolev B. 1994. Ph.D. Thesis., Sofia, pp. 10-35.
[3] Kolev, B., et al. 2007. Using GIS of Soil Resource for Soil Fertility Estimation in Razlog Municipality., Annual of Shumen University "K. Preslavski" t. XVII B 3 „Natural Science", Shumen, pp. 182-201.
[4] Kolev, B. et al., 2006. The Geographic Information System of Soil Resource Using for Sustainable Agriculture Realization In: International Conference on Cartography and GIS, January 25-28, 2006, Borovets, BULGARIA.
[5] Kolev, B., et al., 1996, Derivation of Soil Water Capacity Parameters from Standard Soil Texture Parameters for Bulgarian Soils, Ecological Modelling (84), N^{o} 1-3, Elsevier, Amsterdam, Holland, pp. 315-319.
[6] Soil Resources Agency. http://www.soils-bg.org/
[7] The municipality plan for Yakoruda Municipality development 2007 – 2013.

Reducing the induction of scattering inside the measuring current transformers during the simulational process of transitional magnetization by the use of *Chip Corder ISD1400*

Vasil Milovanski, Emil Radev, Krasimir Stoyanov
South-West University "Neofit Rilski", Blagoevgrad, Bulgaria
HMS “Acad. S. P. Corolov", Blagoevgrad, Bulgaria

Abstract: *The simulation of transitional processes in the current transformers by the use of specialized integral scheme – ISD 1400 is reviewed by the authors of several publications. The aim of this one is to review a change in the constructional parameters of the current transformers in order to achieve a more accurate measurement of their magnetic characteristics.*

Key words: *transformer, magnetic, hysteresis cycles, harmonious components*

1. INTRODUCTION

The use of current transformers for precise measurements in the electrical circuits encounters many problems today due to the non-linear ambiguous relation between the strength of the magnetic field H and the magnetic induction $B \to B = B(H)$ inside their ferromagnetic cores. The process becomes even more difficult when the current transformers [*CT*] are used to analyze electrical circuits in a transitional state. In this case, the magnetic induction $B(H)$ is generally moving on private hysteresis cycles. There isn’t any common solution to the problem, so private solutions must be determined that can create models with different degree of accuracy, which are related to specific working conditions. Some of the models use a simplified presentation of the hysteresis – taking in mind only three of the base parameters – coercive force - $H_C, A/m$, residual magnetic induction - B_r, T and saturation induction - B_m, T [2]. However, this approach can’t produce satisfactory results during the analysis of an electrical circuit in a transitional state.

Therefore, other methods are developed to capture the families private hysteresis cycles for a specific ferromagnetic material. One of them is

created by the use of direct computer simulation of transitional processes inside the magnetic core of the current transformers.

The method evolves [3] by making the data of the transitional characteristics to power a specialized integral scheme *Chip Corder ISD1400* [5] by the use of which bigger mobility of the experimental process can be achieved. The risk of technical failure is reduced in the cases of electrical break in the power of the simulator.

The extrapolation of the magnetic characteristics in the mentioned model requires good practical design and precise manufacturing of the current transformer. For the purpose, a set of strictly defined rules are usually followed by the use of the specified magnetic parameters and characteristics, if there are any. It is no secret that in the recent practice a difference can be found between the used magnetic materials and information given for them. Moreover, in some implementations the working conditions, like operating frequency, temperature and others, are not analyzed or described in the attached documentation. Therefore, the process of extrapolation of the private hysteresis cycles by the method described in [3] requires a correct and balanced manufacturing of the referenced *TT.*

2. CHOICE OF AN APPROPRIATE CURRENT TRANSFORMER AND A METHOD OF INVESTIGATION – AN EXPERIMENTAL MODEL

The presented work aims to determine a suitable method for preliminary analysis of ferromagnetic cores designed for the manufacturing of measuring transformer. It uses an existing low-powered mains transformer with Π figurative band magnetic core, which shape is similar to a toroidal one. It is comprised of three coils, placed on two reels with a total number of windings as follow windings of transformers - $w_1 = 150,tur$, $w_2 = 150,tur$ and $w_3 = 2000,tur$ (w_3 is not used in the calculations).

The dynamic resistance of the first and the second coils are also equal - $R_1 = R_2 = 0.4,\Omega$. The section of the magnetic core is $S = 512 * 10^{-6},m^2$ and the length of the average magnetic power line is $l_{av.} = 0.198,m$. The equivalent scheme for the transformer is presented in Figure 1, and the equations that describes it - in (1).

The determination of private hysteresis cycles by the method of computer simulation that uses the integral scheme *Chip Corder ISD1400* is done by quasi-static state of magnetization [1]. This means that the period of full re-magnetization of the ferromagnetic material is exceeding - $T \geq 50,ms$ ($f = \frac{1}{T} \leq 20,Hz$). For that purpose, a generator is used, which has an adjustable frequency and a linear power booster. For the illustration of

the specified method, another decision pattern is utilized, shown on Figure 2. It most accurately concords with the used for testing mains transformer at a frequency $f = 50, Hz$.

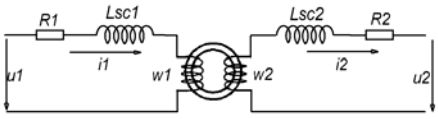

Fig. 1. Equivalent scheme for nonlinear transformer

(1)

$$\begin{cases} u_1 = R_1 i_1 + Lp_1 \dfrac{di_1}{dt} + w_1 \dfrac{dF}{dt} \\ u_2 = -R_2 i_2 - Lp_2 \dfrac{di_2}{dt} + w_2 \dfrac{dF}{dt} \\ i_1 w_1 - i_2 w_2 = i_0 w_1 = l_{av.} H \end{cases}$$

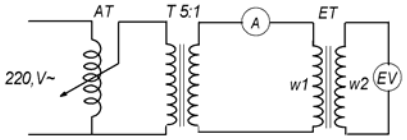

Fig. 2. Scheme of experimental platform with mains power and autotransformer

Scheme legend:

AT - autotransformer;

T - an extra transformer with turns ratio $k_U = 5:1$;

A and EV - digital devices that measure the electrical current and voltage.

The measuring transformer is in state of “idle”, because its second coil is connected to the high-ohm electric voltmeter. Therefore, the system of equations (1) turns into (2).

(2)

$$\begin{cases} u_1 = R_1 i_1 + w_1 \dfrac{d\Phi}{dt} \\ u_2 = w_2 \dfrac{d\Phi}{dt};\ i_2 = 0 \\ i_1 w_1 = l_{av.} H \Rightarrow H = \dfrac{i_1 w_1}{lav.} = \dfrac{i_0 w_1}{lav.} \end{cases},$$

Due to the low electrical current, the induction of scattering - Lsc_1 of the first circuit and the electrical current - i_2 of the second circuit of the transformer are both ignored. In the third equation of (2) $i_0 = i_1$ it represents the current that is magnetizing the magnetic core.

The analysis of the magnetic flow can be done most accurately by measuring the voltage of the second coil, because that way the reduction of the dynamic resistance in the first coil can be eliminated - $u_{R1} = R_1 i_1$.

The way the measuring transformer is connected to the generator of the sinusoidal voltage (Figure 2) points to the conclusion that the magnetic flow in the core is also sinusoidal - $\Phi(t) = \Phi_m \sin(\omega t)$, $\frac{d\Phi}{dt} = \omega\Phi_m \cos(\omega t)$. The same applies to the magnetic induction - $\frac{dB}{dt} = S\omega B_m \cos(\omega t)$, where S is the section of the magnetic core.

After taking into account the last two dependences from (2) the following results are generated:

(3) $\begin{cases} B_m = \dfrac{U}{4.44fwS} \\ H = \dfrac{w_1}{l_{av.}} I \end{cases}$, where U and I are the readings from the devices.

3. RESULTS FROM THE EXPERIMENT

On Figure 3. the graphical representation of the magnetization process for the analyzed magnetic core is shown. It presents the dependencies the measured current has on the applied voltage - $I = I(U)$ and the magnetic induction has on the intensity - $B_m = B_m(H)$.

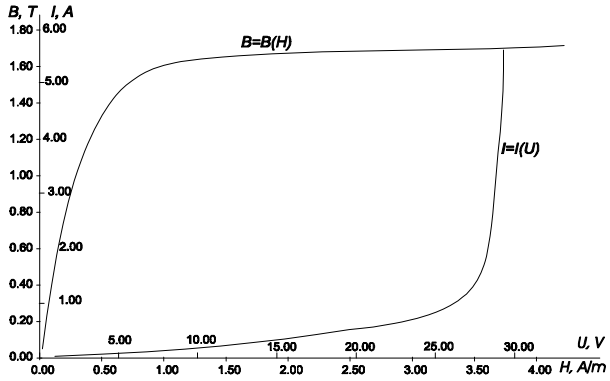

Fig. 3. Graphs for the current $I = I(U)$ and the magnetic induction - $B_m = B_m(H)$

The first graph $I = I(U)$ shows that during the initial growth of the voltage, the electrical current, operating on „idle", is increasing in a slow linear manner, while the voltage reaches the value of $U = 23,V$. When $U = 29,V$ the magnetic core comes to state of saturation. The same process can be seen on the other graph $B_m = B_m(H)$. The magnetic induction is changing linearly

until $B = 1.4, T$, and when $B = 1.7, T$, the magnetic core reaches a saturation state.

The maximum value of the working induction can be determined by both graphs by choosing an area of the characteristic with a relatively high linearity. It must also be noted that the extrapolation of private hysteresis cycles using the simulation method in conjunction with the specialized integral scheme *Chip Corder ISD1400* is done in one of the areas of magnetization. This means that, it lacks the full re-magnetization of the ferromagnetic core. Therefore, the maximum jump of the magnetic induction can’t be more than half of the measured linear area and in this case $\Delta B_m \le 0.6, T$ is chosen.

4. DEFINING THE LINEAR AREA OF MAGNETIZATION AND THE INDUCTION OF SCATTERING

The determination of the linear area of magnetization is done by a measuring transformer, which works in a state of „idle”. The process of finding families of private hysteresis cycles, by the use the simulation method, requires the change of the magnetic induction to be achieved stepwise. This method of magnetization is affected by the induction of scattering, which must be as low as possible. In order to be determined, another experimental platform must be utilized - Figure 4. Here the transformer has a secondary coil, of a "short circuit". On the scheme R_1 and R_2 are shown as separate elements, which represent the dynamic resistance of each one of the coils, as well as Lsc_1 - Lsc_2, which stand for their corresponding inductions of scattering. The readings that were measured by the devices during the experiment are as follow - $A_1 = 1.04, A$, $A_2 = 1.0, A$ and $EV = 2.3, V$.

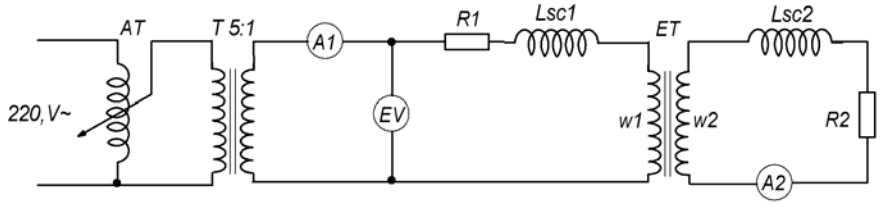

Fig. 4 Experimental platform for determining the inductions of scattering Lsc_1 and Lsc_2

On Fig. 5. an equivalent scheme of transformer with an equal number of windings in the first and in the secondary coil - $w_1 = w_2$ is shown. In this case, the parameters - R'_2, Lsc'_2 and i'_2 are brought to the first one, where

$R_1 = R'_2 = R$ and $Lsc_1 = Lsc'_2 = Lsc$. The voltage $u_{\Phi 1} = w_1 \frac{d\Phi_0}{dt}$ represents the magnetic flow in the core. The electrical current i_0 is the current that magnetizes the magnetic core - $i_0 = i_1 - i'_2$.

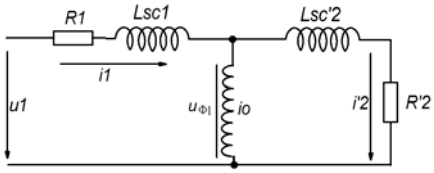

Fig. 5. Equivalent scheme of the transformer when $w_1 = w_2$

The determination of the induction of scattering can be done approximately after applying a complex representation of the parameters of the scheme in the calculation process and also after comprising an equation using the second law of Kirchhoff.

(4) $\dot{U} = \dot{I}_1(R_1 + j\omega L_{sc1}) + \dot{I}'_2(R'_2 + j\omega L'_{sc1}) = (\dot{I}_1 + \dot{I}'_2)(R + j\omega L_{sc})$, if the phase shift between the two currents is ignored the following can be concluded from the equation:

5) $U = (I_1 + I'_2)\sqrt{(R^2 + \omega^2 L_{sc}^{\ 2})}$.

After processing the above expression, the induction of scattering can be evaluated:

(6) $L_{sc} = \frac{1}{\omega}\sqrt{\frac{U^2}{(I_1 + I_2)^2} - R^2} = 3.36, mH$.

The equation end value is higher than the normal one that can be achieved by transformers with that type of construction and size. This is a result of the two coils being placed on separate reels.

5. CONCLUSION

1. The extrapolation of private hysteresis cycles using the method of computer simulation in conjunction with the integral scheme *Chip Corder ISD1400* has the special feature that the magnetization is done in one area of the hysteresis cycle, in which the state of saturation can be achieved easily. Therefore a good knowledge of the magnetic properties of the utilized material is necessary. The catalogue data is only used for initial orientation. The material needs to be analyzed and the methods are not complicated.

2. Taking into account the stepwise way of change of the magnetic induction, the errors that can be made during its determination can be caused by the magnitude of the induction of scattering. The described method can be used to approximately evaluate it and also to search for constructive solutions for its reduction.

6. REFERENCES

[1] *Milovanski V.* (1997), An interface transformer for computer simulation of transitional processes in the current transformers, A collection of scientific labours, Varna, part 2, p. 8-11

[2] *Milovanski V.* (1999), One method of examining of transitional processes in the current transformers by using a computer simulation, A collection of scientific labours, Shumen, part 3, p. 53-57

[3] *Milovanski V., Radev E.* (2003), Simulation of transitional processes in the current transformers by using an integral scheme from the series ISD 1400., Scientific labours, Veliko Tarnovo, part 73-I, p. 510-516

[4] *Milovanski V., Radev E.* (2009), Simulation Reducing the impact of the generated noises by the integral scheme ISD1400 in the process of simulation of transitional magnetization of electrical transformers., Scientific labours – FMNS, Blagoevgrad, V-1, p. 171-176

[5] www.winbond.com

On Some Properties of Quasi-Essential Variables of the Boolean Functions

Ivo Damyanov
South-West University, Blagoevgrad, Bulgaria

Abstract: *In the paper we continue the study of the properties of quasi-essential variables and quasi-separable sets of variables. Some properties of strongly quasi-essential variables and quasi-separable sets of variables are discussed.*

Keywords: essential variables, separable sets, strongly essential variables.

1 Introduction

Let the Boolean function $\Phi(y_1, y_2, x_i)$ is a such a function that any arbitrary Boolean function $f(x_1, x_2, ..., x_n)$ of -variables can be represented as $\Phi(f_0, f_1, x_i)$, where f_1 and f_2 does not depend on x_i. Then we say that we have *decomposed* f to f_1 and f_2 with respect to variable x_i using Φ. In [4] J.Denev called such a function Φ, *universal*. Here f_1 and f_2 are called Φ-subfunctions of f. If the set of obtained Φ-subfunctions with respect to variables $x_{i_1}, x_{i_2}, ...x_{i_k}$ does not depends on the order of decomposition then the function Φ will be called *proper*.

The most popular proper universal function is known as Shannon Expansion.

$$\Phi(f_1, f_2, x_i) = x_i f_1 + \bar{x} f_2. \qquad (1)$$

Many properties of variables and sets of variables, such as essentiality and separability, are introduced using Shannon expansion [1], [5], [8], [7].

Here $f_1 := f^{sh}(x_i = 0)$ and $f_2 := f^{sh}(x_i = 1)$ are functions of $n-1$ variables (the functions which are obtained by substituting variable x_i in f with the Boolean constants 0 and 1) and are called *sh-subfunctions* of $f(x_1, \ldots, x_n)$.

Another widely used proper universal functions are

$$f = xf_1 \oplus f_2 \quad positive\ Davio\ (positive\ polarity)$$
$$f = \bar{x}f_1 \oplus f_2 \quad negative\ Davio\ (negative\ polarity)$$

The positive and negative Davio are also known as Reed-Muller expansions.

Since definition of fictive/essential and strongly essential variables and separable sets of variables can be extracted by properties of obtained sh-subfunctions it is possible to introduce similar definitions using another proper universal function. In [2], I. Damyanov introduced quasi-fictive and quasi-separable sets of variables using Positive Davio Decomposition. The transfer of results to Negative Davio Decomposition is straightforward.

Essential inputs and separable sets of inputs for Tree automata was introduced by Sl. Shtrakov and others in [11] and further observed in [10], [3] and [12]. Sl. Shtrakov and K. Denecke in [9] introduced essential variables and separable sets of variables in Universal algebras.

2 Basic Definitions and Notations

The function $f(x_1,\ldots,x_n)$ can be decomposed with respect to (w.r.t.) the variable x_i as follows:

$$f(x_1,\ldots,x_n) = x_i f_1 \oplus f_2. \qquad (3)$$

Here f_1 and f_2 are functions of $n-1$ variables and we will call them *rm-subfunctions* of $f(x_1,\ldots,x_n)$, or *Reed-Muller's subfunctions* and will denote them by $f^{rm}(x_i = 1)$ and $f^{rm}(x_i = 0)$ respectively.

Let

$$f^{rm}(x_i = c_i) = \begin{cases} f_2, if\ c_i = 0 \\ f_1, if\ c_i = 1 \end{cases}. \qquad (4)$$

If $g = f^{rm}(x_{i_1} = const,\ldots,x_{i_k} = const)$, where $M = \{x_{i_1},\ldots,x_{i_k}\}$ then we will write $g \prec_{rm}^{M} f$.

Definition 1 *Let f be a Boolean function and its Shannon decomposition w.r.t. variable x_i is $f = \bar{x}_i f_1 + x_i f_2$. The variable x_i is called sh-fictive (or fictive) for $f(x_1,\ldots,x_n)$ iff $f_1 = f_2$ and sh-essential (or essential) iff $f_1 \neq f_2$.*

The set of all essential variables for $f(x_1,\ldots,x_n)$, will be denoted by $shEss(f)$. The set of all functions that depend essentially exactly on n variables will be denoted by $F^{sh}(n)$. It is clear that if we get a function and all its variables are sh-fictive then this function is *constant.*

Definition 2 *Let f be a Boolean function and its Reed-Muller decomposition w.r.t. variable x_i is determined by the equation $f = x_i f_1 \oplus f_2$. The variable x_i is called rm-fictive (or quasi-fictive) iff $f_1 = f_2$. The variable x_i is rm-essential (or quasi-essential) for $f(x_1,\ldots,x_n)$ iff $f_1 \neq f_2$.*

The set of all quasi-essential variables for $f(x_1,\ldots,x_n)$, will be denoted by $rmEss(f)$. The set of all functions which depend quasi-essentially exactly on n variables will be denoted by $F^{rm}(n)$.

Example 1 Let $f = x_1x_2 \oplus x_1 \oplus x_2 \oplus 1$. The Reed-Muller decomposition of f w.r.t. x_1 is: $f = x_1(\overline{x}_2) \oplus \overline{x}_2$. Hence $x_1 \notin rmEss(f)$. Analogously, Reed-Muller decomposition of f w.r.t. x_2 is $f = x_2(\overline{x}_1) \oplus \overline{x}_1$, i.e. $x_2 \notin rmEss(f)$. So, $rmEss(f) = \varnothing$, but f is not constant.

Some of essential variables of the Boolean function alone ca determine the function value. For example, if $f(x_1,...,x_n) = x_1 g(x_2,...,x_n)$, and the variables x_1 has value 0 then the function f has value 0 no matter what the other variables values are.

Definition 3 [13] *If the Boolean function $f \in F(n)$ is such that $f = \dot{x}_i f_{\dot{x}_i}$ (or $f = \dot{x}_i + \overline{\dot{x}_i} f_{\overline{\dot{x}}_i}$), then the variable x_i is called 0-single-faced variable of f (or 1-single-faced variable) and the function f -- single-faced function. Here by $\dot{x}_i$ we denote either x_i or $\overline{x_i}$.*

In [13] Wang and others show that functions with single-faced variables have more compact representations with OBDD. It is easy to see that in our case a quasi-fictive variables actually are 0-single-faced variables for Reed-Muller expansion. We focus on studying the properties of quasi-essential variables since their behavior is more complex.

Definition 4 *If* $f \in F^{rm}(n),\ n \geq 1$ *and* $\varnothing \neq M \subseteq rmEss(f)$ *then the variable* $x \in M$ *is called rm-strongly essential (quasi-strongly essential) for* f *w.r.t.* M, *if there exists value* c, *such that* $M \setminus \{x\} \subseteq rmEss(f^{rm}(x = c))$.

If $f \in F^{rm}(n),\ n \geq 1$ and $\varnothing \neq M \subseteq rmEss(f)$ then the set of all quasi-strongly essential variables for f w.r.t. M will be denoted by $rmEss^{*}(f, M)$.

Definition 5 *If* $f \in F^{rm}(n),\ n \geq 1$ *and* $\varnothing \neq M_1 \subseteq rmEss(f)$, $M_2 \subseteq rmEss(f),\ M_1 \cap M_2 = \varnothing$, *then we say that the set* M_2 *is rm-separable (quasi-separable) for* f *w.r.t.* M_1, *if for the variables from* M_1 *there exist values such that when replacing them by Boolean constants, the new rm-subfunction* g *obtained from* f *satisfies* $M_2 \subseteq rmEss(g)$. *This will be denoted by* $M_2 \in rmSep(f, M_1)$.

Definition 6 *For the Boolean function* f *we say that the set* M $(M \subseteq rmEss(f))$ *is quasi-separable for* f, *if* M *is quasi-separable for* f *w.r.t.* $rmEss(f) \setminus M$.

3 Properties of Quasi-Essential Variables

The basic properties of quasi-essential (quasi-fictive) variables can be proved easily.

Lemma 1 *Let* x_i *and* x_j *be two variables of Boolean function* $f(x_1, \ldots, x_n)$. *If* $g = f^{rm}(x_i = \alpha_i)$ *and* $h = f^{rm}(x_j = \beta_j)$ *for* $\alpha_i, \beta_j \in \{0,1\}$ *then* $g^{rm}(x_j = \beta_j) = h^{rm}(x_i = \alpha_i)$.

Lemma 2 *If* x_i *is quasi-fictive for the Boolean function* $f(x_1, \ldots, x_n)$, *then* x_i *is quasi-fictive for each rm-subfunction of* f.

Lemma 3 *If* $f \in F^{rm}(n),\ g \prec_{rm} f$ *and* $M \in rmSep(g)$ *then* $M \in rmSep(f)$.

In [2] the first results for quasi-strongly essential variables was obtained.

Theorem 1 *If* $f \in F^{rm}(n), \quad n \geq 2$ *and* $M_1 \in rmSep(f, M_2)$, $M_2 \neq \emptyset$, *then there exists at least one variable from* M_2 *which is quasi-strongly essential for* f *with respect to* $M_1 \cup M_2$.

Corollary 1 *If* $f \in F^{rm}(n), \quad n \geq 2$ *and* $M \in rmSep(f)$, *where* $M \subset rmEss(f)$ $(M \neq rmEss(f))$, *then there exists at least one variable* $x_t \in rmEss(f) \setminus M$ *such that* $M \cup \{x_t\} \in rmSep(f)$.

In [6] the following theorem is proven for strongly essential variables.

Theorem 2 [6] *If the Boolean function* $f(x_1,...,x_n)$ *depends essentially on at least two variables, then for every set of variables* $M = \{x_1,...x_m\}$, $M \subset shEss(f)$ *and for every set of values* $C = \{c_1,...,c_m\}$ *the set* $shEss(f) \setminus shEss(f_1)$ *contains at least one strongly essential variable for the function* f. *Here* $f_1 = f^{sh}(x_1 = c_1,...,x_m = c_m)$.

The following two examples shows that this statement is not always true if we try to state it respectively for quasi-essential variables.

Example 2 *Let* $f = x_1(x_2 \oplus x_3) \oplus x_2x_3$. *Here* $rmEss(f) = \{x_1, x_2, x_3\}$. *Let the set* $M = \{x_3\}$. *We observe two cases:*

Case 1: Let $x_3 = 0$. Then $f^{rm}(x_3 = 0) = x_1x_2$ and from where we have
$rmEss(f^{rm}(x_3 = 0)) = \{x_1, x_2\}$, *i.e.* $rmEss(f) \setminus rmEss(f^{rm}(x_3 = 0)) = \{x_3\}$.

Case 2: Let $x_3 = 1$. Then $f^{rm}(x_3 = 1) = x_1 \oplus x_2$ and from where we have
$rmEss(f^{rm}(x_3 = 1)) = \{x_1, x_2\}$, *i.e.* $rmEss(f) \setminus rmEss(f^{rm}(x_3 = 1)) = \{x_3\}$.

From *Case 1* and *Case 2* follows that x_3 is quasi-strongly essential variable for f. If we observe x_1 or x_2 we get similar results.

Example 3 *Let* $f = x_1x_2 \oplus x_3$. *Here* $rmEss(f) = \{x_1, x_2, x_3\}$. *Let the set* $M = \{x_1\}$. *We observe two cases:*

Case 1: Let $x_1 = 0$. Then $f^{rm}(x_1 = 0) = x_3 = x_3.1 \oplus 0$ and from where we have

$rmEss(f^{rm}(x_1 = 0)) = \{x_3\}$, *i.e.* $rmEss(f) \setminus rmEss(f^{rm}(x_1 = 0)) = \{x_1, x_2\}$,

but neither x_1 or x_2 are quasi-strongly essential variables.

Case 2: Let $x_1 = 1$. Then $f^{rm}(x_1 = 1) = x_2 = x_2.1 \oplus 0$ and from where we have

$rmEss(f^{rm}(x_1 = 1)) = \{x_2\}$, *i.e.* $rmEss(f) \setminus rmEss(f^{rm}(x_3 = 1)) = \{x_1, x_3\}$,

and here x_3 is quasi-strongly essential variable.

Next we will prove invariance of quasi-essentiality under projection of variables.

Theorem 3 *If* $f \in F^{rm}(n)$, $n \geq 3$ *and* x_1 *forms quasi-separable pairs with* $x_2,...x_{r+1}$, *then any rm-subfunction of* f *with respect to variables in* $rmEss(f) \setminus \{x_1, x_2,..., x_{r+1}\}$, *depends quasi-essentially on* x_1.

Proof: Since x_1 is quasi-essential for f from Lemma 2 follows that we can choose a constants $c_2,...,c_{r+1}$ such that

$$f_1(x_1, x_{r+2},..., x_n) = f^{rm}(x_2 = c_2,..., x_{r+1} = c_{r+1}).$$

From x_1 - quasi-essential for f_1, follows that f_1 does not depends quasi-essentially from the variables in $\{x_{r+2},..., x_n\}$. This is true, since otherwise if we assume that f_1 depends quasi-essentially from at least one variable $x_j \in \{x_{r+2},..., x_n\}$, from Corollary 1 will follows that $\{x_1, x_j\}$ forms quasi-separable pair for f. Therefore, from Lemma 3 follows that x_1 forms quasi-separable pairs not only with variables in $\{x_2,..., x_{r+1}\}$, which is a contradiction with the conditions of the theorem.

Consequently, whatever values $c_{r+2},...,c_n$ we take, the rm-subfunction $f_1^{rm}(x_{r+2} = c_{r+2},..., x_n = c_n)$ will depends quasi-essentially on x_1.

Therefore from $f_2 = f^{rm}(x_{r+2} = c_{r+2},..., x_n = c_n) \succ f_1^{rm}$, follows that $\{x_1\} \in rmEss(f_2)$, from where follows the truth of the proposition.

Conclusions

Proper universal functions are widely exploited in data structures for representation and manipulation of the Boolean functions. Since definition of fictive/essential and strongly essential variables and separable sets of

variables can be expressed by properties of obtained subfunctions it is possible to introduce similar definitions using another proper universal functions. In addition to the results obtained in [2] we have investigated invariance of quasi-essentiality under projection of variables.

References

[1] Брейтбарт, Ю.Я., *О существенных переменных функций алгебры логики*, Доклады АНСССР, **172**, (1967), 9-10

[2] Damyanov, I., *On Some Properties of Variables in Reed-Muller Decompositions*, Mathematics and education in mathematics, (2001), 258-262

[3] Damyanov, I., Sl. Shtrakov, *Essential inputs and minimal tree automata*, Discrete mathematics and applications, (2002), 77-85

[4] Денев, Й.Д., *Върху едно обобщение на понятието подфункция*, Математика и математическо образование, Доклади на Четвъртата пролетна конференция на БМД, (1978), 98-104

[5] Chimev, K., *Separable sets of arguments of functions*, MTA SzTAKI, Budapest, 180, (1986), 1-173

[6] Чимев, К. *Дискретни функции и подфункции*, ВПИ, Благоевград, 1991

[7] Chimev, K., Iv. Mirchev *Separable and dominating sets of varables*, SWU, Blagoevgrad, (1993)

[8] Shtrakov, Sl., *Dominating and Anuling Sets of Variables for the Functions*, Blagoevgrad, 1987

[9] Shtrakov, Sl., K. Denecke, *Essential Variables and Separable Sets in Universal Algebra*, Multiple-Valued Logic, An International Journal 8/2, (2002), 165-181

[10] Shtrakov, Sl., Vl. Shtrakov, Tree Automata and Separable Sets of Input Variables, FILOMAT 2001, Nis, Yugoslavia, (2001), 61-69

[11] Shtrakov, Sl., Tree automata and essential input variables, Contributions to general algebra, 13, Heyn, Klagenfurt, (2001), 309-319

[12] Shtrakov, Sl., Essential variables and positions in terms, Algebra Universalis, Vol. 61, No. 3-4, (2009), 381-397

[13] Wang, Y., C.McCrosky, X.Song, Single-faced Boolean Functions and their Miminization, The Computer Journal, Vol. 44, No. 4, (2001), 280-291

Laboratory course development for teaching DSP and digital filters implementations on FPGA

Sotirios Pouros[*], Angel Popov[**], Valentin Hristov[***]
[*]*Alexander Technological Institute of Thessaloniki, Greece*
[**]*Technical University, Sofia, Bulgaria*
[***][3]*South-West University, Blagoevgrad, Bulgaria*

***Abstract**: This paper presents block design based laboratory courses on IIR and FIR digital signal processing. The proposed course on DSP is implemented with field-programmable gate arrays (FPGA) devices. By using FPGAs, students are given the opportunity to design and explore custom hardware implementations. The goal is to develop signal processing experiments in which students are asked to design and implement FIR and IIR digital filters on FPGA boards. The students in the limited amount of time available for labs must learn to develop digital filtering systems using MatLab, Simulink and Xilinx System Generator. Finally, the students should know how to test the programmed FPGA and to determine the characteristics of implemented digital filters.*

***Keywords:** Electronic engineering education, Field programmable gate arrays. Signal processing, FIR, IIR, DSP, Digital filters*

1. INTRODUCTION

The digital signal processing (DSP) industry requires engineers capable of developing DSP solutions to applications. The FPGAs understanding can provide an essential tool for all electronic engineers. The students must have a basic knowledge and understanding of the latest technology available in the market. The combined knowledge of MatLab, Simulink and Xilinx System Generator on FPGAs can result in solutions in FIR and IIR applications which are very common. The main target is to simplify the process of the FPGA programming for students to acquire a solid base to evolve later on in the industry. Programming languages as Verilog, VHDL or even C can

[3] This paper is sponsored by Research project No SRP-B4 at South-West University- Blagoevgrad, Bulgaria

provide capabilities for DSP but the students will have to experiment on basic system design before entering traditional programming [1].

2. METHODOLOGY

This course is designed for students specializing in electronics and DSP. However, in practice, the majority of students are electronics students [2]. Students taking this course are expected to be familiar with Matlab, Simulink, and ISE Xilinx tools. Previous knowledge of DSP theory and FPGA implementation of digital circuits is also required.

Before the enrolment at the lab the students should have a basic knowledge of all the themes mentioned below [3].

- FPGA structure
    - Configurable Logic Blocks (CLB)
        - Look-up Table (LUT),
        - D Flip-Flop,
        - Multiplexer 2:1 (MUX)
- Differences between FPGAs and CPUs
- Basic Work Flow
    - Specification, Verification, Implementation, System Debug
- DSP Introduction
    - Digital Filters, FIR, IIR

2.1 Using Simulink

The lab professor should introduce the basic functions and tools of MatLab and Simulink before starting the digital filters design. The elementary steps to follow are illustrated below:

- Basic use of Simulink
- Step1: Introduction to design
- Step2: The effect of the sample period
- Step3: Low level filter design
- Step4: Creating a subsystem

2.2 Using Xilinx System Generator

Furthermore, an Introduction of the Xilinx System Generator [4] for the Xilinx FPGA devices in essential. The elementary steps to follow are illustrated below:

- Basic use of System Generator
- Step1: Simulation of a prototype circuit
- Step2: Redesign with Xilinx Blocks

- Step3: Implementation of the Xilinx design
- Step4: Experimenting on different architectures

Step1: The prototype system is designed by Simulink libraries. Based upon this system, a Xilinx FPGA system will be designed and then it will be compared to the prototype.

The students must implement the design in Figure 1 and then start the simulation. The result should be like the one in Figure 2.

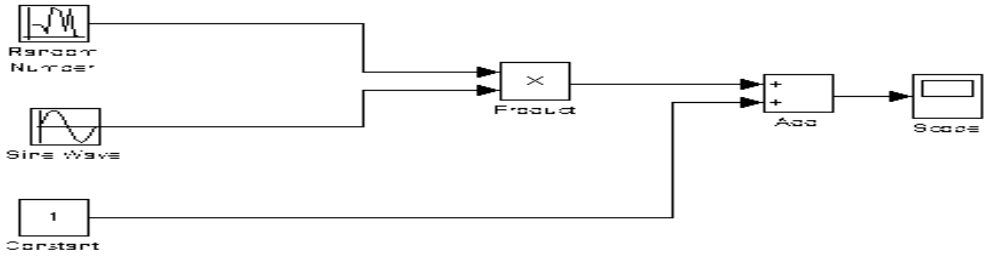

Fig. 1: Step 1 Design

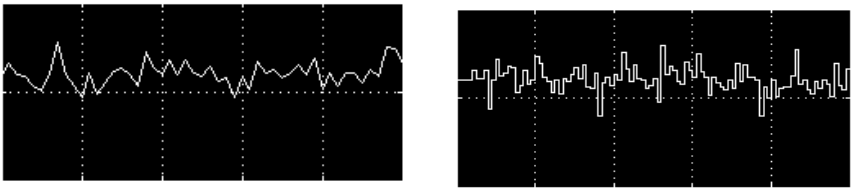

Fig. 2: Step 1 and Step 2 graphs

Step 2: Evolving the previous system, as in Figure 3, using the Xilinx Blockset Library

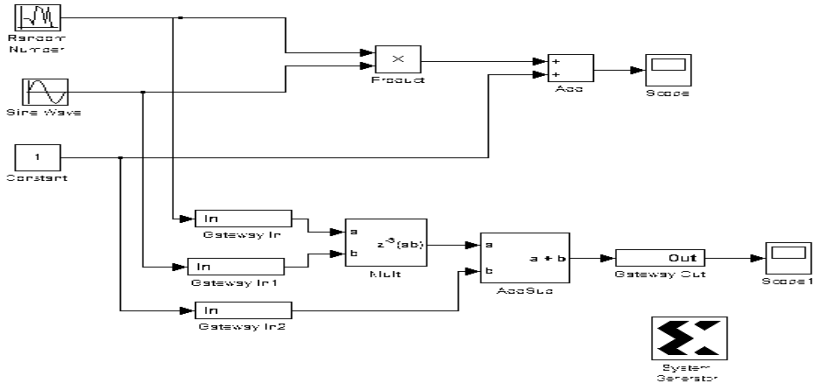

Fig. 3: Step 2 Design

The students should start the simulation and compare the results between the two systems output in Figure 2. The output signal of the Xilinx FPGA system is scaled because the System Generator forces sampling to the input signals and presents the real behavior of the FPGA.

The results of the simulations can be observed by the use of a Subtractor. For the students further experimentation, 3 unit of delay blocks can be connected to the output of the Add block.

Step 3: The bitstream generation is an essential step to the FPGA programming. By double clicking the System Generator Block the output FPGA device can be selected from the dropdown menu. Then, by clicking the Generate command button, automatically all the stages of the synthesis will be executed.

Step 4: This step is experimenting on different architectures.

The students have to create a subsystem, using all the Xilinx blocks including the System Generator block, as shown in Figure 4.

By copying the subsystem, a second subsystem is created. The students change the initial design as illustrated in Figure 4:

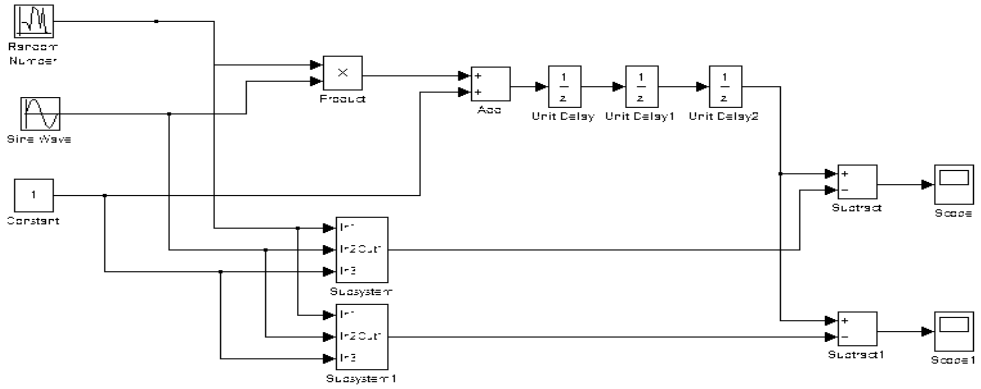

Fig. 4: Architecture with two subsystems

At this time, the design includes two subsystems, each one with its own System Generator Block. This design can be implemented with two FPGA devices or inside one FPGA device, as parts of a wider system. So, each System Generator block results in the creation of an entity, which represents the relevant subsystem. The use of subsystems is a useful technique, where different architectures may be used to implement a specific design [5].

In addition to the above, the students should modify the design, so that the same functionality is achieved by the DSP48 macro block of Xilinx. The set up of the parameters takes place by double clicking the DSP48 macro block. An equation like A*B+C can be inserted to the instructions field. Final steps are: the simulation, the functionality check up of the design and the generation of the bitstream.

2.3 Digital Filters IIR and FIR Theory

Before the development of the filters, the students should be familiar with the basic rules and terms of digital filtering in FIR and IIR implementations. The calculation of the H(z) transfer function and the difference equation is fundamental to develop these filters.

2.4 Digital Filters implementation with System Generator

An example of an IIR peak filter will illustrate the basic steps of the implementation.

The students should develop the design of the Figure 5 and in the Filter block the Figure 6 design should also be developed.

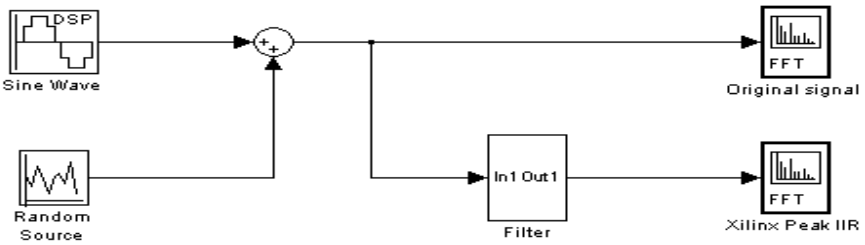

Fig. 5: Initial design of digital filters

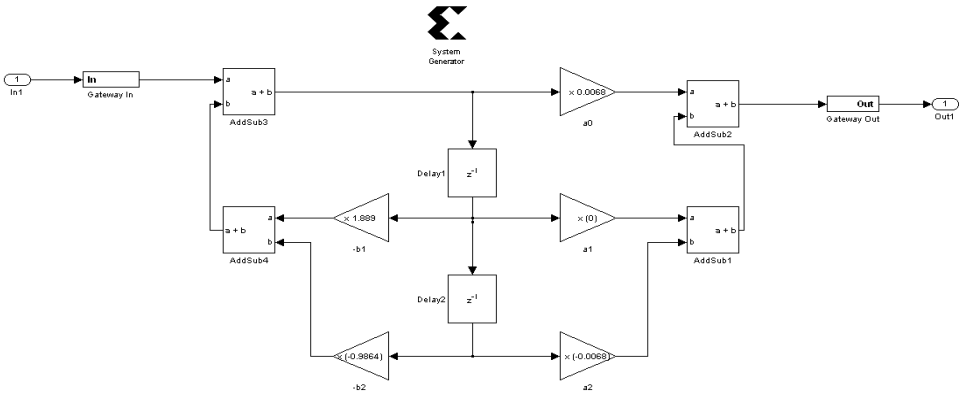

Fig. 6: IIR peak filter design

This is the implementation of an IIR filter with the transfer function:

(1) $$H(z) = \frac{0.0068 - 0.0068z^{-2}}{1 - 1.889z^{-1} + 0.9864z^{-2}}$$

Finally, by simulating the system the results should appear as in Figure 7.

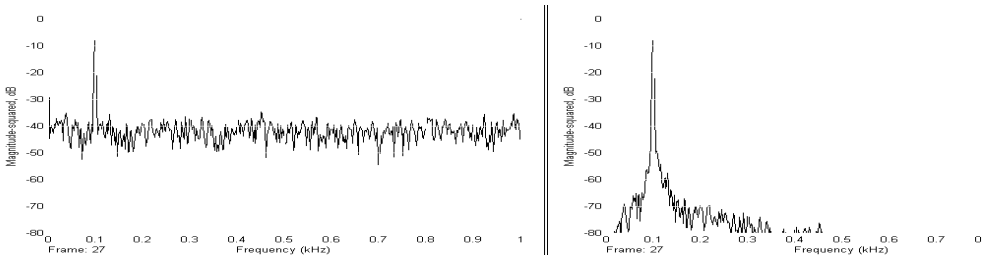

Fig. 7: Result graphs of a peak filter

At least two more exercises should be fulfilled by the students. An IIR Low Pass filter and an FIR Low Pass filter are recommended. The design of a FIR filter should be similar to the one in Figure 8.

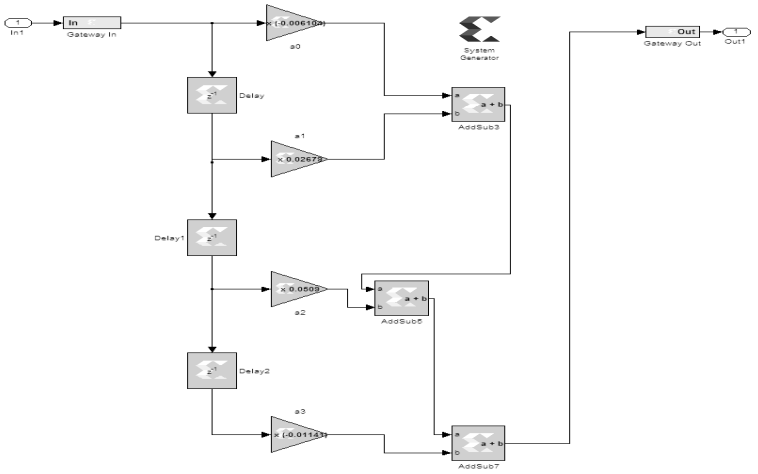

Fig. 8: Basic design of FIR Filters

2.5 Automated FIR filter design using FDATool & FIR Compiler

The MatLab FDATool [6] is an easy to use signal processing tool widely known to the scientific community. The significance of this experiment is to present the ability of the Systems Generator FIR Compiler to cooperate with the FDATool.

2.5.1 Using the FDATool

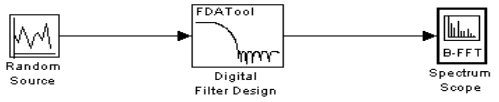

Fig. 9: FDATool digital filters design

The students are required to develop the system illustrated in Figure 9 and run the simulation after setting the parameters.

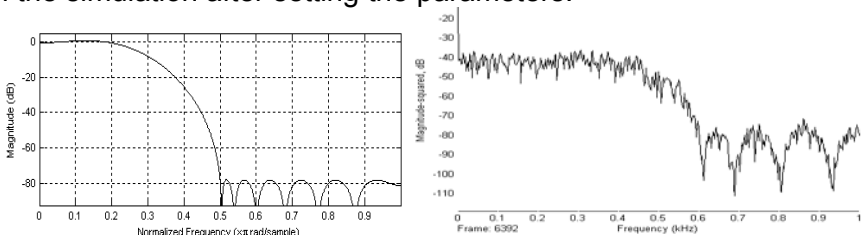

Fig. 10: Result graphs using the FDATool

The FDATool and the Scope should result in Figures 10 graphs.

2.5.2 Using the FDATool and the FIR Compiler

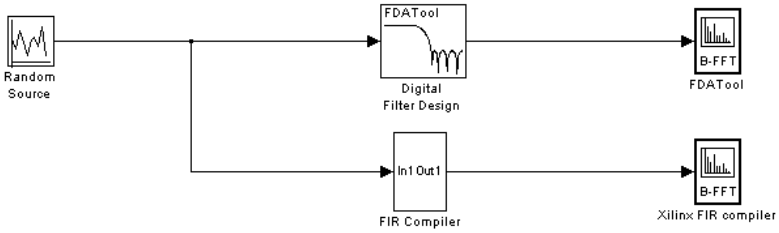

Fig. 11: Step 1 and Step 2 grafs

The system should evolve ,as in Figure 11, accordingly and the Figures 12 design must be implemented in the FIR Compiler .

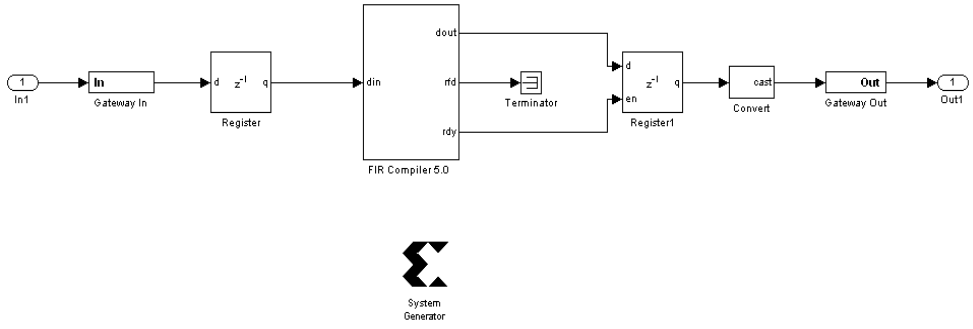

Fig. 12: Step 1 and Step 2 grafs

The results of the two scopes should be identical.

There are two ways to acquire the coefficients for the FIR Compiler.

1. The coefficients from the FDATool are stored at the Num variable of the MatLab workspace and the Num variable must be specified at the Coefficient Vector in the Filter Specification Tab.
2. By the Xilinx Blockset/Index library the Xilinx block FDATool should be added to the subsystem. After the setting of the parameters in the

FDATool properties window the xlfda_numerator('FDATool') value should be added to the Coefficient Vector in the Filter Specs Tab.

Finally, the bitstream can be generated.

2.8 Testing

After the programming of the FPGA device, a real time testing procedure should take place so that the students may realize the result of a digital filtering system. A function generator should be used as an input source and an oscilloscope at the output of the FPGA device to observe the result of the processing on the screen. Different values of the frequency will result in different outputs depending on the filter specifications. Using the obtained values [7], a figure will be designed to be compared to the diagram of the simulation.

3. CONCLUSIONS

Students realize that just by using the software tools is difficult to understand what has been achieved with the programming and the simulation until it is used in real time and the results are obvious. Even though the DSP FPGA course is difficult, the combined knowledge of MatLab, SImulink and System Generator at a preliminary level is enough to be a solid base for an engineer to start building more complex digital systems.

4. REFERENCES

[1] Kang J, Olson B, Felzer A, Chandra R, Oldak S.,(2007), "*Simulink Based Real-Time Laboratory Course Development",* IEEE International Conference on Microelectronic Systems Education (MSE'07)

[2] Sansaloni T, Pérez-Pascual A,Torres V, Almenar V, Toledo J, Valls J.(2007), *"FFT Spectrum Analyzer Project for Teaching Digital Signal Processing With FPGA Devices*", IEEE Transactions on Education, vol. 50, No. 3

[3] Vainio O, Salminen E, Takala J., (2010), *"Teaching Digital Systems Using a Unified FPGA Platform"*, 12th Biennial Baltic Electronics Conference (BEC2010), Estonia

[4] Xilinx, FPGA and CPLD Solutions from Xilinx, Inc. Available: *http://www.xilinx.com/index.htm* (accessed March 27, 2011)

[5] Mentor Graphics, The EDA technology Leader. Available: *http://www.mentor.com* (accessed March 27, 2011)

[6] MathWorks, MATLAB and Simulink for Technical Computing. Available: http://www.mathworks.com (accessed March 27, 2011)
[7] Meyer-Baese U., (2007), *Digital Signal Processing with Field Programmable Gate Arrays*. Springer, USA

Neurotherapy and Neurofeedback, as a research field and evidence-based practice in applied neurophysiology, are still unknown to Bulgarian population

Vezenkov, S.R.
Department of Language and Speech Pathology, South West University “Neofit Rilski”, e-mail: vezenkov.stoyan@swu.bg

Abstract: *Neurofeedback and Neurotherapy, an ultramodern computerized evidence-based practice worldwide, was shown here to be a completely unknown to Bulgarian population. The powerful combination of modern computerized signal processing of neurophysiological parameters (qEEG, amplitude, frequency bands, coherence), applied statistics (neurometrics and its normative databases) and principles of applied neurosciences opened a novel research field for Bulgarian scientists and practitioners. These novel methods could be used widely as supplementary therapy to many drug and other therapies, especially in the field of psychopathology and language-speech pathology. Several related methods such as neurotherapy, neurofeedback, neurometrics, etc. are shortly reviewed here and their relationship discussed.*

Key words: *neurotherapy, neurofeedback, BCI (brain-computer interface), evidence-based practice, applied neurosciences*

Short overview of the methods in applied neurophysiology

Neurotherapy includes electrophysiological based methods of modulating the state of the brain. The well-known methods until now are transcranial direct current stimulation (tDCS), AC-stimulation including deep brain stimulation (DBS), transcranial magnetic stimulation (TMS) and neurofeedback. Neurofeedback in turn can be divided into two discovered methods: EEG biofeedback and DC (or infra slow wave) biofeedback. EEG biofeedback is a method for modulating the brain activity by mean of neurophysiological feedback using such parameters as power of given brain

waves (delta, theta, alpha, beta etc.), intercortical coherence, beta theta ratio etc. (Buzsaki, 2006)

Neurotherapy should be distinguished from eastern methods of self-regulation, confined by relaxation, and placebo effect, which has distinct neuronal mechanism. Placebo had been shown could amount up to 30 % from the effects even of medical drugs.

Any physiological parameter measured within the body could be fed back to the patient and modified in inherently learning process. The latter is the concept of biofeedback method in general. In particular, neurofeedback uses EEG parameters such as spectral characteristics (absolute amplitude, relative amplitude of a given frequency band, amplitude ratio etc.), coherence measures (recordings from different points of the scalp, C3 to F3, for example), intracranial current density processed by LORETA or s-LORETA.

LORETA, low resolution electromagnetic tomography, is an EEG imaging technology allows for a tomographic representation of EEG sources in 3D space.

QEEG method as a main part of neurofeedback is computing spectral characteristics (amplitude, frequency bands, coherence) of recorded EEG signal.

Several types of neurofeedback have been developed depending on the parameter fed back:

- ERD-based neurofeedback (ERD – event related desynchronization, measures the percentage change of the EEG amplitude in response to a given event); (Pfurtscheller et al., 2006)
- ERP-based neurofeedback (ERP – event related potential);
- Self-regulation of HEG (hemoencephalography, measures the oxygenation of local blood flow by spectrophotometry); (Toomim et al., 1999)
- Self-regulation of fMRI (functional magnetic resonance imaging, dependent on the level of blood oxygen); (Fox et al., 2007; Weiskopf et al., 2004)
- Self-regulation of evoked slow cortical potentials, in response to warning stimuli; (Strehl et al., 2006)

If the modulating of neuronal activity might be directed to control of computer, the approach has been called “brain-computer interface” (BCI). (Bayliss et al., 2004) For example, a patient has been learned to control a computer cursor by self-regulation of his EEG slow cortical potentials (Birbaumer, 2006). The idea of BCI is similar to the basics of neurofeedback.

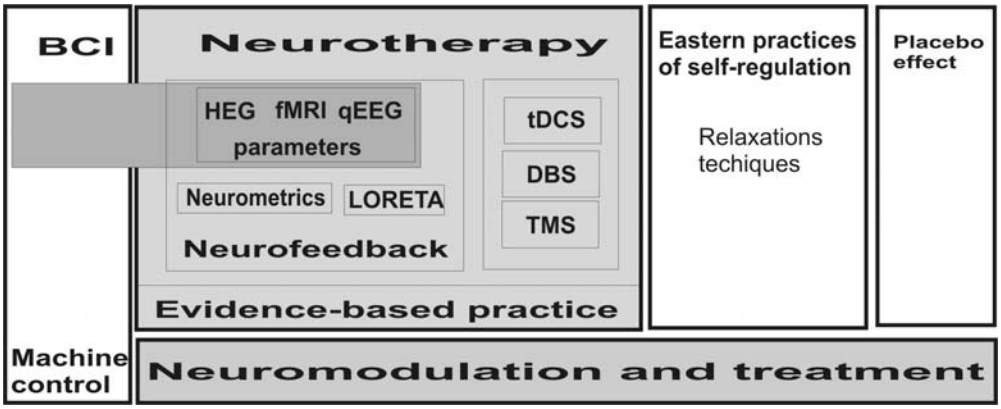

Fig.1. Relationship between the methods. *BCI – brain computer interface; HEG – hemoencephalography; fMRI – functional magnetic resonance imaging; qEEG – quantitative electroencephalography; LORETA - low resolution electromagnetic tomography; tDCS – transcranial direct current stimulation; DBS – deep brain stimulation; TMS – transcranial magnetic stimulation*

Neurometrics was born from applied statistics and has defined the neurophysiological basis of brain dysfunction and brain normative functioning. The normative databases developed in neurometrics are used nowadays as a basis of defining neurofeedback protocols of treatment each particular case as evidence-based practice.

To ensure the evidence-based practice the top Labs developed normative databases and give us opportunity to compare the computed parameters (qEEG) of recorded individual signal to the normative values.

There are several known databases developed – HBI, NxLink, Neurorep AQR, Novatech LORETA, SKIL, BRC and Neuroguide.

The relationship between the above mentioned methods is presented in **Fig. 1**.

The purpose of this study was to gather preliminary data in what degree Bulgarian population is informed to the following terms EEG, neurotherapy, neurofeedback and evidence-based practice.

Method

A preliminary simple on-line questionnaire was composed and distributed to 1000 persons randomly. The obtained data was imported and analyzed in MS Excel 2010 (Microsoft corp.) and put into tables and figures.

Results

From the distributed 1000 questionnaires, were obtained 295 fully finished (57,63% women, 42,37%). Sex and age frequencies (in %)

within the gro up are shown in **Fig. 2**. The geographic diffusion of the tested persons is presented in **Fig. 3**.

The responses of the questions are presented in **Table 1**.

Table 1. The responses to the main questions.

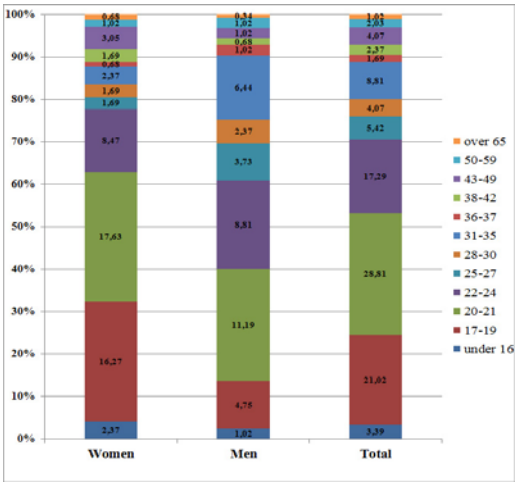

Fig.2. Frequencies (in %) of the sex and age of the tested persons

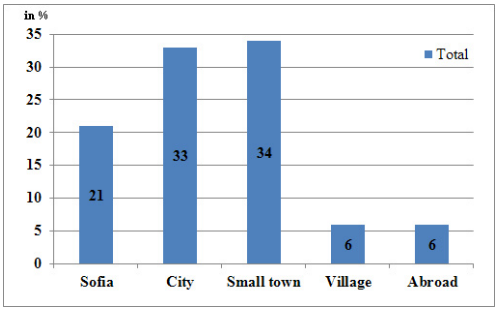

Fig.3. Geographic spreading of the tested persons (in %)

	Question	Yes *(in %)*	No *(in %)*
1	Do you know what EEG is?	37*	63*
2	Do you know what Biofeedback is? *	21*	79*
3	Do you know what Neurofeedback is? *	19*	81*
4	Do you know what Neurotherapy is?	54	46
5	Is there any difference between Neurofeedback and Neurotherapy?*	38*	62*
6	Do you know what evidence-based practice is? *	23*	77*

**The questions were followed by the open text box with the instruction to write down the meaning of the terms*

Only 35%, 5,01%, 15,25%, 3,34% and 3,39% of the test persons tried to describe the terms respectively to the questions 1, 2, 3, 5 and 6 in the following open text boxes. From them only 34%, 4,4%, 6,1%, 0% and 0,34% respectively answered right. 3,73% from the answers to question 3 were that neurofeedback is identical to neurotherapy. 1,36% from the respondents of question 5 said that neurotherapy is part of the neurofeedback method and nobody answered correctly. The most correct answers were obtained to the question 1 – 34%.

Conclusions

Except to the abbreviation EEG (34% correct answers) to all other questions the correct answers were less than 5%. These results suggested that the terms neurotherapy, neurofeedback and evidence-based practice are completely or partial unknown for Bulgarian people. A tremendous educational work lies before the research and public health institutions in Bulgaria to inform the population about the methods of applied neurosciences including biofeedback, neurotherapy, neurofeedback and the relevant evidence-based practices.

References

[1] Birbaumer, N. (2006) Breaking the silence: brain-computer interface (BCI) for communication and motor control. Psychophysiology 43(6), 517-532
[2] Buzsaki, G. (2006) Rhythms of the brain. Oxford University Press
[3] Bayliss, J.D., S.A. Inverso and A.Tentler (2004) Changing the P300 brain computer interface. Cyberpsychol. Behav. 7(6), 694-704
[4] Fox, M.D. and M.E. Raichle (2007) Spontaneous fluctuations of brain activity observed with functional magnetic resonance imaging. Nat. Rev., Neuroscience 8, 700-711
[5] Weiskopf, N., K. Mathiak, S.W. Bock, F. Scharnowski, R. Veit, W. Grodd, R. Goebel and N. Birbaumer (2004) Principles of a brain-computer interface (BCI) based on real-time functional magnetic resonance imaging (fMRI). IEEE Trans. Biomed.Eng. 51(6), 966-970
[6] Strehl, U., U. Leins, G.Goth, C.Klinger, T. Hinterberger and N. Birbaumer (2006) Self-regulation of slow cortical potentials: a new treatment for children with ADHD. Pediatrics 118(5), 1530-1540
[7] Toomim, H. and J. Carmen (1999) Hemoencephalography (HEG). Biofeedback 27(4), 10-14
[8] Pfurtscheller, G. and C. Neuper (2006) Future prospects of ERD/ERS in the cortex of brain-computer interface (BCI) developments. Prog. Brain Res. 159. 433-437

Active Learning's Approach to the Physics Education

Plamen S. Gramatikov[1], Maria I. Gramatikova[2]
1-The Neofit Rilski South-West University, Blagoevgrad, Bulgaria
2-The Ichko Boichev Vocational High School, Blagoevgrad, Bulgaria

***Abstract**: Basic characteristics of traditional and active schools are presented and comparison between their didactic models is made.*
***Keywords:** Active Learning, Pedagogical Interactions, Interactive Methods.*

1. INTRODUCTION

In Democracy the citizens, acting on their own knowledges and opportunities and not as followers of a "gifted leader", are supposed to participate actively to the decisions taken. As these decisions are increasingly dependent upon Science and Technology developments, the active citizen's participation implies that he not only should be Science and Technology literate but also that he must have cognitive skills permitting decisions on incomplete knowledge, i.e. also in areas he (she) is not an expert. Formation of models developing such skills is (or should be) an integral part of Science teaching, particularly of Physics.

2. TRADITIONAL OR ACTIVE SCHOOL?

Traditional school is based on a very old conception, but many of its characteristics are still present in education in almost all countries. These basic characteristics are [1]:

- a curriculum and syllabi defined in advance;
- the aim of teaching is to acquire the curriculum;
- the basic teaching method is the lecturing (verbal transmission), with or without some didactic aids;
- the student role is to listen, to try to understand and memorize the compulsory academic subject matter;
- grading (in writing or orally) consists of checking to what extent the compulsory academic subject matter has been acquired;
- the motivation for learning is external (grades, praise, prizes-punishments);

- the child is treated in school only as a student, i.e. the person who should with understanding repeat the lectured material.

Active school is a school which is more centred and oriented toward a child who is treated as a person and not only as a student, i.e. different aspects of his/her personality are engaged in the instructional process.

Basic characteristics of the active school are:

- a detailed curriculum defined in advance is not obligatory - only guidelines are given;
- the children's interest is taken as a starting point and the learning process is developed on the basis of this interest;
- the academic subject matter is connected to the child's personal experience;
- the learning motivation is personal, internal;
- the basic teaching method is aimed to increase chances for gaining personal experience, i.e., active methods are dominant - practical working, manual activities, expressive activities (such as drawing or literary essays), lab experiments, social activities, field work, observation of natural phenomena, etc.

The aim of the active school is to develop the individuality of each child, and not only to acquire a specific school curriculum. Children's satisfaction with the undertaken activities is assessed, as well as children's progress compared to their initial state, their motivation and interest in work and activities, and the development of their personality.

Didactic difference between these both types of schools can be seen when compare the both models of pedagogical relations in them on Figures 1 and 2.

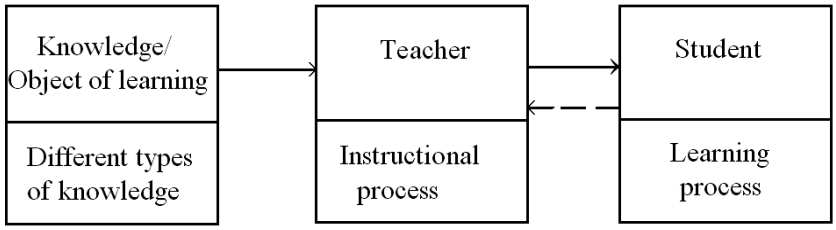

Fig. 1: Linear model scheme of pedagogic interactions in traditional school

The model of pedagogic interactions in traditional school is characterized by the following:

- the process of learning is linear, moving in the direction indicated by the arrows (the dotted arrow shows a minimal possibility of action going that way). A teacher, professionally trained in some academic discipline, occupies the central place in this interaction. Here there is a possibility of latent danger (usually turned into the reality) for the entire school to be organized around professional activities of the teacher (thus the theories of school learning are often reduced to theories of teaching).

- the most negative consequences of this model of pedagogic interaction is the possibility to jeopardize the essential aspect of school learning - the very interaction. In the theory and in practice, this unique process of interaction has been broken down (almost as a rule) into two isolated parts: that what the teachers are doing (that is teaching), and that what the children are doing (learning process), with deadly consequences for the efficiency of school learning. Besides, one fundamental human relationship is deformed and dehumanized.

- this linear relationship stops a direct interaction between the knowledge and the student, an important component of the pedagogic interaction (the knowledge is usually mediated by the teacher, it comes through him). By doing that, some higher, fruitful forms of learning are eliminated from the practice.

The more complex and nonlinear model of active learning (Fig. 2) introduces a lot of innovations and demonstrates one of the possibilities of overcoming the traditional school model.

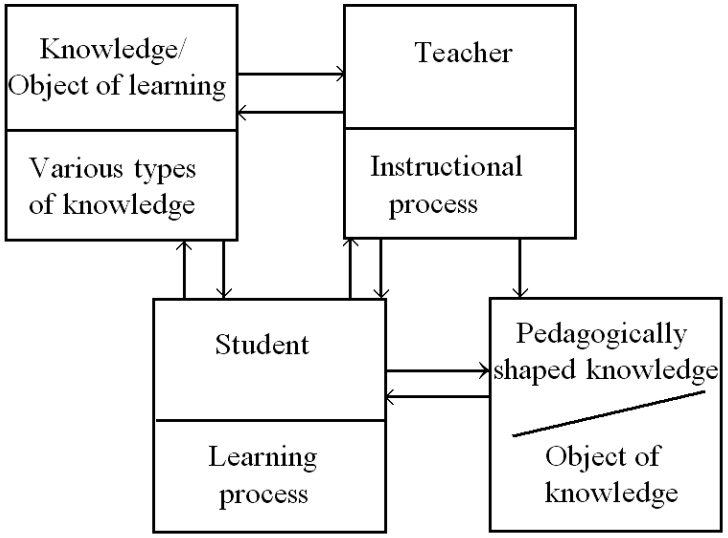

Fig. 2: Nonlinear model of pedagogical interaction of active learning

Its basic advantages are:

- to the educational process an intrinsic and fundamental quality has been preserved - it is one of the basic forms of human relationships, which means that it is a two-way process of interaction and communication. Therefore, it is truly a process of teaching/learning.

- a feedback from teacher to knowledge has been established, and a teacher is not just an agent of knowledge transmission but also plays important partner roles in a direct pedagogic interaction with students.

- an indirect interaction with students is being introduced in the form of pedagogically shaped knowledge (where the teacher is in the role of an organizer and a director, and students are left with the possibility of cooperative learning and of direct interaction with knowledge).

At the moment the following actions can be practically applied:

- abandoning some characteristics of traditional school (lecturing as the only form of teaching, students' passivity, grading only exact reproduction of knowledge, etc.);

- respecting the child in school, taking into consideration his/her age and individual characteristics, expanding the scope of teaching methods in the implementation of programs defined in advance, paying attention to child's motivation for learning, encouraging development as one of the learning goals, and not only acquiring the academic subject matter.

These innovations in the model of pedagogic interaction represent a basis for all those models of learning present in the modern educational theory and practice such as: independent assessment (in the lab, field work, independent observation and analysis of the observed, individual problem solving, learning by discovery, cooperative learning, individual construction of knowledge, social construction of knowledge - co-construction, children to children learning, reciprocal learning (including the reciprocal learning where teachers partly learn from students).

The model of active learning gives a possibility of departure from the classical mission of school - a transmission of ready-made knowledge. This mission still remain one of the school missions, but new functions are introduced such as: intellectual autonomy (training for independent work, independent assessment, individual problem solving, learning to learn, LLL), encouraging development of thinking (by studying some domains of human knowledge, the modes of thinking characteristic of those fields are acquired), initiative (which can be developed only through the mentioned models of independent and direct interaction between the one who learns and knowledge/object of knowledge, the ability to evaluate knowledge, the ability for social interaction, exchange and cooperation can be developed only through a lasting process of participation in social interactions.

It is important to emphasize that within the classical linear model, basically, the models of learning which go beyond the transmission of ready-made knowledge can't be developed, but are extremely needed in modern society.

3. INTERACTIVE METHODS OF EDUCATION IN NATURAL SCIENCES

The basic idea for introducing of interactive methods of education in teaching of natural subjects is to engage students in meaningful activities

adequate for the nature of the material they need to learn. Some initial ideas in this area are [1].

a) *Independent use of mathematical formulas*.
b) *Semantic comparison of two concepts*.
c) *Logic of Natural Laws*.
d) *Pro and Con*.
e) *Laboratory experiment*.

Many other interactive and innovative methods of active learning like brainstorming, data base search, guest in class, natural science centre creation, environmental educational workshop, etc. is possible to apply in education in natural subjects.

Very important is teacher training how to use different interactive and innovative methods of active learning in their practice. Towards this end, valuable resources are polymorphic practice, new and flexible methods of training and project based teaching [2].

Lately a trend to unification in international networks of different scientists and groups working on development and introduction of innovative and interactive methods of education in natural sciences can be seen. This activity is financed by won international projects. Good examples in this area are the Network of Youth Excellences (NYEX) in Hungary with members from 13 countries, "Hands-on Science" in Portugal with its 28 educational institutions and transnational consortium of 10 European countries and others. Especially physicists from Roumania are very active in these organisations. Unfortunately bulgarian attendance in such international networks is completely absent and the first precedent was participation of Prof. Dr. Plamen Gramatikov [3] in the conference of NYEX in Balatonfured, Hungary in 2007.

4. ROLE OF PHYSICS KNOWLEDGE IN LEARNING INFORMATION TECHNOLOGIES (IT)

The origin and increasingly growing progress of information technology as a science with many applications was the product of multiple forces operating during decades prior to 1980s, when a wide use of PCs indicated the beginning of the IT era. Physics creates a strong foundation for IT literacy. The portion of the physical knowledge involved in teaching IT can only increase in the near term, which raises a question concerning how teachers can provide efficient access to the relevant information within IT courses.

Knowledge of relevant physics information is important to students for a variety of reasons:

- it makes the link between the theory and the practice meaningful for students;
- it reinforces comprehension of how IT hardware work;

- it enables students to understand current trends in IT and see the principal limits of those trends;
- it provides support for decision making regarding the proper selection and use of IT hardware;
- it allows seeing new ways in future IT.

Traditional physics courses provide a good primary basis, but a stronger accent on the potential of many physical phenomena, effects and concepts in IT would be useful. Few efforts can be made to refresh the physical knowledge in students' memory. When faced with forgotten facts, students will often bypass their old textbooks and seek rapid access to easier understandable information. Web-based instruction model with its deep linking strategy that links students directly to the structured components of online courseware provides a potential roadmap to a solution. This can be illustrated by the next example [4].

Entropy is a cornerstone concept in information theory in the context of a probabilistic model for a data source. However students are likely having heard this word and have learned the entropy concept while were studying physics and thermodynamics in particular. Indeed, both concepts of entropy, information and thermodynamics, have deep links with each other. Then the sensible approach is to provide a link from IT courseware to a relevant physics resource, for example "Introduction to thermodynamics" developed at the Physics Department, Murcia University [5], and benefit from its opportunities including simulation. This facilitates achieving more pragmatic teaching goals, e.g. explaining what the amount of information is, why one binary element contains a unit of information named a bit, when loss-less data compression is possible etc.

5. CONCLUSIONS

Current teaching models especially for science subjects have reached a high state of collaboration. In this regard, establishing the content of and providing the access to cross-subject courseware components should be a profession-wide undertaking. However, such an undertaking would necessarily require profession-wide discussion on the scale of current practices in science teaching.

In such variable environment as the science and the Internet, successful support for teaching requires flexibility and creativity that may be an iterative process. New technologies may enhance courseware but also introduce problems because much in education remains more of an art than a science. Better technologies will certainly help us, but very often we will continue to rely on the expert opinion of our professional colleagues who know the science and, most important of all, know the needs of students we teach.

6. REFERENCES

[1] Ivic I., A. Pesikan, S. Antic. (2002) *Active Learning - manual for implementation of active learning/teaching methods*. Institute of Psychology, Novi Sad.

[2] Michaelides P. (2003) *An affordable and efficient in-service training scheme for the Science Teacher*, Proc. of the 6th Int. Conf. on Computer Based Learning in Science (CBLIS03), University of Cyprus, Nicosia, pp. 792-799.

[3] Gramatikov P., D. Todorina, M. Gramatikova. (2007) *Bulgarian Education's Reform and Strategy for Diagnostics of Gifted Children*, in the book "Science Education: Models and Networking of Student Research Training under 21", NATO Security through Science Series E: Human and Societal Dynamics, vol. 16, IOS Press, Amsterdam, pp. 254-264

[4] Berezovska I., N. Berchenko. (2005) *Web-based Instruction in IT Hardware*. Proc. of the 2nd Int. Conf. on Hands-on-Science, HSci 2005, Rethimno, Crete, pp. 83-86.

[5] *Introduction to Thermodynamics*. (1996) Physics Department, Murcia University, Spain.

Digitalised experiment, computer programs and e-platforms in the process of chemistry curriculum acquisition

Mitko Stoev [a], Pavel Teply [b] and Jan Čipera [b]

[a] Dept. of Chemistry
Faculty of Mathematics and Natural Sciences
South-West University “N. Rilski”
2700 Blagoevgrad, Bulgaria
E-mail: mstoev@mail.bg

[b] Dept. of Didactic in Chemistry
Faculty of Natural Science
Charles University
Prague, Czech Republc
E-mail: cipera@natur.cuni.cz

Abstract

The creation of interactive computer programs in chemistry using mostly HTML, digitalised experiments in the process of chemistry curriculum acquisition in education programs, e-platforms, distance education, and self-instruction methods are presented. The research of efficiency of applied instruments using various feedback resources is discussed.

Key words

Education objectives, computer programs, digitalisation of chemical experiments, e-platform, verification of program efficiency, regulation of created educational aids

1. Introduction

The applications of computers in the process of chemistry curriculum acquisition included four steps: (i) simple use of computers [1], (ii) creation of various interactive computer programs [2-4], (iii) writing and applying in education process of advanced hypermedia computer programs [5] and (iv) using e-platforms [6]. Commencement of the Internet and computer networks later enabled dissemination of created programs and other multimedia instruments, incl. learning process regulation, even to distance

education and self-instruction methods, training of talented chemistry students, etc. In the course of time, computers and programming languages used have been changing. The digitalised experiment was introduced as inseparably part of advanced digital lecture cources at Dept. of Chemstry, Faculty of Mathematics and Natural Sciences, South-West University "N. Rilski" using Internet and a file exchange e-platform [7].

The decision to use computer programs in the curriculum acquisition process was based on side studies demonstrating unambiguously that this instrument enables to create such curriculum structure that can be maximally interactive, flexible and responding to changes in the curriculum acquisition process. Such instrument also enables to individualise the learning process, to respect different abilities and knowledge structure of individual students for self-study and different learning styles. Modification of computer programs e.g. modified setting of learning tasks, integration of other information into programs, is possible thanks to the fact that these programs are carriers of the source code. This code can be modified not only in HTML editors, but also for example in Notepad, which is part of the operating system Windows. FrontPage offers easier program modification, since we do not have work with the source code in this case.

Among others, modifications enable to prepare various content of the curriculum for different groups of students that differ by initial knowledge and activity structure, aspiration level to the chemistry, etc. Chemical structure of programs is derived from generalized results of chemistry curriculum structure on the primary and secondary school level, which also serves as a base for setting learning tasks. The main lectures for bachelor degree level in Inorganic Chemistry are using Power Point software and are uploaded on www.dox.bg fail exchange platform. The digitalised experiment is uploaded on e-platform as a short and representative films connected to the main lecture. This kind of organization of the lecture course is attractive for the students and they can actively support the new flexible digitalised lectures by theirs digitalised students' projects. In this way students are active part of the creation and refreshment of advanced lecture courses in chemistry.

We first applied an initial test of students' abilities to create various modified programs in practice. The students' ability to modify the flexible program is 42 % unable to modify the program, 45% capable of modifying using editors and 13% capable of modifying directly in the source code. It was thus apparent from test results that it is advisable to prepare students for such activities. Therefore also lectures and seminars oriented in the use and modification of flexible programs have been integrated within various events [8].

After completion of individual courses, results showed that the ability of students to modify flexible programs in applied editors or source code increased approximately by 45%, or 15% respectively.

Handling learning tasks assigned and subsequent regulation of their results is the base for acquisition of the chemistry curriculum. To reduce complicacy of problem solving, digitalised chemical experiments, hypertext dictionary, series of empirical data (substance structures, diagrams, etc.), auxiliary information, feedback, practical use of chemical processes, electronic browsers, flexible text utilisation and e-platforms are used.

2. Preparing a computer program

For any material didactic instrument, incl. computer programs, objectives of its application in specific training are crucial. Creating didactic objectives is not a single event but includes a few steps. In these steps, e.g. when we deal with relations between educational objectives and pedagogical (didactic) categories, these objectives or their variants are gradually specified. After correct definition of the didactic objective, the curriculum should for example be determined not only by its content but also by its level and method of acquisition, since we cannot define more precisely how the curriculum would contribute to the development of general students’ abilities, such as digitalised experiment application, logical reasoning ability, further education ability, etc. until deciding on the level and method of curriculum acquisition. Our research in this area showed that it is advisable to distinguish following three components of educational objectives**: informative**, **methodological**, and **formative**. Objective components stated not only determine what curriculum are students to acquire (informative component of the objective) and by what activities they would acquire the planned curriculum (methodological component of the objective), but also how their personalities would form through the acquired curriculum and methods of its acquisition (formative component).

The results from scheme presented on Fig. 1 are:

- activities, individual curriculum components are transformed into know-how, knowledge, skills, and habits;
- acquired curriculum and activities, students’ abilities are developed, forming their personalities;
- teaching methods applied, i.e. curriculum acquisition methods, students’ abilities and characteristics are developed, etc.

Fig. 1 The scheme of educational objectives

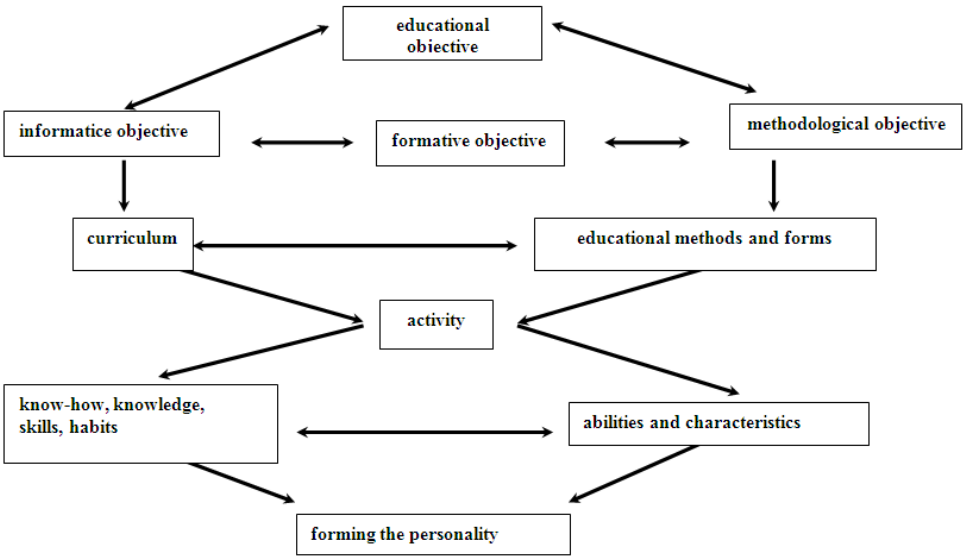

At the same time, there is a hierarchy of objectives when the lowest objectives relate to acquisition of individual knowledge and activities. To create the hierarchy of educational objectives, a broader predicate logic method is used. The literature describes also simpler and not so objective methods of curriculum structure, e.g. matrix method [9]. Relations between individual partial objectives, i.e. between knowledge and activities, can be quite objectively determined using simpler mathematical methods - methods of simple propositional and predicate logic. In doing so, we always first record the piece of knowledge using mathematical logic means.

It is apparent from the demonstration that students may derive independently this finding based on acquisition of the following curriculum components: total atom charge, definition of atomic nucleus and shell, size and polarity of electron, proton, and neutron charge, and determination of the total nucleus charge and electron shell. In addition, schematic notation of these findings given by mathematical logic instrument defines also their content and scope. Students may also acquire the finding through other material instruments provided, e.g. from the table of elementary charge polarities, on the Internet, or directly from the teacher, etc.

Oriented diagram is the final result of determined relations between individual chemical findings in the thematic complex. “Logically related” findings in the oriented diagram are linked by the so-called oriented diagram edge. The logic relation of findings is understood that the information, which

the oriented diagram edge is based on, is necessary for derivation of the finding, which the oriented diagram edge points to.

The oriented diagram consists of definitions, sentences, propositions, and facts arranged in logical sequences. Definitions are indicated with Arabic or Roman numerals. Definitions and sentences indicated with Arabic numerals specify the content and scope of acquired information from the previous curriculum, and definitions and sentences indicated with Roman numerals specify the content and scope of new information acquired. Information from other subjects of study, e.g. physics, mathematics, etc., are indicated as propositions. Empiric information from chemistry and other scientific disciplines are indicated as non-derivable facts adopted in the teaching process.

3. Digitalisation of chemical experiments

The chemistry is a science of chemical experiments that verify theoretical findings, or that bring empiric findings with the possibility of their theoretical assessment. Although the real experiment execution is optimal, it is however impossible in many cases to apply this method of knowledge acquisition, since it is “prevented” by their time-consuming execution, availability of chemical substances, safety aspects, etc., regardless of impossibility to use them directly in distance education and self-study. Therefore we have made a research of how to substitute simulated chemical experiments for their digitalisation. Digitalisation was made using a video camera (Sony-Handycam), edited in Premiere Pro 1.5 or Pinnacle programs, and compression of the material recorded in VirtualDub program. The above recording can be replayed, stopped, resumed, or zoomed at any time, which is impossible in case of the real experiment. We use digital chemical experiment with its empiric version at lectures in Chemistry. Since the practical research showed that most students are unable to evaluate theoretically empiric data derived from chemical experiments, we have supplemented recorded experiments with partial control tasks.

Partial tasks stated enable to create different variants of theoretical solution of the learning task according to students’ capabilities. The student selects such variant of the control task that would help him/her solve the problem, e.g. to record the chemical process as a chemical equation. Students may eventually ask for other control task or tasks, and finally they can verify the notation with the equation mentioned [10].

Fig. 2 Digital process recording – comparing reduction characteristics of atomic and molecular hydrogen, and one of the control task variants.

Efficiency of digitalised experiments used was examined by analysis of results of tested learning tasks, results of discussions and talks with students. In doing so, results were always compared with students who did not use digitalised learning instruments. In all cases, these are results achieved with participation of more than 200 students. Results of empiric efficiency investigation of such processed program experiments can be summarized into following points:

- Time demand for acquisition of anticipated knowledge and skills was reduced by 65%,
- Students'ability to interpret the essential of monitored chemical processes and their regularities increased approximately by 50%,
- Efficiency of acquired knowledge and activity permanence measured for the period of 6 months after using study aids increased by 80%,
- It emerged from the discussion among others that students' interest in the chemistry and its investigation subject matter also increased.

4. Distance education

In distance education courses [11], we have used the system LMS MOODLE – DVPP, and also LearningSpace. The advantage of this approach is that students may acquire the curriculum at any time and in any place, if they have ideally access to the Internet. Learning tasks presented included also a digitalised chemical experiment, which could be "recalled" by students at any time to help them resolve the assigned task. Students

then sent their answers to the tutor who either approved the correct solution or indicated what tasks were resolved incorrectly, and what was the essential of their incorrect results. In these cases, the tutor sent them auxiliary information to remove the defects found. In case of further incorrect solution of assigned learning tasks, students are provided with a flexible program with the topic in question. Practical results showed that virtually all defects were removed after providing students with the flexible program and e-platform in Internet.

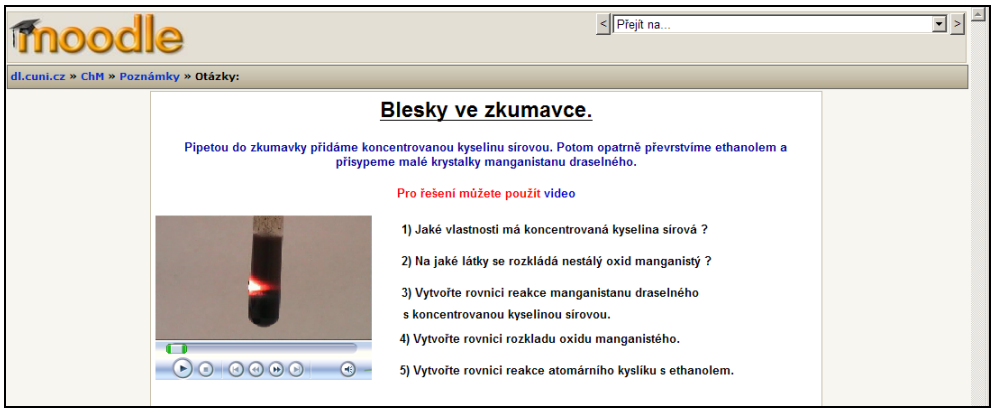

Fig.3. Problem solving related to clarification of processes running in the system of concentrated sulphuric acid – ethanol – potassium permanganate.

Conclusion

Examples stated herein document the fact that the use of computer programs contributes greatly to higher efficiency of the curriculum acquisition process. In addition, this approach also increases interest of students in the chemistry curriculum and in problems of processes the chemistry deals with. So far the greatest disadvantage of this approach is that preparation of basic program and modification of flexible program is very time-consuming. Therefore we search for the way how to reduce complicated creation, modification and use of such programs by their development in HTML editors (FrontPage) instead of source code, by improving teachers’ preparation within various lectures and seminars. The goal is to acquire skills necessary for application and modification of flexible programs, and for creating various school educational programs with respect to actual conditions of the pedagogical practice. It is common knowledge that any instrument for curriculum acquisition cannot be quite optimal, but includes always some deficiencies. Fundamental deficiency of

this approach is that students using digitalised experiment do not develop their motor skills.

References

[1] ČIPERA, J.: Rozpravy o didaktice chemie I,II. Karolinum, UK v Praze 2000,2001.Praha
[2] ČIPERA, J.: Chemische Programme mit variabler Struktur. NiU - Chemie6, (1995), Nr. 28, pps 32-35
[3] DVOŘÁK, M.: Flexibilní program – Chemie manganu, PřF UK, Praha 2005
[4] KAMLAR, M.: Flexibilní program – Chemie rtuti, PřF UK, 2004
[5] TEPLÝ, P.: Hypermediální výukový program Chemie halogenů a jeho využití ve vzdělávání nadaných žáků v chemii, Praha 2010
[6] STOEV, M., VL. YURUKOV: E-platform for PV education, International Workshop on Teaching in Photovoltaics, TU-Prague, 2006, 24-30.
[7] STOEV, M: Applied photovoltaics as a practical education in Renewable Energy Technologies, FMNS-2009, Blagoevgrad, Bulgaria
[8] ČIPERA, J.: Kurz přípravy učitelů na tvorbu ŠVP. SEF-Český Šternberk, Šternberk 2006
[9] NAJMONOVÁ, R.: Vodík. Praha, PřF UK,1978
[10] MIČKA,Š.: Digitální chemické experimenty. PřF UK, Praha, 2003
[11] MALČIK M. a kol.: Chemická knihovna – objekty 200 chemických experimentů. CIT, OU v Ostravě, Ostrava, 2006

Reading the Individual Context of Web Message

Gergana Apostolova
SWU "Neofit Rilski" – Blagoevgrad, Bulgaria

The Active E-art Product: Part 1

Abstract*:The offered paper is based on a study of the cultural interferences of a pragmatic nature in the perception of the text as a complex cultural sign where conventional language signs translate into picture-sound icons serving as indexes of the mental state of the user and go further into an active dialogue aiming at achieving an integrity of the individual mental display.*

Keywords: *complexity of text symbol; e-art, e-pictogram, synchronization of cultural realia, individual context, situational context.*

1. INTRODUCTION

Lost in the Infosphere

> ***The computerized description and control of the physical environment, together with the digital construction of a synthetic world, are, finally, intertwined with a fourth area of application, represented by the transformation of the encyclopaedic macrocosm of data, information, ideas, knowledge, beliefs, codified experiences, memories, images, artistic interpretations and other mental creations into a global infosphere.***
> ***The infosphere is the whole system of services and documents, encoded in any semiotic and physical media whose contents include any sort of data, information and knowledge, with no limitations either in size, typology or logical structure.***
> ***The symbolic-computational power of ICT tools is employed for ends that go beyond the solution of complex numerical problems, the control of a mechanical world or the creation of virtual models.***
> Luciano Floridi, *Philosophy and Computing*

Since 2008 I have been using the tool of *course product* as a clearer source for cultural study than direct web-derived feedback to verify the application of certain methodology for intercultural studies of the internet. It is a task set to all the *real individuals* on a course. I have been teaching *Persuasive discourse* and related courses to various groups of undergraduate students of English studies (philology and applied linguistics), Bulgarian Studies, and Economics, and to graduate groups of

English Philology. The students are often asked to trace certain item of information in the Internet. The results form a curious host of data and inferences:

1. Out of 1000 randomly picked lines from Bulgarian chat groups and forums, where the undergraduates participate, there are extracted only 68 different words and phrases in Bulgarian and English, while emoticons, keyboard signs, and links reach up to half of the exchange. The dialogue of non-academic web-communities is based on a complex unit which I have called *e-pictogram* [1] where communication runs at the level of context.
2. English-speaking users of the Internet are more apt to enter Bulgarian communities the globe over than users of Bulgarian only.
3. The web-based research results in mere recognition of surface facts (most visited sites) and general failure in tracing a host of key-words on topics beyond the area of synchronized youth-culture interest. It is not merely the binary assessment tools for likes and dislikes that produce insufficiency of key words for approaching certain topic, neither is insufficiency of web ontology-design. The fact that elder trainees (aged 40-50) look up information, following their own line of picking up key-words, based on associations running deeper in an educational and cultural background of broader nature than the young undergraduates (aged 20 - 40) whose search is contextually dependent on their web-communities, has come to suggest a reconsideration of the stereotype-based approach to the problems of *e-illiteracy*.
4. The use of web-translators is still limited by the lack of sufficient database of Bulgarian text-corpora on the one hand, and on the lack of clear classification of text-types and situational analyses, on the other.
5. We have a very limited number of web-linguists trained in both applied linguistics and COS – most of them living in non-Bulgarian environment.
6. There is a vast space still for filling in Bulgarian cultural contribution to both – educational and business purposes.

2. STORY-TELLING AS THE ROMANTIC ASPECT OF CASE-STUDY

> *If there is a continuum of hypertext from my note pad, through the diaries and letters and notes of my family and my groups, into the world of selected edited and published material, then we have a world in which the regular person*

has been re-enabled as a writer, a thinker and a linker, rather than just a clicker.

Tim Berners-Lee

The storyteller, the individual, the artisan, many tools in one box to be applied to widely different tasks and the power of personal use to reveal the beauty of these kinds of communication - these are the core images that can help in understanding the enchanting utility of the Web.

J. Madox

Cultural and respectively intercultural studies are based on case-study producing correspondent texts. Internet text is a complex sign-structure where story-telling is hyper-textual while mind work in the process of communication goes far beyond the traditional limitations in text-weaving.

In previous papers I have extrapolated on the nature of the e-pictogram, which can be used as the *toolbox* for the study of the individual paths through the Internet. [2]

The subject of this paper is focused on the design of a complex product of art where text, picture and sound are interwoven in the message reality where the encoder and the decoder are interchangeable depending on their interaction with the sensitive message.

A bigger objective is the design of e-art products based on Bulgarian realia, synchronized culturally on the levels of global web-metaphor and on Bulgarian Y-generation cultural e-exchange.

2.1. Contexts v/s Statistics in designing an e-art product

Statistics are based on cultural stereotyping whether there be binary or multi-agent functioning. However, the Internet is where cultural context is used to simultaneous application with situational context of synchronic exchange by the individual members of a community. While a community can be taken as a statistical unit, it takes care that its members are about the statistically average or reasonable functioning.

The regulation of communicative contexts is carried out through the use of the complex communicative sign or the e-pictogram where the agents, the situational elements and the messages form an entity of uniquely interwoven contexts relying on a series of clicks where a set of signals S is sent to a set of recipients S1, whose individual perception forms a set of perceived signals S2. In this procedure the contents of the signals depend on the mental state of the users, as well as their individual reading of the links, which can be single, or multiple – individual or related.

Each community has its own way of connection based on its own story-telling, where the values of that community are supported by a number of stored contents reached through links of audio and video messages.

Even if we do not take into consideration the contents of those messages, it is clear that the user is passively exposed to their effect since they have been chosen and sent by the initiator of that situational exchange.

Our purpose here is to find a way of restructuring the complex sign of the message so that it becomes active in searching its users.

To start with, we do not need all but the optimal situation markers in designing an active e-art product through writing, linking and editing of color and sound through clicking. To this purpose undergraduates of Applied linguistics contribute with their final course products for the spring semester of 2011.

The next step is to make it web-interactive. To that purpose we shall need web-designers.

The third step is to design single e-art product that recognizes its user and is activated by the individual body-signaling to call him or her on their approach. It shall rely on forming a team of professional people from a broader scope of areas. The work in progress of the FMNS at the SWU has provided sufficient background for further cooperation. [3]

A parallel running verification process is being in procedure, involving social web-communities and communities of younger web-users where the projects in virtual rhetoric of the Sofia University Department of Rhetoric [4] and the integrated education in web-studies project at the High Language School in Blagoevgrad [5] provide control groups of users.

3. APPLICATIONS OF THE ACTIVE E-ART PRODUCT

Besides its market value, the successful e-art product has educational attractiveness for the involvement of our undergraduate and graduate students in active training for professional career upon leaving the University. The nearest estimated applications in the training of linguists are:

- Reassessment of Bulgarian cultural heritage in weaving picture, sound and word in e-realia.
- Improvement of web-translation mechanisms for intercultural exchange through employing graphs for the text-type and situation-type recognition.
- Keeping the e-learner's mental balance through reconstruction of the integrity of ethos, pathos and logos
- Bridging methodologies and translating tool-applications in further web-product design.

4. CONCLUSION

Integrity of e-art requires integrity of effort running vertically across generations, and extensionally – across areas of training. An active e-art product can serve to this purpose as both means and an end.

5. PERSPECTIVE

Texts as cultural codes contain the parameters of environment that in its extensions forms Worlds. An active e-art complex product can turn into the next generation of Virtual Worlds carrier, closely concerned with the emotional recharging of the user, or achieving integrity of the independent human individual functioning multi dimensionally in the virtual reality.

6. REFERENCES

[1] Apostolova, G., Internet, Intertext, Interculture, SWU PRESS, upcoming 2011

[2] Apostolova, G., E-Illiteracy, SU online journal of Philosophy and Rhetoric, upcoming 2011

[3] Chimev, K., *Structural Properties of Functions,* FMNS 2009, Vol. 1, p.17 – 20, Shtrakov, S., *On the number of functions in a class of k-valued logic,* FMNS 2009, Vol. 1, p. 22 – 26, Vezenkov, S.R., E.L. Karashtranova, *Models for the measurement of Bulgarian speech Rhythm*, FMNS 2009, Vol. 1, p. 61 – 67; Yordjev, K. and team papers for the FMNS 2009, Vol. 1.

[4] Mavrodieva, I., Virtual Rhetoric, SU PRESS, 2010

[5] Milcheva, Integrated Methods in the Web-studies Classroom, presentation proposal to the current Conference.

[6] Maddox, J., The Storyteller's Tool-box http://pespmc1.vub.ac.be/Cybspasy/JMAB.html (latest visit: 04-20-2011)

EDUCATION FOR HEALTH AND PERSONAL DEVELFPEMENT IN BULGARIA

Roumen Bostandjiev
Burgas Free University, Department of Humanitarian Sciences

Abstract: *Health Education is integrated in the subject "Biology and health education" in Bulgarian schools. The challenge now is to develop theoretical framework for conceptualization of this education in concordance with contemporary trends. In this relation we analyze concept and practise of Social and Emotional Learning in USA and some countries in EU. Here we propose a brief concept of Education for health and personal development which integrates health issues with creation of social and emotional competence. Development of specific educational programs as well as creation of supportive school climate and activities, involving parents, is a part of this idea.*

INTRODUCTION

A key challenge for 21st-century schools is to maintain a creative climate wherein **all students can develop intellectually, emotionally and socially to their fullest potential**. As a result, students will experience the joy of learning, academic and personal growth and acquire the skills that exemplify **successful professional realisation, responsible citizenship, meaningful family life and responsible parenthood**.

Effective schools, those that prepare students not only to pass tests at school but also to pass the tests of life, are finding that **social–emotional competence and academic achievement are interwoven** and that integrated, coordinated programs in both areas maximize students' potential to succeed in school and throughout their lives.

Also schools are now seen as ''an important if not central arena for **health promotion and primary prevention .** . . in addition to the education of students'' (Roeser, Eccles, & Samoroff, 2000, p. 467). These findings are not surprising, as shown in the work of Wang, Haertel, and Walberg (1997). They examined 28 categories of influences on learning, which they based on reviews of 179 handbook chapters, 91 research syntheses, and surveys of 61 national experts. Wang et al. found that 8 of the 11 most influential categories involved

social and emotional factors (e.g., student–teacher social interactions, classroom climate, and peer group).

Among the major reasons for **dropping out of schools**, according to the National Center for Education Statistics in USA (2002), several involve social and emotional factors: not getting along with teachers or peers (35.0% and 20.1%, respectively), feeling left out (23.2%), and not feeling safe (12.1%). Thus, it is understandable that Wang et al. concluded that ‘‘direct intervention in the psychological determinants of learning promises the most effective avenues of reform’’ (p. 210), which supports providing social and emotional learning in schools (Zins et al , 2006).

Because many students lack social-emotional competencies and become less connected to school as they progress from elementary to middle to high school, this negatively affects their academic performance, behavior, and health (Blum & Libbey, 2004). There are no sufficient researche on this topic in Bulgaria, but results from studies in USA are clear. From a national sample of 148,189 sixth to twelfth graders, only 29%–45% of surveyed students reported that they had social competencies such as empathy, decision making, and conflict resolution skills, and only 29% indicated that their school provided a caring, encouraging environment (Benson, 2006). By high school as many as 40%–60% of students become chronically disengaged from school (Klem & Connell, 2004). Furthermore, approximately 30% of high school students engage in multiple high-risk behaviours (e.g., substance use, sex, violence, depression, attempted suicide) that interfere with school performance and jeopardize their potential for life success (Dryfoos, 1997; Eaton et al., 2008).

In conclusion - there is a broad agreement in USA among educators, policy makers, and the public that teaching and learning in contemporary schools have strong social, emotional, and academic components (Zins, Weissberg, Wang, & Walberg, 2004). Students typically do not learn alone but rather in collaboration with their teachers, in the company of their peers, and with the encouragement of their families. Emotions can facilitate or impede children’s academic engagement, work ethic, commitment, and ultimate school success. Because relationships and emotional processes affect how and what we learn, schools and families must effectively address these aspects of the educational process for the benefit of all students (Elias et al., 1997).

SOCIAL AND EMOTIONAL COMPETENCE AND EDUCATION IN EUROPE

Unfortunately the idea of social and emotional learning as basis of Health Education and Health Promotion is not so popular in Europe. Regardless of some pioneering efforts in Spain, The United Kingdom, Germany, Netherlands and Sweden (see http://educacion.fundacionmbotin.org/index.php?a=educacion_responsable_emocional_social) this concept is not yet accepted as leading framework in educational and youth politics on administrative level in the European Union. Activists in this field become more and more. They are organized in European Network for Social and Emotional Competence in Children (ENSEC). This year the third biennial conference of ENSEC will be held in Manchester (UK).The theme of the 2011 conference is "Social and emotional education across the world: celebrating diversity in theory, research and practice".

HEALTH EDUCATION AND SOCIAL AND EMOTIONAL LEARNING IN BULGARIA

The terms Social and Emotional Learning (SEL), as well as socio-emotional competence and education are relatively new in Bulgaria. Main political documents, concerning young people in Bulgaria – "National strategy for youth 2010 – 2011 and "Programme for development of education, sciences and politics for youth in Republic of Bulgaria 2009 – 2013 (see http://www.minedu.government.bg/left_menu/documents/strategies/) declare that care for youth is a priority task for our government. Realization of this responsibility is linked with whole spectrum of administrative and economical measures, oriented mainly toward professional development of children. Personal development and health prevention presents in those documents but without clear design who, how and after what kind of professional education will offer systemic programs, services and other educational activities to pupils in this connection.

In real practise Health Education is integrated in subject "Biology and Health Education", but this covers only small amount of topics, regarding mainly health knowledge. Since last three decades a lot of different health and preventive programs are running in Bulgarian school system. Usually they are implementing by nongovernmental organizations which works directly with pupils or make seminars and trainings for involved teachers. Most of this initiatives are for short term, not mutually coordinated, without scientific approval of their effectiveness and with no sustainability. Traditionally health is accepted in Bulgaria mainly as "absence of illness". That's why

traditional “Health education or health instruction” is associated primary with information about different illnesses and their prevention. Concepts of Health Promotion and Wellness are not very clear among teachers and usually they are not ready to link them with social and emotional literacy, intelligence and competence. Educational efforts are focused mainly on negative results of “risk behaviours”. Usually they are defined as “fight against” HIV/AIDS, venereal infections, school violence and bulling, drug, tobacco and alcohol addiction, unwanted pregnancies, traffic of girls, injuries. As reasons for all this troubles public opinion is inclined to blame mainly outside conditions - poverty, unemployment, crisis, lack of social perspective, pure political management. It’s not difficult to find traces of post communist learned helplessness behind this common mentality.

WHAT CHANGE WE NEED?

At firs we need consensual understanding of the term “Health Education” which will give as fruitful ground for joined plans and actions in this field.

The World Health Organization defined health as “state of complete physical, mental and social well-being and not merely the absence of disease or infirmity.”(WHO, 1948). This definition clearly focuses on personal and social aspects of health. From contemporary point of view it means that if we want to be healthy, we ought to be in harmony with ourselves, with other people and with Nature.

Concepts of Emotional literacy, intelligence, competence and education as well as concept of Social intelligence, competence and education gives as perfect tool for understanding health behaviour, health promotion and health education. There are a lot of empirical researches last two decades that prove positive effects of Social and Emotional learning (SEL) not only on health parameters, but also on improving school success, school discipline and prevention of risk behaviours (Durlak et al., 2011). This shoes that Health Education must include Social and Emotional Learning as integrative elements. We could name this holistic education – EDUCATION FOR HEALTH AND PERSONAL DEVELOPMENT (EHPD). Its goal could be – development of Health, Personal and Social competence. These three key competences are interwoven and they are interdependent with so called “academic competence”, measured by school marks and test in different subjects. Implementation of EHPD will improve effectiveness of our educational system and will put appropriate accent on personal grout and social competence of our children.

WHAT COLD INVOLVE EDUCATION FOR HEALTH AND PERSONAL DEVELOPMENT?

When we create our new school programs and initiatives for improvement of health and prosperity of our children, we can use huge experience accumulated in USA and other countries developing SEL in last twenty years. The most powerful and influential organisation of educators, researchers, developers of educational programs and politicians in USA is Collaborative for Academic, Social and Emotional Learning (CASEL). Their mission and vision is " to promote children's success in school and life". They work for a "world where families, schools, and communities work together to promote children's success in school and life and to support the healthy development of all children. In this vision, children and adults are engaged life-long learners who are self-aware, caring and connected to others, and responsible in their decision-making. Children and adults achieve to their fullest potential, and participate constructively in a democratic society."(http://casel.org/about-us/mission-vision/). In their site http://casel.org we can find a brief explanation of Social and Emotional Learning (SEL): "SEL is a process for helping children and even adults develop the fundamental skills for life effectiveness. SEL teaches the skills we all need to handle ourselves, our relationships, and our work, effectively and ethically. These skills include recognizing and managing our emotions, developing caring and concern for others, establishing positive relationships, making responsible decisions, and handling challenging situations constructively and ethically. They are the skills that allow children to calm themselves when angry, make friends, resolve conflicts respectfully, and make ethical and safe choices. Many of the programs that teach SEL skills have now been rigorously evaluated and found to have positive impacts. According to reliable research, schools are a highly effective setting for teaching SEL skills. SEL is also a framework for school improvement. Teaching SEL skills helps create and maintain safe, caring learning environments. The most beneficial SEL programs provide sequential and developmentally appropriate instruction in SEL skills. They are implemented in a coordinated manner, schoolwide, from preschool through high school. Lessons are reinforced in the classroom, during out-of-school activities, and at home. Educators receive ongoing professional development in SEL. And families and schools work together to promote children's social, emotional, and academic success."(http://casel.org/why-it-matters/what-is-sel/).

CASEL identified **five core groups of social and emotional competencies**: "

- **Self-awareness**—accurately assessing one’s feelings, interests, values, and strengths; maintaining a well-grounded sense of self-confidence
- **Self-management**—regulating one’s emotions to handle stress, control impulses, and persevere in overcoming obstacles; setting and monitoring progress toward personal and academic goals; expressing emotions appropriately
- **Social awareness**—being able to take the perspective of and empathize with others; recognizing and appreciating individual and group similarities and differences; recognizing and using family, school, and community resources
- **Relationship skills**—establishing and maintaining healthy and rewarding relationships based on cooperation; resisting inappropriate social pressure; preventing, managing, and resolving interpersonal conflict; seeking help when needed
- **Responsible decision-making**—making decisions based on consideration of ethical standards, safety concerns, appropriate social norms, respect for others, and likely consequences of various actions; applying decision-making skills to academic and social situations; contributing to the well-being of one’s school and community “(http://casel.org/why-it-matters/what-is-sel/skills-competencies/)

To these five competences, in our EHPD we cold add also **Competence for family life and parenthood**. For us tis is a key competence not only for individual success and health, but for prosperity and wellbeing of future generations.

RELATION BETWEEN EHPD SCHOOL CLIMATE AND PROFFESIONAL QALIFICATION OF TEACHERS

Application of EHPD could have two interdependent trends in school education. The first one is development of original or adaptation of existing foreign specific educational programs for children from kindergarten to grade 12, concerning different elements of Social and Emotional competence. These programs could deliver additional knowledge, work with attitudes and create specific skills in each separate area of competence. Engagement in implementation of these specialized programs could have only teachers with appropriate training and qualification. The setting could be facultative, inset in free from obligatorysubjects time.

The second trend concerns whole interaction between students, teachers and parents in school system. The role in this process could have each teacher who is a leader of a class. It means that he will need some more fundamental qualification, skills and personal support (at university or post graduated level). The core of this new

competence for teachers could involve knowledge of group process, group dynamic and group roles, as well as skills in group leadership.

More effective participation of parents in process of education for health and personal development of their children will need additional activities from our educational system. For health education and personal development this is critical because most of healthy life styles and conditions for personal grout are family dependent. That means that whole EHPD must involve specific programs, supporting and educating parents.

Special attention in EHPD ought to be given to children in risk situation and children with specific educational needs.

The task to improve health and personal growth of our children is complex and needs our comol efforts. I am deeply convinced that together we will succeed.

REFERENCES

1. Benson, P. L. (2006). All kids are our kids: What communities must do to raise caring and responsible children and adolescents (2nd ed). San Francisco: Jossey-Bass.
2. Blum, R. W., & Libbey, H. P. (2004). School connectedness—Strengthening health and education outcomes for teenagers. Journal of School Health, 74, 229–299.
3. Dryfoos, J. G. (1997). The prevalence of problem behaviors: Implications for programs. In R. P. Weissberg, T. P. Gullotta, R. L. Hampton, B. A. Ryan, & G. R. Adams (Eds.), Healthy children 2010: Enhancing children's wellness (pp. 17–46). Thousand Oaks, CA: Sage.
4. Durlak, J.A., Weissberg, R., Dymnicki, A., Taylor, R., Schellinger, K. The Impact of Enhancing Students' Social and Emotional Learning: A Meta-Analysis of School-Based Universal Interventions. Child Development, January/February 2011, Volume 82, Number 1, Pages 405–432.
5. Eaton, D. K., Kann, L., Kinchen, S., Shanklin, S., Ross, J., Hawkins, J., et al. (2008). Youth risk behavior surveillance—United States, 2007. MMWR Surveillance Summaries, 57(SS04), 1–131. Retrieved November 29, 2010, from http://www.cdc.gov/mmwr/preview/mmwrhtml/ss5704a1.htm?s_cid=ss5704a1_e
6. Elias, M. J., Zins, J. E., Weissberg, R. P., Frey, K. S.,Greenberg, M. T., Haynes, N. M., et al. (1997). Promoting social and emotional

learning: Guidelines for educators. Alexandria, VA: Association for Supervision and Curriculum Development.
7. Klem, A. M., & Connell, J. P. (2004). Relationships matter: Linking teacher support to student engagement and achievement. Journal of School Health, 74, 262–273.
8. Roeser, R. W., Eccles, J. S., & Samoroff, A. J. (2000).School as a context of early adolescents’ academic and social–emotional development: A summary of research findings. The Elementary School Journal, 100, 443–471.
9. Wang, M. C., Haertel, G. D., & Walberg, H. J. (1997). Toward a knowledge base for school learning. Review of Educational Research, 63, 249–294.
10. WHO, Preamble to the Constitution of the World Health Organization as adopted by the International Health Conference, New York, 19-22 June, 1946; signed on 22 July 1946 by the representatives of 61 States (Official Records of the World Health Organization, no. 2, p. 100) and entered into force on 7 April 1948.
11. Zins, J. E., Weissberg, R. P., Wang, M. C., & Walberg, H.J. (Eds.). (2004). Building academic success on social and emotional learning: What does the research say? New York:Teachers College Press.
12. Zins, J. E., & Elias, M. J. (2006). Social and emotional learning. In G. G. Bear & K. M. Minke (Eds.), children’s needs III: Development, prevention, and intervention (pp. 1–13). Bethesda, MD: National Association of School Psychologists.

Developing Key Competences in Secondary School

Stefan Manev, *Reneta Petkova, **Adriana Tafrova
SOUTH-WEST UNIVERSITY NEOFIT RILSKI
**MINISTRY OF EDUCATION, YOUTH AND SCIENCE*
*** University of Sofia St. Kliment Ohridski*

***Abstract**. In this paper a brief overview of the science key competences along with the traditions in Bulgarian education referring to these competences is made. The need of application of some key competences is shown off by several examples of tasks from Bulgarian ancient and modern textbooks. It is outlined the importance for young people to develop key competences in school. The necessary methodological ground for mastering of such competences is considered. Some problems and possible ways to resolve them are highlighted.*

***Keywords:** key competences, science education, European Reference Framework, problem solving*

1. INTRODUCTION

The rapid pace of changes in the 21st century way of life and in the organisation of work require certain new abilities and skills of young people. The goal of secondary school education is not merely to achieve subject-specific knowledge skills but to develop the needed key competences which help people to cope with the new demands. "Young people must not only keep their specific job-related skills up-to-date, but also possess the generic competences that will enable them to adapt to change. People's competences also contribute to their motivation and job satisfaction in the workplace, thereby affecting the quality of their work." [1].

The need to equip students with necessary key competences call for education system to be adapted in response to new competence requirements through better identification of key competences.

2. WHAT ARE KEY COMPETENCES

The concept of competences could be defined as a combination of knowledge, skills and attitudes that are particularly necessary for personal fulfillment and development, and social inclusion.

Key competences are those competences which are essential in a knowledge society and guarantee more flexibility in the labour force, allowing it to adapt more quickly to constant changes in an increasingly interconnected world. They are also a major factor in innovation, productivity and competitiveness, and they contribute to the development of active citizenship, social integration and job satisfaction in the workplace, thereby affecting the quality of work.

A recommendation on key competencies for lifelong learning has been developed and was adopted by the Council and the European Parliament in December 2006 (Education

Council, 2006). The Recommendation is known as European Reference Framework [1,2] and sets out eight key competencies:

1) Communication in the mother tongue;
2) Communication in foreign languages;
3) Mathematical competence and basic competences in science and technology;
4) Digital competence;
5) Learning to learn;
6) Social and civic competences;
7) Sense of initiative and entrepreneurship;
8) Cultural awareness and expression.

These key competences are all considered equally important. Most of them overlap and interlock: aspects essential to one domain will support competence in another. Nearly all of these eight key competences involve critical thinking, creativity, initiative, problem-solving, decision-taking etc.

According to the recommendation of the EU Reference Framework the key competences are to comprise components as sociability, interactivity and individual activity which make them effective and useful for the development of individuals (Fig. 1).

Bulgaria as an EU member has to focus its education on the identifying and development of key competences and therefore to ensure that young people have developed the competences to a level that equips them for adult life. It should be of special concern that the acquired knowledge, skills and competences form a basis for further learning and working life and that people would be able to develop and update their key competences throughout their lives.

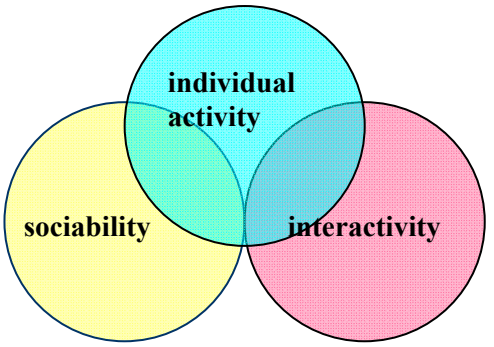

Fig. 1. Basic components of the key competences

According to the European Reference Framework competences in science refers to the ability and willingness to use the body of knowledge and methodology employed to explain the natural world, in order to identify questions and to draw evidence-based conclusions.

Key competences in science comprise the following essential knowledge, skills and attitudes:

Knowledge
➢ knowledge of the basic principles of the natural world
➢ knowledge of the fundamental scientific concepts, principles and methods
➢ understanding of the impact of science knowledge on the natural world

Skills
➢ ability to use scientific data to: ➢ achieve a certain goal ➢ reach an evidence-based decision ➢ communicate conclusions based on evidences
➢ ability to recognise the essential features of scientific inquiry and to communicate the reasoning and conclusions that led to them

Attitudes
➢ critical appreciation and curiosity to the scientific progress
➢ understanding of the progress along with the scientific limitations and risks
➢ interest in ethical issues интерес към етични въпроси
➢ respect for both safety and sustainability of the scientific progress
➢ understanding the scientific progress in relation to the individual citizen, and communities

The system of school education can play a big role in developing the key competences. As a general, they are included in the National Educational Content Standards and decomposed in the Programmes of Study.

Each school subject in conformity with its content, teaching methods, approaches and applied techniques could contribute to the development of some of the components of key competences. The total mastering of all key competences could be reached in all school years and all subjects in their integrity.

3. ARE KEY COMPETENCES A NOVELTY IN BULGARIAN SCHOOL?

A textbook “Bulgarian Arithmetic” is published in Istanbul in 1856 (36 years later than Dr. Petar Beron’s “Fish Primer”[1)]). The problems included in this textbook require not only mathematical operations but stimulate the development of key competences [3,4]. A few examples are given below.

Task 1[2)].

В. Ко́ломбъ на́нде Аме́рика на 1492 по Р. Х. ко́лко годи́ны са ѿ тога̀ до дне́сь;

1856
1492
―――
ѿ. То́лко са годи́ны . 364

One of the first tasks in this textbook concerns the subtraction of numbers. Beside arithmetical operations this task pays attention to some historical facts: whom and when America has been discovered. Students learn as well to find a time interval.

Task 2.

Еди́нъ прѫтъ 4½ арши́на высо́къ, пра́ви сѣнка 3 арши́на: ко́лко е высо́къ гра́дскïо часо́вникъ на кого́то е сѣнката 153 арши́на ?

In this case a practical skill – to determine the height of an object (without measuring it), is aimed to be developed. Based on the similar

triangles the theory is more or less complicated. Not to go deep into this theory, students learn a comparatively important skill.

Modern textbooks, including those published after 2006, also include elements of key competences. Fig. 2 illustrates a model of the research approach presented and explained in a chemistry textbook [5].

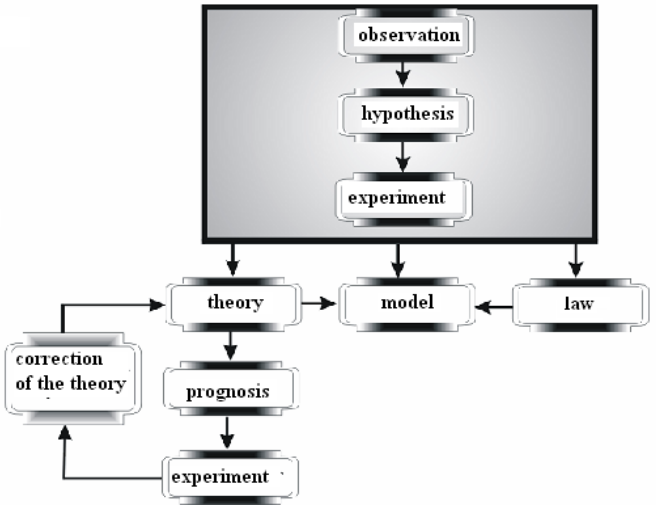

Fig. 2. A model presentation of the research approach

Another task in the same textbook [5] is based on an everyday life case:

A student decides to check the potentialities of the research method. Below you can follow the procedure of his/her inquiry:	
Observation:	A new bakery is open. On Monday at 3 p.m. the student buys there bread which is hot and delicious**.**
Hypothesis:	In this bakery one can buy hot and delicious bread every day at 3 p.m.
Experiment:	The student buys bread in that bakery for three days running.
Finding:	All of these three days bread is cold and burnt.
Conclusion:	The initial hypothesis is not true.
New hypothesis:	Only on Monday at 3 p.m one can buy hot and delicious bread in this bakery.
Experiment:	The experimenter buys bread at 3 p.m. for three Mondays running.
Finding:	Once bread is hot and twice is cold.
Conclusion:	Therefore the second hypothesis is not true as well. It is better to ask the baker when one can buy hot bread.
Observation:	The baker's answer is that hot bread is available at

	4 p.m. and on rare occasions at 3 p.m.
New hypothesis:	The baker’s answer is correct: hot bread is available at 4 p.m. and very rarely earlier than 3 p.m.
Experiment:	The student buys bread for three days running at 4 p.m.
Conclusion:	Bread is hot and delicious all of these three days.
Theory:	First you have to gather information and then to start an experiment.
Verification of the theory:	The verification of the theory shows that the theory is true.

At first sight this task appears to be a little bit airy but in fact it relates the research methods to the solutions of everyday life problems which everyone encounters in his/her life, or in other words the task aims at the development of core competence.

Textbooks in Biology and Health Education school subject also comprise topics related to the development of key competences. Some examples of such topics are: “Psychosexual Development” and “Sexual and Reproductive Health” [6]. There are permanent columns as well, such as “How to be Healthy”. Different aspects of health competences are described in these columns, for example: “Do not allow having sexual intercourse without your agreement, under influence of other people, of alcohol, psychoactive drugs, or having sex just to satisfy your curiosity or because you think all your friends are doing it. What is important is that you must use or require from your partner to use condoms to prevent unwanted pregnancy and sexually transmitted diseases (STDs), including HIV [6].

Appropriate ways to develop key competences of young people are such forms of informal education as learning and practice out of class and out of school environments. Examples of good practice for developing key competences are the National Competition on Key Competences [7,8] and European Union Science Olympiad [9,10].

4. PEDAGOGICAL REQUIREMENTS FOR DEVELOPMENT OF KEY COMPETENCES IN TEACHING-LEARNING PROCESS

Nowadays it is obvious that traditional pedagogical approaches, methods and educational means cannot provide key competences and therefore do not reach educational results necessary for the development of a socially mature person who is capable of full self-realization in the modern society. This is obviously true taking into account the essential features of these specific combinations of knowledge, skills and attitudes. A variety of studies prove that [7,8, 10-13].

On the basis of the theoretical analysis of the key competences and proceeding from our experience with National Competition on Key Competences we believe that the most important pedagogical requirements can be stated as follows:

- the activity-based approach has to be applied in teaching and learning
- interactive methods and techniques have to be widely implemented in the learning process
- cross-curricular relationships have to be used
- wide implementation of problem solving involving key competences
- implementation of student-centered education; the teacher has to act as coach and facilitator rather than instructor.

5. PROBLEMS RELATED TO THE DEVELOPMENT OF KEY COMPETENCES

As stated up to here, in the secondary school there are favourable factors for developing of key competences. Such helpful factors are the legislative norms, educational documentation, traditions. Nevertheless, the competence-based approach is not among the priorities of the school education. Which are the major problems facing the developing of key competences?

Problem 1. Developing of key competences as a necessary educational priority is not recognized by all education policy-makers and educators. This fact was confirmed at a series of meetings of regional education experts and science teachers. These meetings were carried out in 2010/2011 school year. The essential features, necessity and ways of implementation of key competences throughout the educational system were identified and discussed during these meetings.

Problem 2. National Educational Content Standards, educational curriculum, particularly Programmes of Study and textbooks do not embed a full range of needed key competences. Their representation in these documents should be increased.

Problem 3. A great deal of teachers does not master the necessary pedagogical abilities to develop key competences of their students. The point is that the activity, interactivity and cross-curricular-based as well as problem-solving and student-centered approaches must be applied in teaching and learning. However, teachers still act as instructors, as a source of information, which in many cases could be found in textbooks.

Problem 4. National external assessment does not target at key competences. On one hand that is fair because students are not taught purposefully how to apply key competences. On the other hand the external assessment could contribute to bring the key competences to the fore and

therefore to solve *Problem 1*. The move to testing competence rather than testing knowledge is important in the fast-changing world.

The successful solving of problems related to mastering of key competences by the secondary school students can be achieved only with the participation of all actors in the field of secondary and higher education. It is possible in collaboration with all institutions concerned including NGO, public organizations, parents, as well as educators and policy makers from other European countries.

6. CONCLUSIONS

In this paper reasons for the importance of developing key competences are given. It is made a brief overview of the science key competences along with the traditions in Bulgarian education referring to these competences. Authors present their perceptions about the needed methodological ground for efficient development of such competences. Some problems and possible ways to resolve them are highlighted.

To date, little attention has been given to the circumstances in which the process of developing key competencies may take place both in formal and informal education. We are convinced that a spotlight has to be put on the mastering of key competences. Citizens must be able to cope with the increasingly rapid changes in the work market, and to adapt to the changing societal needs in the context of globalization. The world is changing so fast that it is no longer possible to know what knowledge is relevant in the future and therefore what people need is a learning environment able to provide them with “life skills”. Such an environment will contribute to the improvement of the Bulgarian school education and its synchronization with European education.

7. NOTES

1) Dr. Petar Beron (1799 – 1871) is an eminent Bulgarian educator, physician and natural scientist who created the first modern Bulgarian primer, erroneously called the Fish Primer (*Riben bukvar*) because of a dolphin drawn in the end of the book.

2) The original appearance of Tasks 1 and 2 is intact.

8. REFERENCES

1. Key Competences. European Reference Framework. *Ministry of Education and Science*, (2007), [In Bulgarian].

2. http://www.euso.dcu.ie/euso/home/index.htm

3. Николов, О., (1856), Болгарска аритметика, Цариград.

4. Manev, S., V.Dimitrova (2009) The Tasks in „Bulgarian Arithmetic" from 1856 – an example of Development of Key Competences, *Chemistry*, **18** (5), , 340 – 348. [In Bulgarian]

5. Manev,S.,L.Mihova, M.Tsavkova, D.Lazarov, G.Petrov. (2009) Chemistry and Environmental Protection, Year 9, second level. *Prosveta*, Sofia, [In Bulgarian].

6. Bostandjiev,R., S.Tomova ets. (2009) Biology and Health Education, Year 8. Azbuki - Prosveta, Sofia, [In Bulgarian].

7. Manev,S.,S.Tomova,A.Tafrova,M.Gaidarova,K.Tiutiulkov, K.Jotovska. (2010) About Key Competences in Science. *IV National Conference in Biological Education „ Quality of the Biological Education".* Lovech, November, [In Bulgarian].

8. Manev, S.,A.Tafrova-Grigorova,S.Tomova,K.Jotovska, M. Gaidarova, K.Tiutiulkov (2009) First National Competition in Key Scientific Competences, *Chemistry* **18** (2-3) 195 –206 [In Bulgarian].

9. Tomova, S., A.Tafrova-Grigorova**,** M. Gaidarova (2009) VII European Union Science Olympiad. Biology, Ecology and Biotechnology,. *Chemistry* **18** (5-6), 57 – 90, [In Bulgarian].

10. Petkova, R., S. Manev, S. Tomova (2010) Development of Key Competences: A Priority in science Education. *IV National Conference in Biological Education „Quality of the Biological Education"*. Lovech, November, [In Bulgarian].

11. Manev, S., (2007) On The Spirit of Problems and Tasks, *Chemistry*, **16**, (3), 1, [In Bulgarian].

12. Gushterova, P., (2011) Developing Key Competences in Chemistry and Environmental Protection, Year 8. *Graduate thesis.* South-West University Neofit Rilski, Blagoevgrad, [In Bulgarian].

13. Manev, S.,S. Tomova, A.Tafrova, M. Gaidarova, K. Tiutiulkov, K. Jotovska, R. Petkova. (2011) Science Tasks and Problems for Years 5-8. *Azbuki - Prosveta*, Sofia, [In Bulgarian].

Lewis Acid Catalyzed Rearrangement of 1,1'-Diphenyl-2,2'-spirobiindane-1,1'-diol

Jane Bogdanov
Sts. Cyril and Methodius University, Republic of Macedonia

Abstract: *It is well established that 2,2’-spirobiindane ketones are susceptible to nucleophile-induced retro-Claisen condensations that lead to molecular rearrangements destroying the spiro connectivity. In the course of functionalization of the 2,2’-spirobiindane skeleton, 1,1'-diphenyl-2,2'-spirobiindane-1,1'-diol was prepared as a versatile synthetic intermediate. However, most of the conventional reactions failed because this spirodiol undergoes a facile Lewis-acid catalyzed dehydration. The structure of the rearrangement product was determined and a mechanism for this transformation is proposed.*

Keywords*: Lewis acid, rearrangement, 1,1'-diphenyl-2,2'-spirobiindane-1,1'-diol*

1. INTRODUCTION

As a part of our systematic study of spirobiindane derivatives as potential precursors for reactive intermediates [1] (such as diradicals), we have focused our attention on introduction of groups that would increase the persistency of the diradicals [2]. We have chosen to build the spirocenter early in our synthetic sequence and then to functionalize the 2,2-spirobiindan framework. Work done by Maslak and co-workers [3] clearly indicated the sensitivity of 2,2’-spirobiindan1,1’-dione (**1**) and similar systems to nucleophiles (Figure 1). It is important to keep this in mind in terms of synthetic planning, because once at least two ketones are present ,one should avoid strong nucleophiles. Preliminary attempts of bis-alkylation of 2,2’-spirobiindan-1,1’-dione, **1**, with phenylmagnesium bromide and phenyllithium resulted in the destruction of the spirosystem. Herein, we would like to report an interesting rearrangement we have encountered of one of the synthetic intermediates (1,1'-diphenyl-2,2'-spirobiindane-1,1'-diol, **2**)

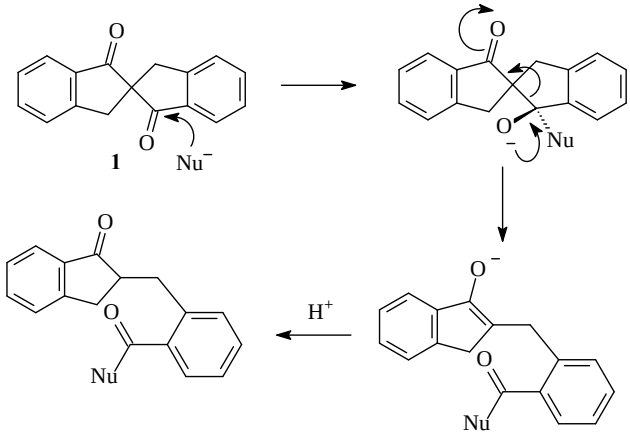

Fig. 1: Nucleophile-induced retro-Claisen condensations of 2,2'-spirobiindan-1,1'-dione that leads to molecular rearrangements destroying the spiro connectivity

2. MATERIALS AND METHODS

The title compounds were purified and characterized using standard procedures. NMR spectra were recorded on Bruker DRX-400 spectrometer (400 MHz for proton) in deuterated chloroform ($CDCl_3$) and were reported in ppm with respect to tetramethylsilane (2 drops per 100 g $CDCl_3$). Infrared spectra were recorded on Perkin Elmer Model 1600. as thin films between sodium chloride plates (reported as film). Gas chromatography was performed on a Varian 3700 with packed columns 1/8" diameter packed with 5% OV-101 on Supelcoport with helium as the carrier gas with a flow rate of 30 mL/min. High resolution mass spectrum was obtained on Waters GC-TOF with Agilent 6890 GC. 1,1'-Dihydroxy-1,1'-diphenyl-2,2'-spirobiindanes were prepared by literature procedure [10].

Acid induced rearrangement of 2a. A 100 mg sample of **2a** was dissolved in 0.7 mL of deuterated chloroform, transferred into an NMR tube and allowed to stand for a week on a bench top. The traces of acid in the deuterated chloroform induced a rearrangement (that could be conveniently monitored via ^{1}H NMR) to phenyl-[2-(3-phenyl-1-*H*-indene-2-ylmethyl)-phenyl]-methanone, **3**: (400 MHz, $CDCl_3$): 7.77 (d, J = 8.0 Hz, 2 H), 7.56 (t, J = 7.4 Hz, 1 H), 7.42 (t, J = 7.9 Hz, 4 H), 7.38 (m, 11 H), 7.38 (s, 2 H), 3.33 (s, 2 H). The sample was evaporated to dryness, dried *in vacuo* to give analytically pure **3** as yellow oil; GC R_t = 14.12 min (Varian temp. program: 160 °C, 3 min, 8 °C/min 280 °C); HRMS ($C_{29}H_{22}O$): Calc. 386.1671, found 386.1672 ^{1}H NMR (400 MHz, C_6D_6): 7.79 (m, 2 H), 7.36 – 6.96 (m, 15 H), 6.88 (dt, J = 7.3 Hz, J = 1.5 Hz, 1 H), 3.98 (s, 2 H), 3.20 (s, 2 H); IR (liquid film): 1665 cm^{-1} (C=O).

3. RESULTS AND DISCUSSION

After careful inspection of the reaction conditions, we found that in all cases the Grignard or phenyllithium was added to **2** (i.e normal addition). We speculated that once the phenyl adds to the ketone, the resulting tetrahedral intermediate collapses in analogous manner to that illustrated in Figure 1, resulting in ring opening. To remedy this problem, we decided to do a “reverse addition” i.e. slowly add a solution of the dione to a slight excess (2.1-2.3 equivalents) of a pre-cooled phenyllithium solution. If the ring opening is slower than the second addition of phenyllithium, then we have a chance to obtain the elusive diphenylspirodiol. We assumed that the dilithium dialkoxide should be stable under the reaction conditions and protonation should yield the desired product.

Indeed, the reverse addition gave the desired product, **2** in 69% yield (mixture of two diastereomers, **2a** : **2b =** 2.5 : 1.0). Several attempts of obtaining X-ray quality crystals of **2a** have failed. The stereochemistry of **2a** and **2b** was established based on ^{1}H NMR data and via structural correlation with the 1,1'-dimethoxy-1,1’-diphenyl-2,2'-spirobiindane, for which we have obtained single crystal X-ray crystallographic data.

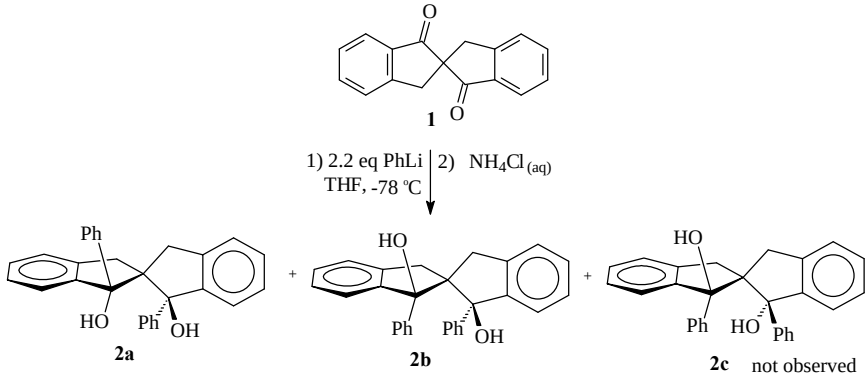

Fig. 2: Synthesis of 1,1'-diphenyl-2,2'-spirobiindane-1,1'-diols (**2a** and **2b**).

We have come to a conclusion, based on the spectral data, that the spirodiol, **2**, is sensitive to the acidic impurities in the deuterated chloroform. The ^{1}H NMR spectroscopy indicated quantitative conversion of **2a** (or **2b**) to **3**. The proposed rearrangement mechanism of this acid-catalyzed dehydration of 1,3-spirodiols is depicted in Figure 3.

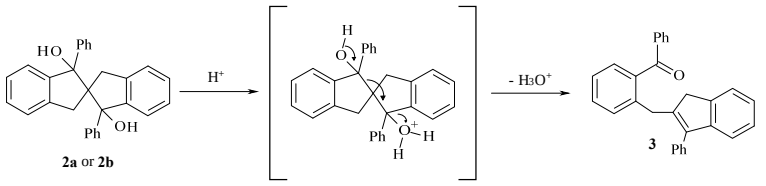

Fig. 3: Lewis-acid catalyzed rearrangement of 1,1'-diphenyl-2,2'-spirobiindane-1,1'-diol to give

We decided to proceed to find alternative protective groups for the tertiary alcohols, possibly such that could serve as radical precursor (Barton-type deoxygenation chemistry[4]). If we use acetyl chloride directly on the dialcohol, **2**, the liberated hydrogen chloride would promote rearrangement to **3**. An example from the literature supported this claim: Schonberg and co-workers refluxed a mixture of the spirodiol and excess of acetyl chloride [5] and after work-up they obtained 5,11-diphenylbenzo[b]fluorene, **4**. They rationalized its formation by the mechanism described in Figure 4 where the protonated **3** (**3H$^+$**) was involved as an intermediate. Our approach to diacetylation of the diol was rather simple. After the addition of spirodione to phenyllithium, we attempted to trap the dialkoxide with acetyl chloride. Unfortunately, even after several attempts we were not able to isolate the diacetate. This result implied that transformation would be very difficult if not impossible. This outcome revealed to us that the preparation of Barton-type esters would be very difficult or perhaps maybe not be feasible.

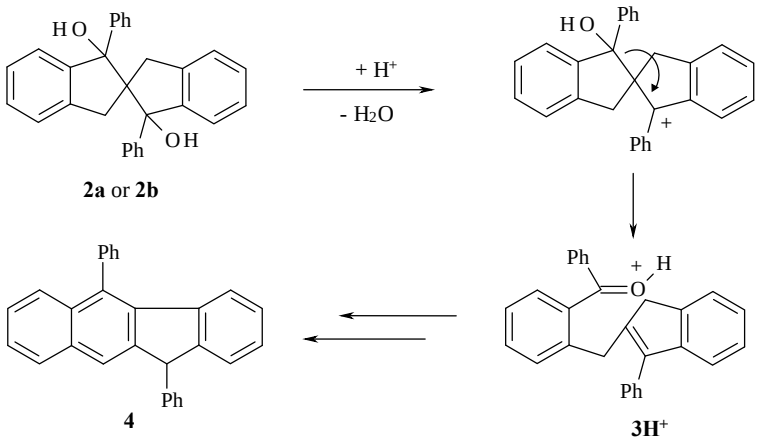

Fig. 4: Schonberg's proposed mechanisam for rearrangement of **2** to 5,11-diphenylbenzo[b]fluorene, **4**.

We have attempted preparation of the cyclopropane derivative using the methodology developed by Walborsky [6] involving reductive coupling of 1,3-diols using low valent titanium (McMurry reagent,[7,8] $TiCl_3/LiAlH_4$) to afford the cyclopropane. Subjecting **2a** to these conditions resulted in rearrangement product **3**. The presence of traces of Lewis acid, (we suspect unreacted $TiCl_3$) was sufficient to trigger the rearrangement. Additionally, we have attempted to deoxygenate **2a** using the procedure by Lau and co-workers [9], utilizing $NaCNBH_3$ in presence of ZnI_2, and instead the desired product we obtained the rearrangement product **3**. In this case the Lewis acid, ZnI_2, was responsible for the rearrangement. The dialcohols (**2a** and **2b**) were found to be too sensitive for the desired synthetic manipulations.

4. CONCLUSION

Functionalization of 1,1’-diphenyl-2,2'-spirobiindane-1,1'-diols are severely limited using standard reactions because this spirodiol undergoes a facile Lewis-acid catalyzed dehydration. Based on the identity of the rearrangement product, phenyl-[2-(3-phenyl-1-*H*-indene-2-ylmethyl)-phenyl]-methanone, a mechanism for this transformation was proposed. The dialcohols (**2a** and **2b**) were found to be too sensitive for the desired synthetic manipulations, which severely limits their usefulness as synthetic precursors.

ACKNOWLEDGEMENT

The author expresses deep gratitude to Dr. Pshemak Maslak (Pennsylvania State University) for his help and valuable advices and to Dr. Alan Benesi and Dr. Robert Minard from Pennsylvania State University for their help with the acquisition of NMR and mass specta.

5. REFERENCES

[1] Moss, R.A., Platz, M.S., Jones, M., Jr., and Editors. (2004). *Reactive Intermediate Chemistry*.

[2] Platz, M.S. (1982) Diradicals. In *Diradicals*. W.T. Borden, editor. New York: Wiley 195.

[3] Maslak, P., Varadarajan, S., and Burkey, J.D. (1999) Synthesis, Structure, and Nucleophile-Induced Rearrangements of Spiroketones. *J. Org. Chem.* 64:8201-8209.

[4] Barton, D.H.R., and McCombie, S.W. (1975) New method for the deoxygenation of secondary alcohols. *J. Chem. Soc., Perkin Trans. 1*:1574-1585.

[5] Schoenberg, A., and Sidky, M.M. (1974) Formation of 11*H*-benzo[b]fluorene from (±)-2,2'-spirobiindan-1,1'-dione. Dehydration of 1,3-diols. *Chem. Ber.* 107:2341-2344.

[6] Walborsky, H.M., and Murari, M.P. (1980) Coupling of nonvicinal glycols by low-valent titanium. *J. Am. Chem. Soc.* 102:426-428.

[7] McMurry, J.E., Fleming, M.P., Kees, K.L., and Krepski, L.R. (1978) Titanium-induced reductive coupling of carbonyls to olefins. *J. Org. Chem.* 43:3255-3266.

[8] McMurry, J.E., Silvestri, M.G., Fleming, M.P., Hoz, T., and Grayston, M.W. (1978) Some deoxygenation reactions with low-valent titanium (titanium trichloride/lithium tetrahydroaluminate). *J. Org. Chem.* 43:3249-3255.

[9] Lau, C.K., Dufresne, C., Belanger, P.C., Pietre, S., and Scheigetz, J. (1986) Reductive deoxygenation of aryl aldehydes and ketones and benzylic, allylic, and tertiary alcohols by zinc iodide-sodium cyanoborohydride. *J. Org. Chem.* 51:3038-3043.

[10] Bogdanov, J.B. (2005) Electron Delocalization in Spiroconjugated Systems. *Ph. D. Thesis, The Pennsylvania State University*.

Synthesis and Structural Characterization of 3,3’-Dihalo-2,2’-spirobiindan-1,1’-diones

Jane Bogdanov
Sts. Cyril and Methodius University, Republic of Macedonia

Abstract: *Starting from 2,2’-spirobindan-1,1’-dione, 3,3’-dibromo-2,2’-spirobiindan-1,1’-dione, 3,3’-dichloro-2,2’-spirobiindan-1,1’-dione and 3,3’-difluoro-2,2’-spirobiindan-1,1’-dione were prepared using standard chemical transformations. For each of these derivatives six stereoisomers are possible (three pairs of enantiomers). In some cases one or more of the diastereomers were separated and purified and using ^1H NMR and single crystal X-ray crystallography their relative configuration was determined*.

Keywords*: 3,3’-Dihalo-2,2’-spirobiindan-1,1’-diones, relative configuration, synthesis*

1. INTRODUCTION

As a part of our systematic study of 2,2’-spirobiindane-1,1’-dione derivatives as potential diradical precursors [1,2], we have focused our attention on introduction of photolabile substituents such as halides. A convenient starting material was the “parent” compound, 2,2’-spirobiindan-1,1’-dione. Its synthesis is well documented in the literature [3] and we had experience with its preparation in our laboratory [4].

Our primary goal was to focus on the preparation of the 3,3’-Dihalo-2,2’-spirobiindan-1,1’-diones (**X(HH)** systems, where X=F, Cl, Br), in order to gain understanding of the stereochemical and reactivity issues and apply it to the more challenging precursors (spirocyclopropane derivatives). The choice of photoremovable **X** substituents was chlorine or bromine, because these are known in the literature to give diradicals either by direct photolysis [5,6] or by photolysis in the presence of amines [7,8], and there are many reliable benzylic halogenation procedures. Once the 1,3-dihalides are prepared they can serve as convenient diradical precursors and synthetic precursors for the spirocyclopropanes.

2. MATERIALS AND METHODS

The title compounds were purified and characterized using standard procedures. All NMR spectra were recorded on Bruker DRX-400 spectrometer (400 MHz for proton) in deuterated chloroform ($CDCl_3$) using TMS as internal standard. The reported X-ray structures were obtained using X-ray intensity data measured at 98 K (cooled by Rigaku MSC X-

Stream 2000) on a Bruker SMART APEX CCD area detector system equipped with a graphite monochromator and a MoKα fine–focus sealed tube (λ = 0.71073 Å) operated at 1600 W (50 kV, 32 mA).

3. RESULTS AND DISCUSSION

3.1 Practical assignment of relative stereochemistry

In the course of this study no optically active spiro compounds or reagents were used, so both enantiomers are always present in equal amounts (all materials are racemates). Since the tetrahedral stereogenic centers on the carbons 3 and 3' are equivalent in terms of their substituents, only six stereoisomers (three pairs of enantiomers) are, in fact, expected for the idealized geometry of these spiro compounds. When one deals with racemic mixtures with several chiral centers, the naming scheme becomes quite cumbersome. However, for racemic compounds only the relative configurations are important. Such relative configurations should be quickly recognizable and be rich in stereochemical content pertinent to the system under study. The crucial stereochemical concern is the relative orientation of the **X** and **H** substituents. To completely state the relations between these substituents, it is sufficient to relate just two (one on carbon 3, and one on carbon 3'). Since one pair (the hydrogens) of the substituents will be the permanent fixture of the spirosystem, while the other will be removed to generate the radical center, it would be desirable to indicate the relative stereochemistry of the "permanent" pair (i.e. in this specific case the hydrogens). The three diastereomeric racemates of the synthetic precursors should in principle have different enough physico-chemical properties, both chromatographically and spectroscopically, to be separable and identifiable. From the point of view of the NMR techniques, inspection of models indicates that there are two symmetrical and one non-symmetrical diastereomers (symmetrical in terms of chemical shift equivalency of the "halves"). The non-symmetrical isomers would yield two sets of signals (the two spiro sub-systems will be non-equivalent). The non-symmetrical isomer (C_1 space group), will always correspond to mixed label, **X(mHH)**. On the other hand, the two symmetrical isomers will have only one set of signals (for both subunits). These isomers are C_2 symmetric, and will always have the designation anti, **X(aHH)** or syn **X(sHH**). The only method to distinguish between the anti and syn stereoisomers is the one that is unrivaled in structural chemistry-single crystal X-ray crystallography.

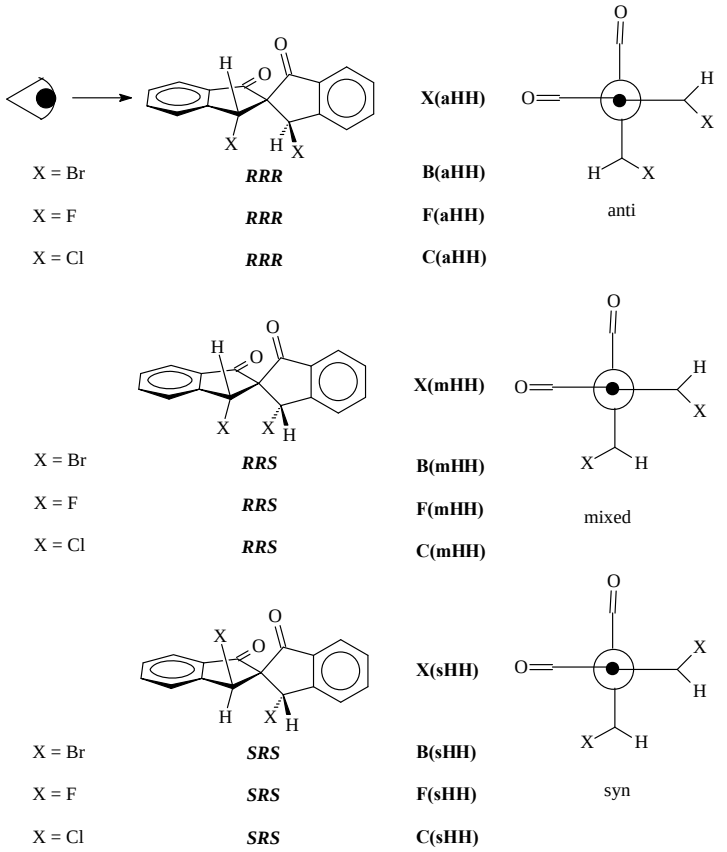

Fig. 1: Three possible diastereomers of 3,3’-(dihalo)-2,2’-spirobiindan-1,1’-dione, **X(HH)** system. Only one enantiomer of each pair is shown.

Additional potential complications arise from the fact that in the non-idealized structures five-membered rings are not flat but adopt a so-called “envelope” conformation This deviation from planarity becomes evident from structural calculations and literature X-ray structure of 2,2’-spirobiindan-1,1’-dione [9] as well as those obtained in our laboratory [4]. In solution, however, there is conformational flexibility. The energy differences between extreme conformers are low [10,11], so the interconversion in solution at 25 ºC is rapid [12,13]. As indeed was observed, the rings rapidly (faster than the NMR time-scale) swing between the extremes, giving “time averaged” signals simplifying the analysis based on the idealized “flat” structures (Fig. 5).

3.2. Synthesis of the 3,3’-Dihalo-2,2’-spirobiindandione Systems

The synthesis of the simplest precursors, **B(HH)**, started with *N*-bromosuccinimide bromination of 2,2’-spirobiindan-1,1’-dione, **2**. Based on

the ^{1}H NMR spectrum of the crude reaction mixture, only two isomers of the 3,3'-dibromo-2,2'-spirobiindan-1,1'-dione were obtained (**B(aHH)** and **B(mHH)**). This is a peculiar finding, because in free-radical reactions the intermediate benzylic radicals are expected to be planar, there should not be any differentiation between the faces, and one would expect all three diastereomers (Figure 2). The reason for this behavior has not been investigated. The isomers were separated by chromatographic means and were further purified via recrystallization. The **B(aHH)** and **B(mHH)** isomers gave crystals suitable for X-ray crystallography (Figure 6) .

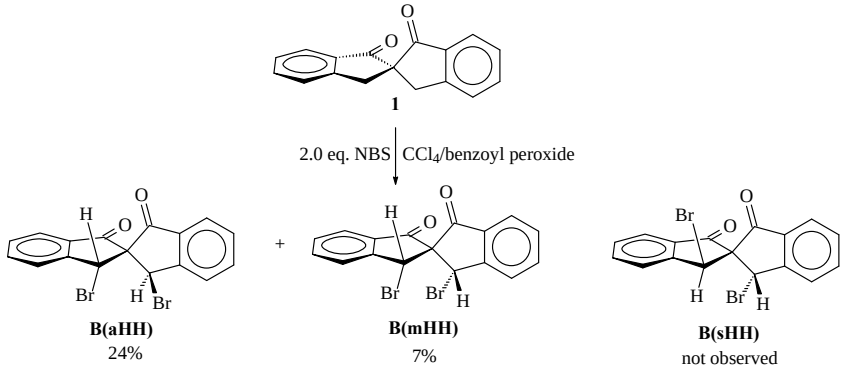

Fig. 2: Synthesis of 3,3'-dibromo-2,2'-spirobiindan-1,1'-diones (**B(aHH)** and **B(mHH)**) via NBS bromination of 2,2'-spirobiindan-1,1'-dione.

The **B(aHH)** isomer served as a valuable intermediate (most abundant and easily separable). Silver tosylate assisted hydrolysis in dioxane/water resulted in a mixture of three dialcohol isomers, whose stereochemistry was not determined. Treatment of the dialcohols with thionyl chloride gave a mixture of three dichlorides, of which two were successfully separated and purified (**C(aHH), C(mHH)**) and their relative stereochemistry established by X-ray crystallography (Fig. 3).

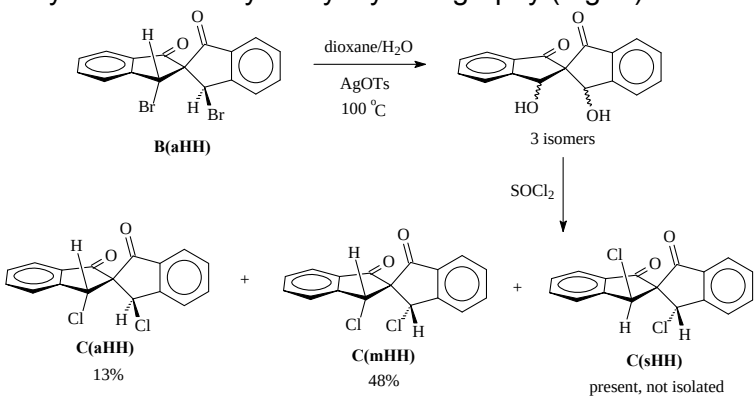

Fig 3.: Synthesis of 3,3'-dichloro-2,2'-spirobiindan-1,1'-diones.

We intetended to prepare the 3,3’-difluoro-2,2-spirobiindan-1,1’-dione, **F(HH)**, and subject it to benzylic bromination in order to obtain system should provide increased stability of the diradical. The synthetic approach was rather simple. We subjected crude 3,3’-dibromo-2,2-spirobiindan-1,1’-dione (~ 84% pure) **B(aHH)** to fluoride-bromide exchange using silver fluoride [14-16]. This kind of exchange is believed to proceed via carbocation mechanism. Since the carbocations are planar and there is no preferential face of attack by the fluoride, one would expect three difluoro isomers. Indeed, the crude reaction mixture contained three difluoro isomers, of which two (**F(sHH)** and **F(mHH)**) were isolated by chromatographic means (Figure 4). Further purification via recrystallization resulted in X-ray quality crystals, and the relative stereochemistry was firmly established.

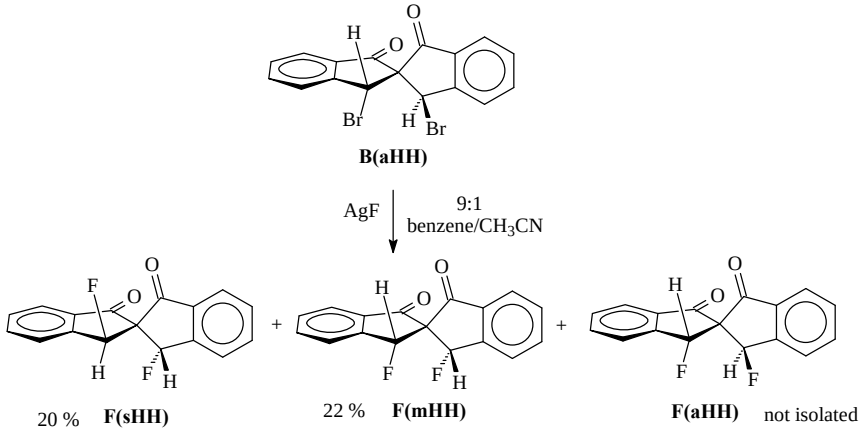

Fig. 4: Synthesis of 3,3’-difluoro-2,2’-spirobiindan-1,1’-diones.

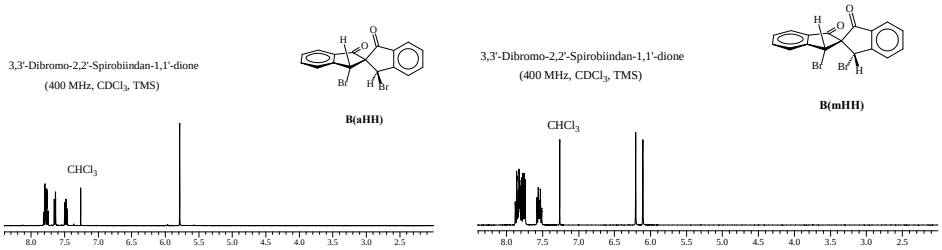

Fig. 5: ^{1}H NMR spectra of two diastereomers of 3,3’-dibromo-2,2’-spirobiindane-1,1’-dione, **B(aHH)** (left) and **B(mHH)** (right) in $CDCl_3$ (400 MHz).

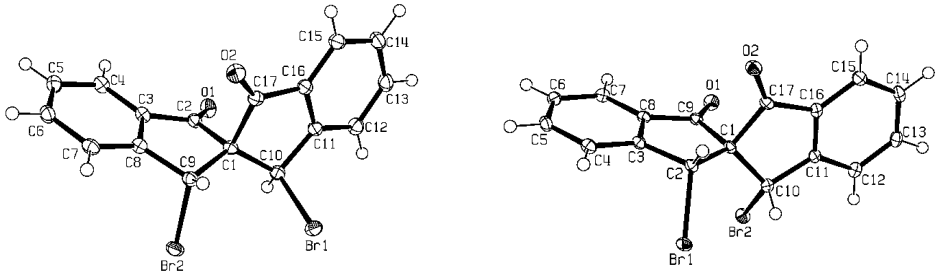

Fig. 6: ORTEP drawings of **B(aHH)** (left) and **B(mHH)** (right)**.** Displacement ellipsoids are drawn at 50% probability level.

ACKNOWLEDGEMENT

The author expresses deep gratitude to Dr. Pshemak Maslak (Pennsylvania State University) for his help and valuable advices and to Dr. Alan Benesi and Dr. Hemant Yennawar from Pennsylvania State University for their assistance in obtaining the NMR and X-ray crystallographic data.

4. REFERENCES

[1] Moss, R.A., Platz, M.S., Jones, M., Jr., and Editors. (2004) *Reactive Intermediate Chemistry*.

[2] Platz, M.S. (1982). Diradicals. In *Diradicals*. W.T. Borden, editor. New York: Wiley. 195.

[3] Neudeck, H., and Schlogl, K. (1977) *Chem. Ber.* 110:2624-2639.

[4] Bogdanov, J.B. (2005) Electron Delocalization in Spiroconjugated Systems. *Ph. D. Thesis, The Pennsylvania State University*.

[5] Biewer, M.C., Biehn, C.R., Platz, M.S., Despres, A., and Migirdicyan, E. (1991) *J. Am. Chem. Soc.* 113:616-620.

[6] Goodman, J.L., and Berson, J.A. (1985) *J. Am. Chem. Soc.* 107:5409-5424.

[7] Wright, B.B., and Platz, M.S. (1983) *J. Am. Chem. Soc.*105:628-630.

[8] Haider, K., Platz, M.S., Despres, A., Lejeune, V., Migirdicyan, E., Bally, T., and Haselbach, E. (1988) *J. Am. Chem. Soc.* 110:2318-2320.

[9] Petersen, K.B., and Danielsen, J. (1974) *Acta Crystalogr. B* 30:338-341.

[10] Legon, A.C. (1980) *Chem. Rev.* 80:231-262.

[11] Fuchs, B. (1978) *Topics in Stereochemistry* 10:1-23.

[12] Adams, W.J., Geise, H.J., and Bartell, L.S. (1970) *J. Am. Chem. Soc.* 92:5013-5019.

[13] Lambert, J.B., Papay, J.J., Khan, S.A., Kappauf, K.A., and Magyar, E.S. (1967) *J. Am. Chem. Soc.* 89:7036-7044.

[14] Bhandari, K.S., and Pincock, R.E. (1974) *Synthesis*:655-656.

[15] Heumann, A. (1979) *Synthesis*:53-54.

[16] Ruzziconi, R., and Sebastiani, G.V. (1980) *J. Heterocyc. Chem.* 17:1147-1148.

Estimating Acute Toxic Action of Sulfur Containing Compounds in the Petroleum

Yana Koleva[1], Yordanka Tasheva[2]

[1]Department of Organic Chemistry, University "Prof. Assen Zlatarov", 1 Prof. Yakimov str., 8010 Bourgas, Bulgaria

[2]Department of Industrial Technology and Management, University "Prof. Assen Zlatarov", 1 Prof. Yakimov str., 8010 Bourgas, Bulgaria

***Abstract**: Sulfur being the third most abundant element next to carbon and hydrogen poses a serious threat in view of both economy and environment. Acute toxicity is one of a batch of tests used in environmental risk assessment to determine the safe use and disposal of organic chemicals. Estimation methods based on readily available chemical properties that can be correlated with acute toxicity are useful for identifying compounds likely to present the greatest environmental risk and for gaining an understanding of the mechanism of toxicity. It is necessary to distinguish between general toxicity (or narcosis) and specific (or reactive) toxicity. General toxicity occurs by non-specific disruption of the functioning of the cell membrane. Specific toxicity refers to chemicals that interact with or disrupt the function of a defined receptor site. The aim of this work is to define the acute toxic action of sulfur containing compounds which can be found in the petroleum.*

***Keywords:** acute toxicity, sulfur compounds, petroleum*

1. INTRODUCTION

Petroleum is one of the most complex mixtures known with respect to the number of individual species. The composition of crude oil can vary greatly from source to source. However, all crude oils are mainly composed of carbon and hydrogen in the form of alkanes, naphthenes and aromatics, i.e. hydrocarbons. In addition, minor amount of sulfur-, oxygen- and nitrogen-containing heterocycles, and trace amount of metals like vanadium and nickel are also found. The abundance of heteroatoms rises with increase in average molecular weight of the sample, which in turn is related to boiling point of distillation. Although heterocycles containing S, O and N represent a minor portion in most crude oils, they are of crucial importance for exploration, production and refining of petroleum. Generally, sulfur content in crude oils varies from 0.05 to 13.95 wt %. Oils containing, however, more than 1 wt % are considered as sulfur rich oils [8].

The trend for limits on sulfur content in transportation fuels, due to environmental pollution, is gradually declining. SOx, a major air pollutant causing acid rain, from petroleum-derived fuels also poses a serious threat to the environment. Sulfur compounds also affect the emission of NOx and hydrocarbons from automobile engines by reducing the activity of catalytic converters. Moreover, sulfur oxides have detrimental effects on human health, wildlife and agricultural productivity. Therefore, most countries have defined the limits on sulfur in transportation fuels, being the major source of SOx, in order to protect the environment [8].

The price of crude oil, the major backbone of a developed economy, is largely decided by the amount of sulfur in it. Moreover, sulfur being the most abundant hetero element in crude oil is of more concern than other heteroatoms. However, the source of such high amount of sulfur in fossil fuels still remains a mystery. Sulfur exists both in aliphatic and aromatic form in crude oil. All are collectively termed organic sulfur compounds (OSC) [8].

Sulfur is in the same column of the periodic table as oxygen, but being the third-period element means that sulfur is less electronegative and more polarizable than oxygen. Thus, thiols and sulfides bear an obvious resemblance to alcohols and ethers, respectively. Sulfides are easily oxidized; initially to produce sulfoxides, whereas further oxidation leads to the formation of sulfones. Sulfoxides and sulfones are typically represented as having sulfur–oxygen double bonds and thus an expanded octet around the sulfur. However, the sulfur-oxygen double bond is not a double bond in the same sense as a carbon–carbon or carbon-oxygen double bond. In the latter two cases, the “second bond” arises from -overlap of p-orbitals. Because sulfur has lower energy d-orbitals, it is thought that the sulfur–oxygen double bond is a result of an overlap of an oxygen p-orbital with a sulfur d-orbital. It was hypothesized that this atypical double bond may affect the toxicity of sulfur-containing compounds [10]. The aim of this work is to define the acute toxic action of sulfur containing compounds which can be found in the petroleum.

2. MATERIAL AND MEYHODS

Compounds. The organic sulfur compounds for acute toxicity (aquatic and terrestrial species) were collected. The name of compounds are presented (Table 1).

Acute Aquatic Toxicity Data. Toxicity values of sulfur compounds to *Tetrahymena pyriformis* were obtained from the literature [10] and reported in Table 1. Population growth impairment was assessed after 40h with the common ciliate *T. pyriformis*.

Acute Terrestrial Toxicity Data. The experimental data for rat (oral LD_{50} values) were collected from the literature [3].

EcoSAR software. EcoSAR is a user-friendly computer programme developed and routinely applied by the US EPA for predicting aquatic toxicity to fish, daphnids and algae [4]. This software was used for grouping of the chemicals.

Log P. Data for the logarithm of the 1-octanol-water partition coefficient (log P) were obtained from the KOWWIN software [5]. Where possible measured log P values were verified and used in preference to calculated values.

Baseline models. In this study several models were used for non-polar compounds to aquatic and terrestrial species to determine the acute toxicity of organic sulfur compounds (Tables 1).

Baseline model (saturated alcohols and ketones) of *Tetrahymena pyriformis* [2]:

(1) $\log(1/IGC_{50})=0.78*\log P–2.01$

n = 87 R^2 = 0.96 s = 0.20 F = 2131

Baseline model (saturated alcohols and ketones) of Rat (oral LD_{50}) [6]:

(2) $\log(1/LD_{50}) = 0.805*\log P – 0.971*\log(0.0807*10^{\log P}+1) + 0,984$

n = 54 R^2 = 0.824 s = 0.208 F = 35.3

Excess toxicity. The property - excess toxicity - was used to define the toxicity of chemicals (reactive or nonrective) [6]. The extent of excess toxicity was determined as the toxic ratio (TR), which was calculated by the following equations 3-4 [6, 7]:

(3) $TR = \log(1/C)exp – \log (1/C)calc$

(4) TR=(predicted baseline toxicity)/(observed toxicity)

Mode of action. For environmental toxicants four broad classes of mode of action have been identified – from class I to class IV [9, 11].

3. RESULTS AND DISCUSSION

There are several modes of action for acute toxicity. The sulfur compounds were classified as neutral organics, thiols (mercaptans), thiophenes, vinyl/allyl sulfones from the EcoSAR software. For the organic sulfur compounds mode(s) of toxic action, where toxicity is observed to be (or not to be) in excess of narcosis, the possible mechanism is (ir)reversible, i.e. the toxicity is (not) observed to be related to hydrophobicity and is (not) in excess of baseline toxicity for the compounds (Fig. 1).

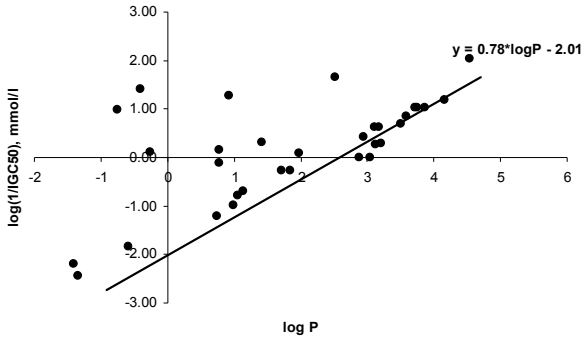

Fig. 1: Plot of toxicity to *Tetrahymena pyriformis* vs log P for sulfur compounds showing baseline toxicity.

Therefore, among sulfur compounds are recognized narcotics and reactive chemicals.

Tab. 1: Experimental and predicted values of organic sulfur compounds

Name of compound	logP	Exp. T. pyriformis log(1/IGC_{50}), Mmol/l	Pred. T. pyriformis log(1/IGC_{50}), Mmol/l /TR	Exp. oral Rat LD_{50} Mmol/Kg	Pred. oral Rat LD_{50} Mmol/Kg / TR
Cycloheanethiol	3.05[b]	-0.004	0.369/-0.37		
1-Heptanethiol	3.72[b]	1.02	0.892/0.13		
Hexane-1,6-dithiol	3.18[b]	0.63	0.470/0.16		
Octane-1,8-dithiol	4.16[b]	1.19	1.235/-0.04		
1,4-Dithiane	0.77[a]	-0.11	-1.409/1.30	23.02	27.54/1.20
2,2'-Bithiophene	3.75[a]	1.04	0.915/0.13		
Propyl sulfide	2.88[b]	-0.003	0.236/-0.24		
n-Butyl sulfide	3.87[b]	1.04	1.009/0.03	15.18	25.25/1.66
Sulfurous acid, diethyl ester	0.99[b]	-0.99	-1.238/0.25		
Di-n-propyl sulphite	1.97[b]	0.09	-0.473/0.56		
Diethylsulfate	1.14[a]	-0.70	-1.121/0.42	5.71	38.55/6.75
Sulfuric acid, dibutyl ester	3.11[b]	0.62	0.416/0.20		
Dimethyl sulfoxide	-1.35[a]	-2.44	-3.063/0.62	185.59	0.79/0.004
Dipropyl sulfoxide	0.74[b]	-1.22	-1.423/0.21	3.72	26.60/7.14
1,1'-sulfinylbisbutane	1.72[b]	-0.26	-0.668/0.41		
Dimethyl sulfone	-1.41[a]	-2.20	-3.110/0.91	53.12	0.70/0.013
Diethyl sulphone	-0.59[a]	-1.84	-2.470/0.63		

1,1'-sulfonylbis butane	1.84[b]	-0.26	-0.575/0.31		
Vinyl sulfone	-0.40[b]	1.41	-2.32/3.73	0.27	4.45/16.44
Methyl vinyl sulfone	-0.75[b]	0.99	-2.59/3.59	5.37	2.37/0.44
Ethyl vinyl sulfone	-0.26[b]	0.11	-2.213/2.32		
Thiophenol	2.52[a]	1.66	-0.044/1.70	0.42	40.89/97.51
Thianaphthene	3.12[a]	0.26	0.424/-0.16		
Phenoxathiin	4.54[a]	2.04	1.531/0.51		
(Ethythio)benzene	3.20[a]	0.30	0.486/-0.19		
Benzene, (propylthio)- (9CI)	3.58[b]	0.86	0.782/0.08		
(Allylthio)benzene	3.51[a]	0.69	0.728/-0.04		
Phenyl vinyl sulphide	2.95[b]	0.42	0.291/0.129		
Phenyl vinyl sulphoxide	0.78[b]	0.16	-1.402/1.56		
(Ethylsulphonyl)benzene	1.05[b]	-0.79	-1.191/0.40		
Allyl phenyl sulfone	1.41[b]	0.31	-0.910/1.22		
Phenyl vinyl sulphone	0.92[b]	1.28	-1.292/2.57		

[a]Experimental value of logP; [b]Calculated value of logP.

A number of reliable baseline equations are available for different organisms (aquatic (*Tetrahymena pyriformis*) and terrestrial (Rat)) and endpoints (IGC_{50}, LD_{50}). Baseline models (eqs 1-2) for different species (aquatic and terrestrial) were applied to organic sulfur compounds (Table 1). On the basis of calculated and experimental values for acute toxicity, the toxicity ratio (TR) as the ratio of the calculated baseline toxicity over the experimentally determined value was calculated. A TR-value less than one could indicate rapid hydrolysis and/or biotransformation of the parent compound by the organism to non-toxic metabolites [1].

4. CONCLUSION

A series of aliphatic and aromatic sulfur-containing compounds were evaluated in the *T. pyriformis* population growth impairment assay (IGC_{50}) and oral Rat (LD_{50}) for acute toxicity. The endpoints are a result of different

routes of exposure in various species. The effect of a chemical is dependent on the species, route of exposure, and dose. The structure of sulfur compounds is varied, suggesting a different reactivity (non-covalent and covalent interactions).

5. REFERENCES

[1] Aptula, A.O. and Roberts D.W. (2006) Mechanistic applicability domains for non animal-based prediction of toxicological end points: General principles and application to reactive toxicity, *Chem. Res. Tox.* 19, 1097-1105.

[2] Ellison, C.M., Cronin, M.T.D., Madden, J.C., Schultz, T.W. (2008) Definition of the structural domain of the baseline non-polar narcosis model for *Tetrahymena pyriformis*, *SAR and QSAR in Environmental Research* 19, 751-783.

[3] http://chem.sis.nlm.nih.gov/chemidplus/

[4] http://www.epa.gov/oppt/newchems/tools/21ecosar.htm

[5] http://www.epa.gov/oppt/exposure/pubs/episuite.htm

[6] Lipnick, R.L. (1991) Outliers-Their origin and use in the classification of molecular mechanisms of toxicity, **Science** *of the* **Total Environment** 109, 131–153.

[7] Nendza, M. and Müller, M. (2007) Discriminating toxicant classes by mode of action: 3. Substructure indicators, *SAR and QSAR in Environmental Research* 18, 155–168.

[8] Panda, S.K. (2006) Liquid Chromatography and High Resolution Mass Spectrometry for the Speciation of High Molecular Weight Sulfur Aromatics in Fossil Fuels, NRW Graduate School of Chemistry University of Münster Germany.

[9] Russom, C.L., Bradbury, S.P., Broderius, S.J., Hammermeister, D.E. and Drummond R.A. (1997) Predicting modes of toxic action from chemical structure: Acute toxicity in fathead minnow *(Pimephales promelas)*, *Environ. Toxicol. Chem.* 16, 948–967.

[10] Schultz, T.W., Sinks, G.D., Miller, L.A. (2001) Population Growth Impairment of Sulfur-Containing Compounds to *Tetrahymena pyriformis, Environmental Toxicology* 16, 543-549.

[11] Verhaar, H.J.M., van Leeuwen C.J., Hermens J.L.M. (1992) Classifying environmental pollutants. 1. Structure activity relationships for prediction of aquatic toxicity, *Chemosphere* 25, 471-91.

Predicting the Acute Toxic Potential of Michael Acceptors for Mammalian

Yana Koleva
Department of Organic Chemistry, University "Prof. Assen Zlatarov", 1 Prof. Yakimov str., 8010 Bourgas, Bulgaria

***Abstract**: QSAR models based upon a narcosis mechanism represent baseline (minimum) toxicity which can be applied for defining excess toxicity of reactive chemicals and their interpreted in terms of Michael addition mechanistic domain. The aim of the researching was made an attempt to form mechanistic category for mammalian acute toxicity with regard to their excess toxicity based on baseline acute toxicity models for rat with routes of administration oral and an attempt to be applied quantitative and mechanistic read-across using an electrophilicity index (ω) for Michael acceptors. This study also demonstrates the utility of ω to make predictions of Michael acceptors of unsaturated aldehydes and ketones using a mechanism-based read-across model. The mechanism-based read-across is a powerful, transparent, mechanistically interpretable methodology suitable for risk assessors and regulators to make computational predictions as part of an intelligent testing strategy.*

***Keywords:** Michael acceptor, acute toxicity, mammalian*

1. INTRODUCTION

The use of QSAR in ecotoxicology is well established, and predictions can be made with sufficient accuracy for a number of endpoints and wide variety of chemicals. The situation in mammalian toxicology is rather different. There are a number of reasons for this, namely the wide variations in the quality and source of experimental data, in the organisms used, combined with a limited understanding of the biological mechanisms involved. Thus, although a considerable amount of data is available, the modelling can be problematic [3]. Often the problem is related to the different laboratories and different protocols used. Despite this, there have been numerous efforts for developing QSAR models for acute mammalian toxicity [2, 13].

Non-testing data can be provided by the following approaches: a) structure-activity relationships (SARs) and quantitative structure-activity relationships (QSARs), collectively called “(Q)SARs”; b) expert systems

incorporating (Q)SARs and/or expert rules; and c) grouping methods (categories and read-across). These approaches can be used to assess acute toxicity if they provide relevant and adequate data for the chemical of interest [14]. At the moment there is little information about the formal use of (Q)SARs in support of regulatory decisions related to acute toxicity. Read-across has been used to a limited extent, and on a case by case basis [10]. Nevertheless, the spirit of REACH for increased safety of chemicals by more comprehensive use of existing information and utilization of non-testing methods where possible is driving the development of reliable (Q)SAR models and grouping approaches.

The observation that in the field of mammalian toxicity the QSAR models are strictly limited to a well-defined class of chemicals is outlined in a number of studies [2, 7]. It is reasonable taking into account that a QSAR generally presumes identical modes of action of the compounds under the study. In contrast to the aquatic toxicity where often there is a predominance of non-specific effects and log P (octanol-water partition coefficient) is a sufficient predictor of the toxicity, the situation in mammalian toxicity is rather different and even small changes in chemical structure can result in different modes of toxic action [7].

Reactive electrophilic chemicals fall naturally into several mechanistic domains based on classic organic reaction chemistry. The major domains are Michael type acceptor, S_NAr, S_N1, S_N2, Schiff base formation, and acyl transfer [1]. Of these, Michael type addition is proving to be important in toxicity and is well-studied. The basic criteria for a compound to be a Michael type acceptor are summarized in Scheme 1.

Mechanistic domain **Protein binding reaction** **Modified protein**

Michael acceptors

Scheme 1: Michael type addition reaction and applicability domain

With regard to the activating group X on the double or triple bond in Scheme 1, the effectiveness (or strength of reaction) is related to the ability of the functional group to stabilize a positive charge on the carbon atom to which it is bound. Substituents on the α- and *β*-carbon atoms of the unsaturated chemicals can have a strong influence on Michael reactivity [1].

The aims of this study were to be defined possible mechanistic domain of chemicals to mammalian, to evidence excess toxicity of the possible reactive chemicals (Michael acceptors) through a baseline toxicity narcosis QSAR models for rat with routes of administration oral LD_{50} and to apply a

method for computational mechanistic read-across utilizing the ω parameters, having assessed its domain of applicability.

2. MATERIAL AND METHODS

Experimental details. For oral rat LD_{50} toxicity data were collected 9 unsaturated reactive chemicals (toxicity data are listed in Table 1) [6, 9]. The data were obtained from different labs, and with different strains of animals, hence, some uncertainty exists in the robustness of these values. The same factors will also contribute to the uncertainty in the read-across derived predictions of toxicity. All LD_{50} [Mg/Kg] values were converted into log ($1/LD_{50}$) [Mmol/kg] values.

Mechanistic domain of acute toxicity for mammalian. Nine chemicals for oral rat containing a polarized alkene and alkyne moiety were identified as potentially belonging to the Michael addition domain using the structural rules defined recently [1,8,12]. The chemicals studied are listed in Table 1.

Calculation of (baseline) minimum toxicity effect and excess toxicity. Compounds acting by a more specific mechanism than narcosis can be identified by comparing their toxicity with that predicted by a baseline narcosis equation, according to equation (1). Chemicals with TR values that are less than 2 may be considered as acting by a narcosis mechanism. By contrast, chemicals for which TR is greater than 2 are assumed to be acting by a more specific mechanism (Table 1) [8].

(1) $TR=LD_{50}pred/LD_{50}exp$

Baseline model (saturated alcohols and ketones) of Rat (oral) [8]:

(2) $\log(1/LD_{50}) = 0.805*\log P - 0.971*\log(0.0807*10^{\log P}+1) + 0,984$

$n = 54 \quad R^2 = 0.824 \quad s = 0.208 \quad F = 35.3$

Computational chemical calculations. All calculations on chemical structure were performed using the Gaussian03 package of programs utilizing the B3LYP/6-31G(d) level of theory [5]. The global electrophilicity parameter (ω) was then calculated for each optimized chemical as shown by eqs 3-5 [11].

(3) electrophilicity index $(\omega) = \mu^2 / 2\eta$

in which

(4) $\mu = (E_{HOMO} + E_{LUMO})/2$

(5) $\eta = E_{LUMO} - E_{HOMO}$

where E_{HOMO} and E_{LUMO} are the one-electron energies of the highest occupied and lowest unoccupied molecular orbitals respectively.

Read-across predictions. Read-across predictions for the chemicals in Table 1 were made using the following methodology [4].

3. RESULTS AND DISCUSSION

The chemicals as unsaturated aldehydes and ketones, which containing a polarized alkene or alkyne moiety (or their combination) were identified as potentially belonging to the Michael addition domain using the structural rules defined recently [1, 12]. Michael acceptors acting by more specific mechanisms and exhibit excess toxicity. Perhaps the largest class of chemicals showing excess toxicity are those that act by undergoing covalent binding to nucleophilic sites on one or more biological macromolecules and act as electrophile toxicants. Michael acceptors are covalent binding chemicals and are reactive for rat oral LD_{50} in Table 1.

The equation 2 for saturated monohydric alcohols and monoketones for oral rat LD_{50} was applied into Michael acceptors of Tables 1, which are reactive than narcosis mechanism. Their TR values can be seen in Table 1. The chemicals were defined in a mechanistic category according to TR – Michael addition. In general in this reactive category are chemicals with excess toxicity greater than 2 (TR > 2).

In this study, the electrophilic index (ω) was used to rank ‘excess’ chemicals in Michael mechanistic domain for rat oral LD_{50} based on their electrophilicity, with the rationale being that chemicals that have similar ω values should have approximately similar acute toxicity potential (Table 1).

Examination of the Michael acceptor chemicals in Table 1 for rat oral LD_{50} reveal that a relationship suitable for traditional QSAR development does not exist between log ($1/LD_{50}$) and ω (Fig. 1).

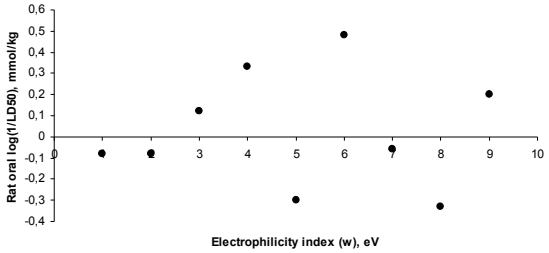

Fig. 1: Plot of log ($1/LD_{50}$) vs ω for rat.

Tab. 1. Structures of the chemicals for rat oral LD_{50} used in this study ranked by electrophilicity index (ω) and their prediction by read-across

CAS number	NAME	Structure	Exp Rat Oral LD_{50} [Mg/Kg]	TR	ω	Pred LD_{50} by ω
106-51-4	1,4-Benzoquinone	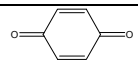	130	10.33	3.8937	NP
130-15-4	1,4-Naphthoquinone		190	38.96	2.9767	186.23
13061-80-8	4-Hexen-1-yn-3-one	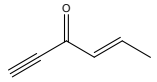	71	27.36	1.9747	60.46
107-02-8	2-Propenal	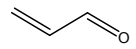	26	18.95	1.8433	29.91
78-85-3	2-Methyl-2-propenal	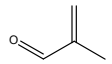	140	13.32	1.7061	141.18
78-94-4	3-Buten-2-one	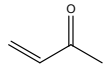	23.1	52.07	1.6605	39.88
123-73-9	2-Butenal, (E)-	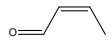	80	19.52	1.6578	87.73
814-78-8	3-Methyl-3-butene-2-one		180	15.63	1.5576	88.46
64011-46-7	4,5-Epoxy-2-pentenal	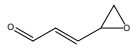	62	7.70	1.5227	NP

4. CONCLUSIONS

The read-cross method is a powerful, transparent, mechanistically interpretable methodology suitable for risk assessors and regulators to make computational predictions as part of an intelligent testing strategy. Importantly, the study has also demonstrated the ability of ω to be used, within carefully considered mechanistic applicability domains, to perform mechanism-based read-across to predict acute toxic LD_{50} values for mammalian.

5. REFERENCES

[1] Aptula, O.A. and Roberts, D.W. (2006) Mechanistic applicability domains for nonanimal-based prediction of toxicological endpoints: General principles and application to reactive toxicity, *Chem. Res. Toxicol.* 19*,* 1097-1105.

[2] Cronin, M.T., Dearden, J.C. (1995) QSAR in toxicology. 2. Prediction of acute mammalian toxicity and interspecies correlations, *Quant. Struct.-Act. Relat.* 14, 117-120.

[3] Cronin, M.T., Dearden, J.C., Walker, J.D., Worth, A.P. (2003) Quantitative Structure-Activity Relationships for human health effects: Commonalities with other endpoints, *Environ. Toxicol. Chem.* 22, 1829-1843.

[4] Enoch, S.J., Cronin, M.T.D., Schultz, T. W., Madden, J.C. (2008) Quantitative and mechanistic read across for predicting the skin sensitization potential of alkenes acting via Michael addition, *Chem. Res. Toxicol. 21,* 513–520.

[5] Frisch, M.J., Trucks, G.W., Schlegel, H.B., Scuseria, G.E., et al. *(2003) Gaussian03*, Revision B.04, Gaussian, Inc., Wallingford, CT.

[6] Guilian, W., Naibin, B. (1998) Structure-activity relationships for rat and mouse LD_{50} of miscellaneous alcohols, *Chemosphere* 35, 1475-1483.

[7] Jäckel, H., Klein W., (1991) Prediction of mammalian toxicity by Quantitative structure-activity relationships: Aliphatic amines and anilines, *Quant. Struct. Act. Relat.* 10, 198-204.

[8] Lipnick, R.L. (1991) Outliers-Their origin and use in the classification of molecular mechanisms of toxicity, **Science** *of the* **Total Environment** 109, 131–153.

[9] NIOSH/RTECS; website: http://chem.sis.nlm.nih.gov/chemidplus/

[10] OECD (2006). Report on the Regulatory Uses and Applications in OECD Member Countries of (Q)SAR Models in the Assessment of New and Existing Chemicals.

[11] Parr, R.G., Szentpaly, L.V., and Liu, S. (1999) Electrophilicity index, *J. Am. Chem. Soc.* 121, 1922-1924.

[12] Schultz, T.W., Yarbrough, J.W., Hunter, R.S., and Aptula, A. O. (2007) Verification of the structural alerts for Michael acceptors, *Chem.Res. Toxicol. 20*, 1359–1363.

[13] Tsakovska, I., Netzeva, T., Worth, A. (2006) Review of (Q)SARs for Mammalian Toxicity, JRC report EUR 22486 EN, Ispra, Italy, European Commission, Joint Research Centre.

[14] Worth, A.P., Bassan, A., Gallegos, A., Netzeva, T. I., Patlewicz, G., Pavan, M., Tsakovska, I., Vracko M. (2005) The Characterisation of (Quantitative) Structure-Activity Relationships: Preliminary Guidance, JRC report EUR 21866 EN, European Chemicals Bureau, Joint Research Centre, European Commission, Ispra, Italy.

Sn(II)-ion-selective electrode based on chalcogenide glasses

Lilia Aljihmani, Venceslav Vassilev
Department of Non-Ferrous Metals and Semiconductors Technology, University of Chemical Technology and Metallurgy, 8 Kliment Ohridski blvd., 1756 Sofia, Bulgaria e-mail: venciv@uctm.edu

***Abstract**: Sn(II)-ion-selective-electrodes (Sn(II)-ISE) were created on the base of new chalcogenide glasses from the As_2Se_3-Ag_4Sse-SnTe system. (Sn(II)-ISE) include composite membranes and a construction from the coated wire-type. The basic analytical characteristics of ISE: linear range, slope of the electrode function, working pH-range, limits of detection, results reproduction and response time were studied. The influence of some mono-charged and double-charged interfering ions on the response of Sn(II)-ISE is investigated. A mechanism, which explains the studied dependencies, is proposed.*

***Keywords:** ion-selective-electrode, chalcogenide glasses, glassy electrode.*

1. INTRODUCTION

Trachtenberg and co-workers [1,2] applied chalcogenide glasses (ChG) as ion-selective electrochemical sensors. Recently, many glassy sensors for detection of Ag^+ [3], Cu^{2+} [4], Pb^{2+} [5], Cd^{2+} [6], Fe^{3+} [7], Zn^{2+} [8] and other ions have been developed. ChG are widely spread in application as membrane material of ISE [9].

The aims of this paper are creation of solid-state Sn(II)-ions on the base of ChG of As_2Se_3-Ag_4SSe-SnTe system [10] and investigation of their analytical characteristics.

2. EXPERIMENTAL

Two types of ion-selective electrodes (ISEs) were constructed: a coated wire-type (type A) and a liquid membrane-based type (type B). For this purpose the active component (ChG) was introduced to an inert polymeric matrix (epoxy resin) at a concentration of 1 mass%. The compositions of the used ChG were indicated with numbers in the glass-forming region of the system As_2Se_3-Ag_4SSe-SnTe (Fig. 1). The inner com-parative electrode

was made the following way: a Ag-wire (∅=1 mm) was cleaned with a 10 % HNO_3 solution, then it was immersed in a 0,5 M $FeCl_3$ solution for 24 hours (the surface got covered with a thick AgCl layer).

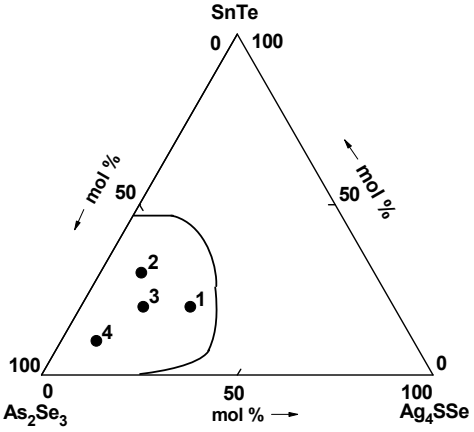

Fig. 1. Glass-forming region in the As_2Se_3-Ag_4SSe-SnTe system [12].

1. Coated wire-type ISEs - the composyte (ChG+epoxy resin) is laid as a thick layer on the Ag/AgCl-electrode surface.

2. Liqiud membrane-type ISEs – the composite was moulded in cylindrical form (∅=6 mm, h=3-4 mm). By means of grinding and polishing h is reduced to ≈2 mm. The ISEs body was made of a small quartz pipe.

Potentiometrical measurements are carried out with cells with inner solution or with direct contact. The standard calibration solutions were obtained from an initial solution (1M $SnCl_2$). The electrode potential was measured during a constant dilution of the solutions with velocity 200 rev min^{-1}. The ISEs conditioning was made in a 10^{-3} M solution of the potential-determi-ning (pd) ion. The pH effect on the electrode function was studied in solutions with constant concentration of Sn(II)-ion (10^{-1}, 10^{-2} and 10^{-3} mol l^{-1}) as concentrated HCl was added thereto or a 25 % NH_3 solution. The response time and the limits of detection were determined in solutions with concentration of Zn(II)-ions from 10^{-4} to 10^{-1} M.

3. RESULTS AND DISCUSSION

3.1. Stability, Linearity and Slope of the Electrode Function. Limits of detection

As an evaluation criterion for the ISEs function, the following analytical characteristics were used: slope (S) and length (L) of the linear range of the calibration function, limits of detection (LD), response time (τ) and working pH-range.

From the initial measurements made it was established that ISE-A.3 (A.4, B.3 and B.4) do not respond. No equilibrium potential was established with these ISEs both prior to and after their conditioning and that is why further work with them was stopped.

In the case of ISEs – p. 2 (fig. 1) we received a stable response only with the A-type. The ISE-A.2 potential prior to conditioning is negative and 30 min after conditioning is positive as the slope of the linear range is close to the theoretical one of Sn(II)-ions.

ISEs with ChG-based membranes corresponding to p. 1 gave a promising response.

The time necessary for establishing the equilibrium electrode potential is approximately 2 min. The conditioning for 15 min stabilized and improved the parameters of the electrode function of ISE-A.1 (A.2 and B.1).

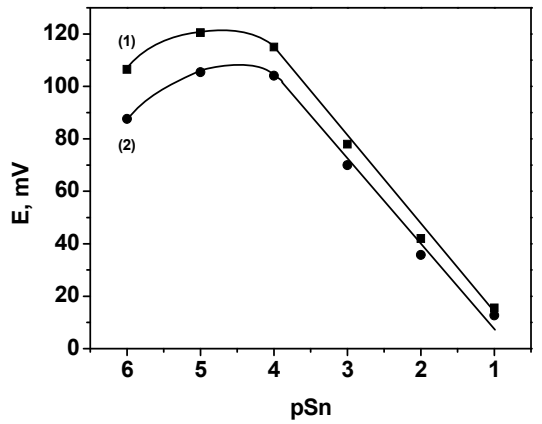

Fig. 2. Calibration functions of ISE-A.1;1 – 15-min conditioned; 2 – non-conditioned.

The results of measuring S, L and LD after the initial measu-rements of the conditioned electrodes were summarized in Table 1.

Tab. 1. Analytical characteristics of the studied Sn(II)-ISE.

Type of ISE	Composition of ChG in the membrane, mol %	S, mV dec^{-1}	L, mol l^{-1}	LD, mol l^{-1}
ISE-A.1.	$(As_2Se_3)_{52}(Ag_4SSe)_{28}(SnTe)_{20}$	28,4	$10^{-4} \div 10^{-1}$	$7{,}1.10^{-5}$
ISE-B.1.	$(As_2Se_3)_{52}(Ag_4SSe)_{28}(SnTe)_{20}$	38,8	$10^{-4} \div 10^{-1}$	$7{,}9.10^{-5}$
ISE-A.2.	$(As2Se3)_{59,5}(Ag4SSe)_{10.5}(SnTe)_{30}$	30,2	$10^{-4} \div 10^{-1}$	$6{,}5.10^{-5}$

The slope of the electrode function S of ISE-A.1 (B.1 and A.2) is 29,58 mV dec^{-1}. S changes within the range from 28,4 to 38,8 mV dec^{-1}. Tests were carried out on the same ISE after 60 days since their production (Table 2).

Tab. 2. Test results of ISE after 60 days since their production.

	ISE-A.1		ISE-B.1		ISE-A.2	
	1st day	60th day	1st day	60th day	1st day	60th day
L,mol l^{-1}	10^{-4} ÷ 10^{-1}	10^{-4} ÷ 10^{-1}	10^{-4} ÷ 10^{-1}	10^{-4} ÷ 10^{-1}	10^{-4} ÷ 10^{-1}	10^{-4} ÷ 10^{-1}
S, mV dec^{-1}	28,4	28,3	38,8	36,7	30,2	33,8
LD, mol l^{-1}	$7{,}6.10^{-5}$	$7{,}3.10^{-5}$	$7{,}8.10^{-5}$	$7{,}5.10^{-5}$	$6{,}3.10^{-5}$	$6{,}8.10^{-5}$

These data (tab. 2) show that ChG of the system As_2Se_3-Ag_4SSe-SnTe, on the basis of which Sn(II)-ISEs were developed, are an appropriate membrane material.

3.2. pH effect on the Electrode Function

The exact pH value of the solutions was determined through measurement in an electrochemical cell. A glass electrode was used as an indicating electrode. It was discovered that the working pH-range for the studied Sn(II)-ISEs is at pH<2. At pH=2 a sediment of $Sn(OH)_2$ is formed.

3.3. Response Time (τ_{95})

We measured ISEs at pH=1 in solutions within the concentration range from 10^{-1} to 10^{-6} mol l^{-1} $SnCl_2$. The ChG composition did not have a significant effect on τ_{95}, i.e. with ISE-A.1 (A.2 and B.1) the exchange reaction of Sn(II)-ions between the membrane and the analyzed solution runs with the same velocity. Sn(II)-ISEs showed relatively quick response (τ_{95}≤150 s).

3.4. Selectivity Coefficients ($K_{i,j}^{pot}$)

It was studied the impeding effect of monocharged (Cl^-, NO_3^- and CH_3COO^-), and bicharged (Zn^{2+}, Cd^{2+} and Pb^{2+}) ions on the response of ISE-A.2 in the presence of Sn(II)-ions (Table 3).

Tab. 3. Values of selectivity coefficients (* Concentration of the impeding ion).

ISE-A.2	$K^{Pot}_{Sn,K}$	$K^{Pot}_{Sn,Zn}$	$K^{Pot}_{Sn,Cd}$	$K^{Pot}_{Sn,Pb}$	K^{Pot}_{Sn,NO_3}	$K^{Pot}_{Sn,Cl}$	K^{Pot}_{Sn,CH_3COO}
10^{-3} mol l^{-1}*	$6{,}7.10^{-2}$	$4{,}9.10^{-2}$	1.10^{-3}	$6{,}3.10^{-2}$	$4{,}9.10^{-11}$	$1{,}0.10^{-12}$	$6{,}3.10^{-11}$

4. CONCLUSIONS

(i) Coated wire-type Sn(II)-ISE with membranes (a plate type with liquid relation) were developed on the base of a chalcogenide glass from the As_2Se_3-Ag_4SSe-SnTe system. The suggested construction and technology of Sn(II)-ISE guarantee a high reproducibility of the analytical characteristics as well as a very good selectivity about the ions: Cl^-, NO_3^-, CH_3COO^-, Zn^{2+}, Cd^{2+} and Pb^{2+}.

(ii) The Sn(II)-ion-selective membrane does not exhibit indication of aging due to negative processes, such as crystallization, oxidation or reduction of the chalcogenide glass, polymer destruction and others.

5. REFERENCES

[1] Baker, C. T., Trachtenberg, I. (1971) J. Electrochem. Soc. 118, 571-576.
[2] Jasinski, K., Trachtenberg, I. (1972) Anal. Chem. 44, 2373-2376.
[3] Vlassov, Yu. G., Bychkov, E. A., Seleznev, B. L. (1990) Sens. Actuators B 2, 23-26.
[4] Vlassov, Yu. G., Bychkov, E. A., Medvedev, A., (1986) Anal. Chim. 185, 137-158
[5] Vlassov, Yu. G., Bachkov, E. A., Legin, A. V. (1985) J. Anal. Chimii. 40, 10, 1839-1941 (in Russian).
[6] Zhukov, A. F., Vishniakov, A. V., Harif, Ia. L., Urusov, Iu. I., Bolinets, F. K., Rizhikov, E. I., Gordievskii, A. V. (1975) J. Analit. Chimii 30, 9, 1761-1763 (in Russian).
[7] Koenig, C.E., Grabner, E. W. (1995) Electroanalysis 7, 11, 1090-1094.
[8] Vassilev, V. S., Hadjinikolova, S. H., Boycheva, S. V. (2005) Sensors and Actuators B 106, 401-406.
[9] Vassilev, V. S., Boycheva, S. V. (2005) Talanta 67, 1, 20-27.
[10] Aljihmani, L., Vassilev, V., Petkov, P. (2003) J. Optoelectr. and Adv. Materials 5, 5, 1187-1192.

Crystallization of chalcogenide glasses from the $GeSe_2$-Sb_2Se_3-PbTe system

Temenuga Hristova-Vasileva, Venceslav Vassilev, Mira Radonova

Department of Non-Ferrous Metals and Semiconductors Technology, University of Chemical Technology and Metallurgy, 8 Kliment Ohridski blvd., 1756 Sofia, Bulgaria e-mail: venciv@uctm.edu

***Abstract**: The crystallization temperatures of chalcogenide glasses from the $GeSe_2$-Sb_2Se_3-PbTe system at heating rates of 10, 15, 25 and 35 K/min were determined using differential thermal analysis. Al_2O_3 and Se were used as reference substances. The activation energy of crystallization was calculated by the Kissinger and the Augis & Bennett models. The values, obtained by the two independent models, coincide. A correlation between them and the glasses' composition is established.*

***Keywords:** chalcogenide glasses, crystallization, activation energy.*

1. INTRODUCTION

The chalcogenide glasses are useful medium for information storage, as material for optical windows in the IR part of the spectrum, for functional elements in the integrated micro-, nano- and optoelectronics, etc. From the point of view on the practical application of the chalcogenide glasses, it is important to know both their physicochemical characteristics and their steadiness, crystallization ability, in particular the kind and the number of the crystallized phases, as well as their crystallization energy.

As a rule, two methods are used for studying of the crystallization kinetics: isothermal and non-isothermal [1]. In the first case the sample is subjected to thermal treatment at $T \approx T_{cr}$ for a short time and the physicochemical properties are revealed as a function of time. In the second method the sample is heated with constant rate up to the crystallization temperature and the investigated properties are measured as a function of the temperature.

The crystallization kinetics is subject of many investigations [2-9]. Different methods are used for its study (DSC or DTA), which are based on investigation of the exothermal peaks obtained during heating.

The glassforming region in the $GeSe_2$-Sb_2Se_3-PbTe system was investigated in our previous work [10]. It lies partially on the $GeSe_2$-Sb_2Se_3 (0-70 mol % Sb_2Se_3) and $GeSe_2$-PbTe (15.0-57.5 mol % PbTe) sides of the

Gibbs' concentration triangle – Fig. 1. No glasses were obtained in the Sb_2Se_3-PbTe system.

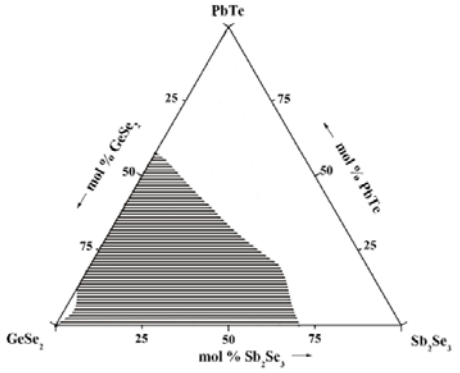

Fig. 1. Region of glassformation in the $GeSe_2$-Sb_2Se_3-PbTe system.

The aim of the present work is to determine the crystallization temperatures of chalcogenide glasses from the $GeSe_2$-Sb_2Se_3- PbTe system at different heating rates and their activation energy of crystallization, as a main parameter characterizing this process.

2. EXPERIMENTAL

The initial compounds ($GeSe_2$, Sb_2Se_3 and PbTe), as well as the glassy phases from the $GeSe_2$-Sb_2Se_3-PbTe system, are obtained by direct monotemperature synthesis in evacuated (up to residual pressure of 1.10^{-3} Pa) and sealed quartz tubes. For this purpose are used: Ge and Se with purity of 5N, as well as Sb and Pb with purity of 4N. The materials are sintered in crucible furnace with vibration device for homogenization of the melt.

The samples from the $GeSe_2$-Sb_2Se_3-PbTe system are obtained using the following time-temperature line: increase of the temperature up to 500, 800 and 950 °C and isothermal steps at these temperatures of 0.5, 0.5 and 2.0 h, respectively. During the final step a vibration stirring of the melt is performed. Then the melt is tempered at 800 °C (0.5 h) and quenched in a water + ice mixture. The obtained glassy samples are with black color and shiny surface with well expresses shell-like crack.

DTA apparatus from the F. Paulik - J. Paulik - L. Erdey, which guarantees measurement accuracy of ± 5 °C, was used for determination of the thermal characteristics. As reference substances Al_2O_3 (preliminary tempered at 1000 °C) and Se (with known thermodynamic crystallization parameters) were used. The investigated compositions, powdered to grain size of 63-

125 μm, and the reference materials were put in quartz Stepanov's vessels, which were vacuumed and sealed under residual pressure of 1.33×10^{-2} Pa.

Two independent models, based on DTA data, were used for determination of the activation energy of crystallization (E_a):

1. The Kissinger (K) model [11]:

$$\ln\frac{b}{T_{cr}^2} = -\frac{E_a}{RT_{cr}} + \text{const}, \quad (1)$$

where b - heating rate, T_{cr} - crystallization temperature.

2. The Augis and Bennett (A&B) model [12]:

$$\ln\frac{b}{T_{cr} - T_o} = -\frac{E_a}{RT_{cr}} + \text{const}, \quad (2)$$

where T_o is the initial temperature in the DTA furnace (T_o = 298 K).

3. RESULTS AND DISCUSSION

For determination of the crystallization activation energy, data about the characteristic temperatures at different heating rates is required. At this investigation the crystallization temperatures are measured at heating rates of 10, 15, 25 and 35 K/min. The results are presented in Table 1.

The values of the activation energy E_a of the crystallization process of glasses from the $GeSe_2$-Sb_2Se_3-PbTe system, determined by the Kissinger and the Augis & Bennett models, are very close - Table 1.

For convenience during the analysis of the composition-property dependencies the z and m coefficients are included. z is the molar content of the third component in the glasses (in this case this is PbTe) and m = y/(x+y) renders an account on the ratio between the other two components (in this case m = Sb_2Se_3/($GeSe_2$+Sb_2Se_3)).

The activation energies, calculated by the Kissinger and the Augis & Bennett, coincide in the accuracy limits (Table 1). Strong impression makes the fact, that the activation energy of the crystallization process depends weakly on the glasses’ composition and the deviation does not exceed ± 15 % (Fig. 2). The dependence E_a(m) has linear path and is described by the equation y=-27.9x+453.5 (at $0.1 \leq m \leq 0.65$). This trend of the E_a(m) dependence shows that one and the same phase crystallizes, which most probably corresponds to Sb_2Se_3.

From the application point of view this dependence widens the possibilities for usage of the glasses from this system without taking into account their composition. Furthermore, the fact that only one phase crystallizes determines one of the real applications of these materials as information storage media, based on the phase transition glass-crystal-glass.

Tab. 1. Composition, crystallization temperatures and activation energy of glasses from the $GeSe_2$-Sb_2Se_3-PbTe system.

№	Composition	T, K	m	E_a (K) kJ/mol	E_a (A&B) kJ/mol
1	$(GeSe_2)_{81}(Sb_2Se_3)_9(PbTe)_{10}$	660 664 667 670	0.1	661	507
2	$(GeSe_2)_{72}(Sb_2Se_3)_{18}(PbTe)_{10}$	655 659 662 666	0.2	416	416
3	$(GeSe_2)_{54}(Sb_2Se_3)_{36}(PbTe)_{10}$	645 649 653 656	0.4	395	396
4	$(GeSe_2)_{36}(Sb_2Se_3)_{54}(PbTe)_{10}$	617 620 624 625	0.6	466	466
5	$(GeSe_2)_{31.5}(Sb_2Se_3)_{58.5}(PbTe)_{10}$	615 618 621 625	0.65	400	400
6	$(GeSe_2)_{63}(Sb_2Se_3)_7(PbTe)_{30}$	619 620 624 628	0.1	361	412
7	$(GeSe_2)_{56}(Sb_2Se_3)_{14}(PbTe)_{30}$	612 616 618 621	0.2	447	447
8	$(GeSe_2)_{42}(Sb_2Se_3)_{28}(PbTe)_{30}$	590 592 593 597	0.4	509	509
9	$(GeSe_2)_{48}(Sb_2Se_3)_{12}(PbTe)_{40}$	589 592 595 598	0.2	406	406
10	$(GeSe_2)_{45}(Sb_2Se_3)_5(PbTe)_{50}$	603 606 609 611	0.1	472	472

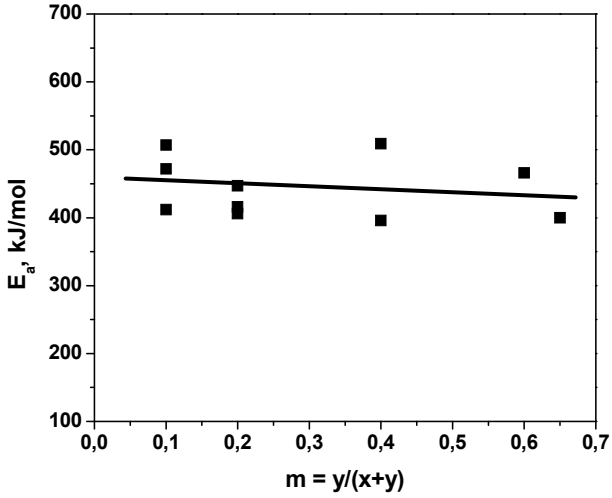

Fig. 2. Compositional dependence of the activation energy of crystallization.

4. CONCLUSIONS

The crystallization temperatures of chalcogenide glasses from the $GeSe_2$-Sb_2Se_3-PbTe system are determined at heating rates of 10, 15, 25 and 35 K/min. They vary between 589 and 670 K. The activation energies of this process, determined by two independent models, coincide. The E_a values change between 361 and 661 kJ/mol. A correlation between the investigated properties and the glasses' composition is established.

5. ACKNOWLEDGEMENTS

The authors express their gratitude to the Ministry of Youth, Education and Science – Bulgaria ("Scientific investigations" Fund – contract DO 02-123/15.12.2008) for the financial support of this study.

6. REFERENCES

[1] Mehta, N., Zulfequar, M., Kumar, A. (2004) J. Optoel. Adv. Mat. 6, 2, 441.
[2] Satyam, S., Krishnan, K. (2004) Physica B. 348, 1-4, 310.
[3] Wakkad, M. M. (2001) J. Therm. Anal. Cal. 63, 533.

[4] Abdel-Rahim, M. N., Abdel-Latif, A. Y., Soltan, A. S. (2000) Physica B 291, 41.
[5] Málek, J. (2000) Thermochim. Acta, 355, 1-2, 239.
[6] Abu El-Oyoun, M. (2000) J. Phys. Chem. Solids 61, 10, 1653.
[7] Málek, J. (1999) J. Therm. Anal. Cal. 56, 763.
[8] Pamukchieva, V., Savova, E., Baeva, M. (1998) Phys. Chem. Glasses 39, 6, 328.
[9] Abu El-Oyoun, M. (2000) J. Phys. D: Appl. Phys 33, 2211.
[10] Vassilev, V., Radonova, M., Boycheva, S., Fidancevska, E. glass formation in the multicomponent chalcogenide $GeSe_2$-Sb_2Se_3-PbTe system, J. Optoel. Adv. Mat., in press, accepted for publication.
[11] Kissinger, H.E. (1957) Anal. Chem. 29, 1702.
[12] Augis, J.A., Bennett, J.E. (1978) J. Thermal Anal. 13, 283.

Comparison of sodium borohydride hydrolysis kinetics on Co-based nanocomposite catalysts

Georgi Hristov[1], Elitsa Chorbadzhiyska[1], Rashko Rashkov[2], Yolina Hubenova[3], Mario Mitov[1]

[1]Department of Chemistry, South-West University, Blagoevgrad, Bulgaria
[2]Insitute of Physicochemistry – Bulgarian Academy of Sciences, Sofia, Bulgaria
[3]Department of Biochemistry and Microbiology, Plovdiv University, Bulgaria

***Abstract**: In this study, we compared the results, obtained with several Co-based nanocomposites (CoMnB, CoNiMnB and CoNiMoW) produced by electrodeposition on Ni-foam, as catalysts for the sodium borohydride hydrolysis reaction. Based on the comparative analyses, we propose CoNiMnB electrodeposits as most proper catalysts for development of Hydrogen-on-Demand (HOD) system, while CoNiMoW ones as potential anodes for Direct Borohydride Fuel Cells (DBFCs).*

***Keywords:** Hydrogen-on-Demand (HOD), Nanocomposites, Hydrolysis, Catalyst, Kinetic.*

1. INTRODUCTION

The prospect of peaking world-wide oil production has motivated the development of alternative energy sources and energy carriers. Hydrogen has been claimed as a likely replacement energy carrier and renewable energy source [1]. A hydrogen energy economy would be less dependent on limited fossil fuel supplies. Nevertheless, many critical technical challenges remain to be addressed before hydrogen-based energy can become widely available and economical [2]. The main problems of using hydrogen as a fuel are connected with its storage and transportation [3]. Two promising hydrogen storage material categories are metal hydrides and chemical hydrides, both of which rely on catalysis to improve kinetics. Chemical hydride systems always involve reactions between the storage medium and a solvent, in most cases water. The reaction can be catalyzed by solid catalysts. At room temperature, the reaction between sodium borohydride and water is very slow [1]. For sodium borohydride systems, the chemical hydride is dissolved in alkaline solution. A pH level of 14 is the most likely for practical applications involving stabilized solutions [4].

Ruthenium and rhodium salts showed the best catalytic activity. Chloride salts of manganese, iron, cobalt, nickel and copper were also exhibited good catalytic properties for hydrolysis of sodium borohydride to

produce hydrogen gas at room temperature [5,6]. Although these homogeneous catalysts are active, the metal ions dissolved in aqueous solution cause serious contamination concerns for discharged fuel recycling or disposal. In this regard, heterogeneous catalysts offer distinct advantages of ease separation of catalyst from discharge fuel and for controllable generation and delivery of hydrogen on demand [4]. Cobalt and nickel metals, and also metal oxide supported Pt, Pd, Rh, Ru, Ir, Os, Au, Ag catalysts were reported to be active for catalytic hydrolysis of sodium borohydride in an aqueous alkaline solution at near room temperature conditions [7].

In the present study, three different types of newly synthesized Co-based nanocomposites: CoMnB, CoNiMnB and CoNiMoW, produced by electrodeposition on nickel foam, were investigated as potential catalysts for borohydride hydrolysis reaction. The hydrogen generation rates and activation energy values, obtained with the examined nanocomposite materials, were compared and discussed.

2. EXPERIMENTAL

Composite CoMnB coatings were obtained by potentiostatic electrodeposition from electrolyte, containing 5 g/l Co^{2+}, 5 g/l Mn^{2+}, 5 g/l Ni^{2+} and 35 g/l boric acid. The CoNiMnB nanocomposites were obtained from similar electrolyte, but with different amounts of Co^{2+} and Ni^{2+}. The electrolysis continued 30 min at 40 ^{o}C. Co-electrode was used as an anode and Ni-foam (RECEMAT, RCM-Ni-4753.016 pore diameter d=0.4 mm, SSA=5800m^2/m^3 and RCM-Ni-2733.03, pore diameter d=0.6 mm, SSA=2500m^2/m^3) as a cathode.

Composite CoNiMoW coatings were obtained by galvanostatic electrodeposition from alkaline electrolyte, containing 72g/l sodium citrate, 24g/l $Na_2WO_4.2H_2O$, 6g/l Na_2MoO_4, 16g/l $Ni(SO_3NH_2)_2$, 16g/l $Co(SO_3NH_2)_2$. pH 10 was fixed by addition of NH_4OH. The composites were electrodeposited on nickel foam under different galvanostatic regimes (1A, 2A, 3A, 4.8A) for 30 min and electrolyte stirring at 250 min^{-1}.

Varying the electrolysis conditions nanocomposites with different content, structure and morphology have been produced. Scanning electron microscopy (SEM) using Leo 1455VP and Leo Supra 55VP microscopes with Energy dispersion X-ray (EDX, Oxford Inca 200 instrument, Software INCA-Vers.4) was applied for examination of the surface morphology and elemental analysis of the electrodeposited coatings. XRD spectra for structure identification of layers was recorded in the angle interval 10–100° (2θ) by using Philips PW 1050 diffractometer, equipped with Cu Kα tube and scintillation detector.

The catalytic properties of the investigated nanocomposites towards the borohydride hydrolysis were also studied. The examined sample was placed into a reaction vessel, which was then hermetically closed. 10 ml of 5% (w/v) $NaBH_4$/6M KOH solution was injected in the vessel and the volume of the generated hydrogen was measured with time by means of water-displacement method [8]. The reaction temperature was kept constant by thermostat in the range from 15 ^oC to 45 ^oC. The rate constants at different temperatures were estimated from the slopes of the obtained kinetic curves and the activation energy was calculated from constructed Arrhenius plots.

3. RESULTS AND DISSCUSION

3.1. SEM investigation of the Co-based electrodeposits

SEM images of the investigated nanocomposites are shown on Fig. 1. All of the three types of the Co-based electrodeposits have a dendrite structure. The bright spots on the SEM image were mainly Co.

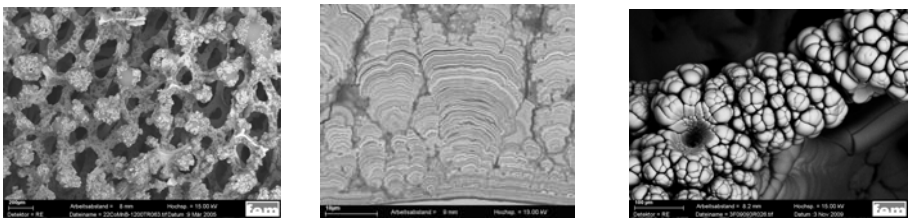

CoMnB CoNiMnB CoNiMoW

Fig. 1: SEM images of the CoMnB, CoNiMnB, CoNiMoW nanocomposites.

Detailed SEM investigations proved that there was different elemental distribution on the Ni-foam surface. For example, significant amount of Co (70%) was found in the center than on the edge of the electrode (50%). Also the amount of Co enriched, but that of Ni decreased with increasing the current applied under galvanostatic deposition regimes.

3.2. Catalytic hydrolysis of sodium borohydride

A gaseous bubbling started immediately after immersion of investigated sample (CoMnB, CoNiMnB or CoNiMoW) into sodium borohydride solution, which proved that the examined materials catalyzes the sodium borohydride hydrolysis process [9]:

(1) $$NaBH_4 + 2H_2O \rightarrow NaBO_2 + 4H_2$$

The hydrolysis followed an apparent zero order kinetics with all studied materials. The estimated from kinetic curves rate constants and activation energy values, obtained with the examined nanocomposite materials, are presented in Table 1.

Two types of Ni-foam with different pore diameter were used as a pad for the CoMnB deposits. The hydrogen generation rate was about 4 times higher on the nanocomposites, electrodeposited on Ni-foam with bigger pore diameter. That can be explained with better mass transfer through the catalysts pores and easy diffusion of the reagents and the obtained products. That is why all of the other nanocomposites were electrodeposited on the Ni-foam pad with bigger pores.

Two types CoNiMnB electrodeposits were prepared under potentiostatic conditions (-1.5V and -1.8V) and the samples were also investigated as catalysts for the sodium borohydride hydrolysis. For the both types of CoNiMnB electrodeposits, the examined hydrogen generation rates and the calculated activation energy were the same in practice, which indicated that the potential regime did not exert any influence on the catalytic properties of these nanocomposites.

Four types CoNiMoW electrodeposits were prepared under galvanostatic conditions (1.0A, 2.0A, 3.0A and 4.8A). The bigger current in the galvanostatic regime applied, the less catalytic activity showed the examined CoNiMoW nanocomposite. The best catalyst for the sodium borohydride reaction was the CoNiMoW electrodeposit, produced under 1.0A galvanostatic regime.

All of the examined nanocomposites exhibited lower activation energy than Ru (56,0 kJ/mol), which is known as one of the best catalysts for sodium borohydride hydrolysis process [9]. Including Ni in the nanocomposite increased sufficiently the activity of the catalyst. Comparing the results from the Ni-foam as a catalyst with those obtained with CoMnB and CoNiMnB, we can purposed that the size of the composite is in a correlation with the activity – the smaller composite, the higher activity.

Table 1: The hydrogen generation rate using different Co-based catalysts, ml/s.

Temperature, °C / Sample	**15**	**25**	**30**	**40**	**E_a, kJ/mol**
CoMnB small pores	0,06	0,16	0,21	0,28	54,5

CoMnB big pores	0,37	0,68	0,80	1,34	54,9
CoNiMnB -1,5V	0,86	1,24	1,50	2,20	35,7
CoNiMnB -1,8V	0,90	1,30	1,47	2,12	36,9
CoNiMoW 1,0A	0,06	0,08	0,12	0,25	37,8
CoNiMoW 2,0A	0,04	0,05	0,07	0,12	33,8
CoNiMoW 3,0A	0,02	0,03	0,05	0,09	38,9
CoNiMoW 4,8A	0,02	0,02	0,04	0,07	35,6

Although the calculated activation energy for the sodium borohydride reaction catalyzed by CoNiMoW had the lowest value, the hydrogen was generated with the slowest rate, which indicated that there were other factors that limited the reaction, for example, diffusion. Additional experiments are needed to prove such hypotheses.

4. CONCLUSIONS

The catalytic properties of three different types newly synthesized Co-based nanocomposites towards sodium borohydride hydrolysis reaction were studied. The obtained order of descending catalytic activity is CoNiMnB>CoMnB>CoNiMoW. The best catalyst among the examined nanocomposites is CoNiMnB (1.8 V) with 1.3 ml/s generated hydrogen (at 25 ^{o}C). Besides the elemental composition, the catalytic activity of the investigated nanocomposites also depends on the applied deposition regime as well as pore size of Ni-foam used as a support. The galvanostatic regime used influences more significantly the catalytic properties of the examined materials, while those obtained under potentiostatic regime exhibit almost the same activity. The bigger pore sized Ni-foam improves the catalytic activity of investigated electrodeposits, probably due to facilitated mass transport of reagents and products through the catalysts. Based on the comparison of results, we consider that CoNiMnB nanocomposites can be used in newly designed Hydrogen-on-Demand generators, while CoNiMoW electrodeposits, exhibited the lowest catalytic activity towards sodium borohydride hydrolysis, can be potentially applied as anodes in Direct Borohydride Fuel Cells.

5. REFERENCES

[1] Zhang, J., Delgass, W., Fisher, T., Gore J. (2007) Kinetics of Ru-catalyzed sodium borohydride hydrolysis, *Journal of Power Sources* 164, 772–781

[2] U.S. Department of Energy, Office of Basic Energy Sciences, Basic research needs for the hydrogen economy, report available at: http://www.sc.doe.gov/bes/hydrogen.pdf, 2003.
[3] Ross, D. (2006) Hydrogen storage: The major technological barrier to the development of hydrogen fuel cell cars, Vacuum, 80(10), 1084-1089.
[4] Zhang, Q., Smith, G., Wu, Y., Mohring, R. (2006) Catalytic hydrolysis of sodium borohydride in an auto-thermal fixed-bed reactor, *International Journal of Hydrogen Energy* 31, 961 – 965
[5] Schlesinger, H., Brown, H., Finholt, A., Gilbreath, J., Hoekstra, H., Hyde, E. (1953) Sodium borohydride: hydrolysis and its generation of hydrogen. *J Am Chem Soc*;75, 215–9.
[6] Amendola, S., Kelly, M., Wu, Y. (2003) Process for synthesizing borohydride compounds. *US Patent* 6,524,542
[7] Kojima, Y., Suzuki, K., Fukumoto, K., Sasaki, M., Yamamoto, T., Kawai, Y., Hayashi, H. (2002) Hydrogen generation using sodium borohydride solution and metal catalyst coated on metal oxide, *Int J Hydrogen Energy* 27,1029–34
[8] Mitov, M., Hristov, G., Hristova, E., Rashkov, R., Arnaudova, M., Zielonka, A. (2009) Complex performance of novel CoNiMnB electrodeposits in alkaline borohydride solutions. *Environm Chem Lett* 7 (2),167-173
[9] Jeong, S., Kim, R., Cho, E., Kim, H., Nam, S., Oh, I., Hong, S., Kim, S. (2005) A study on hydrogen generation from NaBH4 solution using the high-performance Co-B catalyst. *J Power Sources* 144(1),129-134

Electrochemical modification of graphite with Prussian Blue - characterisation and electroanalytical application

Dochko Dochev, Jivko Denchev, Nina Dimcheva
Faculty of Chemistry, Plovdiv University, 24, Tsar Assen st.; BG-4000 Plovdiv, Bulgaria

Abstract: *An optimised procedure for electrochemical deposition of iron III hexacyano-ferrate (Prussian blue) and its stabilisation on the surface was elaborated. Catalytic activity towards the electroreduction of hydrogen peroxide at pH 5,5 and working potentials around zero mV was examined both under static conditions and in flow-injection mode. Further stabilisation of the electrodeposits was achieved through coverage of the electrocatalyst with a thin polymeric film cast from 1% solution of the fluorine-sulphate ionomer Nafion™. The results suggest that the electrocatalyst retains high catalytic activity for more than a month and therefore has a prospective application as peroxide sensor in acidic and neutral media.*

Introduction

Prussian blue, $Fe_4[Fe(CN)_6]_3 .nH_2O$ is a classical mixed valence compound [1]. There are two proposed formulae of Prussian Blue (PB) that have been called “insoluble PB” $Fe^{III}_4[Fe^{II}(CN)_6]_3$ and “soluble PB” $KFe^{III}Fe^{II}(CN)_6$ [2,3]. It is believed that the degree of hydration affects the conducting properties of these compounds. If deposited onto the electrode surface the insoluble form of PB can be oxidized to Prussian Green as well as reduced to Prussian White at approximately +0.7 V and -0.1 V vs. SCE, respectively. The reduced form of PB (Prussian White) has a catalytic activity for the reduction of molecular oxygen and of hydrogen peroxide in aqueous acidic electrolytes and can act as an electrocatalyst for hydrogen peroxide electroreduction present in solution or formed in the course of an enzymatic reaction [4,5]. Since this electrocatalytic process proceeds at a low electrode potential (ca. -0.1 V vs. SCE), it is possible to eliminate the effect of interfering species and hence to develop a selective and sensitive hydrogen peroxide sensor working at a low operational potential [5,6]. In this connection, the electrochemical deposition of PB film has been studied over diverse electrode materials such as carbon paste [4], Pt [5] and

glassy carbon [6]. Under sertain deposition conditions the PB film can selectively catalyse the electrochemical reduction of hydrogen peroxide in the presence of molecular oxygen [6].

Hydrogen peroxide is present in countless biological reactions as the main by-product from the enzyme-catalysed oxidation of organic substances [7, 8] and is an important indicator for the monitoring of these bio-processes [7-10]. Variety of analytical techniques to assay H_2O_2 are currently in use including fluorometry [11], chemiluminescence [12], photometry [13] and voltammetry [14]. The monitoring of hydrogen peroxide has been realized in different complex matrices such as food samples [15], pharmaceuticals [16] or environment [17]. In recent years, one of the most promising electroanalytical techniques employed in H_2O_2 assay is biosensing with peroxidase-based enzyme electrodes [8, 10, 18]. A number of Prussian Blue modified electrodes and also electrodes modified with similar transition– metal cyanide complexes have been reported and recommended for highly selective monitoring of hydrogen peroxide. However, these electrodes still face different drawbacks mostly associated with their long-term stability and sensitivity to pH changes.

Therefore, the present work deals with the optimisation of the procedure for Prussian Blue electrodeposition on spectroscopic graphite and stabilisation of the film by means of the formation of a protective thin polymeric layer over the electrode surface. The catalytic activity of produced electrode with respect to hydrogen peroxide electrochemical reduction was examined under static and hydrodynamic (in a flow-injection system) conditions.

Experimental

Chemicals used for electrode modification and solutions preparation: $FeCl_3$, $K_4[Fe(CN)_6]$, potassium phosphate monobasic and dibasic, HCl, KCl, and H_2O_2, were of analytical grade. The polymeric solutions of the ionomer Nafion™ (Fluka, commercially available as 5% solution in mixture of low-weight aliphatic alcohols) were obtained through dilution of the solution with bi-distilled water to the desired concentration. Rods of spectroscopic graphite, pressed into Teflon cylinder and with copper current leads were used as working electrodes. Before modification, the graphite surface was polished with fine emery paper with gradually decreasing grit size (P800, P1200, and P2000) and sonicated in bi-distilled water for at least 3 min after each polishing step. Then the electrode surface was washed thoroughly with bi-distilled water and allowed to air-dry. The electrode was modified trough potentiodynamic cycling at 20 mV/s between 0,4 and 0,75 V vs.

Ag/AgCl, 3M KCl in the electrochemical bath, containing the following electrolyte: 2 mM $K_3[Fe(CN)_6]$ + 2 mM $FeCl_3$ in 0.1 M KCl and 0.1 M HCl [19]. Further the electrode was activated by performing 20 voltammetric cycles between +0.35 and –0.05 V at 0.04 V s^{-1} in a solution of 0.1 M KCl and 0.1 M HCl [20]. The activation step was followed by a brief air-drying of the surface and spreading over the PB film of a 10 µL drop of the Nafion™ solution. A similar electrode, but without polymeric coverage was used for comparative studies.

All electrochemical studies were performed in a three-electrode electrochemical setup with graphite as working electrode, saturated calomel electrode as reference and platinum wire as counter electrode. Only for PB deposition and activation steps a Ag/AgCl, 3M KCl was used as reference electrode. For the fabrication of the PB-modified electrode and the examination of its electrocatalytic activity under static conditions a computer controlled electrochemical workstation PalmSens (Palm Instruments BV, The Netherland) and software PS Trace 2.13 was used. The flow-injection measurements were performed with an analogue potentiostat Tacussel (Tacussel Electronique, France), equipped with a peristaltic pump and lab-made three-electrode flow cell, connected with silicon tubing with 1 mm inner diameter. All measurements related to the catalytic activity of PB-modified electrode with respect of H_2O_2 electroreduction were performed in a 0,1 M phosphate buffer solution (pH = 5,5) at. The current variation was monitored at a constant potential of -100 mV vs. SCE by adding aliquots of 0,01 M H_2O_2 stock solution. The pH of buffer solutions was adjusted by means of a Hanna Instruments 211 pH-meter. The solutions were prepared with bi-distilled water.

Results and Discussion

Although the procedure for Prussian Blue onto the electrode surface is generally well documented in the literature, the change of the electrode material requires some further optimisation as related to the homogeneity of the formed film, its mechanical stability as well as the reproducibility of the catalytic activity observed. Our experiments showed that the temperature of the electrodeposition bath considerably affects both the mechanical stability of the PB-film and the resulting electrocatalytic activity towards hydrogen peroxide electroreduction. On Fig. 1 are depicted the cyclic voltammograms (CVs) of the bare graphite in the electrodeposition bath at room temperature (21˚C, Fig.1 a) and thermostated at 45 deg (Fig.1 b). The shape of the voltammograms recorded in the thermostated bath is indicative for the formation of a homogeneous and with high catalytic

activity film that was further confirmed by the studies of their catalytic activity. It has to be mentioned that differences were noted also in the cyclic voltammetric curves recorded during the activation stage of the PB-film formation (Fig. 2). While the film deposited at the warmed bath possessed all the characteristics of a fully reversible redox transformation of the film (Fig. 2b), the deposition at room temperature requires much longer activation process until a quasi-reversible voltammogram is obtained – the activation of the film was carried out several times by repeating cycles of 20 CVs between -0,05 and 0,4 V until a reversible CV is recorded (Fig.2a)

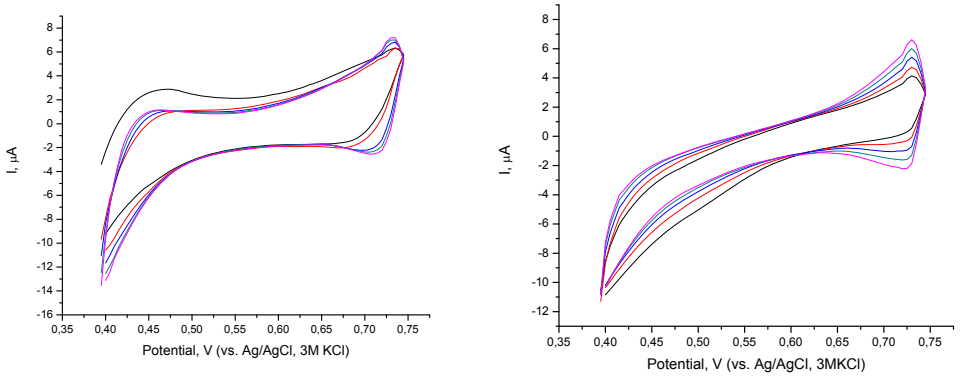

Fig. 1. Cyclic voltammograms of clean spectroscopic graphite in the PB-electrodeposition bath: a) left at 21 deg; b) right, at 45 deg.

Despite the repetitive cycling at the activation step yielded a nearly reversible CV, the observed catalytic activity of thus obtained PB-film was much lower than the desired one and the electrodes were not usable for electroanalytical purposes. Therefore as optimal deposition conditions were selected the potentiodynamic electrodeposition of the film in a warmed up to 45 deg. electrodeposition bath followed by an activation step consisting of 20 cycles between -50 and +400 mV in an electrolyte consisting of 0,1 M HCl and 0,1 M KCl, showing reversible electrochemistry of the deposited film.

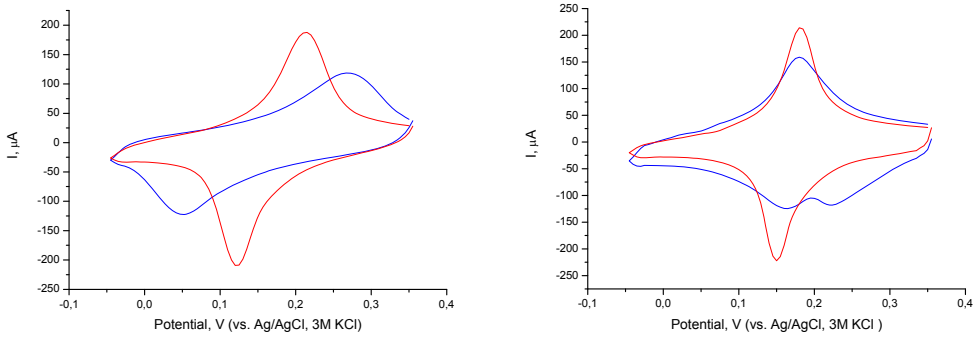

Fig. 2. The first (blue) and the last (red) CVs of the PB-modified graphite upon continuous cycling in 0,1 M HCl and 0,1 M KCl at room temperature: a) left, PB-electrodeposition at 21 deg; b) right, at 45 deg.

The test of the electrocatalytic activity in neutral medium (pH = 7) of so produced electrodes showed rapid deactivation of the electrocatalyst. As the most probable reason for that observation was hypothesised the dissolution of the iron electrocatalyst in presence of hydroxylic groups that are more abundant in neutral medium as compared to acidic one. This motivated our next step – to form a protective layer over the electrocatalyst that will be capable of electrostatically repulsing the negatively charged OH^- ions and this way to prevent the damages of the PB-film. For that purpose the ionomer Nafion™ – a fluorine-sulfonated polymer was chosen. When the polymeric film formed on the electrode surface is immersed in aqueous solution its surface charges negatively thus repulsing the hydroxyl ions away from the PB film. On the next Figure (Fig. 3) is presented the authentic chronoamperometric curve representing the current change of a PB-modified graphite electrode upon addition of 10 mM portions of hydrogen peroxide. The vertical lines on the graph are a result of stirring of the solution after each addition. It is obvious that the electrode response goes more negative (reduction process) upon addition of each portion H_2O_2. The resulting calibration curve is presented on Fig. 4.

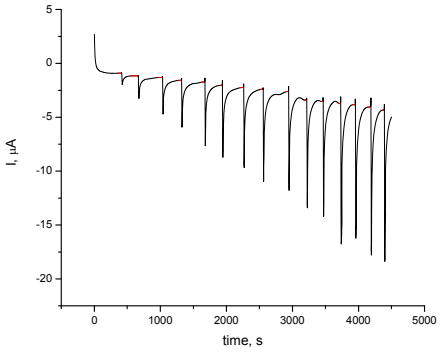

Fig. 3. Authentic record of the electrode response with time upon addition of H_2O_2 portions; E = - 0,1 V.

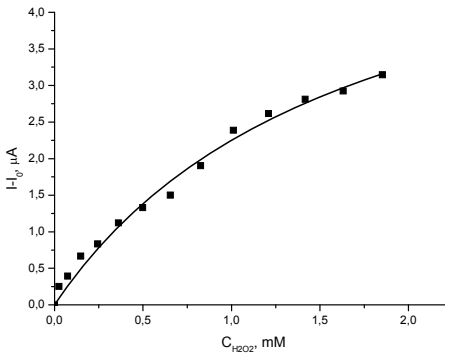

Fig. 4. Calibration graph for the PB-modified graphite covered with a thin Nafion film in presence of H_2O_2; E = - 0,1 V; $r^2 = 0,98_3$.

The calibration graph is not linear but has a linear dynamic range of up to about 500 mM H_2O_2 . Its shape reminds an adsorption isotherm – most probably the penetration of peroxide is impeded after reaching certain concentration and this causes the deviations of the graphs from linearity. At least four independent measurement yielding similar results (± 8%) were recorded, proving that the electrode fabrication is fully reproducible and leads to the formation of a highly active electrocatalytic layer on the electrode surface. Under static conditions there was no possibility to determine precisely the detection limits that is why we examined the operational characteristics of the electrocatalytic PB-film electrode under enhanced hydrodynamic conditions - in a flow-injection system. All the working conditions were equivalent, and in order to reach the best sensitivity the flow rate was varied from 1,0 to 5,5 ml/min. The best experimental results were obtained with 5,25 ml/min flow rate, which was chosen as the optimal for further experiments. On Fig. 5 is presented an authentic record of the current variation with several equal additions of hydrogen peroxide stock solution. It could be seen that the current peaks reach almost identical values for each particular concentration. All the records are characterised with a very low noise level and sharp peaks.

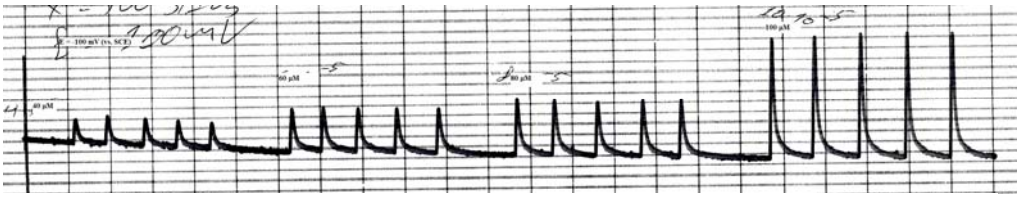

Fig.5. Authentic record of the response of PB-film modified electrode upon additions of several equal portions of peroxide in flow-injection system; working potential -100 mV vs. SCE.

As an approximate limit of detection in flow-mode 20 μM concentration of peroxide could be stated. In addition to the good sensitivity and reproducibility, the PB-polymeric film modified graphite shows enhanced stability as compared to the non-covered with a polymer electrode. After a period of 30-days exploitation (ca. 10-12 calibration measurements) the retained catalytic activity of the discussed electrode exceeded 50%, while the non-covered electrode was capable of performing only two consecutive measurements before the activity drops to 30% of the initially registered.

Acknowledgements

Authors acknowledge the support from the Bulgarian National Science Fund (grant DVU-02/38).

References

1. P. Day, F. Herren, A. Ludi, H. Gudel, F. Hulliger, D. Givord, Helv. Chim. Acta. 63 (1980)148.
2. D. Ellis, M. Eckhoff, D. Neff, J. Phys. Chem. 85 (1986)1225.
3. K. Itaya, T. Ataka, S. Toshima, J. Am. Chem. Soc. 104 (1981) 4767.
4. R. Gayonite, A. Malinauskas, Sens. Actuat. B 46 (1998) 236.
5. R. Gayonite, A. Malinauskas, Sens. Actuat. B 56 (1999) 93.
6. A. Karyakin, E. Karyakina, L. Gorton, Electrochem. Comm. 1 (1999) 78.
7. L. Gorton, E. Csoregi, E. Domingues, J. Emneus, G. Jonsson-Pettersson, G. Marko-Varga, B.Persson, Anal. Chim. Acta 250 (1991)203.
8. H.B. Dunford, “Heme Peroxidases” (1999) Wiley-VCH, New York.
9. A. Amine, G. Patriarche, G. Marrazza, M. Mascini, Anal. Chim. Acta 242 (1991) 91.
10. K. Matsumoto, T. Tsukatani, Y. Okajima, Electroanalysis 7 (1995) 527.

11. T. Holm, G. George, M. Barcelona, Anal. Chem. 59 (1987) 582.
12. K. Hool, T. Neiman, Anal. Chem. 60 (1988)834.
13. I. Vieira, O. Fatibello, Analyst 123 (1998) 1809.
14. P. Westbroek, B. VanHaute, E. Temmerman, Fres. J. Anal. Chem. 354(1996) 405.
15. F. Miyamoto, M. Saeki, T. Yoshizawa, Japanese J. Toxic Environ. Health 39 (1993) 336.
16. J. Wang, Y. Lin, L. Chen, Analyst 118 (1993) 277.
17. J. Lee, I. Tang, J.-B. Weinstein-Lloyd, Anal. Chem. 62 (1990) 2381.
18. T. Ruzgas, E. Csoregi, J. Emneus, L. Gorton, G. Marko-Varga, Anal. Chim. Acta 330 (1996) 123.
19. I. L. de Mattos, L. Gorton, T. Ruzgas, A. A. Karyakin, Analytical Sciences 16 (2000) 795.
20. K. Itaya, T. Ataka, S. Toshima, J. Am. Chem. Soc. 104 (1982) 4767.

STEREOCHEMISTRY OF CALIXARENES

Pavel Vojtisek, Jana Klimentova and Jiri Ludvik
Dep. of Inorg. Chemistry, Faculty of Science, Charles University, Prague, Czech Republik;
J. Heyrovský Institute of Physical Chemistry, Academy of Sciences, Prague, Czech Republic
pavojt@natur.cuni.cz; jiri.ludvik@jh-inst.cas.cz

In 1872 Adolph von Baeyer heated aqueous formaldehyde with phenol and observed a reaction that yielded a hard, resinous, noncrystalline product.However, the chemistry of the day was not sufficiently advanced to allow characterization of such materials, and the structure remained unprobed. The nature of the materials was studied by Alois Zinke's group at the University of Graz. In 1944 Zinke[1] obtained high melting solids from the reaction of para-substituted phenols and formaldehyde, and they assigned a cyclic tetrameric structure to these compounds. This assignment has gained acceptance as the result of X-ray crystallographic data by Cornforth et al. and the stepwise synthesis of Hayes and Hunter, repeated and extended by Kammerer.[1]

Until extensive works of David Gutsche (in the 7th and 8th decade of the 20th cent.) have led to simple and reproducible syntheses giving calixarenes in good yields, and have start a wide chemistry of the compounds.[2]

Calix[4]arenes are a class of macrocyclic compounds which has attracted a lot of attention because of their possible utilization in many areas of research and industry. Because of their potential, the chemistry of calixarenes has in the last few years developed into a wide and well-explored area.[2] These macrocycles have been used principally as spacers bearing functional groups in a well-defined arrangement, allowing their desired cooperation.

The utilization of calix[4]arenes as molecular platforms possesses a few advantages. First, the synthesis of these macrocycles can be easily accomplished by a well-known procedure in good yields. The size of the macrocycle can be successfully controlled by the reaction conditions.[2] The starting materials are inexpensive and common. Calix[4]arenes can be easily modified both on their upper and lower rim, the chemical and physical properties of these molecules can be therefore changed as required. Finally, the four possible conformations

of the calix[4]arene macrocycle, easily immobilized by lower rim substitution, are the main reason for the advantage of using calix[4]arenes as molecular platforms.

The four possible conformations for calix[4]arenes are depicted in Fig. 1.

In order to design functional molecules based on calix[4]arenes, effects causing deformation of the calix[4]arene scaffold and rigidity/flexibility of the calix[4]arene molecule should be evaluated. It is therefore necessary to find simple parameters to describe the geometry of the calix[4]arene scaffold.

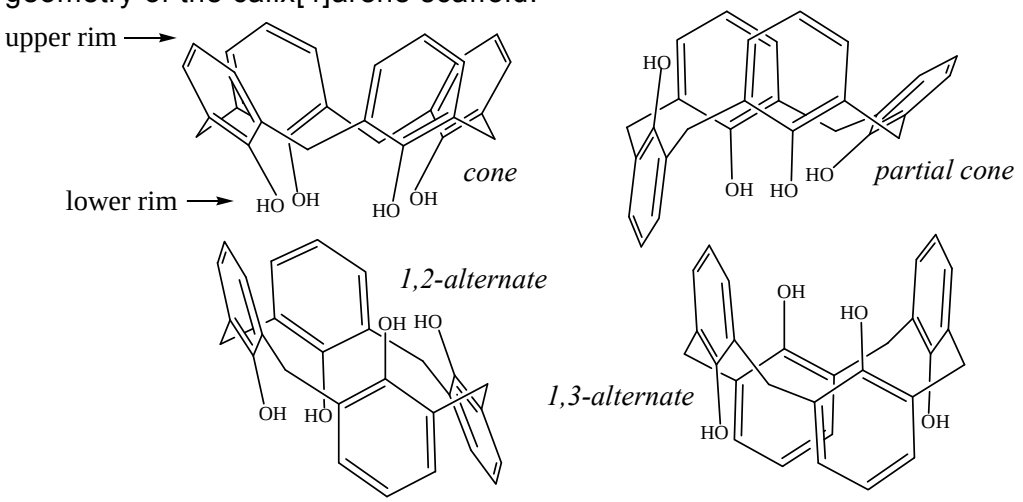

Fig.1: Conformations of calix[4]arenes

The conformation of the calix[4]arene base frame (i.e. hydrocarbon skeleton without upper rim and lower rim substituents) is fully described by the values of torsion angles at the C_{arom}-C_{bridge} bonds. For calix[4]arenes, the relevant torsion angles visible in Fig. 2 are the angles C28-**C1-C2**-C3, C24-**C1-C2**-C3, C1-**C2-C3**-C4 and C1-**C2-C3**-C25. There are obviously two torsion angles at each bond C_{arom}-C_{bridge}, so there are altogether 16 relevant torsion angles to describe the conformation of the calix[4]arene backbone. It is necessary to reduce the number of relevant parameters.

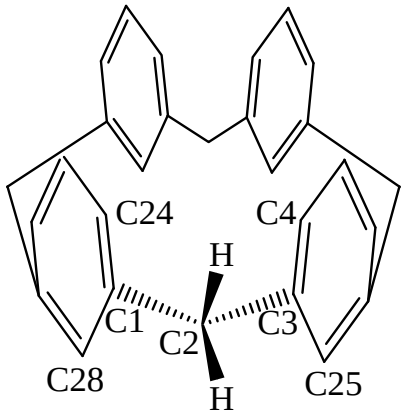

Fig. 2: Torsion angles at the calix[4]arene scaffold

The Arnaud-Neu's approach[3] has been utilized by the definition of a reference plane to which the angles ω_1, ω_2, ω_3, ω_4 of the four calix[4]arene phenyl rings are related. This reference plane is the plane of the four bridge carbon atoms (the deviations of the bridge atoms from this plane are below 0.1 Å). The angles of the phenyl rings (ω_i, i = 1-4) are calculated in the scale 0-360°, see Fig. 3

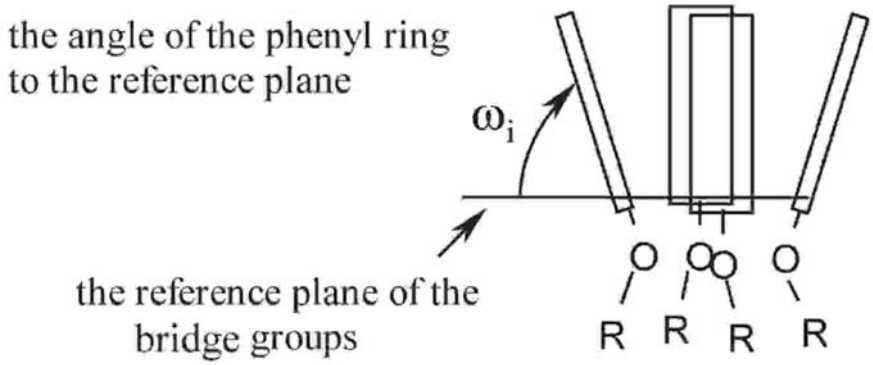

Fig. 3: The definition of the phenyl ring angles ω_i

The previous sixteen torsion angle parameters have been successfully reduced by this approach to four parameters ω_1, ω_2, ω_3 and ω_4. However, the assignment of these four parameters is not unambiguous and depends on the numbering of the calix[4]arene base

frame, e.g. there is a question which calix[4]arene phenyl ring should be assigned as ω_1. Moreover, four parameters form a four-dimensional space that is very difficult to imagine and work with. It would be therefore more convenient to reduce the number of the parameters from four to three, since 3D space is much easier to describe. To achieve these two objectives, new parameters **α, β, δ** (in °) have been introduced:[4]

$$\alpha = 0.25*(\omega_1 + \omega_2 + \omega_3 + \omega_4)$$ *(average value of the phenyl ring angles ω_1 - ω_4)*

$$\beta = | (\omega_1 + \omega_3) - (\omega_2 + \omega_4) |$$ *(distortion of the calix[4]arene towards C_{2v} symmetry)*

$$\delta = | \omega_1 - \omega_3 | + | \omega_2 - \omega_4 |$$ *(distortion of the calix[4]arene towards C_s symmetry)*

The 2D β-δ plot showing the deformation of the calix[4]arene scaffold is the most informative one; this plot is depicted in Fig. 4. Average values of the parameters (with s. d.) in the groups of *cone*, *partial cone*, *1,2-alternate* and *1,3-alternate* conformers in Table (AV = average value, SD = standard deviation) also give us useful information. The AVs reflect the distribution of parameters **α, β, δ** whereas the values of the SD represent the rigidity or flexibility of the calix[4]arene scaffold, not a only experimental and calculation errors.

Since there are fewer structures in CSD[5] for calix[4]arenes in other conformations than *cone*, the *partial cone*, *1,2-alternate* and *1,3-alternate* calix[4]arenes are not presented in this work. In the following parts, the influence of substitution and inter- and/or intramolecular interactions on the stereochemistry of the *cone* calix[4]arene moiety (described by parameters **α, β, δ**) is discussed.

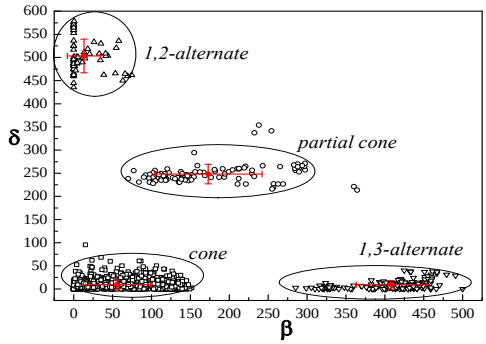

Fig. 4: Distribution of α β, δ values for calix[4]arenes

conformation	par.	AV	SD	SD/AV
cone	α	59.19	6.46	0.11
	β	55.61	43.03	0.77
	δ	9.29	9.59	1.03
partial cone	α	119.37	7.36	0.06
	β	172.99	69.2	0.40
	δ	248.26	21	0.08
1,2-alternate	α	182.73	4.34	0.02
	β	13.14	21.24	1.62
	δ	503.36	36.25	0.07
1,3-alternate	α	182.71	6.11	0.03
	β	408.02	44.79	0.11
	δ	9.1	9.28	1.02

SUMMARY

The final geometry of the calix[4]arene scaffold in symmetrically tetrasubstituted free *cone* calix[4]arenes results from combination of the following three effects.

1. Effects of lower rim substituents

The effect of lower rim OH groups is predominant over other effects, especially over the effect of a filled/empty cavity.

Lower rim OH-substituted calix[4]arenes are significantly more rigid than calix[4]arenes alkylated or acylated at the lower rim due to narrow ranges of parameters α, β. In order to prepare more flexible calix[4]arenes, alkylation or acylation of the calix[4]arene lower rim phenolic oxygen atoms should be performed.

More rigid cavity in lower rim OH-substituted calix[4]arenes also enables formation of filled-cavity compounds. In lower rim alkylated/acylated calix[4]arenes, intramolecular π-π and hydrophobic interactions between one pair of calix[4]arene phenyl rings predominate and formation of filled-cavity compounds is therefore not favored.Calix[4]arenes with four hydroxyl groups at the lower rim possess larger cavities with α < 60; calix[4]arenes with alkylated/acylated lower rim phenolic oxygen atoms have more narrow cavities with α > 60. The value of parameter α tends to increase with increasing size of the lower rim substituents.

Deprotonating in lower rim hydroxyl-containing calix[4]arenes disrupts the cyclic array of hydrogen bonds present at the lower rim; therefore, the values of parameters β, δ tend to be slightly increased in such calix[4]arenes.

2. Effect of upper rim substituents

The values of parameter β in calix[4]arenes with unsubstituted upper rim and calix[4]arenes substituted by polar groups at the upper rim tend to be higher than the values of parameter β in calix[4]arenes with bulky nonpolar upper rim substituents.

3. Effect of a filled/empty cavity

In lower rim OH-substituted calix[4]arenes, this effect is insignificant because the effect of lower rim substitution predominates.

In lower rim alkylated/acylated calix[4]arenes, the values of parameter β in filled-cavity calix[4]arenes tend to be lower than the values of parameter β in empty-cavity calix[4]arenes.

The type, size and flexibility of the molecule inside the cavity affect the final geometry of the calix[4]arene scaffold.

Calixarene frame able to bear various substituents – e.g. redox centers. Tetra-nitro derivatives of calix[4]arenas are an example of molecules with more redox centers. The presence four nitro groups (on upper rim) in one molecule provokes many principal questions: What is the intramolecular electronic interaction between them? Are they reduced simultaneously or stepwisely? What is the influence of the lower rim substitution on the reduction of the nitro groups? What is the influence of the reduction on the molecular geometry? Can we able to see in solution any effects observed in solid state?

Electrochemical reduction of the tetranitrocalix-[4]-arenes starts with two 2-electron reversible waves corresponding to the presence of two different couples of equivalent nitro groups. This result reflects well the finding of the x-ray structural analysis, that the "calix" is in fact not circular, but pinched with a strong "π-stacking" of the opposite benzene rings. It correspons with relatively high value of the parmeter **β**. The electrochemical properties of the systems was discussed and interpreted in terms of molecular geometry and intramolecular electronic communication between the redox centers through the space; in the terms of the „**stereoelectrochemistry**".

The first two waves are followed by a single 12-electron wave, indicating that the generated tetrakis-radical anion intermediate involves four equivalent non-communicating nitroradical anions. This result provokes questions about an electron-transfer induced change in geometry of the calix arene due to the change in the reduction state.

to a circular one. The experimental results are correlated with quantum chemical calculations.

REFERENCES

[1] *a)* A. Zinke and E. Ziegler, Chem. Ber., 77, 264 (1944). *b)* J. W. Cornforth, et al., Tetrahedron, 29, 1659 (1973). *c)* E. T. Hayes and R. F. Hunter, Chem. hd., 193 (1956); *J. Appl.* Chem., 8,743 (1958). *d)* H. Kammerer, G. Happel, and F. Caesar, *Makromol.* Chem., 162, 179 (1972).

[2] e.g. *a)* Gutsche C. D., *Top. Curr. Chem*., **1984**, 1-47; Gutsche C. D., Calixarenes (Monographs in Supramolecular Chemistry), the Royal Society of Chemistry, Stoddart J. F.; Cambridge 1989; *b)* Vicens J., Böhmer V., Calixarenes: A Versatile Class of Macrocyclic Compounds, Kluwer Academic Publishers 1991; *c)* Shinkai S., *Tetrahedron*, **1993**, 49(40), 8933-8968; *d)* Gutsche C. D., Calixarenes Revisited (Monographs in Supramolecular Chemistry), RSC Publishing, Cambridge 1998; *e)* Mandolini L., Ungaro R., Calixarenes in Action, Imperial College Press 2000; *f)* Asfari Z., et al., Calixarenes 2001, Kluwer Academic Publishers 2001; *g)* Gutsche C. D., Calixarenes: An Introduction (Monographs in Supramolecular Chemistry), RSC Publishing, Cambridge 2008;

[3] Arnaud-Neu F., et al., *J. Am. Chem. Soc.*, **1989**, 111, 8681-8691;

[4] *a)* Klimentová J., Vojtíšek P., *Materials Struct.*, **2005**, 12, 151; *b)* Klimentová J., Vojtíšek P., *J. Mol. Struct*., **2007**, 826(1), 48-63; *c)* Klimentová J., Vojtíšek P., Sklenářová M., *J. Mol. Struct*., **2007**, 871(1-3), 33-41;

[5] Cambridge Structural Database Version 2.3.6 (update January 2011), Cambridge Crystallographic Data Centre (CCDC);

N-acetyl-methyl amides of some amino acids - synthesis and IR- spectral analysis of the initial compounds

Atanas Chapkanov[1*], Tatyana Dzimbova[2], Bojidarka Ivanova[3], Atanas Marvakov[1]

[1]Department of Chemistry, FMNS, SWU "N. Rilski", 66 "I. Mihailov" Str., 2700 Blagoevgrad, Bulgaria, chapkanov@swu.bg

[2]Institute of Molecular Biology, Bulgarian Academy of Sciences, 21 Acad. G.Bonchev str., 1113 Sofia, Bulgaria

[3]Faculty of Chemistry, Sofia University, 1 J. Boucher Boulevard, Sofia 1164, Bulgaria

***Abstract**: The development of simple and efficient method for synthesis of N-Acetyl derivatives of α-amino acids (L-glycine, L-valine, L-proline and L-cysteine) and IR-spectral analysis for characterization was the purpose of the present work. The simple method for the preparation of these compounds was developed. Two step procedure was applied – acetylation in basic condition at room temperature and mixed anhydride amidation. The conventional and IR-LD spectral analysis of oriented solid sample as a nematic liquid crystal suspension of amino acid L-Valine (L-Val) and L-cys as zwiterionic structure and intermediates compounds was carried out. On the base of the obtained spectroscopic data the IR-characteristic bands of the investigated compounds accompanied with structural prediction were assigned.*

***Key words:** ά-amino acids, N-acetyl-methyl amides, IR - spectral analysis*

1. INTRODUCTION

Nature has continuously provided mankind with a broad and structurally diverse arsenal of bioactive compounds that have been utilized as new drugs or as lead structures for the development of novel synthetically derived analogues. The ordinarily free amino groups of N-terminal residues in polypeptide chains are blocked in some instances by acetyl groups, e.g., in melanocyte-stimulating hormone (α-MSH), and in the following proteins: horse heart cytochrome c, hemoglobin F1, egg albumin, histones, turnip yellow

mosaic virus (TYMV), and tobacco mosaic virus (TMV) proteins. N-acetyl cysteine is derived from cysteine found in food and synthesized in the body. It helps the body to synthesize glutathione. It is used as a mucolytic agent to reduce the viscosity of mucous secretions. It has also been shown to have antiviral effects in patients with HIV due to inhibition of viral stimulation by reactive oxygen intermediates. There are many examples for N-acetylated amino acids in living organisms. N-Acetyl aspartic acid is a derivative of aspartic acid. It is the second most concentrated molecule in the brain after the amino acid glutamate. It is synthesized in neurons from the amino acid aspartate and acetyl coenzyme A. The various functions served by N-acetylaspartic acid are still under investigation, but the primary proposed functions include: 1) A neuronal osmolyte that is involved in fluid balance in the brain 2) A source of acetate for lipid and myelin synthesis in oligodendrocytes, the glial cells that myelinate neuronal axons 3) A precursor for the synthesis of the important neuronal dipeptide N-acetylaspartylglutamate 4) N-Acetyl aspartic acid may also be involved in energy production from the amino acid glutamate in neuronal mitochondria [1]. The synthesis of different N-acetyl amino acid derivatives were synthesis, evaluated and reported earlier [2-7] as well as and the corresponding spectral study [8,9].

2. EXPERIMENTAL PART

2.1. Synthesis

Amino acids and solvents were obtained from Fluka and were used without further purification. Melting points were measured on Büchi (Switzerland) model 535. Optical rotation was determined on Polarimeter 141, Perkin Elmer (USA). For TLC silicagel plates (Merck, $60F_{254}$) were used and following systems: A) $CHCl_3$:MeOH:H_2O(80:30:5); B) CH_3CN:H_2O (4:1).

N-Acetyl amino acids. Amino acid (0.1 g) was dissolved in 5N NaOH (3 ml) and acetic anhydride (2 x 0.2 ml) was added over 15 minute periods. Reaction mixture was stirred at room temperature for 1 hour. Water was evaporated under reduced pressure. Residue obtained was dried and was used without further purification on the next step.

N-Acetyl amino acid methyl amides. To the solution of N-Acetyl amino acid (3 mM) in DMF (2 ml) and THF (2 ml) NMM (0.33 ml, 3 mM) was added, and the reaction mixture was cold to -10^{o}C. Piv-Cl (0.37 ml, 3 mM) was added dropwise and after 10 minutes solution of methyl

amine hydrochloride (1 g, 15 mM) and Et_3N (0.415 ml, 15 mM) in water (2 ml). Process completed after 1.5 at -10^oC and solvent was evaporated under reduced pressure. The residue was dissolved in $CHCl_3$ (10 ml) and was washed with water (2 x 10 ml). Organic layer was dried over Na_2SO_4, and $CHCl_3$ was evaporated. Pure product was obtained after column purification (silicagel) and eluent: CH_3CN : H_2O (4 : 1, v/v).

2.2 Methods

The IR-spectra were measured using a Bomem-Michelson 100 FT-IR-spectrometer (4000 – 400 cm-1, 2 cm-1resolution, 150 scans) equipped with a Perkin Elmer wire-grid polarizer. Non-polarized solid-state IR spectra were recorded, using the KBr disk technique. The oriented samples were obtained as a colloidal suspension in a nematic 4'-cyano-4'-alkylbicyclohexyl mixture (ZLI-1695, Merck), whose poor IR-spectrum allows the recording of the guest-compound bands in the whole 4000 - 400 cm^{-1} range. The presence of the isolated nitrile stretching IR-band at about 2230 cm^{-1} additionally serves as an orientation indicator. The effective orientation of the solid samples was achieved by the next procedure: the investigated compound (5 mg) was mixed with the liquid crystal substance until obtaining of a slightly viscous suspension. The phase prepared thereby was pressed between two KBr-plates, which in advance were rubbed out in one direction by fine sand-paper. The grinding of the prepared mull in the rubbed direction promotes in addition the sample orientation [10, 11]. For polarized IR-spectra interpretation, the IR-LD spectroscopy used stepwise reduction procedure [12-15]. The IR-LD data interpretation was consisted in subtraction of the perpendicular spectrum (IRs - a result of the 90° angle between the polarized light beam electric vector and the orientation of the sample) from the parallel spectrum (IRp) obtained with a co-linear mutual orientation. The recorded difference (IRp-IRs) spectrum divided the integrated absorbance into positive and negative bands. Positive bands originate from transition moments which formed average angles with the orientation direction (n) between 0° and 54.7° (magic angle) and negative bands corresponding to transition moments, which were directed between 54.7° and 90°. In the reducing-deference procedure, the perpendicular spectrum, multiplied by the variable parameter **c**, was subtracted from the parallel spectrum and parameter **c** was varied until at least one band or set of bands is eliminated in the obtained (IRp - cIRs) reduced IR-LD spectrum. The simultaneous disappearance of these bands in the reduced spectrum provided information about the mutual disposition of the molecular

fragments. This elimination method was carried out graphically using the attached subtracting procedure for processing of IR spectra.

3. RESULTS AND DISCUSSION

The work could be considered as a part of systematic synthetic, spectroscopic and structural investigations on amino acids and their derivatives, small peptides and their possibilities for application as potential medicaments [16-19]. The synthesis of the desired N-acetyl amino acid methyl amides was done according to the Scheme 1.

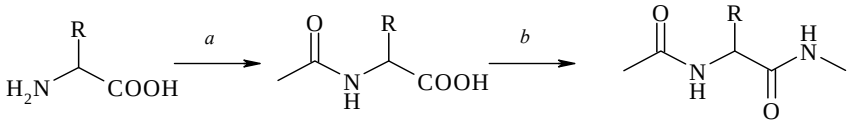

1 **2** **3**

a) 5N NaOH, $(CH_3CO)_2O$; *b*) NMM, PivCl, CH_3NH_2. HCl, Et_3N, THF+DMF

Scheme1. Synthesis of N-acetyl amino acid methyl amides.

On the first step N-acetyl amino acid was prepared using acetic anhydride in basic conditions (5N NaOH) in aqueous solution at room temperature for 1 hour. N-Acetyl amino acids were used on the next step after evaporation of the solvent, drying of the crude product, without further purification. N-Acetyl amino acid methyl amides were obtained in mixed anhydride procedure – Piv-Cl was the reagent used. The reaction was made at -10^{o}C and in mixture of THF and DMF as solvents. Process continued for 1.5 hour and the desired N-acetyl amino acid methyl amide was obtained after column purification (silicagel, CH_3CN **:** H_2O, 4 : 1, v/v). Some physical constants and chemical characteristics of the synthesized compounds were presented in Table 1.

Tab. **1.** Some physical data and characteristics of amino acid derivatives

Amino acid derivative	Melting point (mp), °C	Optical rotation $[\alpha]_D^{20}$	Yield (%)
Ac-Val	124-125	+7,4 (water)	82%
Ac-Gly	207-209	_	80
Ac-Cys	109 -112	-35 (water)	81
Ac-Val- NH-CH_3	oil	-94° (water)	31
Ac-Gly-$NHCH_3$	oil	_	27
Ac-Cys-$NHCH_3$	81	-24 (MeOH)	31

IR-spectral analysis

The obtained results about the investigated compounds were assigned on the basis of known IR-data about similar systems [20 - 28]. The characteristic IR-bands of the pure amino acids L-Val were

listed and assigned in Table (2). The comparison and assignment of the solid-state IR-spectra (Figs. 2.1) of the systems studied was done, using the statement that pure amino acids stabilize H_3N^+,-R-COO^-(L-Val) zwitterions with characteristic IR-spectral bands of -NH_3^+ and -COO^-groups. The polarized IR-method was appeared to be unique for the experimental proving of the vibrational bands to corresponding modes.

Tab. 2. IR-characteristic bands in 1700 – 1350 cm^{-1} region of $_L$-Val

Assignment	$_L$-Val ν [cm^{-1}]
ν_{NH3+} stretching	3200 – 2700
δ^{as}_{NH3+}	1629
$\delta^{'as}_{NH3+}$	1612
δ^{s}_{NH3+}	1567
ν^{as}_{COO-}	1585
ν^{s}_{COO-}	1508

*IR-data obtained after applied deconvolution and curve-fitting procedures

The comparative analysis showed the presence of bands assigned to the stretching vibrations of the protonated amino group -NH_3^+ in the 3200 – 2700 cm^{-1} region for amino acid L-Val, as well as two bands at 1629 и 1612 cm^{-1} characterized asymmetric banding vibrations (δ^{as}_{NH3+}). The band at 1567 cm^{-1} was assigned to the symmetric banding vibrations (δ^{s}_{NH3}+). The typical -COO-maxima are in the 1600 – 1500 cm^{-1} spectral range. The character of the band at 1585 cm^{-1} and 1508 cm^{-1} were assigned and belonging to the asymmetric and symmetric stretching modes of COO-fragment (ν^{as}_{COO-} and ν^{s}_{COO-}) in the molecule of L-Val. Moreover, the last peaks disappeared in the spectrum of protonated form of L-Val hydrochloride, accompanied with a new peak at 1720 cm^{-1}, corresponding to $\nu_{C=O}$ stretching mode of –COOH. The simultaneously elimination of pairs of peaks at 1629 cm^{-1} and 1612 cm^{-1} (Fig. 1.2) confirmed their character as δ^{as}_{NH3+} and $\delta^{'as}_{NH3+}$ (Table 1) due to their possession of the same symmetry class.

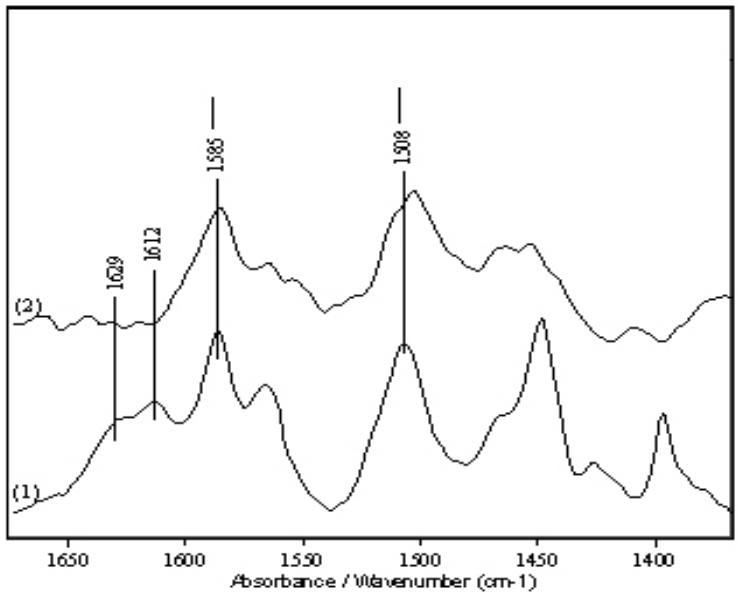

Fig. 1. Non-polarized IR-(1) and reduced IR-LD spectra of $_L$-Val after elimination of 1629 cm^{-1} (2)

The protonation leds to disappearance of the typical -COO-maxima in 1630 – 1550 cm^{-1} spectral range as well as about 1405 cm^{-1}. The character of the 1585 cm^{-1} and 1508 cm^{-1} band as ν^{as}_{COO-} and ν^{s}_{COO-} in $_L$-Val was confirmed in addition by the obtained IR-spectrum of protonated L-Val as hydrochloride salt. It is characterized with the disappearance of the maxima at 1585 cm^{-1} and 1508 cm^{-1} and a new peak at 1735 cm^{-1} appeared, which corresponded to $\nu_{C=O}$ stretching vibration of the restored COOH group in the salt. The precise elucidation of the L-cysteine required a comparison with the neutral amino acid data (Fig.2). The broad absorption band within whole 3320 – 1800 cm^{-1} belong to ν^{as}_{NH3+} and ν^{s}_{NH3+} stretching vibrations. The highest frequencies sub maximum at 3170 cm^{-1} belonging namely to the asymmetric stretching vibrations of ν^{as}_{NH3+}. The IR-band observed at 2069 cm^{-1} corresponded to $\delta^{as}_{NH3+} + \tau_{NH3+}$ combination mode. The intensive band at 2551 cm^{-1} corresponded to ν_{SH} stretching vibration of the SH-group. The bands at 1589 cm^{-1} and 1397 cm^{-1} corresponded to ν^{as}_{COO-} and ν^{s}_{COO-} stretching vibrations of COO-fragment, while the bands at 1654 cm^{-1}, 1610 cm^{-1} and 1530 cm^{-1} – to bending vibrations δ^{as}_{NH3+}, $\delta^{as'}_{NH3+}$ and δ^{s}_{NH3+} of NH_3^+- of NH_3^+-group. To ν_{C-N} stretching mode belonged the band at 1349 cm^{-1}.

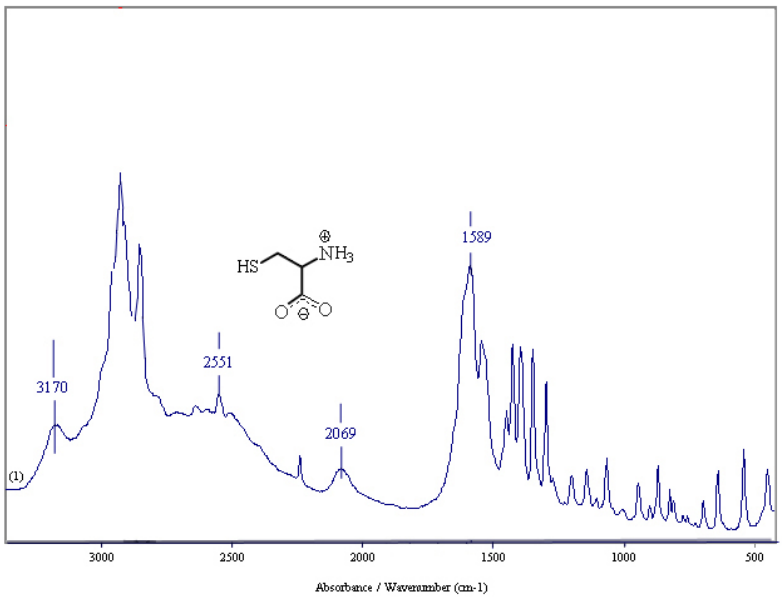

Fig. 2. Non-polarized IR-spectrum of L-cysteine

4. CONCLUSION

The N-acetyl-methyl amides derivatives of ά-amino acids L-Gly, L-Val, and L-Cys were synthesized by a new efficient and simple method using acetic anhydride in basic conditions at room temperature and following mixed anhydride procedure. The spectral investigation, inclucuding IR-characteristic bands determination of the starting amino acids as zwitterions L-Val and L-Cys were carried out. The method of linear polarized vibrational IR-spectroscopy of oriented colloids in nematic host was applied on L-Val and L-Cys, with a view to obtain experimental bands assignment and local structural elucidation in solid-state. The obtained experimental IR-LD results confirmed the applicability of the used spectral method for structural determination.

ACKNOWLEDGEMENTS

This investigation was supported by the project: SRP-A8 “Synthesis and spectral characterization of biological-activated substance - amino acids and their N-substituted derivatives”- SWU”N. Rilski”, 2011.

ABBREVIATIONS

DMF – *N*,*N*-dimethylmethanamide, THF – tetrahydrofuran, NMM – 4-methylmorpholine, Piv-Cl – pivaloyl chloride, Et – ethyl.

5. REFERENCES

[1] Do, K.Q., Lauer, C.J., Schreiber, W., Zollinger, M., Gutteck-Amsler, U., Cuenod, M., Holsboer, F.(1995) Gamma-Glutamylglutamine and taurine concentrations are decreased in the cerebrospinal fluid of drug-naive patients with schizophrenic disorders. J. Neurochem. 65(6), 2652-62.

[2] Harris, W.T., Tenjarla, S.N., Holbrook, J.M., Smith, J., Mead, C., Entrekin, J., (1995) N-pentyl N-acetylprolinate. A new skin penetration enhancer. J. Pharm. Sci. 84, 640–642.

[3] Haddox, J.L,, Pfister, R.R., Muccio, D.D., Villain, M., Sommers, CI., Chaddha, M., Anantharamaiah, G.M., Brouillette, W.J., DeLucas, L.J., (*1999)* Bioactivity of peptide analogs of the neutrophil chemo attractant, N-acetyl-proline-glycine-prolyne., Invest. Ophthalmol. Vis. Sci. 40(10), 2427-2429.

[4] Sijpkes, A.H. and Somsen, G., (1990) Chiral interactions of some *N*-acetyl-*N′*-methyl amino acid amides dissolved in *N*,*N*-dimethylformamide, J. Chem. Soc., Faraday Trans. 86, 1461-1466

[5] Cooke, A., Bennett, J. and McDaid, E. (2002) A facile synthesis of N-benzyl-4-acetylproline via a tandem cationic aza-Cope rearrangement-Mannich reaction, Tetrahedron Letters, 43, 903–905

[6] Tenjarla, S.N., Kasina, R., Puranajoti, P., Omar, M., Wayne, S., Harris, T., (1999) Synthesis and evaluation of N-acetylprolinate esters —novel skin penetration enhancers, International Journal of Pharmaceutics, 192, 147–158.

[7] Kuvaeva, Z.I., Lopatik, D.V., Nikolaeva, T.A., Knizhnikova, A. N., Najdenov, V.E. and Markovich, M.M., (2010) Drug synthesis methods and manufactoring technology. Preparation and use of N-acetyl-ά-amino acids. Pharmaceutical Chemistry Journal, 44(6), 22-23.

[8] Nemec, I., Micka, Z., (2001), Tri- L-val selenate – study of vibrational spectra and structural phase transition, Journal of Molecular Structure, 563-564, pp. 289-294.

[9] Beulah J. Rajkumar, M., Ramakrishnan, V. (2002) Infrared and laser Raman studies of L-phenylalanine, L-phenylalaninium perchlorate and bis (DL-phenylalaninium) sulphate monohydrate, Spectrochimica Acta Part A, 58 1923–1934.

[10] Ivanova, B., Tsalev, D., Arnaudov, M. (2006) Validation of reducing-difference procedure for the interpretation of non-polarized infrared spectra of n-component solid mixtures. Talanta, 69, 822-836.

[11] Ivanova, B., Simeonov, V., Arnaudov, M., Tsalev, D. (2007) Linear-dichroic infrared spectroscopy – validation and experimental design of the orientation technique as suspension in nematic liquid crystal. Spectrochim. Acta, Part A, 67(1), 66-75.

[12] Thulstrup, E., Eggers, M. (1968) J. Moment directions of the electronic transitions of fluoranthene. Chem. Phys. Lett., 1, 690–692.

[13] Thulstrup, E., Michl J. (1986) Spectroscopy with Polarized Light, VCH, Wienheim,

[14] Jordanov, B., Nentchovska R., Schrader, B. (1993) FT-IR linear dichroic solute spectra of nematic solutions as a tool for IR-band assignment. J. Mol. Struct., 297, 401-406.

[15] Jordanov, B., Schrader, B. (1995) Reduced IR-LD spectra of substances oriented as nematic solutions. J. Mol. Struct., 347, 389-398.

[16] Chapkanov, A.G., Miteva, Y., Kolev, T., Spiteller, M., Koleva, B. (2010,) New Au (III), Pt (II) and Pd (II) complexes with pentapeptide gly-cyl-glycyl-L-methyonyl-glycyl-glycine and their interaction with calf thymus DNA. Protein & Peptide Letters, 17(2), 228-237

[17] Chapkanov, A.G., Zareva, S.Y. (2009**)** Structural and IR-spectroscopic elucidation of dipeptide L-threonyl-L-methionine in solid-state. Protein & Peptide Letters*,* 16(11), 1277-1280.

[18] Kolev, T., Spiteller, M., Koleva, B. (2010) Spectroscopic and structural elucidation of amino acid derivatives and small peptides: experimental and theoretical tools. Amino Acids, 38, 45-50.

[19] Kolev T., Koleva B., Stoineva I., Jakimova B., Tchorbanov B. (2009) Stabilization of Neutral NH_2-R-COOH Form of the Antihypertensive Peptides L-Valyl- L-Prolyl- L-Proline and L-Isoleucyl-L-Prolyl- L-Proline, Protein & Peptide Lett., 16, 112-115.

[20] Pandiarajan, S., Umadevi, M., Rajaram, R., Ramakrishnan, V. (2005) Infrared and Raman spectroscopic studies of l-valine l-valinium perchlorate monohydrate. Spectrochim. Acta, Part A, 62(1-3), 630-636.

[21] Jacob, R., Fischer, G. (2003) Infrared spectra and structures of the valyl-alanine and alanyl-valine zwitterions isolated in a KBr matrix. J. Phys. Chem. A, 107(32), 6136-6143.

[22] Basiuk, V., Douda, J. (2001) Analysis of less-volatile products of polyvaline pyrolysis by gas chromatography/Fourier Transform infrared spectroscopy/mass spectrometry. J. Anal. Appl. Pyrolysis, 60(1), 27-40.

[23] Rajkumar, B., Ramakrishnan, V. (2000) Infrared and Raman spectra of L-valine nitrate and L-leucine nitrate. J. Raman Spectrosc. 31(12), 1107-1112.

[24] Stepanian, S., Reva, I., Radchenko, E., Adamowicz, L. (1999) Combined matrix-isolation infrared and theoretical DFT and ab Initio study of the nonionized valine conformers. J. Phys. Chem. A, 103(22), 4404-4412.

[25] Basiuk, V. (1998) Pyrolysis of valine and leucine at 500°C: identification of less-volatile products using gas chromatography -

Fourier transform infrared spectroscopy-mass spectrometry. J. Anal. Appl. Pyrolysis, , 47(2), 127-143.

[26] Cappelli, C., Monti, S., Rizzo, A. (2005) Effect of the environment on vibrational infrared and circular dichroism spectra of (S)-proline. Int. J. Quantum Chem., 104(5), 744-757.

[27] Schweitzer-Stenner, R., Eker, F., Perez, A., Griebenow, K., Cao X., Nafie, L. (2003) The structure of tri-proline in water probed by polarized Raman, FTIR, VCD and ECD spectroscopy. Biopolymers (Peptide Science), 71, 558-568.

[38] Koleva B.B, Kolev T.M, Simeonov V, Spassov T, Spiteller M. (2008) Linear polarized IR-spectroscopy of partial oriented solids as a colloid suspension in nematic liquid crystal - new tool for structural elucidation of the chemical compounds, J. of Inclusion Phenomenon, 61, 319-333.

PHENYLPROPANOIDS AS NATURALLY OCCURRING AND SYNTHETICAL ANTIOXIDANTS: FROM PLANT DEFENSE TO HUMAN HEALTH

Maya Chochkova, Lyubomir Georgiev, Tsenka Milkova
South-West University “Neofit Rilski”, Blagoevgrad 2700, Bulgaria

***Abstract**: Oxidative stress plays a key role in initiation of many degenerative processes in humans, related to cardiovascular disease, inflammatory disease, aging, and to DNA damage, mutation and promotion leading to cancer. The simplify functionality of hydroxycinnamic acids as esters, amides has gripped our attention, because of displaying a broad spectrum of properties as: antibacterial, antiviral, antiinflammatory, antioxidative, antiproliferative, neuroprotective and etc. The diversity of pharmacological properties of similar compounds are associated with either their properties to act as antioxidants. In order to study the radical scavenging activity, a series of hydroxycinnamic acid amides has been synthesized.*

1. INTRODUCTION

Cinnamic and hydroxycinnamic acids and their derivatives (esters, amides and glicosides) belong to phenylpropanoids - the largest group of secondary metabolites produced by plants in response to UV irradiation, wounding, infections, pollutions, exposure to ozone and other environmental conditions. The main representatives of natural hydroxycinnamic acids are:

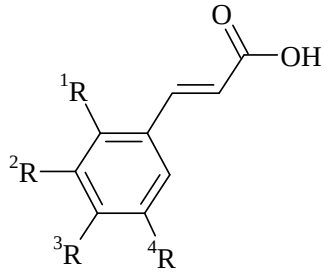

$^1R = {}^2R = {}^3R = {}^4R$ = H; **Cinnamic acid;**
$^1R = {}^2R = {}^4R$ = H, ^3R =OH ; ***p*-Coumaric acid**;
$^1R = {}^4R$= H, ^2R = OCH_3, ^3R = OH; **Ferulic acid**;
^1R = H, $^2R = {}^4R$ = OCH_3, ^3R =OH ; **Sinapic acid**;
^1R = H, $^2R = {}^3R$ = OH, ^4R = H ; **Caffeic acid**

Fig.1.

In the past 10 years there is an emerging interest in the use of dietary and synthetic hydroxycinnamic acids and their derivatives for their effect on human health [1]. It is thought that the protective role in plants and therapeutical effects on humans is due to the antioxidant and free radical scavenging properties of these compounds.

I. Antioxidant and radical scavenging activity

Hydroxycinnamic acids and their derivatives are able to act as antioxidants in a number of ways.

- Phenolic hydroxyl groups are good hydrogen donors: they can react with reactive oxygen and reactive nitrogen species in a termination reaction, which breaks the generation of new radicals. As a result, a stable radical form of the antioxidant is produced. Phenolic hydroxyl groups often have the potential to inhibit the lipid peroxidation and strongly to interact with proteins, inhibiting some enzymes involved in radical generation, such as various cytochrome P450 isoforms.

- The considered phenolics are able to chelate metal ions involved in the production of free radicals.
- These compounds are able to absorb ultraviolet light and can be used as stabilizers for cosmetics and polymeric materials.
- Hydroxycinnamic acids and derivatives act as synergists with other antioxidants.

II. Anti-cancer effect [2-4]

The compounds with antioxoidant activity are regarded as potential inhibitors of several cancers as the free radicals are considered as important factors in the etiology of cancer. Important mechanisms for the anticarcinogenic effects of polyphenols include the reduction of proliferative activity and the induction of apoptosis in cancer cells.

III. Radioprotective effect

Radiation therapy is a form of cancer treatment that uses ionizing radiation to kill cancer cells and shrink tumors. It also injures or destroys the normal cells. Although radiation damages both cancer cells and normal cells, the goal of radiation therapy is to kill as many cancer cells as possible, while limiting the damage to nearby healthy tissue . The deleterious effects of ionizing radiation in biological systems are mainly mediated through the generation reactive oxygen species (ROS) including superoxide anion ($O2^{\bullet -}$), hydroxyl radical ($OH^{\bullet *}$) and hydrogen peroxide H2O2. These ROS are known to cause oxidative stress in several critical cellular molecules like DNA, proteins and lipid membranes. Since ferulic acid and its esters prevents the formation of ROS, it can be used as a radioprotectors [9].

IV. Anti-inflammatory effect

Chronic or acute inflammation is a multiple process, which is mediated by activated inflammatory or immune cells. It has been reported that a number of antioxidants including hydroxycinnamic acids and related ester derivatives decrease the levels of some inflammatory mediators [5]. These findings suggest that these phenolics might have potential as an anti-inflammatory drug and reveals at least in part the mechanisms of its anti-inflammatory effect.

V. Use in cosmetics

UV radiation could influence the generation of reactive oxygen/nitrogen species [6] resulting in oxidative damage of the skin. The exposure to sun rays promotes premature skin ageing, erythema, inflammation, immunodepression and photo-carcinogenesis. UV absorbtion of hydroxycinnamic acids and derivatives resulted in formation of a resonance stabilized phenoxyl radicals, wich are able to terminate free radical chain

reactions. Therefore, compositions containing the hydroxycinnamoyl derivatives can be effectively used as cosmetic compositions with anti-aging effect, skin pigmentation improving effect and anti-wrinkle effect by promoting collagen synthesis [7].

VI. Antidiabetic effect

Experiments with diabetic rats showed that supplementation of ferulic acid and its amides at relatively low doses increased the activities of antioxidant enzymes, thereby neutralizing free radicals which, in diabetics, are primary causes of accelerated tissue damage. Ferulic acid also decreased blood glucose and lipid levels [8].

VII. Hepatoprotective and immunostimulating effect

Intake of alcohol results in excessive generation of free radicals, which alter the biomembrane and cause severe damage. The regular ingestion of hydroxycinnamic acids and derivatives may provide substantial protection against alcohol and polyunsaturated fatty acid (PUFA) induced toxicity [10].

Tissue culture experiments in Taiwan have shown that ferulic acid and derivatives stimulate the production of human white blood cells and increases the secretion of IFN-gamma (gamma-interferon), an immune-system stimulatory protein. This suggests a possible value of FA as an immune stimulant.

VIII. Neuroprotective effect [11]

By virtue of their antioxidant properties, the considered phenolics greatly reduce free radical damage to the external and internal membranes of nerve cells without causing nerve cell death. They also appear to encourage the proliferation of at least some types of nerve cells, such as retinal cells. These properties have attracted the interest of researchers looking for treatments for Alzheimer's and other neurodegenerative diseases, and for certain diseases of the retina such as macular degeneration.

IX. Anti-Atherogenic Effect

As a result of their antioxidant properties hydroxycinnamic acids and derivatives effectively reduced the lipid levels (free fatty acids, triglycerides, cholesterol and phospholipids). FA was found to be effective in treating ischemic stroke in China. Moreover, reports have shown that γ-oryzanol, a mixture of feruloyl esters of plant sterols, can lower the cholesterol level in blood and lower the incidence of coronary heart disease [12].

X. Bone generation (anti-osteoporosis) effect

Studies of bone metabolism suggest that ferulic acid prevents bone loss by a mechanism different from that of estrogens. In an era when hormone

replacement therapy is under fire from anti-technology crusaders, ferulic acid may be a welcome addition to the osteoporosis treatment arsenal.

XI. Pulmonary Protective Effect

Nicotine of cigarette smoke increases lipid peroxidation and thus causes oxidative cellular injury, which is believed to play a major role in the pathogenesis of several smoking-related diseases. Administration of phenolic acids protects the cells from oxidative damage [13].

XII. Antimicrobial effect

Phenylpropenoic acids derivatives are known to inhibit various pathogenic microorganisms. The antibacterial effect of free hydroxycinnamic acids, their esters ad sugar analogues are well known [14]. Recently the same effect was reported for the synthetic halogenated cinnamoyl amides [15]. There is limited information about antimicrobial activity of naturally occurring cinnamoyl amides.

XIII. Antiapoptotic Effect

Apoptosis is a certain type of cell death in multicellular organisms. It is suggested that dietary phenolic compounds cause apoptosis in various cancer cells [16] and exhibit anti-apoptotic activity in normal peripheral blood mononuclear cells (PBMCS) [17].

XIV. Athletic performance

Hydroxycinnamic acids and their derivatives have been widely used to enhance athletic performance, both in humans and in race horses. They reduce fatigue by neutralizing free radicals that would otherwise damage the energy-producing structures in cells. This concept has merit theoretically, but has yet to be demonstrated in clinical trials.

2. RESULTS AND DISCUSSIONS

In searching of new biological active phenylpropenoid analogues, we synthesize cinnamic and hydroxycinnamic acid amides and esters and study some of their properties. The obtained compounds are depicted in the Fig. 2. The compounds were synthesized by the standard methods in peptide chemistry, as well as by sonochemical- and microwave accelerated Wittig reaction. Most of the synthesized compounds were tested for their radical scavenging property using DPPH* test. Some of them show activity near to that of the free phenylpropenoic acids, accepted as standard antioxidants.

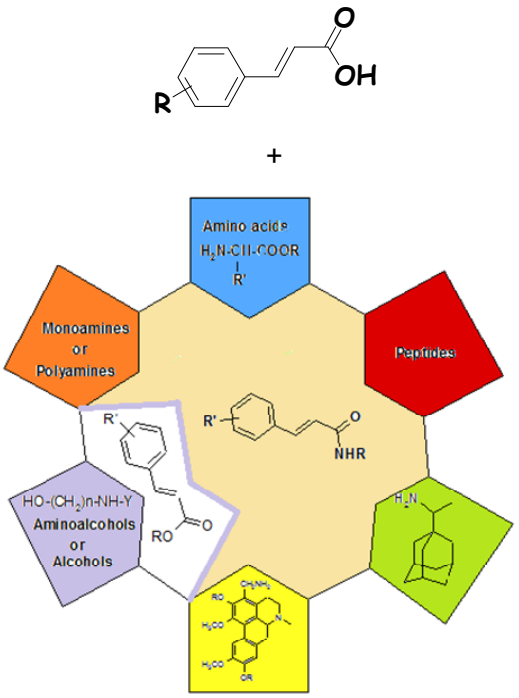

Fig.2.

For example, the aporphine alkaloid- glaucine is known as a natural antioxidant. We synthesized new glaucine derivatives by its coupling with hydroxycinnamic acids and phenylalanine – compounds, containing three structural fragments with a proved antioxidative activity. The N-feruloyl – and sinapoyl-phenylalanyl-3-aminomethyl amides show two times higher radical scavenging activity compared to those amides without phenylalanine rest. Among all the tested compounds, sinapoyl-phenylalanyl-3-aminomethyl glaucine amide possesses the highest activity, even higher than the standard antioxidant –tocopherol [18] (Fig. 3.) On the other hand we established that the radical scavenging activity of the synthesized sinapoyl- and caffeoyl amides of cysteine against DPPH* are superior to the standards as ferulic acid, eugenol and isoeugenol. The same amides showed antibacterial activity against Streptococcus pyogenes, even higher in comparison with the free hydroxycinnamic acids.

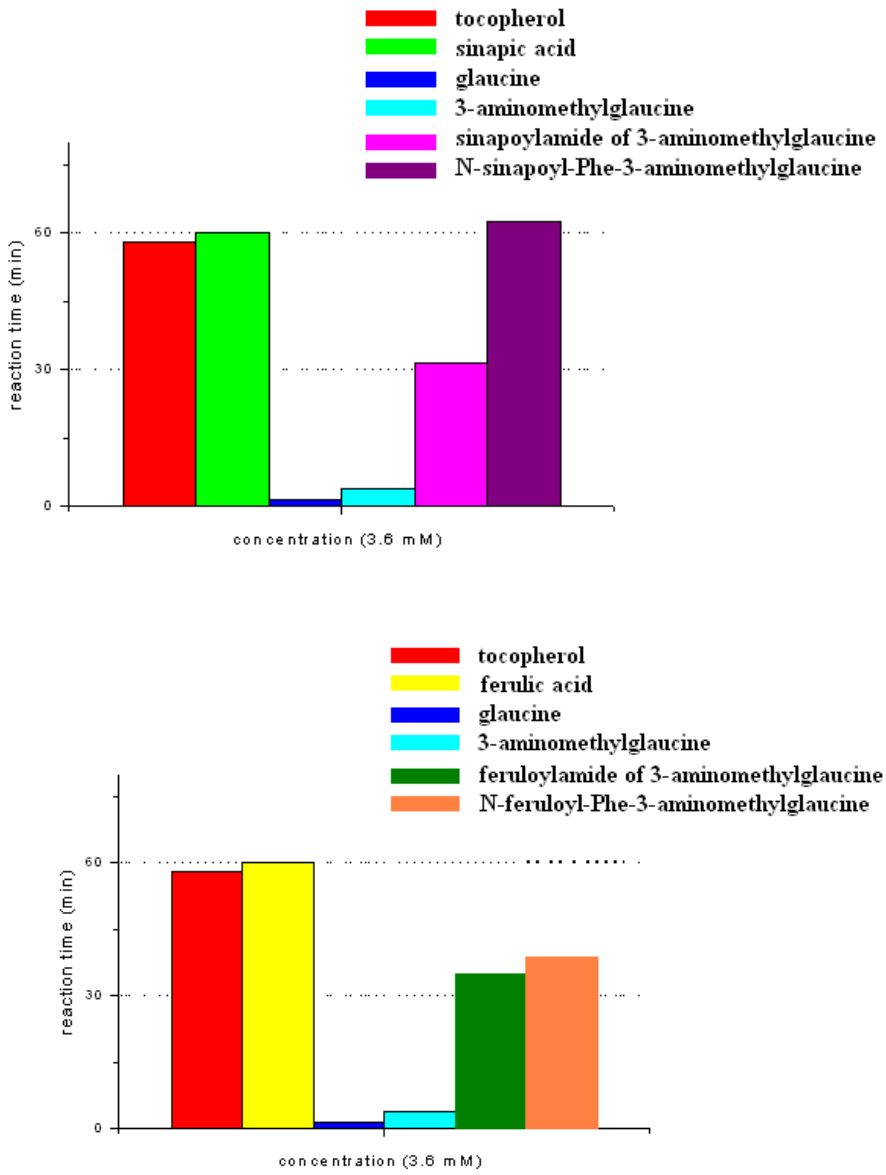

Fig. 3.

Our last investigations concern the synthesis of cinnamoyl and hydroxycinnamoyl amides of some biogenic amines (tryptamine, tyramine, phenylethylamine). The radical scavenging properties of these compounds are compared to that of the corresponding amides of their amino acid precursors (Table 1). It is evident that the amides of aromatic amines are more active than those of their precursors. The synthesized compounds are more active than the listed in the table standards.

Table 1.

	(%) RSA	
	3.6 mM	
	Reaction time (min)	
AH	10'	20'
Quercetin	**76.01±0.08**	**78.05±0.06**
D,L α-Tocopherol	**62.91±0.05**	**73.31±0.03**
Isoeugenol	**17.56±0.01**	**19.04±0.01**
Caffeic acid	**88.04±1.52**	**91.83±0.65**
Caffeoyl tryptophan methyl ester	80.1±0.8	87.9±0.3
Caffeoyltryptamine	90.41±0.37	90.82±0.36
Caffeoyl tyrosine methyl ester	89.61±0.33	90.20±0.18
Caffeoyltyramine	89.75±0.13	89.95±0.22
Caffeoyl phenylalanine methyl ester	90.34±0.11	90.49±0.15
Caffeoylphenylethylamine	93.43±0.09	94.21±0.96

DPPH radical scavenging activity of HCA-amides. Each experiment was performed in triplicate. The values are given as the mean ± standard error.

The antimicrobial activity of the synthesized amides of amino acids is tested against Bacillus subtilis, Escherichia coliD1 and Klebsiella pneumonia. Among the tested compounds the highest activity is shown for feruloyl- and sinapoyl amides of phenylalanine and tyrosine. Feruloyl tyrosine amide is active against Bacillus subtilis, and the most active against Escherichia coliD1 are feruloyl- and sinapoyl phenylalanine amides [19].

3. ACKNOWLEDGEMENTS

We gratefully acknowledge the financial support from the South-West University “N.Rilski” – Blagoevgrad, Bulgaria (project SRP-A7).

4. LITERATURE

[1] Srinivasan, M., Sudheer, A.R., Menon, V. P. (2007) Ferulic Acid: therapeutic potential through its antioxidant property. *J Clin Biochem Nutr.*; 40, 92–100.

[2] Loo, G. (2003) Redox-sensitive mechanisms of phytochemical mediated inhibition of cancer cell proliferation. *J. Nutr. Biochem.* 14, 64–73.

[3] Vermeulen, K., Van Bockstaele, D.R., Berneman, Z.N. (2003) The cell cycle: a review of regulation deregulation and therapeutic targets in cancer. *Cell Prolif.* 36, 131–149.

[4] Kawabata, K., Yamamoto, T., Hara, A., Shimizu, M., Yamada, Y., Matsunaga, K., Tanaka, T., Mori, H. (2000) Modifying effects of ferulic acid on azoxymethane-induced colon carcinogenesis in F344 rats. *Cancer Lett.* 157, 15–21.

[5] Murakami, A., Nakamura, Y., Koshimizu, K., Takahashi, D., Matsumata, K., Hagihara, K., Taniguchi, H., Noumura, E., Hosoda, A., Tsuno, T., Maruta, Y., Kim, H.W., Kawabata, K., Ohigashi, H. (2002) FA 15, a hydrophobic derivative of ferulic acid, suppresses inflammatory responses and skin tumor promotion: comparison with ferulic acid. *Cancer Lett.* 180,121–129.

[6] Graf, E. (2000) Antioxidant potential of ferulic acid. *Free Radic. Biol. Med.* 28,1249–1256.

[7] WO/2008/018683. Hydroxycinnamic acid derivatives and preparation method thereof and cosmetic composition containing it.

[8] Noumura, E., Kashiwada, A., Hosoda, A., Nakamura, K., Morishita, H., Tsuno, T., Taniguchi, H. (2003) Synthesis of amide compounds of ferulic acid and their stimulatory effects on insulin secretion *in vitro*. *Bioorg. Med. Chem.*11, 3807–3813.

[9] Sultana, R., Ravagna, A., Mohmmad-Abdul, H., Calabrese, V., Butterfield, D.A. (2005) Ferulic acid ethyl ester protects neurons against amyloid beta-peptide (1-42)-induced oxidative stress and neurotoxicity: relationship to antioxidant activity. *J. Neurochem.* 92, 749–758.

[10] Rukkumani, R., Aruna, K., Varma, P.S., Menon, V.P. (2004) Influence of ferulic acid on circulatory prooxidant antioxidant status during alcohol and PUFA induced toxicity. *J. Physiol. Pharmacol.* 55, 551–561.

[11] Scapagini, G., Butterfield, D.A., Colombrita, C., Sultana, R., Pascale, A., Calabrese, V. (2004) Ethyl ferulate, a lipophilic polyphenol, induces HO-1 and protects rat neurons against oxidative stress. *Antioxid. Redox Signal.* 6, 811–818.

[12] Hiramatsu, K., Tani, T., Kimura, Y., Izumi, S.I., Nakane, P.I. (1990) Effect of γ-Oryzanol on atheroma formation in hyper-cholesterolemic rabbits.*Tokai. J. Exp. Clin. Med.*15, 299–306.

[13] Sudheer, A.R., Kalpana, C., Srinivasan, M., Menon, V.P. (2005) Ferulic acid modulates lipid profiles and prooxidant/antioxidant status in circulation during nicotine-induced toxicity: A dose dependent study.*Toxicol. Mech. Methods.* 15, 375–381.

[14] Narasimhan, B., Belsare, D., Pharande, D., Mourya, V., Dhake, A. (2004) Esters, amides and substituted derivatives of cinnamic acid: synthesis, antimicrobial activity and QSAR investigations *Eur. J. Med. Chem.* 39, 827-834

[15] Fu, J., Cheng, K., Zhang, Z., Fang, R.,. Zhu, H. (2010) Synthesis, structure and structure–activity relationship analysis of caffeic acid amides as potential antimicrobials *Eur. J. Med. Chem.* 45, 2638-2643

[16] Taraphder, A.K., Roy, M., Bhattacharya, R.K. (2001) Natural products as inducers of apoptosis: implication for cancer therapy and prevention. *Curr. Sci.* 80, 1387–1396.

[17] Khanduja, K.L., Avti, P.K., Kumar, S., Mittal, N., Sohi, K.K., Pathak ,C.M. (2006) Anti-apopototic activity of caffeic acid, ellagic acid and ferulic acid in normal human peripheral blood mononuclear cells: A Bcl-2 independent mechanism. *Biochim. Biophys. Acta.* 1760, 283–289.

[18] Spasova, M., Philipov, S., Avramov, G., Milkova, Ts., (2008) In *Peptides*: Hilkka Lankinen (Ed.) Conjugation of glaucine to hydroxycinnamoyl amino acid amides**,** 48-49.

[19] Spasova, M. (2006) PhD Thesis “Synthesis of new derivatives of substituted cinnamic acids with potentional biological activity”.

Inductively coupled plasma atomic emission spectrometry - determination of platinum and palladium in environmental materials after pre concentration/separation procedure

Petranka P. Petrova[a], Serafim V. Velichkov[b], Ivan P. Havezov[b], Paunka Vassileva[b], Penka Tzvetkova[b], Nonka N. Daskalova[b],

[a]South-West University “Neofit Rilski” Blagoevgrad, Bulgaria
[b]Institute of General and Inorganic Chemistry, Bulgarian Academy of Sciences, Acad. G. Bontchev Str. bl. 11

***Abstract**: Platinum group elements (PGEs) were doped in automobile catalytic converters. Since the introduction of catalytic converters, there has been a clear link between their use and the increasing emissions of these elements in the environment. By using a radial viewing 40.68 MHz inductively coupled plasma atomic emission spectrometry and selected analysis lines the following detection limits in ng g^{-1} were obtained: Pt -1700 and Pd-1440. Improvement of the detection limits in the determination of platinum and palladium in environmental materials was achieved by pre concentration of analytes and by separation of matrix elements Al, Ca, Fe, Mg and Ti. The separation and pre concentration procedure was carried out at pH=1. A new column method with **2-** mercaptobenzimidazole immobilized on an activated carbon was proposed. The following detection limits in ng g^{-1} were obtained: Pt – 3.3 ng g^{-1} and Pd - 4 ng g^{-1}.*

***Keywords:** ICP-AES, detection limits, platinum, palladium, activated carbon, sorption, and column method*

1. INTRODUCTION

Platinum group elements (PGEs) were included in automobile catalytic converters and the converters have been used in many car exhaust systems [1]. Since the introduction of catalytic converters, there has been a clear link between their use and the increasing concentration of these elements in the environment [2]. PGEs and their complex salts cause allergy, asthma, rhino-conjunctivitis and different serious health problems [3].

The progress in the study of the occurrence and distribution of PGEs in environmental materials depends on the possibilities of their

quantitative determination. With introduction of ICP-AES and ICP-MS the possibilities for determination of PGEs were extended [4 - 6].

The basic problems in the determination of PGEs in environmental materials by ICP-AES are trace element concentrations and complex sample matrices. The spectral interferences in the presence of complex matrices influence on the accuracy and detection limits in the determination of trace of elements by ICP-AES. In the direct ICP-AES determination of PGEs the following detection limits (in ng g^{-1}) can be reached: Pt -1700 and Pd-1440 [6].

Improvement of the detection limits can be achieved by pre concentration of platinum and palladium after separation of matrix constituents [7-11]. The interest in activated carbons is determined by their unique properties such as large specific surface area, strongly developed micro porosity and the possibility to modify their surface and texture [12- 18].

The purpose of the present paper is to improve the detection limits in the determination of Pt and Pd in environmental materials by ICP-AES below 10 ng g^{-1} by developing a new column method with **2-**mercaptobenzimidazole immobilized on an activated carbon for separation of matrix elements Al, Ca, Fe, Mg, Ti and pre concentration of analytes.

2. EXPERIMENTAL

2.1. Instrumentation

The experiments were performed with a 40.68 MHz ICP HORIBA Jobin Yvon Ultima 2 ICP system (Longjumeau, France). The sample solutions were introduced in ICP- AES by Meinhard, concentric glass and ultrasonic nebulizers (Courtesy of Cetac Thechnologies, Omaha, Nebraska, USA). The operating conditions are given in Table 1.

Tab. 1: Operating conditions

Incident power /(kW)	1.00
Outer argon flow rate/(l min^{-1})	13
Auxiliary gas /(l min^{-1})	0
Sheath gas flow rate/(l min^{-1})	0.2
Liquid uptake rate/(ml min^{-1})	1.0
Carrier gas flow rate (l min^{-1})	0.4

2.2. Reagents, buffer solutions, certified reference material

Reagents of highest purity grade were used: 30% HCl, 65% HNO_3, 47 % HBr (Suprapur, Merck), and bi-distilled water from quartz

apparatus. Activated carbon GAS 1240 (Norit N.V. Netherlands) with specific surface area 1240 $m^2 g^{-1}$.

Buffer solutions (Merck): pH = 1 (0.1 M HCl), pH =2 (0.01 M HCl), pH = 3 (citric acid- hydrochloric acid), pH =4 (citric acid- hydrochloric acid), pH = 5 (citric acid – sodium hydroxide).

Certified reference material BCR-723 for the determination of platinum and palladium in road dust.

2.3. Modification of activated carbon

2-mercaptobenzimidazole-modified activated carbon was prepared by the following steps: First step: The carbon was heated in a furnace at 600^0C for 3 h in inert atmosphere. Then the sample was cooled down to room temperature in argon. Second step: 3 g of activated carbon were heated for 1 h at 200^0C in vacuum, whereupon 10 ml of a 2 % (wt) solution of 2-mercaptobenzimidazole in ethanol were added and the mixture was allowed to stand at 20^0C for 2 h to facilitate better penetration of the modifier into the pores of activated carbon. Then the solvent was evaporated at 90–100^0C. Then heated for 1 h at 200^0C in vacuum again and treated the sample as described above. This procedure is repeated three times. The modified carbon was washed with distilled water and 1M HCl until attaining a constant pH value of the washing water, and then dried at 100^0C for 6 h.

2.4. Decomposition procedure

Extraction procedure of traces of Pt and Pd in acid mixture (HBr /HNO_3) in an apparatus, described in [ISO 11466:1995 (E)] was used for digestion of certified reference material BCR-723 (road dust). A total of 3.0 g subsample was weighed in a reaction vessel; 3 ml of bi-distilled water was added to obtain slurry, followed by 15 ml of HBr and 15 ml HNO_3. The sample was allowed to stand for 16 h at room temperature for slow oxidation of the organic matter and reduction of the gases. Then it was heated under reflux until boiling for 2 h and allowed to cool slowly at room temperature. The supernatant solution was filtered through a filter (blue band), the solution was collected in a 100 ml graduated flask, the residue was washed with 0.1 M HCL and final solution was filled up to the 100 ml with 0.1 M HCL.

3. RESULTS AND DISCUSSION

3.1. Detection limits in the determination of Pt and Pd in pure solvent

The detection limit of the analytes in pure solvent (or dilute acid) is defined by Eq. (1):

$$C_L = 2\sqrt{2} \times 0.01 \times RSDB \times BEC \quad (1),$$

where BEC is background equivalent concentration in pure solvent; RSDB=1% is the relative standard deviation of the pure solvent [11]. Table 2 shows the detection limits for Pt and Pd under optimal operating conditions (Table 1) by using the most prominent lines.

Tab. 2: Detection limits for Pt and Pd in pure solvent, obtained by 40.68 MHz ICP and different nebulizers

Analysis lines, λ, nm	Detection limits, ng ml^{-1}	
	Meinhard, concentric glass nebulizer	Ultrasonic nebulizer
Pt II 203.646	7.0	1.0
Pd II 229.651	11.0	1.2

3.2. Investigation of the conditions for sorption of platinum and palladium on 2-mercaptobenzimidazole -modified activated carbon

The sorption behavior of the 2- mercaptobenzimidazole-modified activated carbon towards Pt and Pd was studied. A 50 mg portion of the activated carbon was weighed and transfered in glass bottles with stoppers (volume 25 ml). 0.1 ml of solution with concentration 100 μg ml^{-1} for platinum and palladium separately in 0.1 M HCl were added. Sorption behavior was studied in an acidity range between pH =1 and pH =5. The acidity was measured using automatically pH – meter. The final volume was 10 ml and each bottle contains 50 mg activated carbon and 10 μg platinum or palladium at corresponding acidity. All bottles were fixed vertically on the platform and were shaken on the shaken machine for 2 h at room temperature. In order to eliminate possibility for reduction of Pt and Pd ions, the experiments were carried out in room without direct sun light. Five parallel experiments for each analyte for pH =1, 2, 3, 4 and 5 were carried out. The activated carbon was allowed to settle. The concentration of Pt and Pd in supernatant solution was determined by ICP-AES under experimental conditions, shown in Table 1. The analytes are not detected in solution only at pH = 1. The detection limits for Pt and Pd are shown in Table 2. Hence, at pH =1, 100 % Pt and 100 % Pd are sorbed on the activated carbon immobilized with 2-mercaptobenzimidazole.

3.3. Method for extraction of platinum and palladium, sorbed on activated carbon immobilized with *2*- mercaptobenzimidazole at pH =1

Different acids and acid mixtures were used for efficient extraction of Pt and Pd from activated carbon. An appropriate procedure, which

ensure 100 % extraction of the analytes was not found. In the present paper a procedure including dry-ashing was selected. The following parameters were optimized: temperature conditions for dry-ashing, the material of the vessel and conditions for dissolution of the residue. The following procedure was used: the resulting solution obtained in Section 3.2 was filtrated through a filter (blue band); the filter with activated carbon was dried in drying-oven at 90 ^{0}C; the activated carbon along with a filter was transferred in quartz crucible and the sample was heated at 450 ^{0}C (1 h) and 850 ^{0}C (1 h) in furnace; the quartz crucible was allowed to cool slowly at room temperature and after that the crucible is get into reaction flask of an apparatus, described in ISO 11466:1995 (E); an acid mixture HNO_3/HBr (3 ml HNO_3+ 3 ml HBr) was used for dissolution of the so prepared residue; the sample was heated under reflux until boiling for 1 h and allowed to cool slowly at room temperature. The content of the reaction container was transferred quantitatively to a 10 ml graduated flask and filled up to the mark with 0.1 M HCl. The solution was introduced in ICP-AES. Table 3 shows the mean values for five replicates and the confidence interval of the mean value ΔX for statistical confidence P=95%.

Tab. 3: Exctraction of Pt and Pd from activated carbon immobilized with ***2***-mercaptobenzimidazole

Element	Total content of platinum or palladium in activated carbon, μg	
	Added	Found - mean value (X) ± ΔX from five replicates
Pt	10.0	10. 0 ± 0.37
Pd	10.0	9.98 ± 0.60

3.4. Determination of major elements by ICP–AES in final sample solution, derived after dissolution of certified reference material BCR 723 (road dust).

A certified reference material was dissolved using procedure given in Section 2.4.One ml of the basic sample solutions were diluted (dilution factor = 25) in order to eliminate the multiplicative interference. The concentrations of Al, Ca, Fe, Mg and Ti are shown in basic sample solution (Table 4.)

Tab. 4: Content of Al, Ca, Fe, Mg and Ti in solution (in μg ml^{-1}) derived after dissolution of the certified reference material

Analysis lines, nm	Concentration of matrix elements, in ***μg ml^{-1}***
Al II 394.401	660
Ca I 422.673	1656

Fe II 238.204	1030
Mg II 279.806	760
Ti II 334.941	26

3.5. Investigation of the conditions for sorption of Pt and Pd in the presence of matrix elements Al, Ca Fe, Mg and Ti on *2*-mercaptobenzimidazole -modified activated carbon

A 50 mg portion of the activated carbon was weighed and transfer in glass bottles with stoppers (volume 25 ml). To the activated carbon were added: 1 μg ml^{-1} Pt + 1 μg ml^{-1} Pd and matrix elements in concentrations shown in Table 4. The experiment was carried out at pH =1. The final volume was 10 ml. The mixture was shaken on the shaken machine for 2 h at room temperature. Five replicates were obtained. The sample solution was filtered through a filter blue band.

Tab. 5: Contents of Pt, Pd, Al, Ca, Fe, Mg and Ti in basic sample solution

Elements	Concentrations, in μg ml^{-1}
Pt	1
Pd	1
Al	600
Ca	1410
Fe	1000
Mg	760
Ti	25

The concentrations of Pt and Pd were determined in basic sample solution. The matrix elements were determined in solution which was diluted 25 times. The concentrations of Pt, Pd, Al, Ca, Fe, Mg and Ti in basic solution are show in Table 5. Hence, under these experimental conditions Pt and Pd cannot be sorbed on the activated carbon.

The influence of concentration of matrix elements on the sorption efficiency was investigated. The experimental results show that for concentration of matrix elements 10 times lower in comparison of the corresponding values shown in Table 4, the matrix elements were delectated 100 % in solution and Pt and Pd were sorbed 100 % on the activated carbon.

3.6. Column method with *2*- mercaptobenzimidazole immobilized on an activated carbon

By using column containing activated carbon immobilized with *2*-mercaptobenzimidazole *and by varying the size of the column (bore and length), the amount of the activated carbon, the linear flow rate of the solution the optimal conditions for the separation of matrix*

elements from the analytes and pre concentration of Pt and Pd were established. *The parameters are: column with bore = 3 mm, length = 9 mm, amount of activated carbon = 0.4 g, flow rate of the solution =4 mil* min^{-1}*. The experiments were carried out at room temperature. The* preliminary investigations were carried out by using solution, containing 1 μg ml^{-1} Pt + 1 μg ml^{-1} Pd and concentration of matrix elements 10 times lower in comparison of the corresponding values shown in Table 4 (Section 3.6). The column was washed with 0.1 HCl. The matrix elements were quantitatively detected in solution. *The column with activated carbon* was dried in drying-oven at 90 ^{0}C. The procedure for dry ashing and dissolution was applied in accordance with (Section 3.3). The final sample solution was 10 ml. The solution was introduced in ICP -AES.

The new column method with *2*- mercaptobenzimidazole-immobilized on an activated carbon was applied for pre concentration/ separation in the determination of Pt and Pd in *certified reference material BCR -723* (road dust). The final sample solution was introduced in ICP-AES with ultrasonic nebulizer. The final solution, obtained in Section 2.4 was diluted up to the 1000 ml. The final acidity was pH =1. The acidity was measured by using automatically pH-meter.

Table 6 shows the detection limits in the determination of Pt and Pd with respect to the dissolved solid sample, in ng g^{-1} (column 2) by using above pre concentration/separation procedure, content of Pt and Pd in the certified reference material BCR-723, obtained by ICP-AES (mean values X, for n=4 replicates and the confidence interval of the mean value ΔX for statistical confidence P=95% and f=n−1 =3 (column 3), as well as the RSD of the analytical results (column 4). Column 5 lists the certified values.

Tab. 6: Detection limits with respect to the dissolved solid sample in ng g^{-1} in the determination of Pt an Pd in certified reference material BCR-723 (road dust) by using the present method, contents of Pt, Pd in ng g^{-1}, RSD of the analytical results and certified values in ng g^{-1}

Element	Detection limits, ng g^{-1}	Concentration, ng g^{-1}	RSD, %	Certified values, ng g^{-1}
Pt	3.3	80.9 ± 0.05	3.0	81.3
Pd	4.0	6.2 ±0.0.04	2.5	6.0

The results obtained by the present method agree well with the certified values of the reference material BCR-723. Therefore, this method can be used successfully in the determination of Pt and Pd in environmental material.

REFERENCES

[1]. Kindon A.I. and Davis R.F, in Engineered Materials Handbook, Volume 4 (1991), Ceramic and glasses, Thechnical Chaiman, Schneider S.J., ASM International, Metal park,OH

[2]. Zereini F,. Skerstupp B., Alt F, Helmers E.,Urban H., (1997) Geochemical behavior of platinum-group elements (PGE) in particulate emissions by automobile exhaust catalysts: experimental results and environmental investigations, Sci. Total Environ. 206, 137-146.

[3]. Merget R., Rosner G. (2001) Evaluation of the health risk of platinum group metals emitted from automotive catalytic converters, Sci. Total Environ. 270, 165–173.

[4]. Rauch S., Motelica-Heino M, Morrison G.M.,. Donard O.F.X (2000), Critical assessment of platinum group element determination in road and urban river sediments using ultrasonic nebulisation and high resolution ICP-MS, J. Anal. Atom. Spectrom. 15 329–334.

[5]. Wiseman C.L.S., Zereini , F.(2009) Airborne particulate matter, platinum group elements and human health: a review of recent evidence, Sci. Total Environ. 407, 2493–2500.

[6]. Petrova P. Velichkov S. Velitchkova N. Havezov I., Daskalova N. (2010) Problems, possibilities and limitations of inductively coupled plasma atomic emission spectrometry in the determination of platinum, palladium and rhodium in samples with different matrix composition, Spectrochimica Acta Part B 65, 130–136.

[7]. Liska I., Fifty years of solid-phase extraction in water analysis-historical development and overview, J. Chromatogr. A 885 (2000) 3 - 13

[8].Kilian K., Pyrzynska K., (2001) Preconcentration of metal ions on porphyrin-modified sorbents as pretreatment step in AAS determination, Fresenius J. Anal. Chem. 371, 1076 –1078

[9]. Chakrapani G., Mahanta P.L., Murty D.S.R. , Gomathy B. (2001) Preconcentration of traces of gold, silver and palladium on activated carbon and its determination in geological samples by flame AAS after wet ashing, Talanta 53, 1139–1147

[10]. Pribylov A. A., Kalinnikova I. A., and Regent N. I. (2003*)* Features of sulfur hexa fluoride adsorption on carbon adsorbents, Russian Chemical Bulletin, International Edition 52, 882—888

[11]. Walczyk A., Svatowski A., Pakula M., and Biniak S.(2005) Electrochemical studies of the interaction between a modified activated carbon surface and heavy metal ions, Journal of Applied Electrochemistry 35, 123–130

[12]. Jankowski K., Jackowsk A.,Łukasiak P. (2005) Determination of precious metals in geological samples by continuous atomic emission spectrometry after preconcentration on activated carbon, Analytica Chimica Acta 540 197–205.

[13]. Someda H. H. , Sheha R. R.(2008) Solid Phase Extractive Preconcentration of Some Actinide Elements Using Impregnated Carbon, Radiochemistry. 50, 56 - 63.

[14]. Mikuła B, Puzio B., (2008) Determination of trace metals by ICP-OES in plant materials after preconcentration of 1,10-phenanthroline complexes on activated carbon, Talanta 71, 136–140

[15]. Ghaedi M., Shokrollahi A., Kianfar A.H., Pourfarokhia A., Khanjaria N.,. Mirsadeghia A.S, Soylak M. (2009), Preconcentration and separation of trace amount of heavy metal ions on bis(2-hydroxy acetophenone)ethylendiimine loaded on activated carbon, Journal of Hazardous Materials 162 1408–1414.

[16]. Ensafi A.A., Khayamian T., Karbasi M. (2003) On-line preconcentration system for lead (II) determination in waste water by atomic absorption spectrometry using active carbon loaded with pyrogallol red, Analytical Sciences 19, 19 953 -956.

[17]. Ferreira A.C., Korn M.A., Ferreira S.L.C. (2004), Multivariate Optimization in Preconcentration Procedure for Manganese Determination in Seawater Samples by FAAS, Microchim. Acta 146, 271 -278

[18]. Gentsheva G., Vasileva P., Tzvetkova P, Lakov L., Peshev O, Ivanova E.(2008)Activated carbon sorbent with thioetheric sites- preparation and characterization, J. Porous Mater., 15, 331-334.

Voltammetric Determination of Diphenyl ether herbicides in natural waters.

Vít Novotný, Jiří Barek
Faculty of Science, Charles University in Prague, Department of Analytical Chemistry,
UNESCO Laboratory of Environmental Electrochemistry, Prague, Czech Republic, Hlavova 8, CZ-128 43
E-mail: novotny1@natur.cuni.cz

Abstract: *The determination of Aclonifen, Acifluorfen, Nitrofen and Oxyfluorfen by Differential Pulse Voltammetry at a meniscus modified silver solid amalgam electrode is discused. The optimum conditions regarding pH are found. The detection limit for the determination of Aclonifen in deionised water is $2 \cdot 10^{-7}$ mol·L^{-1}. The detection limit for the determination of AC in Vltava river water is $3 \cdot 10^{-8}$ mol·L^{-1}. The detection limit for the determination of Acifluorfen is $3 \cdot 10^{-6}$ mol·L^{-1}. The detection limit for the determination of Nitrofen is $9 \cdot 10^{-7}$ mol·L^{-1}. The detection limit for the determination of Oxyfluorfen is $7 \cdot 10^{-7}$ mol·L^{-1}. AgSAE is therefore a suitable sensor for the determination of these substances. Furthermore, a method of determination of Acifluorfen at a carbon paste electrode is developed and the detection limit reached is $5 \cdot 10^{-7}$ mol·L^{-1}. So this sensor proves to be even more efective for aclonfen determination.*

Kewords: *Aclonifen Acifluorfen, Oxyfluorfen, Nitrofen, Differential pulse voltammetry, Silver solid amalgam electrode, Carbon paste electrode, River water.*

1. Introduction

Diphenyl ether herbicides (DPhEHs) are a group of pesticides that destroy weeds by inhibiting the enzyme protoporfyrinogen oxidase [*1*]. The are being used for crop protection in the cultures of cultures of rice, soy, corn, potatoes, peas, carrot, and sunflowers [*2*]. The representatives of this group studied in this work are Aclonifen, Acifluorfen, Nitrofen and Oxyfluorfen. Although not very toxic toward mammals, they have some worrying side effects such as high toxicity for aquatic organisms and hepatotoxicity in mammals in high doses [*3*]. Many are listed as a suspected human carcinogens and many substances from this group are endocrine disruptors and have adverse effects on blood formation [*4, 5*]. Nitrofen is not used anymore for

agricultural purposes but is an important model substance for the study of chemicaly induced birth defects [*6*], the other substances enjoy widespread agricultural use. Considering the wide use of the substances in focus, and the risks connected with their usage, it is highly desirable to develop reliable analytical methods for determination of these substances. Many methods already exist, but most use laborious and expensive sophisticated techniques, such as HPLC-MS and GC-MS [*7-10*]. Voltammetry proves to be an efficient and cheap method for the determination of electroactive substances in trace amounts and Nitrated DPhEs are easily reducible [*11, 12*]. A suitable electrode has to be found however. Mercury dropping and hanging electrodes offer perfect performance but are not popular anymore due to issues with mercury toxicity and mechanical stability of the sensor [*13*]. Meniscus modified Silver Solid Amalgam Electrodes (m-AgSAE) turn out to be an excellent replacement [*14*]. They are slightly less sensitive, but no mercury is consumed during measurements and the silver amalgam used is nontoxic. Problems with electrode passivation can be overcome by suitable means of regeneration of the electrode surface. Overall they are reliable, cheap, easy to handle and sensitive sensors for various pollutants in trace amounts [*14, 15*]. Carbon paste electrodes (CPE) also offer high sensitivity, mechanical robustness and a great potential for chemical modification [*16*]. If carbon microspheres are used as a part of the paste the are also suitable for measuring in matrices containing high proportion of organic solvent.

2. Materials and methods

The stock solution of Oxyfluorfen (2-chloro-1-(3-ethoxy-4-nitrophenoxy)-4-(trifluoromethyl) benzene 99%, Sigma – Aldrich Laborchemikalien, Germany) in methanol (c = 1·10-3 mol·L-1) was prepared by dissolving 0.0362 g of the substance in 100 mL of methanol (Lachema, Brno, Czech Republic).

The stock solution of Nitrofen (2,4-dichlorophenyl 4-nitrophenyl ether 99%, Sigma – Aldrich Laborchemikalien, Germany) in methanol (c = 1·10-3 mol·L-1) was prepared by dissolving 0.0284 g of the substance in 100 mL of methanol (Lachema, Brno, Czech Republic)

The stock solution of Acifluorfen (5-[2-chloro-4-(trifluoromethyl)phenoxy]-2-nitrobenzoic acid 99%, Sigma – Aldrich Laborchemikalien, Germany) in deionized water (only 2·10-4 mol·L-1 concentration due to low solubility in water) was prepared by dissolving 0.0182 g of the substance in 250 mL of deionized water (Milipore, USA) All solutions were kept in a freezer at 4°C.

The stock solution (c $1 \cdot 10^{-3}$ mol·L^{-1}) of Aclonifen (2-chloro-6-nitro-3-phenoxybenzenamine 99%, Sigma–Aldrich Laborchemikalien, Germany.) has been prepared by dissolving 0,02648 g of AC in 100 mL of methanol. Solutions of lower concentrations were prepared by precise diluting of the stock solution with methanol. The stock solution was kept in the dark in the refrigerator. The stability of the stock solutions has been checked by UV-VIS spectrophotometric measurements. The stock solution of AC was stable for at least 6 months in the conditions under which it was kept, other stock solutions were stable for more than 18 months. Other used chemicals were boric acid, acetic acid (99%), phosphoric acid (85%), sodium hydroxide, potassium chloride, all chemicals p. a., Lachema Brno, Czech Republic. Methanol p.a. Merck, Germany was used. Britton-Robinson buffers of the desired pH were prepared by mixing of 0,2 mol·L^{-1} NaOH with a solution containing 0,04 M boric acid, phosphoric acid and acetic acid. Measurements of pH were performed on a Jenway 3510 (Jenway, Essex, Great Britain) pH-meter with a combined glass membrane electrode (type 924 005) The electrode was calibrated by standard buffer solutions in water. Deionized water (Millipore, USA) was used as a solvent. Palmsens Electrochemical Sensor Interface (Palm Instruments BV, Ruitercamp, The Netherlands) and the PalmsensPC software was used for differential pulse voltammetric determination of Aclonifen at m-AgSAE. The software was running under the Windows XP (Microsoft Corp.) operating system. Other voltammetric measurements were performed on Eco-Tribo Polarograph using PolarPro 4.0 software (all Polaro-Sensors, Prague, Czech Republic). The software was driven by the operational system Microsoft Windows 98 (Microsoft Corporation) Pulses of width of 80 ms and height of –50 mV were used while performing DPV. A polarization rate of 20 mV/s, and potential resolution of 2 mV were used. All measurements were performed using a three electrode system. A silver chloride electrode (1 mol·L^{-1} KCl) type RAE 113, Monokrystaly, Turnov, Czech Republic, a platinum wire auxiliary electrode and a meniscus modified silver solid amalgam electrode that was purchased from Polaro Sensors, Prague, Czech Republic. After extended periods of storage and if the behavior of the electrode starts changing the meniscus is renewed by immersing the electrode in a vial containing a small quantity of mercury, the process is called amalgamation. Each day at the start of using the electrode it was activated in 0.2 M KCl solution by applying of a potential of -2200 mV for 300s, as described in [*17*]. Measured solutions of AF were prepared by adding an appropriate amount of the stock solution to a 10 mL volumetric flask, and then filling the flask up to 10 mL with BR buffer of the desired pH.

Measured solutions of AC, NF and OF were prepared by adding an appropriate amount of the stock solution to a 10 mL volumetric flask, filling with methanol to a total volume of 5 mL and then filling the flask up to 10 mL with BR buffer of the desired pH. Model samples of AC in the concentration range ($2 \cdot 10^{-6}$ - $1 \cdot 10^{-5}$) mol·L^{-1} in drinking water were prepared by making a $1 \cdot 10^{-5}$ mol·L^{-1} solution of AC in drinking water. The drinking water was taken after letting it flow for 5 minutes to remove any impurities or gas pockets in the tubing. The apropriate amount of the stock solution was then added to a 10 mL volumetric flask, filled to 5 mL with pure drinking water and then filled up to 10 mL by BR buffer pH 12. The same was true for the ($2 \cdot 10^{-7}$ - $1 \cdot 10^{-6}$) mol·L^{-1}concentration range, but a $1 \cdot 10^{-6}$ mol·L^{-1} stock solution has been used instead. Analogous procedure was used for the determination in Vltava river water. The river water was taken from the surface of the river into a clean PET bottle and was stored in a refridgerator in a glass vessel for about 2 days during the experiments. Values of points in calibration curves are arithmetic averages of 3 measurements. Error bars are derived from the same data. Detection limits are calculated according to the formula LOD = $3{,}3 \cdot \sigma / S$ where σ is the standard deviation of 10 measurements of the lowest concentration when the signal can still be evaluated and S is the slope of calibration curve in the vicinity of that concentration [*18*].

3. Results and discussion

Voltammetric behavior of AC (c 10^{-5} mol·L^{-1}) at m-AgSAE was studiend in a mixture of methanol and BR buffer of the desired pH (1:1) in the BR buffer pH range 2-12. The pH chosen for the determination of AC at m-AgSAE is 12, as the AC peak is the highest and best developed under these conditions. This pH was also used for all the model samples of real matrices. The voltammograms of AC in the concentration range ($2 \cdot 10^{-8}$ - $1 \cdot 10^{-7}$) mol·L^{-1} in Vltava river water can be seen in Fig. 1. The calibration dependence is linear in the concentration range from $2 \cdot 10^{-7}$ mol·L^{-1} to $10 \cdot 10^{-5}$ mol·L^{-1} and lower concentrations could not be determined. The detection limit reached is $2 \cdot 10^{-7}$ mol·L^{-1}.

Voltammetric behavior of AF (c 10^{-5} mol·L^{-1}) at m-AgSAE was studied in a solution of BR buffer of the desired pH (1:1) in the BR buffer pH range 2-12. The peak height and shape at pH are optimal and so pH 12 has been chosen for quantitation. The DP voltammograms of AF in the concentration range $2 \cdot 10^{-6}$ – $1 \cdot 10^{-5}$ mol·L^{-1} are shown in Fig. 2.

Voltammetric behavior of AF (c 10^{-5} mol·L^{-1}) using DPV at CPE has been studied in BR buffer in the pH range 2-12. The optimum BR

buffer pH for the determination is 2, as the peak of the substance is highest under these conditions. The DP voltammograms of AF at CPE in the concentration range $2 \cdot 10^{-7}$ – $1 \cdot 10^{-6}$ mol·L^{-1}can be seen on Fig. 3.

Voltammetric behavior of OF (c 10^{-5} mol·L^{-1}) using DPV at AgSAE has been studied in a methanol - BR buffer solution 1:1 in the pH range 2-12. The optimal pH for determination of OF is 12. DP voltammograms of OF at m-AgSAE in the concentration range $2 \cdot 10^{-7}$ – $1 \cdot 10^{-6}$ mol·L^{-1} can be seen in Fig. 4.

The voltammetric behavior of NF (c 10^{-5} mol·L^{-1}) using DPV at AgSAE has been studied in a methanol - BR buffer solution 1:1 in the pH range 2-12. The optimal pH for determination of NF is 3. DP voltammograms of NF at m-AgSAE in the concentration range $6 \cdot 10^{-7}$ – $6 \cdot 10^{-6}$ mol·L^{-1} can be seen in Fig. 5.

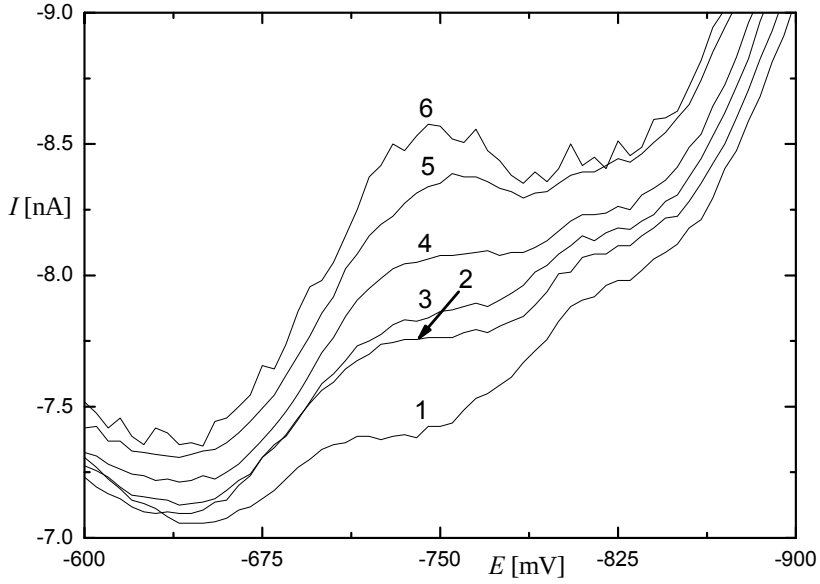

Fig. 1. DP voltammograms of AC at m-AgSAE. Measured in a solution of BR buffer pH 12 and Vltava river water (1:1). AC concentration in river water 0 (1), $2 \cdot 10^{-8}$ (2), $4 \cdot 10^{-8}$ (3), $6 \cdot 10^{-8}$ (4), $8 \cdot 10^{-8}$ mol·L^{-1} (5), and $1 \cdot 10^{-7}$ mol·L^{-1} (6).

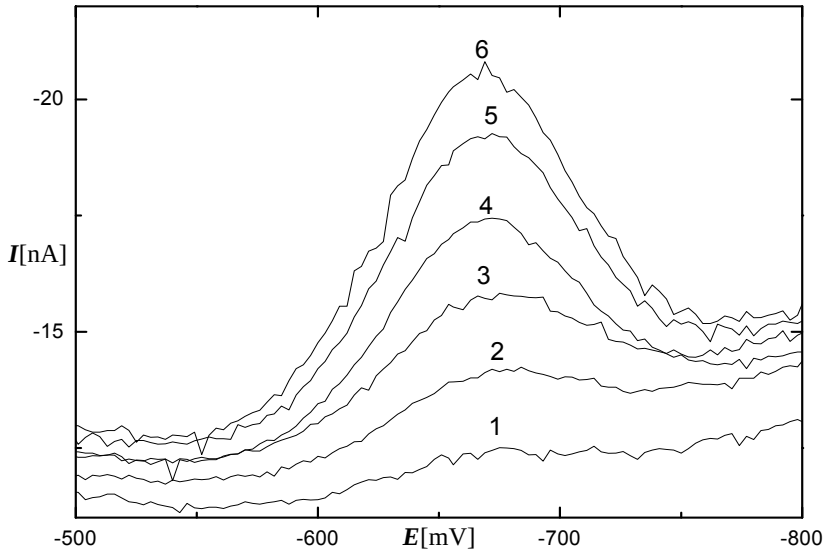

Fig 2. DP voltammograms of AF at m-AgSAE in the concentration range $2 \cdot 10^{-6}$ – $1 \cdot 10^{-5}$ mol·L^{-1} measured in BR buffer pH 12. AF concentration: 0 (1), $2 \cdot 10^{-6}$ (2), $4 \cdot 10^{-6}$ (3), $6 \cdot 10^{-6}$ (4) $8 \cdot 10^{-6}$ (5). and $1 \cdot 10^{-5}$ mol·L^{-1} (6).

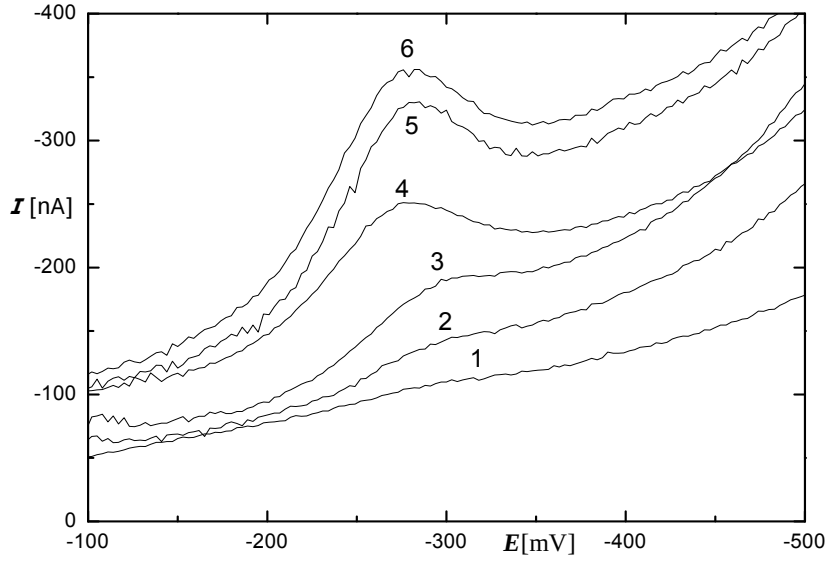

Fig. 3. DP voltammograms of AF at CPE in BR buffer pH 2 . Concentration: 0 (1), $2 \cdot 10^{-7}$ (2), $4 \cdot 10^{-7}$ (3), $6 \cdot 10^{-7}$ (4), $8 \cdot 10^{-7}$ (5) and $1 \cdot 10^{-6}$ mol·L^{-1} (6).

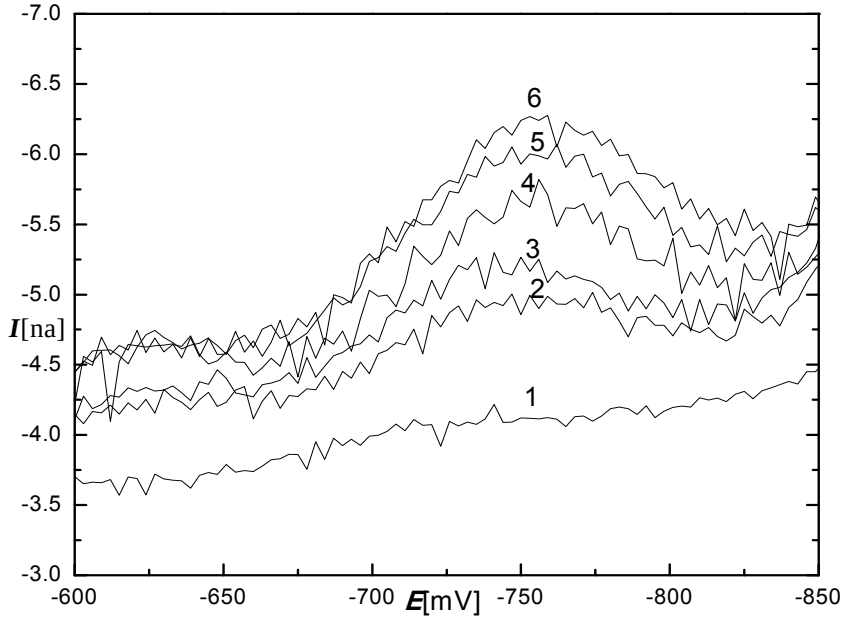

Fig. 4. DP voltammograms of OF at in a mixture of BR buffer pH 12 – methanol 1:1, concentration range $2 \cdot 10^{-7}$ – $1 \cdot 10^{-6}$ mol·L^{-1}. Concentration: 0 (1), $2 \cdot 10^{-6}$ (2), $4 \cdot 10^{-6}$ (3), $6 \cdot 10^{-6}$ (4), $8 \cdot 10^{-6}$ (5), $1 \cdot 10^{-5}$ mol·L^{-1} (6).

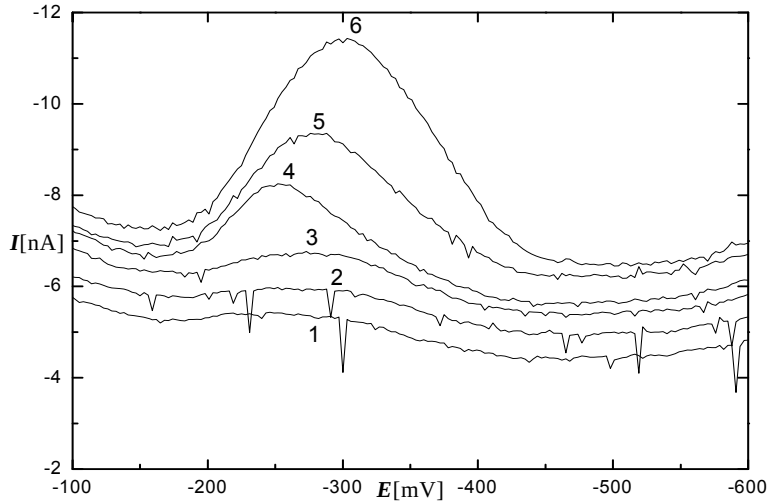

Fig. 5. DP voltammograms of NF at m-AgSAE in a mixture of BR buffer pH 3 – methanol 1:1. NF concentration: 6·10-7 (1), $8 \cdot 10^{-7}$ (2), $1 \cdot 10^{-6}$ (3), $2 \cdot 10^{-6}$ (4), $4 \cdot 10^{-6}$ (5) and $6 \cdot 10^{-6}$ mol·L^{-1} (6).

4. Conclusions

The methods for the determination of AC, AF, NF and OF by DPV at m-AgSAE have been successfully developed. The calibration dependences are linear in the studied concentration ranges. The detection limit reached for the determination of AC in a solution of BR buffer pH 12 – methanol (1:1) is $2 \cdot 10^{-7}$ mol·L^{-1}. The detection limit reached for the determination of AF in a solution of BR buffer pH 12 is $3 \cdot 10^{-6}$ mol·L^{-1}. The detection reached for the determination of NF in a solution of BR buffer pH 12 – methanol (1:1) is $9 \cdot 10^{-7}$ mol·L^{-1}. The detection reached for the determination of OF in a solution of BR buffer pH 12 – methanol (1:1) is $7 \cdot 10^{-7}$ mol·L^{-1}. A method for the direct determination of AC in Vltava river water by DPV at m-AgSAE has been successfully developed. The calibration dependence is linear in the concentration range from $2 \cdot 10^{-8}$ to $1 \cdot 10^{-5}$ mol·L^{-1}. The detection limit reached is $3 \cdot 10^{-8}$ mol·L^{-1}. A method for the determination of AF by DPV at CPE has been successfully developed. The detection limit reached for the determination of AF in a solution of BR buffer pH 12 is $5 \cdot 10^{-5}$ mol·L^{-1}. Further work will focus on adapting the methods for the determination of the studied substances in real samples using solid phase extraction as a preconcentration technique.

5. Acknowledgements

The financial support of The Czech Ministry of Youth and Sports (project LC06035, MSM 021620857 and RP14/63) and of the Technological Agency of Czech Republic (Project TA01020565), and by the Project SVV 2011-263204, is gratefully acknowledged.

6. References

[1.] Lee, H. J., Duke, S. O. (1994) Protoporphyrinogen IX-Oxidizing Activities Involved in the Mode of Action of Peroxidizing Herbicides? *J. Agric. Food Chem.* 42**,** 2610-2618.

[2.] Zhang, Z. P. (2003) Development of chemical weed control and integrated weed management in China *Weed Biol. Manage.* 3**,** 197-203.

[3.] Scrano, L., Bufo, S. A., D’Auria, M., Meallier, P., Behechti, A., Shramm, K. W. (2002) Photochemistry and Photoinduced Toxicity of Acifluorfen, a Diphenyl-Ether Herbicide *J. Environ. Qual.* 31**,** 268-274.

[4.] Teshima, R., Nakamura, R., Nakajima, O., Hachisuka, A., Sawada, J.-I. (2004) Effect of two nitrogenous diphenyl ether pesticides on mast cell activation *Toxicol. Lett.* 150**,** 277–283.

[5.] Francis, B. M., Metcalf, R. L., Lewis, P. A., Chernoff, N. (1999) Maternal and Developmental Toxicity of Halogenated 4'-Nitrodiphenyl Ethers in Mice *Teratology* 59**,** 69-80.

[6.] Baglaj, S. M., Czernik, J. (2004) Nitrofen-Induced Congenital Diaphragmatic Hernia in Rat Embryo: What Model? *J. Pediatr. Surg.* 39**,** 24-30.

[7.] Laganà, A., Fago, G., Fasciani, L., Marino, A., Mosso, M. (2000) Determination of diphenyl-ether herbicides and metabolites in natural waters using high-performance liquid chromatography with diode array tandem mass spectrometric detection *Anal. Chim. Acta* 414**,** 79-94.

[8.] Fenoll, J., Hellian, P., Marian, C., Martinez, C. M., Flores, P. (2005) Multiresidue Analysis of Pesticides in Soil by Gas Chromatography with Nitrogen-Phosphorus Detection and Gas Chromatography Mass Spectrometry *J. Agric. Food Chem.* 53**,** 7661-7666.

[9.] Patil, S. H., Banerjee, K., Dasgupta, S., Oulkar, D. P., Patil, S. B., Jadhav, M. R., Savant, R. H., Adsule, P. G., Deshmukh, M. B. (2009) Multiresidue analysis of 83 pesticides and 12 dioxin-like polychlorinated biphenyls in wine by gas chromatography–time-of-flight mass spectrometry *J. Chromatogr. A* 1216**,** 2307-2319.

[10.] Gilbert-López, B., García-Reyes, J. F., Fernández-Alba, A. R., Molina-Díaz, A. (2010) Evaluation of two sample treatment methodologies for large-scale pesticide residue analysis in olive oil by fast liquid chromatography-electrospray mass spectrometry *J. Chromatogr. A* 1217**,** 3736-3747.

[11.] Rupp, E. B., Zuman, P., Šestáková, I., Horák, V. (1992) Polarographic Determination of Some Pesticides. Application to a Study of Their Adsorption on Lignin *J. Agric. Food Chem.* 40**,** 2016-2021.

[12.] Orr, G. L., Elliott, C. M., Hogan, M. E. (1983) Determination of Redox Behavior in Vitro of Nitrodiphenyl Ether Herbicides Using Cyclic Voltammetry *J. Agric. Food Chem.* 31**,** 1192-1195.

[13.] Vyskočil, V., Barek, J. (2009) Mercury Electrodes–Possibilities and Limitations in Environmental Electroanalysis *Crit. Rev. Anal. Chem.* 39**,** 173-188.

[14.] Yosypchuk, B., Barek, J. (2009) Analytical Applications of Solid and Paste Amalgam Electrodes *Crit. Rev. Anal. Chem.* 39**,** 189-203.

[15.] Vyskočil, V., Daňhel, A., Fischer, J., Novotný, V., Deýlová, D., Horáková, E., Barek, J., Yosypchuk, B., Wang, J., Silver Amalgam Electrodes – A Look Back at the Last Five Years of Their Development and Applications. In *Sensing in Electroanalysis*, 2010; Vol. 5, pp 13-32.

[16.] Zima, J., Švancara, I., Barek, J., Vytřas, K. (2009) Recent Advances in Electroanalysis of Organic Compounds at Carbon Paste Electrodes *Crit. Rev. Anal. Chem.* 39**,** 204-227.

[17.] Yosypchuk, B., Novotny, L. (2002) Electrodes of Nontoxic Solid Amalgams for Electrochemical Measurements *Electroanalysis* 14**,** 1733-1738.

[18.] Hayashi Y, M. R., Ito K, Nishimura W, Imai K, Maeda M. (2005) Detection Limit Estimated from Slope of Calibration Curve: An Application to Competitive ELISA *Anal. Sci.* 21.

Determination of toxic elements in biological materials by inductively coupled plasma atomic emission spectrometry

Serafim Velichkov, Pavel Markov, Nonka Daskalova

Institute of General and Inorganic Chemistry, Bulgarian Academy of Sciences, Acad. G. Bontchev Str., bl.11, 1113 Sofia, Bulgaria

Abstract *The possibilities of different ICP-systems with radial viewing and different types of nebulizers in the determination of traces of toxic elements As, Hg, Se, Cd, Sb, Pb and Tl in biological materials were studied. The analysis of these materials is important in medical and forensic science applications. By using equipment including 40.68 MHz ICP, spectrometer with vacuum ultraviolet spectral region and optimal excitation conditions in inductively coupled plasma the detection limits in the determination of As, Hg, Se, Cd, Sb, Pb and Tl satisfy the requirement of medicine and forensic sciences.*

Kaywords: *ICP-AES, toxic elements, animal tissues, hair, brain, normal concentration levels*

1. INTRODUCION

The need for elemental analysis of biological materials has been well documented [1]. The determination of toxic trace elements in animal tissues is interrelated with cases of acute toxic poisoning of people and animals This problem is very important for medicine and forensic sciences [2].

Comprehensive reviews of instrumental techniques (atomic absorption spectrometry, atomic emission spectrometry, mass spectrometry) and applications include developments in the analysis of clinical and biological materials were published as part of the series of Atomic Spectrometry Updates [3, 4]. Inductively coupled plasma atomic emission spectrometry is a powerful analytical technique combating the following features: trace analytical methodology with muli-element capability; the possibility of element determinations in a broad concentration range including detection limit levels [5].

Providing accurate results about the different biological samples requires a major effort. There have to pay attention to the factors affecting the accuracy of elemental trace analysis: choice of sample preparation procedure and accurate measurements by using a given instrumental technique [1].

The purpose of the present paper was to show the possibilities of 40.68 MHz ICP, spectrometer with vacuum ultraviolet spectral region and optimal excitation conditions in the determination of As, Hg, Se, Cd, Sb, Pb and Tl in biological materials.

2. EXPERIMENTAL

2.1. Instrumentation

The experiments were performed with two equipment of Jobin Yvon (Longjumeau, France): JY ULTIMA 2, 40.68 MHz ICP and JY 38, 27.12 MHz ICP. The characteristics of JY ULTIMA 2 and JY 38 are specified in Table 1. The operating conditions are given in Tables 2 and 3, respectively. The prominent lines with wavelengths below 200 nm were measured by a nitrogen-purged spectrometer. (JY ULTIMA 2). The excitation temperature (Texc) was evaluated by the Boltzmann plot method using titanium lines [6]. The Mg II 280.270 nm/Mg I 285.213 nm line intensity ratio was measured to characterize the robustness of the plasma [7]

Tab. 1: Specification of two type ICP systems, HORIBA Jobin - Yvon ULTIMA 2 (France)

Monochromator	HORIBA Jobin - Yvon ULTIMA 2	JY 38 Jobin Yvon, France
Mounting	Czerny - Turner, focal length 1 m	Czerny - Turner, focal length 1
Grating	Holographic, 2400 grooves mm^{-1}	Holographic, 2400 grooves mm^{-1}
Wavelength range	170-800 nm	200-700 nm
Entrance slit	0.015 / 0.02 mm	0.04 mm
Exit slit	0.02 / 0.08 mm	0.04 mm
Practical spectral bandwidth	from 160 nm to 320 nm pm in the 2-nd order 10 pm in the 1-st order from 320 To 800 nm	15.6 pm (1-st order)
Detectors	High Dynamic Detectors based on PMT's	Photomultiplier, Humamatsu TV, R 446 HA
Rf generator	Solid state	Plasma Therm, model HFP 1500
Frequency	40.68 MHz	27.12 MHz
Power output	0.5 – 1.5 kW	0.5 – 1.3 kW
Nebulizers	Meinhard, concentric glass Ultrasonic nebulizer, Courtesy of Cetac Technologies, Omaha	Meinhard, concentric glass

	Nebraska, USA	
Spray chamber	JY Glass cyclonic spray chamber	JY Glass Scott spray chamber
Plasma torch	Fully demountable torch	Not demountable;
Pump	Two channels, twelve-roller	Peristaltic, ten-roller, Gilson Minipuls (Gilson Medical Electronics, France)

Tab. 2: Operating conditions in the determination of toxic elements in biological materials

Incident power /(kW	1.00
Outer argon flow rate/(l min^{-1})	13
Auxiliary gas /(l min^{-1})	0
Sheath gas flow rate/(l min^{-1})	0.2
Liquid uptake rate/(ml min^{-1})	1.0
Carrier gas flow rate (l min^{-1})	0.4
Mg II 280.270 nm /Mg I 285.213 nm line intensity ratio	11.4
Excitation temperature (T_{exc}), K	7200

Tab. 3: Operating conditions of 27.12 MHz ICP JY 38 (Jobin Yvon, France)

Incident power /(kW	1.00
Outer argon flow rate/(l min^{-1})	13
Liquid uptake rate/(ml min^{-1})	1.0
Carrier gas flow rate (l min^{-1})	0.45
Mg II 280.270 nm /Mg I 285.213 nm line intensity ratio	11.4
Excitation temperature (T_{exc}), K	7200

2.2. Reagents and reference solutions

All reagents were of analytical--reagent grad (Merck, Darmstadt, Germamy) and doubly distilled water was used throughout. The stock solutions of the elements (1 mg ml^{-1}) were prepared from Merck Titrisol solutions. The reference solutions for the determination of the analytes were prepared by precise matching of sample acidity.

2.3. Sample digestion procedures

Human liver

A 10 g sample was treated with 30 ml acid mixture HNO_3/H_2SO_4 by a wet decomposition procedure. The wet digestion was carried out in a close system by using an autoclave with Teflon vessel (Perkin – Elmer, Norwalk, CT, USA, No 3) with working volume = 0.12 l, pressure = 50 bar and maximum temperature =160^{o}C.A notable advantage of digestion carried out in closed systems is that volatilization losses can be minimized [1].. The final volume of the sample solution was 100 ml. The solvent blank had a concentration of 183 mg ml^{-1} H_2SO_4.

Hair

The digestion was performed in a microwave digestion system (Milestone 1200, USA) at at pressure of 70 bar. A samples of hair was washed consecutively with doubly distilled water, acetone, nitric acid (1%), doubly distilled water at room temperature. After that the sample was dried at room temperature. A 0.500 g dry sample was weighted in a PTFE vessel. The digestion was performed in a microwave digestion system procedure in two steps was used: – First step - 3 ml nitric acid (65%) and 2 ml doubly distilled water were added. The sample was heated at temperature 130 ^{o}C for 3 min, cooling period 10 min.; Second step — the sample was heated at 175^{o}C for 10 min. The final sample solution was 5 ml.

3. RESULTS AND DISCUSSION

3.1. Influence of multiplicative interferences on the intensity of prominent line of analytes

The multiplicative interferences on the most prominent lines of As, Hg, Se, Cd, Sb, Pb and Tl in the presence of 183 mg ml^{-1} H_2SO_4 and in the presence of biological matrix were investigated. The influence of H_2SO_4 and biological matrices was studied at the concentration levels equal to that in the final sample solutions. The results show the following:

(a) The net line signals in the presence of 183 mg ml^{-1} H_2SO_4 decreased by 30% in comparison with the corresponding values in pure aqueous solution. This is in accordance with reference data [8, 9];

(b) A biological matrix at the same acidity did not change the slope of the calibration graphs.

3.2. Detection limits in the presence of 183 mg ml^{-1} H_2SO_4 by using different ICP systems and different nebulizers

The detection limit of the analytes in pure solvent (or dilute acid) is defined by Eq. (1):

$$C_L = 2\sqrt{2} \times 0{:}01 \times RSDB \times BEC \quad (1),$$

where BEC is background equivalent concentration in pure solvent; RSDB=1% is the relative standard deviation of the pure solvent [10]. Table 3 shows the detection limits for Pt and Pd under optimal operating conditions (Table 2, 3) by using the most prominent lines.

Tab. 4: Detection limits of As, Hg, Se, Cd, Sb, Pb and Tl in the presence of 183 mg ml^{-1} H_2SO_4 in solutions

Analysis lines.λ, nm	Detection limits, ng ml^{-1}		
	Meinhard, concentric glass nebulizer		Ultrasonic nebulizer
	JY 38	JY ULTIMA 2	JY ULTIMA 2
Hg I 194.277	-	2.7	-
Hg I 253.652	50. 0	2.7	
As I 193.695	-	4.0	0.5
As I 200.334	120.0	12.0	-
Se I 196.026	-	5.2	0.9

Se I 203.985	156.0	16.0	-
Cd II 214.438	40.0	9.0	4.0
Sb I 206. 838	65.0	13.0	2.6
Pb II 220.353	37.0	7.0	1.5
Tl I 190.852	-	9.0	2.6
Tl I 276.787	280	26. 0	-

The following conclusion can be drowning:

(a) The detection limits, obtained by 27 MHz ICP are higher in comparison with corresponding values, obtained with 40.68 MHz ICP. This is in accordance with reference data [11] ;(b) The detection limits in the determination of As, Se and Tl were improved by using prominent lines below 200 nm; (c) The detection limits can improve up to 8 times by using ultrasonic nebulizer instead Meinhard, concentric glass nebulizer.

3.3. Determination of As, Hg, Se, Cd, Sb, Pb and Tl in human liver

The sample of human liver was dissolved by using procedure, described in Section 2.3. Table 4 shows the detection limits with respect to the dissolved sample of the wet tissue, obtained in the present paper, content of As, Hg, Se, Cd, Sb, Pb and Tl in human liver and the range of “normal values” of trace element concentrations in the human liver. In case of chronic poisoning with toxic elements, their concentrations are several times higher than the “normal values”. Modern biological and forensic sciences maintains a interest in techniques which ensure multi-element analysis and have possibilities to detect large number of element at threshold concentration levels.

Tab. 5. Detection limits with respect to the dissolved samples of wet tissues (in ng g^{-1}) obtained in the present paper by 40.68 MHz ICP, content of element in a sample and range of “normal values” of trace element concentrations in human liver of clinical interest in accordance with Ref.[12]. The detection limits are shown by Meinhard, concentric glass nebulizer (MGN) and ultrasonic nebulizer (UN)

Analysis lines, λ, nm	Detection limits, ng g^{-1}		Content, ng g^{-1}	“Normal values” , ng g^{-1}
	MGN	UM		
Hg I 194.277	27.0	-	48.0 ±1.0	30-150
As I 193.695	40.0	5.0	10.2 ± 0.2	5 -15
Se I 196.026	52.0	9.0	225 ± 5.0	250 – 400
Cd II 214.438	90.0	40.0	180 ± 5.0	300
Sb I 206. 83 8	130.0	26.0	35.0 ± 2.0	no data
Pb II 220.353	70.0	15.0	390.0 ± 5.0	350-550
Tl I 190.852	90.0	26.0	< 26.0	no data

* Confidence interval of the mean value ΔX for statistical confidence P=95% for four replicates

The results in Table 5 show that the detection limits obtained by 40.68 MHz ICP and Meinhard, concentric glass nebulizer can satisfy the requirements of medicine and forensic sciences.

3.4. Determination of Hg in Human hair

The sample of human liver was dissolved by using procedure, described in Section 2.3.

Table 6 lists the detection limits with respect to the dissolved solid sample of the hair, obtained in the present paper, the content of Hg in human hair and the range of "normal values" of trace element concentrations in the human hair.

Tab. 6: Detection limits with respect to the dissolved solid samples (in ng g^{-1}) obtained in the present paper by 40.68 MHz ICP with Meinhard, concentric glass nebulizer (MGN), content of element in a sample and range of "normal values" of trace element concentrations in human liver of clinical interest .

Analysis line, λ, nm	Detection limits, ng g^{-1}	Content, ng g^{-1}	"Normal values" , ng g^{-1}	
Hg I 194.277	MGN		[13]	[14]
	27.0	50.2 ±1.0	0.45 – 1.2	0.1-1.33

In this case the concentration of Hg in human hair is significantly higher in comparison with "normal values" and therefore there have example for poisoning with Hg.

4. **Conclusion**

By using equipment including 40.68 MHz ICP, spectrometer with vacuum ultraviolet spectral region and optimal excitation conditions in inductively coupled plasma the detection limits in the determination of As, Hg, Se, Cd, Sb, Pb and Tl satisfy the requirement of medicine and forensic sciences.

REFERENCES

[1]. [2] Maessen F.J.M.J (1987) in: P.W.J.M. Boumans (Ed.), Inductively Coupled Plasma Emission Spectroscopy, Part 2, Applications and Fundamentals, Chapter 3, Wiley, New Yorkp. 48

[2]. Schwartz K.S. (1977) Essentiality versus toxicity of metals in: S.S. Brown, Ed., Clinical Chemistry and Chemical Toxicology of Metals, Elsevier/North Holland Publ. Comp.., New York-Oxford, vol. 1, p. 3.

[3]. Taylor A.,Branch S., Day M.P.,Patriarea M, White M. (2009),Atomic spectrometry update. Clinical and biological materials, Foods and beverages, J. Anal. At. Spectrom. 25, 535-579

[4]. Taylor A.,Branch S., Day M.P.,Patriarea M, White M. (2010),Atomic spectrometry update. Clinical and biological materials, Foods and beverages, J. Anal. At. Spectrom. 25, 453-492

[5]. P.W.J.M. Boumans, Inductively Coupled Plasma Emission, in: P.W.J.M. Boumans (Ed.), Inductively Coupled Plasma Emission Spectroscopy, Part 1, Methodology, Instrumentation, and Performance, Inductively Coupled Plasma Emission Chap.3, Wiley, New York, 1987, p. 69.

[6]. Mermet J.M, Spectroscopic diagnostics: basic concepts, in: P.W.J.M. Boumans (Ed.), Inductively Coupled Plasma Emission Spectroscopy, Part 1, Methodology,Instrumentation and Performance, Wiley, New York, 1987, p. 353, Chapter 10.

[7]. Dennaud J. , Howes A., Poussel E., Mermet J.M. (2001) Study of ionic-to atomic line intensity ratios for two axial viewing-based inductively coupled plasma atomic emission spectrometrs, Spectrochim. Acta Part B 56, 101–112.

[8].Chudinov E.G., Ostroukhova I.I.,. Varvanina G.V. (1989) Acid effects in ICP-AES, Z. Anal. Chem. 335 (1989) 25 - 33.

[9]. Todolı´ J.L., Mermet J.M. Acid interferences in atomic spectrometry: analyte signal effects and subsequent reduction, Spectrochim. Acta Part B 54 (1999) 895 – 905

[10]. Velitchkova N., Velichkov S., Daskalova N. (2007), Inductively coupled plasma atomic emission spectrometry — Optimization of the operating conditions in the determination of trace of elements in line-rich emission matrices Spectrochim. Acta Part B 56 , 101–112.

[11].Boumans P.W.J.M. (1987) Basic concepts and characteristics of ICP-AES, in: P.W.J.M. Boumans (Ed.), Inductively Coupled Plasma Emission Spectroscopy, Part 1, Methodology, Instrumentation, and Performance, Wiley, New York, p. 100, Chap. 4.

[12]. Iyengar G.V. (1985) Concentrations of 15 Trace elements in some Selected Adult Human Tissues and Body Fluids of Clinical Interest from Several Conuntries:Results from a Pilot Study for the Extablishment of Reference Values, Report No1974 oj the Institute of Medicine, Julich Nuclear Research Center.

[13] Tzalev D.L.(1984) Atomic Absorption Spectrometry in Occupational and Environmental Health Practice, vol. II. Detrmination of Individual Elements, CRS Press, Boca Raton, Florida, p.128.

[14] Tzalev D.L. (1995) Atomic Absorption Spectrometry in Occupational and Environmental Health Practice, vol. III. Progress in Occupational and Environmental Health Practice, CRS Press, Boca Raton, Florida, p.152.

Electrostatic Instability of a Conductive Charged Drop and a Conductive Solid Sphere

P.A. Polyakov, N.E. Rusakova, Yu.V. Samukhina
Lomonosov Moscow State University, Moscow, Russia
M.A. Tassev
South-West University ‘Neofit Rilski’, Blagoevgrad, Bulgaria

Abstract*: The instability of spherical and ellipsoidal charged drops of a conductive incompressible liquid is under investigation by means of the energy and dynamic methods. In the paper the decay conditions for the two forms of a charged drop are obtained. The influence of the ellipticity criterion on the charged drop stability and the character of surface density of the resultant force on the Rayleigh instability criterion is analyzed. Another problem considered in the work is a condition of charge stability on a conductive solid sphere inside a dielectric shell that appears to differ from that for a liquid drop.*

Key words*: Rayleigh instability, drop instability, charge stability*

INTRODUCTION

An electrostatic instability of a charged drop known since XIX century draws scientific attention till nowadays. The phenomenon theory basic was developed by Lord Rayleigh and have being refined till up to date since the phenomenon can be used in numerous applications ([1], [2]). The instability appears when the surface density of Coulomb repulsion force of electric charges within the conductive liquid exceeds the surface tension pressure The analysis of instability of non-umbilic charged drops is a complicated problem since one has first to derive the electrostatic problem of charge distribution on a drop surface and the drop shape, surface distribution of charge and surface tension value are dependent.

The usual way to derive charged drop instability problem is a perturbation method. However the method allows to find out only a linear stage of instability and cannot precisely predict the further development of the charged drop shape that can result in a new equilibrium state or a drop decay into daughter drops.

Another approach is based on an analysis of free energy of a charged drop in an initial and a final states, the latter is governed by instability development. And if the final state energy e.g. after a decay is less than the initial one than the former state is energy-profitable. But this fact does not

guarantee the drop transition to the new state since there can be a potential barrier preventing the drop decay or its shape change. A complete solution of non-linear hydrodynamic equations is necessary to answer the question definitely [3].

INSTABILITY OF A SPHERICAL CHARGED DROP OF AN INCOMPRESSIBLE CONDUCTIVE LIQUID

Dynamic approach. Rayleigh electrostatic criterion

Let us consider a conductive liquid spherical drop of radius *a* that has charge q homogeneously distributed on its surface with charge density σ. The surface force density is determined by Coulomb repulsion pressure f_q directed from the drop centre is ([4], [6]) and surface tension p directed to the drop centre [7]

(1) $$f_q = \sigma^2/(2\varepsilon_0) = q^2/(8\pi\varepsilon_0 a),\ p = \alpha\cdot(1/R_1 + 1/R_2)$$

where α is the surface tension coefficient, R_1 and R_2 — principal radii of curvature. The equilibrium is unstable at the points of the surface where $f_q > p$ then the drop tends to change its shape and this can result in a drop splitting into smaller daughter drops [1].

According to the papers [2], [3] we introduce a dimensionless Rayleigh instability criterion

(2) $$W = q^2/(16\pi^2\varepsilon_0\alpha a^3)$$

that is a ratio of a surface density of Coulomb energy to that of the energy of surface tension.

Then for the spherical drop the critical condition of instability can be written as

(3) $$W > 4$$

Energy approach

Let us consider a probable way of splitting of the spherical incompressible liquid drop considered above. Suppose that the drop of radius a has split into daughter drops of different radii b and c ($b >> c$).

Then a splitting condition expressed through the initial drop energy E and daughter drop energy values E_b and E_c after splitting turns to

(4) $$E > E_b + E_c,$$

Total energy of every drop is a sum of its Coulomb energy E_q and surface tension energy E_α

(5) $$E_q = (1/2)\cdot\left(q^2/4\pi\varepsilon_0 R\right),\ E_\alpha = \alpha S = \alpha\cdot 4\pi R^2,$$

where R is the drop radius.

If the daughter drops scatter to sufficiently long distance then Coulomb interaction is very weak and a surface charge densities of the drops are inversely proportional to the drop radii. Denote the radii fraction as $\xi = c/b$. Taking into account that $\xi << 1$ one can obtain the following condition for the splitting of the spherical drop of a conductive incompressible liquid into two daughter drops of different radii

(6) $$(1/4\pi\varepsilon_0)\cdot\left(q^2/a\right) > \alpha\cdot 4\pi a^2\cdot\xi\cdot(1-(2/3)\xi)$$

The condition for the Rayleigh instability criterion [8] can be written as

(7) $$W \geq (c/b)\cdot(1-(2/3)(c/b))$$

Hence it is more energy-efficient for the spherical drop to split to the drops of rather different radii. And the final state of the drops is the more efficient the less the smaller drop radius is. Furthermore the big daughter drop can also split into a big and small drops and thus the initial drop can split into the finest droplets as a result of consequent numerous splittings [2]. However the energy approach shows only the energy efficiency of the final state. The drop transition to the state is in doubt. It can be impossible e.g. because of a potential barrier.

ELECTROSTATIC INSTABILITY OF A CHARGED LIQUID DROP ONTO A SHAPE CHANGE FROM SPHERICAL TO ELLIPSOID

Let us consider the possibility of change of the charged drop shape from spherical to ellipsoidal as a result of the electrostatic instability. In general case the problem is not solved and one have to consider some certain scenarios of Rayleigh instability development according. A scenario proposed in the paper can be analytically derived [4]. Let us consider the an ellipsoid of revolution with semiaxes $a < b$. Its surface area is determined by [4])

(8) $S = 2\pi a^2 + 2\pi(ab/\varepsilon)\arcsin\varepsilon$ with eccentricity $\varepsilon = \sqrt{1-\beta}$, $\beta = (a/b)$

If one charge the ellipsoidal drop with charge q, then its resulting energy (sum of electrostatic energy and surface tension energy) expressed through the radius r of the initial spherical drop is ([8])

$$(9)\quad E = \frac{1}{8\pi\varepsilon_0}\frac{q^2}{\beta^{2/3}r}\frac{\beta}{\varepsilon}\ln\frac{\beta}{1-\varepsilon} + \alpha\cdot\left(2\pi\beta^{2/3}r^2 + \frac{2\pi\beta^{2/3}r^2}{\beta\varepsilon}\arcsin\varepsilon\right)$$

According to the above energy approach the necessary condition of the drop shape change is

$$(10)\quad E < (1/2)\cdot\left(q^2/4\pi\varepsilon_0 r\right) + \alpha\cdot 4\pi r^2$$

The formula (10) can be written as

$$(11)\quad W > 2\eta\text{, where}$$

$$(12)\quad \eta = \left(1-(1/2)\cdot\left[\beta^{2/3} + \left(1/\beta^{1/3}\varepsilon\right)\arcsin\varepsilon\right]\right)/\left(1-\left(\beta^{2/3}/\varepsilon\right)\ln\left(\beta/(1-\varepsilon)\right)\right)$$

So it is energy profitable for the charged conductive drop of incompressible liquid to change its spherical shape to ellipsoidal when the Rayleigh criterion exceeds 2η. It is easy derived that the dependency has minimum at $\beta = 0{,}3$ hence the shape change is possible at Rayleigh criterion value $W = 3.6$.

INSTABILITY OF THE ELLIPSOIDAL CHARGED DROP OF AN INCOMPRESSIBLE CONDUCTIVE LIQUID

Let us consider the an ellipsoid of revolution with semiaxes $a < b$.

Taking α/a as normalization factor and using the dynamic approach we obtain the normalized force surface density in a point of the ellipsoidal surface

$$(13)\quad \frac{f}{\alpha/a} = \left(W\frac{\beta}{2}\frac{1}{\left(1-\varepsilon^2\cos^2\theta\right)} - \frac{1}{\sqrt{\sin^2\theta+\beta^2\cos^2\theta}}\cdot\left(1+\frac{\beta^2}{\sin^2\theta+\beta^2\cos^2\theta}\right)\right)$$

where β and ε are expressed with formulae (9), α is the surface tension coefficient, θ is the angle between the semiaxis b and a normal in the point, W is the Rayleigh criterion.

On can derive from (13) that when $3.5 < W < 3.9$ the dependency of normalized surface force density on θ is non-monotonic. If $W = 3.7$ the dependency has minimum at $\theta \approx \pi/6$ ([8]). Hence the ellipsoidal surface is most unstable in the angle range. This can result in toroidal daughter drop birth and its further detach from the initial drop as a result of a secondary instability or further splitting to several drops or only in surface shape change without any splitting. The exact result can be obtained only by

accurate development of the complete system of the hydrodynamic equations as mentioned above.

CHARGE INSTABILITY OF A CONDUCTIVE SOLID SPHERE

According to (3) the charge of liquid spherical drop can not exceed $q = \sqrt{64\pi^2\varepsilon_0\alpha a^3}$, otherwise the charge instability appears. But if the surface distribution of charge is discrete the charge instability condition is rather different from that given by formula (3) since the Rayleigh model considers a continuous approximation.

Let us consider a conductive solid sphere of radius a surrounded by a dielectric shell of thickness δ ($\delta << a$) with three discrete charges $+q$ (tiny charged grains) on its surface. We do not take the polarization charges of the shell and molecular attraction of the grains to the shell into account.

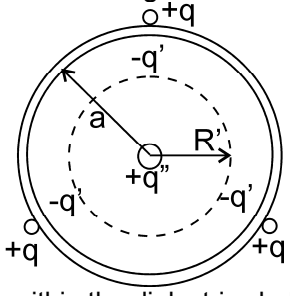

Fig. 1. Conductive solid sphere within the dielectric shell with discrete charges on the surface

The induced charges $-q'$ and $+q''$ appear as shown at Fig. 1. Let us denote the distance between $+q''$ and $-q'$ as R'.

Then if $\delta \to 0$ the resulting force of Coulomb interaction between all the charges $+q$, $-q'$, $+q''$ is

$$F \approx \left(3q^2/a^2\right) - \left(q^2/4\delta^2\right) \tag{15}$$

and the charge stability criterion is

$$\delta^2 < a^2/12 \tag{16}$$

If we take N grains the resulting force is

$$F_q \approx -\left(q^2/\delta^2\right) + N\left(q^2/a^2\right) \tag{17}$$

and the charge instability appears at

$$N > \left(a/\delta\right)^2 \tag{18}$$

So the instability criterion does not explicitly depend on the total charge of grains though the latter depends on N. That is completely different from the Rayleigh criterion for liquid drop.

Let us estimate maximum possible total charge of grains according to the conditions of charge instability derived from Rayleigh mechanism and the one developed in our work.

Consider the conductive solid sphere of radius 1 mm covered with a thin dielectric layer of the thickness 10 nm. As the Rayleigh criterion shows that the instability of liquid charged drop appears when its total charge is $6.4 \cdot 10^{-10}$ C ($N \approx 4 \cdot 10^{9}$). At the same time for conductive solid sphere from formula (18) one can obtain that the charge instability appears when the grains' quantity N is 10^{10} and that corresponds to the total charge which is 2.5 times greater than the former value.

REFERENCES

[1] Schukin, S.I., Grigor'ev, A.I. (2000) Energeticheskiy analiz vozmozhnykh kanalov raspada zaryazhennoy kapli na dve chasti. *ZhTF*, 70(4), 1-7 (in Russian).

[2] Grigor'ev, A.I. (2000) Kapillyarnye elektrostaticheskie neustoychivosti. *So*rosovskiy obrazovatelny zhurnal, 6(7), 37-43. [in Russian]

[3] Belonozhko, D.F., Grigor'ev, A.I. (2000) Nelineyniye kapillyarniye kolebaniya zaryazhennoy kapli. vozmozhnykh kanalov raspada zaryazhennoy kapli na dve chasti. *ZhTF,* 70 (8), 45-52

[4] Schukin, S.I., Grigor'ev, A.I. (1998) Ustoychivost zaryazhennoy kapli, imeyuschey formu tryokhosnogo ellipsoida. *ZhTF.* 68(11), 48-51.

[5] Korn, G. A. and Korn, T. M. (2000) *Mathematical Handbook for Scientists and Engineers*, Second Edition, Dover, New York.

[6] Landau, L.D. Lifshitz, E.M. (1984) *Electrodynamics of continuous media*. Oxford, Pergamon Press

[7] Landau, L.D. Lifshitz, E.M. (1970) *Hydrodynamics*. Oxford, Pergamon Press

[8] Polyakov, P.A., Rusakova, N.E., Samukhina, Yu. V. (2010) *Proc. of XVIII International Conference «Electromagnetic Field and Materials»*, Russia, 237-251.

Application of conformal mapping technique to problems of direct current distribution in thin film wires

P.A. Polyakov, T.N. Gerasimenko
Lomonosov Moscow State University, Moscow, Russia
Ilia Giudjenov
South-West University ‘Neofit Rilski’, Blagoevgrad, Bulgaria

Abstract*: A conformal mapping technique was applied to find direct current distributions in thin film wires of various shapes. A wire with a rectangular defect and a wire angled at 60^o were considered. For both cases we have obtained analytical expressions for mapping of the upper complex half-plane onto the considered domain and found a current distribution. An approximate method of finding current distributions in thin film conductors of complex shape was suggested.*

Keywords: *current distribution, conformal mapping, Schwarz–Christoffel transformation.*

1. INTRODUCTION

Thin film wires are important elements of integrated circuits and various on-chip devices. For the construction and application of such devices it is often necessary to know current distributions inside thin film conductors. In most cases the pattern of thin films contains various angles and constriction or expansions, the calculation of current distribution is therefore a difficult mathematical problem. Complications arise because numerical solution of the boundary-value problem produces nonphysical singularities in corners. To avoid these difficulties research in analytical methods is very useful.

One of the approaches is application of conformal mapping to find a solution of the Laplace equation arising in the required domain. In terms of resistance calculations it was investigated by P. M. Hall [2] and L. N. Trefethen [5], who studied the dependency between the resistance of a conductor and various parameters.

We have used conformal mapping to find direct current distributions in thin film wires of different shapes.

2. A CONDUCTOR WITH A RECTANGULAR DEFECT.

The first problem of interest is current distribution in a conductor with a defect that has a shape of rectangular cut (fig. 1). This model may be used to investigate real wires with defects or constrictions. In the case of direct current, Maxwell's equations can be reduced to the Laplace equation for scalar potential

(1) $$\Delta\varphi = 0.$$

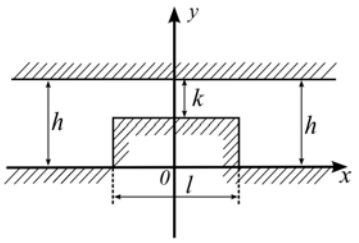

Fig. 1 The geometry of considered wire

According to [4], one can use a complex potential $W(z) = U(z) + iV(z)$ instead of scalar and consider the equation:

(2) $$\frac{\partial^2 W}{\partial x^2} + \frac{\partial^2 W}{\partial y^2} = 0\,,$$

$V(x,y)$ represents the scalar potential, and $U(x,y)$ is the stream function [4].

Since these functions are not independent but constrained by Cauchy–Riemann equations, boundary conditions can be defined for only one of them. For the problem being considered, these are conditions of regularity at an infinite distance and the absence of current flow through lateral boundaries of the conductor:

(3) $$\begin{cases} V(x \to -\infty, y) = V_1 = const, \\ V(x \to +\infty, y) = V_2 = const, \\ U(x,h)\big|_{(x,y)\in\Omega_1} = U_1 = const, \\ U(x,y)\big|_{(x,y)\in\Omega_2} = U_2 = const, \end{cases}$$

where Ω_1 and Ω_2 denote the upper and lower boundaries of the conductor respectively.

To solve problem (2)-(3) we have first considered the solution of Laplace equation in the upper complex half-plain with the boundary conditions corresponding to a point charge placed at the origin. This solution is well known: the force lines are radial straight lines and the

equipotent lines are concentric half-rounds. Then the conformal mapping that maps the upper complex half-plain onto the considered domain (fig. 1) was found.

(4) $$z = C\int_0^{z_1} \frac{1}{z_1}\sqrt{\frac{(z_1-a)(z_1-b)}{(z_1-1)(z_1-c)}}dz_1$$

This integral cannot be taken in elementary functions but its numerical calculation appears to be a difficult problem in the case of complex variables, therefore we suggest an approximate solution.

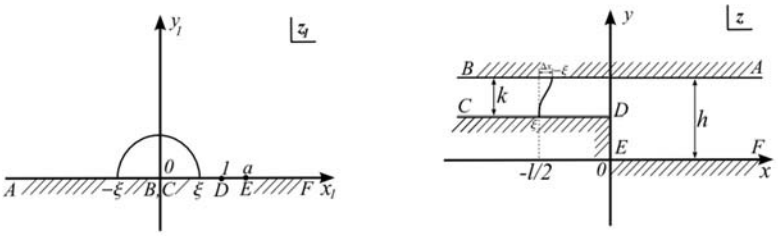

Fig. 2 The correspondence between points of upper complex half-plain and these of a band with a stub.

We have considered a mapping of the upper complex half-plane onto the band $0 < y < h$ with the stub $0 \le y \le h-k$ at the point of the origin (fig. 2) and reflected the obtained picture over a hand-picked line $x = -l/2$. The upper half-plane is mapped onto this band with Schwarz-Christoffel mapping [1]:

(5) $$z = C\int_0^{z_1} \frac{1}{z_1}\sqrt{\frac{z_1-1}{z_1-a}}dz_1 \ .$$

This integral can be taken in elementary functions. The result is the following:

(6) $$z = \frac{h}{\pi}\left(\ln\left(\frac{1+t}{1-t}\right) - \frac{1}{b}\ln\left(\frac{b+t}{b-t}\right)\right), \text{ where } t = \sqrt{\frac{z_1-b^2}{z_1-1}} \text{ and } b = \frac{h}{k}$$

Because of the symmetry of the conductor considered it is clear that the equipotent line at the point $-l/2$ is a straight line orthogonal to its lateral boundaries. The obtained solution is not exact, therefore this line moves aside from the perpendicular to some value Δx. We have used this value divided by a typical size of the system as an estimate of inaccuracy $\alpha \equiv \Delta x/(h-k)$. The dependencies of α and of the length of the cut (fig. 1) on arbitrary point $(\xi \le 1, 0)$ of the z_1-plane (fig. 2) were obtained using (6).

(7) $$l = 2\,\mathrm{Re}(z(\xi)) = 2\frac{h}{\pi}\left[\ln\left(\frac{\sqrt{b^2-\xi}+\sqrt{1-\xi}}{\sqrt{b^2-\xi}-\sqrt{1-\xi}}\right)-\frac{1}{b}\ln\left(\frac{\sqrt{b^2-\xi}+b\sqrt{1-\xi}}{\sqrt{b^2-\xi}-b\sqrt{1-\xi}}\right)\right];$$

(8) $$\alpha = \frac{1}{\pi}\frac{b}{b-1}\left\{\ln\left(\frac{\sqrt{b^2+\xi}+\sqrt{1+\xi}}{\sqrt{b^2+\xi}-\sqrt{1+\xi}}\right)-\ln\left(\frac{\sqrt{b^2-\xi}+\sqrt{1-\xi}}{\sqrt{b^2-\xi}-\sqrt{1-\xi}}\right)+\right.$$
$$\left.+\frac{1}{b}\ln\left(\frac{\sqrt{b^2-\xi}+b\sqrt{1-\xi}}{\sqrt{b^2-\xi}-b\sqrt{1-\xi}}\right)-\frac{1}{b}\ln\left(\frac{b\sqrt{1+\xi}+\sqrt{b^2+\xi}}{b\sqrt{1+\xi}-\sqrt{b^2+\xi}}\right)\right\}.$$

Solving this system of equations numerically, one can estimate the value of α for arbitrary values of parameters h, k and l. For example, when $h = 2k$ and $l = 4k$ then $\alpha \approx 2\%$. Lines of the current in this case are depicted in Figure 3.

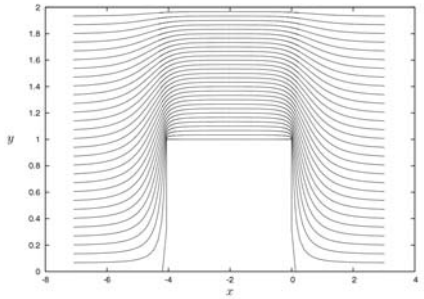

Fig. 3 Lines of the current for $h = 2k$, $l = 4k$.

3. THE CONDUCTOR ANGLED AT 60°.

The second problem of interest is current distributions in thin film wires angled at various angles (fig. 4). The mapping of the upper complex half-plain onto this domain is the following:

(9) $$z = C\int \frac{1}{z_1}\left(\frac{z_1-1}{z_1+a}\right)^{1-\beta} dz_1$$

(10) $$\beta = \frac{\alpha}{\pi},\ a = \left(\frac{h}{k}\right)^{\frac{1}{1-\beta}},\ C = \frac{h}{\pi}(\sin\alpha - i\cos\alpha).$$

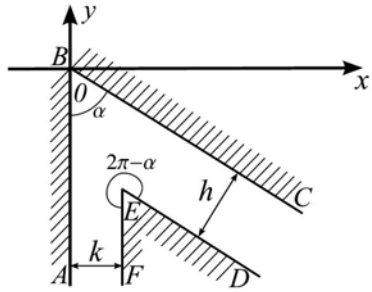

Fig. 4 The geometry of an angled conductor.

The integral (9) can be taken in elementary functions if $1-\beta = P/Q$ where $0 < \mathrm{P} < \mathrm{Q}$, *P* and *Q* are integers [3]. Thus, for $\alpha = 60^o$ the following expression for conformal mapping was obtained

$$z = C\left\{\frac{1}{b^2}\ln(t+b) - \ln(t-1) - \frac{1}{2b^2}\ln(t^2 - bt + b^2) + \frac{1}{2}\ln(t^2 + t + 1) + \right.$$
$$\left. + \frac{i\sqrt{3}}{2b^2}\ln\left(\frac{-2t+b-i\sqrt{3}b}{2t-b-i\sqrt{3}b}\right) + \frac{i\sqrt{3}}{2}\ln\left(\frac{-2t-1-i\sqrt{3}}{2t+1-i\sqrt{3}}\right)\right\} + C_1 \quad , \tag{11}$$

$$C_1 = -\frac{h+k}{4} - i\frac{\sqrt{3}}{12}(7k-h)\,,\ t = \left(\frac{z_1+b^3}{z_1-1}\right)^{\frac{1}{3}}. \tag{12}$$

Using Ohm's law and the dependency between the magnetic field strength and the scalar potential, the expression for current density was obtained:

$$j = j_0\left|\frac{\partial W}{\partial z}\right| = j_0\left|\frac{1}{C}\left(\frac{z_1(z)+a}{z_1(z)-1}\right)^{\frac{P}{Q}}\right|, \tag{13}$$

$j_0 = I/k$, *I* is the current strength, applied to the conductor. The dependency $z_1(z)$ is given by expressions (11), (12) in an implicit form and can be calculated numerically. The lines of the current and the dependency between current density and the scaled distance from point *B* along line *BE* (fig. 4) are depicted in Figure 5.

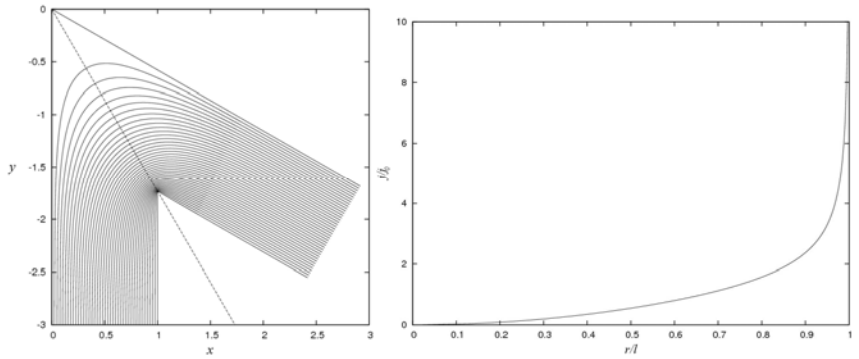

Fig. 5 The lines of the current in a conductor angled at the angle 60^{o} and the dependency between current density and the scaled distance from the point B along the line BE (fig. 4)

4. CONCLUSION.

The suggested method of obtaining an approximate picture of current lines may be used to derive current distributions in various complex patterns of thin film wires. Moreover, the results can be used to find resistance of such conductors, to estimate heat dissipation near defects or to obtain magnetic field strength created by the current.

5. REFERENCES

[1] Gerasimenko, T. N., Ivanov, V. I., Polyakov, P. A., Popov, V. Yu. (2011) Application of a conformal mapping technique to a boundary-value problem of current distribution in plain conductors, *Journal of Mathematical Sciences, Vol. 172, No. 6*

[2] Hall, P. M. (1997) Resistance calculations for thin film rectangles, *Thin Solid Films*, 300 256-264.

[3] Kober, H. (1957) *Dictionary of Conformal Representations*, Dover Publ., New York.

[4] Smythe, W. R., (1950) *Static and dynamic electricity*, New York, Toronto, London.

[5] Trefethen, L. N. (1984) Analysis and design of polygonal resistors by conformal mapping, *Journ. Appl. Math. and Phys. (ZAMP)*, Vol. 35, September.

Non Linear Optical Effects in Quartz fibers

L.M. Ivanov

South West University, 66 Ivan Mihailov st., 2700 Blagoevgrad, Bulgaria
Institute of Electronics, Bulgarian Academy of Sciences, 72 Tzarigradsko shossee, 1784, Sofia, Bulgaria
mihovli@abv.bg

Abstract: *Because of their ability to maintain high energy density over long distances due to the cross sections and low optical losses the fused quartz fibers are very appropriate media for observation of nonlinear optical effects. In this article is examined the possibility by using nonlinear optical processes occurring in the fused quartz fibers to determine their geometrical*

Introduction

One of the most rapidly advancing areas in optics during the last few decades was nonlinear optics. As a result was explained not only the fundamental dependencies of the nonlinear processes but also a lot of applied devices were developed. The nonlinear optics gives wide possibilities for frequency conversion of coherent radiation thus strongly enlarging the laser technology abilities to create new coherent sources of light. We can hardly imagine the modern scientific researches without using the parametric light generators, without generating second and third harmonic, Raman’s lasers and a lot of other devices. Due to several reasons which we will discuss later the fused quartz fibers turn out to be very appropriate media for observation the nonlinear optical processes. The following article is devoted to clarifying the possibilities for determining the geometrical parameters of the fibers by means of occurring nonlinear optical processes.

Geometrical parameters of the fused quartz fibers

The phenomenon of the total internal reflection, responsible for guiding of light in the optical fibers, has been known since 1954. Although glass fibers were made in the 1920s their use was practical in 1979, when the losses of the optical fibers were reduced to $0{,}5dB/km$. Since this year the optical fibers become the most important communication media and begin the building of the optical

fibers communication systems. In its simples form an optical fiber consists of a cylindrical core of silica glass surrounded by a cladding whose refractive index is lower than that of the core. This requirement is need to ensure the total internal reflection of the light on the core-cladding interface. The entire structure is covered by a protected jacket. Because of an abrupt index change at the core-cladding interface, such fibers are called step index fibers. Fig. 1. shows schematically the index profile and the cross section of such fiber.

The fibers are characterized with there geometrical parameters such as core diameter $2a$, cladding diameter $2b$, core refractive index n_1, cladding refractive index n_2, and respectively core cladding refractive index difference $\Delta n = n_1 - n_2$. These parameters are very important because they determine the fiber communication parameters, in particular the information speed. There is a most important, integral parameter that describes the fiber properties. It is called the normalized frequency or simply the V parameter and is defined as:

$$V = \frac{2\pi a}{\lambda}\sqrt{n_1^2 - n_2^2} \approx \frac{2\pi a}{\lambda}\sqrt{2n_1\Delta n} \quad (1)$$

We have to mention that two fibers with different geometrical parameters are identical if their V parameters are equal. It means that their information properties are the same.

There is another different type of fiber, known as graded-index fiber. In these fibers, the refractive index decreases gradually inside the core.

Considerable insight in the guiding properties of the optical fibers can be guiding by using a ray picture based on geometrical optics. The geometrical optics description, although approximate is valid when the core radius a is mush larger than light wavelength λ. When the two become comparable it is necessary to use wave propagation theory. Both of the approaches predict the formation of mode structure of the light as the individual beams travel under different angle compared to the axis of the fiber and therefore with effective propagation constant β. The number of excited waveguide modes depends on the parameter V of the fiber. When a parameter V is less than 2.405 only one mode is formed in the fiber. Such fibers are classified as single-mode fibers. With parameter $V > 2.405$ more than one mode gets excited and these fibers are classified as multi-mode fibers. As can be seen from formula (1) each fiber can be single-mode for one wave length and multi-mode for other shorter wave length. Therefore with appropriate choice of the light launched the fiber multiple modes can

get excited. By the means of wave analysis the propagation constants for the different modes can be calculated in dependence to the parameter of the fiber. The result is shown on fig. 1a. Furthermore the wave analysis gives information about the distribution of the light intensity in the cross section of the fiber. Fig. 1b shows the results for the first two modes marked as LP_{01} and LP_{11}. As can be seen at the figure the axially symmetrical LP_{01} mode has maximum intensity at the center of the core. This conclusion turns out to be true for all the axially symmetrical modes (all modes with first index 0). On the contrary axially nonsymmetrical mode LP_{11} has minimum intensity at the center of the fiber. This also turns out to be correct for all the other modes with first index different from zero.

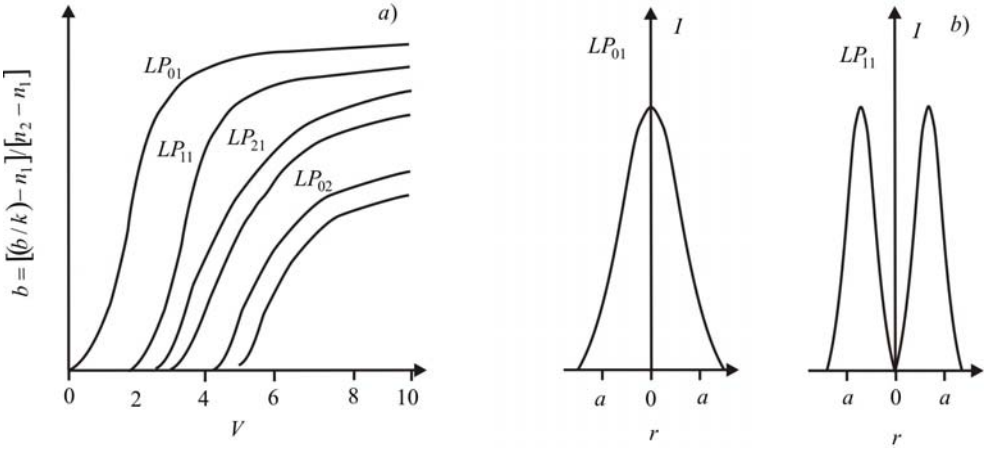

Figure 1. Normalized propagation constant (a) and field distribution (b) for first few modes.

Fused quartz fibers as nonlinear media

It is well known that fused quartz, a material used to made the communication fibers has very low coefficients of nonlinearity in comparison to the other conventional nonlinear media. This fact is the main disadvantage of the quartz as a nonlinear medium. However the fibers have a lot of other advantages over the conventional nonlinear volumetric media. The small cross sections of the cores of the fibers give them the ability to maintain high density of the energy also the small losses and the great lengths of the fibers guarantee a great interaction length between the waves. As a result in the fibers the product of the coefficient of nonlinearity and the length of interaction which determine the effectiveness of the nonlinear process exceeds

many times those of the volumetric media. This makes the fibers very effective media for a nonlinear processes [1]. The nonlinear processes occurring in the fibers are quite numerous. We will focus our attention on two of them only – Stimulated Raman Scattering (SRS) and Four-Wave Mixing (FWM) with an accent on the second one which allows determining the geometrical parameters of the fibers. The stimulated Raman scattering is a nonlinear process where a new wave length in the Stokes area is generated which frequency displacement from the pumping radiation corresponds to the vibrational spectrum of the nonlinear medium. The amplification line of spontaneous Raman scattering in the fused quartz is quite wide but has maximum at $\Delta\nu = 440cm^{-1}$ and that is why the occurring stimulated Raman scattering has the mentioned above frequency displacement. The process is very effective because phase synchronism is not required and that is why it often occurs as cascaded Raman scattering as the new Raman frequency components act as pumping for the next process of Raman scattering.

As it is well known, the stimulated FWM is a non linear process, when two pump photons of frequency ν_p are transformed in Stokes and anti-Stokes pair of frequency respectively ν_s and ν_a, which obey the energy balance

$$\nu_p - \nu_s = \nu_a - \nu_p$$

The process is efficient if the phase matching condition is fulfilled.

$$\Delta k = k(\nu_s) + k(\nu_a) - 2k(\nu_p) = 0$$

Perfect phase-matching can not be achieved in optical glasses because in the normal (anomalous) dispersion region Δk is always greater (less) than zero. Exact phase-matching is possible in optical fibers, when the material is compensated by the modal dispersion for a suitable combination of the modes (see fig. 1a), i.e.

$$\Delta\beta = \beta_{p1} + \beta_{p2} - \beta_a - \beta_s \quad (2)$$

where, β_{p1}, β_{p2}, β_a, and β_s are the propagation constants of the waves in the respective waveguide modes.

The dynamics of both processes versus the power of the pumping pulses is shown on fig. 2. The fiber is pumped with second harmonic radiation of Q switched Nd:YAG laser.

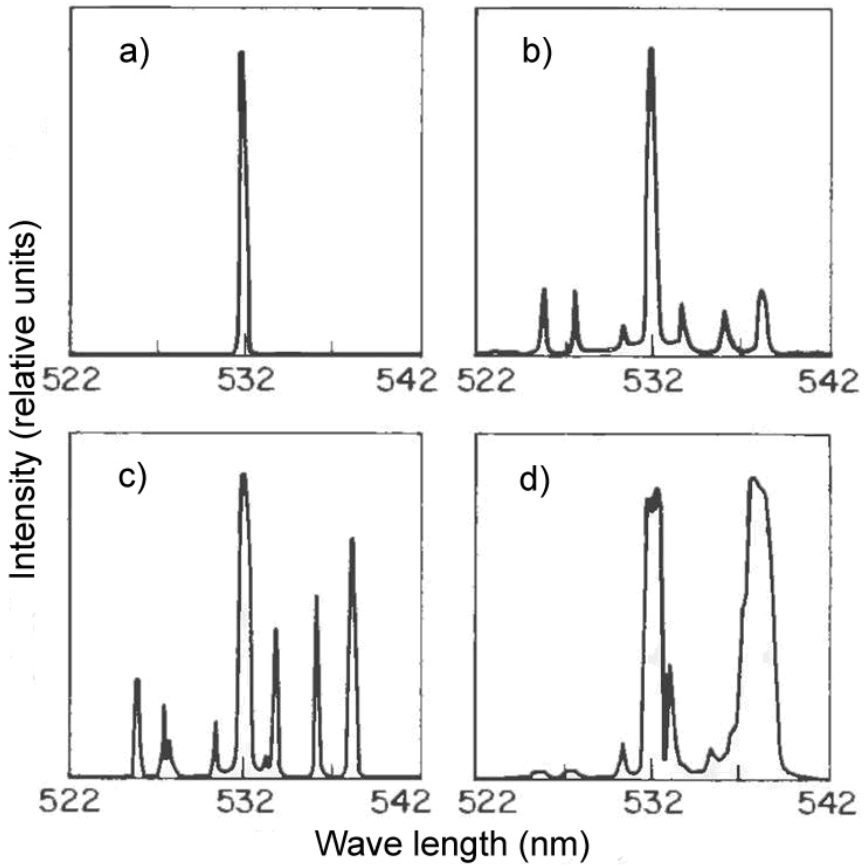

Figure 2. Dynamics of SRS and FWM processes versus the power of the pumping pulses.

On fig 2a the power of the stimulating radiation is low and at the out of the fiber only the pumping radiation is registered. With the increasing of the pumping radiation’s power on fig. 2b several new symmetrical to the stimulating radiation frequency components appear. These spectrum lines occur as a result of the FWM process. The energy of the Stokes and anti-Stokes components is approximately equal. Further increasing of the pumping power (fig. 2c) leads to increased power of the Stokes components because they get additional amplification as a result of the SRS process because these lines are within the spontaneous Raman scattering. The last fig.2d presents the spectrum of a very high pumping power. In this case the SRS process occurs. The energy of the pumping frequency almost

completely transforms into Raman line and there is not enough energy left for the FWM process.

Non linear method for determining of fiber parameters.

The frequencies ν_s and ν_a generated by a FWM process can be accurately predicted, if the parameters of the fiber, including the refractive index profile, are precisely known. For a fixed modal combination, they can be calculated by varying frequency shift $\Delta\nu = \nu_p - \nu_s = \nu_a - \nu_p$, and looking for a $\Delta\nu$, at the phase-matching condition, expressed by eq. 2.

The solving of the inverse problem – to fine the fiber parameters from the given FMW frequencies – have to deal with difficulties, connected mainly with the influence of the refractive index profile. Most of the fibers produced by the MCVD technique have a central dip in the profile. The shape and the depth of this central dip substantially modify the dispersion properties of the fiber. In this work we demonstrate the possibility for substantial reduction of the error, associated with the FWM method.

For the case of weakly guided fibers [2] in a divided pump process (that is the Stokes and one of the pump wave propagate in one fiber mode, while the anti-Stokes and other pump wave propagate in another fiber mode) the frequency shift $\Delta\nu$ is determinate by Δn, V, $2a$, and n_1 as it follows [3,4]:

$$\Delta\nu\lambda_p D(\lambda_p) = \Delta n\left[\frac{d(B_s V)}{dV} - \frac{d(B_{as} V)}{dV}\right] \quad , \tag{3}$$

where V is the normalized frequency, λ_p is the pump wavelength, $D(\lambda) = \lambda^2\left(\frac{d^2 n}{d\lambda^2}\right)$ is the core material dispersion and $\frac{d(BV)}{dV}$ are differential mode delays of the propagating Stokes and anti-Stokes waves. These modal delays depend only on the V parameter and on the real profile of the refractive index of the waveguide core. For two distinct combinations of modes the following characteristic equation for the parameter can be written [5].

$$(4)\quad \frac{\Delta\nu^{(1)}}{\Delta\nu^{(2)}} = \frac{\dfrac{d(B_s^{(1)}V)}{dV} - \dfrac{d(B_{as}^{(1)}V)}{dV}}{\dfrac{d(B_s^{(2)}{}_sV)}{dV} - \dfrac{d(B_{as}^{(2)}V)}{dV}} = R(V)$$

In eq.4 indices 1 and 2 denote the first and the second modal combination respectively. If the refractive index profile is already known, the right side of the eq.4 depends only on the V parameter. This fact established the possibility to obtain V parameter, and after that – the other fiber parameters. However, the various refractive index profiles yield different value for the normalized group delays [6], and therefore substantially different function $R(V)$. As a result, the error of the obtained V parameter can be quite large. In order to find the conditions for minimizing this error we investigated the $R(V)$ function for various refractive index profile and modal combinations. The main concept of our approach is straightforward. The central dip of the refractive index profile influences substantially on the normalized group delays of the axially symmetrical only (the LP_{lp} modes with first index $l=0$) [6]. The latter is a consequence of the fact that the intensity maximum of these modes, for the fiber without a dip must lay in the center of the fiber. Hence, the presence of the dip changes radial field distribution and the group velocity of the wave. The influence of the refractive index profile on the axially anti-symmetrical modes (the first index $l>0$) is much less pronounced, because their intensity at the center of the fiber is zero.

Fig. 3 shows the dependencies $R(V)$ for the rectangular refractive index profile (continuous line) and the rather extreme case when the radius of the rectangular central dip is 15% of the core radius and the refractive index in the center of the fiber equals to the refractive index of the cladding (dotted line). The dependencies $R(V)$ are show for three different combinations of the pump wave modes, including respectively 0, 1 and 2 axially symmetrical modes. Curve 1 correspond to $\Delta\nu^{(1)}$ obtained with the pair $LP_{31}-LP_{21}$ and to $\Delta\nu^{(2)}$ obtained with $LP_{21}-LP_{11}$, curve 2 to $\Delta\nu^{(1)}$ obtained with $LP_{21}-LP_{11}$ and $\Delta\nu^{(2)}$ obtained with $LP_{11}-LP_{01}$, curve 3 to $\Delta\nu^{(1)}$ obtained with $LP_{02}-LP_{11}$ and $\Delta\nu^{(2)}$ obtained with $LP_{11}-LP_{01}$. It is interesting to mention that these are combinations of the lowest order modes.

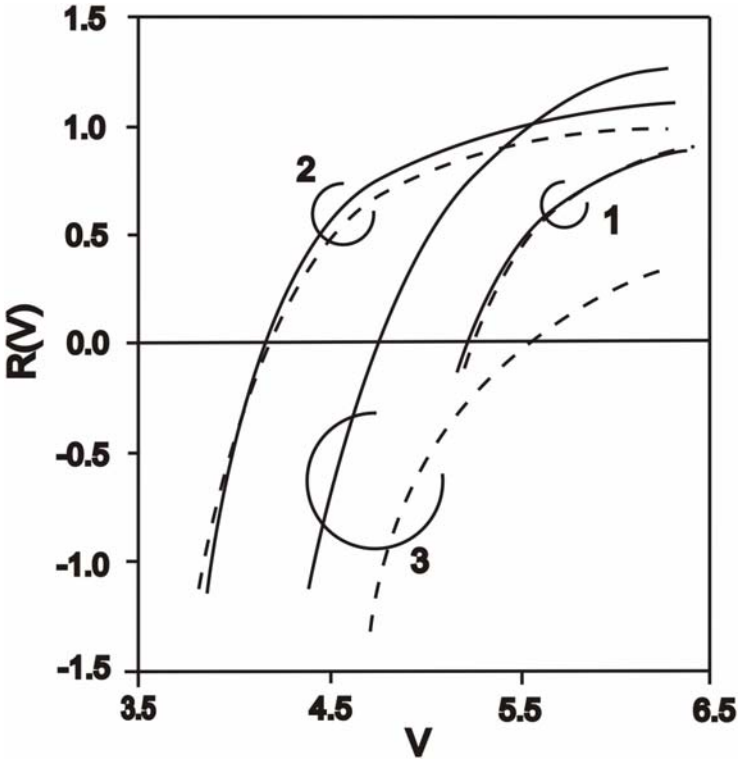

Figure 3. Dependencies $R(V)$ for the rectangular refractive index profile (continuous line) and for refractive index profile with rectangular central dip in the center of the fiber. (dotted line).

From fig.3 it is seen that $R(V)$ has zeros for certain values of V. Consequently, for those values of V the normalized group delays participating in numerator of eq. 4 are equal. The negative value of $R(V)$ correspond to the case when the anti-Stokes wave of the modal combination in the numerator of eq. 4 propagate in the higher mode, that the Stokes wave. The positive values correspond respectively to the case when the Stokes wave is in the higher mode. As it seen from the given curves, if only axially anti-symmetrical modes are used, the function $R(V)$ for the cases of rectangular refractive index profile and profile with a central dip almost completely coincide. Hence, using such modal contribution, the value of the V parameter can be determined with remarkable precision without considering the type of profile. In the case of only one symmetrical mode participating in the process, an interval of V value, where the two curves coincide enough precisely, can be found too. This is the interval around the point where

the function $R(V)$ becomes zero. For the concrete case when the first frequency is obtained for LP_{21} and LP_{11} fiber modes, while the other – for LP_{11} and LP_{01} modes in the interval $3.9 < V < 4.3$ the error of the obtained value of V is less than 1%. However, for larger values of V the error becomes considerable. Suitable interval of V values does not exist in the case of two axially symmetrical modes, so such modal combination is not preferable to be use in determining of the V parameter.

If the V parameter is already known, the determination of the other parameters (core radius a and the core cladding refractive index difference Δn) requires information about the doping composition of the fiber, or equivalently, about refractive index $n(\lambda)$ and the dispersion $D(\lambda)$. Using the data for the pure fused quartz in this case we can obtain good accuracy of such approximation [7]. The error due to this exchange is especially negligible, if λ_p is far from the point of zero material dispersion of the fused silica. After that, the derivation of Δn and a is straightforward.

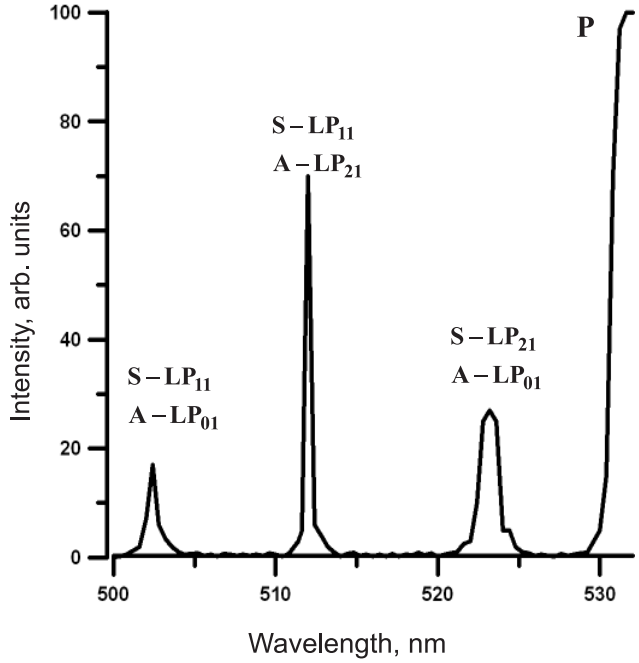

Figure 4. Anti-Stokes components of the FWM spectrum.

In order to prove experimentally the feasibility of determining the fiber parameter using FWM process with one axially symmetrical mode, we studied a fiber with known V parameter, which was approximately 3.9 at $\lambda_p = 532nm$. An experimental set up, which is widely used for studying non-linear phenomena in optical fibers, was employed for obtaining the stimulated FWM spectra. The fiber was pumped by the second harmonic of a Q-switched and mode-locked CW Nd:YAG laser. The fiber had been produced by the MCVD technique and had pure silica cladding and Ge-doped cores with different molar concentration.

In the experiments the excitation of the different groups of modes was accomplished by varying the launching conditions for the pump beam. The modal structure of the generated radiation was identified visually, after splitting a fraction of the fiber output with a grating. FWM were recorded by OMA.

In Fig. 4 the anti-Stokes sides of the FMW spectra is shown. For this fiber the refractive index profile differ substantially from rectangular one. fig. 4 shows also the modal combination of the Stokes and anti-Stokes components for the respective frequency. The Stokes sector of the spectra expect the symmetrical Stokes frequency, contains also the stimulated Raman scattering (SRS) line with frequency shift 440 cm^{-1} from the pump. It complicates the spectra and increases the uncertainty of the adjacent FWM frequencies. For this sample we used $\Delta\nu^{(1)} = 722cm^{1}$ obtained with $LP_{21} - LP_{11}$ and $\Delta\nu^{(2)} = 1089cm^{-1}$ with $LP_{11} - LP_{01}$. The frequency shift $\Delta\nu^{(1)} = 722cm^{1}$ was obtained when anti-Stokes component was in the higher mode. That's why we take this value as a negative. Via eq. 4 we found that the V value of the pump wavelength is 3.96.

Using this value, the parameters of the fiber were easily calculated. The standard optical fibers are made from SiO_2 with Ge-doped core. But the doping concentration weakly effects to core refractive index n_1, core material dispersion $D(\lambda) = \lambda^2\left(\frac{d^2n}{d\lambda^2}\right)$ and differential mode delays $\frac{d(BV)}{dV}$ [7]. Then if we use the data for pure silica the error will be negligible. Solving eq. 3 we obtain for the core-cladding refractive index difference $\Delta n = 3{,}04.10^{-2}$. From eq. 1 we find out for the core diameter $2a = 2.25\mu m$ when. We have to mention that the passport data are correspondingly $\Delta n = 3.2.10^{-2}$ and $2a = 2.2\mu m$.

Conclusion

In conclusion, non-linear optical frequency-resolved method is proposed to determine simultaneously most of the important fiber parameter, without accounting for the specific refractive index profile, which were experimentally demonstrated. The accuracy of the obtained data is satisfactory.

References

[1] G. Agrawal, , *Nonlinear Fibre optics*, (London, Prentice-Hall International, 2001).

[2] . D. Gloge, “Weakly Guided Fibers”, *Applied Optics*, Vol. 10, pp. 2252-2258, 1971.

[3] R. H. Stolen, “Phase-matching-stimulated four-photon mixing in silica-fiber waveguide”, *IEEE J. Quantum Electron.*, Vol. QE-11(3), pp. 100-103, 1975.

[4] R. H. Stolen, J. Bjorkholm, “Parametric amplification and frequency conversion in optical fibers”, *IEEE J. Quantum Electron.,* Vol. QE-18(7), pp. 1062-1072, 1982.

[5] S. J. Garth, C. Pask, G. E. Rosman, “Stimulated four photon mixing in bent few-mode optical fibres”, *Optical and Quantum Electronics*, Vol. 20(1), pp.79-86, 1988.

[6] R. H. Stolen, “Modes in fibre optical waveguides with ring index profiles”, *Applied Optics,* Vol. 14(7), pp. 1533-1537, 1975.

[7] J. W. Fleming, “Dispersion in $GeO_2 - SiO_2$ glasses”, *Applied Optics*, Vol. 23(24), pp. 4486-4493, 1984

Growth, structural and dielectrical investigations of $Bi_2Fe_4O_9$ single crystals

D. Petrova [a], M. Kalitzova [b], V. Tomov [b], O. Petrov [c]

[a] South-West University, 66 Ivan Mihailov str., 2700 Blagoevgrad, Bulgaria.
[b] Institute of Solid State Physics, Bulgarian Academy of Sciences, 72 Tzarigradsko Chaussee Blvd., 1784 Sofia, Bulgaria.
[c] Central Laboratory of Mineralogy and Crystallography, Bulgarian Academy of Sciences, G. Bonchev Str., Building 107, 1113 Sofia, Bulgaria.

Abstract: *$Bi_2Fe_4O_9$ single crystals were successfully grown by the High Temperature Solution Growth Method (HTSGM). Powder X-ray diffraction shows that $Bi_2Fe_4O_9$ crystallized in space group Pbam, has orthorhombic structure with unit cell parameters: a = 7.965 Å; b = 8.440 Å; c = 5.994 Å. Differential thermal analysis (DTA) of $Bi_2Fe_4O_9$ single crystals detected a second phase transition in the region of 550^o C. The anomalies in the dielectric constant values around the phase transition temperature increase with frequency decreasing. This behavior can be associated with the nanostructure regions in the investigated crystals.*

Keywords: *Crystal symmetry, Electrical measurements, Phase transitions, X-ray spectroscopy*

1. INTRODUCTION

$Bi_2Fe_4O_9$ is important material with various applications, e.g., semiconductor in gas sensors [1], electrode material in reduction of oxygen [2, 3] and catalyst for ammonia oxidation to NO [4, 5]. Significant characteristic of $Bi_2Fe_4O_9$ is the second phase transition from paraelectric to ferroelectric state.

In this study the dielectric behavior of $Bi_2Fe_4O_9$ single crystals is investigated. Determined are the temperature and the diffuseness of the observed phase transition at various frequencies of the applied AC-voltage.

2. EXPERIMENT

$Bi_2Fe_4O_9$ single crystals were successfully grown by the High Temperature Solution Growth Method (HTSGM). The starting materials were Bi_2O_3, Fe_2O_3 and Bi_2O_3 flux with minimum purity of 99.999% and the ratio between the flux and the crystallizing compound 7:1. The crystallizing compound was placed in a platinum crucible (R=60 mm, L=75 mm) covered with a platinum lid and melted at 1150^o C. The crystal growth was accomplished by cooling the high temperature solution to 870^o C with a cooling rate of 1^o C/h. As a result $Bi_2Fe_4O_9$ has been crystallized on the wall of the crucible.

Various techniques – X-ray diffraction, DTA and dielectric measurements were used to investigate the structural properties of $Bi_2Fe_4O_9$ single crystals.

X-ray diffraction measurements carried out on DRON 3M powder X-ray diffractometer (Fe-filtered CoK_α radiation).

Differential thermal analysis (DTA) of $Bi_2Fe_4O_9$ sample was carried out with Perkin Elmer (Diamond TG/DTA) at 10 ^{o}C/min heating rate by using Pt crucibles and single monocrystal with weight of ~50 mg.

For the dielectric measurements flat-parallel crystal plates were used. On their opposite sides circular silver electrodes with diameter of 2.3 mm were deposited, the samples being thick 0.7 mm. The measurements were carried out by the means of Hewlett-Packard 4284A RLC bridge at frequencies of 10 kHz, 100 kHz and 1 MHz in the temperature range from 200^o C to 570^o C. For all measured frequencies the relative error of the bridge was 3 %.

3. FORMAT RESULTS AND DISCUSSION

Fig. 1 shows X-ray diffraction spectrum of $Bi_2Fe_4O_9$ single crystals.

From experimental data analyses can be concluded that $Bi_2Fe_4O_9$ crystallized in space group *Pbam* with orthorhombic structure and unit cell parameters as follows: *a* = 7.965 Å*; b* = 8.440 Å*; c* = 5.994 *Å*. The peaks (d-spacing) in the XRD pattern (fig. 1) fully match the data for $Bi_2Fe_4O_9$ (PDF №250090) in the ICDD – data base.

DTA experimental traces show change in the slope at about 540^o C. This increasing of the value of specific heat capacity might be interpreted as a second order phase transition.

Figure 2 shows the temperature dependence of the dielectric constant of $Bi_2Fe_4O_9$ single crystals.

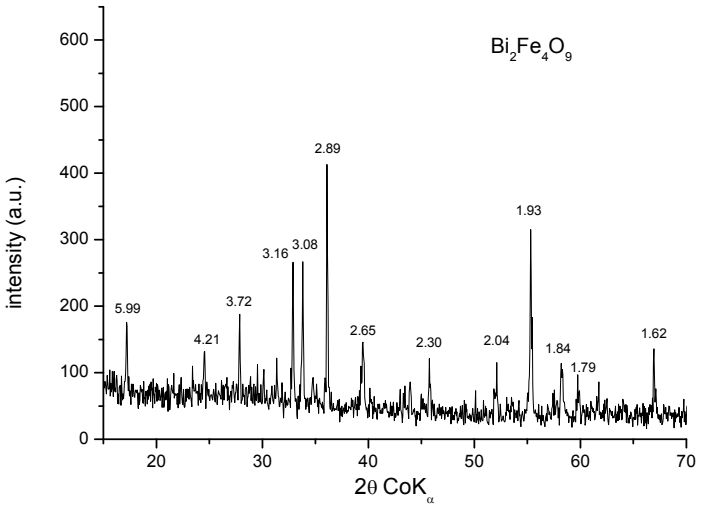

Fig. 1. X-ray diffraction pattern of $Bi_2Fe_4O_9$ single crystals.

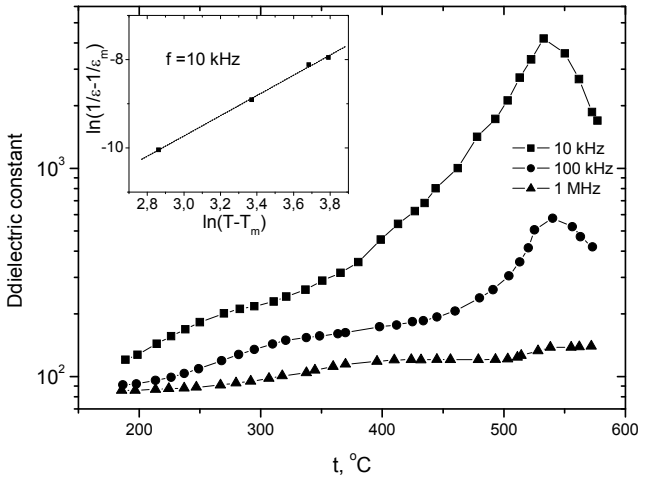

Fig. 2. Temperature dependence of the dielectric constant of $Bi_2Fe_4O_9$ at 10 kHz, 100 kHz and 1 MHz. The inset shows $\ln(t-t_m)$ as a function of $\ln(1/\varepsilon - 1/\varepsilon_m)$ at 10 kHz.

The anomalies in the dielectric constant values around the phase transition temperature are more pronounced with frequency decreasing. To describe the diffuseness of the phase transition, the following empirical modification of the Curie-Weiss Law [6] is used:

$$\frac{1}{\varepsilon} - \frac{1}{\varepsilon_m} = \frac{(T - T_m)^{\gamma}}{C^*} \quad (1)$$

where γ is the critical exponent, which describes the degree of diffuseness of the transition, C^* is a Curie-Weiss constant, ε_m is the maximum value of the dielectric constant and T_m is the temperature at which the maximum dielectric constant is attained. The value of γ for investigated crystals was calculated from the slope of the $\ln(1/\varepsilon - 1/\varepsilon_m)$ vs. $\ln(T - T_m)$ graph. For γ we obtained a value closed to 2 by fitting a curve to the experimental data. The fitting curve at 10 kHz is shown in the inset of Fig. 2.

4. SUMMARY AND CONCLUSIONS

The broad maxima in the temperature dependence of the dielectric constant from Fig. 2 are attributed to the phase transition from ferroelectric to paraelectric state. For a sharp transition the critical exponent in equation (1) is $\gamma = 1$. For a diffuse-like transition γ is in the range $1 < \gamma \leq 2$ [7]. For $\gamma = 2$ equation (1) reduces to the one given by Smolensky [8] and represent ideal relaxor ferroelectrics [9, 10]. This behavior can be associated with the nanostructure regions in the investigated crystals at frequency 10 kHz.

5. ACNOWLEDGEMENTS

This study was supported by Grant No. ВУХ-308/07 from the Ministry of Education and Science of Bulgaria.

6. REFERENCES

[1] A. S. Poghossian, H.V. Abovian, P. B. Avakian, S. H. Mkrtchian, V. M. Haroutunian, Bismuth ferrits: new materials for semiconductor gas sensors, Sens. Actuators B 4 (1991) 545-549.

[2] G. Gokagac, B. J. Kennedy, L. Electroanal. Chem. 368 (1994) 235.
[3] J. B. Goodenougth, R. Manoharan, M. Paranyhaman, J. Am. Chem. Soc. 112 (1990) 2076.
[4] N.I. Zakharchenko, Kinet. Catal. 43 (2002) 95–98.
[5] Y. Xiong, M. Wu, Z. Peng, N. Jiang, Q. Chen, Chem. Lett. 33 (2004) 502–503.
[6] M. E. Lines and A. M. Glass, Principles and Applications of Ferroelectrics and Related Materials, Oxford Classic in the Physical Sciences, 2001.
[7] B. P. Pokharel, D. Pandey, J. Appl. Phys. 88, (2000) 5364.
[8] G. A. Smolensky, J. Phys. Soc. Jpn. Suppl. 28 (1970) 26.
[9] A. A. Bokov, Z. G. Ye, Solid State Commun. 116 (2000) 116.
[10] A. A. Bokov, Y. H. Bing, W. Chen, Z. G. Ye, Phys. Rev. B68, (2003) 052 102.

Invariant analysis of the fragmentation of relativistic nuclei ^{8}B

R. Zh. Stanoeva
South West University, Blagoevgrad, Bulgaria

Abstract*: The pattern of the fragmentation of relativistic nuclei of energy above 1 A GeV in emulsion is represented in invariant variables. Data extracted from emulsions exposed to 1.2 A GeV ^{8}B nuclei suggest the advantages of the emulsion technique in obtaining unique information on the decay of light nuclei to a few fragments.*

Keywords: *invariant analysis, relativistic nuclei, fragmentation, emulsion.*

1. INTRODUCTION

The fragmentation of relativistic nuclei is a source of information about their structure. The nuclear photo-emulsion method makes it possible to study in detail the fragmentation of a projectile thanks to a high resolution capability of emulsion and the detection of secondaries in a 4π geometry. The registration of all charged particles and their identification enable one to explore the isotopic composition of fragments and the projectile fragmentation channels. In the present paper, we give a detailed examination both of the decays conventionally called “white” stars (fig.1) because they have no target-nucleus fragments and of the decays involving the production of several target-nucleus fragments (fig.2). The main criterion for selecting the appropriate events used for the study of the projectile fragmentation is the requirement of conservation of the primary charge in a narrow fragmentation cone and the absence of produced charged particles.

2. RESULTS

A detailed study of relativistic fragment systems formed in the dissociation of nuclei of energy above 1 A GeV provides a qualitatively better understanding of the structure of nuclear excitations above the decay thresholds. In accordance with the classification developed in paper [2],

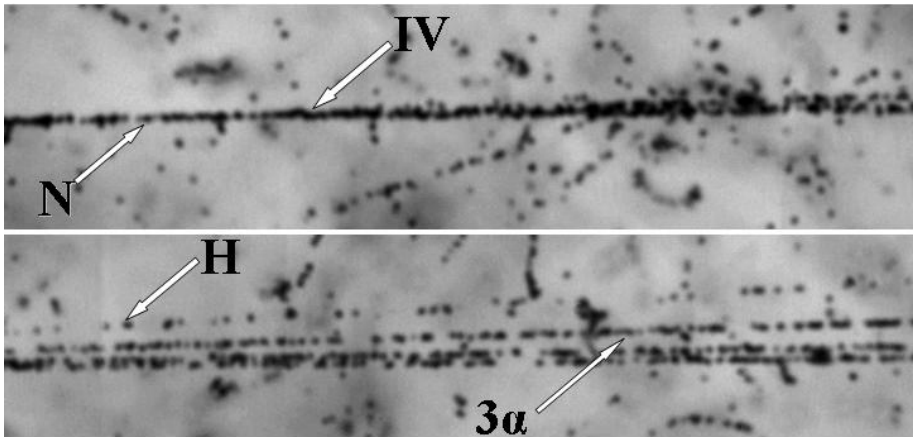

Fig. 1: Example of peripheral interaction of a 2.1 A GeV ^{14}N→3He+H in a nuclear track emulsion ("white" star). The interaction vertex (indicated as **IV**) and nuclear fragment tracks (**H** and **He**) in a narrow angular cone are seen on the upper microphotograph. Following the direction of the fragment jet, it is possible to distinguish 1 singly and 3 doubly charged fragments on the bottom microphotograph.

fragmentation results in the production of fragment jets which are determined by the invariant variable region concentrated within $10^{-4}<b_{ik}<10^{-2}$, where

$$b_{ik} = -(u_i - u_k)^2 = -\left(\frac{P_i}{m_i} - \frac{P_k}{m_k}\right)^2,$$

u_i, u_k are 4-velocities of the fragments i and k, $P_{i,k}$ and $m_{i,k}$ are their 4-momenta and masses.

The lower limit corresponds to the decay ^{8}Be→2α (decay energy 92 KeV), while the upper one — to the upper limit of non-relativistic nuclear processes as suggested by A. M. Baldin. The latter go at the level of nucleon-nucleon interactions without inclusion of the meson degrees of freedom. The expression of the data via the relativistic invariant variable b_{ik} makes it possible to associate in a common form data on multiple target-nucleus and relativistic projectile fragmentation.

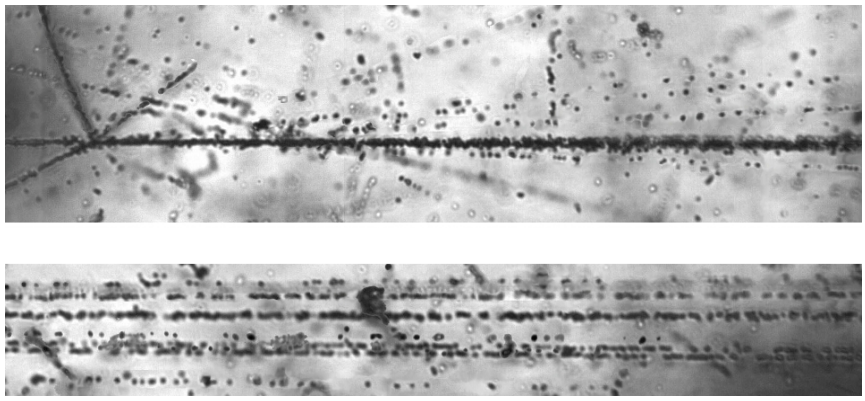

Fig. 2: Example of peripheral interaction of a 3.65 A GeV ^{28}Si in a nuclear track emulsion.

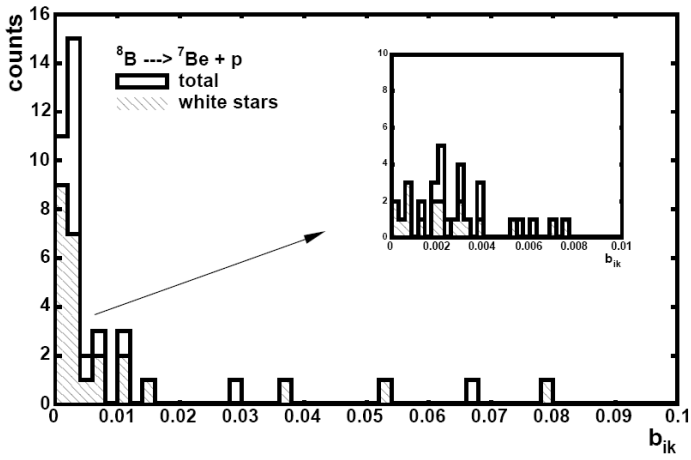

Fig. 3: The b_{ik} distribution for the fragmentation $^{8}B \rightarrow {}^{7}Be + p$ channel. The inset shows the analogous distribution with respect to b_{ik} in the range 0-0.01. The shaded part of the histogram represents the contribution of white stars.

A leading role of the channel 4+1 in the ^{8}B fragmentation implies that the exploration at $b_{ik}<10^{-2}$ is prospective. For the sake of illustration, we consider several events for which angular measurements have been already performed. The b_{ik} distribution (fig. 3) is of the same nature as for the above-considered $^{22}Ne \rightarrow n\alpha$ events [3]. The range 0-0.01 (see fig.3) includes 80% of peripheral interactions.

There is a close connection between b_{ik} variables and the invariant mass of the system of fragments.

$$M^{*2} = (\Sigma P_j)^2 = \Sigma(P_i \cdot P_k)$$

and the excitation energy $Q = M^* - M$, where M is the mass of the ground state of the nucleus corresponding to charge and weight of the system being analyzed.

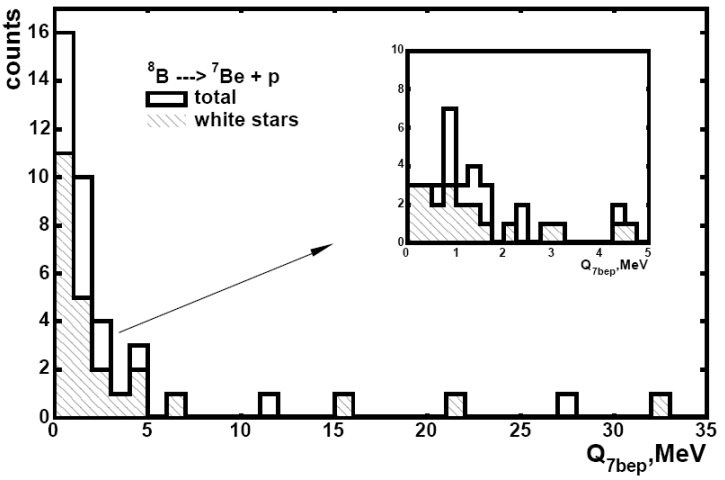

Fig. 4: Excitation-energy distributions for the channel $^8B \rightarrow {}^7Be + p$ in the ranges 0–35 MeV and 0–5 MeV (on the inset). The shaded part of the histogram represents the contribution of white stars.

To estimate the excitation energy of ^{8}B nucleus, the distribution of the difference of the invariant mass M* of ^{7}Be +p system and the sum of the masses of ^{7}Be nucleus and proton, M, is displayed in Fig.4. The mean value of this distribution is $\langle Q_{pBe} \rangle = 4.3 \pm 1.5$ MeV. The majority of the events are grouped in the range $Q_{pBe} < 2$ MeV. A more detailed pattern of the distribution in this range is given in Fig. 4. It includes 64% of white stars characterized by a mean value of $\langle Q_{pBe} \rangle = 0.9 \pm 0.1$ MeV. This value is compatible with the assumption of the decay of the ^{8}B nucleus through the first excited state above the threshold for ^{7}Be + p decay channel at 0.8 MeV with a width of 35 keV. The energy of the next excited state is 2.3 MeV. In just the same way as in the case of "white" ^{22}Ne [3] stars, it is indicated that there is a concentration of events in the region of very low energies.

3. CONCLUSIONS

In the paper was used the invariant approach to analyzing the fragmentation of relativistic ^{8}B nuclei at an energy of 1.2 A GeV in emulsion. In spite of limited statistics it can be asserted that the use of relativistic invariant approach to the analysis of multiple fragmentation of light nuclei in emulsion, suggested by A.M.Baldin in a rather general form, is an effective means of obtaining sufficiently clear conclusions about the behavior of systems involving a few lightest nuclei at energies typical of quantum coherence.

Relativistic fragments are concentrated in a cone defined by $b_{ik}<10^{-2}$ and their differential distributions in this domain are alike. This approach makes it possible to explore the particular features of decay of individual nuclei. The excitation energy of a system involving a few fragments over the ground state with the same baryon number can be estimated in an invariant form up to ^{8}Be nucleus decays.

The work was supported by the Russian Foundation for Basic Research (Grants nos. 96-1596423, 02-02-164-12a, 03-02-16134, 03-02-17079, 04-02-16593 and 04-02-17151), VEGA 1/9036/02 Grant from the Agency for Science of the Ministry for Education of the Slovak Republic and the Slovak Academy of Sciences and Grants from the JINR Plenipotentiaries of Bulgaria, Czech Republic, Slovak Republic, and Romania in 2002-20011.

4. REFERENCES

[1] R. Stanoeva, V. Bradnova, S. Vokr'al, P.I. Zarubin, I.G. Zarubina, N.A. Kachalov, A.D. Kovalenko, A.I. Malakhov, G.I. Orlova, N.G. Peresadko, P.A. Rukoyatkin, V.V. Rusakova, E. Stan, M. Haiduc, S.P. Kharlamov, I. Tsakov, T.V. Schedrina. (2007). Peripheral fragmentation of ^{8}B nuclei in nuclear emulsion at an energy of 1.2 GeV per nucleon. *Physics of Atomic Nuclei*, vol. **70**, No. 7, pp. 1216–1221.

[2] A. M. Baldin and L. A. Didenko. (1990). *Forscht. Phys*. **38**, pp. 261-332.

[3] Web site of the BECQUEREL project: http://becquerel.jinr.ru.

CASE STUDY OF THE RISK OF EXPLOSIONS AND FIRES IN GASIFICATION SETTLEMENTS IN EARTHQUAKE

Lyubomir Direkov
South West University "Neofit Rilski" – Blagoevgrad (Bulgaria)

Abstract: *In the recent years, almost two thirds of the bigger populated places in Bulgaria were gasified. In the region of Southwest Bulgaria gasification is carried out by the Italian - Bulgarian joint stock company "Rila gas. " Despite the existing rules and regulations for safety and installation of equipment andthe exploitation of natural gas, in many places including the region of Blagoevgrad, local incidents occurred due mainly to the fact that there was no coordination between the Rila gas ", CEZ , Vivacom and other companies, having the gas and electrical installations under ground. This creates a real danger for the people living in these populated locations of fires and explosions due to earthquakes, where the entire infrastructure would be destroyed.*

Keywords: *Natural gas, gas, accidents, explosions, fires, earthquakes, destruction, poisoning, basic steps, people injured, first aid*

1. INTRODUCTION

Natural gas (methane) is a multicomponent mixture, containing mainly methane and hydrocarbons of its homologues and non-carbon components that form the natural underground accumulations. Natural gas is classified into three main groups:Gas produced from pure natural gas field, consisting mainly of methane (82% - 98%);Gas - condensed origin, a mixture of gas and heavy hydrocarbons, which under normal conditions consist of fluid and contain significant quantities of methane (80% - 95);

Gas produced from oil and oil fields (petroleum gas), comprising a mixture of petrol vapor gas and propane - butane fractions containing only 30% to 70% methane.Natural gas from underground formations is transported to consumers primarily through gas pipelines for high pressure, which in addition by land, cross water reservoirs ("Blue Stream"), swamps and deserts. Besides through pipelines, natural gas is transported by tankers or tanks in compressed form, at high

pressure or liquid at temperatures below -161 ° C. In the process of liquefaction of natural gas, it reduces its volume 600 times the volume, occupying the same volume of gas under normal conditions. Natural gas in the earth stata is saturated with water vapor to the movement of methane mixture condense, accumulate in the lower parts of the pipeline, breaking technological mode of transportation of gas. Coupling of water with acid gas containing methane in the mixture, contributes to the intensive formation of corrosion. Moreover, in certain pressures in the presence of moisture in gas, crystal-hydrates are formed, which obstructs or reduces the section of pipeline and valve, thus causing an emergency, such as explosions and fires.

Fig. 1. Ignition and explosion of gas pipeline.

2. EXHIBITION

The purpose of this study is to analyze the risk of occurrence of explosions and fires in gasified cities in earthquakes and to propose combined measures to protect people. Natural gas forms explosive mixtures in the air. Gas mixture can ignite and explode when the gas content in the air in the emergency zone is between the lower and upper concentration limits of ignition. The lower concentration limits of ignition corresponds to the minimum percentage of methane in the air (4% - 5%), in which the explosion is now possible, and the upper - the maximum concentration (15%) where it an explosion is still possible. It

should be considered that the concentration of ignition of gas continues to exist for a certain time, even after the gas flow is terminated.

Causes of explosions could be mainly the following: an abrupt change in physical condition of the system - evaporated liquefied gas, instantaneous burst of the walls of the facility, which is natural gas under high pressure and others. Thus in 2007 when increasing the pressure in the gas distribution system in an apartment block, explosion occured ,in which the explosion wave caused the collapse of two of the four entrances in the 10 - storey building, in which 33 people died and 18 were seriously injured.

Fig. 2. Gas explosion in an apartment block in the city of Dnipropetrovsk.

Gasification of Blagoevgrad and other towns in the area started in 2009 by Italian-Bulgarian joint stock company "Rila gas. Although existing rules and regulations for safety and installation of equipment, in many places, including in the region of Blagoevgrad, local accidents occurred due mainly to the fact that there was no coordination between the Rila gas ", CEZ , Vivacom and other companies having the gas and electrical installations under ground. So in 2010 in Blagoevgrad Street »Ivan Mihailov» № 6 a fire occurred, due to interfacial fire break and short circuit in low voltage cables laid underground. Later it is found that gas pipelines had been laid beneath, and the the two structures almost touch each other without intermediate isolation. And according to Regulation № 6 for safe exploitation of such facilities, spacing must be at least 50 cm of cables with voltage up to 1 kV and 60 cm of cables with voltage of 35 kV. With an average load of such cables from the grid they are heated to 50-70 ° C, which creates a real danger to

melt polyethylene pipes for the pipeline and the risk of explosion is very high.

Fig. 3. Explosion of gas pipeline to Greece near the village Bulgarchevo, Blagoevgrad Municipality

Extremely high risk for people living in cities with natural gas pipelines is created in case of severe and catastrophic earthquakes. Such earthquakes can destroy electrical, gas, plumbing and sewage systems; roads and bridges, buildings and equipment; can create massive fires and serious accidents at industrial sites and nuclear power stations, in which hazardous substances can induce the air and the environment . The area of southwestern Bulgaria is one of the most dangerous,regarding an occurrence of severe and catastrophic earthquakes in the Alpine-Himalayan seismic belt. In this region the risk to humans is highest t in the direction Blagoevgrad - Simitli - Kresna. In the region of Kresna Gorge in 1904 emerged the strongest earthquake in Europe for the past 100 years.

In such degrees of possible earthquakes in gasified populated areas, from the destroyed gas pipelines in the streets and gas installations as well as the equipment in residential and municipal buildings would create explosions and fires that would directly affect the people and cause serious injuries and death. Moreover, in the houses and other enclosed spaces could appear dangerous concentrations of gas, which when inhaled by humans could result in poisoning and death. Symptoms of severe poisoning from natural gas

are mainly the following: difficulty in breathing, drowsiness, nausea, dizziness, pain in the area of temples, loss of consciousness due to oxygen deficiency.

3. CONCLUSIONS

1. The risk to the health and lives of people from fires and explosions in gas, supplied in the cities in the event of severe and catastrophic earthquakes is much greater than in not gasified.
2. Due to the toxic properties of the emitted gas components in the ignition of gas, people before leaving the premises must be placed in the mouth and nostrils, gauze masks or handkerchiefs, soaked in an aqueous solution of sodium bicarbonate for respiratory protection.
3. Should not perform any action and do not use items that could cause sparks in the area of the accident with natural gas, including lights, bells, intercoms, inclusion and speaking with mobile phones and similar devices, starting and movement of vehicles and others.

4. REFERENCES

[1]. Direkov, L. Protection of human and environmental extreme conditions. 1996.

[2]. Regulation № 6 For technical rules and standards for design, construction and use of facilities and equipment for transmission, storage, distribution and supply of natural gas. 2004.

[3]. Voskresenskiy, Yu. Study seysmicheskih reflection amplitude change for searching and exploration of hidrocarbons. 2002.

[4]. Proselkov, Yu; Bulatov, A. Complication and emergencies in the drilling of oil and gas drilling holes. 2000.

[5]. Bob Shively, John Ferrare. Understanding Today's Natural Gas Business. 2009.

[6]. European Natural Gas Demand, Supply, and Pricing: Cycles, Seasons, and the Impact of LNG Price Arbitrage

[7]. Boyun Guo, Ali Ghalambor. Natural Gas Engineering Handbook. Boyun Guo, Ali Ghalambor. 2006

[8] Arthur J. Kidnay, William R. Parrish, Daniel G. McCartney Fundamentals of Natural Gas Processing. 2009.

INVESTIGATION OF BRAIN FUNCTIONAL ASYMMETRY THROUGH MEASUREMENT OF ENERGY SPECTRUM OF WATER AS A SENSOR

Stoyan R. Vezenkov[1], Krasimir Damov[2] and Anton S. Antonov[2]
[1] Department of Language and Speech Therapy, South West University Neofit Rilski, Ivan Mihailov str. 66, Blagoevgrad, e-mail: vezenkov.stoyan@swu.bg
[2] Department of Physics, South West University Neofit Rilski

Abstract: *In current study was suggested a new application of Antonov’s method, which is described in details. The energy spectra of water, put on the left and the right half of the human scalp (water filled test-glasses on positions C3 and C4), were altered differently during fulfillment of different cognitive tasks. These preliminary results demonstrated that the method could be applied to investigate the functional asymmetry of brain. It was supported the term ‘water sensor’, in the sense of the suggested new application, that together with the classical electrophysiological sensors and the relevant signal processing could reveal a new aspects of the brain activity – the electromagnetic emissions and their respective information, affecting the molecular structure of water respectively its intermolecular energy spectrum, which could be measured objectively.*

Key words: *energy spectrum of water, “water sensor”, functional asymmetry of brain, cognitive tasks, neurophysiology*

Introduction

A unique physics method for measurement the energy spectra of intermolecular H-bonds of the water has been developed from Antonov and colleagues over decades.

A specific mechanism for water structure stabilization was proposed to take a place under different influences. (Antonov etc., 1982, 1985, 1995, 1997, 2000, 2002, 2004; Yuskesselieva&Antonov, 1973) The water energy spectrum was observed as a measurable parameter of relative stable intermolecular water structures as an informational recordings of these influences – physical, chemical and even biological. (Antonov etc., 2001, 2002; Lavrenko etc., 2007)

Due to the high sensitivity of Antonov’s method it was suggested for estimation the influence of radio, TV and media products on the man, characterizing itself that the media product could act on person,

holding in his hands a bottle with water, drop from which was taken and further evaluated. (Antonov etc., 2004)

In all studies which have been conducted to determine the influence of biophysical fields of man in given conditions on the water energy spectrum, the water bottle was hold in his hand.

The purpose of this work is to investigate whether there will be a difference in the energy spectrum of water put on the both sides of the scalp of a person, who fulfills different cognitive tasks.

The brain asymmetry has been studied more than hundred years since Paul Broca in XIX century has been described the verbal areas in left brain hemisphere. A huge number of methods and methodology has been developed to study the asymmetrical phenomenon of the brain functioning.

The idea was to use the water sensors (Antonov etc., 2004) in neurophysiological context, namely to see its sensibility to brain asymmetric functioning.

The preliminary results are presented here.

Antonov's experimental method

For investigating the time dependence of the wetting angle we used the optical method developed according Antonov (1973, 1985, 1995, 2000). In **Fig. 1** is shown the basic scheme of this method. A plane-parallel beam of monochromatic light (shown by arrows) falls on the water drop lying on the horizontal plate and forms a dark ring at the plate exit. This ring is fixed on a photographic plate and is shown in **Fig. 2**.

The ring thickness ***a*** is related to the wetting angle θ by means of the relation (1). The experiments were carried out on destilled water drops placed on a plate of polymethylacrilate with 4 mm thickness. During the evaporation of the drops a constant temperature T=22.5±0.2^{o}C and a constant relative humidity f=38.4±0.6% of the environment were maintained. The boundary wetting angle and the basic diameter of the drops were measured as function of time until complete evaporation of the drops under conditions of an open space above the evaporating drops. The wetting angle and the base diameter of the drops were determined with an error minor to 1%.

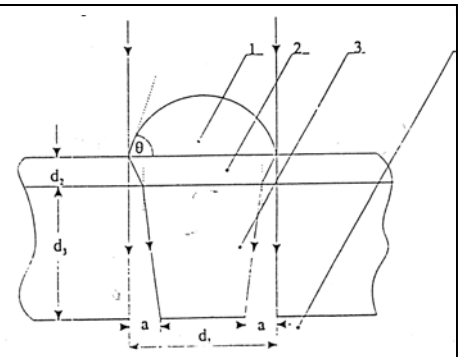

Fig. 1. Scheme of the optical method for determination of the boundary wetting angle θ:
1- water drop; 2- transparent hydrophobic plate; 3 – photographic plate; ← - light flux

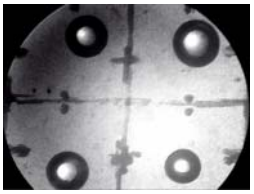

Fig. 2. Photographic recording of the dark rings representing the evaporating water drops.

(1) $$\theta = arctg \frac{n_3}{\left[n_1^2 \left(1 + \frac{d_3^2}{a^2} \right) - n_3^2 \right]^{1/2} - \left(1 + \frac{d_3^2}{a^2} \right)^{1/2}}$$

n_1, n_3 – are the coefficients of light deflection of water and plate, respectively.

The method is precise since it is reduced to determination of the width of certain light patterns when light beam passes through the drop. A typical error assessment in a precise E measurement is less than 3%. The dependence of the energy E of the hydrogen bonds on the wetting angle θ is shown in (2), (3), (4):

(2) $\theta = arccos\ (-1 - 14{,}33E) = arccos\ (-1 - bE)$; b=14,33 eV^{-1}

The mean energy is:

(3) $$\overline{E} = \int_{E_o}^{E(O)} Ef(E)dE,$$

E_o – E at the starting angle θ_0, a E(O) – E at the final angle θ=0.

Calculated by:

(4) $$E = -\frac{\gamma_2^0(1+\cos\theta)}{Y(1+\cos\theta_0)}$$

(5) $b = Y(1 + \cos\theta_0) / \gamma_2 = 14{,}33\ eV^{-1}$

$\gamma_2 = 0{,}0723\ Nm^{-1}$ – the surface tension of deionized water

θ_0 – wetting angle in the beginning

Considering θ as a stochastic parameter and f(θ) to be the distribution function, we used the dependences (6) and (7) is valid.

(6) $$f(E) = f(\theta)\frac{d\theta}{dE}$$

f(θ) – distribution function of θ.

(7) $$f(E) = \frac{bf(\theta)}{\sqrt{1-(1+bE)}};\quad b = 14{,}33\ eV^{-1}$$

Experimentally we measured ***f(θ)= ΔN(θi)/$\Sigma\Delta$N(θi)***, where N(θi) is the number of measured θ in the interval $\Delta\theta$. The quantity *f(θ)* was called the state spectrum of water (Antonov etc., 1995). As it is seen it is directly connected via formula (7) with $\bar{f}$(E) – the nonequilibrium energy spectrum of water and could be calculated.

This function was postulated as a function of water intermolecular bonds energies or of H-bonds in the group H-O···H (Antonov etc., 2000).

The water structure is influenced by the global geophysical factors. To eliminate the effect of other possible factors not in the scope of investigation it was necessary to compare the treated water sample with the difference of both the sample and control (called differential energy spectrum).

To characterize the influence of a given factor on the water structure was used the Renyi's formula for the informational growth (Antonov etc., 2004).

Neurophysiological Methods

To monitor the neurophysiological state of the tested person the following setup were used: respiratory sensor (RSP Sensor, 128 SPS, measures the relative expansion of the abdomen or thorax during inhalation and exhalation), sensor for skin conductance (SC/GSR, 128 SPS, measures the sweat gland activity, relative changes in skin conductance); temperature sensor (NX-TMP, 0.001^{o}C), blood volume pulse sensor (NX-BVP, 128SPS, measures relative blood flow, using optical electronics that measure near-infrared light), hardware Blue Tooth Wireless Link; ADCard data precision (24 bit); computer Core 2CPU, T7200, 2GHz, 2GB of RAM with graphic card NVIDIA 1024x768 resolution, 256 MB; Windows XP-SP3, software for physiological monitoring and biofeedback BioTrace+ for NeXus-10 from Mind Media B.V. Netherlands.

The sensors were put as it is shown in **Fig. 3** and the signals were monitored during the whole experiment and stored for further analysis.

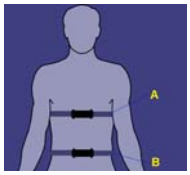

Fig. 3. Neurophysiological sensors and setup. Respiratory

Experimental design

The novelties of applying the Antonov’s method were, firstly, to put the water filled two test-glasses on positions C3 and C4 of the scalp of the tested person in comparison to the classical way to hold it into the hand and second, to monitor his physiological state simultaneously. The person was put in two distinct conditions, fulfilling two different tasks:

1. Reading a scientific text;

2. Listening music ("Idiliya", written by P.Dunov, performed by viola) with closed eyes.

Both tasks were conducted for 10 minutes. Than the measurements of water energy spectrum were performed.

Results

Water energy spectrum data

The results from the first task "Reading" are shown in Fig. 4. As can be seen, the peak of the left hemisphere's (LHS) water spectrum was shifted to the lower values but its amplitude remained the same. To visualize better the obtained difference was built differential energy spectrum (Fig. 4, to the left).

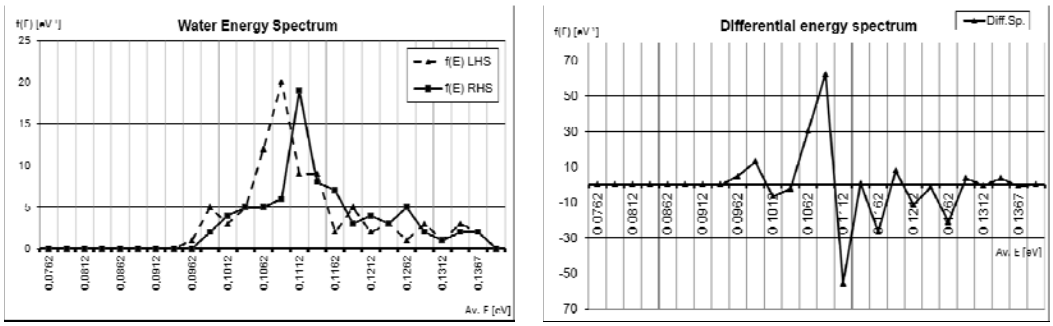

Fig. 4. Differences of water energy spectrum put on the left hemisphere (LHS) and on the right hemisphere (RHS) after reading. Differential water energy spectrum between water put on the LHS and RHS (to the right)

The results from the second task "Listening music with closed eyes" are shown in Fig. 5.

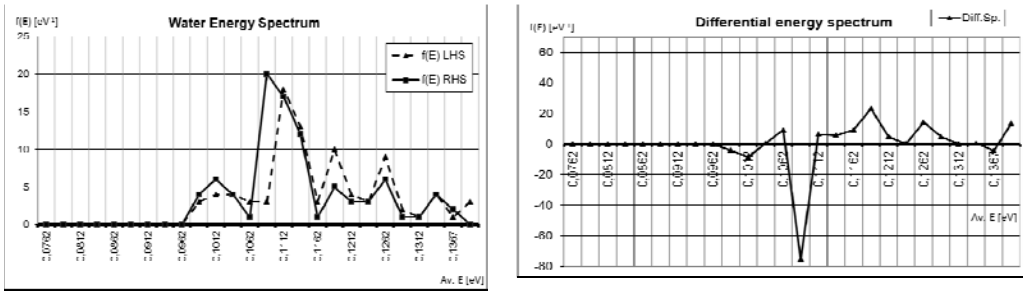

Fig. 5. Differences of water energy spectrum put on the left hemisphere (LHS) and on the right hemisphere (RHS) after listening music with closed eyes. Differential water energy spectrum between water put on the LHS and RHS

Interestingly the peak in energy spectrum of the right hemisphere's (RHS) water after the second task was shifted also to the left with

lightly increase in amplitude (Fig. 5, to the right). Thus the differential spectrum in the second case has the same peak as the first one but with the opposite sign minus.

The mean energy of both left and right waters for both tasks are shown in **Table 1**. Interestingly this data showed reciprocal asymmetry too.

Table 1. Mean Energy (E) for both left and right waters during the two tasks.

	Mean E_{LHS}	**Mean E_{RHS}**
Reading text (open eyes)	0,1121	0,1143
Listening music (closed eyes)	0,1164	0,1136

Physiological Data

The results obtained from the both tasks are shown in **Table 2**. Two distinct physiological states could be observed. During the first task “Reading” scientific text an overall excitation was evoked – increase of the skin conductance, heart and respiration rates, head temperature, on one hand, and decrease of respiration amplitude and coherence or synchronous action of heart and respiratory systems, on the other hand, in comparison to the second task “Listening music” with closed eyes.

Table 2. Physiological variables and statistics during the first task “Reading” (1, in gray) and second task “Listening music” (2, in white)

Parameter	Mean 1**	Mean 2	Var. 1	Var. 2	StdDev 1	StdDev 2	Coeff.V 1	Coeff.V 2
Skin Conductance	12,63	11,67	0,13	0,09	0,31	0,36	0,03	0,03
Temperature	35,3	34,92	0,02	0,02	0,13	0,14	0	0
Heart Rate	94,53	92,18	4,36	5,78	2,09	2,4	0,02	0,03
Respiration Rate	19,22	12,21	14,68	31,58	3,83	5,62	0,2	0,46
Heart Variability LF%	59,9	72,7	273,36	254,16	16,53	15,94	0,28	0,22
Respiration Amplitude	19,65	29,04	227,25	196,64	15,07	14,02	0,77	0,48
Respiration/ Heart Rate Coherence	-0,22	-0,01	0,06	0,09	0,24	0,3	-1,07	-58,54

* *Abbr.:* Var. – Variability; StdDev – Standard deviation; Coeff. V – Coefficient V

** *index 1* – values during the first task; 2 – values during the second task

Discussion and conclusions

It's known today from the EEG recordings and the new qEEG method that the brain emits electromagnetic waves, called brain rhythms, generated from the bioelectrical activity of the neurons in cortex and in subcortical areas.

The brain rhythms after a spectral analysis have been divided in the following frequencies bands: delta (1-4 Hz), theta (4-8), alpha (8-13), SMR or μ-rhythm, or Rolandic alpha (8-13), beta (>13 Hz). The amplitudes of the brain waves are in the range of 5-10 μV, for delta to 20 μV. The relative amplitudes of the brain rhythms appeared on the sagittal line are: delta (~30%), theta (~21%), alpha (~30%), beta (~19%) (Kandel etc., 2000).

The grand average spectra of the brain rhythms are quite symmetrical for different age groups. However, it is not uncommon for a healthy person to reveal an asymmetry in alpha rhythms at the range of 10-50% (to the advantage of RHS) in other words the power of this asymmetry could be big enough (more than 50% is a marker for pathology). The question aroused whether this asymmetry might be a measure of some individual character, for example, intro/extroversion, negative/positive affects etc., has not yet fully revealed. The studies of Davidson have shown asymmetry of the alpha spectra in frontal lobes during different emotional reactions (Davidson, 2004). During relaxed wakefulness in eyes closed condition the brain exhibits electromagnetic activity in alpha frequency band, predominantly from the RHS. The power of alpha activity has been shown to be inversely correlated to methabolic function of the corresponding brain area, thus have obtained the name "idling" rhythms of the cortex.

On the other hand inhibitory neuronal networks have shown to be involved in generating beta rhythms. They were shown to be positively correlated with metaboloic activity in the recorded brain area.

Interestingly the activation of a given cortical area is related to a high oxygen and glucose consumption in inhibitory neuronal network, emitted at beta frequencies.

The question arises which processes might be involved in altering the water energy spectrum put on the scalp in our experiments?

The energy of the emission of the brain activity might be related to the power, the amplitude of the brain rhythms, to the blood dynamics and to the biochemical processes, respectively the heat produced. The amplitudes of the alpha and slower rhythm as was shown upper are bigger than the beta ones. Thus, the idling brain might emit more energy than the working. On the other hand the blood dynamics and the metabolism, respectively the heat produced in activated brain areas could affect more powerful the water than the electromagnetic

field of the beta rhythms, which are energetic weaker than the alpha emissions from the idling areas.

The neuronal networks for reading have been proved to be in the left hemisphere for the right-handed persons. The RHS has been reported to be responsible for music recognition, especially the rhythm and melody.

Brain area activity as discussed previous is related to beta rhythms, which have twice weaker amplitudes than the alpha rhythms, generated by idling areas. The energy of the electromagnetic wave produced is proportional of the square of its amplitude.

Our empirical data, shown in **Table 1** suggests that the activated brain areas produced less energy than the idling, which our water sensors detected in the two distinct task conditions, determined also physiologically (**Table 2**).

On the other hand, the activated brain area shifted the peak in water energy spectrum to the left (**Fig. 4 and 5**). For the latter results we don’t have any explanation and should be further proved and researched.

Our preliminary results showed clear that the Antonov’s method could be applied for investigation of the functional asymmetry of brain in addition to the classical methods.

References

1. Antonov, A.S and T.D. Galabova (2004) Water as a sensor of superweak physical and chemical influences on man. Proceeding of the Ninght National Conference on Biomedical Physics and Engineering, 14-16 Oct. 2004, Sofia, 303-308
2. Antonov, A.S. and L.Todorova (1995) On the Effect of –rays treatment on the water state spectrum. Comptes rendus de l’Academie bulgare des Sciences, Tome 48, N 1, 21-24
3. Antonov, A.S. and T.D. Galabova (2000) Water-Chemical Compounds Interaction in Biological Systems. Proceedings of the Eight National Conference on Biomedical Physics and Engineering, 12-14 Oct. 2000, Sofia, 97-99
4. Antonov, A.S. and Yuskesselieva (1982) Dissipative Structures in Water. System. Studia biophys. 91, 93-94
5. Antonov, A.S. and Yuskesselieva (1985) Experimental Study of Dissipative Stuctures in Water Systems Owing to Evaporation. Acta Hydrophysica, Berlin, XXIX, H.1, 5-14
6. Antonov, A.S., T. Cholakov, T. Galabova, P. Gramatikov (1995) Nonequilibrium Energy Spectra of Rain and River Water from Rila Mountain. OM2, N3, 39

7. Davidson, E.J. (2004) What does the prefrontal cortex “do” in affect: perspectives on frontal EEG asymmetry research. Biol. Psychol. Vol. 67, (1-2), 219-233
8. Gramatikov, P.S. and A.S.Antonov (1997) On the two conditions model of water structure. Comptes rendus de l’Academie bulgare des Sciences, Tome 50, N 3, 13-16
9. Kandel, E., J. Schwartz and T. Jessel (2000) Principles of Neural Science. Mc-Graw-Hill, New York
10. Lavrenko S., A. Antonov, V. Tsetlin, T. Galabova, K. Damov, V. Tanchev (2007) Information treated water energy spectrums and biological properties, Proceedings International Conference CSIT’2007, 09-2007, Lviv, Ukraine
11. Yuskesselieva, L.G. and A.S. Antonov (1973) Optical Method for Determination of Liquid – Solid Substrate Boundary Angle. C.R.Acad.bul.Sci. 26, 35-38
12. Антонов, А., В. Въчков, П. Граматиков, К. Дамов, В. Ковачев, Д. Манолев, Л. Тодорова, С. Тодоров, Т. Гълъбова, (2002) Водата като универсална среда за запис и запаметяване на информация в природата и у човека, Първа национална научна конференция по психология, май 2002, ЮЗУ-Благоевград, 16-17

Nonlinear spectroscopy of second- and third-order susceptibility in Magnesium Sulfite Hexahydrate single crystal

L. I. Pavlov[a*], D.I.Kaisheva[a], Z. Bunzarov[b]

[a]Department of Physics, South-West University, 66 I.Mihailov str., Blagoevgrad-2700, Bulgaria
[b] Dept.of Cond.Matter, Fac.of Physics, Sofia University, 5 James Bourchier Blvd., 1164 Sofia, Bulgaria

***Abstract**: The second- and third-order nonlinear optical properties of single crystals of Magnesium Sulfite Hexahydrate ($MgSO_3.6H_2O$) were studied by Second-Harmonic Generation (SHG) and Degenerate Four-Wave Mixing (DFWM). Nanosecond pumping by special type Nd:YAG laser having a variable reflection output coupler was used. The effective quadratic ($\chi^{(2)}$) and cubic ($\chi^{(3)}$) nonlinear susceptibility values of the examined crystals are obtained at room temperature. The dispersion of the nonlinear optical susceptibility of $MgSO_3.6H_2O$ is also discussed.*

***Keywords:** nonlinear optical materials, second-harmonic generation, degenerate four-wave mixing, $MgSO_3.6H_2O$*

1. INTRODUCTION

The increasing variety of applications of nonlinear optical (NLO) materials for second harmonic generation (SHG), sum- or difference-frequency mixing, optical parametric oscillation or amplification and other NLO processes have resulted in the development of numerous NLO materials. Especially the crystals, where the second-order NLO properties are strongly influenced by the molecular structure and their arrangement, have been the subject of increasing interest[1] since the discovery of the first inorganic NLO material KB5 in the series of borates[2].

The crystal magnesium sulfite hexahydrate ($MgSO_3.6H_2O$) belongs to a specific crystal symmetry (C_3) and its crystal structure is rhombohedral. Crystallographic data of this inorganic crystal have been reported[3]. The $MgSO_3.6H_2O$ crystal has the property of being strongly birefringent (necessary to obtain phase matching for NLO processes). Moreover, it is transparent in a wide spectral range,

particularly for the 1064-nm output from Nd:YAG laser and at doubled frequency (532 nm), and resistant against a high-intensity irradiation. The linear optical properties of $MgSO_3.6H_2O$ single crystals formed by method[4] have been studied[5], as well as the second-order NLO properties. In the latter case, a phase-matchable SHG of both Type 1 (o_1-o_1-e_2) and Type 2 (o_1-e_1-e_2) interactions has been performed. The birefringence of this material favours its use for SHG, but the SHG-conversion efficiency is limited by the optical quality of the crystals.

The growth of single crystal materials is complicated by a lot of effects which lead to fluctuations of the quality in the volume of the growing crystal, and, which in turn leads to degradation of its material properties and of NLO response. Growth under low gravity conditions, significantly reduces the poor crystalline perfection. Here, we examine a new group of $MgSO_3.6H_2O$ single crystals produced by improved growth and optimized crystallization method[6] which allows single crystals with large sizes to be obtained; additional Ni concentration is inserted within the sample, as well. Possessing an optical high quality, the NLO response of this material is probed by SHG and Degenerate Four-Wave Mixing (DFWM) under nanosecond regime of pumping. Especially, a higher input fundamental frequency energy close to the saturation is used for both nonlinear processes.

2. EXPERIMENTAL

Well polished samples of $MgSO_3.6H_2O$ single crystals with cross-sectional area of 20 $\times$ 15 mm^2 and various lengths from 8 to 18 mm were prepared. The large crystal aperture is of advantage when the phase-matching angle for SHG is sizable. The samples were oriented by polarized light using a polarization microscope. Raman spectra of the crystals were recorded in the spectral region from 100 to 1100 cm^{-1}. In this range the Raman spectra depend significantly on the crystal orientation and polarization.

The SHG and DFMW measurements were performed in a non-focused optical setup. The light source was a computer-controlled high-power *Q*-switched Nd:YAG laser with variable reflectivity dielectric mirror[7] (λ = 1064 nm) with 0.1 nm spectral width, pulse duration 10 ns (FWHM) and energy of 60 mJ/pulse. The beam divergence was 0.18 mrad (HWHM at e^{-2} intensity-level). The laser, utilizing unstable resonators with variable output coupler, provides a Gaussian and super-Gaussian profiles with various mirror spot sizes. The advantages of this laser are: (i) reduction of the diffraction losses; (ii) radially symmetric output profile which results in an uniform output beam in the near- and far-field and increases the transverse mode

discrimination; and (iii) high second-harmonic conversion efficiency (up to 50% using a 15-mm long KDP nonlinear crystal, Type 1 interaction). In fact, such cavities are very effective for Q-switched lasers when high-energy frequency doubling is needed[7,8].

In the experiments, the linearly polarized laser output was divided into two parts by a beam splitter and the reflected beam was employed as a reference. The pulse energies of the incident and nonlinearly generated beams were controlled simultaneously by energy meter Rj-7200 (Laser Precision Corporation). The incident laser beam spot size was of about 1.3 mm^2 corresponding to a peak intensity in the sample ~ 350 MW/cm^2. The energy density per pulse was approximately 3.5 J/cm^2. To prevent the influence of thermal effects, we used single-pulse measurements with a repetition rate of 1 Hz. It should be noted that the magnesium sulfite hexahydrate is in a stable equilibrium solid phase at temperatures below 42°C, otherwise its stability drastically decreases[9]. To overcome the pulse-to-pulse fluctuations in the input beam when measuring, and in order to get well reproducible and conclusive data, an averaging by use of 50 laser shots up to hundred, was used. In the course of our experiments we have not observed any optical damage of the samples proved by irradiation with at least 10^4 laser shots - the single crystals did not undergo any changes.

Colored glass filters were used for spectral separation of the signals. In DFWM measurements, not only the fundamental output at wavelength 1064 nm but also the frequency-doubled laser output (532 nm, 45 mJ) were used. Transmittance spectra were recorded by Specord UV-VIS spectrophotometer (within the spectral range 180 – 800 nm) and Specord IR (800 – 1800 nm). All measurements were carried out at room temperature.

3. RESULTS

Fig. 1 presents the optical transmission spectrum of $MgSO_3.6H_2O$ single crystal. Trasmittances up to 85 % at 532 nm and 71 % at 1064 nm were measured, slightly varying for various samples. The crystals are phase-matchable, but did not require a very crucial adjustment for the frequency-doubling of the 1064-nm output from Nd:YAG laser. Nevertheless, the on-axis phase-matching conditions between the fundamental beam and second harmonic were carefully optimized in our measurements. The angle for a maximum SHG-conversion of Type 1 (o-o-e) phase matching was 12.4°.

Upon optimal phase match, we have measured the SHG-conversion efficiency $\eta = I_2/I_1$, where I_2 and I_1 denote the second-harmonic and fundamental laser intensities, respectively. This quantity

depends on I_0 and varies with the crystal samples. Corrected to the reflection, the maximum η measured was as high as 0.5 % (at 60 mJ fundamental). The measurement of SHG output for various sample L lengths (the NLO interaction length, optical path) shows an increasing SHG with *L*, but it is not proportional to L^2 (Fig. 2). The deviation from the quadratic dependence suggests the influence of both linear and two-photon absorption losses on the SHG efficiency with the two-photon one prevailing .

The second harmonic emission generated in the crystals can be used to estimate the effective quadratic ($\chi^{(2)}$) nonlinear susceptibility value. The SHG intensity is determined by[10]:

$$I_2 = \frac{128\,\pi^5}{c\,\lambda_1^2}\frac{\left|\chi^{(2)}\right|^2}{n_1^2 n_2} I_1^2 \left\{\frac{\sin(\Delta kL/2)}{\Delta kL/2}\right\}^2 L^2 \qquad (1)$$

where $\Delta k = k_2 - 2k_1$ is the phase mismatch. Thus, the SHG-efficiency η at optimal phase match is proportional to the squared modulus of $\chi^{(2)}$ of the NLO material:

$$\eta \propto \left|\chi^{(2)}\right|^2 L^2 \qquad (2)$$

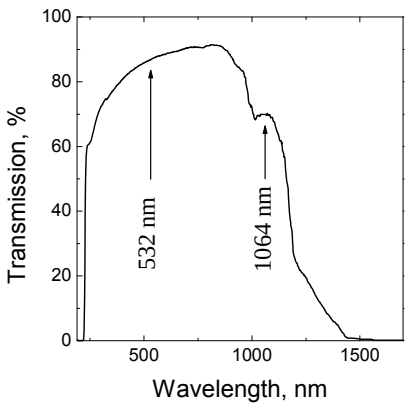

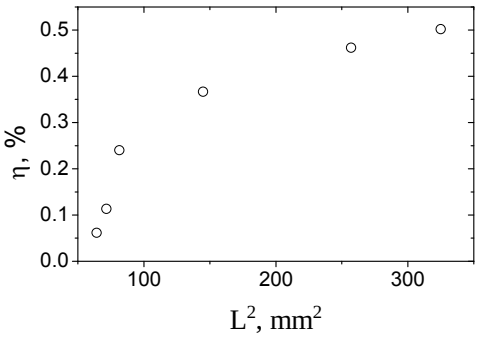

Fig. 1. Optical transmission of $MgSO_3.6H_2O$ single crystal (15-mm long sample).

Fig. 2. The observed variations of the conversion efficiency η as a function of the squared optical path L^2.

Related to the inorganic SHG-crystal KDP (potassium dihydrogen phosphate) of the same length *L*, e.g. 16 mm, η of the $MgSO_3.6H_2O$ single crystals is of about 20 times less. According to the Eq. (2), $|\chi^{(2)}|$

of $MgSO_3.6H_2O$ at 1064 nm is of about 22 % that of KDP. The experimental uncertainty of this estimation is of about ± 15 %. Compared to the commonly used SHG crystals at present, this second-order optical nonlinearity is relatively low. However, we have to point out that the $MgSO_3.6H_2O$ single crystals possess a relatively high optical damage threshold; reference to the one of KTP (potassium titanyl phosphate) gives ~ 15 J/cm², which is a very useful option.

In addition to $\chi^{(2)}$ NLO, the $\chi^{(3)}$ of the single crystal of magnesium sulfite hexahydrate is also of interest. Especially, the Raman-active vibration at 954 cm^{-1} is very strong in a XX scattering configuration (Fig.3) which suggests the possibility for the use of this sharp resonance for Raman laser action. However, in our experiments we have not observed a stimulated Raman scattering (SRS), pumping with 1064 nm (up to 750 MW/cm^2) and 532 nm (up to 450 MW/cm^2), most probably because the threshold for SRS has not been reached, or due to suppression of such an emission by the competing NLO processes like the two-photon absorption.

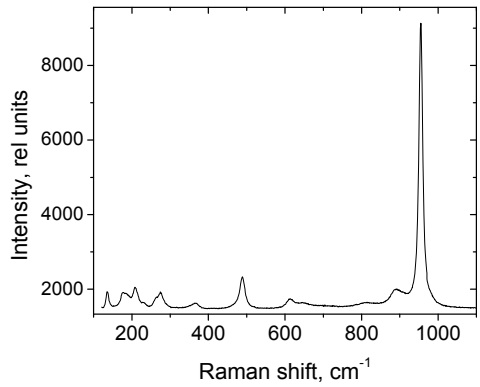

Fig.3. Raman spectrum of $MgSO_3.6H_2O$ single crystal in a XX scattering configuration.

We estimated the effective cubic ($\chi^{(3)}$) nonlinear susceptibility for the used $MgSO_3.6H_2O$ single crystal. For the purpose, the backward DFWM was performed by collimated beams and in a conventional pump-probe configuration (Fig. 4). The three laser beams - two opposite-travelling strong pump waves $\boldsymbol{E_1}$ & $\boldsymbol{E_2}$ and the probe wave $\boldsymbol{E_P}$, were directed onto the sample at a small angle. The generated signal wave $\boldsymbol{E_S}$ is coherent because the phase-matching condition is automatically fulfilled. The process is described by $\chi^{(3)}(\omega=\omega+\omega-\omega)$ and it is well established in nonresonance case[11].

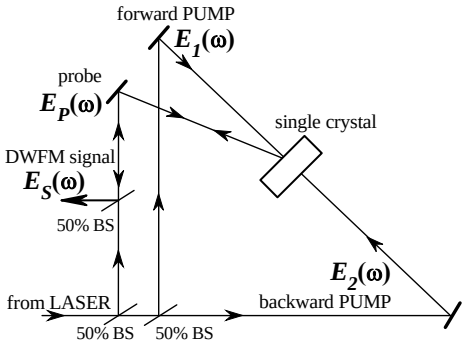

Fig. 4. Schematic illustration of the configuration for DFWM used here.

$\chi^{(3)}$ of $MgSO_3.6H_2O$ was measured relative to $\chi^{(3)}$ of Roshelle salt single crystal (8 mm length) used as a reference. For this material the value $|\chi^{(3)}| = 6\times10^{-15}$ esu has been obtained in our laboratory under 25-ns pump[12].

If the pump has an intensity above the threshold, the intensity of the generated nonlinear signal is be given by[13]:

$$I_S \propto const\ I_1 I_2 I_p \left|\chi^{(2)}\right|^2 L^2 / n_0^4 \qquad (3)$$

where the constant depends on the definitions used. The results from our measurements are: $|\chi^{(3)}| \approx 9.1\times10^{-15}$ esu at 1064 nm and $|\chi^{(3)}| \approx 1.5\times10^{-14}$ esu at 532 nm. Such values are quite comparable to the ones of some centrosymmetrical crystals[14] and some organic polymers, but considerably lower (about five orders of magnitude) than $\chi^{(3)}$ of the commercially available semiconductor-doped glasses in the form of colored glass filters under 10-ns pump[13,15] and, unfortunately, they are insufficient for true NLO use.

Being of importance for the practical application of $MgSO_3.6H_2O$, the dispersion of NLO susceptibilities of this crystal is also of interest. That characteristics is significant under resonant conditions. It is directly related to the proper NLO process and can be derived experimentally. For example, the dispersion $\chi^{(2)}(\omega)$ can be obtained from SHG measurements. Concerning the experimental procedure of the $\chi^{(2)}(\omega)$ measurement, we have to settle, that the traveling-wave optical amplifier appears to be the most preferable optical system to measure $\chi^{(2)}(\omega)$. In this case, the real gain coefficient G which is not influenced by the positive feedback of the resonator, depends on

$\chi^{(2)}(\omega)$. Thus, the measurement of G can be used to determine $\chi^{(2)}(\omega)$ instead of measurements of the SHG signal as a function of ω.

The small gain increment of parametric amplifier can be expressed as follows[10]:

$$G_2 = \frac{1}{4}\exp\left[\left(\frac{16\omega_1^2 \Phi d_{eff}^2}{\varepsilon_0 n_1^2 n_2 c^3} - \Delta k^2\right)^{1/2}\right] \qquad (4)$$

where Δk is the phase mismatch, ε_0 is the vacuum permittivity, Φ is the pump fluence, and d_{eff} is the second-order NLO coefficient. As a result, using the data for the refractive index disperison of $MgSO_3.6H_2O$ crystal[5], an information about the $\chi^{(2)}$ dispersion of this material can be obtained within the visible and near-infrared region 0.6 – 1.2 μm.

4. CONCLUSIONS

In conclusion, we have applied Nd:YAG laser with variable reflectivity mirror to study the NLO properties of the single crystals of magnesium sulfite hexahydrate. It was found that this inorganic non-centrosymmetrical crystal exhibits moderate $\chi^{(2)}$ and relatively low $\chi^{(3)}$ values. While the quadratic NLO response is promising and can be applied in case of good crystal quality, the cubic response seems to be still very weak for NLO use, e.g. for an optical parametric oscillator.

Data measured for various kinds of $MgSO_3.6H_2O$ single crystal will allow to optimize the crystallization process of the growth in order to improve the nonlinear optical properties of this NLO crystal. At present, such work is in a progress.

5. REFERENCES

1. D. Xue, K. Betzler, H. Hesse and D. Lammers, “Nonlinear optical properties of borate crystals,” *Solid State Commun.* 114(1), 21-25 (2000).
2. C. F. Dewey Jr., W. R. Cook Jr., R. J. Hodgson and J. J. Wynne, *Appl. Phys. Lett.* 26(12), 714-719 (1975).
3. H. D. Lutz, S. M. El-Suradi and B. Engelen, “Zur Kenntnise der Sulfite und Sulithydrate des Zinks, Mangans, Magnesiums and Cobalts – Roentgenographische, spektroskopische und thermoanalytische Untersuchungen,” *Z. Naturforsch.,* 32b(7), 1230-1238 (1977).
4. Ts. Kovachev, Republic of Bulgaria, Patent No.3und4515.

5. Z. Bunzarov, S. Saltiel, Ts. Kovachev, L. Ljutov and D. Russev, "$MgSO_3.6H_2O$ a new crystal for nonlinear optics," *Proc. SPIE* Vol. 3052, 197-200 (1996).
6. Z. Bunzarov, to be published.
7. I. P. Nikolov, I. Buchvarov, L. A. Gubanova and E. N. Putilin, "High Power Nd:YAG Laser With Variable Reflectivity Mirrors," *Proc. SPIE* Vol. 4397, 49-53 (2001).
8. A. Parent and P. Lavigne, "Increased frequency conversion of Nd:YAG laser radiation with a variable-reflectivity mirror," *Opt. Lett.* 14(8), 399-401 (1989).
9. J. Nyvlt, "Solubilities of Magnesium Sulfite,"J *Therm. Anal. Cal.,* 66 (2) 509-512 (2001).
10. S. A. Akhmanov and R. V. Khokhlov, *Problems of Nonlinear Optics*, Moscow, 1964.
11. A. Yariv and D. M. Pepper, "Amplified reflection, phase conjugation, and oscillation in degenerate four-wave mixing,"*Opt. Lett.* 1(1), 16-18 (1977).
12. G. B. Hadjichristov, P. P. Kircheva and N. Kirov, "Multiplex CARS spectroscopy of Rochelle salt crystal," *J. Molec. Struc.* 382(1), 33-37 (1996).
13. R. A. Fischer, *Optical Phase Conjugation*, Academic Press, New York, 1983.
14. M. D. Levenson and N. Bloembergen, "Dispersion of the nonlinear optical susceptibility tensor in centrosymmetric media," *Phys. Rev. B* 10(10), 4447-4463 (1974).
15. R. K. Jain and R. C. Lind, "Degenerate four-wave mixing in semiconductor-doped glasses," *J. Opt. Soc. Am.* 73(5), 647-653 (1983).

Some features about obtaining of ecological dark fuel

Yordanka Tasheva, Petko Petkov
Main assistant, PhD., Professor DSc., Bourgas, Bulgaria

***Abstract**: Waste protected vulcanizate utilization demands working out environmentally safe technologies, affording valuable goods. One of possible solutions of this problem is destructive thermal processes. Thermal solution of waste vulcanizates in dark fuel products affords as asphalt-like materials. These products may use in road building or as anticorrosive, waterproofing and other materials.*

***Keywords:** thermal cracking, utilization, waste tires, and fuel oil*

1. INTRODUCTION

The aim of the present paper is to described some features about obtaining of ecological dark fuel from one hand and from another hand purifying of environment.

The huge quantity of protected vulkanizates gone out of usage every year because of it’s lead to pollution of environment, such as the high resistance toward the effect of sunlight, moisture, oxygen, ozone and et. all. Toward the negative sides of the exported vulканizates may refer their fire hazard, and the products of their uncontrolled burning have harmful effect as well environment as under her occupiers [1].

Environmental and economic concerns have led a number of governments to introduce legislation for plastic wastes [1] and caused much interest in disposal and recovery developments. Land filling, incineration, and remelting require predisposal while chemical recycling does not. The latter method converts polymer waste into fuel or other high value products.[2] An example of this approach is thermal degradation which has been studied by many researchers [3 – 11].

Polymer thermal degradation involves complex reactions dependent on various factors such as the heating rate, pressure, reaction medium, (solution and/or gaseous, oxidative, reductive, or inert) and reactor geometry. The polymer’s high viscosity complicates the process by impeding heat and mass transfer.[12–13]. Solvent addition eases these and lowers operating temperatures. Further advantages of this approach are higher total conversion, higher liquid yields, and easier control.

Recycling process development is particularly important for polyethylene

(PE) since the latter is the major component of plastic wastes. PE pyrolysis is nonspecific under conventional conditions, resulting in a wide range of products including some ethylene oligomers but rather little of the desired output, namely its monomer [14]. Pinto et al. [9] reported that alkane formation was usually favored when a large amount of PE was present in the treated waste and suggested adding polystyrene or polypropylene to the input mixture in order to increase the aromatics and alkene yields. Uemichi et al. [15] improved the aromatic yield by harnessing activated carbon loaded with platinum or iron. Comparing various works with their own, Scott et al.[11] concluded that short residence times and high temperatures (above 700 °C) appeared to improve the liquid yield. Kaminsky and Kim [7] also supported short residence times.

PE thermal degradation in solvent media is scarce in the literature.

The thermal decomposition behavior of polypropylene, oil shale and a 1:3 mixture of the two were investigated in a thermo gravimetric analyzer (TGA) reaction system in an argon atmosphere, with a view to comparing the process of the mixture with those of the individual components. Experiments were conducted at three heating rates of 5, 10, and 15 K min^{-1}, in the temperature range of 30–900°C. The obtained activation energies were 250 kJ kg^{-1} for polypropylene, 63 kJ kg^{-1} for the oil shale organic matter, and 242 kJ kg^{-1} for the mixture. The results indicate that the characteristics of the process depend on the heating rate, and that polypropylene acts as a catalyst in the degradation of oil shale in the mixture [1].

The decomposition of polyethylene and polypropylene over HZSM-5 zeolite catalyst and a catalyst modified with orthophoshoric acid (PZSM-5) have been compared. The gaseous and liquid products depend on the polymer type, its structure, on the catalyst, its acidity and steric effect. The gaseous products contain large C_3 fraction, while the liquid products from both polymers contain mainly aromatic hydrocarbons. Catalytic decomposition increases the amount of gaseous products, lowers the liquid fraction and changes the composition of these products compared to uncatalytic decomposition [2].

Thermogravimetry (TG) and mass spectrometry (MS) combined techniques have been used to investigate the thermal degradation and catalytic decomposition of high-density polyethylene (HDPE) over solid acid catalysts as H-ZSM-5, Al-MCM-41 and a hybrid material with a bimodal pore size distribution (H-ZSM-5/AL-MCM-41). The silicon/aluminum ratio of all catalysts is 15. Both thermal and catalytic processes showed total conversion in a single mass loss step. Furthermore, the catalytic conversion

presents average reduction of 27.4%, in the onset decomposition temperature. The kinetic parameters were calculated using non-isothermal method. These parameters do not indicate significant differences between the thermal and catalytic processes. Even though, the presence of the catalysts changes the reaction mechanism, from phase boundary controlled reaction to random nucleation mechanism.

Important difference in distribution of evolved products was detected when several catalysts were used. However, in all cases the main products were alkanes (C_2, C_3 and C_4), alkenes (C_3 and C_4), dienes (C_4 and C_5) and traces of aromatic compounds [3].

Thermal degradation of low density polyethylene (LDPE) wastes was investigated in this study as a step in chemical recycling. The effects of the degradation temperature, the solvent–LDPE ratio, and the reaction time were researched in the respective ranges 375– 450 °C, 0:1–6:1, and 30–120 min. Experiments at a cyclohexane: LDPE ratio of 6:1 showed that up to 4258C the solid residue decreased whereas the liquid yield and the total conversion increased. There were no significant changes thereafter. Solventless degradation at 425 °C gave the weight percentages of 4.7, 75.6, and 19.7 for solid, liquid, and gaseous products, respectively. The use of cyclohexane as a solvent brought about approximately 20% gain in liquid yield and diminished the solid residue to negligible levels [2].

2. RESULTS, DISCUSSIONS, CONCLUSIONS

For achievement of our purpose we used the laboratory method of thermal cracking, which are described in [13]. In literature [14] are given the laboratory conditions and chemical characteristics of used from us waste tires. It must notice that the protected vulcanizates are produced from manufactory in Yambol and mechanical processes prepared them in advance. The obtained liquid product was investigated such as conventional fuel oil. In Table 1 are given physical-chemical properties of obtained liquid product so called “pyrolysis oil”.

Tab. 1: Physical – chemical properties of pyrolysis oil.

Parameters	Methods	Values
Density at 20 ºC	BSS EN ISO 3675:2004	0.8720
Sulphur, %	BSS EN ISO 8754:2004	0.19
Specific heat /lower/, kJ/kg	BSS EN ISO 1285:2003	40.45
Kinematic viscosity at 50 ºC, mm^2/s	BSS EN ISO 3104:2001	4.45
Ash content, % (m/m)	BSS EN ISO 6245:2004	0.10
Water soluble acids and base	BSS 5252:1984	Neal
Flash point, ºC	BSS EN ISO 2592:2004	105
Freezing point, ºC	BSS 1751:1970	- 14
Water content, ºC	BSS EN ISO 3733:2003	Neal

The present data have shown that pyrolysis oil, which is obtained in laboratory required of ecological norms of BSS for blend fuel oils, from one hand and from another it presented excellent combustion parameters.

We investigated a conventional fuel oil produced from Bulgarian refinery by corresponding parameters to be made a comparison with a new alternative dark fuel, too. The second raw material is commercial fuel oil, which is required to BSS and EU norms. The obtained results are given in Table 2.

Tab. 2: Physical – chemical properties of conventional fuel oil.

Parameters	Methods	Values
Density at 20 ºC	BSS EN ISO 3675:2004	0.9826
Sulphur, %	BSS EN ISO 8754:2004	0.88
Specific heat /lower/, kJ/kg	BSS EN ISO 1285:2003	43.20
Kinematic viscosity at 50 ºC, mm^2/s	BSS EN ISO 3104:2001	7.45
Ash content, % (m/m)	BSS EN ISO 6245:2004	0.12
Water soluble acids and base	BSS 5252:1984	Neal
Flash point, ºC	BSS EN ISO 2592:2004	115
Freezing point, ºC	BSS 1751:1970	- 5
Water content, ºC	BSS EN ISO 3733:2003	Neal

As can see from obtained results conventional fuel oil for trading had worse ecological parameters /sulfur content, ash content/ than alternative fuel.

It must notice as disadvantages the presence of mechanical contaminates and worse smell of obtained from our research team alternative fuel, which will be object of our future investigations.

We conclude that possibility for treatment of protected vulcanizates as such as polymer materials is very perspective – from one hand obtaining of additional quality of fuels from another it's a way to solve a world ecological problem with waste from vulcanizates, tires and polymers.

3. REFERENCES

[1] Galvagno S., Casu, M., Martino E., Portofino S., (2007), Thermal and kinetic study of tyre waste pyrolisis via TG-FTIR-MS analysis. *Journal of Thermal Analysis and Calorimetry*, Vol. 88, (2), p. 507–514.

[2] Rajender S., Varma, Kannan P., at all. (1998), Selective nitration of styrenes with Clayfen and Clayan: A solvent – free synthesis of β–nitrostyrenes. *Tetrahedron Letters*, 39, p. 3977 – 3980.

[3] Robert P., Antony J. at all, (1998), The reactions of nitrogen dioxide with dienes. *J. Chem. Soc., Perkin Trans., (*1), p. 3523 – 3528.

[4] Sakata Y., K.Murata at all., (1999), Catalytic Degradation of Polypropylene into Liquid Hydrocarbons Using Silica-Alumina Catalyst. *Chemistry Letters,* vol. 25,(3), p. 245.

[5] www.springerlink.com

[6] Ali A. A., Garforth D., at all, (2002), Polymer waste recycling over “used” catalysts, *Catal. Today*, 75, p. 247.

[7] Zuev V., Bertini F., Audisio G., (2006),. Investigation on the thermal degradation of acrylic polymers with fluorinated side-chains. *Polymer Degradation and Stability*. Vol. 91, (3), p.512-516.

[8] Zuev V.,, Bertini F., Audisio G, (2005), Fullerene C_{60} as stabiliser for acrylic polymers, *Polymer Degradation and Stability*, 90, p.28 – 33.

[9] Ivanov V., Gribkova O at all., (1998), Filament – like structure formation in vacuum thermally evaporated thin films of polyaniline during oxidation in nitric acid. *Mendeleev communications Electronic Version*, 1, p. 1 – 42.

[10] Kaminsky W, Carsten Mennerich C., Zhang Z., (2009), Feedstock recycling of synthetic and natural rubber by pyrolysis in a fluidized bed. *J. Anal. Appl. Pyrolysis*, 85, p.334 – 337.

[11] Zhibo Z., Nishio S., and all., (2006), Thermal and chemical recycle of waste polymers. *Catalysis Today*, 29, p. 303 – 308.

[12] Mielke Z., (2007), Infrared spectra of the nitric acid – ethylene complex in solid argon. UV irradiation. *J. Phys. Chemistry,* 101, p. 4560 – 4568.

[13] Dimov M., Petkov P., Tasheva Y., (2010), Possibilities for utilization of waste protected vulcanizates and obtaining of additional quantity of energy sources, TU- Sofia, Sozopol, p.125.

[14]Tasheva Y., Petkov P., Dimov M., (2010), Utilization of waste protected vulcanizates by thermal cracking, 29, (1), p. 34.

Microbial electrolysis cells as innovative technology for hydrogen production

Elitsa Chorbadzhiyska[1], Yolina Hubenova[2], Georgi Hristov[1], Mario Mitov[1]

[1]Department of Chemistry, South-West University, Blagoevgrad, Bulgaria
[2]Department of Biochemistry and Microbiology, Plovdiv University, Plovdiv Bulgaria

***Abstract**: Hydrogen production is becoming increasingly important in view of using hydrogen in fuel cells. However, most of the production of hydrogen so far comes from the combustion of fossil fuels and water electrolysis. Microbial Electrolysis Cell (MEC), also known as Bioelectrochemically Assisted Microbial Reactor, is an ecologically clean, renewable and innovative technology for hydrogen production. Microbial electrolysis cells produce hydrogen mainly from waste biomass assisted by various bacteria strains. The principle of MECs and their constructional elements are reviewed and discussed.*

***Keywords:** microbial Electrolysis Cells, hydrogen production, waste biomass purification*

1. INTRODUCTION

One of the major global problems nowadays is to satisfy the rapidly rising energy demands. The existing energy system has two main disadvantages: first, the energy is produced mainly from fossil fuels, whose resources are limited and second, the use of hydrocarbon fuels causes dangerous environmental pollution due to the huge emissions of CO_2. That's why the need of using alternative power sources, which can gradually replace the traditional energy fuels, is widely discussed [1].

The opinion of more scientists is that the hydrogen will be the main power source in the future [2]. The hydrogen has three times more caloricity than petrol and it has not corrosive effect on the metals. The producing of hydrogen is still expensive and that is limiting its wide application [3]. Conventional electrolysis is one of the two most common methods currently used to produce hydrogen. Hydrogen production by electrolysis is not connected with CO_2 emission. The insufficiency of this method is that it needs large quantity of electricity.

Microbial electrolysis cells (MECs) could be a partial solution of the problem. A MEC is an electrolyzer that oxidizes organic matter at the anode,

while the cathode carries out the abiotic reduction of water in the usual way [4]. Using microorganisms in electrolysis systems decreases the overpotential, makes easier the electron transfer and reduces the necessary quantity of electricity for the electrolysis. Theoretically, the hydrogen evolution on the cathode needs a potential of E_{CAT} = − 0.41 V (vs.SHE). The anode potential of most MFCs reaches around E_{AN} = − 0.30 V (vs.SHE). Therefore, the minimum overall cell voltage needed is E=-0.11 V [5].

$$E = E_{CAT} - E_{AN} = (-0.41) - (-0.30) = -0.11V \quad (1)$$

The most important thing is that the MECs use substrates from renewable sources and have high conversion efficiency. That’s why MEC is an appropriate technology for potential application in local power plants and also for simultaneously wastewater treatment and hydrogen generation.

The development of microbial electrolysis cells (MECs) represents an exciting new area of environmental biotechnological research, exploiting common wastewater as a fuel source to produce hydrogen. The first demonstration of the renewable method for hydrogen production from wastewater using a microbial electrolysis system is underway at the Napa Wine Company in Oakville [6].

The MEC has been intensively investigated and developed for the last five years. For the progress of this innovative technology the generalization of achievements is of a big importance. In this paper, the principles and construction elements of MEC are reviewed and discussed.

2. MEC

2.1. Structure and operating principle

Microbial electrolysis cell is a technology for hydrogen production closely related to Microbial fuel cells (MFCs). Whilst MFC's produce an electric current from the microbial decomposition of organic compounds, MEC's partially reverse the process to generate hydrogen or methane from organic material by applying an electric current. The anode process of an MEC is the same as that of a MFC and the cathode process is the same as that of a water electrolyzer [7]. In principle, MEC can be divided into three major components: anode chamber, cathode chamber and separator [8] (Fig.1).

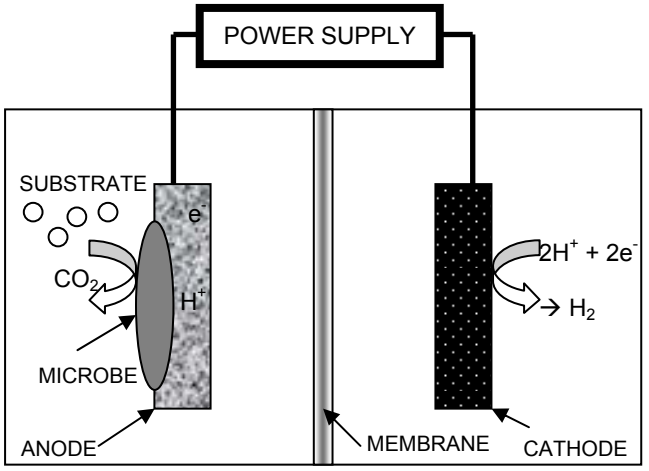

Fig.1: The working principle of a microbial electrolysis cell

In an MEC, electrochemically active microbes growing on the surface of the anode break down organic matter into CO_2, electrons and protons. The electrons and protons pass through the external electric circuit and the electrolyte, respectively, and combine at the cathode to generate hydrogen. The oxidation at the anode is supported by a microbial biofilm on the electrode, which acts as an electrocatalyst. MEC proposes to design specific microbial biofilms for the development of MEC anodes by identifying new sources of inoculum, adapting the microbial population and determining the structural characteristics of biofilm that will optimize its electroactive properties [9].

The most investigated microbial cultures for application in MECs are Archaea, the single-celled cyanobacterium Cyanothece 51142 [9], Dechlorinating bacteria (Dehalococcoides spp. and Desulfitobacterium spp.) and also methanogens and homoacetogens microorganisms [10]. Biowaste and wastewater provide immediate profits and the greatest likelihood for success of MEC technology. Abundant and renewable cellulosic biomass can potentially produce enough hydrogen for transportation and industrial use [5]. The identity of the specific microorganisms determines the products and the efficiency of the MEC. Electrogenic microorganisms consuming an energy source (such as acetic acid) release electrons and protons, creating an electrical potential of up to 0,3 V. In a conventional MFC, this voltage is used to generate electrical power. In a MEC, an additional voltage is supplied to the cell from an outside power source. The combined voltage is sufficient to reduce protons, producing hydrogen gas. The efficiency of hydrogen production depends on which organic substances are used. Lactic and acetic acid achieve 82% efficiency, while the values for unpretreated cellulose or glucose are close to 63%. The efficiency of normal water

electrolysis is 60 to 70 percent. As MEC’s convert unusable biomass into usable hydrogen, they can produce 144% more usable energy than they consume as electrical energy. Depending on the organisms presented at the anode, MEC’s can also produce methane by a related mechanism [11].

2.2. Electrode catalyst materials

The anode material in a MEC can be the same as in a MFC, such as carbon cloth, carbon paper, graphite felt, graphite granules or graphite brushes. The development of highly efficient anode materials is critical for enhancing the current output of microbial electrochemical cells. Au and Pd nanoparticle decorated graphite anodes were developed and evaluated in a newly designed multi-anode microbial electrolysis cell (MEC). On the contrary, no significant correlation was evident between the current density and the particle density based on area fraction and particle counts. These results demonstrated that nano-decoration can greatly enhance the performance of microbial anodes while the chemical composition, size and shape of the nanoparticles determined the extent of the enhancement [13]. Use of carbon cloth or thin graphite felt as anode materials may provide great advantages over other materials for scale-up.

Platinum is well known as the best cathode catalyst material used in MEC, but it is too expensive [7,14]. The high cost of platinum is driving research into bio-cathodes as an alternative. Extensive studies have been also carried out on precious metal-free catalysts for MEC. Low-cost materials as stainless steal and carbon based NiMo-, NiW-nanocomposites showed good performance as cathode in MEC [15]. Penn State researchers have found a way to replace the platinum catalyst in their hydrogen generating microbial electrolysis cells with stainless steel brushes without losing efficiency. The trapped hydrogen also remains in the reactor longer and is therefore available to microbes that consume hydrogen [12]. The limitation of extending these results to MECs is that they have been only examined under highly acid or alkaline conditions [16,17] Investigation of cathode materials that are efficient catalysts at neutral pH is needed [4].

2.3. General MEC design

MEC can be developed as a single-chamber or a two-chamber system. A MEC lacking a membrane can produce high hydrogen and energy recoveries. Operating without a membrane can allow for more cost effective and simpler designs [5]. Use of a membrane in two-chamber MEC systems can reduce the amount of impurities in the biogas but increase the internal resistance. Removal of the membrane in single-chamber systems simplifies

the reactor design but increases the possibility for hydrogen consumption by methanogenic bacteria [4].

3. PERSPECTIVES FOR MEC APPLICATION

Research on the innovative and novel MEC technology is in its infancy. As the bioanode reactions are much more extensively studied in MFC, crucial for the MEC practical application and commercialization is the development of cost-effective cathodes for near-neutral pH and low temperature conditions as well as the minimization of the internal resistance by improvement of the cell design.

MECs can potentially be used for different applications. The main application of MEC is to produce hydrogen, which can be used in different directs. Other application is for effective wastewater treatment. MEC have the potential to convert waste organic matter into a valuable energy source [18].

4. REFERENCES

[1] Kotay, S., Das, D. (2008) Biohydrogen as a renewable energy resource—Prospects and potentials, *Int. J. Hydrogen Energy* 33, 258 – 263.

[2] Mitov, M., Kondev, I., Petrov, Y., Bliznakov, S., Popov, A. (2003) Fuel cells – achievements and perspectives, *Chemistry* 12, 455 – 465.

[3] Rozendal, R., Hamelers, H., Euverink, G., Metz, Buisman, C. (2006) Principle and perspectives of hydrogen production through biocatalyzed electrolysis, *Int. J. Hydrogen Energy* 31, 1632 – 1640.

[4] Hu, H., Fan, Y., Liu, H. (2008) Hydrogen production using single-chamber membrane-free microbial electrolysis cells, *Water research* 42, 4172–4178.

[5] Call, D., Logan, B. (2008) Hydrogen production in a single chamber microbial electrolysis cell (MEC) lacking a membrane, *Environ. Sci. Technol.* 42, 3401–3406.

[6] Logan, B., Renewable hydrogen production becomes reality at winery, report available online at: http://www.physorg.com/news173451507.html

[7] Liu, H., Hu, H., Chignell, J., Fan, Y. (2010) Microbial electrolysis: novel technology for hydrogen production from biomass, Biofuels 1(1), 129–142.

[8] Jeremiasse, A., Hamelers, H., Buisman, C. (2010) Microbial electrolysis cell with a microbial biocathode, *Bioelectrochemistry*, 78, 39–43.

[9] Bandyopadhyay, A., Stöckel, J., Min, H., Sherman L., Pakrasi, H. (2010) High rates of photobiological H_2 production by a cyanobacterium under aerobic conditions, *Nature Communications*, 1, 139.

[10] Cheng, S., Xing, D., Call, D., Logan, B. (2009) Direct Biological Conversion of Electrical Current into Methane by Electromethanogenesis, *Environ. Sci. Technol.*, 43 (10), 3953–3958.

[11] Cheng, S., Logan, B. (2007) Sustainable and efficient biohydrogen production via electrohydrogenesis, report available online at: http://www.pnas.org/content/104/47/18871.full.pdf

[12] Olivares-Ramirez, J., Campos-Cornelio, M., Uribe Godinez, J., Borja-Arco, E., Castellanos, R. Studies on the hydrogen evolution reaction on different stainless steels, *Int. J. Hydrogen Energy* 32, 3170–3173.

[13] Fan, Y., Xu, S., Schaller, R., Jiao, J., Chaplen, F., Liu, H. (2011) Nanoparticle decorated anodes for enhanced current generation in microbial electrochemical cells, *Biosensors and Bioelectronics,* 26, (5), 1908-1912.

[14] Freguia, S., Rabaey, K., Yuan, Z., Keller, J. (2007) Electron and carbon balances in microbial fuel cells reveal temporary bacterial storage behaviour during electricity generation, *Environ. Sci. Technol*. 41(8), 2915–2921.

[15] Hu, H., Fan, Y., Liu, H. (2009) Hydrogen production in single chamber tubular microbial electrolysis cells using non-precious metal catalysts (NiMo, NiW), *Int. J. Hydrogen Energy* 34, 8535–8542.

[16] Navarro-Flores, E., Chong, Z., Omanovic, S. (2005) Characterization of Ni, NiMo, NiW and NiFe electroactive coatings as electrocatalysts for hydrogen evolution in an acidic medium, *J. Mol. Catalyst A: Chemical*. 226, 179–197.

[17] Olivares-Ramirez, J., Campos-Cornelio, M., Uribe Godinez, J., Borja-Arco, E., Castellanos, R., (2007) Studies on the hydrogen evolution reaction on different stainless steels, *Int. J. Hydrogen Energy* 32, 3170–3173.

[18] Rozendal, R., Hamelers, H., Rabaey, K., Keller, J., Buisman, C. (2008) Towards practical implementation of bioelectrochemical wastewater treatment, *Trends in Biotechnology* 26, 450–459.

Comparative Investigation of CoMnB, CoNiMnB and CoNiMoW-supported Anodes for Direct Borohydride Fuel Cells

Georgi Hristov[1], Elitsa Chorbadzhiyska[1], Rasho Rashkov[2], Yolina Hubenova[3], Mario Mitov[1]

[1]Department of Chemistry, South-West University, Blagoevgrad, Bulgaria
[2]Insitute of Physicochemistry – Bulgarian Academy of Sciences, Sofia, Bulgaria
[3]Department pf Biochemistry and Microbiology, Plovdiv University, Plovdiv, Bulgaria

***Abstract**: A direct borohydride fuel cell (DBFC) is a device that converts chemical energy of alkaline borohydride electrooxidation into electricity. Many materials are object of investigation with the importance of operating parameters on the fuel cell performance. In this study, we investigated and compared the results, obtained with DBFC using Co-based nanocomposites (CoMnB, CoNiMnB and CoNiMoW) as anodes and air gas-diffusion electrodes as cathodes. The Co-based nanocomposite electrodes were prepared by electrodepositon on Ni-foam.*

***Keywords:** Direct borohydride fuel cell (DBFC), Electrooxidation, Nanocomposites*

1. INTRODUCTION

Fuel cells constitute an attractive class of renewable and sustainable energy sources. Fuel cells are considered as promising power sources because of their high-energy conversion efficiency, environmental compatibility, reliability, and quiet operation. The typical fuel cells use hydrogen as a fuel. There are several types of fuel cells, depending on their construction and the fuel [1]. A direct borohydride fuel cell (DBFC) is a device that converts chemical energy of borohydride into electricity. Borohydrides are a group of compounds with high hydrogen contents. For example, $NaBH_4$ contains 10.6 wt% hydrogen. The direct anodic oxidation of borohydride provides more negative potential than that of hydrogen. During electrooxidation one BH_4^- ion generates eight electrons. The theoretical energy density can reach as high as 9.3 Wh/g of $NaBH_4$ if using sodium borohydride as the fuel. The theoretical energy conversion efficiency

of the DBFC is 0,91 [2]. The best electrocatalysts for the electrochemical oxidation reaction are Ni, Pt, and Pd, but they also have good catalytic activity towards the hydrolysis reaction [3]. That is why the research is focused on searching for a material, which is a good catalyst for the sodium borohydride electro-oxidation, but has low affinity to sodium borohydride hydrolysis process. Au and Ag show high utilization efficiencies towards borohydride electrooxidation because of their low activity towards hydrolysis [4]. However, Au and Ag are too expensive as electrodes in commercial devices. Among the non-precious metals, nickel has received maximum importance as catalyst for electrooxidation of BH_4^- [3]. Also, Ni is a major component of hydrogen storage materials such as AB_2 and AB_5-type alloys [5]. Hydrogen storage alloys are metallic materials that have a unique ability to reversibly absorb and release significant amounts of hydrogen gas. These materials show good performance as anodes in DBFC [6].

Appropriate nanocomposites should be very promising materials as anodes in DBFC as they perform high specific surface area, which may compensate a low catalytic activity.

In this study, three different types of newly synthesized Co-based nanocomposites: CoMnB, CoNiMnB and CoNiMoW, produced by electrodeposition on Ni-foam, were investigated as anodes in DBFC.

2. EXPERIMENTAL

Composite CoMnB coatings were obtained by potentiostatic electrodeposition from electrolyte, containing 5 g/l Co^{2+}, 5 g/l Mn^{2+}, 5 g/l Ni^{2+} and 35 g/l boric acid. The CoNiMnB nanocomposites were obtained from similar electrolyte, but with different amounts of Co^{2+} and Ni^{2+}. The electrolysis continued 30 min at 40 °C. Co-electrode was used as an anode and Ni-foam (RECEMAT, RCM-Ni-4753.016 pore diameter d=0.4 mm, SSA=5800m^2/m^3 and RCM-Ni-2733.03, pore diameter d=0.6 mm, SSA=2500m^2/m^3) as a cathode.

Composite CoNiMoW coatings were obtained by galvanostatic electrodeposition from alkaline electrolyte, containing 72g/l sodium citrate, 24g/l $Na_2WO_4.2H_2O$, 6g/l Na_2MoO_4, 16g/l $Ni(SO_3NH_2)_2$, 16g/l $Co(SO_3NH_2)_2$. pH 10 was fixed by addition of NH_4OH. The composites were electrodeposited on nickel foam under different galvanostatic regimes (1A, 2A, 3A, 4.8A) for 30 min and electrolyte stirring at 250 min^{-1}.

Varying the electrolysis conditions nanocomposites with different content, structure and morphology have been produced. Scanning electron microscopy (SEM) using Leo 1455VP and Leo Supra 55VP microscopes with Energy dispersion X-ray (EDX, Oxford Inca 200 instrument, Software INCA-Vers.4) was applied for examination of the surface morphology and elemental analysis of the electrodeposited coatings. XRD spectra for

structure identification of layers was recorded in the angle interval 10–100° (2θ) by using Philips PW 1050 diffractometer, equipped with Cu Kα tube and scintillation detector.

Initially, the examined materials were investigated as electrodes in three electrode cell using 5%$NaBH_4$/6M KOH electrolyte. The nanocomposite sample was connected as a working electrode and Ni-wire was used as a counter electrode. The working electrode potential was measured against Hg/HgO reference electrode. Polarization curves were obtained by means of chronopotentiometry using PJT 35-2 potentiostat-galvanostat (Radiometer, Tacussel).

Round shaped samples of electrodeposited electrodes with diameter 3 cm were applied as anodes in DBFC. Air gas-diffusion electrodes (GDE), developed for metal-air systems [7], were used as cathodes. The investigations were performed in single-chamber DBFC (10 ml working volume). 5%$NaBH_4$/6M KOH solution was served as an electrolyte. Polarization measurements at variable load resistances in a borohydride-containing electrolyte were carried out. From recorded values of voltage, U, and current, I, the power output was calculated by equation P=UxI, and the polarization and corresponding power curves were plotted.

3. RESULTS AND DISSCUSION

All of the polarization curves obtained with studied materials began at more negative potential than the typical hydrogen reaction in alkaline media (-0.926 V vs. Hg/HgO) [8], which indicated a direct electrooxidation of the sodium borohydride.

Anodic polarization curves, obtained with CoMnB and CoNiMnB electrodeposited samples in borohyride-containing electrolyte, are presented in Fig. 1. For both types of electrodes, the overpotentials are fewer than 100 mV even at high current loadings (up to 100 mA/cm^2). However, the CoNiMnB exhibited better performance expressed as smaller overpotentials at equal currents. The behavior of the CoNiMoW electrodes was similar to that of CoMnB and CoNiMnB ones. In another experiments, we discovered that the examined materials also catalyzed the sodium borohydride hydrolysis reaction. The hydrolysis began immediately after immersion of investigated sample (CoMnB, CoNiMnB or CoNiMoW) into sodium borohydride solution. Hydrogen release decreases sufficiently with increasing current density and above 100 mA/cm^2 its rate is reduced approximately by half compared to the value in the absence of polarization. This result indicated an existing competition between borohydride hydrolysis and electrooxidation reactions. In our previous investigations [9], we found out that the relative share of sodium borohydride consumed in hyhydrolysis process on CoNiMnB electrodes was about 45% of the total depletion,

which was close to the relative share on Ni-electrode (50%) [10]. By this reason, we concluded that CoNiMnB-nanocomposites are better to use in Hydrogen-on-Demand systems than in DBFC.

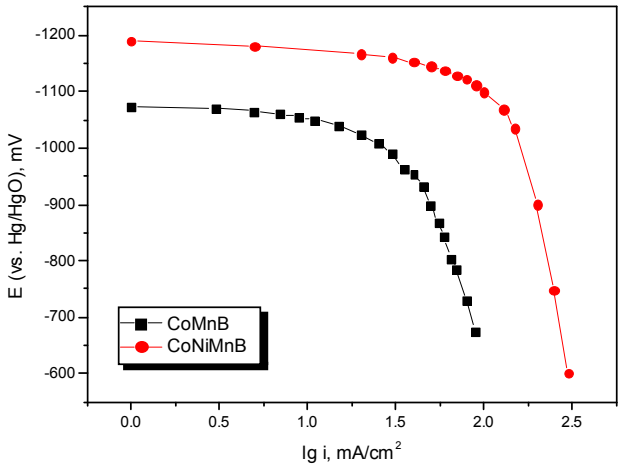

Fig. 1: Polarization curves obtained with CoMnB and CoNiMnB electrodes in 5%$NaBH_4$/6M KOH electrolyte.

In comparison with the other examined types of Co-based nanocomposites, CoNiMoW exhibited the smallest catalytic activity towards sodium borohydride hydrolysis. That is why the most investigations in DBFC were performed with CoNiMoW anodes, produced under the upper described four regimes of electrodeposition. Typical polarization and power curves with this type of electrodes are shown in Fig. 2. A tendency for improvement of DBFC outputs with the decrease of the current applied during electrodepositions is observed from the obtained results. The maximal power of 90 mW was obtained with CoNiMoW anode, produced at 1A.

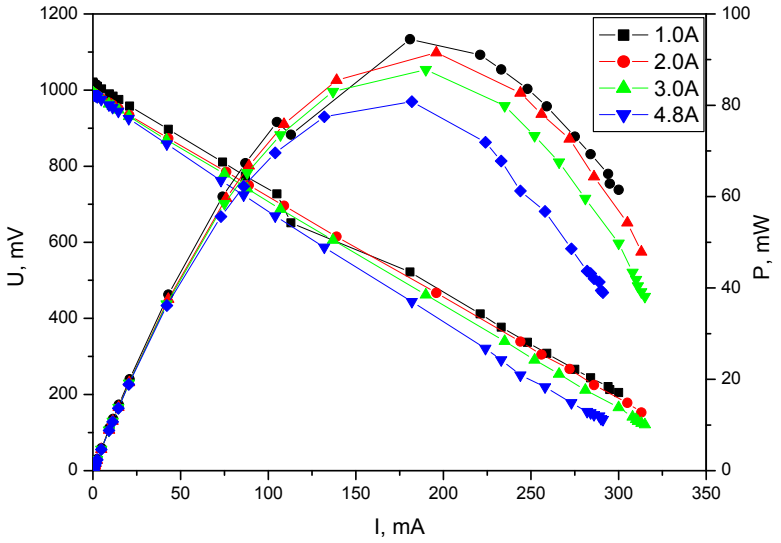

Fig. 2: Polarization and power curves, obtained with a single-chamber DBFC using air gas-diffusion cathode and CoNiMoW/Ni-foam anodes, prepared under different galvanostatic conditions.

4. CONCLUSIONS

The electrocatalytic properties of three types newly synthesized Co-based nanocomposites towards sodium borohydride electrooxidation were studied. The performance of CoNiMnB electrodes overcomes that of CoMnB ones. However, both nanocomposite materials exhibit relatively high catalytic activity towards sodium borohydride hydrolysis process, which makes them more suitable for development of Hydrogen-on-Demand (HOD) generators or hybrid DBFC–HOD systems. The best performance in DBFC, combined with the lowest catalytic activity towards borohydride hydrolysis, propose CoNiMoW electrodeposits as the most appropriate electrocatalysts for direct borohydride electrooxidation among studied electrode materials.

5. REFERENCES

[1] Mitov, M., Kondev, I., Bliznakov, S., Popov, A. (2003) Fuel cells – achievements and perspectives, *Chemistry* 12, 455 – 465.

[2] Li, Z., Liu, B., Arai, K., Suda, S. (2005) Development of the direct borohydride fuel cell, *Journal of Alloys and Compounds,* 404-406, 648-652

[3] Liu, B., Li, Z., Suda, S. (2004) Electrocatalysts for the anodic oxidation of borohydrides, *Electrochim Acta*, 49:3, 097–105.

[4] Chatenet, M., Micoud, F., Roche, I., Chainet, E. (2006) Kinetics of sodium borohydride direct oxidation and oxygen reduction in sodium hydroxide electrolyte Part I. BH_4^- electro-oxidation on Au and Ag catalysts. *Electrochim Acta,* 51:54, 59–67.
[5] Choudhury, N., Raman, R., Sampath, S., Shukla, A. (2005) An alkaline direct borohydride fuel cell with hydrogen peroxide as oxidant. *J Power Sources,* 143, 1–8.
[6] Ma, J., Choudhury, N., Sahai, Y. (2010) A comprehensive review of direct borohydride fuel cells, *Renewable and Sustainable Energy Reviews*, 14, 183–199.
[7] Kaisheva, A., Iliev, I., Gamburzev, S. (1984) Comparative methods for estimation of the activity and the transport hindrances of air gas-diffusion electrodes, *J Power Sources* 13, 181-195.
[8] Mitov, M., Hristov, G., Hristova, E., Rashkov, R., Arnaudova, M., Zielonka, A. (2008) Complex performance of novel CoNiMnB electrodeposits in alkaline borohydride solutions, *Environmental Chemistry Letters*, 7, 167-173.
[9] Hristov, G., Hristova, E., Mitov, M. (2009) Investigation of Metal Hydride Electrodes for Application in Direct Borohydride Fuel Cells, *In: Proceedings of the Thirds International Scientific Conference FMNS-2009*, 2, 167-173.
[10] Liu, B., Li, Z., Suda, S. (2003) Anodic oxidation of alkali borohydrides catalyzed by nickel. *J Electrochem Soc*, 150:A, 398–402.

Application of renewable energy sources in an integrated heating systems for individual house

Anna Majchrzycka, Tadeusz Kozak

West Pomeranian University of Technology, Szczecin, Poland

Abstract. *The paper is aimed at cost analysis of an integrated house heating systems in an individual house. Energy demand was determined from a home energy audit. Based on energy demand the appliances for house heating and preparing of hot water were selected. An existing heating system with gas fuelled boiler was compared with the following integrated heating systems: gas boiler and ground heat pump, gas boiler and flat-plate solar collectors, gas boiler, flat-plate solar collectors and ground heat pump. Then, analysis of investment and operating costs and profitability of the systems in question was performed. To determine an environmental impact of an integrated house heating systems emission of CO2, CO, NOx and dust was determined.*

1.INTRODUCTION

Increasing interest in renewable energy sources (RES) utilisation follows from EU and the Polish energy policy aimed at increasing share of energy from RES. The target is for energy produced in Poland from RES to account for 15% of total energy consumption by 2020. Moreover, according to Kyoto Protocol in 2008-2012 Poland is obligated to reduce greenhouse gases of 6% emissions compared to 1988. Due to high cost of fossil fuels (FF) and the necessity to switch from FF to RES, many homeowners are seeking for solutions leading to reduce energy consumption, upgrade energy facilities and save energy costs. There is an increasing interest in modern RES facilities and integrated heating systems combining FF and RES facilities. There are many different solutions of an integrated systems meeting energy demand for house heating and preparation of hot water. Usually, such system consists of FF boiler and heat pump or FF boiler integrated with thermal solar collectors. Heat pump meets energy demand to the predicted level that follows from an assumed outside temperature. In case of not sufficient energy being delivered by heat pump, peak FF boiler should be switched on. Very often such installations are integrated with thermal solar collectors for water heating.

The paper is aimed at cost analysis of the different integrated heating systems that are possible to apply in an individual house (replacement or new installations).
The following heating systems will be discussed: gas boiler fuelled with 2E-G20,gas boiler and ground heat pump, gas boiler and thermal solar collectors, gas boiler, thermal solar collectors and ground heat pump. Energy demand will be determined from an energy audit of the house [1]. Based on energy demand, the house heating and water heating appliances will be selected. Then, analysis of capital and running costs and profitability (NPV) of the systems in question will be performed. Environmental impact of an analysed systems will be evaluated from emission of CO_2, CO, NO_x and dust.

2. ENERGY DEMAND FOR THE HOUSE HEATING AN7D PREPARATION OF HOT WATER

An analysis is performed for one floor detached individual house with cellar and loft, covered with the gable roof.. The house of usable area of 134 m^2 is equipped with heating system that consists of an individual energy source - gas boiler of efficiency η_b = 0,8. Water heating system consists of individual gas heaters of efficiency η_{bw} = 0,8. The house has been built in seventies of XX century, according to actual building engineering standards. Replacement of an existing heating systems needs analysis of possible technical solutions and their capital and running costs and profitability (NPV). To select an applicable house heating appliances an energetic audit of the house has been performed, [1]. Energy demand for water heating was determined at the following assumptions: N = 4 inhabitants, mean twenty-four hours water demand per capita g_w=60 kg/capita, the hot water temperature t_w=60ºC, mean outside operating temperature of t = -16^{o}C. Energy demand for house and water heating is Q = 44 606 kWh/a and Q_w = 4 063 kWh/a, respectively. Fig.1 shows the scheme of analysed systems.

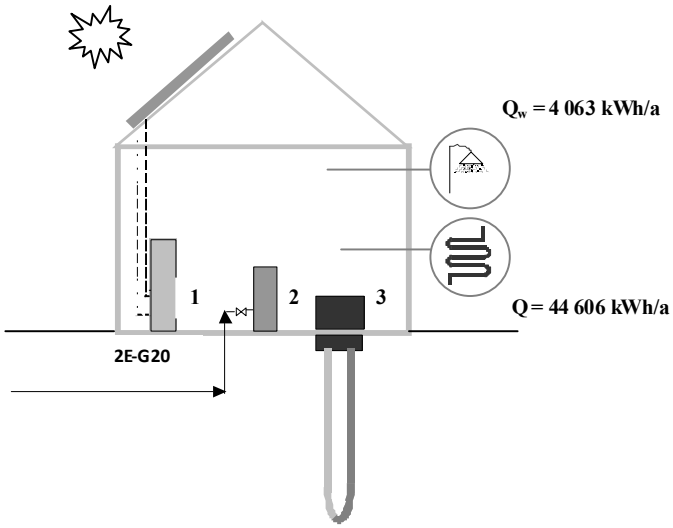

Fig.1: Scheme of the systems for house and water water heating: 1-thermal solar collectors , 2-gas boiler, 3-ground heat

3.SELECTION OF HEATING APPLIANCES

Gas boiler installation provides heat to meet energy demand for house and water heating either exclusively or additionally as a peak appliance of an integrated house heating system. Double-function gas (fuelled with 2E-G20) boiler of type Vaillant VUW 242-3 Plus, thermal power of N=8,9 kW and efficiency of η_k = 0,9 has been selected, [7] as an individual energy source or peak facility in an integrated house heating system. Heat pump is to meet energy demand to the predicted outside temperature (in the system in question: bivalent heat pump and bivalent point of t=0^{o}C). In case of outside temperature lower than bivalent point, gas boiler will be switched on into the heating system as a peak boiler. Selection of heat pump consists in many factors, however, here an economic factor was prevailing. Based on recent prices, the most accessible ground heat pump manufactured by Solis, type SO-110X has been selected, [6]. Operating parameters of selected ground heat pump are as follows: heating power of 10,8 kW, cooling power of 6800 kW, input electric power 2,5 kW, water outlet temperature of 55°C, working fluids ethylene glycol and water. Selected thermal solar installation consists of flat –plate solar collectors manufactured by Aquasolar, typ E KS 2000S, total surface area of 2,09 m^2 and absorber net effective surface area of 1,83 m^2, [5]. There are four flat-plate collector modules of the total absorber net effective surface area of 7,2 m^2 placed on the roof.

4.ECONOMIC ANALYSIS

To analyse profitability of the different house heating systems capital, annual running and unit heat production costs and net predicted value (NPV) were determined. It was assumed hereto, that capital costs of the systems in question refer only to heat source and pipelines, fittings and heaters are not included.Fig.2 shows capital costs of the different house heating systems.

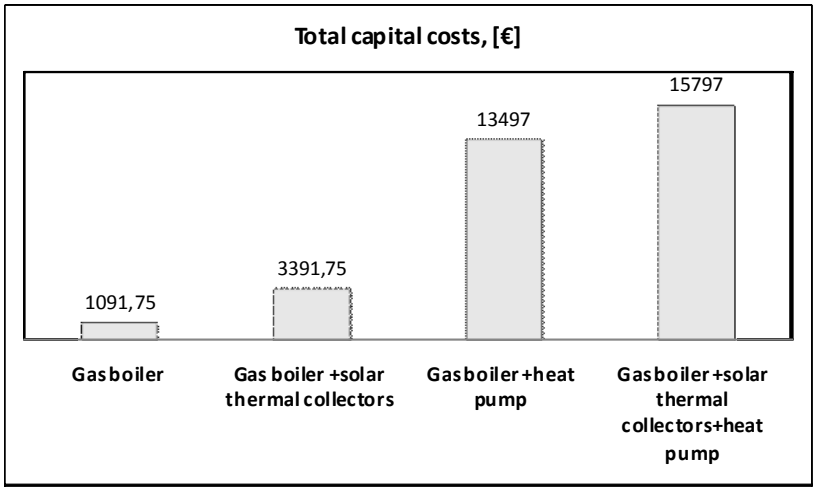

Fig.2: Capital costs of the different heating systems

As it follows from Fig.2, the system integrating gas boiler with thermal solar collectors and ground heat pump providing both hot water and heat is characterised with the highest capital costs. Capital costs of heating systems based exclusively on gas boiler are the lowest one. Annual running costs of the house and water heating systems follow from annual consumption of heat-carrying agents and their unit costs. Annual running costs of the heating systems in question are presented in Fig.3.

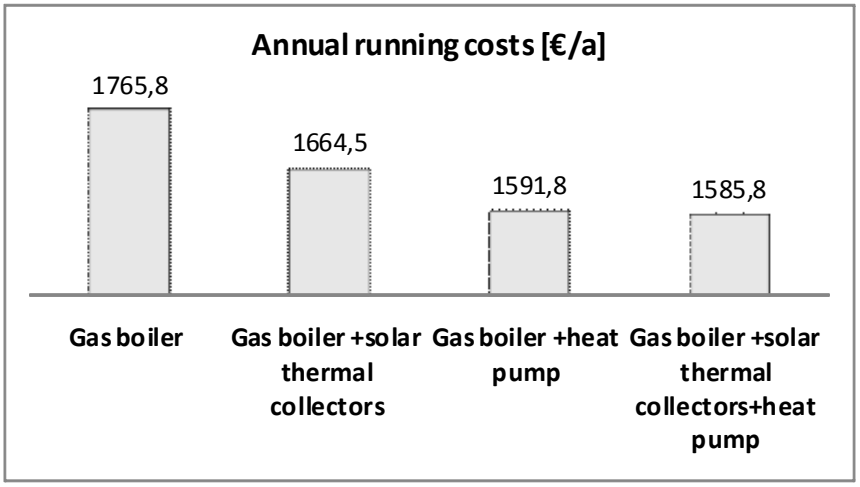

Fig.3: Annual running costs of the different heating systems

As it follows from Fig.3 the house and water heating by means of gas boiler is costly. Considering running costs it can be concluded that an integrated system consisting of gas boiler, thermal solar collectors and ground heat pump is the most advantageous. Cost of heat production consists of supply energy costs (fuels, electricity) and costs resulting form an investment outlays. Evaluation of supply energy costs should account heat source efficiency. Cost resulting from the investment outlays depends upon purchase and facility installation costs, annual heat consumption and the investment outlay service rate. Annual service rate of the investment expenditures includes the rates of discount and depreciation. The real rate of discount was assumed to be 8 %, depreciation rate was assumed to be 5,1 %.
The unit cost of heating produced by the different heat sources can be written as follows, [2]:

$$k_c = \frac{k_z}{\eta} + \frac{p \cdot l}{Q_a} \tag{1}$$

In case of an integrated heating system, heat unit costs were determined as weighted average of each heating appliance in the system. Fig.4 shows heat unit costs for the different house heating systems.

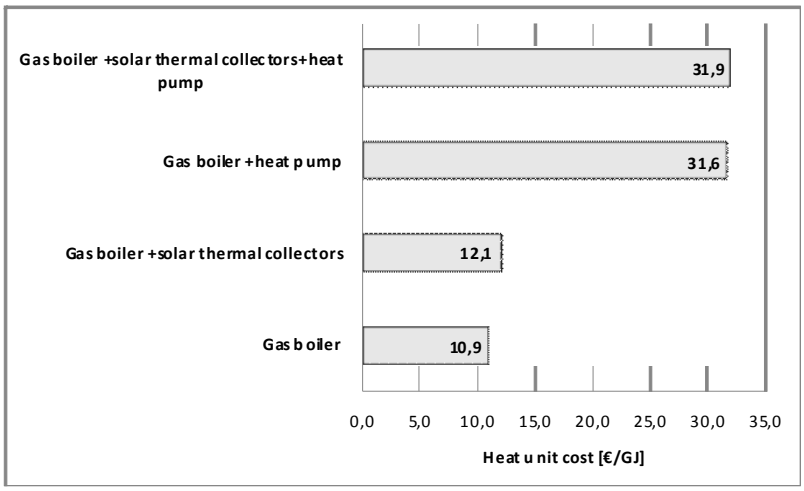

Fig.4: Heat unit costs for the different house heating systems.

As it follows from Fig.4 integrated heating system consisting of gas boiler and solar thermal collectors and ground heat pump has the highest unit costs of heat production, compared to the other systems. Analysis of investment outlays, annual running costs and unit heat production costs is not sufficient to evaluate profitability of the house heating system. To analyse profitability of the heating system it is necessary to determine economic effect covering the total work time of the heating system. It is described as Net Predicted Value, NPV, in fact, it is total predicted profit discounted to year zero, expressed in currency of this year. It is an objective function of an analysis in question, [3]. The heating system of the lowest NPV is considered to be the most cost-effective:

$$NPV = \sum_{t=0}^{t=n} \frac{(CI_t - CO_t)}{(1+r)^t} \tag{2}$$

Fig.5 illustrates relationship between Net Predicted Value (NPV) and work time of the different house heating systems at assumption that exploitation work time of the systems equals 10 years.It is evident from Fig.5 that house and water heating exclusively by means of gas boiler is the most profitable one as NPV reached the lowest level compared to the other heating systems. Integrated heating system that consists of gas boiler combined with thermal solar collectors and ground heat pump is less profitable because of the high capital costs but the system is environmentally friendly.

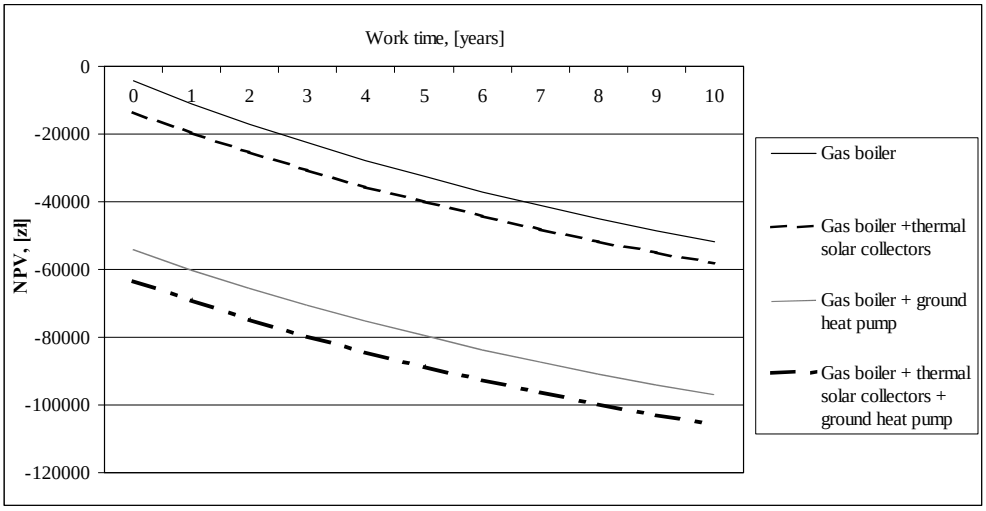

Fig.5: NPV for the different house heating system

5. ENVIRONMENTAL IMPACT

To evaluate environmental impact of analysed heating systems, it is necessary to determine output of the most important pollutants. Based on fuel consumption (gas GZ-50) and emission factors, [4] emission of CO_2, NO_x, CO and dust was determined. Table 1 shows emission of CO_2, NO_x, CO and dust from house and water heating systems in question.

As it follows from Table 1 carbon dioxide output produced by analysed heating systems is prevailing. Because of low CO_2, NO_x, CO and dust output, integrated heating system consisting of gas boiler combined with thermal solar collectors and ground-heat pumps is much more environmentally-friendly solution than the other systems being analysed. In spite of high capital costs, integrated heating systems containing heat pump and thermal solar collectors are recommended everywhere, where environment protection is of utmost importance.

Table 1. Emission of CO_2, NO_x, CO and dust from the house and water heating systems.

No.	Heating system	Emission [kg/a]			
		CO_2	NO_x	CO	Dust
1	Gas boiler	10 923	7,11	2,00	0,08
2	Gas boiler + heat pump	3 835	2,50	0,70	0,03
3	Gas boiler + thermal solar collectors	10 297	6,71	1,88	0,07
4	Gas boiler + heat pump+ thermal solar collectors	3 798	2,47	0,69	0,03

6. CONCLUSIONS

Selection of an optimum house heating system providing heat and hot water depends upon many factors: practical requirements, technical and investment potential, running costs and the other factors. From analysis that has been performed the following conclusions can be drawn:

- four integrated systems for house and water heating were discussed: gas boiler, gas boiler and ground heat pump, gas boiler and thermal solar collectors, gas boiler, thermal solar collectors and ground heat pump were compared regarding capital costs of the system, unit cost of heat production, running costs and NPV,
- based on the lowest unit cost of heat production and NPV, heating system with gas boiler was found as the most profitable one, however, running costs of the system are high
- because of variable solar conditions in Poland, application of thermal solar collectors for exclusive house heating and providing hot water is not recommended, installation of thermal solar collectors is cost-effective only in case of exclusive water heating,
- heat pump can be alternative heat source for the different heating systems provided that there are technical and investment potentials for utilization of the low temperature heat sources,
- however, capital costs of an integrated systems with solar thermal collectors and ground heat pump are high but running costs , moreover because of low CO_2, CO, NO_X, and dust emission the systems are considered as environmentally friendly,

- it is worth to accentuate that depending on the kinds of low temperature heat sources, ground heat pump can be replaced by the other types of heat pumps, for example air heat pump ,as such solution is less costly because there is no need to install ground heat exchanger of high capital cost.

NOMENCLATURE

Cl_t, CO_t - cash inflow ,cash outflow,[[€]
k_z - unit cost of supply energy, [€/GJ],
n - operating time of the installation. (time of cash flow),[year],
p - annual investment outlays service rate,[%],
r - discount rate,[%],
I - heat source investment expenditures, [€]
Q_a - annual heat demand ,[GJ/a],
t - successive year of exploitation

REFERENCES

[1] Górzyński J.:*Audyting energetyczny*, Narodowa Agencja Poszanowania Energii, Warszawa 2000,
[2] Rubik M.: Współpraca sprężarkowych pomp ciepła z instalacjami odbiorczymi. *,,Ciepłownictwo, Ogrzewnictwo, Wentylacja"*, nr 7(1997), pp.25-29,
[3] Skorek J., Kruppa R.: Analiza ekonomiczna zastosowania pompy ciepła w typowym budynku jednorodzinnym, *Gospodarka Paliwami i Energią,* No.4 (2000), pp.9-17.
[4] Wskaźniki emisji substancji zanieczyszczających wprowadzanych do powietrza z procesów energetycznego spalania paliw, (1996) Materiały informacyjno-instruktażowe, MOSZNiL, seria 1/96, Warszawa,
[5] http://www.aquasolar.pomp.pl/
[6] http://www.solis.pl/
[7] http://vaillant.pl/

Electrochromic thin films optical coatings - functional elements in “Smart windows”

K. A. Gesheva and T. M. Ivanova
Central Laboratory of Solar Energy and New Energy Sources at Bulgarian Academy of Sciences, Blvd. “Tzarigradsko chaussee” 72, 1784 Sofia, Bulgaria

Abstract: *Transition metal oxides exhibit electrochromic (EC) effect, consisting in changing of film optical transmittance under a small voltage applied across the film. Film goes from color to bleach state, if the polarity of the voltage is changed. These films are developed to be applied as working electrodes in smart windows. Smart windows are the real windows in future low-energy architectural solar building.*

Atmospheric pressure chemical vapor deposition (APCVD) technology was used, utilizing CVD carbonyl process, employing pyrolitic decomposition of metal hexacarbonyls at temperature of 150 - 200^{o}C in oxygen reactive gas media.

The microstructure and optical and properties are studied as a result of technological parameters change, and the resulted electrochromic performance is evaluated.

Keyword: *Thin film optical coatings, Transition metal oxides, Electrochromic effect, Smart windows, Color efficiency, Optical modulation*

1. INTRODUCTION

The “smart window” is a multilayered system consisting of conductive glass surface, coated by electrochromic (EC) transition metal oxide thin film (WO_3, MoO_3 or mixed films based on these oxides), and laminated with a second conductive glass by a polymeric electrolyte, in which in advance Lithium ions are inserted. If a small voltage is applied to the conductive glass electrodes, electrons from the electrode get injected in the film, ions from the polymer intercalate also in the film, Fig.1. The building block of film structure, namely the metal octahedron in presence of electron, ion, and photon (the EC effect makes sense only in light, it is effect provoked by light, human eye is a detector of it) form absorptive structure. As a result the film absorbs part of the solar light, and what we see as a

color of the film is the complementary color. If the polarity is changed, electrons and ions go back to the initial places and film, respectively the device, is bleached.

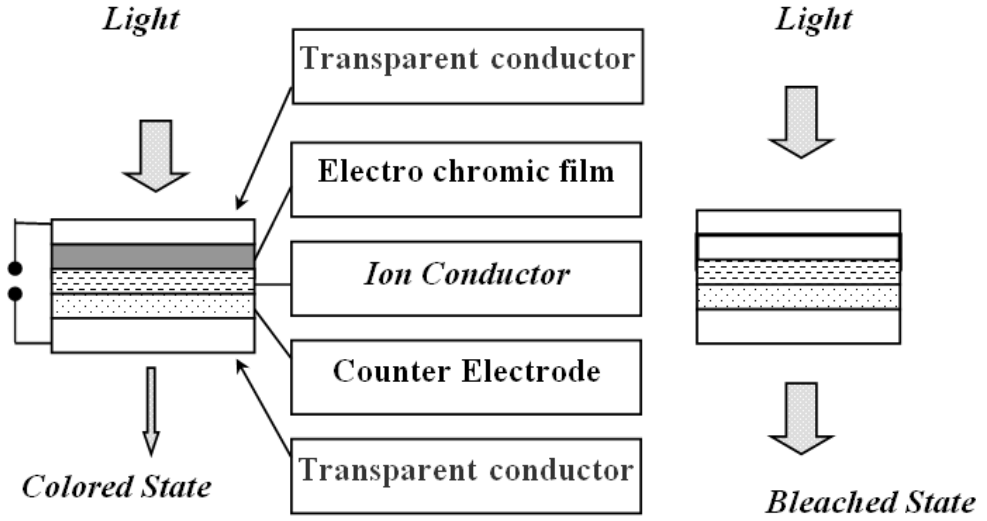

Fig. 1. Electrochromic device - smart window

EC effect in case of tungsten oxide as functional layer is explained as follows: in presence of a photon, a reversible reaction takes place in the EC device hv

(Transparent phase) WO_3 + xe- + xM^+ ↔ Mi_xWO_3 (Colored phase)

M^+ can be H^+, Li^+, Na^+ etc. – small alkali ions or protons. The effect goes in presence of a photon (hv).

The microstructure plays considerable role, for instance in its orthorhombic modification MoO_3 has the unique layered structure (right side of Fig. 2), facilitating the intercalation of ions in between the double layers connected with each other only with bridging oxygen atoms. The monoclinic MoO_3 (left side on the figure) has also an arrangement of its structure forming free spaces where ions can intercalate.

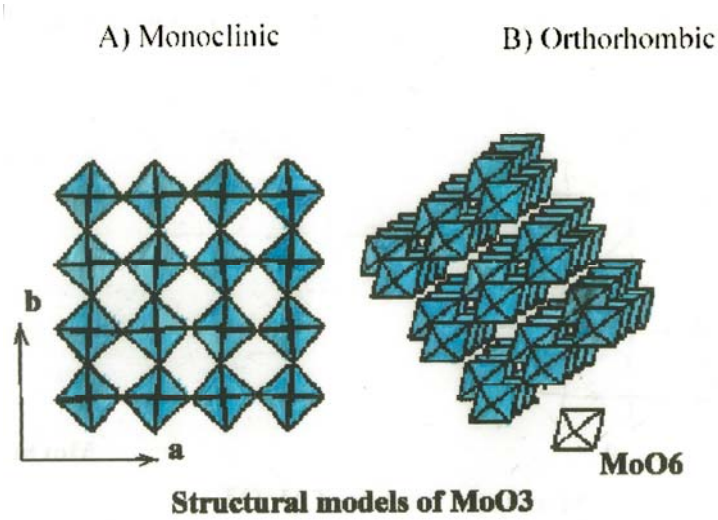

Fig. 2 Crystalline modifications of molybdenum oxide structure

Surface morphology of the films is especially important for the intercalation of ions in the film, thus defining the kinetics of the switching process from colored to bleached state.

Field emission scanning electron microscopy (FESEM) was used to study the films structure. Such structure facilitates the ions intercalation and de intercalation processes. As it can be seen in the orthorhombic MoO_3 there are double layers, between them channels are formed, and ions can easily propagate in these channels.

Optical transmittance of the films is measured by UV-VIS-NIR Spectroscopy. The results show high initial transparence of the films (oxides are large-band semiconductors). Cyclic voltammetry is used for determination of color efficiency, and optical modulation. Raman and FTIR spectroscopy were used to find the specific Raman bands for a certain crystalline modification. Centering the bands on the X axis corresponds to modes of vibration of atoms at specific chemical bonds, characteristic of material crystalline modification.

Optoelectronic properties of transition metal oxides are of great research interest especially concerning their electrochromic properties [1, 2]. These materials find applications in controllable devices for optical information and storage, anti-glare automobile rear and side-view mirrors, sunglasses, glare reduction systems for offices and “smart windows” for buildings and cars [3]. Examples of successful electrochromic devices already exist in rear-view mirrors for cars and in smart windows [4].

Tungsten oxide is the first and most extensively studied electrochromic material [5-7]. However, for practical electrochromic devices, further improvement in some of the EC properties (reversibility, stability,

optical modulation, color, etc.) is needed. The mixture of two electrochromic oxides possessing different desired properties can lead to oxide films combining of the good characteristics of the single oxides [2]. In mixed metal oxide films a stronger optical absorption is expected in result of more intense electron transitions between electronic states like W^{5+}, W^{6+}, and the corresponding lower energy electronic states of Mo, leading to better expressed electrochromic effect [2].

MoO_3 as added to WO_3 was expected to improve the adhesive ability, coloring efficiency, and prolong the cycling life [8]. Improved photoelectrochromic behavior was reported for MoO_3-WO_3 films [9] due to the occurrence of the maximum optical absorption of mixed films at 2.15eV, which is significant because it is very close to the maximum of the eye sensitivity. Gas sensing properties can also be modified by mixing these two metal oxides [10].

An important issue for the readymade electrochromic window device is the polymer electrolyte. This specific layer in the EC device should possess suitable electrochemical stability, good ionic conductivity, and long term durability. Various systems have been investigated during the last three decades and applied in high-energy lithium-ion batteries.

The present status of the problem is related to the practical application of the “smart windows”, the purpose is to decrease the still high price, around 850 -1200$/m^2 down to around 200$/m^2. The effect is well studied, and now the efforts are concentrated on cost-effective technologies.

Demonstration projects were developed, one of which is the Lawrence Berkeley National Laboratory test room project (Fig.3).

Fig 3 Interior view of test room, the electrochromic windows are in the clear state (left side) in the morning under a diffuse light, and in active coloured mode when the sun shines through the window (after Eleanor S. Lee, Dennis L. Di Bartolomeo, and Stephen E. Selkowitz, Lawrence Berkeley National Laboratory, (11).

Atmospheric pressure chemical vapour deposition technology, which the Optical coatings group at the Central laboratory of Solar Energy and New Energy Sources at the Bulgarian Academy of Sciences (CL SENES-BAS) has employed through the years for developing of different optical coatings for effective solar energy utilization, is promising since it can assure flow through process. No vacuum system is required. In industrial type APCVD reactor, by assuring homogenous heating of the window-size glass substrate (usually disposed on heated graphite susceptor), and developing a coating deposition process of high growth-rate, a continuous, flow-through production process is possible.

In this paper we show a representative study, part of the research related to APCVD technology for electrochromic “smart window”, developed at CL SENES-BAS.

2. Experimental

By atmospheric pressure CVD, utilizing carbonyl process with precursor metal hexacarbonyls, mixed oxide films based on molybdenum and tungsten, as well as molybdenum and chromium were obtained. The microstructure of the coatings is studied by electron microscopy techniques, and field emission microscopy. The films optical properties were characterized by UV-VIS-NIR, and vibration properties were studied by analyzing FTIR spectra in the range 4000 cm^{-1}-350 cm^{-1}. Electrochromic characteristics, color efficiency and optical modulation were derived from the voltametric curves measured by a voltammetry set-up especially installed.

A larger-area electrochromic device is constructed, and by Ellipsometry the homogeneity of the coating is evaluated by measuring and determining the optical constants for different areas over the coating surface. The area is 75/75 mm, which is the standard size researchers use for comparison of the results, published in literature.

Polymeric electrolyte is developed to laminate the two glasses. The electrochromic characteristics of the ready-made device are studied.

Mixed oxide films based on Mo and W are deposited using atmospheric pressure CVD method [12, 13], employing a horizontal quartz reactor with cold walls. High frequency generator (HFG) was heating a graphite plate covered with silicon carbide layer. Over the plate in advance, glass substrates are placed. The glass is conductive, indium-tin-oxide covered. The mixed Mo/W oxides based coatings require substrate heating up to 200^{o}C. Single MoO_3 grows at lower substrate temperature (150^{o}C). The growth-rate of these films is much higher than of WO_3 films. The chemical precursors, are the metal hexacarbonyls, $W(CO)_6$ and $Mo(CO)_6$. The mixed precursor powder was placed in a sublimator, immersed in a silicon oil bath,

heated by a magnetic stirrer heater to sublimation temperature of 90^{o}C. The carbonyls vapors were carried by Ar flow from the sublimator to the CVD reactor, and this Ar flow rate is related to the flow rate of separately running oxygen flow (the reactive gas), and to this specific gas flow ratio we refer as to a definition of the oxygen content. Here in the paper some results for two different ratios are presented - ratio of 1/16 and 1/32. After deposition, the samples were additionally annealed at elevated temperatures, reaching the most of 500^{o}C, for 1 hour in air. The larger area substrates were covered by W/Mo based mixed oxide film obtained at the above described technological conditions with the purpose to make an electrochromic device - smart window.

Optical transmittance and reflectance spectra were measured with UV – VIS 3600 Shimadzu spectrophotometer in the range of 300 to 1200 nm. Reflectance spectra are performed by using 5^{o} incident reflectance attachment and the reference sample is aluminum mirror.

Cyclic voltammetry experiments were performed in a standard three-electrode cell arrangement. The three electrodes are: the working electrode-glass with the film above, reference electrode is calomel electrode (SCE) and the counter electrode Platinum. The voltage sweep potentials were provided by a computer controlled Bank-Electronic Potentiostat. Monochromatic light was providing by a monochromator. Chopped light source and lock-in amplifier were available in the system, as well. A quartz cuvette with three electrodes inside was filled with electrolyte used, namely either 1mol/l $LiClO_4$ in propylene carbonate (PC) or acid types electrolytes like 1 M H_2SO_4+ 50% glycerin. The glycerin is necessary to prevent film deterioration by the acid electrolyte.

Surface morphology was observed by ultra-high resolution field emission FE-SEM Hitachi S-4800.

3. RESULTS AND DISCUSSION

3.1 *Microscopy study*

Columnar structure, typical for the CVD thin films was proved by Field Emission microscopy (FE-SEM) study. The micrograph on Fig.4 presents the image of a substrate-film system, observed by the beam falling under angle on the cross section surface. Columns would favor easy intercalation and deintercalation of ions at the place of their boundaries.

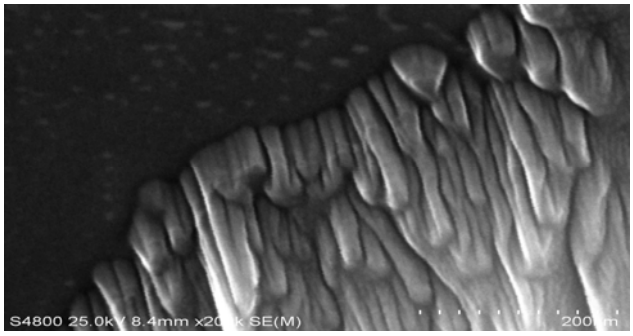

4. Field Emission SEM (at angle) micrograph of CVD as-deposited MoO_3-WO_3 слоеве, oxygen 1/16 on Si substrate.

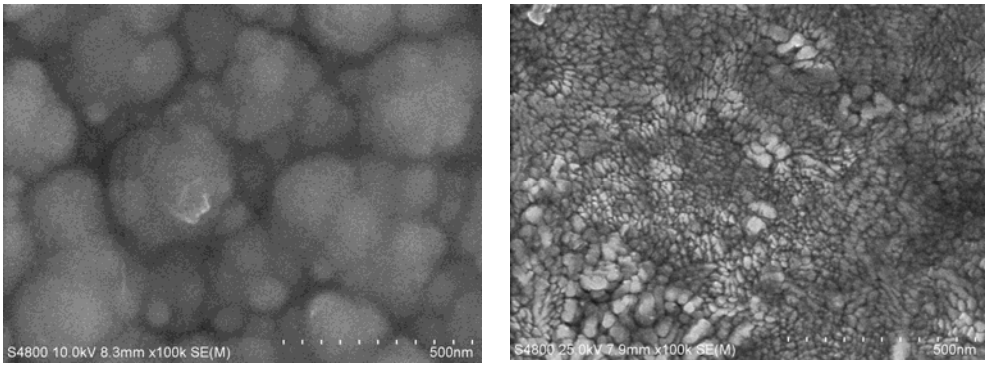

a b

Fig.5. FESEM micrographs of CVD MoO_3-WO_3 thin films, grown on conductive glass at: a) gas flow ratio 1/16 and b) 1/32 in as deposited state.

The two groups of samples deposited at different oxygen amounts show different features. The first set samples grown at lower oxygen concentration contains grains, on the surface of which a contrast change is observed. These grains look like clusters. The inter-grains areas could also facilitate the ions intercalation process. Higher amount of oxygen (b) leads to smaller size of the grains, part of them look brighter than others. The brightness is probably connected with existence of sub oxide phase.

3.2 Optical transmittance and reflectance

The optical behavior of the studied films was monitored by transmittance and reflectance measurements.

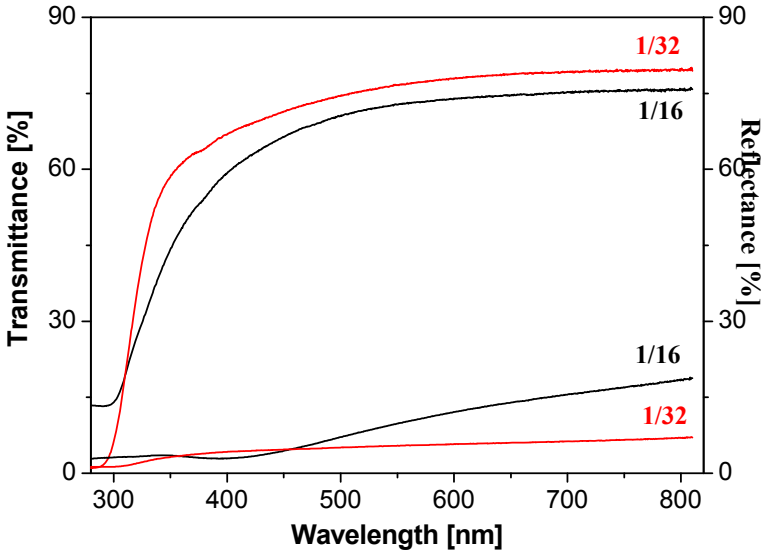

Fig.6. UV-VIS transmittance and reflectance spectra of MoO_3 -WO_3 oxide films, grown on glass at different oxygen flow-rates. As-deposited films are additionally treated at 500^{o}C.

Figure 6 presents the UV-VIS spectra of annealed at 500^{o}C films, obtained at the two gas flow ratios. As it can be observed, the transmittance of film grown at higher oxygen amount is higher than the other set. Respectively, its reflectance is lower. This is due to the fact that the films growing at higher oxygen content are probably more stoichiometric and visually they are more transparent.

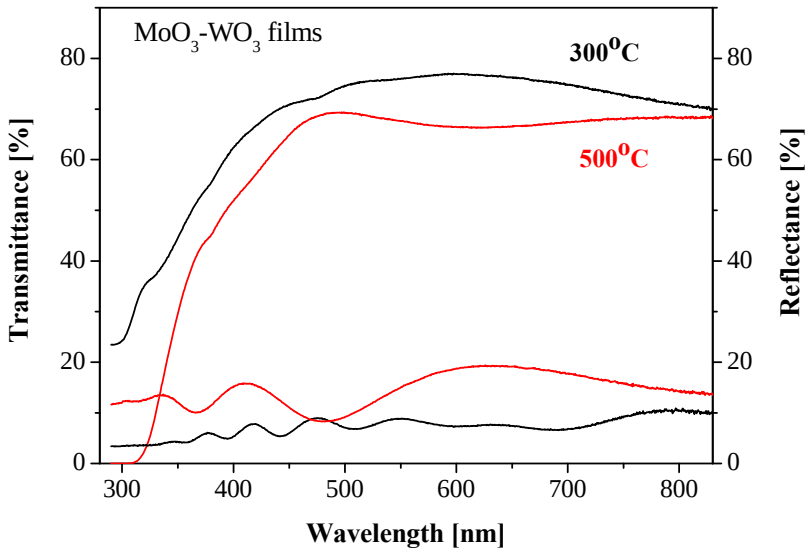

Fig.7. UV-VIS spectra of CVD MoO_3-WO_3 thin films, grown at gas flow ratio 1/32 and additionally annealed at 300 and 500°C. The substrates used are conductive glass.

As it is seen from the two curves on Fig. 7 the transmittance of mixed oxide films deposited at lower oxygen amount considerably decreases with annealing temperature. Transmittance of 500°C annealed film is lower than that of 300°C (close to deposition one, 200°C) treated sample. This shows that the second stage of the overall technology, namely the annealing of as-deposited films is not necessary. A number of other our studies have proved this result. This is a good technological result, makes the technology more simple, more cost-effective

The optical properties of the mixed oxide films are suitable for electrochromic applications, as they manifest high transmittance in the visible spectral range, reaching 80 % even in case of the conductive glass substrates.

3.3 Electrochromic properties – color efficiency and optical modulation

Color Efficiency (CE) is determined:

$$CE = \Delta (OD) / \Delta Qinj. \qquad (1)$$

Where the optical density is related to extinction and film thickness:

$$OD = (4\pi/\lambda)kd \qquad (2)$$

Experimentally, $\Delta(OD)$ is determined from the relation:

$$\Delta (OD) = - \log 10 (Tcolored/Tbleached) \qquad (3)$$

Tcolored – transmittance measured after ion injection, and Tbleached – transmittance of bleached film (extraction of alkali ions). These values are determined by a computer program running the voltammogram (current-voltage dependence) measurements. The surface area of the voltammogram gives the charge transferred through the system, and injected in the film (Δ Qinj).

From the volammograms measured (not presented here) in the three-electrode configuration cell, the determined values of the color efficiency and optical modulation (see Table 1 below) are high enough for the films to serve as working electrodes in practical electrochromic devices [5].

Table 1. Electrochromic characteristics of CVD MoO_3-WO_3 films, obtained at gas flow ratio 1/16 and 1/32 derived from cyclic voltammetric data.

MoO_3-WO_3 films	**λ [nm]**	**CE [cm^2/C]**		**ΔT [%]**	
		As deposited	**Ann. 500°C**	**As deposited**	**Ann. 500°C**
Ar/O_2=1/16	500	32,7	28,8	17,8	28,8
	550	37,3	43,7	20,0	43,7
	600	29,0	23,4	15,9	23,4
Ar/O_2=1/32	500	51,6	51,6	20,3	26,9
	550	140,8	86,3	73,2	20,0
	600	75,6	75,6	29,7	28,1

In Table 1 the colour efficiency (CE) and the optical modulation (ΔT), derived from cyclic voltammetry data are summarized. Other authors reported that mixed oxide systems show better electrochromic performance, when the single oxides are in the optimal range of ratios [2]. The annealing leads to decreased values of the colour efficiency and optical modulation. The annealed films show considerably lower optical modulation. The wavenumber dependence of the colour efficiency is obvious. The highest value of 140, 8 cm^2/C is obtained for the colour efficiency of as-deposited films for λ = 550nm, which is the maximum of the solar spectrum. The three digital value of the colour efficiency, and optical modulation of around 73% (see the table) are very promising results for practical application. Thermal treatment seems not necessary, since the transmittance is decreased, and the measured electrochromic characteristics for as-deposited films are superior compared to the ones of annealed films. The technological process

for deposition of MoO_3 - WO_3 thin films can be shortened by avoiding the second stage of annealing process. This would result in energy saving, cost-effective “smart window” technology.

3.4 Optical constants evaluation

The larger area substrate of Donnelly type conductive glass was covered by mixed Mo/W oxide film. Three samples were prepared, a larger area one, and two control ones The Data for the refractive index at different places of the coating are evidence how the homogeneity of the graphite susceptor heating assures homogeneity of the films disposed over its surface. The 75/75 mm sample, refractive index calculated in result of measurements, N_1=2.117; sample smaller area 25/25 mm, N_2=2.205; second sample smaller surface area 25/25mm, N_3=2.2; The corresponding film thicknesses are: 534nm, 515nm, and 505nm. We should note that the substrate was conductive glass and the evaluation of the coating is made considering the substrate as a glass covered by ITO film, the optical constants for which were in advance evaluated, as follows: n=1.859, and the extinction coefficient $K=2.16.10^{-5}$, showing too small absorption value.

4. CONCLUSION

The chosen CVD technology is suitable for preparation of smooth and transparent MoO_3-WO_3 thin films. Different flow-rate of the oxygen entering the CVD reactor produces different structure and optical performance of Mo/W mixed oxide films. The higher amount of oxygen leads to crystalline films with columnar structure even in as deposited state. The optical and electrochromic properties are superior for the case of as deposited MoO_3-WO_3 films. Their microstructure and optical characteristics facilitate the electrochromic effect.

The proposed APCVD MoO_3-WO_3 films are promising materials for application in electrochromic devices. The obtained values of color efficiency and the optical modulation are high enough for the films to be applied as working electrodes in smart windows.

The authors acknowledge the help of Stefan Boyadjiev (TU–Sofia), our coauthor in previous publications, for FESEM micrographs, made in Japan, and of Zoya Nenova (CL SENES-BAS) for the ellipsometry measurements.

5. REFERENCES

[1]. Granqvist, C.G. Niklasson, G.A , Azens A., (2007) Appl. Phys A 89, 29.

[2]. Granqvist C.G., (1995), Handbook of Inorganic Electrochromic Materials, Elsevier, Amsterdam.

[3]. Papaefthimiou S., Leftheriotis G., Yianoulis P.,. Hyde T.J, Eames P.C., Fang, Y.. Pennarun P.-Y,. Jannasch P, Energy and Buildings, (2006) 38, 1455–1467.

[4]. Rodrigues L.C., Barbosa P.C., Silva M.M,. Smith M.J, Gonçalves A., Fortunato E., (2009), Opt. Mater., doi:10.1016/j.optmat.2009.02.004.

[5]. Deb S.K, Philos. Mag. (1973).27, 801.

[6]. Leftheriotis G, Yianoulis P., Solid State Ionics, (2008)179, 2192.

[7]. A.A, Joraid, Current Applied Physics, (2009) 9, 73.

[8]. Wei Luo, Xiang Kai Fu *, Li Hua Ma, Chinese Chemical Letters, (2007) 18 883–886.

[9]. He T., Yao J., Progress in Materials Science, (2006) 51, 810–879.

[10]. Morandi S., Ghiotti G., Chiorino A., Bonelli B., Comini E., Sberveglieri G., Sensors and Actuators (2005), B 111–112 28.

[11]Eleanor S. Lee, Dennis L. Bartolomeo, and Stephen E. Selkowitz, " Electrochromic Windows for Commercial Buildings: Monitored Results from a Full-Scale Testbed", Proc. 2000ACEEE Summer Study on Energy Efficiency in Buildings, August 20-25, 2000, Pasific Grove, CA

[12]. Gesheva K.A., Ivanova T., Marsen B., Zollo G., Kalitzova, J M., J. Crystal Growth, (2008), 310 (7-9) 2103.

[13]. Gesheva K. A. , Ed. "Thin Film Optical Coatings for Effective Solar Energy Utilization: Spectrally selective surfaces and Energy control coatings", (2008) N. Y. USA, Nova Science Publishers.

ASSESSEMENT OF RENEWABLE ENERGY POTENTIAL
Calculation model “AREP-LP”

Eng. Alexander Penchev, MSc.
Managing director – ESD-Bulgaria Ltd.
www.esdb.bg alexander@esdb.bg

Key words: *Renewable Energy (RES), Renewable Technologies (RET), Theoretical Potential, Technical Potential, Municipalities, Regions, Energy Planning(EP), Emission Reduction (EmR), Market Assessment (MA), Data base(DB).*

Introduction

Bulgaria is a country rich in renewable energy sources. There are all types of RES including: solar, geothermal, biomass, wind energy and hydropower. Per capita it ranks among the top in Europe. Bulgaria's target for 2020 is 16% of final consumption of electricity should be from renewable energy. To achieve this goal, the first and most important task is assessing the potential of renewable energy and its geographical distribution. Creating a database of renewable energy is essential for implementation of investment projects in this area.

Models for assessment of RES potential

Currently there are different models for the assessment of RE potential. One of the first is **SAFIRE** (**S**trategic **A**ssessment for **I**mplementation of **R**ational **E**nergies). It was developed in the early 90's of last century by ESD Ltd. UK and Freiburg University Germany. The model assesses the macro level.

It has a complex structure and is designed to work on renewable energy experts with high experience. Evaluate: the technical and theoretical potential, financial and economic indicators including market potential and market penetration. Results are intended for policy makers and decision makers. The results do not give a response where the resource is located and what are the investment opportunities. SAFIRE has been used in over 40 countries worldwide. During the period 1995-1997 it was made a first assessment of the potential of renewable energy in Bulgaria.

Another group of models such as: RETScreen, Energy software, Renewable software and others. They are designed for pre investment studies for specific RET. They work with a detailed database on specific RE technologies. From the foregoing it appears that at present there is no

model for the assessment of renewable energy potential and its geographic distribution in a given area and / or region.

Calculation model AREP-LP. General description.

(**A**ssessment of **R**enewable **E**nergy **P**otential - **L**ocal **P**lanning)

The lack of a suitable model for assessment of RES potential has forced our company (ESD-Bulgaria Ltd) to develop their own calculation program. The computational model AREP-LP was established.

The main objectives of the model were:

• To fill the gap between assessment models on the macro level and to those for investment research (Figure 1).
• Evaluate the theoretical and technical potential, depending on the RET
• Evaluate the commercial applicability of the RET
• Evaluate the market potential and market penetration
• Evaluate under different scenarios
• To be able currently to introduce modifications
• Be friendly (can be used by non professionals)
• Ability to make evaluations at the macro level and feasibility studies for investment projects.
• To serve to create a database of renewable energy potential of municipal, regional and national level.

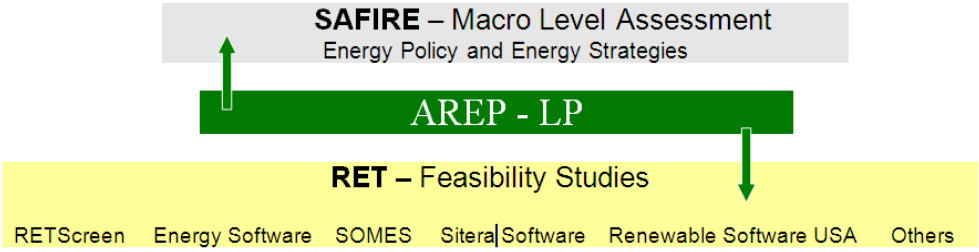

Fig.1.

On Table 1 is a comparative assessment of different computational models made by a team of TU - Sofia. Comparison is based using the following criteria:

- Range of models - a variety of categories and components of the model (1)
- Structure of the model - allowing easy access and use its various modules (2)
- Functionality of the model - flexibility of the model (3)
- Sensitivity and accuracy of model (4)
- Applicability (universality) of the model (5)
- Accessibility for use by non-specialists (6)

• Number of RET, which can be used to model their energy assessment (7)

Tabl.1

Calculation model	*Criteria*						
	1	*2*	*3*	*4*	*5*	*6*	*7*
RETScreen	♦♦	♦♦♦	♦♦♦	♦♦♦	♦♦♦	♦	8
Energy software	♦	♦	♦	♦♦	♦♦	♦	2
SOMES	♦	♦	♦♦	♦♦	♦	♦	2
Siterra software	♦	♦	♦♦	♦♦	♦♦	♦	2
Renewable software	♦♦♦	♦♦	♦♦♦	♦♦♦	♦♦	♦	5
Renewable fuels module	♦♦♦	♦♦	♦♦♦	♦♦	♦♦	♦♦	5
SAFIRE	♦♦♦	♦♦♦	♦♦♦	♦♦♦	♦♦	♦♦	8
AREP - LP	♦♦♦	♦♦♦	♦♦♦	♦♦♦	♦♦♦	♦♦♦	**9**

AREP-LP – Structure

The model includes three main groups: input data, computation part and generate results. Input data is consistent with the format in which are represented by official institutions. Computational part is designed based on precise engineering methods of calculation.

The results are generated in tabular and graphic form.

On Figure 2 presents the type of input data.

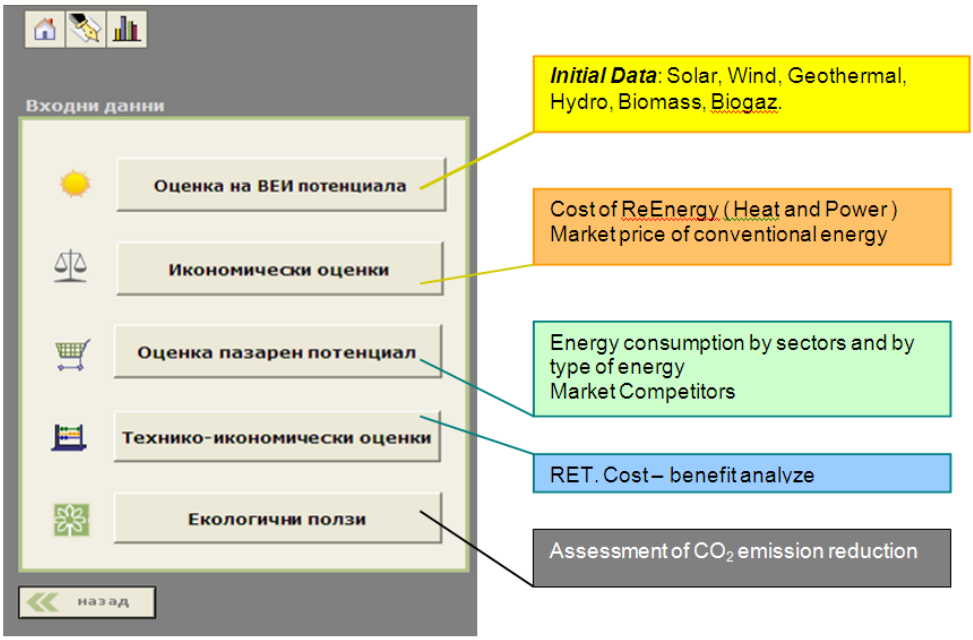

Fig.2

The model make the following groups of evaluations - *Fig.3.*

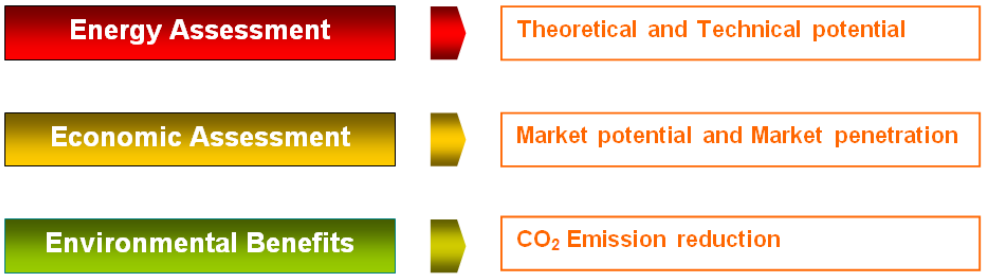

Fig.3

Input data and results

All inputs and outputs are presented in tabular and graphic form. Examples are given in fig.4 and fig.5

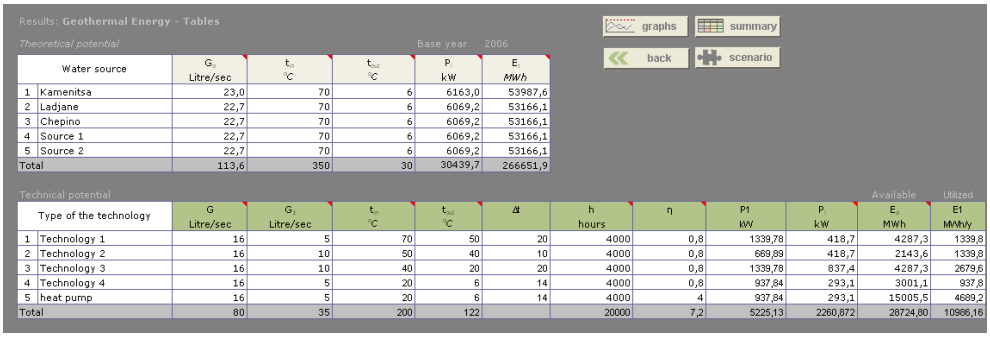

Results: Geothermal Energy - Tables

graphs summary back scenario

Theoretical potential Base year 2006

	Water source	G_{in} Litre/sec	t_{in} °C	t_{out} °C	P_t kW	E_t MWh
1	Kamenitsa	23,0	70	6	6163,0	53987,6
2	Ladjane	22,7	70	6	6069,2	53166,1
3	Chepino	22,7	70	6	6069,2	53166,1
4	Source 1	22,7	70	6	6069,2	53166,1
5	Source 2	22,7	70	6	6069,2	53166,1
Total		113,6	350	30	30439,7	266651,9

Technical potential Available Utilized

	Type of the technology	G Litre/sec	G_1 Litre/sec	t_{in} °C	t_{out} °C	Δt	h hours	η	P1 kW	P_t kW	E_t MWh	Et MWh/y
1	Technology 1	16	5	70	50	20	4000	0,8	1339,78	418,7	4287,3	1339,8
2	Technology 2	16	10	50	40	10	4000	0,8	669,89	418,7	2143,6	1339,8
3	Technology 3	16	10	40	20	20	4000	0,8	1339,78	837,4	4287,3	2679,6
4	Technology 4	16	5	20	6	14	4000	0,8	937,84	293,1	3001,1	937,8
5	heat pump	16	5	20	6	14	4000	4	937,84	293,1	15005,5	4689,2
Total		80	35	200	122		20000	7,2	5225,13	2260,872	28724,80	10986,16

Fig.4. *Geothermal energy potential – Velingrad municipality*

Резултати: Геотермална енергия - графично представяне

Годишен теоретичен и технически потенциал на геотермалната енергия, за всеки водоизточник

Каменица Ъджане Чепино Извор 4 Извор 5

Водоизточник

Теоретичен потенциал

Технически потенциал

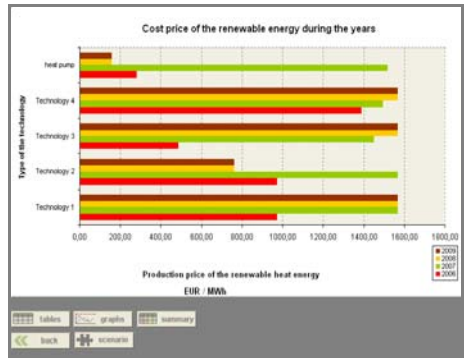

Cost price of the renewable energy during the years

heat pump Technology 4 Technology 3 Technology 2 Technology 1

Type of the technology

0,00 200,00 400,00 600,00 800,00 1000,00 1200,00 1400,00 1600,00 1800,00

Production price of the renewable heat energy

EUR / MWh

Fig.5. *Data present in graphs - Examples*

Applicability

Computational model "AREP-LP" was established as a universal tool for development of municipal energy plans

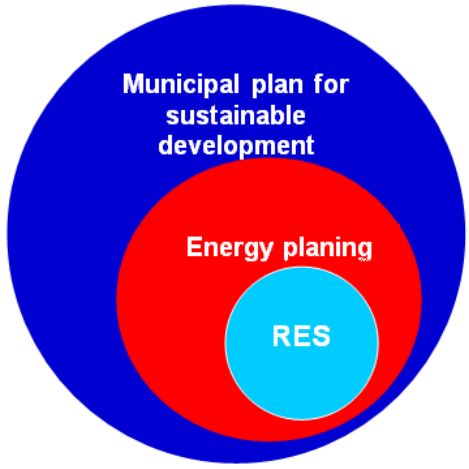

Fig.6.

Estimates with him are extremely effective in applying the bottom up method. First, evaluate the potential of municipal level and then aggregating the results of regional and national level - fig.7

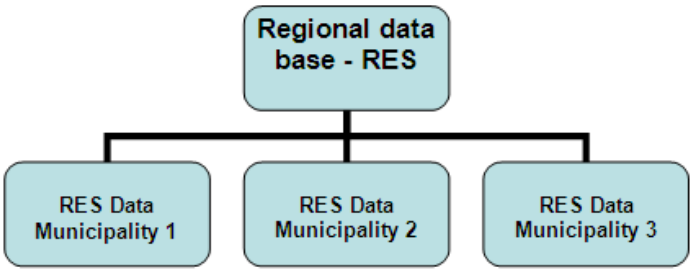

***Fig.7**. Assessment of RES potential. The method bottom-up*

Computational program is a type of "open source", which gives the model greater opportunities. Based on the basic model different versions were developed such as AREP-Geothermal, REScan and others. REScan version was specifically developed for use by municipal and regional administrations.

Where used

AREP-LP and its various versions began to be used by 2001
Most important applications

- 2010. Assessment of renewable energy potential in all 11 municipalities in Stara Zagora. Establishment of municipal and regional database.
- 2009. Assessment of renewable energy potential of the municipality of Sofia. Establishment of a municipal database
- 2008. Assessment of RE potential of the municipality of Petrich. Establishment of a municipal database
- 2006. Assessment of RE potential in all nine municipalities of Smolyan. Establishment of municipal and regional database.
- 2001 – 2008. Assessment of RE potential in municipalities: Silistra, Kyustendil, Kocherinovo, Teteven, Velingrad and others
- 2002 –Poland
- Sins 2005 in UK

Why AREP-LP

The model give opportunities to estimate:

- The energy equivalent of theoretical and technical potential of RES
- The market potential and commercial applicable RET
- Assessments may be made under different scenarios
- Ability to create and maintenance of database

Key tool in the development of local sustainable energy plans
Flexible - with the possibility to include additional modules in the model, depending on the specific task

A universal - can be applied in all countries, allows to obtain information additional to that implied by the model
It can be used for pre investment studies and also for the ***development of investment project***

It has ***high sensitivity and accuracy*** of assessment of the results.
Easy to use
Identify investment projects in renewable energy and energy efficiency areas
Assessment of CO2 emission reduction.

Conclusions

Computational models AREP-LP and its versions: AREP-Geothermal and REScan are with proven qualities.
It can be widely used at home and abroad.

References

1. PHARE Energy Program. Project “Technical and Economic Assessment of RES Potential in Bulgaria” . 1995-1997.
2. SAFIRE - Description of calculation model for assessment of RES potential. ESD Ltd.UK. 1991.
3. Project “Local sustainable energy planning”. Donor DFID. 2002
4. Project “ Development of calculation model AREP-LP”. ESD-Bulgaria. ESD-Bulgaria. 2004-2005
5. Project “Assessment of RES potential – Smolian municipality” ESD-Bulgaria. 2006
6. Project “ Sofia municipality – development of municipal renewable energy program” ESD-Bulgaria. 2009.
7. Project “Public Private Partnership: Building the capacity for municipal sustainable energy development, Municipality of Petrich” ESD-Bulgaria. 2008
8. “REScan – calculation model for assessment of RES potential in the territory of Stara Zagora region” ESD-Bulgaria. Project 2009.
9. Petkova.S and collective. Article. “Analysis of models for assessment of RES energy potential” 2009.

Linking Geography With Ecology: A Case Study From India

S.K. Sharma
Carman Residential and Day School, India

ABSTRACT

The study of Geography in India encompasses the **Physical Geography :** consisting mainly of ***Geomorphology -*** factors controlling landform development, geo-hydrology, economic geology and environment ; ***Climatology -*** temperature and pressure belts of India and the world and heat budget of the earth ; ***Oceanography -*** bottom topography of the Atlantic, Indian and Pacific Oceans, temperature and salinity of the oceans, heat and salt budgets and ocean deposits ; ***Biogeography -*** genesis of soils, causes of soil erosion and conservation measures; ***Environmental Geography -*** principle of ecology; human ecological adaptations; influence of man on ecology and environment; global and regional ecological changes and imbalances; ecosystem their management and conservation; environmental degradation, management and conservation; biodiversity and sustainable development; environmental policy; environmental hazards and remedial measures; environmental education and legislation and the **Human Geography :** perspectives in human geography, economic geography, population and settlement geography, regional planning and models, theories and laws in human geography. However, **for raising the socio-economic level of the country, India has over exploited its** resources including land, surface and ground water, energy, minerals, biotic and marine resources; forest and wild life resources. **This has endangered the environment and ecology with disastrous consequences to natural resources.** Some of the **Contemporary Ecological** issues which have arisen from these activities are : environmental hazards - landslides, earthquakes, tsunamis, floods and droughts, epidemics. The Government of India is going high-tech in issuing early warning system against to these natural calamities. The Government has enacted the Environmental Protection Act, 1986 to deal with the issues pertaining to environmental pollution due to increased industrial activities. Keeping in view the principles of environmental geography, the Government has now constituted the environmental impact assessment committee (EIA) under the patronage of Ministry of Environment and Forest to deal with the changes in patterns of land use owing to increased urbanization. The Government has now further enforced the Forest Conservation Act in 1980 more vigorously to check the environmental degradation, deforestation, desertification and soil erosion. India, being an agrarian county, is facing serious agricultural problems, specially after adopting the Green Revolution – the Government has now banned the faulty agricultural practices such as shifting cultivation and use of chemical fertilizers / pesticides and promoting the organic farming. The principles of Human Geography has helped in creating an

environmental awareness - in this regard, Chipko (literally means sticking to the trees) movement initiated in 1973 in which a human chain around the tree was made by the local people, specially the women, to save the trees/ forest from cutting by the loggers, has played an important role in restoring ecosystem of the Himalayan region. The top soil did not lose its contact with underlying layer when the area remained forested. The roots of the plants held the soil from sliding down. The approach of involving and educating the local women in the protection and management of forests and environment proved to be a great success in India. Thus, it is very logical to study geography to understand and resolve the ecological problems.

Key words : Chipko movement, environmental hazards, human geography, physical geography

INTRODUCTION

The total forest cover of India as per State of Forest Report 2003 is 678,333 km², which constitutes 20.64 % of the geographic area of the country, plays a significant role in biodiversity protection (gene / species protection - harboring more than 45,000 floral and 81,000 faunal species of which 5150 floral and 1837 faunal species are endemic), global environment conservation (global warming mitigation, global climate stabilization and air purification), landside prevention and soil preservation (soil erosion prevention, surface landslide/soil run-off and other natural disaster prevention), headwater conservation (flood mitigation, water resource reserve, water flow control and water quality purification), health, recreational and cultural (cure, recreation, landscape and scenic beauty, religious festivals and traditional culture), material production (timber, food such as mushroom etc, fertilizers, feeds, raw material for pharmaceutical and other industrial products, extracted ingredients, greening materials etc) and poverty alleviation. The nation has established 597 Protected Areas comprising 95 National Parks, 500 Wildlife Sanctuaries 2 conservation reserves covering 1.56 million ha area or 4.75 per cent geographical area of the country for in-situ and ex-situ conservation of flora and fauna. The ***Environmental Geography*** **comprising the** principles of ecology; human ecological adaptations; influence of man on ecology and environment; global and regional ecological changes and imbalances has helped the country to understand the ecosystem its management and conservation; environmental degradation, management and conservation; biodiversity and sustainable development; environmental policy; environmental hazards and remedial measures; environmental education and legislation. India is a fortunate country for having rich and varied heritage of biodiversity representing almost all the bio geographical regions of the world. It

has a variety of habitats of ranging from tropical rainforests to alpine vegetation and from temperate forests to coastal wetland. Fig. 1 shows the rich biodiversity regions of India which is a center of agro biodiversity. It is a homeland of nearly 167 cultivated species and the global exchange of biota existed since historical times. The restrictedness of Indian biodiversity is very high. About 33% of the country’s recorded flora and fauna are endemic to the country and are concentrated in four regions which are represented by green color in the figure viz: North-East, Western Ghats (UN Heritage Site), North-West Himalaya and the Andaman Nicobar islands [1].

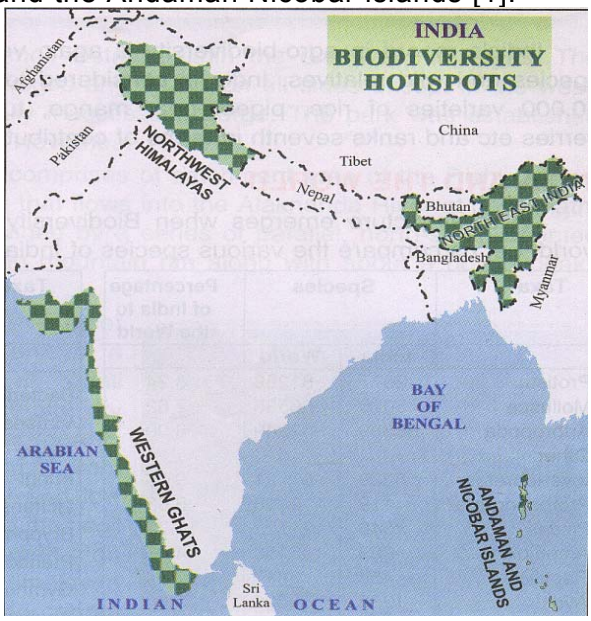

Fig. 1 Rich biodiversity Hot Spots in India

The biodiversity is used for different values : primarily as - Direct values – for food and medicinal values which are the most important assets of biological diversity.

HUMANS, NATURE AND ECOLOGY - THE VITAL CONNECTIONS

It is a well known fact that the humans are a part of nature, dependent on natural systems for a variety of economically important resources and ecological services essential to our survival and long-term prosperity whereas the Ecology is a field of science that seeks to describe relationships between organisms and their chemical and physical environment.

IMPACT OF HUMAN ACTIVITY ON ECOSYSTEM AND FORESTS

Ecosystem which Function for the Photosynthetic organisms such as plants and algae produce food within ecosystems. Their well-being is essential to the survival and well-being of all other species. However, the rising demand for forest based products and resultant deforestation and encroachment has led to a severe loss of natural resources and destruction of habitat, Fig.2 and 3.

Fig. 2 Forests are the natural habitat of India's rich fauna and flora

Fig.3 Deforestation for meeting various human needs

In the northern most states of India, forests meet nearly 40% of the energy needs in the form of fuel wood which is of the order of about

235 million m^3 annually and the green fodder for livestock which is also of the order of 882 million tons per year making it 50% of the requirement while remaining is met by destructive over-grazing within forests [3]. This has lead to massive deforestation, fig. 4.

Fig. 4 Fuelwood collection by local villagers

Deforestation is one of the major reasons for wildlife loss and an increase in Global Warming leading to Climate Change. The Gangotri glacier is now has been receding since 1780 and started retreating rapidly after 1971 due to climate change attributed mainly to the deforestation, Fig 5. The expected danger of the melting down the glaciers is the widespread flooding followed by irreversible droughts, threatening the livelihood of millions of people. The climate pattern change is bringing in the variability in monsoon and seasonal rainfall is leading to 10-40% fall in agricultural food production as the water balance is disrupted leading to droughts in traditionally fertile zones. This would not only mean unprecedented food shortage but also a massive water crisis**.** The Indo-Gangetic basin in North India alone is

a home to more than 500 million people. Nearly 70% of the discharge into the Ganga is from the rivers in Nepal, which means that if the Himalayan glaciers dry up by 2050, as predicted, so will the Ganga downstream in India causing water shortages for nearly 37 % of India's irrigated land. The Himalayan glaciers receding at "an alarming rate, influencing the stream run-off of Himalayan rivers." Six per cent, or 63.2 million, of India's population live in low elevation coastal zones that are vulnerable to sea-level rise.

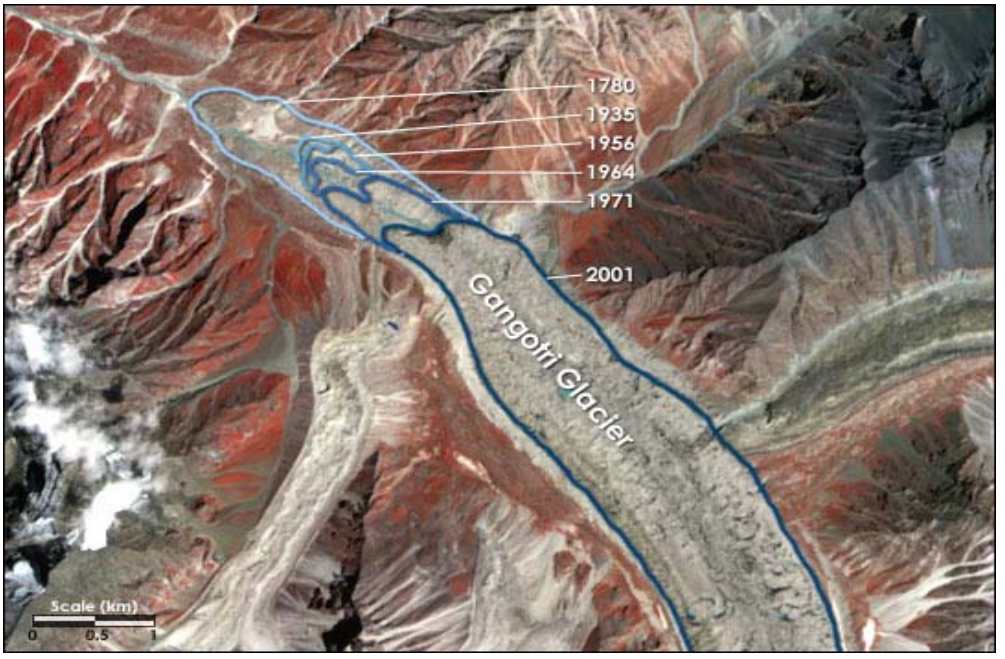

Fig 5 Retreat of Gangotri Glacier

However, despite large-scale tree planting programs, forestry is one arena in which India has actually regressed since independence. Annual felling at about four times the growth rate are a major cause. Widespread pilfering by villagers for firewood and fodder also represents a major decrement. In addition, the forested area has been shrinking as a result of land cleared for farming, inundations for irrigation and hydroelectric power projects, and construction of new urban areas, industrial plants, roads, power lines, and schools, Fig. 6.

Fig. 6 Forested area cleared for faulty way of farming

CONSERVATIONS MEASURES

Since the early 1970s, as they realized that deforestation threatened not only the ecology but their livelihood in a variety of ways, people have become more interested and involved in conservation. The best known popular activist movement is the Chipko Movement In India, in which local women decided to fight the government and the vested interests to save trees. The women of Chamoli District, Uttarakhand, declared that they would embrace--literally "to stick to" (*chipkna* in Hindi)--trees if a sporting goods manufacturer attempted to cut down ash trees in their district, Fig. 7. Since initial activism in 1973, the movement has spread and become an ecological movement leading to similar actions in other forest areas. The movement has slowed down the process of deforestation, exposed vested interests, increased ecological awareness, and demonstrated the viability of people power [2].

Fig. 7 Tree hugging to save forests

A few years later the news of this movement crossed the international boundaries and 'Chipko-Day' was observed at New York in USA on the 29th April, 1983. In addition to it, number of eco-task force have been created by the Government of India by enacting "The Forest Conservation Act, 1980" to conserve the forests for protecting the valuable soil cover, acquiring fresh water and air, shelter, and a clean and healthy environment in which we live.

LONG-TERM PREVENTIVE MEASURES

India's long-term strategy for forestry development reflects three major objectives: to reduce soil erosion and flooding; to supply the growing needs of the domestic wood products industries; and to supply the needs of the rural population for fuelwood, fodder, small timber, and miscellaneous forest produce. To achieve these objectives, the

National Commission on Agriculture in 1976 recommended the reorganization of state forestry departments and advocated the concept of social forestry. The commission itself worked on the first two objectives, emphasizing traditional forestry and wildlife activities; in pursuit of the third objective, the commission recommended the establishment of a new kind of unit to develop community forests. Following the leads of Gujarat and Uttar Pradesh, a number of other states also established community-based forestry agencies that emphasized programs on farm forestry, timber management, extension forestry, reforestation of degraded forests, and use of forests for recreational purposes.

The role of India's forests in the national economy and in ecology was further emphasized in the 1988 National Forest Policy, which focused on ensuring environmental stability, restoring the ecological balance, and preserving the remaining forests [4]. Other objectives of the policy were meeting the need for fuel wood, fodder, and small timber for rural and tribal people while recognizing the need to actively involve local people in the management of forest resources. Also in 1988, the Forest Conservation Act of 1980 was amended to facilitate stricter conservation measures. A new target was to increase the forest cover to 33 percent of India's land area from the then-official estimate of 23 percent. In June 1990, the central government adopted resolutions that combined forest science with social forestry, that is, taking the socio-cultural traditions of the local people into consideration.

In addition, Government of India has now started encouraging the Eco-Tourism in the country which is still at a very nascent stage, but there are for sure conscious efforts to save forests and its biodiversity specially, the fragile Himalayan Eco System and culture and heritage of the indigenous people, which is probably the largest concentration in the world. But in the recent past, the movement of Eco-tourism in Garhwal Himalayas in the northern part of India, is gathering momentum, not only for geological reasons but also by virtue of its archaeological, ecological and cultural values. Eco-tourism involving traveling to this relatively undisturbed natural areas with the specific objectives of studying, admiring and enjoying nature and its wild plants and animals as well as existing cultural aspects found in these areas. It stresses on the total environment while making an economic contribution and local community and is distinguished from mass tourism and general resort tourism by having a lower impact on the environment and require less infrastructure development. Such responsible travel to natural areas conserves the environment and improves the well-being of local people. Eco-tourism has played a

significant role in reducing the dependence of local communities on the forests.

CONCLUSIONS

Human well-being is highly dependent on ecosystems and the benefits they provide such as food and drinkable water. Over the past 50 years, however, humans have had a tremendous impact on their environment. The principles of Physical Geography and Environmental Geography has helped the government to opt for Long-Term Preventive Measures and to better understand the consequences of current changes to ecosystems and to evaluate scenarios for the future and what actions could be taken to limit harmful consequences of ecosystem degradation.

ACKNOWLEDGEMENTS

Thanks are due to a large number of people who have helped with the collection of data, reviewing of drafts, and patient explaining and clarification.

REFERENCES

[1] Dhamija, S.K. (2005) Environmental Science, Kataria Publishers, New Delhi, pp 217

[2] Mathew, K.M. (2008) Manorama Year Book, Kottayam, Kerala, pp 285-87

[3] Rai, A.N. (2005) I.S.C. Environmental Education, Part 1, Goyal Brothers Prakashan, New Delhi, pp 15-17

[4] Shah, S.A. (1988) Forestry for people, Indian Council of Agriculture Research, New Delhi, pp 2-3.

Population density modeling of the Blagoevgrad district using ArcGIS tools

Penka Kastreva, Emilia Patarchanova, Galina Kuleva
South –West University, Blagoevgrad, Bulgaria

Abstract: *This paper presents the theoretical and practical use of nonparametric techniques for creating a surface model of population and population density. This surface is modeled as a raster data set in grid cells. In this way data for each point from the territory of mapping is ensured. ArcGIS tools (Simple density and Kernel density) are used. These methods ensure more accurate representation of the population into territorial units in comparison with traditional choropleth techniques.*

Keywords: *population density, density surface, interpolation, ArcGIS tools.*

1. INTRODUCTION

Census data are used for determination of various social indices such as population density. Many of these indices are related to government policy. Most of them conventionally are derived from the decennial population censuses and are normally computed at the administrative level as the spatial unit. This unit in Bulgaria is the settlement. The data are gathered and manipulated from the Institute of National Statistic (INS). The coverage of Bulgaria is spatially complete, and the data are spatially comprehensive in all censuses units. The increasing use of information technology in such administrative level has greatly expanded the volume of such data and its potential use for spatial analysis.

The advantages of indicators based on a census are that the data are available as a regular series and that they are immediately available in machine readable form. However there are some difficulties.

As we mentioned the settlement with its belonging land is the basic unit for which data are published involving the assembly of information for persons. It is known that urban and rural areas include areas of ‘un-populated’ land, such as commercial and uncultivated areas and farmland. The traditional cartographical method for representation of such statistical data as choropleth doesn’t show this specific. For practical purposes, standard choropleth techniques are frequently

used to display data at the administrative level as commune, municipality or district instead of a settlement. Such mapping is now very easily produced by many GIS. Such displays can be highly misleading, mainly because of the 'fixed' areas that have no relationship to the distribution of the phenomenon.

The main problem is however more theoretical and concerns the most appropriate way in which population and population-related phenomena, should be represented in a spatial data structure, and hence be portrayed by graphic and cartographic means. One way in which this can be achieved is to transform gathered census data into a data structure that represents population distribution more verisimilar as a continuous surface. This approach requires a change in the basic assumption of data representation, namely that the data value can be seen not as a property of an area or a point, but rather as a property of a location at which the population is distributed. The useful information about this distribution can be derived from a spatial analysis of a set of the basic area or point data values. Using such data, a model can be created as grid surface with fine resolution to represent a spatial distribution of population.

2. A REVIEW OF THE CREATING DENSITY SURFACES

2.1 A DEFINITION FOR A SURFACE

Surfaces represent phenomena that have values at every point across their extent. The values at the infinite number of points across the surface are derived from a limited set of sample values. These may be based on direct measurement, such as height values for an elevation surface, or population values for a population surface. The surface is assigned between these measured location values by interpolation. To create a continuous surface from discrete samples with measured values different interpolation methods are used. Surfaces can be represented using contour or iso-lines, arrays of points, TINs, and rasters; however, most surface analysis in GIS is done on raster or TIN data.

Linear interpolation or TIN: It is applied for territories with known Z-values (for example population values) of the measurement points. This allows precise linear interpolation among the Z-values of the nearest neighbouring points. The idea here is that the unknown value in a given point and is calculated proportionally to the distances among the measured points. This method is standard especially in the production of topographic maps for a relief representation.

GRID interpolation: The non-linear spatial interpolation calculates the unknown values using a set of points with known values that are distributed on the whole area of the territory. The distance from a point with an unknown value to a point with a known one helps to define the unknown value. In the previous paper [6] several interpolation methods of grid interpolation were discussed in detail: Inverse Distance Weighted (IDW), Natural Neighbor, Kriging and Spline.

2.2 CREATING A POPULATION DENSITY SURFACE

Population density is the measurement of the number per unit area. The density can be calculated for countable objects: discrete objects or phenomena (for example trees, car thefts, seismic epicenters) and their attributes (kind of trees, number of stolen cars, and magnitude of earthquakes).

Population density of people is an often reported and commonly compared statistic for places around the world. It is commonly represented as people per square kilometer, which is derived simply by dividing total population to land area in square kilometers. The density can be computed for any area if we know the size of the land area and the population within that area. The population density of cities, states, entire continents, and even the world can be computed.

The density functions in GIS allow to set the highest and the lowest concentration of the object’s data with we are available. Two methods for density calculation are used: simple and kernel. Both methods apply searching into an area (window) with circle form in order to calculate the density. The distance for the density function is measured from each cell to the most neighboring source with known value. The cells’ values always show number of objects per unit area (as people per square km). Surfaces received in this way are best used for visualization of some trends in data that are otherwise invisible.

2.2.1 SIMPLE DENSITY CALCULATIONS

This method for creating a density surface uses circle area for searching in order to calculate cells’ values. This circle is placed into every cell center (pixel) with unknown value. The particular values of cells are calculated by dividing the number of objects contained into the search area (for example observations) to the area size. The obtained result references to the cell. If no points or line sections fall within the neighborhood of a particular cell, that cell is assigned as NoData. Each surface cell is processed in the same way. The result of

the surface calculations depends of search radius size. The smoother surface is obtained with longer radius because probably more points can be included. Smaller values of the radius produce a raster that shows more details.

There are density tools for point and line features in ArcGIS software. We can compute a raster density map from vector point data. Point density function calculates the density of point features around each output raster cell. Units of density are points per unit of area. Line Density calculates the density of linear features (as roads, rivers) in the neighborhood of each output raster cell. Density is calculated in units of length per unit of area.

2.2.2 KERNEL DENSITY CALCULATIONS

Statistical smoothing consists of a range of nonparametric techniques for processing a data set. In a spatial context these may be techniques for identifying possible models and for analysing how well models fit to the observed data. Various simple smoothing ideas are available but more sophisticated methods stem from the idea of kernel smoothing.

The Kernel method is vastly complicated mathematical way of calculating the density surface that is based on the quadratic kernel function described in Silverman in 1986. Kernel Density can be use for point or polyline features.

When applying this method for point features a circle is drawn around every point with known value (not every cell). After that a mathematical function is applied that can take values from 1 to 0. The highest value is at the point location. The value diminishes with increasing distance from the point and is zero for a distance equal to the radius. We can image kernel as smooth bend curve that is fitted to every point. The greater the search radius is the flatter the kernel curve is. The kernel function creates a smoother surface than is created using the simple method. The density at each output grid cell is calculated by adding the values of all the kernel surfaces where they overlay the grid cell center. As we mentioned in the analysis, a window is positioned over each data point (fig.1). The window's size can vary according to the density of points around that location.

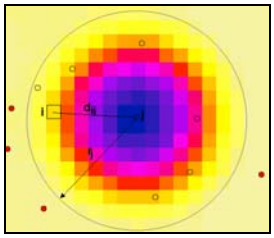

o Known points that participate in the density calculation

● Known points that do not participate in the density calculation

Fig.1 The density of every cell i is calculated using the values of the known points that fall into a circle with a search radius r drown around the known point j and circle size area

The cells falling within this window derive population values, according to weights that depend on their proximity to the data point. The output values for people density are only integers (i.e. whole person). In summary, the assignment of the value to each cell in the grid is obtained as:

$$(1) \quad P_i = \sum_{i=1}^{c} P_j . W_{ij}$$

where Pi is the estimated population of cell i, Pj is the empirical population recorded at point j, c is the total number of data points, and Wij is the unique weight of cell i with respect to point j.

The calculated cell i will not receive population from every point location but only from any points in whose window it falls. Wij will be zero for all other cell-point combinations. The window (it is called kernel) is initially defined as a circle with radius r, and depends on the density of other points falling within this circle. Weights are assigned to every cell whose centre falls within the adjusted kernel by the formula:

$$(2) \quad W_{ij} = f \frac{d_{ij}}{r_j}$$

where f is the distance function; dij is the distance from cell i to point j, and rj is the radius of the circle window defined as average arithmetic means for the distance for the known point j and other known points l in the initial kernel window:

$$(3) \quad r_j = \frac{\sum_{i=1}^{c\ 1} d_{jl} (j \neq 1)}{c \quad 1}$$

Finally we can calculate the density. As we mentioned above the density value for every raster cell i can be computed by dividing Pi (number of objects that are contained into search area) to the area size Si. This can be expressed in the following way:

(4) $D_i = P_i / S_i$

Si is the sum of cells' areas falling into kernel window of the cell i.

The explanations for kernel density calculation for line features are similar.

3 PRACTICAL APPLICATION OF THE METHODS USING ARCGIS TOOLS AND THE RESULTS FROM POPULATION DENSITY GRID OF BLAGOEVGRAD DISTRICT

It is theoretically and practically proven that some interpolation methods are more precise than others. Each of them has a variety of parameters that influence the resulting surface. In our previous paper are given examples of how different interpolation techniques can produce different output surfaces from the same input data. More widespread ways to create raster density surfaces are these discussed above. They are including interpolating values stored at measured point locations, as settlement positions. In this paper we will show the results from using ArcGIS tools to create a surface of the density of a given phenomenon. We use these possibilities of ArcGIS software in order to create raster surface of the density people population. The results of Simple density and Kernel density functions we'll use farther for comparison of the different cartographical techniques.

In the current example, the census tract density can be connected to a "centroid" point (center of gravity) for each settlement. The centroids are determined by specially ArcGIS function that uses the coordinates of boundaries. This function is very useful for extraction of mean center for several settlement formations with the same names which can be always found in the Blagoevgrad district.

Study area: The Blagoevgrad district is located in the southwest part of Bulgaria and has an area constituting 5.9 % of the total area of the country which makes it the third largest district in Bulgaria. The Blagoevgrad district is divided into 14 communes (1 urban, 7 urban-rural and 6 rural according to Eurostat methods). The largest town in the region is Blagoevgrad with 71144 thousand inhabitants (according to the census from 2001 year). The other major towns are: Petrich, around 29606 thousand inhabitants, Sandanski, around 26507 thousand inhabitants, Goce Delchev around 20426 thousand inhabitants and Razlog around 12738 thousand inhabitants.

The Blagoevgrad district is inhabited by 341283 people distributed into 281 settlements (according EKATTE). Rural settlements are dispersed and fragmented. The populated territory of settlements constitutes around 3.6 % of the total area of Blagoevgrad district. Most of the territory out of settlements is uncultivated land. Around 17 882

HA (excluding THE AREA OF THE PIRIN NATIONAL PARK AND PART OF THE AREA OF NATIONAL PARK RILA) of the area of the Blagoevgrad district is under protection. There are two national parks, eight nature reserves, two MAINTAINED reserves, nine protected landscape areas and sixteen NATURAL LANDMARKS.

Data: Population data was obtained from the 2001 Bulgarian Census. The mapping unit for population density was settlement, the lowest level of administrative division in Bulgarian. It is used database with settlement boundary, available in a vector format. The polygon objects were transformed into point ones, in order to apply Simple density and Kernel density functions.

Statistical results: The settlement network consists of 12 towns and 269 rural settlements units. One of the regions where population is distributed unevenly and rarely is in the central part of Blagoevgrad district with north-south direction. This territory is with a significant area of lakes, forests and protected areas limiting inhabited areas.

At present about 57.5% of population Blagoevgrad district lives in towns, and 42.5% is residing in rural areas. The average population density in urban areas amounts to 3188 inhabitants per km^2 in contrast to 1005 people per km^2 recorded in rural areas. The mean population density 1099 persons per sq. km is calculated as an arithmetic mean of all values of the population and the settlement areas. The maximal value is 7702. These data are obtained from calculations for population density for every settlement. The same statistical values are obtained with other raster interpolation method as Ordinary Kriging. The same calculated values for population density are used as input data for creating a raster surface. The mean population density obtained with Simple density and Kernel density functions is different in comparison with the shown methods. These differences are given in table 1.

Tab. 1

Density per sq. km	From calculations	Ordinary Kriging	Simple density	Kernel density
Mean density	1099,0	1099.0	44.6	44.7
Max density	7702.1	7702.1	3429.6	10073.2

As we can see from the data the maximum density values are vastly different. Let us consider a circle window that is drown around point sign which presents Blagoevgrad town with the largest population. The calculated density with the real populated territory is 7702 persons per sq. km. The maximum value in the simple method is significantly less than this value because according the technique of this method the sum of the settlement’s population falling into circle window is divided to its area. It is logical that the total population is

almost the same as that of Blagoevgrad because the other settlements are villages with less population while the circle window area is significantly larger than the town's territory.

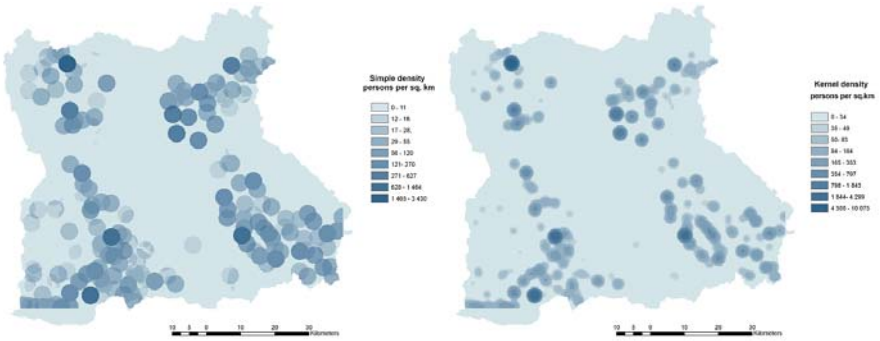

1) Simple density 2) Kernel density

Fig 2. Population density of Blagoevgrad district: The kernel function creates smoother surface than the simple method

The maximum value in the kernel method is larger than the calculated average value for Blagoevgrad. The maximum density value 10073 is obtained for the position of the point sign for Blagoevgrad. All other pixels falling into town's delineation receive smaller values.

These data are generalized and grouped to mapping population density. The most suitable classification method should be chosen depending on the character of the data distribution in order to visualize even the settlements with the least density. Simple density and Kernel density allow the obtaining of values for the population density for every point of the cartographical extent (fig 2).

3. CONCLUSION

Most GIS applications use discrete geographic information. These types of data are represented by point, line and area symbols for mapping. Continuous data can be represented as a continuous surface, generally without sharp or abrupt changes. Such data for example are population concentration dispersed over whole territory of mapping. The new technologies enable to do density mapping using points and to create a raster surface. This method has series of advantages but it is very important to represent precisely the spatial distribution of variables.

It is known that the traditional cartographical method for creating choropleth map for density representation uses administrative units for mapping as municipality or district and it shows the mean population

density in these boundaries. This cartographical technique doesn’t represent the exact distribution of the data. In our research we use the census tracts namely the settlements represented with point cartographical symbols instead of shown territorial units.

The mapping in this way is different from the choropleth map in that the borders of the cartographical representation aren’t arbitrary and they concern the spatial distribution of the variables that will be mapped. Simple density and Kernel density create a surface model of population and population density. This surface is modeled as a raster data set in grid cells and then we calculate values or density for each cell. In this way the data for each point from the territory of mapping is ensured. These methods ensure more accurate representation of the population into territorial units in comparison with choropleth technique. Finally, this method for density mapping is suitable for the cases of small scale thematic mapping because the settlements are presented with point symbols that show only the spatial positions but not their area size.

The shown methods and the obtained results are very suitable for defining the population density of urban territories. They show the density changes of very short distance (from the center to periphery) or into the settlement boundary. This will be useful for the local government during planning and constructing of different types of infrastructure. For example, planning of new kindergartens, school capacity assessment, urban transport construction and others. The effect will multiply – good planning, followed by a developed infrastructure and quality services for inhabitants.

4. REFERENCES

[1] ArcView GIS. Version 9.3. Environmental Systems Research Institute, Inc., Redlands, CA.

[2] ESRI. (2000-2002) *Using ArcGIS™ 3D Analyst*. USA. ESRI

Analysis of the interpolation methods for a geostatistical and spatial modelling of the population density

Penka Kastreva
South –West University, Blagoevgrad, Bulgaria

Abstract: *This paper discusses various techniques for calculating and mapping density population. Density surface of the territory of the Blagoevgrad district is created in two ways. The first is to calculate the density with spread point values over the surface. These points represent settlement positions. The surface is modeled as a raster data set in grid cells and then the values or density is calculated for each cell. In the second way the settlements are used as polygons. They outline the territories that are populated. The conclusions made are based on the comparison of the methods. All interpolation methods for creating density surface with ArcGIS software are used.*

1. INTRODUCTION

Mapping of the density shows the concentration of features per unit area. For example we use density surfaces to represent the distribution of a wildlife population from a set of observations, or the degree of urbanization of an area based on the density of roads. The density mapping is used more often for calculation and mapping population per square kilometers (population / area) in census tracts to calculate density. Mapping density is particularly useful when we compare data in areas of greatly varying sizes. For example, larger census tracts may have more people in total, but smaller census tracts may have higher population density or more people per square kilometers.

We may do density mapping using point or line symbols and area symbols (polygons). Normally when we map densities we create “density surface”. Traditionally for mapping density of point or line features a dot and isoline cartographical techniques are used. Then we must: 1) define the area of mapping; 2) create Z-values that represent the number of features and 3) create a continuous surface (contour map) from the Z-values as we use suitable interpolation methods.

If we map densities by using defined areas, such as census tracts or administrative boundaries (city boundaries, municipality, district or others) normally we use dot and chloropleth mapping. In this way we receive discontinuous surface whose values vary sharply in boundaries. If we use

dot density maps, where a dot represents a specific value, we must determine the number of features for each dot, and a census tract that has a number of definite features (for example people living in it). We have to know that the actual locations of these features are not accurate. This type of map can give us a more detailed visual concept for a density.

Chloropleth map can be created as we divide the total number of features (or the total of their values) by the area of the polygon that contains the features. As a result a density value for each polygon in units of number of people per sq. km is received. The polygons can be shaded according to the number of features contained in each polygon.

The new technologies enable the density to be created as a raster surface. Each cell of the surface receives a density value. In this case like traditional cartography the density values can be created from points or lines. If the features are lines, the density will be in units of length per unit area, for example kilometers per square kilometers.

In the next lines we’ll do a brief review of the techniques for modeling raster density surface. In 1989 Bracken and Martin describe a more sophisticated approach to developing surface representations of demographic data for census enumeration districts in the United Kingdom. Their method is a variant of Inverse Distance Weighted (IDW) interpolation. Population counts are assigned to a set of summary points generated from the centroids of the original areal units. A moving window operation over an ‘‘empty’’ raster grid then assigns to the window kernel a value according to the population values of those centroids contained within the window, with closer centroids having more ‘‘weight’’ than those centroids farther away. The relative density of centroids around the kernel determines the size of the window. This method assumes that population density decreases away from the centroid according to some distance function and allows for some areas of the raster surface to contain zero population.

We can summarize the choice of density modeling: 1). mapping by defined area if the data is already summarized by area; 2). creating a density surface (through TIN or raster creation) if we desire to “see” the concentrations of point (or line) features. As a result we can see that there is a dramatic difference in this example between “census tracts shaded by population” vs “density surface of population”.

2. COMPARATIVE ANALYSIS OF THE METHODS

In order to make the comparison of the basic interpolation methods experiments with one and the same population easier data have been made with different interpolation methods. Let us consider them.

Once Z values are created then they can be used to create a TIN and raster grid. It is known that depending upon that how the points are

distributed - unevenly or evenly it is used respectively TIN and raster models. The TIN and raster grid are modeled via 3D modeling of the population data with ArcGIS functions named “Create TIN from features”, “Point Density” and “Kernel density”. What the GIS do to create a density surface or a raster process is theoretically explained in our preview paper in detail. All rasters are drawn with pixel size 100x100 meters in order to make comparisons. Automated means for modeling the surface with contour lines have been used too.

However the main emphasis will be on that how to create a density surface map from data already summarized by area. This looks to be a useful and not particularly difficult way of creating a density surface map, once the population density field is created into attribute table.

It is better to give the number of the inhabitants who live within the settlement as well as outside of it. This detailed information is needed for precisely cartographical representation. During the last 20 years in Bulgaria some parts of the agricultural and forest lands are assigned for construction aims (for industrial or residential buildings). A small part of them is populated. This means that the territories outside of the settlements have to obtain population distribution from the entire population living into the belonging land of village. It is similar for unpopulated territories within the borders of the settlement with vast areas of parks, industrial areas, and road infrastructure. Generally we can say that the urban territories are more densely populated than the villages’ territories.

The base of this method is dasymetric mapping. The most researches from different authors use land-cover maps produced by satellite images. Working with various land cover classes the key question becomes how to distribute the population among those classes. The basic technique is known as binary classification, wherein all classes are designated as either inhabitable or non- inhabitable. The population is distributed by areal weighting into the inhabitable areas of each enumeration district. This simple method can improve accuracy of traditional choropleth maps. The result is modified choropleth map that presents discontinuous surface. Our idea is to use cadastral map that in detail presents all territories. More details for this method we be given in the next research.

The paragraphs below analyse the used methods:

Choropleth: In the general case for creating choropleth map are used administrative units for mapping as municipality or district and it shows the mean population density in these boundaries. The most densely populated is the Blagoevgrad municipality; the most rarely populated is the Strumiani commune.

Statistical data: Min 16.27 p/km2; Max 125.8 p/km2 ; Mean 49.14 p/km2; Median 35.82 p/km2; Standard deviation – 31.39 p/km2

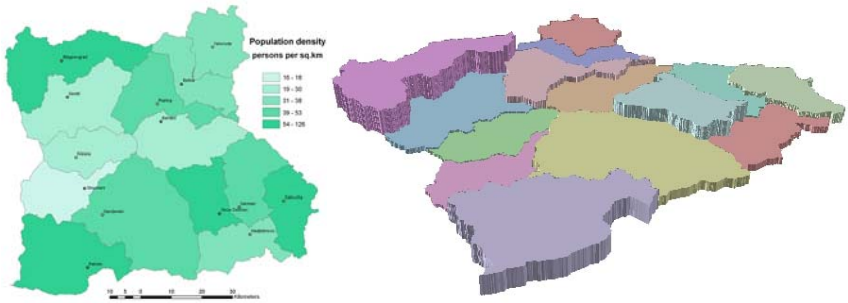

Fig. 1 Choropleth map and 3D model of population data

Modify Choropleth: In this case we use the census tracts namely the settlements except for the unpopulated. In order to outline the borders of the settlement extend the regulation plans are. The approved circular polygons are used for the settlements that do not have such plans. These borders together with advanced modifications (settlement expansions) are drawn on cadastral maps. This method is used to create raster surface model of population and population density and this method ensures more accurate representation of the population into territorial units. In order to obtain continuous raster surface we have to add to the settlement territories all other territories without settlements with population value equal to zero. These data have to be in common map layer. We have to outline again that it is possible to have other population territories with small areas into the belonging land of the settlement as well as there may be unpopulated areas into the settlement. Because such information is missing in our research the unpopulated territories will obtain zero for population values. The aim is to explain the nature of this method that has been implemented due to new technologies.

Statistical data: Min 0 p/km2; Max 7702 p/km2; Mean 1107 p/km2; Median 704 p/km2; Standard deviation – 31.39 p/km2.

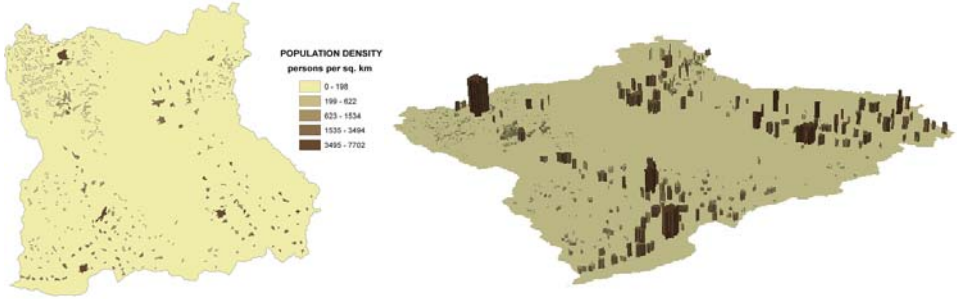

Fig.2.Modified choropleth map and 3D perspective view of population density

TIN method: The TIN model is the basic vector form for presenting a surface with the help of a computer, based on the triangular interpolation

method. A key moment in the modeling of our surface is that the available measured point data are the settlements and they are irregularly distributed on the territory. The connected neighboring points form a network of irregular triangles. Subsequently the TIN model can be converted into a grid surface.

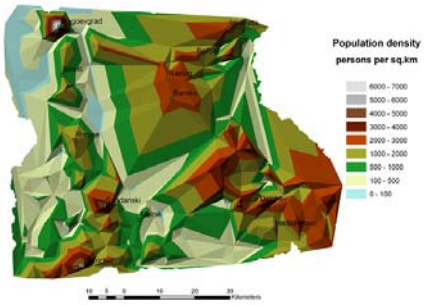

Fig.3. TIN model

Statistical data: Min 0 p/km2; Max 7702 p/km2; Mean 1105 p/km2, Standard deviation –835. 9

Ordinary Kriging: The non-linear spatial interpolation calculates the unknown values using a set of points with known values that are distributed on the whole area of the territory. The distance from a point with an unknown value to a point with a known one helps to define the unknown value. There are some interpolation methods. Four of the most often used methods are weight (Inverse Distance Weighted – IDW), Natural Neighbor, Spline and Kriging. The details for this interpolation method are given in [5].

Statistical data: Min 0 p/km2; Max 7702 p/km2; Mean 1099 p/km2; Median 697 p/km2; Standard deviation –1097.4.

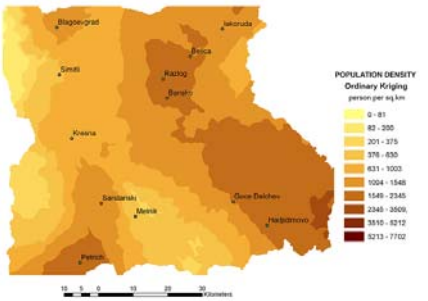

Fig. 4 Grid model: Ordinary Kriging method

Isolines: In order to accomplish comparisons easer isolines, obtained with different methods for density modeling are interpolated. In our example the isolines are obtained from vector point data (the settlements) and grid

surface obtained by Ordinary Kriging method. Both methods use as input data calculated density for every settlement. The isolines in the TIN interpolation are broken lines but as a whole their image is the same as in smooth isolines obtained in Ordinary Kriging method.

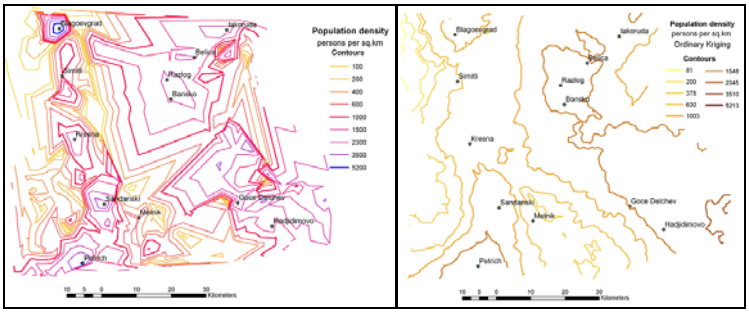

Fig.5. Population density isolines obtained from: 1) TIN model;
2) Ordinary Kriging

Simple and Kernel density: These cartographical techniques represent the exact data distribution. In our research instead of administrative territorial unit municipality or district we use the census tracts namely the settlement. The kernel method gives more detail and smoother surface than the simple method. This depends on the average value that the cell presents.

Statistical data: Simple density: Min 0 p/km2 ; Max 3429.6 p/km2 ; Mean 44.6 p/km2; Standard deviation –218.2

Kernel density: Min 0 p/km2; Max 10073.2 p/km2; Mean 44.7 p/km2; Standard deviation –290.87

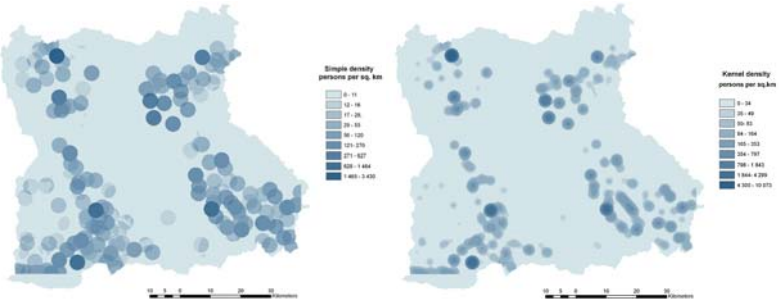

Fig. 6. Density surface: 1) Simple method 2) Kernel method

3. CONCLUSION

As it can be seen there is a rich variety of interpolation methods and the correct choice in their application is especially important. The different methods give different results. It is appropriate the interpolation to be carried out according to two different methods, to analyze the differences.

4. REFERENCES

[1] Demers S. (1989) *Fundamentals of Geographic Information Systems.* (2nd ed.). John Willey&Sons, New York

[2] Longley P., Goodchild M., Maguire D. (2001). *Geographic Information Systems and Science*. John Willey&Sons, New York

[3] Robinson A., J. Morrison, P. Muehrcke, Kimerling A., Gupttile S. (1995). *Elements of cartography* (6th ed.). John Willey&Sons, New York

[4] Slocum T., McMaster R., Kessler F., Howard H. *Thematic Cartography and Geographic Visualization.* 2nd ed. Pearson Prentice Hall. 2005.

[5] Valev G., Kastreva P. Application of the interpolation methods in the modeling of a topographic surface. *International symposium "Modern technologies, education and professional practice in Geodesy and related fields"* Sofia, 5 - 6 November 2009

[6] Valev G., Kastreva P. Analysis of the problems of interpolation in GIS medium. *3rd International conference on cartography and GIS*. 15-20 June, 2010, Nessebar, Bulgaria

Construction wastes – Policy and Management

Stefka Tsekova
South-West University "Neofit Rilski, Blagoevgrad, Bulgaria

***Abstract**: European ecological action programs are regulatory strategic instruments for pursuing policy in the field of sustainable development and environment. Sixth action program 2002 – 2012 of EU has defined four priority fields – climate changes, biodiversity, natural resources and wastes, environment and people's health. Combining categories "natural resources and "wastes" is hardly a coincidence, because the possibility of replacing natural resources for wastes that are valuable scraps is of great importance for the protection and rational use of natural resources. The present report focuses on the management of construction wastes piled in Blagoevgrad Municipality, on the already existing problems and describes the possibilities for their use.*

***Keywords:** construction and building demolition wastes, recycling, use, household wastes landfill, construction wastes landfill*

1. INTRODUCTION

In compliance with Priority Axis 2 – Improvement and development of waste treatment infrastructure of Operational program "Environment" 2007 – 2013, the Ministry of Environment and Waters (MEW) indicates leading priorities as follows: implementation of facilities for use and final disposal of household and construction wastes. While household wastes management on regional principle records a significant progress during the last years (there are 27 regional landfills built), procedures for regulation of environment friendly management of construction and building demolition wastes (CBDW) are being merely now started. MEW is currently developing drafts of National Strategy for CBDW 2010-2020 and Regulation for CBDW Management. At the development of the Strategy there are two stages provided for: Stage 1 – Preliminary research on the current status of construction wastes and building demolition wastes on the territory of the Republic of Bulgaria and assignment of models for building a system for their treatment; Stage 2 – Development of National strategy for CBDW management and Action plan. National aims and priorities are being developed in accordance with the adopted policies, strategic initiatives and good sustainable practices within EC, as well as the engagements undertaken by the country before EU.

2. PURPOSE OF RESEARCH

Analysis of the current condition of construction wastes and building demolition wastes management of Blagoevgrad Municipality and outlining recommendations for reaching a reasonable management with ultimate use.

3. RESEARCH ANALYSIS AND RESULTS

Management and organization order in collection, transportation and landfill of construction and building demolition wastes is specified in the Regulation for waste management on the territory of Blagoevgrad Municipality. As it stipulates, treatment and transportation of earth piles (EP), construction and building demolition wastes (incl. construction wastes from inner reorganizations and current repair of buildings and facilities) shall be made by the owner, investor or contractor of the activity lead to their piling. In cases where CBDW and earth pile treatment and transportation activities are made for sites to which is issued a construction license and a construction line is opened, and/or sites from which total quantity of wastes goes over $1m^3$, physical and juridical bodies shall submit a standard application at Blagoevgrad Municipality and pay a deposit for cleaning and washing of street and sidewalk soiled areas due to the construction and/or demolition of building. Paying the fee due, the body is given tickets for delivered waste from the site as well as a vehicle pass. Tickets shall be given to the depot operator (at depot entrance) for reporting on daily land filled quantity by stamping each course. Amount of washing and cleaning works costs shall be calculated on the basis of actual costs of their execution. At the time the license is issued, the investor shall be given a Precautionary Record, which obliges him to fulfill the requirements of Municipality Regulation, Environment Protection Act (EPA) and Waste Management Act and represents a ground for issuance of a violation ticket if pollution due to the construction or sites demolition has been established. The person, responsible for waste treatment and transportation activities, depot location and its license number shall be filled in the certificate of construction site opening. Obligations for waste treatment and transportation of respective responsible persons shall be in effect until signing a Statement of Ascertainment – Form No. 15, regardless of construction period.

Ninety-two companies carry out construction activity on the territory of Blagoevgrad Municipality, 20 of which have licenses for trucking construction wastes to a depot in Izgrev village. 1670 construction licenses and regularization statements have been issued in the period 2006 – 2009.

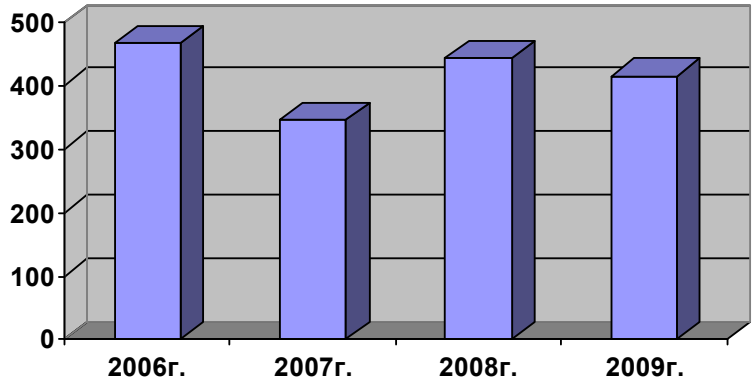

Fig. 1: Construction licenses and regularization statements issued in 2006 - 2009

Most construction licenses and regularization statements we issued in 2006 – 466.

Data from Municipal Administration – Blagoevgrad show that near 70% from wastes piled come from construction companies, 10% from building demolition and near 20% - from construction and building repairs of physical persons. Those 20% include also quantities the Municipality cleans every year because of non-regulated disposal from citizens. Calculations on construct and building demolition waste quantities are based on landfill fee paid at Blagoevgrad Municipality. The existing landfill for inert materials and earth piles of Blagoevgrad Municipality, located on the territory of Izgrev village, are landfilled 7 types of wastes altogether – Table 1 [1] – that fall within group 17 – “Construction and building demolition wastes” of Regulation 3 [2]. This group consists of 44 types of wastes, 16 of which are defined as hazardous. Hazardous wastes generated by Blagoevgrad Municipality and entered for landfilling represent a small part of this flow. They have included the following materials: asbestos, lead pipes, paints, glues, conservative-processed wood, contaminated soil and various materials containing polychlorinated biphenyls. These quantities are relatively small in comparison with the whole quantity of waste flow although special precautionary measures for their management are of great importance to be taken.

Tab. 1: Quantity and type of construction and building demolition wastes (CBDW)

	Waste type	Waste name	Landfilled quantity, t	Piled quantity, t
Waste No. 1	170101	Concrete	5400	8000
Waste No. 2	170102	Bricks	4320	6400
Waste No. 3	170103	Roof-tiles, tiles, faience and ceramic products	2700	4000
Waste No. 4	170107	Mixtures of concrete, bricks and other different from the ones mentioned in 170106	8100	12000
Waste No. 5	170301	Asphalt mixtures	2700	4000
Waste No. 6	170504	Rocks and soil	1080	1600
Waste No. 7	170506	Excavated earth piles	27002	40003

Construction waste quantities disposed at landfill for construction wastes, located on the territory of Blagoevgrad municipality, Izgrev village, and for non-hazardous wastes (household, production and construction) – Buchino village, in the last three years are shown in Fig. 2.

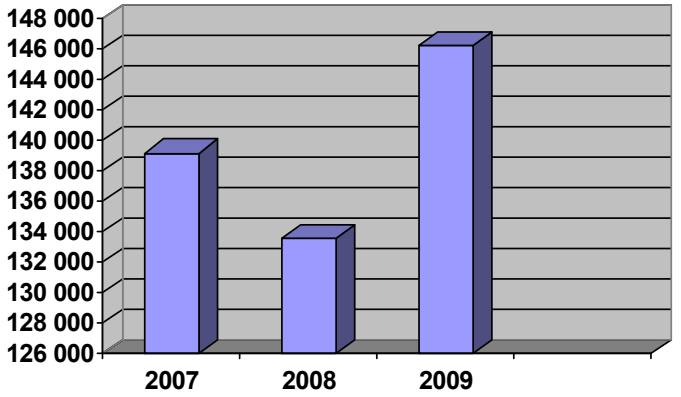

Fig. 2: Generated construction and building demolition wastes in 2007 - 2009

Problems of construction and demolition wastes management:

- insufficient number of employees to control the order stipulated in the Regulation for waste management on the territory of Blagoevgrad Municipality;
- one fee for landfill or recyclable and non-recoverable wastes;

- one fee for companies and physical persons;
- lack of weighing scales to establish the actual quantity of wastes entered for landfill;
- incorrect accounting of construction waste quantities entered together with household wastes at the landfill for hazardous wastes on the territory of Buchino village;
- lack of facility for preliminary treatment of CBDW and their recycling;
- criminal pollutions with construction wastes by citizens in their partial repairs of their homes.

Recycling of construction and building demolition wastes (CBDW) is made predominantly in EU member countries and in USA, Canada, Japan, etc. Significant achievement in CBDW recycling has been made by: Germany, England, France, Italy, Spain, Holland, Belgium, Austria, Portugal, Denmark, Greece, Switzerland, Finland, Ireland, Luxembourg, etc.

Main materials allowing secondary use and/or recycling:

- materials excavated at construction, natural disasters, etc. (soil, gravel, clay, sand, rocks);
- materials from road construction (tar, sand, gravel, bitumen, etc.);
- materials from building construction/demolition (cement, bricks, ceramics, plaster, plastics, wood, metal, glass, cables, etc.);

Fields where construction materials allow re-use with/or without preliminary recycling:

- used as primary substance in the construction of new buildings (for an instance, re-use of bricks, roof-tiles, metal structures, joinery, materials of non-damages insulations);
- road construction or tracing of access roads (for an instance, cement, broken concrete from demolished buildings);
- production of construction materials (brick, roof-tile, wooden structures, insulations);
- grassing and closing of abandoned mines;
- realization of plastic and metal materials;
- utilization of gardens and parks

Considering the upcoming regional development of non-hazardous wastes in Kocherinovo landfill (11 municipalities in Kyustendil and Blagoevgrad region) as well as the great quantities of construction wastes generated by Blagoevgrad Municipality, it is rationally to ultimately use them on the territory of the Municipality, instead of being transported. Pre-investment research is therefore required. As possible grounds for the preliminary sorting, breaking of large-scale construction wastes, recycling through formation of various factions of homogenous waste flows shall be investigated the following:

- Ground planned for transfer station of Blagoevgrad and Simitli Municipality (as of the draft for regional management of hazardous wastes), located in the area of Tserovo village – 9 km away from Blagoevgrad and 13 km away from Simitli. Ground area is 20,545 decares. The property is owned by the Mayor hall of Tserovo village;
- Existing landfill for construction wastes – Izgrev village – after reconstruction and expansion

4. CONCLUSIONS

- Realization of investment intention will prerequisite the creation of conditions for fulfilment of the national and European legislation requirements that will be of help for Blagoevgrad and Simitli Municipalities at the establishment of integrated system of facilities and installations securing environment friendly waste management;
- Putting into operation the regional installation for recycling of construction and building demolition wastes will reduce the volume of received for landfilling wastes, and after putting into operation the Regional landfill in Kocherinovo – it will result in reduce in transported quantities;
- Part of recycled wastes can be realized on the construction market after proving good technical and economic characteristics, and the other part – for technical re-cultivation of broken terrains representing grounds for road construction, etc;
- Development of normative municipal regulation to provide clear rules for interrelation between the issuance of construction licenses and waste separation requirement.

5. REFERENCES

[1] Blagoevgrad Municipality (2005) *Plan for making inert wastes landfill comply with normative requirements*. Blagoevgrad; Country: Bulgaria.
[2] State Gazette 44 (25.05.2004) *Classification of wastes* (Regulation No. 3 of Ministry of Environment and Waters)

UNUSUALLY WARM WEATHER IN LATE AUTUMN OF 2010 IN BULGARIA

Ivan Yotov Drenovski
Faculty of Mathematics and Natural Science
South-West University "Neofit Rilski"
Blagoevgrad, 2700, Bulgaria

Abstract: *Very prolonged period (for about 40 days) of abnormally warm weather was observed in late autumn 2010 in Bulgaria. Mean monthly temperatures in November in all stations in Bulgaria were significantly above the norm. Using meteorological maps and satellite images an analysis of atmospheric circulation is made. Regardless the change of NAO+ with NAO- phase, the advection of air masses in SE Europe retains for all the time predominantly from S-SW to N-NE. Giving in account this quick alternation of NAO index, preservation of almost constant atmospheric circulation pattern in SE Europe for more than a month may be defined as a very occasional event.*

Key words: *Atmospheric circulation, North Atlantic Oscillation (NAO) phases, East Atlantic – Western Russia (EAWR) pattern, Mediterranean (MR) storm track*

INTRODUCTION

In November and first decade of December 2010 in Bulgaria was observed unusually prolonged period of abnormally warm weather. In November 2010 in all meteorological stations in Bulgaria very significant excess of mean monthly temperatures was recorded. Predominantly it is between 4 to 7 ^{0}C, with minimal values in SW Bulgaria, and maximal in NE Bulgaria. At the same time a very low monthly amount of precipitations was measured in the whole country. It varies from 11% to 78% for different stations. As a rule the bigger rainfall sums were recorded in the western part of the country with considerable decrease in the East. Simultaneously in many stations a significant number of days (5 to 10) with strong wind (speed ≥14 m/s) were registered.

All abovementioned is very rare phenomenon for the weather in late autumn in Bulgaria. The explanation of this case is connected with a unique long lasting pattern of atmospheric circulation in Europe and Mediterranean and it periodical variations.

DATA

The official data from Monthly November and December hydro-meteorological bulletin 2010 of National Institute of Meteorology and Hydrology in Bulgaria [8] are used. The analysis of atmospheric circulation is made on the basis of satellite images and meteorological maps from the Wetterzentrale website [9] (for the temperature at 850 hPa level and geopotential height from 500 hPa level).

WARM ADVECTIONS IN BULGARIA

Warm advections in our country may occur in three typical situations [7] – with zone circulation (from West to East), or with two subtypes of meridional circulation (from North or from East). The mean duration of warm advections is about 3,8 days (from 1 to 8 days). Under the terms of circulation conditions the warm current is caused by North Atlantic cyclones, moving from West, or by Mediterranean cyclones, moving by South-West to North-East. In both cases Bulgaria is situated in eastern part of the cyclones and get into its warm sections. Winds blow from South-West or from South.

There were very rare occasions, when extremely warm weather lasted whole month as in February 1966 [4]. The mean monthly temperatures were about 5 to 9 ^{0}C above the norm with average value of 6,7 ^{0}C.

ATMOSPHERIC CIRCULATION IN LATE AUTUMN 2010

Many scholars were pointed that the decisive factor for preservation of uniform atmospheric circulation in Euro-Atlantic sector has NAO index (NAO+, or NAO-) [1, 5, 6].

In the first half of the examined period NAO phase is positive and atmospheric circulation pattern with strong westerlies exists. There is alternation between deep Atlantic depressions, with centers moving far north from Bulgaria and shallow Mediterranean cyclones (Fig.1). As [3] mentioned during the positive NAO phases, the EAWR storm track is intensified and shifted northward, produces increased wind activity over the middle and eastern part of the Mediterranean basin.

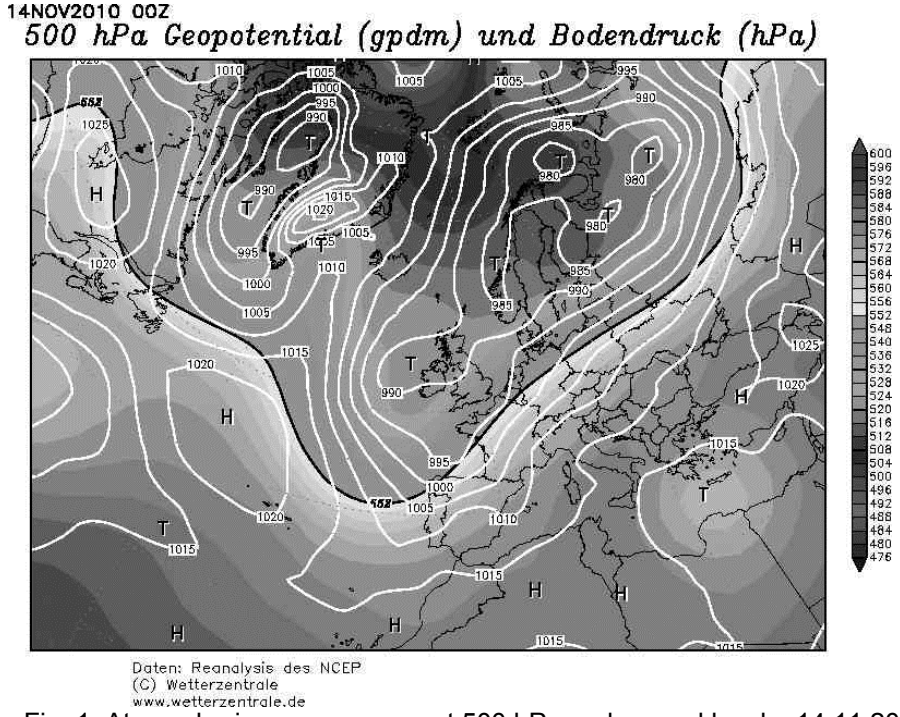

Fig. 1: Atmospheric pressure map at 500 hPa and ground level – 14.11.2010

In the beginning of second part of the examined period a quick change in NAO index is observed from NAO+ to NAO-. During the negative phase of the NAO westerlies weaken, often accompanied with blocking anticyclones occurring over Iceland or Scandinavia, and the Atlantic cyclone tracks move further south (circulation become predominantly meridional) resulting in more cyclonic activity in the MR (Fig.2). This can be explained by strengthen of energy transfer from divergence zone of the North Atlantic and northern Europe to the convergence zone in southern Europe in the NAO- phase [2].

In such cases the duplication of 500 hPa level frontal zone over Europe is observed. The northern one lied from British Isles through Baltic Sea to northern Ural. The southern one is stretched from Azores Islands toward coast of North Africa to Black and Azov Sea.

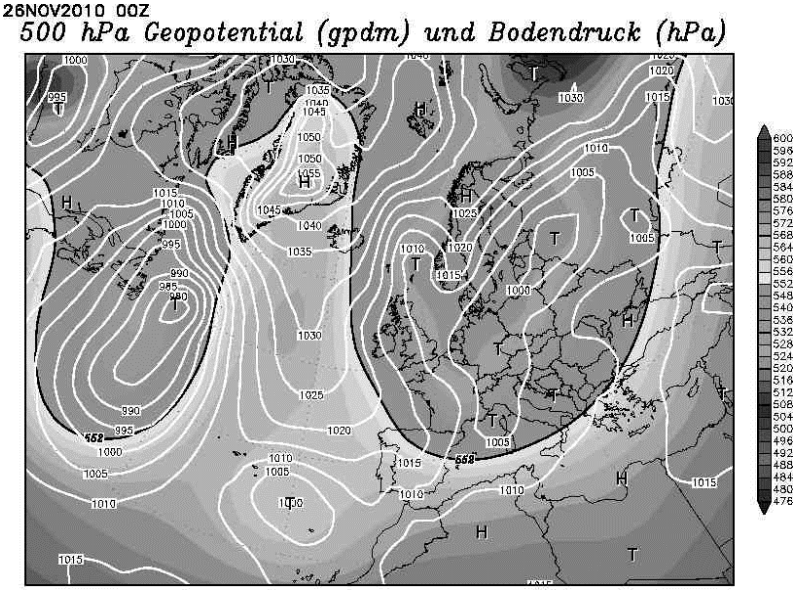

Fig. 2: Atmospheric pressure map at 500 hPa and ground level – 26.11.2010

In the beginning of December inpouring of cold air to South reaches his maximum (Fig.3) and in the north coast of Africa cyclogenesis takes place.

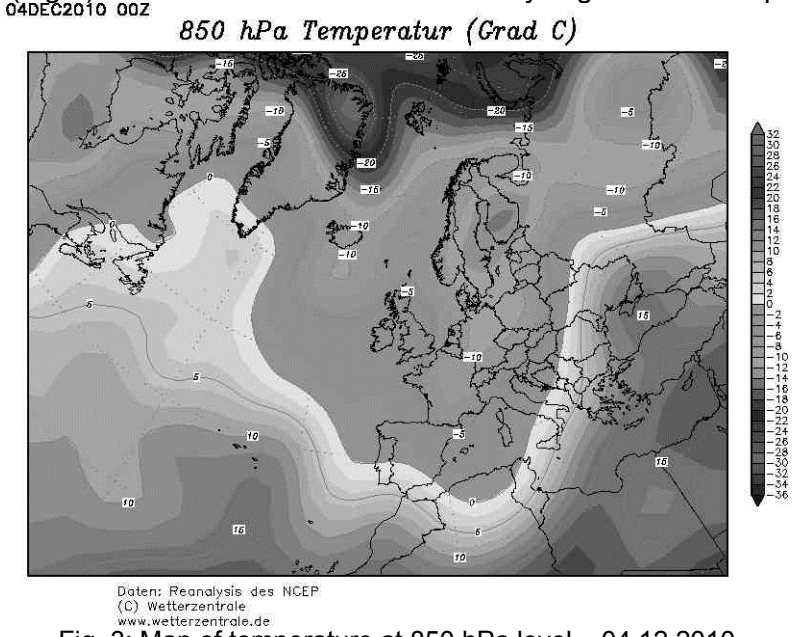

Fig. 3: Map of temperature at 850 hPa level – 04.12.2010

Formed Mediterranean cyclone moves quickly to NE through territory of Bulgaria and causes pelting rains and river floods. In it back crest of high pressure moves warm air from North Africa and in prefrontal zone of new Atlantic cyclone the maximal temperatures in Bulgaria for five days (from 5-th to 9-th December) overcome 20 ^{0}C (Fig.4), marking the end of the period with extremely warm weather.

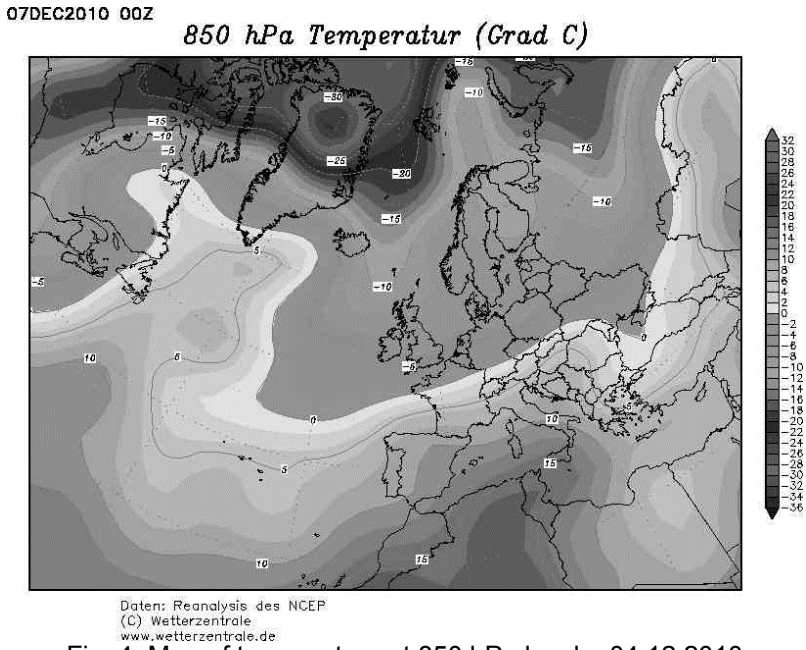

Fig. 4: Map of temperature at 850 hPa level – 04.12.2010

COMMENTS

The observed case is interesting because two main reasons: 1) the period of abnormally high temperatures for the season lasts about 40 days and 2) regardless the change of NAO+ with NAO- phase, the advection of air masses in SE Europe retains for all the time predominantly from S-SW to N-NE. Nevertheless that in the both NAO phases exists a band of energy convergence over the southern Europe, extended from divergence area in the eastern edge of the North Atlantic to the western Caspian Sea [2], preservation of almost constant atmospheric circulation pattern in SE Europe for more than a month is very occasional event.

CONCLUSIONS

In the most research works on NAO, the emphasis is made only on the changes in atmospheric circulation over the North Atlantic and Europe in winter or spring, but not in late autumn. Obviously nevertheless of alternation of two opposite NAO phases within short time, the atmospheric circulation in SE Europe (southerly convergence flow) can remain similar for a sufficiently long period, independently of its untypical character for the season.

REFERENCES

[1] Hurrell, James W., Yochanan Kushnir, Geir Ottersen, and Martin Visbeck (2003) An Overview of the North Atlantic Oscillation in "The North Atlantic Oscillation: Climatic Significance and Environmental Impact", Geophysical Monograph 134 (2003)

[2] Nasr-Esfahany, M., F. Ahmadi-Givi and A. R. Mohebalhojeh (2010) An energetic view to the relation between the Mediterranean storm track and the North Atlantic Oscillation - Q. J. R. Meteorol. Soc. 00: 1.11 (2010), Published online in Wiley InterScience (www.interscience.wiley.com) DOI: 10.1002/qj.000

[3] Nissen, K. M., G. C. Leckebusch, J. G. Pinto, D. Renggli, S. Ulbrich, and U. Ulbrich (2010) Cyclones causing wind storms in the Mediterranean: characteristics, trends and links to large-scale patterns - Nat. Hazards Earth Syst. Sci., 10, 1379–1391, 2010 www.nat-hazards-earth-syst-sci.net/10/1379/2010/ doi:10.5194/nhess-10-1379-2010

[4] Martinov, M. (1966) Extremely warm weather in Febryary 1966 - Hydrology and Meteorology, 3, 1966, p. 55-57 (in Bulgarian)

[5] Martinov, M. (1970) Peculiarities of cyclones moving over Balkan peninsula and Mediterranean region – News of IHM, v. XVIII, 1970, p. 27-70 (in Bulgarian)

[6] Rodwell, M. J., D. P. Rowell & C. K. Folland (1999) Oceanic forcing of the wintertime NorthAtlantic Oscillation and European climate NATURE, VOL 398, MARCH 1999 (www.nature.com)

[7] Stefanov, St., M. Martinov, V. Atanasova (1968) Warm advections in Bulgaria – News of IHM, v. XV, 1968, p. 17-50 (in Bulgarian)

[8] Monthly meteorological bulletins for November and December 2010 - NIMH, Bulgaria

[9] Wetterzentrale website (http://www.wetterzentrale.de)

Unemployment in Blagoevgrad region in terms economic crisis

Emilia Patarchanova
SWU ” Neofit Rilski ”, Blagoevgrad, Bulgaria

Abstract *The material presents the state of unemployment in times of economic crisis in one administrative area. It Analyzes the impact of economic crisis on unemployment in Blagoevgrad region, which traditionally has a very low unemployment rates below the national average. The emphasis is on the dynamics of unemployment in 2009 and several key structures of the registered unemployed are characterized.*

Keywords: *unemployment, economic crisis, labor market*

INTRODUCTION

As in the U.S. and Western Europe and in Bulgaria the manifestation of the economic crisis on the labor market is observed with some delay. The first signs of slowdown in economic growth and negative effects on certain sectors and activities are noted at the end of 2008. Throughout 2009 was marked by the economic crisis. Crisis that hit the positive results in terms of employment and unemployment in the country in recent years. It has changed the labour market and raise serious unemployment in the country. At the end of the year under usually unemployment rises under the influence of factors such as end of seasonal employment in agriculture, tourism, construction and manufacturing, the negative effects of the crisis have superimposed. The negative impact of deteriorating economic situation has begun to feel more and more sensibly. At employment offices have been registered more persons exempt from companies from all areas and industries for reducing the workload and insufficient demand for manufactured goods and services.

MATERIALS AND METHODS

The aim of this paper is to analyze the situation of unemployment in times of economic crisis in the Blagoevgrad region. For us it is interesting to investigate the impact of economic crisis on unemployment in one area which has traditionally been characterized by very low levels of unemployment below the national average. At the same time it is one of the largest in area (third place) and population (V-place) areas in Bulgaria.

It is used statistics provided by the Department of Regional Employment Service "- Blagoevgrad, Department of Labour Offices (LO) and Regional Statistical Office (RSO) - Blagoevgrad.

RESULTS AND DISCUSSIONS

In 2009 in result of the global financial and economic crisis business climate in industry, construction, retail trade and services fell. Growth of consumption and investment was slowing; the rate of foreign trade and markets are lower. These factors influence the increase in unemployment in the area. At LO on its territory in 2009 the registration of unemployed job seekers increased (Fig. 1). Most often they are released after the end of seasonal employment in economic activities (logging, construction, tobacco processing, etc.). Registered persons are exempted as a result of mass layoffs or in connection with reducing the volume of work in some industries (clothing industry, construction, woodworking). During the year, the share of newly registered persons who have worked abroad and returned in the country because of their loss of employment increase has increased.

• Unemployment State

The comparative analysis of unemployment between the two adjacent years clearly shows the increase in 2009 as a result of the economic crisis of 6.7% to 9.3%. i.e. by 2,6 percentage points (Figure 1). In absolute figures these are 15,877 people average number of unemployed persons in 2009 compared with 11 420 people in 2008. There is an increase of 4,457 persons or 39% over the same period last year. Total number of registered unemployed increased throughout 2009 and at the end of December their number reached 18,998 people. Amid the continuing trend of declining population in the area (and country) the problem is even more of a social nature (Table 1).

Territorial analysis of change in the number of unemployed persons showed an increase of this magnitude in all Directorates Labour Office (LO) in the field. Compared to the period of the previous year, the unemployment rate has increased as follows: LOD - Blagoevgrad - an increase of 2.25 points, LOD - Razlog 6.57 points, LOD 1.21 points, Petrich, Sandanski 2.05 LOD-point LOD - Gotse Delchev 1.65 points. For Blagoevgrad region with the highest unemployment rates remain Belitsa municipalities (38%) and Yakoruda (32.9%) [1].

Tab. 1 General characteristics of unemployment in Blagoevgrad region

Blagoevgrad region	***The year of 2009***	*The year of 2008*	*change (+ or -)*
Unemployment rate (%)	***9.3***	*6.7*	***+ 2.6***
Registered unemployment (average annual)	***15 877***	*11 420*	***+ 4 457***
Long-term unemployed (%)	***26.2***	*41.0*	***- 14.8***
Unemployed women (%)	***54.5***	*59.5*	***-5.0***
Unemployed youths under 29 years of age (%)	***17.8***	*16.7*	***+ 1.5***

Among the newly registered unemployed for more than half have worked in the private sector. The largest share are of newly registered unemployed in activities of the service sector - 41.6%, next is the industry sector - 38.4% and after them - Agricultural sector 3.6%.

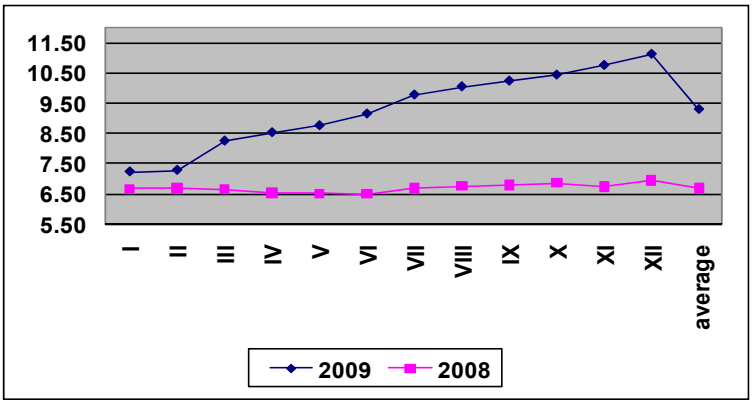

Fig.1 Dynamics of registered unemployed in Blagoevgrad region

Long-term unemployed persons (staying in the LOD over one year) in 2009 were 26.2 percent of the total unemployed. Compared with same period of 2008 we count greater reduction (41%), amounting to 14.8 points (Table 1). However, the proportion of group long-term unemployed to all registered jobseekers in persons remains high. Lack of training and education is a major obstacle for these individuals to find permanent employment. Against the background of the limited number of vacancies and the additional negative effects of economic crisis on employment and unemployment it has made substantial progress in this group.

• Structure of unemployed by age

The age structure of registered unemployed persons is characterized by relative uniformity of the distribution of values of different groups, and during the period the trend of previous years. The largest is the group of registered unemployed aged over 55 years - 3554 annual average (22.4%)

should the group of persons from 50 to 54 years - 2421 annual average (15.2%) and the group of persons aged 45 to 49 years - 2129 annual average (13.4%). In the age structure of the unemployed it is reflected directly observed tendency for an aging of population during the past two decades in which age group over 45 years remains as the most numerous of the labor market (Table 2).

Average number of people over the age of 50 is 5975 or 37.6 percent of all unemployed. In previous years it was shown an increase of registered unemployed in the group of people over 50 years by about 1500 people on average, or about 10%.

Government policy implemented through the regional structures of the LOD is directed mainly to support the return of the labor market of the disadvantaged, namely the young people at age of under 29 and people over 50 years – the first group begins and the other ends their employment activity.

Reducing youth unemployment is among the main strategic priorities of employment policy at home. In recent years there is a trend of greater demand for youths under 29 years of labor market compared to other age groups. One of the important factors for the employment of young people is that they have good language skills demanded by employers who have said jobs. This gives them more chances to realize on the labor market. The share to all registered unemployed was 17.8% and compared to the period of 2008 we register an increase by 1.5 percentage points (Table 1).

Tab. 2 Structure of registered persons by age in Blagoevgrad

Age groups	Absolute value ality (average annual)	Ratio (%)
under the age of 19	230	1.45
from age of 20 to 24	1 098	6.9
from age of 25 to 29	1 503	9.5
from age of 30 to 34	1 571	9.9
from age of 35 to 39	1 604	10.1
from age of 40 to 44	1 767	11.1
from age of **45 to 49**	**2 129**	**13.4**
from age of **50 to 54**	**2 421**	**15.2**
over the age of 55	**3 554**	**22.4**
TOTAL	**15 877**	**100%**

• Structure of unemployed by sex

Still in 2009 the steady trend observed for years continues, the number and proportion of women in the sex structure of the unemployed to be predominant. Registered unemployed women in Blagoevgrad region are 54.5% of the entire group of unemployed. With regard to the same period of

the previous year the unemployment by sex declined by 5 percentage points, which is positive given the appearance that overall unemployment increased in 2009. compared to 2008. (Table1). It should hot however be ignored that issue indicator of female unemployment was 54.5 percent higher by about 10 points of the value of the indicator for unemployed men 45.5%.

Direct and substantial impact on the number of unemployed people of both sexes have an age, qualifications and education, profession, specialty and more.

• Structure of unemployed by occupation

The trend typical for the previous years remains and during the analized period – 2009, namely the share of the group of individuals without specialty (54%) is the largest; followed by the group of individuals with working occupations (25. 2%) and the smallest remains the share of individuals with specialty (20.8%) (Table 3). Therefore, obtaining higher education, the acquisition of additional qualifications and skills is the surest way to secure employment during the working life of each person. On the other hand we should consider the fact that it is "desired" structure of the unemployed rather than the reverse i.e. to dominate those with specialties that have already invested in the acquisition of the profession. It will be very strong indicator of the gap between business in general on the one hand and educational institutions on the other, and between relevant government institutions and coordination among them. Unemployed people who have no profession could (depending on their age) to obtain such consistent with offering of employment of the regional labor market. This would be the multiplier effect - solving the unemployment problem as a person and reduce the unemployment rate in the studing area.

Table 3 Structure of registered unemployed people according to their professional qualification

Indicators	**2009г. (%)**	2008г. (%)
with working professions	**25,2%**	22.4%
specialists	**20,8%**	19.9%
without specialty	**54,0%**	57.7%
Registered-total	**100%**	100%

In 2009, the average number of registered persons with working occupation on the territory of Blagoevgrad region increased comparing to 2008. Share of this group was 25.2%, to all registered in labor offices.

Compared to the same period last year Blagoevgrad was up 2.8 points. Stagnation in the economy led to a reduction of production and release of staff from construction, carpentry and tailoring businesses as a result of this during the year in the Labour offices an increase in the number of registered persons with working occupation is observed.

Registered professionals in 2009 were 20.8%. The share of total registered professionals compared to the same period of last year also marked increase in the value of the index by 0,9 percentage points (Table 3).

• Structure of unemployed by educational sign

The educational structure of registered unemployed in Blagoevgrad region is characterized by the highest proportion of those with primary or lower education. In total number of registered their share was 44.8% (Table 4). The trend of decreasing of their share the previous year is positive. However it is due to the increase in the share of other groups compared to 2008. This is evidenced by the higher absolute value of the unemployed in the same educational degree. The reason for their large number is in the limited capacity of that group of unemployed people to find work and namely that is due to poor education and lack of qualifications.

The educational structure of unemployment in the area is relatively unchanged compared to previous periods.

Tab. 4 Educational structure of registered unemployed persons in Blagoevgrad (%)

Indicators	**2009г.**	2008г.
Higher education	**8.9%**	8.9%
secondary special and vocational education	**37.8%**	35.0%
with general secondary education	**8.5%**	8.1%
with primary or lower education	**44.8%**	48.0%
egistered-total	**100,0%**	100,0%

Registered persons with higher education during the period have almost the lowest share of 8.9% and it remains unchanged by the actions of the economic crisis. It can be assumed that these are people with long-term unemployment due to the one part of their advanced age and to the other part of their specific occupations for which there is no demand in the labor market in the area.

Most affected by the effects of economic crisis are those with secondary special and vocational education. By them we observe the largest increase in absolute and relative value of the unemployed during the analyzed period compared to the previous year (Table 4). It is Not only the

second largest group (37.8%), but these are people with relatively high educational level, which is very disappointing.

• Demand for labor

When comparing data on the labor market in the region with those for 2008, the following conclusions are drawn:

» Trend of priority demand of unskilled labor in labor offices is maintained;

» At the end of the studied period, it is observed even an increase in the proportion of seats for the unemployed without qualifications and with low education to all advertised vacancies;

» Also appear a trend of decrease of jobs advertised for working occupations and the number of seats for specialists.

In the group of announced vacancies for professionals traditionally has a large share of seats for people with technical degrees about 30%, followed by those in the service sector 27% -28% and education 12%. In Blagoevgrad for the researched period vacancies are 6442. Of these, 5320 were on the primary labor market and 112 are in employment programs. New jobs for 2009 are 1237.

The pressure on the labor market (number of unemployed per vacancy) in Blagoevgrad region in 2009 is 15 in the indicator value 9 for the previous year.

There are significant differences between municipalities within the area in terms of economic development. These differences have a very strong influence on local labor markets. It should also not be ignored the influence of factors such as the traditions of the population in employment, specific sectoral structure of local economies, and seasonality, which determines the demand for labor in the primary market.

CONCLUSIONS

Economic crisis affects the labor market and unemployment in the Blagoevgrad region. The number of registered unemployed increased throughout 2009 not only in general, but in all LOD working within its the level of unemployment continues to be the highest in the municipialities of Belitsa and Yakoruda. The newly registered unemployed people who were exempted from the private and public sector are almost equal. The distribution of newly registered unemployed persons by sector shows almost equal shares of the service sector and industry.

Compared to the previous year unemployment in the group of persons over age 50 increased by about 10%. Unemployment among women increased, too.

In the professional structure of the unemployed the trend, characterized for the previous years remains the largest is the proportion of people without qualification and with the lowest degree.

As positive trends occurring throughout the period in the region we can point the reduction of unemployment among young people under age of 29 years and preservation i.e. not increasing of unemployment among people with higher education.

Announced vacancies on the primary labor market and employment measures for the period were 36 less than the same period of 2008. And in 2009 the trend of reduction of stated in the Labour offices seats for non-subsidized employment continues. The dominant influence of seasonal factors on the primary labor market [1].

REFERENCES

[1] Status and development of regional labor market in the Blagoevgrad region. Directorate for Regional Employment Service, Blagoevgrad.

[2] Statistical handbook 2008, Regional Statistical Office, Blagoevgrad.

[3] Statistical handbook 2009, Regional Statistical Office, Blagoevgrad.

Fuzzy logic application for assessment of the environmental risk in SW Bulgaria

Plamena Zlateva[1], Lyubka Pashova[2]
[1]*Institute of System Engineering and Robotics - BAS, Sofia, Bulgaria*
[2]*National Institute for Geophysics, Geodesy and Geography - BAS, Sofia, Bulgaria*

***Abstract**: Assessing the environmental risk can be considered as a fundamental factor for the responsible management and the sustainable regional development of southwestern Bulgaria. The paper presents a fuzzy logic approach for complex estimation of the environmental risk, based on the available information sources and the expert knowledge. The risk assessment problem is defined as a multicriterial task that evaluates several input variables (indicators). A hierarchical system is developed, which generates a complex estimation of the environmental risk. The system is designed in the MATLAB environment using Fuzzy Logic Toolbox and Simulink. The simulation investigations are done.*

***Keywords:** Fuzzy logic, risk assessment, environmental risk, natural hazards, sustainable development, SW Bulgaria*

1. INTRODUCTION

In the last two decades significant global, regional, and local indications of the increasing vulnerability and the changes of environmental conditions have occurred worldwide. Many efforts are underway for the improving environmental risk assessment, the forecasting, the natural disaster preparedness and the risk management to mitigate the negative environmental, social and economic effects.

Bulgaria is exposed to a variety of natural hazards and as a result, the public awareness of this exposure is increasing [5]. Southwestern (SW) Bulgaria is the region with the most expressed tectonic and seismotectonic activity on the whole territory of the country [1, 2, 6]. Besides with the seismic activity, which is concentrated in the Krupnik-Kresna and Mesta river areas, the combination of many endogenous and exogenous factors (recent vertical crustal movements, erosion, surface and ground water level fluctuations) provoke the activation of gravitational processes like landslides, creep, mud-rock flows, and etc. The greater part of the landslide

phenomena occur in the basic landslide regions - the Simitli graben and the landslides along some of the faults in the Strouma zone.

The particular information and the expert knowledge for the natural hazards mentioned above are available in the form of the thematic maps (for example: seismic hazard, geological hazard, gravitational processes), the quantity statistical data and the quality expert evaluations.

There are many qualitative and quantitative methods for the risk assessment. However, it is necessary to point out, that the environmental risk assessment is done under the subjective and uncertain conditions. For this reason, it is required to use the intelligent assessment methods. An intelligent method to assess the risk using the fuzzy logic theory is proposed. This approach provides adequate processing the subjective qualitative and uncertain quantitative data [8].

In this paper a fuzzy logic approach for a complex estimation of the environmental risk, based on the available information and the expert knowledge is applied. The environmental risk for the SW Bulgaria region is assessed only for the seismic and geological hazards taking into account the population density. The simulation results using Matlab environment for three local areas (Dupnitsa, Blagoevgrad, and Sandanski) are presented.

2. SW BULGARIA REGION AND DATA SETS

The territory of Bulgaria is highly vulnerable to a variety of the natural hazards and the climate change. The southwestern region is exposed to the potential damages due to the high seismic risk hazard. The present-day weak seismicity, as monitored by the National Operational Telemetric System for Seismic Information network indicates the formation of two seismic zones with obvious differentiation as one of them is a large active polygon spread over the southwestern one-third of Bulgaria [2, 6, 7].

Over the last century several big and destructive landslides have been observed with different degree of the landslide hazard, as part of them are happened in SW Bulgaria. In this region the manifestation of active landslides and mud-rock falls can be closely connected with the contemporary tectonic activity, the erosion and the rainfalls [1, 3].

The actual to 01.02.2011 data from the NSI express census conducted in early 2011 are used for the three local regions in the Blagoevgrad and Kyustendil districts [4].

3. FUZZY LOGIC SYSTEM FOR ENVIRONMENTAL RISK ASSESSMENT

An approach based on the fuzzy logic expert system for decision making is applied for the environmental risk assessment [9]. The used fuzzy

system has a hierarchical structure with several inputs and one output. The number of inputs corresponds to the linguistic variables, which described the natural hazards and the regional vulnerability. The output represents a quantitative complex assessment of the environmental risk.

Here, four indicators for the environmental risk assessment for the SW Bulgaria region are defined using the published thematic maps for the seismic hazard, gravitational and geological risks, as well as the population density data [1, 3, 4, 6]. The input indicators of the fuzzy logic system are as follow: 1. Landslides (landslips, creep, falls, flows); 2. Mud-rock flows; 3. Seismic hazard; 4. Population density.

A fuzzy logic system with two hierarchical levels and the defined four inputs is proposed. The first level includes two fuzzy logic subsystems each of them with two inputs. The fuzzy subsystem output of the second level gives the complex risk assessment. A scheme of the two-level hierarchical fuzzy logic system is presented on Fig. 1.

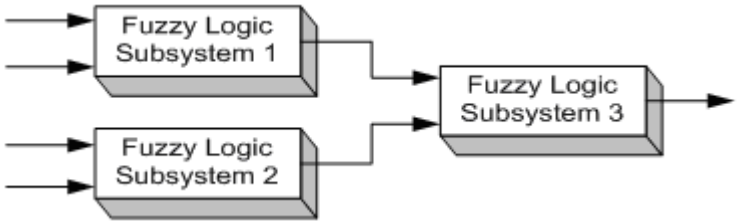

Fig. 1: Two-level hierarchical fuzzy logic system

The inputs of the first fuzzy logic subsystem are: 1) “Landslides”; 2) “Mud-rock flows”. The linguistic variable - the output from this level - is defined as “Gravitational processes risk”.

The inputs of the second fuzzy logic subsystem are: 1) “Seismic hazard”; 2) “Population density”. The linguistic variable - the output from this level - is defined as “Seismic risk”.

The two output variables “Gravitational processes risk” and “Seismic risk” represent the inputs for the third fuzzy logic subsystem. The output of this subsystem gives the complex environmental risk assessment relevant to the defined input indicators. The output value is a criterion for final decision making about the degree of environmental risk for the studied region. The higher value corresponds to the higher risk degree.

4. DESIGN OF FUZZY LOGIC SYSTEM

Different criteria exist for each type of the natural hazards, which are used to define the levels of the hazard characteristics. Inherently qualitative

features of these characteristics are rather than quantitative values, which are usually represented by linguistic variables.

Here, all the input linguistic variables (four indicators and two intermediate) are represented by three fuzzy membership functions: “Low“, “Middle”, and “High”. The input variables are assessed in the interval [0, 10] using trapezoid membership functions as it is shown on Fig. 2a.

The fuzzy logic system output (complex risk assessment) is described by five fuzzy membership functions: “Very low”, “Low”, “Middle”, “High”, and “Very high”. The complex environmental risk is assessed in the interval [0, 100] using triangular membership functions as it is shown in Fig. 2b.

a) trapezoid membership functions for inputs

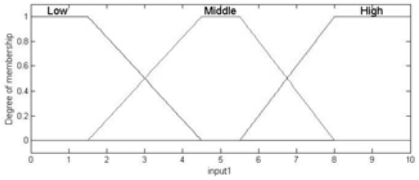

b) triangular membership functions for output

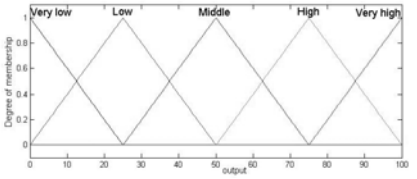

Fig. 2. Membership functions of the input indicators (a) and the output (b)

The inference rules in the fuzzy logic system are defined through “IF - THEN”-clause. In three fuzzy logic subsystems the rule numbers of the knowledge base are 9. Some of the inference rules are defined as follow:

IF “Landslides” is “High” and “Mud-rock” is “Low” THEN “Gravitational processes risk” is “Middle”;

IF “Seismic hazard” is “Middle ” and “Population density” is “Low” THEN “Seismic risk” is “Low”;

IF “Seismic hazard” is “High” and “Population density” is “Low” THEN “Seismic risk” is “Low”;

IF “Gravitational processes risk” is “Low” and “Seismic risk” is “Low” THEN “Complex environmental risk” is “Very low”;

IF “Gravitational processes risk” is “Middle” and “Seismic risk” is “High” THEN “Complex environmental risk” is “High”;

IF “Gravitational processes risk” is “High” and “Seismic risk” is “High” THEN “Complex environmental risk” is “Very high”.

The fuzzy logic hierarchical system is design in Matlab environment using Fuzzy Logic Toolbox. The three fuzzy subsystems are built in the Mamdani type fuzzy inference system. The inference surfaces in 3D for the three fuzzy logic subsystems are given on Fig. 3 and Fig. 4.

a) Surface of input 1-“Landslides” and input 2-“Mud-rock” and output – “Gravitational processes risk”

b) Surface of input 1-“ Seismic hazard” and input 2-“Population density” and output – “Seismic risk”

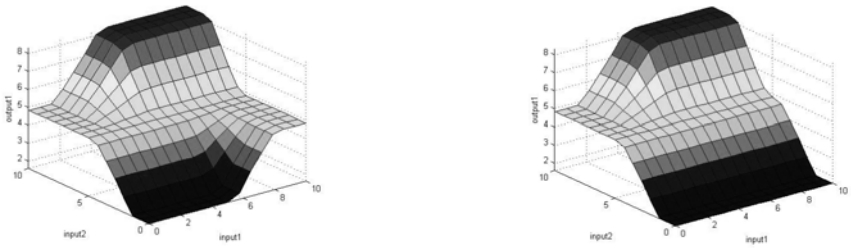

Fig. 3. Surface of the fuzzy logic subsystem 1a) and subsystem 2b)

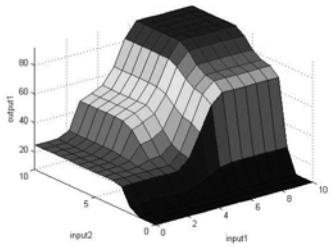

Fig. 4. Surface of input 1-“ Gravitational processes risk” and input 2-“ Seismic risk” and output – “Complex risk assessment”

5. FUZZY LOGIC SYSTEM APPLICATION

The designed fuzzy logic system is used to assess the environmental risk of three areas in the SW Bulgaria region. These areas - Dupnitsa, Blagoevgrad and Sandanski - are exposed to the several types of the natural hazards. They have different density of the population. In this region of the country many tourist destinations are located, like Bansko, Dobriniste, Rupite, Melnik, and etc. Input data indicators for the three local areas and the obtained simulation results are presented in Table 1.

The obtained simulation results for the three local areas in SW Bulgaria show that the Dupnitsa area has the highest value of the complex environmental risk according to the defined input indicators. For the Blagoevgrad and Sandanski areas the risk assessments are comparatively equal, but the first region has a little higher risk value. Therefore, the Dupnitsa area is more vulnerable to the studied natural hazards. For this reason, the stakeholders have to take the relevant management decisions to mitigate the potential dangerous consequences by priority for this local area.

Tab. 1: Input data and simulation results

Criterion	Dupnitsa area	Blagoevgrad area	Sandanski area
Input 1	8	6	8
Input 2	9	5	4
Input 3	8	9	7
Input 4	6	7	6
Evaluation	85	61	56

6. CONCLUSIONS

An approach based on the fuzzy logic for complex evaluation of the environmental risk of three local areas in the SW Bulgaria is proposed. A hierarchical fuzzy logic system which has two levels and comprises three fuzzy subsystems is developed. Four indicators that are interpreted as input linguistic variables are chosen. The system output gives the complex environmental risk assessment. This assessment can support the stakeholders to take more informed decisions for the sustainable regional development of SW Bulgaria.

7. REFERENCES

[1] Bruchev, I., Dobrev, N., Frangov, G., Ivanov, Pl., Varbanov, R., Berov, B., Nankin, R., Krastanov, M. (2007) The landslides in Bulgaria - factors and distribution, *Geologica Balcanica* 36 (3-4), 3-12.

[2] Georgiev, I., Dimitrov, D., Belijashki, T., Pashova, L., Shanov, S, Nikolov, G. (2007) Geodetic constraints on kinematics of southwestern Bulgaria from GPS and levelling, *Geological Society*, London, 291, 143-157.

[3] Jelínek, R., Hervás, J., Wood, M. (2007) *Risk Mapping of Landslides in New Member States*, Luxembourg, EC, JRC41245.

[4] NSI - Bulgaria (2011) Express results from Bulgarian population and housing census 2011, http://www.nsi.bg.

[5] Pashova, L., Zlateva, P. Kouteva-Guentcheva, M. (2010) An approach to comprehensive information systematization for complex risk analysis of the natural hazards. *6th Int. conf. "Global change"*, 16-17 April, 2010, Sofia.

[6] Solakov, D., Simeonova, S., hristoskov, L., Asparuhova, I., Trifonova, P., Dimitrova, L. (2009) Seismic zoning of the Republic of Bulgaria, Final report, Contract-170-1, http://www.mrrb.government.bg.

[7] Tzenov, L., Botev, E. (2009) On the earthquake hazard and the management of seismic risk in Bulgaria, *Information&Security* 24, 39-50.

[8] Pokorádi, L. (2009) Risk assessment based upon fuzzy set theory. *15th Int. Conf. "Build. Serv., Mec."*, 15-16 October, 2009, Debrecen, Hungary, 311-318.

[9] Zlateva, P., Kirov, G., Stoyanov, K. (2005) Fuzzy logic application for eco-tourism potential assessment of villages, Automatics&Informatics, 4, 20-23.

The maintenance and protection of soil resources natural balance in Yakoruda municipality

Boyko Kolev
SWU “N. Rilski”, Blagoevgrad, Bulgaria

Abstract: *For potential yield realization from different agricultural crops it is necessary to determine crops species, climatic and soil conditions, as well as to manage soil cultivations and soil water use efficiency. Modern agricultural ecosystems approach the moment when the cost and the resulting production will be equal. Therefore, the most important aim is reducing the energetic investments in agricultural ecosystems i.e. to reduce the expenses. The simulation procedure for soil hydro-physical properties (soil moisture at field capacity, wilting point, effective soil water content) determination was realized by using soil particle size distribution data only. This was realized for the first time for the Bulgarian soils by [2], with developed in his Ph.D. thesis simulation model model. The determination of soil hydro-physical properties is important for soil resources and fertility protection.*

The aim of the study is protection and maintenance of soil resources (agricultural land and forests) and ecological balance in the Municipality Yakoruda.

Keywords: *environment conditions, soil moisture at field capacity, wilting point, effective soil water content, particle size distribution.*

1. INTRODUCTION

Changed as a result of natural human activity (primary) biotsenozi have become secondary in (urban, agricultural lands, plantations) i.e. in anthropogenic biotsenozi. All these biotsenozi featuring the green surface on which develop the so-called biotope formed agricultural ecosystems. According to Odum agricultural ecosystems are semi home systems, i.e. mediate between the natural and urban ecosystems. The main energetic inputs in one agricultural ecosystem found to be divided among the

following groups of costs: investment for machinery and buildings - 14% for seed investments - 6% for manual labour input - 1%, pesticides - 14% potassium fertilizers - 2 %, phosphorus fertilizers - 4% nitrogen fertilizers - 43% fuel - 29%.

Modern agricultural ecosystems approach the moment when the cost and the resulting production will be equal. Therefore, the most important aim is reducing the energetic investments in agroecosystems i.e. to reduce the expenses.

Major structural elements of each agricultural ecosystem are:

- sown or planted by human crop. This is the central element of any phytocenoses including autotrophic photosynthetic plants. This element is largely determined types and numbers of staff heterotrophic agrocenoses organisms;
- weeds;
- microorganisms from rizosphere (the area around the root system) of agricultural plants;
- bacteria in tuberous roots of legumes;
- micro-algae, fungi, bacteria, free living in soil and take part in the cycle of substances and soil formation process;
- microorganisms harboured by higher crop and causing pathological processes;
- vertebrates and invertebrates living in crops of cultivated plants.

They can cause significant damage, but among them there are useful species such as insect pollinators.

The aim of this study is protection and maintenance of soil resources (agricultural land and forests) and ecological balance in the Municipality Yakoruda.

2. OBJECT AND METHODS

2.1. Geographical characteristics

Yakoruda Municipality [4] is located in the north-eastern part of Blagoevgrad an area of 339.3 sq. km. It borders the municipalities of Samokov and Kostenets at Sofia and Velingrad, Belitsa and Belovo from Pazardzhik district. The municipality is composed of eight villages - the municipal centre of Yakoruda seven villages which are located in the south-eastern part of the municipality., single line spacing, 24 pt spacing before and 6 pt spacing after the capital letters.

Relief - Fig. 1 is mountainous and hilly, covered parts of the Rila and the Rhodope Mountains and narrow valley in the upper course of Mesta. The average altitude is 1603 m and average slope is 11.1%, which adversely

affect general economic and infrastructural development of the municipality and the development of the urban network.

The climate is temperate continental with very low Mediterranean influence, penetrating the valley of the Mesta River, the average annual temperature is 8^0C. Winters are cold, with average January temperature is - 2^0C - snow 150 days a year. Summer is short and cool with average temperatures in July 18^0C.

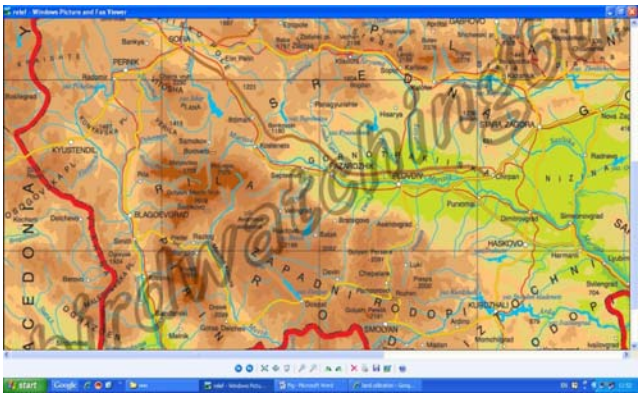

Fig. 1: General form of relief.

2.2. Soil Resources

Soil resources are presented in Fig. 2.

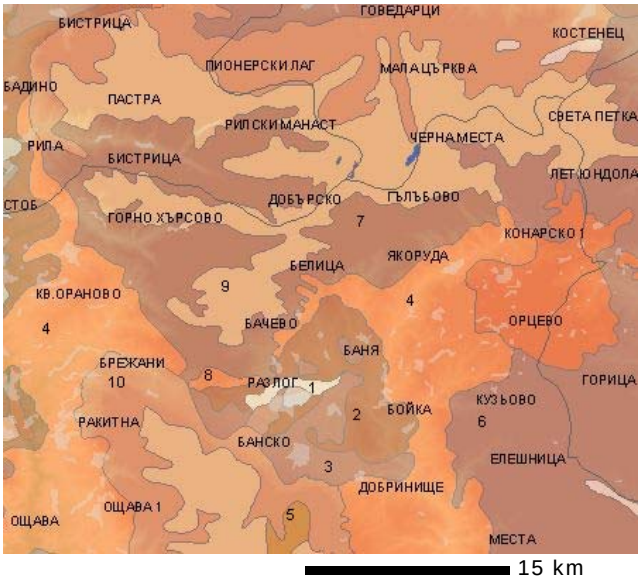

Fig. 2: Soil Map of the object [3].

Legend:

1. Alluvial and Alluvial-Meadow, sandy and loamy soils.
2. Leached cinnamonic forest, eroded;
3. Delluvial and delluvial-meadow sandy and loamy soils.
4. Leached cinnamonic forest soils.Плитки излужени канелени горски;
5. Mountain-meadow soils and rendzinas.
6. Brown forest soils.
7. Brown forest soils, mostly acidly.
8. Leached cinnamonic forest, heavy loamy to slightly clayey soils.
9. Mountain-meadow and alfehumus soils.
10. Dark brown and dark colored forest soils.

The way of sustainable use of soil resources in Bulgaria is presented in Fig. 3, their agro-ecological regions - in Fig. 4 and agro-ecological regions in which the municipality is included - in Fig. 5.

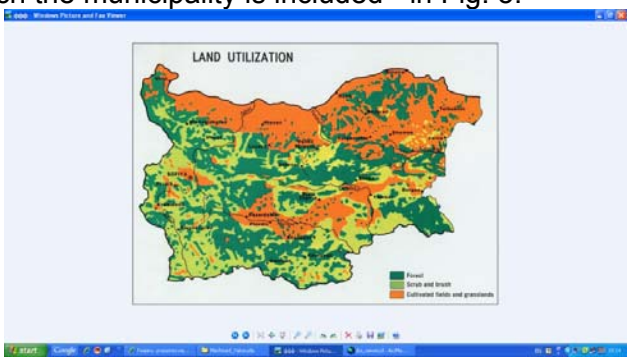

Fig. 3: The way of sustainable use of soil resources

Fig. 4: Agro-ecological regions in Bulgaria [1].

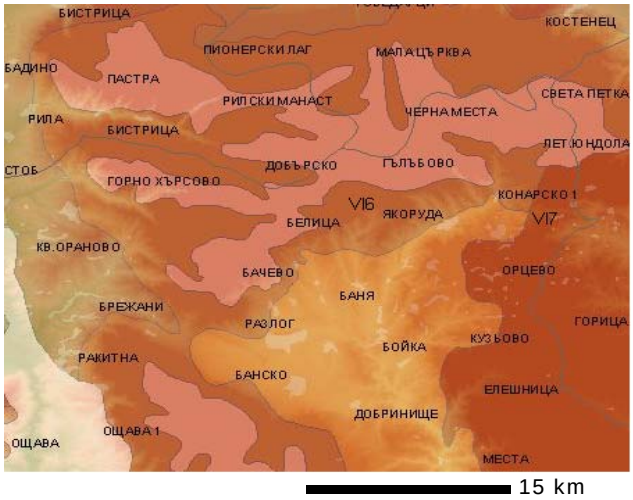

Fig. 5: Agro-ecological regions map for Yakoruda municipality [3].

Legend:
(VI6) Rila-Pirin mountains region;
(VI7) Rodopi mountains region.

2.3. Methods

The survey instruments used ArcGIS 9.3 - ArcMap for objects.

The general view of the object by of ArcGIS 9.3 - ArcMap using is presented in Fig. 6.

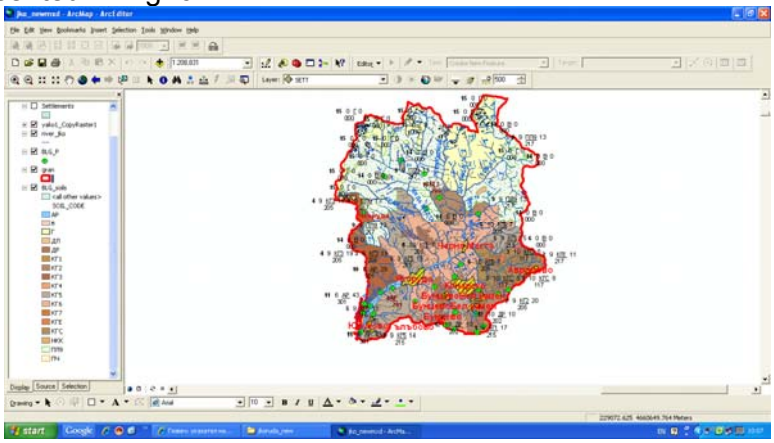

Fig. 6: General view of the object.

Brown forest soils predominate (1-7 KG) - Fig. 6 and found more brown, shallow, middle eroding (KGE) and brown, shallow, high eroded (KGC). They are the most widespread soils in mountain areas and represent 1.7

million ha or 15%. These soils are rich in humus, but the average stock to absorb nitrogen and phosphorus. They need a combination of fertilization. In the high mountains brown forest soils pass into dark colored forest and mountain-meadow soils.

In river beds are found alluvial (AP - alluvial, medium strong) and on the slopes - delluvial (SF - (delluvial, slightly strong) and delluvial (RD - deluvial, medium strong) soils. In the high parts of the municipality the mountain-meadow, shallow, weak and middle eroded soils (PL9) dominated. Cinnamonic soils - Fig. 6 are represented by cinnamonic and immature, shallow, highly eroded and rocks (NCC). Rocks (D), sand and gravel (PM) and gorges and gullies (B) complete the soil resources of the municipality.

3. RESULTS AND DISCUSSIONS

Category of land in the municipality ranges from VI-th to X-th. This does not mean that the lands are not fertile. In Rila-Pirin agro-ecological region (AER) environmental conditions are suitable for potatoes and wheat bonitet 71 and 60 ball and in the Rhodope agro-ecological region (AER) environmental conditions are suitable, respectively, potatoes, pastures and meadows, raspberries, which bonitet score is higher.

According to agroecological assessment of the municipality soil resources can be concluded that although the acquisition of contemporary and modern look of Yakoruda effects on the environment are negligible.

4. CONCLUSIONS

Made by agro ecological assessment of soil resources can be concluded that although the acquisition of contemporary and modern look of the municipality Yakoruda effects on the environment are negligible. Category of land in the municipality ranges from VI-th to X-th. This does not mean that the lands are not fertile. In Rila-Pirin AER environmental conditions are suitable for potatoes and wheat bonitet 71 and 60 ball and in the Rhodope AER environmental conditions are suitable, respectively, potatoes, pastures and meadows, raspberries, which bonitet score is higher.

Of the sites as potential contaminants are not expected to significantly impact on a territorial scale.

The developed self-monitoring system introduction might be used for effective monitoring and strict control of air, soil and water.

5. ACKNOWLEDGEMENTS

Author thanks to Mr. Damian Mihalev - Executive Director of the SRA - Sofia for his assistance in this paper realization. Thanks also to the staff of

General Direction of Agriculture and Forestry in Yakoruda municipality for the information that allowed the elaboration of the study.

6. REFERENCES

[1] Gurov G., Artinova N. 2001. Soil Science, Markus, Plovdiv.
[2] Kolev B. 1994. Ph.D. Thesis., Sofia, pp. 10-35.
[3] Soil Resources Agency (SRA). http://www.soils-bg.org/
[4] The municipality plan for Yakoruda Municipality development 2007 – 2013.

Demographic situation in the villages after implementing the National Plan for Rural Development

Minka Anastasova, Maria Shishmanova
IAE, Sofia, Bulgaria, SWU "N. Rilski", Blagoevgrad, Bulgaria

***Abstract**: The report presents the results for the expected number of rural population in 2013 totally for the country, including for the planning regions and districts. For this purpose the method of extrapolation estimates has been applied on the basis of dynamic series covering the period 2000-2009. In some cases, when necessary, this period is reduced by removing the extreme points from the dynamic series. These so-called "influence" points usually turned out to be for the first 1-2 years from the considered time horizon. The predicted results are analyzed inferring the basic conclusions from them. The human potential in the rural areas will be further diminished in an irregular manner in the different planning regions and districts.*

***Keywords:** prediction, number of rural population, planning regions, districts.*

1. INTRODUCTION

The permanently established negative trends in the development of demographic processes in the villages determine the extremely aggravated situation in the state of human resources in rural areas. A fact of special concern is that even after launching the execution of the measures, envisaged in the National Plan for Rural Development (NPRD), the permanent decline of the rural population number and complete depopulation of entire villages are still continuing. According to prognostic calculations this trend is not likely to change until at least 2013. The outlined diminution of human potential in rural areas in the near future is in line with the preliminary data from the last census.

2. RESULTS, DISCUSSIONS, CONCLUSIONS

The developed prognostic calculations are grouped in two variants. The first option, provisionally called favourable, contains data for the expected number of rural population, which coincide with the upper limit of the respective confidence intervals, and the second one or the so-called pessimistic option includes the predicted values, equivalent to the lower limit

of the confidence intervals. Due to the stochastic character of the forecasting methods, the obtained results are not strictly fixed and fluctuate with a definite guarantee probability within respective ranges. It may be assumed that the first variant would be realized under relatively preserved general socio-economic conditions for the development of rural regions, while the second one – under their eventual further deterioration. The prognostic values are given in Tab. 1.

Tab. 1: Prediction of rural population number towards 2013 according to planning regions.

Planning regions	2009	2013 I variant	Variation 2013 with respect to 2009 (%) I variant	2013 II variant	Variation 2013 with respect to 2009 (%) II variant
Total for the country	2176801	2103567	-3,58	2065630	-5,11
Northwest (NWR)	184393	170306	-7,64	166200	-9,87
North Central (NCR)	335049	316801	-5,76	308761	-7,85
Northeast (NER)	431406	418 026	-3,10	410393	-4,87
Southeast (SER)	225970	221243	-2,09	211091	-6,58
South Central (SCR)	625521	609751	-2,52	598326	-4,35
Southwest (SWR)	374462	370666	-1,01	362996	-3,06

The analysis of the data in the table above shows that further decrease of rural population is to be expected in the next 3-4 years, which will be with 3.6% for the first variant and with 5.1% for the second one. This estimate results from the established permanent trends in the negative demographic development of the rural regions during the previous decades. On the one hand, it is related to the constant diminution of the total population number in the villages (only for the period 2005-2009 it has been reduced with 5.4%). On the other hand, as a result of our previous investigations it has been established that at present migration as a factor exerts lower impact on the dynamics of rural population compared to natural migration. This fact, and the circumstance, that the share of people over the age of 65 exceeds the number of persons younger than 20 (25.7% versus 18.5%) justify that the process of reduction of rural population will continue in the coming years

too. Moreover, this negative trend is characterized by certain fluctuations in all planning regions (Fig.1).

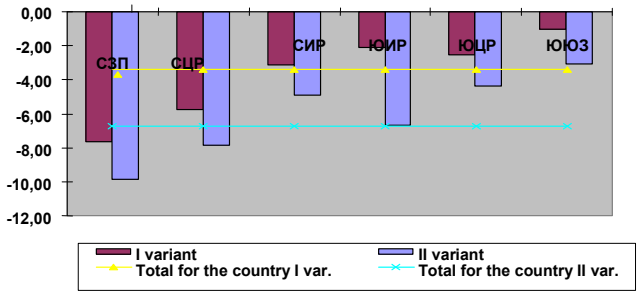

Fig. 1: Expected variation of the number of rural population in 2013 with respect to 2009 in the planning regions (%).

The Northwest region is in the most unfavorable situation. The population reduction rate in this case is higher than the national average (respectively 7.6% and nearly 10%). This is due to the general economic backwardness of this region and better expressed presence of rural population, its share reaching 37.8% from the total population here, while the average relative share of rural population for the country is 28.7%. An additional factor is the more strongly aggravated age structure of rural population in this region. According to some results [1;3;4] NWR is the region with the lowest potential and most numerous difficulties in its development and highest concentration of problematic municipalities. It is expected that the Montana district will suffer the highest loss of human resources in the villages compared to all other districts of the NWR region. It is followed by the Vidin district, where the rural population is expected to reduce by 8.9% and 11.4% respectively. Although the expected reduction in the Vratsa district is lower than that in the other two districts, it remains higher than the average for the country (5.6% and 7.9% for the two variants respectively).

The expected change of the total number of rural population in NCR also indicates negative values, which are higher than those for the country. According to the first variant diminution with 5.8% is envisaged for the first variant and 7.8% - for the second one. The main reasons in this case are also associated with aggravated age structure of rural population. This determines a higher mortality rate and hence – natural migration rate. In NCR 96.5% of the total population are due to natural growth of rural population and the rest 3.5% are due to mechanical migration. Owing to this reason, although there are no weak municipalities in the region [1], in terms of the negative demographic processes in the villages it is ranked immediately after NWR. No substantial differences in the forecast results are observed between the districts included in NCR. The villages situated

within the range of the Ruse district are an exception in positive respect. The lowest reduction of population is expected for these settlements, which amounts to 2.5% for the first and 5.8% for the second variant.

One of the biggest district centers as the town of Ruse represents a relatively insufficiently attractive place for living at least for the population from the neighboring rural municipalities. This may be explained to a certain extent with the serious ecological problems, accompanying the town development in the near past, as well as with the existence of some of the most developed rural municipalities as Vetovo, Byala, Slivo Pole, etc. Diminution of rural population to a higher degree than the average reduction in the villages throughout the NCR is predicted for the Pleven and Veliko Turnovo districts. The main reason for this situation ensues from the very low parameters of natural migration of rural population in these two districts. In the last years (since 2003) the negative natural growth in the villages of the Pleven district varies within the interval minus 14 to minus 18 per 1000 people of the population, and in the Veliko Turnovo district – from minus 17 to minus 20‰.

The changes, which are expected to take place in NER, also outline the features of the general negative trend in the further development of the demographic crisis in the villages, but they are less pronounced in this case. In quantitative respect the aggravation rate of human potential for both variants is lower than the average for the country. The predicted reduction of rural population for the first variant is by 3.1%, and for the second – by 4.9%. The main reason lies in the specificities of the age structure of rural population in the region. This is the area with the most favourable age structure of rural population in the country. The relative share of the persons younger than 20 here exhibits the highest value -21.0%. At the same time the share of elderly rural population above the age of 65 is lower than the average – 22.2%. In its turn this determines the lowest negative values of natural growth of rural population – minus 7.6 per 1000 people. Undoubtedly the relatively better demographic parameters of rural population in NER are due to the presence of a number of large rural municipalities with promising development as Tervel, Krushari, Devnya, Kavarna, Novi Pazar, Veliki Preslav, etc.

The expected reduction of the number of rural population in the single districts found in NER varies within a rather broad range: 0.97% in Varna district to 5.5% in Silistra district for the first variant, and for the second one – from 2.4% to 6.6%. The negative demographic processes for the rural population are expected to be displayed to the lowest extent in the Varna and Shumen districts, while the population in the villages of the Silistra district will be most strongly affected. The negative migration in this district is more important than the natural growth, which is within the range between minus 5 and minus 8‰ in the recent years.

It is natural that the biggest seaside district center Varna attracts more people for tourism and recreation than population for permanent residence from the adjacent rural municipalities. All municipalities included in the Varna district have the status of rural regions and exhibit relatively good characteristics concerning transport infrastructure and the sphere of budget self-financing [1]. This obviously contributes to a certain stabilization of the demographic processes in these rural areas. The relatively low natural-growth coefficient – minus 5.4 per 1000 people, which in its turn is determined by the strong presence of the Turkish ethnic community in the area, is of primary importance for the expected lower decline of rural population in the Shumen municipality.

The reduction of rural population in SER is expected to be by 2.1% for the first variant and by 6.6% for the second. The bigger range between the two predicted variants is explained by the lower stability of the regression model from statistical viewpoint, which leads to higher values of the t-coefficient and respectively broader confidence intervals. However, this does not make the model inadequate and inapplicable, since the values of the empirical F-coefficient (Fisher criterion) are sufficiently high and exceed the value of the theoretical F-characteristic.

Comparing the values of the integral indicator of the overall socio-economic potential for development of the municipalities included in SER, it becomes clear that a part of them are with characteristics exceeding the average ones for the country. These are mainly the municipalities along the seaside – Burgas, Nesebar, Pomorie [1;3]. At the same time, municipalities with limited potential are found here too. A typical example for such municipalities is Malko Turnovo, situated on a large territory in Strandzha, with remote villages and aggravated age parameters of the population. As a whole, the age structure of rural population in the region is more favorable than that in the country, which explains the obtained relatively better prognostic results. SER includes three districts, situated in very different natural-geographic territories with unequal economic basis.

The population in the villages of Burgas district for the first predicted variant is expected to rise, although insignificantly, while the rural population in Sliven and Yambol districts is predicted to decrease by both variants. It is obvious that for the villages adjoined to the Southern Black Sea coast area the demographic problems are not so drastically outlined as in the case with the rest of the villages in SER. Of all the villages in the region the settlements in the Yambol district are with the most unfavorable status, their natural growth reaching minus 18.5 per 1000 people – one of the highest for the country. The expected reduction of population in the Sliven district is lower than the average for Bulgaria because of the Roma community in the area and here one of the lowest levels of negative natural growth are recorded – minus 2.7‰. It may be inferred that the ethnic composition, the

geographic and socio-economic profile of the areas in the region will continue to exert differentiating impact on the development of the quantitative composition of human resources in the adjacent villages.

In general, lower reduction of rural population is expected in SCR, compared to the diminution predicted for the whole rural population in the country. This result is valid for both variants of the forecast: by 2.5% and 4.4% respectively. SCR includes the greatest number of rural municipalities, situated in one of the most fertile plain agricultural lands, as well as municipalities, scattered throughout the whole Rhodopes massif. Stable municipalities (with high values of the integral coefficient) predominate in the Plovdiv district, while municipalities with limited potential are concentrated in the Smolyan district, including Smolyan municipality too [1]. These differences are reflected on the demographic status of the villages in the region and on the further development of the demographic processes in them. According to the forecast, the rural population in the Smolyan district is expected to reduce to a much higher degree. The anticipated diminution of the population in the villages of the Smolyan district is far greater than the average reduction for SCR. Moreover, it is commensurate with the scale of the rural population reduction, typical for NWR. It is expected that the dominating role of migration processes in this district will continue till 2013.

SWP is the region, where the most polar states are observed for the municipalities in it. The main reason for this situation is related to the presence of the Sofia-city district, which is quite reasonably to have the best development parameters in the country, including demographic status too. It is known that the total number of the population in the capital is steadily growing. The positive demographic profile in this area refers to the villages around the metropolitan city too. This is due to the fact that persons migrating from the other parts of the country prefer to settle both in the capital and in the villages close to it. In addition, the natural growth here is also with a negative value (minus 4.5‰), but it is far better than the average natural growth, typical for all villages in the country (more than two times lower). In 2013 it is expected that the population growth in the villages of this area will be preserved for both variants.

In contrast to the Sofia-city area, almost all other districts in SWR are in a different situation. The biggest deviations from the average values for the region are predicted in the villages of the Kyustendil district. It is known that part of the municipalities in the area (Nevestino, Treklyano, Sapareva Banya, etc.) fall within the group of the so-called deprived regions with demographic characteristics exhibiting one of the worst parameters. The predicted values result from the permanently kept trend of constant negative mechanical and natural growth in the district. The absolute value of the coefficient of natural migration of rural population here is one of the highest for the country (in the last years its values are around minus 20‰).

The demographic situation in the villages of SWR in Pernik district is relatively good. Although the natural growth of rural population in the area is quite high (it occupies levels of minus 22-23‰ since 2003 till now), due to the positive mechanical growth in 4 rural municipalities (Kovachevtsi, Breznik, Trun and Zemen) it is expected that the rural population in the district by 2013 will be increased with 0.12% according to the first variant, and that it will be reduced with about 3% according to the second option.

The population in the villages of the Sofia district is expected to diminish according to both variants as a result of the ongoing migration processes in the last years - negative mechanical as well as strongly negative natural processes. The negative natural growth of rural population is higher than the national average (within the range minus 14-16‰). The expected changes in the number of rural population in Blagoevgrad district are close to those, predicted for the population in the villages of the entire Southwest Planning Region.

The following inferences may be drawn on the basis of the analysis of the obtained prediction results concerning the expected changes in the number of rural population by 2013:

- The established trend of permanent reduction of rural population in the recent years will continue until 2013 too. On a national level this reduction will amount to 3.6% according to the first variant and to 5.1% - according to the second variant;
- After launching the implementation of the measures, envisaged by NPRD, in 2007, no substantial positive changes are observed in the development of the basic demographic processes in rural areas that might exert favorable impact on the stabilization of human resources in the rural regions. Regardless of the effect of the measures in NPRD, the villages still continue loosing human potential;
- Especially high negative natural growth of rural population is still observed at present. Moreover, although to a smaller extent, migration of population from the villages to the towns and abroad is still continuing;
- The high negative value of natural growth in the villages, which is far higher than that in the towns, is due to the strong ageing of rural population, leading to high mortality and respectively low birth rates;
- The extent of the expected loss of human potential in the rural areas is different for the single planning regions. The NWR region will continue to be in the most unfavorable situation, followed by NCR;
- Relatively lower deficiency of rural population is expected for SWR, followed by SCR. The values for the villages in SER and NER are almost equal to the average national values of demographic decline;
- The main reasons for the observed differences in the further development of the demographic processes in the villages of the single

planning regions are associated with the unequal degree of socio-economic stability, geographic situation, natural-climatic settings, ethnic composition, established traditions with respect to the reproductive behaviour of the population, etc.;

- Certain differences in the degree of the further expected losses of human potential in the villages are also observed for the districts in the various regions. The following districts will be in the most unfavorable position: Montana and Vidin from NWR, Yambol from CER and Smolyan from SCR;
- The districts Sofia-city, Burgas, Pernik, Varna, Plovdiv, Blagoevgrad and Stara Zagora will continue to be in a relatively more favorable situation with respect to the future demographic status of the villages;
- The outlined differences in the further development of the demographic potential in the villages between the single planning regions and districts require the application of a differentiated approach to determining targeted socio-demographic, economic and migration policy to solve demographic issues.

3. REFERENCES

[1] Kozhuharova, V. et al. (2008) *Municipalities in Bulgaria – development potential*, Sofia, Institute of Sociology.

[2] Yanakieva, I. et al. (2008) *Socio-economic dimensions of the application of EU CAP in rural areas*, Sofia, IAE, AA.

[3] Yankova, N. et al. (2003) *Socio-economic differences between the municipalities in Bulgaria,* Sofia, Economic Research Institute, BAS.

[4] Mihailov, D. et al. (2003) *National Report on human Development*, Sofia, UNDP.

Essence of the Danube Strategy and possibilities for regional development of Bulgaria

Maria Shishmanova
SWU "Neofit Rilski", Blagoevgrad, Bulgaria

***Abstract**: The essence of the Danube Strategy and its basic principles are subjected to consideration. On the basis of this strategy are presented all necessary priorities and management of the Bulgarian Danube territories, with the relevant activities for further development in line with the requirements of the adopted Danube Strategy.*

***Keywords:** Danube Strategy, documents, priorities, activities, management.*

1. INTRODUCTION

The essence of the Danube Strategy and its basic principles are subjected to consideration. On the basis of this strategy are presented all necessary priorities and management of the Bulgarian Danube territories, with the relevant activities for further development in line with the requirements of the adopted Danube Strategy.

2. RESULTS, DISCUSSIONS, CONCLUSIONS

The European Parliament under Article 192 and Article 265, paragraph 5 of the Treaty for the Functioning of the European Union, and also the question of 03.12.2009 to the Commission concerning the European Strategy for the Danube Region (O-0150/2009 – B7-0240/2009), and the European Council conclusions of 18-19.06.2009, called upon the Commission to draw up a European Strategy for the Danube Region before the end of 2010.

The purpose of the macro-regional strategies is to use in a better way the existing resources related to regional development and to find joint responses to common challenges.

The Danube River basin connects ten European countries: Germany, Austria, Slovakia, Hungary, Croatia, Serbia, Romania, Bulgaria, the Republic of Moldova and the Ukraine, six of these countries being EU Member States, and in a broader territorial context the region comprises

also the Czech Republic, Slovenia, Bosnia and Herzegovina and Montenegro. The Danube region represents an interconnected space of heterogeneous economic capacity and is a uniform macro-region, which could contribute to overcoming regional differences in the economic parameters and launching integrated development.

The EU programmes for Cohesion Policy, for the European Neighborhood Policy and the records of the potential candidates should be synthesized for the Danube region. Enhanced interaction will be developed between the different EU policies on cohesion, tourism, agriculture, fishery, power generation, environment, enlargement and neighborhood policy, social development and protection, sustainable economic development transport and energy infrastructure, environmental protection, culture and education.

The document fixes the main directions:

- Evolution via territorial development, closer cooperation in clearly distinguished policy areas, in which all government partners have found a real added value for Europe, and suggest that this strategy should be developed as part of the objective for European territorial cooperation;
- Required action plan that will complement the document. The plan should contain the following elements: environmentally friendly use of the Danube River for inland navigation, intermodality with other transport vehicles along the river course by improving the whole infrastructure, including the existing one, establishing a multimodal transportation system along the entire river flow [1];
- Emphasis on the necessity of diversifying the energy sources and on enhanced cooperation in the sphere of power generation, promotion and implementation of joint projects for energy efficiency and renewable energy sources as bio-, solar-, wind- and hydro-energy;
- Emphasis on accurate strategic evaluations and assessments of the impact on the environment, including estimates of the consequences for the overall river ecosystem;
- Indication of the exceptional economic interdependence of the countries in the Danube region and support of networking for business development and non-governmental organizations for trade promotion by coordination and encouragement of future options of development, mostly of small and medium enterprises, and stimulation the green economy growth in the whole Danube macro-region;
- It is considered that navigation along inland waterways is important for the development of transport in the region and an appeal is made for removing the transport obstacles in single sections along the Rhine-Meuse-Main-Danube navigation axis with the aim of improving the overall intermodal transportation system along the Danube River course. At the same time, the focus is laid on the combination of better

inland ports and logistics, inland navigation and railway transport, as well as additional possibilities for short-distance navigation by sea [2];

- The further development of the trans-European network is proposed, in order to improve the intermodality across the region, as well as the connections with the Black Sea using the road and railway network;
- An appeal is made for broader use of modern communications and information technologies for establishing as soon as possible an effective unified regulation system for the navigation along the Danube;
- It is considered that sustainable tourism is an important tool for encouraging the economic growth in the region. The possibilities of ecotourism are also shown, as well as the economic potential of the bicycle routes along almost the entire Danube River course;
- Support for programmes aimed at improving the multicultural environment in the Danube region by fostering multinational mobility, promoting intercultural dialogue, creating forms of art and communication and training institutions and business incubators in these areas, and preserving the cultural and historic heritage and supporting new cultural industries [3];
- Improvement of education, scientific research and social cohesion by supporting university exchange programmes in the region and enhancing the development of university networks in the region to foster centers of excellence, which are competitive on an international level;
- Mechanisms have been developed for the work of the Commission for more effective and timely coordination of the activities of the individual countries in the Danube region.

The following units fall within the direct influence in the Bulgarian Danube region [4]:

- Two (2) NUTS 2 regions: Northwest and North Central region – population 1 840 330 (24% of the total for the country)
- Eight (8) NUTS 3 territories (districts): Vidin, Montana, Vratsa, Pleven, Veliko Tarnovo, Ruse, Razgrad, Silistra – population 1 554 940 (20% of the total for the country)
- Twenty two (22) NUTS4/ LAU1 territories (municipalities) – population 570 450 (7.5% of the total for the country)

Priority areas

The priority areas for the strategy development are outlined on the basis of the three “milestones” by the Commission:

- **Connectivity** – planning of initiatives for improving the accessibility, transport links and communications along and to the Danube and efficient use of energy resources;

- **Environment** – conducting a policy, including measures for improvement of water quality, biodiversity, risk prevention and management;
- ***“Unlocking the potential”*** – a complex of interventions within a broad spectrum of socio-economic areas with an emphasis on the economic development and increasing the competitiveness of the regions, and on education, culture and tourism, which should ensure cohesion and multicultural and ethnic dialogue, preserving the specifics of regional identity and cultural heritage.

Priority areas

Priority: **Connectivity**

- Development of transport infrastructure (railways, roads, bridges, ports, terminals);
- Power generation networks and facilities;
- Information-communication networks and facilities;

Priority: **Environment and risk prevention**

- Reducing water pollution
- Conservation of nature and biodiversity
- Risk prevention
- Promoting the principles of sustainable development

Priority: **Socio-economic and cultural integration**

- Transnational initiatives and support for innovations
- Promoting trade and investments
- Human resource development
- Priority: Effective use of tourism potential
- Promoting intercultural dialogue

The management of the Danube Strategy within the range of Bulgaria includes:

Connectivity

Priority: **Development of transport infrastructure**

A complex of measures is included for development and modernization of railway, road and port infrastructure, bridges and ferryboat links of the Danube River, the waterway and navigation systems, as well as functional connections providing logistics (intermodal terminals), sustainable mobility and transport safety and security. These measures are integrated in complex design directions along the main trans-European transport corridors.

- Construction and modernization of the infrastructure along the trans-European transport corridors No 7; No 4; No 9; No 10;
- Development and modernization of the transport infrastructure along the destination Danube – Black Sea (Ruse – Razgrad – Shumen – Varna);

- Construction of the Hemus highway and reconstruction and modernization of the first-class roads from the highway to the Danube ports.
- Construction and modernization of the infrastructure along trans-European transport corridor No 7;
- Construction of bridges across the Danube and reconstruction of the existing bridge;
- Construction, reconstruction and modernization of the ferryboat connections;
- Construction and reconstruction of port infrastructure;
- Improving the navigation along the Danube River;
- Construction of the Danube Scenic Road – reconstruction and repair of the road sections parallel to the river from Vidin to Silistra;
- Construction of a bicycle route and alleys along the riparian strip from Vidin to Silistra – Danube cycling trail (part of the e trans-European cycling lane along the Danube.
- Construction and modernization of the infrastructure along trans-European transport corridor No 4;
- Construction of a second bridge across the Danube at Vidin – Calafat (in progress – ISPA);
- Reconstruction and renovation of the first-class road (E79) Vidin – Montana – Vratsa - Botevgrad;
- Renovation and reconstruction of the Northern circular road in Sofia (Northern tangent);
- Construction of the Lyulin highway (in progress);
- Construction of the Struma highway;
- Reconstruction and modernization of the Vidin – Sofia – Kulata railway line.
- Construction and modernization of the infrastructure along trans-European transport corridor No 9;
- Reconstruction of Danube Bridge-1 Ruse – Giurgiu and the adjacent railway line;
- Construction of an intermodal terminal – Ruse;
- Construction of a south-southeast bypass road of the town of Ruse (from highway I-5 – Veliko Tarnovo via main road I-2 Ruse – Varna to main road II-21 Ruse Silistra;
- Improving the access of the Ruse – Giurgiu Euroregion to pan-European corridor No 9;
- Rehabilitation of the transport infrastructure for the development of cross-border cooperation in the Giurgiu – Ruse region;
- Reconstruction and construction of a four-way road I-5 Ruse – Veliko Tarnovo;

- Design and construction of a tunnel under Shipka peak;

Construction and modernization of the infrastructure along trans-European transport corridor No 10

- Construction of the Sofia – Kalotina motorway;
- Construction of the northern tangent of the Sofia City;
- Construction of the Maritsa highway;

Construction of the Hemus highway and reconstruction of roads from the highway to the Danube ports:

- Construction of the Hemus highway from Yablanitsa to Shumen;
- Construction and reconstruction of the first-class road connections from the highway to the ports of Nikopol and Svishtov.

Development and modernization of the transport infrastructure along the Danube – Black Sea destination (Ruse – Razgrad – Shumen – Varna);

- Reconstruction and construction of a four-way road I-2 Ruse – Razgrad – Varna from km 12+208 to 37+300;
- Road I-2 Ruse – Razgrad from km 54+700 to km 61+053 and from km 63+420 to km 69+300;
- Road I-2 Razgrad – Shumen from km 88+010 to km 92+700;
- Restoring the parameters of the Ruse – Varna railway line.

Environment and risk prevention

Priority: **Reducing water pollution**

- Integrated water management and treatment;
- Design and building of the infrastructure for drainage and wastewater treatment of settlements with more than 10 000 eq. residents and preparation stages for the construction of wastewater treatment plants (WWTP) in settlements with population between 2000 and 10 000 eq. residents in the Danube region for basin management;
- Improving the waste management systems and restoring damaged areas and natural landscapes.

Priority: **Conservation of nature and biodiversity**

- Restoring the wetlands and biodiversity conservation along the Danube River course.

Monitoring of the quality of environmental factors in the municipalities of the Danube region.

Priority: **Risk prevention**

- Integrated operational management and prevention of crises, disasters and accidents;
- Establishing a common system for prevention of natural and technological risks, including early warning systems.

Priority: **Promoting the principles of sustainable development**

- Promoting environmental protection and popularizing climate changes and their impact;

- Developing eco-urbanization zones in the Lower Danube Euroregion – models for sustainable urban development;
- Increasing the capacity of municipal and district administrations and NGOs on sustainable development of the regions.

Priority: **Reducing water pollution**

This priority reflects the measures associated with the integrated planning and management of the river area with a number of interventions on infrastructure and technologies for environmental protection as wastewater treatment plants, waste management, sewerage, soil and water treatment, drinking water supply, Danube water use for irrigation;

- Design and construction of the infrastructure for drainage and wastewater treatment of settlements with more than 10 000 eq. residents and preparation stages for the construction of urban wastewater treatment plants (UWWTP) in settlements with population between 2000 and 10 000 eq. residents in the Danube region for basin management;
- Improving the waste management systems and restoring damaged areas and natural landscapes.

Priority: **Conservation of nature and biodiversity**

- Development of new and updating existing plans for management of protected areas along the Danube River course and implementing the activities, envisaged in them;
- Building a network of protected areas Natura 2000 and gradual composition of plans for the management of protected areas along the Danube River course;
- Implementing activities for the protection of endangered animal and plant species, encountered along the Danube River course.

Priority: **Risk prevention**

This priority includes both “soft measures” aimed at monitoring, control and preparedness of the region for united actions, infrastructural components of protective character and basic infrastructure for integrated operational management, and prevention of crises, disasters and accidents [4].

Socio-economic development and intercultural dialogue

Priority: **Transnational initiatives and innovation support**

- Strengthening of the transnational research and scientific exchange, creation and development of research centers and programmes
- Encouraging public-private partnerships, taking into account the heterogeneous nature, needs and potential at all levels in the Danube region

Priority: **Promoting trade and investments**

- Encouraging foreign investments

Improved cross-border and transnational policy for the labor market

Priority: **Human resource development**

- Improving the quality of education, meeting the demand of the labor market, creating opportunities for higher qualification and conditions for development of applied research and scientific work, in order to transfer knowledge and know-how.
- Improving the opportunities for education, retraining and lifelong learning in the region, with emphasis on conservation and development of natural and cultural heritage of the Danube region.

Priority: **Effective use of tourism potential**

- Merging the potential for tourism development in the whole Danube region, formation of joint tourist products and promotional policy;
- Complementing the implementation of all previous priorities of infrastructural development, via economy and ecology to human resources.

Priority: **Promoting intercultural dialogue**

- The promotion of intercultural dialogue is the way to tolerant mutual understanding, allowing the European Community to be united in its diversity;

Accelerating the process of economic and social cohesion of the regions by the development of sustainable partnerships between them.

Priority: **Promoting trade and investments**

- This priority contains initiatives for supporting entrepreneurship, increasing the capacity for conducting effective financial and investment policy on a local level, initiatives stimulating business cooperation and development of small and medium enterprises, infrastructural measures ensuring territorial positioning and logistic support for business;

Construction of industrial and technological parks and transport-logistic and exhibition centers.

Priority: **Human resource development**

- Multidisciplinary projects are identified for the establishment and development of educational and training centers, R&D facilities, projects for marketing of the labor market and student mobility. The development of human resources in the Danube macro-region is based on partnership and transfer of knowledge and best practices;
- Establishment and development of educational and training centers;

Increasing the capacity of municipal and district administrations and NGOs on sustainable development in the region.

Priority: **Effective use of tourism potential**

- The priority covers integrated projects of interregional, cross-border and transnational character, aimed at establishing a common Danube Tourism Strategy, development of a common tourist market, a range of projects for development of Danube tourism products in the field of

cultural, wine, countryside and cruise tourism in the Danube macro-region.

3. REFERENCES

[1] www.europarl.europa.eu/sides/getDoc.do?pubRef=-//...2010
[2] www.vesti.bg/index.phtml?oid=3388631&tid=40
[3] www.bnt.bg/bg/news/view/40420/bylgarija_iska_vodeshta_rolja_v_dunavskata_strategija
[4] www.enterprise-europe-network.bg/plugins/content/content.php?content.1958

Trends in seasonal and annual air temperature within Oltenia Plain, Romania

Alina Vladut, Sorin Avram, Gheorghe Curcan
University of Craiova, Geography Department, str. Al. I. Cuza, nr. 13, Craiova, Romania

Abstract: *On the general warming background, the study of temperature trends gains in importance. Warming is not linear in time and space, but there emerged certain clear regional patterns. The data series analysis revealed that within Oltenia Plain, which is located in the south-west of Romania, air temperature registered a clear upward trend, both at annual and seasonal level, trend supported by the values of positive deviations, linear regression, and 5-years moving averages. Thus, the greatest annual increase occurred in the last decade within most of the analysed region, the highest deviations characterizing especially the western part of the plain. Differentiated temperature increase per seasons might be extremely important in terms of general impact on the environment. Consequently, knowing such trends might help us better cope with future climate-induced problems.*

Key words: *temperature, annual trend, seasonal trend, Oltenia Plain, Romania*

1. INTRODUCTION

Air temperature clearly increased over the past century. Experts stated that, overall, the global warming was of about 0.6ºC [14, 9], but the warming intensity is difficult to be estimated as it did not occur linearly in time and it is not uniformly distributed across the globe. Luterbacher et al. (2004) showed that, in the late 20th and early 21st century, European climate is very likely (>95% confidence level) warmer than that of any time during the past 500 years and 2003 was by far the hottest summer. However, data analysis emphasized that middle and high latitudes of the Northern Hemisphere generally received larger amounts of heat [9, 10], but, at the same time, there were noticed certain cooling trends [5, 6, 7, 8, 11]. In Europe, researchers underline the increase of surface air temperature in most of the regions, especially in the last two-three decades [12]. It is worth mentioning that 11 of the 12 warmest years on record have occurred in the past 20 years [16].

In Romania, the results of the research indicated certain changes observed in the surface air temperature and precipitation regime (mean and extremes), pointing out their direct relation with the changes of large-scale circulation patterns. In the studied area, temperature variability is highly controlled by south-westerly circulation, modulated by the Carpathians. In winter, the region is under the direct influence of moist and warm air masses brought by the cyclones formed above the Mediterranean Sea, which register a maximum intensity in this season, and thermal convection and frontogenesis processes are more frequent than in other areas [2]. Summer is characterized by the reduction of the cyclone activity, but, compared to other regions of the country, it remains quite intense. There was found an interesting connection between NAO phases and Romanian temperature variability in winter [1]. It was also analysed the connection between seasonal mean maximum temperature and various large scale circulation patterns [15]. Starting with 2000, Romania seems to confront itself with ever-increasing air temperatures. In the last decade, there are several problematic years, such as 2000, 2003, and especially 2007. For example, we mention new thermal record values for July (2007, >44°C, at Calafat, which is located within our area of interest), a new record number of consecutive dog days – 10, at all the stations from the region and one case of 10 consecutive tropical nights (Tmin>20°C) at Craiova. There was registered the highest minimum temperature, 25°C at Calafat, on the 23rd of July and 24.6°C at Caracal on the 24th of July [3]. Consequently, the analysis of the trends registered by air temperature in the last 40 years, in the context of global warming, can be highly useful.

2. DATA AND METHODS

The study area is a plain region, representing the western extremity of the Romanian Plain, the largest plain unit in the country. Our choice for the 5 stations (D.T. Severin, Calafat, Bechet, Bailesti, and Craiova, Tab. 1) was based on the quality and continuity of the data. Data were gathered in the form of monthly mean temperatures for the interval 1971-2009. Regarding the completeness of the air temperature records, there were found no missing values. For comparative purposes we also used the mean values of temperature calculated for the interval 1961-1990, which are considered normal.

Tab. 1: *Geographical location of the meteorological stations from Oltenia Plain*

No.	Station	Altitude (m)	Latitude	Longitude
1.	**Calafat**	61	43°59`	22°57`
2.	**Bechet**	36	43°47`	23°57`
3.	**Băileşti**	57	44°01`	23°20`

4.	**Craiova**	192	44°19`	23°52`
5.	**D. T. Severin**	77	44°38`	22°38`

Based on mean annual and seasonal temperature values, we have calculated the deviation corresponding to each year and decade averages. In order to better render the characteristic temperature trends over the region, there were calculated the linear regression (both annual and seasonal time scale) and 5-years moving averages (annual time scale).

3. **RESULTS AND DISCUSSION**

3.1 General features of the thermal regime.

As we have analysed a relatively small and homogeneous landform, the mean annual temperatures do not display extremely high differences. However, they oscillate between 11 and 12°C and the general tendency is to decrease northwards and eastwards [17], the highest value corresponding to the western extremity (11.9°C at Drobeta Turnu-Severin) and the lowest to the northern part (10.9°C at Craiova), due to both higher altitudes and different exposure to air masses. Mean monthly temperatures increase from January (the month with the lowest values of the year) until July (maximum temperatures within the plain) and then the values register a normal decrease. In January, temperature is positive only in the western extremity (0.1°C), while within most of the plain the values are negative due to the more frequent penetration of cold air masses from eastward: -0.4°C at Calafat, -1.1°C at Bechet, -1.1°C at Băileşti and -1,2°C at Craiova (Tab. 2).

Tab. 2: Mean monthly and annual temperatures within Oltenia Plain (1971-2010)

Station	**1**	**2**	**3**	**4**	**5**	**6**	**7**	**8**	**9**	**10**	**11**	**12**	**Mean**
D.T.Severin	0.1	1.9	6.5	12	17.5	21.1	23.2	22.8	17.9	12	5.8	1.5	11.9
Calafat	-0.4	1.5	6.5	12.2	17.7	21.5	23.4	22.7	17.8	11.7	5.3	0.7	11.7
Bechet	-1.1	0.9	6.1	12.1	17.7	21.4	23.1	22.2	17.4	11.2	4.7	0.3	11.3
Băileşti	-1.1	0.9	6.1	12	17.7	21	23.1	22.2	17.4	11.3	4.8	0.3	11.3
Craiova	-1.2	0.7	5.5	11.3	16.9	20.4	22.4	21.9	17.2	11.2	4.8	0.1	10.9

During the year, temperature increases with about 5-6°C from one month to another and the differences among stations are almost similar to the ones registered in January, which means that at Craiova, the northernmost station, mean temperatures are lower than at the rest of the stations. July stands for the highest mean values, above 23°C, except for the northern part: 23.2°C at Severin, 23.4°C at Calafat, 23.1°C at Bechet and Băileşti, and 22.4°C at Craiova. Temperatures are positive even in December, the lowest value, 0.1°C, being registered at Craiova, in the north, while the highest, 1.5°C, at D.T. Severin, in the west. Mean thermal

annual amplitudes also increase form west to east, from 23.3°C at D.T. Severin to 24.2°C Bechet, and decrease northwards (23.6°C at Craiova).

3.2 Trends of the mean annual temperatures

The analysis of the annual temperatures indicates a constant upward trend within the entire perimeter of Oltenia Plain. Thus, compared to the normal (mean temperature of the interval 1961-1990), in the last decade, we notice an increase of about 1°C at D.T. Severin and Băileşti and 0.8°C at Craiova. Generally, the mean temperature increases with 0.2-0.7°C from one decade to another (Tab. 3). The slope of the 20-year increasing trend has consistently been steeper than that recorded over the 1961-1990 period. Comparing the last two decades, the temperature increase reached 0.37-0.54°C within most of the analysed region, except for the northern extremity where the slope is steeper between 1971 and 1990, registering a difference of 0.72°C from one decade to another. As it can be noticed from Fig. 1, the last decade displays the highest positive deviations, generally above 1°C, except for 2005, which was the wettest year registered in 50 years at most of the stations. As shown in Fig. 2, most stations behave quite similarly.

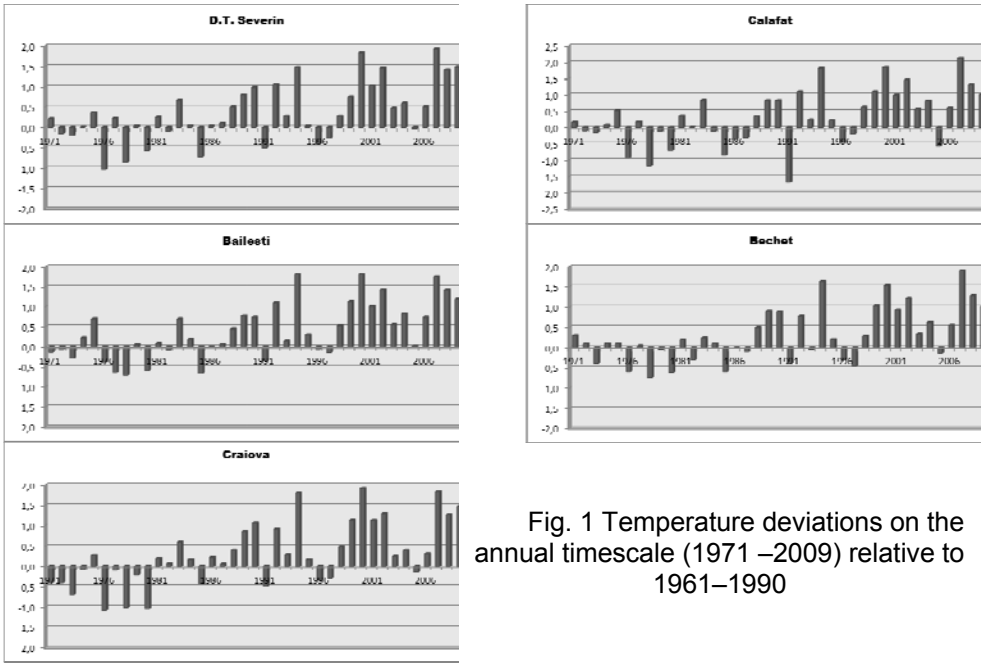

Fig. 1 Temperature deviations on the annual timescale (1971 –2009) relative to 1961–1990

The annual air temperature time series along with 5-years moving average filter and linear models fitting for the five meteorological stations are emphasized in Figure 2. We may notice that the increases are generally

linear over time, with scatter due mainly to interannual variability. The increase in mean temperature shown here is significant at the 99.9% level.

Tab. 3 Mean decade annual temperatures within Oltenia Plain

Decade	D.T. Severin	Calafat	Bechet	Bailesti	Craiova
1961-1990	**11.53**	**11.38**	**11.0**	**10.93**	**10.56**
1971-1980	11.31	11.18	10.83	10.72	10.20
1981-1990	11.76	11.57	11.18	11.13	10.92
1991-2000	11.96	11.87	11.43	11.53	11.16
2001-2009	12.42	12.27	11.80	11.87	11.41

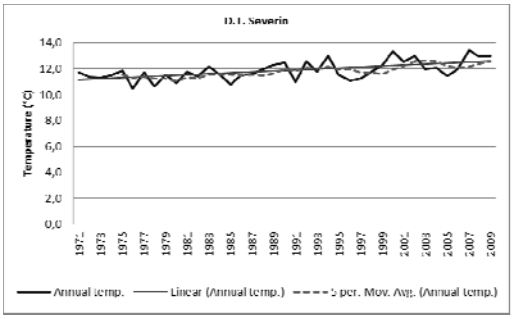

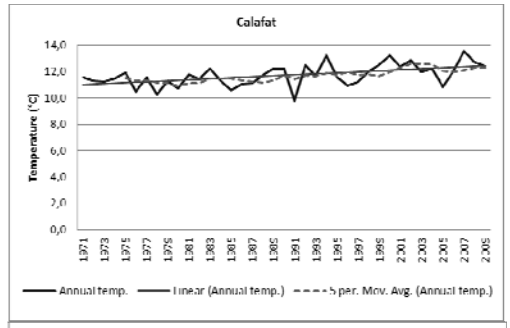

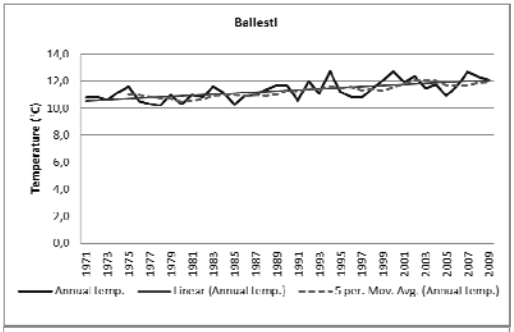

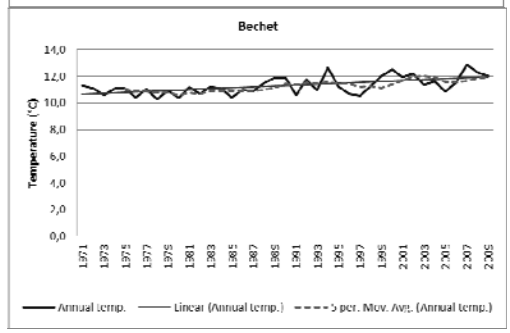

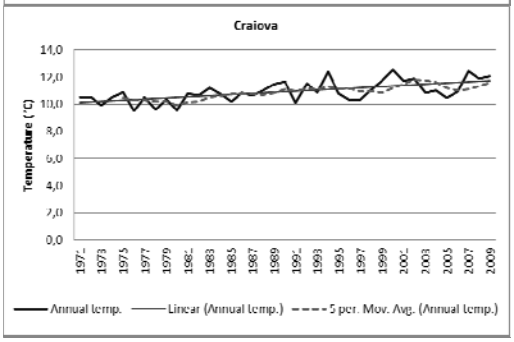

Fig. 2 Annual air temperature time series along with 5-years moving average filter and linear model fitting

3.3 Seasonal trends

From the aforementioned results, it is evident that there is a general pre-dominating positive trend in annual air temperature. However, when the decadal trends are calculated separately for each season, some distinct trends arise (Tab. 4). During the last four decades, winter temperatures have increased by 0.04 to 0.11°C. There emerged certain differences within the region – in the west, there is a gradually increasing trend, the last decade registering the highest value of the entire period and region, 1.39°C at D.T. Severin. However, within most of the plain, this increasing trend is insignificant in winter (Fig. 3), underling the importance of the penetration of warm air from the south-western sector. Starting with spring, the trends become clearly positive within the entire plain.

Tab. 4: Mean seasonal temperatures per decade within Oltenia Plain

Winter					
Decade / Station	**D.T. Severin**	**Calafat**	**Bechet**	**Bailesti**	**Craiova**
1971-1980	0.95	0.56	-0.07	-0.06	-0.07
1981-1990	1.10	0.71	0.02	0.08	0.02
1991-2000	1.25	0.43	-0.16	0.08	-0.16
2001-2009	1.39	0.82	0.21	0.13	0.23
Spring					
Decade/ Station	**D.T. Severin**	**Calafat**	**Bechet**	**Bailesti**	**Craiova**
1971-1980	11.25	11.51	11.67	11.50	11.67
1981-1990	11.87	11.90	11.88	11.74	11.88
1991-2000	11.90	12.22	11.85	11.98	11.85
2001-2009	12.72	12.76	12.49	12.63	12.39
Summer					
Decade / Station	**D.T. Severin**	**Calafat**	**Bechet**	**Bailesti**	**Craiova**
1971-1980	21.32	21.39	21.29	20.80	21.29
1981-1990	22.09	22.12	21.83	21.73	21.83
1991-2000	22.88	23.19	22.87	22.82	22.87

2001 -2009	23.23	23.37	22.94	23.08	22.94
Autumn					
Decade / Station	**D.T. Severin**	**Calafat**	**Bechet**	**Bailesti**	**Craiova**
1971 -1980	11.48	11.28	10.67	10.72	10.67
1981 -1990	11.99	11.54	10.97	11.13	10.97
1991 -2000	11.79	11.62	11.14	11.53	11.14
2001 -2009	12.35	12.12	11.60	11.90	11.68

Thus, spring temperatures have warmed by 0.18-0.37°C per decade. We notice the same difference, namely the western part displays the highest increase. Summer registered the highest positive trends, namely 0.40-0.55°C per decade, while autumn have warmed by 0.21-0.29°C respectively per decade. In autumn, it seems that temperature got higher in the central and western parts of the region. Seasonal warming trends are all significant at the 95% significance level. Consequently, we can claim that the summer air temperature contributes to the annual air temperature much more than winter air temperature does. This is probably the main reason of the annual air temperature increase, especially during the last two decades. So far, it was identified a statistically significant long-term warming trend (up to 0.6ºC on spatial average) of Romanian summers over the last 107 years (1901-2007) [4]. Even if this feature is not linear, as, according to the same authors, two statistically significant changes in the mean summer temperatures were noted, namely an upward shift around 1985, and a downward shift around 1964, overall summer temperature increased.

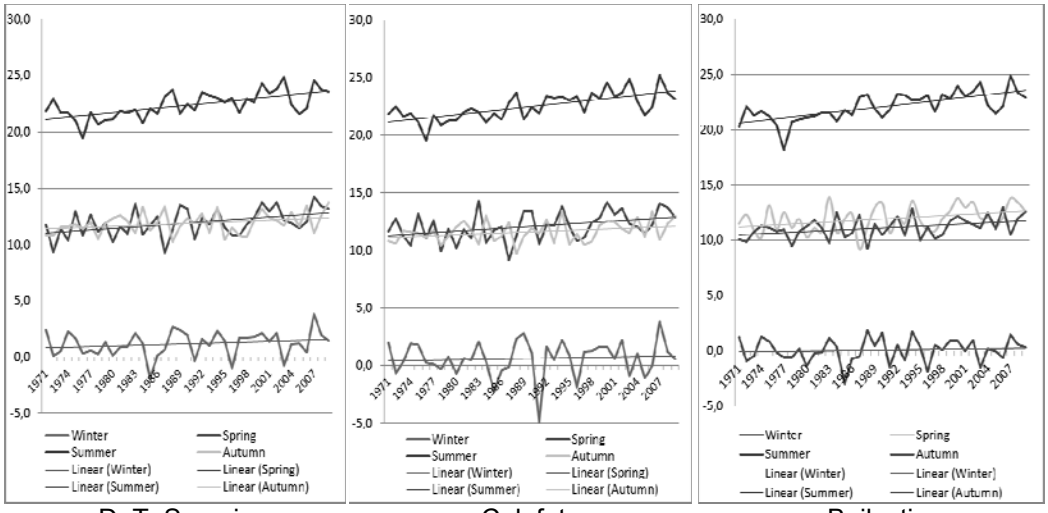

D. T. Severin Calafat Bailesti

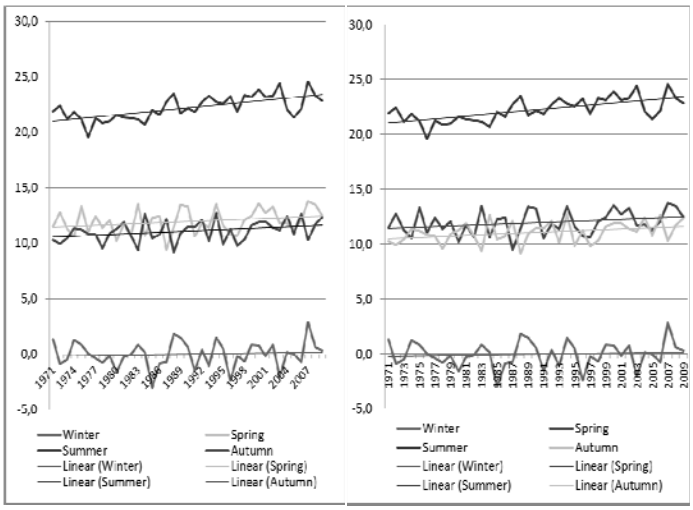

Bechet Craiova

Fig. 3 Seasonal air temperature time series along with linear model fitting

4. CONCLUSIONS

The analysis of temperature data series in Oltenia Plain, each for a period of 39 years long, has revealed that the decadal rate of annual temperature increase has reached up to 0.45ºC. Comparing the means of the last decade with the normal, which is the mean for the interval 1961-1990, there results differences of almost 1ºC. The western part of the plain, which is also more exposed to the penetration of warm air masses coming from the south-western part of the continents, experiences the highest increase and deviation. The temperature increases currently being experienced in the Romania are currently consistent with temperature

patterns over Europe. In spite of certain normal differences induced by a distinct geographic location, the temperature trend registered at the five analysed meteorological stations particularly during the last two decades indicates that the observed patterns are induced by general warming and not by local conditions. During the last two decades (1991–2009), temperatures have increased most in spring and summer and least in autumn, whereas during the 20th century (1901–2000), literature in the field mentions that the seasons warming most rapidly were winter and summer, while trends in spring were lowest. Winter is presently the season that displays the less obvious upward trend, in spite of certain peaks reached in the last decade (for example 2007, with more than 3ºC).

Our analysis emphasized strong rate of temperature increase within Oltenia Plain during the last decades. Warming generally and particularly different seasonal warming patterns generates important impacts on vegetation cycles, energy consumption, and, of course, human health. This is why we suggest that future studies should focus on the analysis of other climatic parameters without ignoring the differentiated seasonal trends.

5. ACKNOWLEDGEMENTS

This work was supported by the strategic grant POSDRU/89/1.5/S/61968, Project ID61968 (2009), co-financed by the European Social Fund within the Sectorial Operational Program Human Resources Development 2007 – 2013.

6. REFERENCES

1. Bojariu, R., Paliu, D. (2001) North Atlantic Oscillation projection on Romanian climate fluctuations in the cold season, *Climate Change and Associated Impacts*, 345-356.
2. Bordei, N.I. (2008) *Fenomene meteorologice induse de configuratia Carpatilor in Campia Romana*, Ed. Academiei Romane, Bucuresti;
3. Burada, C., Sandu, O. (2009) The July 2007 Heat Wave in Oltenia (South-West of Romania) in the Context of Climate Change, *Geographia Technica*, no. 1, Cluj Napoca.
4. Busuioc, A., Dumitrescu, Al., Soare, E., Orzan, A. (2007) Summer Anomalies in 2007 in the Context of Extremely Hot and Dry Summers in Romania, *Romanian Journal of Meteorology*, Vol. 9, No. 1-2, 47-54.
5. Easterling, D.R., Horton, B., Jones, P.D., Peterson, T.C., Karl, T.R., Salinger, M.J., Parker, D., Razuvayev, V., Plummer, N., Jamason, P., Folland, C.K. (1997) Maximum and minimum temperature trends for the globe, *Science*, V. 277, 364-367.

6. Easterling, D.R., Karl, T.R., Gallo, K.P., Robinson, D.A., Trenberth, K.E., Dai A. (2000a) Observed Climate Variability and Change of Relevance to the Biosphere. *Journal of Geophysical Research* 105:20,101-20,114.
7. Easterling, D.R., Meehl, G.A., Parmesan, C., Changnon, S.A., Karl, T.R., Mearns, L.O. (2000b) Climate Extremes: Observations, Modelling, and Impacts. *Science* 289:2068- 2074.
8. Easterling, D.R. (2002) Recent Changes in Frost Days and the Frost-Free Season in the United States. *Bulletin of the American Meteorological Society* 83:1327-1332.
9. Jones, P.D., New, M., Parker, D.E., Martin, S., Rigor, I.G. (1999) Surface Air Temperature and Its Changes over the Past 150 Years. *Reviews of Geophysics* 37:173-199.
10. Karl, T.R., Knight, R.W., Baker, B. (2000) The record breaking global temperature of 1997 and 1998: Evidence for an increase in the rate of global warming? *Geophys. Res. Lett.,* 27, 719–722
11. Karoly, D.J., Braganza, K., Stott, P.A. Arblaster, J.M., Meehl, G.A., Broccoli, A.J., Dixon, K.W. (2003) Detection of a Human Influence on North American Climate. *Science* 302:1200-1203.
12. Klein Tank, A.M.G. et al. (2002), Daily dataset of 20thcentury surface air temperature and precipitation series for the European Climate Assessment. *Int. J. Climatol.,* 22, 1441–1453.
13. Luterbacher, J., Dietrich, D., Xoplaki, E., Grosjean, M., Wanner, H. (2004) European Seasonal and Annual Temperature Variability, Trends, and Extremes, *Science 5,* Vol. 303. no. 5663, pp. 1499 – 1503;
14. Nicholls, N, Gruza, G.V., Jouzel, J., Karl, T.R., Ogallo, L.A., Parker, D.E. (1996) Observed climate variability and change. In *Climate Change 1995: The Science of Climate Change*, Houghton JT, Filho LGM, Callander BA, Harris N, Kattenberg A, Maskell K (eds). Cambridge University Press: Cambridge; 133–192.
15. Tomozeiu, R., Busuioc, A., Stefan, S. (2002), Changes in the seasonal mean maximum air temperature in Romania and their connection with large scale circulation, *Int. Journal of Climatology* 22, 1181-1196;
16. Trenberth, K.E., Jones, P.D., Ambenje, P., Bojariu, R., Easterling, D., Klein Tank, A., Parker, D., Rahimzadeh, F., Renwick, J.A., Rusticucci, M. (2007) Observations: Surface and Atmospheric Climate Change, *The physical science basis. Contribution of Working Group I to the Fourth Assessment Report of the Intergovernmental Panel on Climate Change*, Cambridge University Press.
17. Vladuţ, A. (2007), The pluviometric and thermal regime within the Oltenia Plain*, Analele Universităţii din Craiova, Seria Geografie*, vol. X, Serie Nouă, Editura Universitaria, Craiova, 21-28.

Climatic and Topoclimatic Features within the Rural-Urban Fringe of Craiova City

Sorin Avram, Alina Vladut, Gheorghe Curcan
University of Craiova, Geography Department, str. Al. I. Cuza, nr. 13, Craiova, Romania

***Abstract**: Climatic and topoclimatic features highly influence the inhabitancy potential and the social-economic development of an area. Thus, the analysis of the main climatic features of Craiova urban-rural fringe, illustrated that climate represented a favourability factor in the area. At the same time, human activities influence climate, generating specific topoclimatic conditions, which are more obvious within the urban space, especially in residential and industrial areas.*

***Key words**: climate, topoclimate, rural-urban fringe, Craiova, Romania*

1. INTRODUCTION

The main actor of the settlements system is obviously the *city* that through its position and rank influences, on a greater or smaller distance, all the other settlements. The term rural-urban fringe underwent various mutations until it acquired its present meaning. Thus, the semirural surface located in the immediate proximity of the urban perimeter was characterized by terms as ruralized area [1], ex-urbs [2], semi-urban surface, technoburbs [3], post-suburban surface [4], while presently, urban fringe [5] or even urban-rural interface seem to be the most adequate terms. The Oxford Dictionary of Geography considers the fringe as the urban-rural transition area; however, the fringe also represents the transition area between what is urban and suburban, land use being the defining criteria (sport grounds, airports, malls, parks, which make the rural area acquire an urban aspect). In China, the rural-urban fringe is defined as the surface located out of the urban periphery/the limit of the built surface up to the rural region. The term fringe is preferred instead of peri-urban as it is considered that the city alters the features of the fringe and not vice versa [6].The physical characteristics of the natural environment play an important role in the inhabitancy and social and economic development potential of an area. Thus, by rendering the main climatic features and establishing the topoclimates of Craiova rural-urban fringe we aimed at displaying its favourability for anthropogenic activities.

2. STUDY AREA, DATA, AND METHODS

The metropolitan area of Craiova is mainly located within Dolj Country, except for the secondary urban pole Balş that administratively belongs to Olt County. Even if the city has almost 300,000 inhabitants (together with the 7 suburban settlements that belong to the city), in the near future, Craiova will have to assume numerous local and regional responsibilities. Implicitly, at the level of 182,057 ha and 31 settlements (Fig. 1) (4 urban settlements and 27 rural settlements) of the rural-urban fringe, environmental mutations are complex and continuous and the anthropogenic factor gradually intensifies its print modifying and altering the environment and, of course, climate conditions.

The data used in the present study were supplied by the Statistics Directorate, the Regional Meteorological Center Craiova, the Environment Agency, as well as by own instrumental measurements performed in the last three years. We used topographical maps 1:25,000, orthophotoplans, ArcGis 9.3 for generating topoclimatic maps.

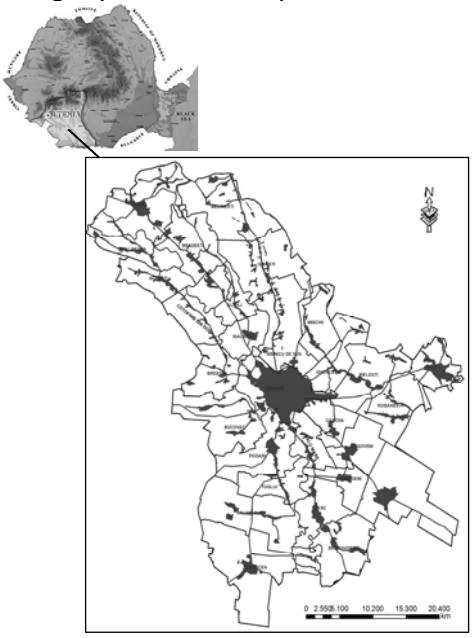

Fig. 1 Craiova rural-urban fringe

3. RESULTS AND DISCUSSIONS

3.1 General climatic features

The general features of the climate within the rural-urban fringe of Craiova are mainly induced by its geographical location and the general

aspect of the relief, characterized by reduced altitudes, generally below 200 m, lack of major obstacles that favours the penetration of various air masses. The presence of the Carpathian Mountains in the north and west imposes certain restrictions for the penetration of western and northern air masses. Thus, the entire region is under the influence of Mediterranean, Euro-Asian, and Atlantic baric centres, with the predominance of the south-European ones [7]. Global radiation reaches 124 Kcal/cm^2, 70-75 Kcal/cm^2 being represented by direct solar radiation. The highest monthly amount is registered in June, about 23 Kcal/cm^2 and the lowest in December, only 5.5-7 Kcal/cm^2. Thus, the radiation balance oscillates between 45 and 48 Kcal/cm^2, being negative (-1.0 Kcal/cm^2) in January and December and positive throughout the rest of the year (7.5 Kcal/cm^2 in spring; 8.0 Kcal/cm^2 in summer).

Main climatic parameters. Air temperature. The mean annual temperature (1970-2009) at Craiova station is 10.9°C (Fig. 2), the month with the highest mean value (22.4°C) being July and the month with the lowest mean (-1.2°C) January. The mean multiannual amplitude is 23.6°C. On the background of some particular synoptic situations, there occur positive and negative deviations. Thus, the highest annual temperature reached 12.5°C in 2000, while the lowest value was 9.5°C in 1976 [8]. With regard to the maximum temperatures mean, the curve is similar to the one of the mean values, meaning a gradual increase from January till July and then a gradual decrease with 4-7°C from one month to another until December. All the values are positive, varying between 2.5°C and 29°C. The minimum temperatures mean is negative in winter (January -4.4°C, February -2.8°C, December -2.9°C) and it remains below 16°C even the July, 15.8°C.

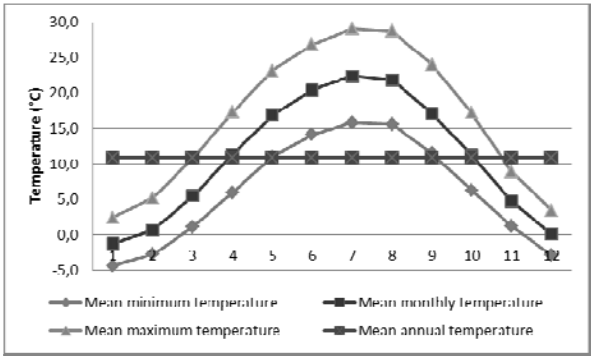

Fig. 2 Mean temperatures at Craiova station (1970-2009)

As absolute maximum and minimum temperatures are concerned, we mention the values of 41.5°C registered on July 5, 1916 and -35.5°C on January 25, 1963. Thus, the absolute maximum amplitude reached 77°C. Generally, the maximum temperatures exceed 33°C, but, in the last ten years, there were numerous cases when temperature was higher than the 40°C

threshold. The minimum temperatures generally oscillate between -13°C and -23°C.

Atmospheric precipitations. The mean annual amount of precipitation, calculated as mean for the interval 1970-2009, is 601.3 mm, 353.8 mm representing 58.83% of the annual mean being registered in the warm season and the rest of 247.5 mm in the cold season (41.17%). Referring to seasonal distribution, the lowest amounts are characteristic in winter (114.1 mm), when anticyclone regime predominates, while in summer, on the background of the intensification of the cyclone activity, as well as of local thermal convection, there is registered the highest amount (192.1 mm). As a particularity of the region, the amounts registered in spring and autumn do not show a great difference (149.8 mm, respectively 142.3 mm), due to the increase of the Mediterranean cyclone activity, especially in November and December. The greatest monthly precipitation amount corresponds to June – 74.2 mm and the lowest to February – 33.5 mm (Fig. 3).

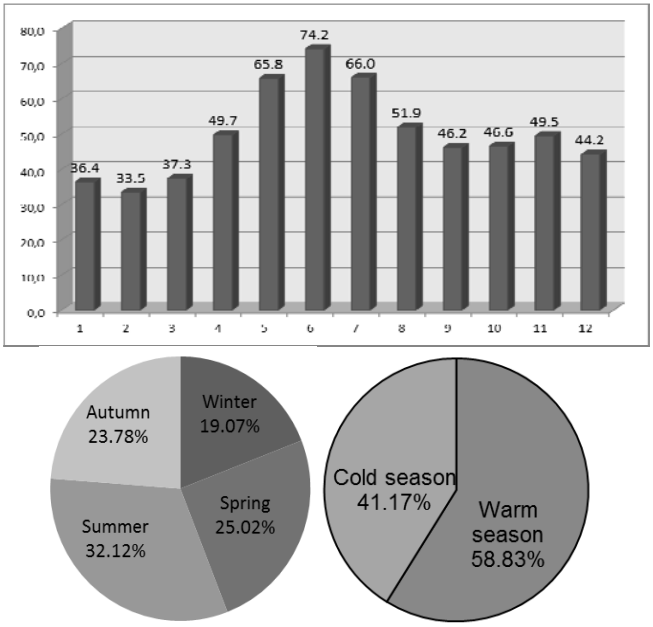

Fig. 3 Mean monthly, seasonal, and semester precipitation amounts at Craiova station (1970-2009)

From the social-economic viewpoint, maximum precipitation amounts in 24 h, as well as drought phenomena have a great impact. The analysis of the climatological data revealed that the frequency of the amounts above 60 mm/24 h increased in the last 20 years. The largest amounts were registered in 1999 (71.9 mm in June and 77.2 mm in September), 2003 (77.6 mm in April) and 2009 (74.2 mm in July) (Fig. 4), which in many cases represents an amount above the multiannual mean. Generally, such

amounts are due to torrential rainfalls characteristic during the warm season. We remark July with about 33% of the number of cases (the greatest amount in 24 h during a year), as well as June and August, which are months characterized by a very active thermal convection that enables the development of local Cumulonimbus clouds.

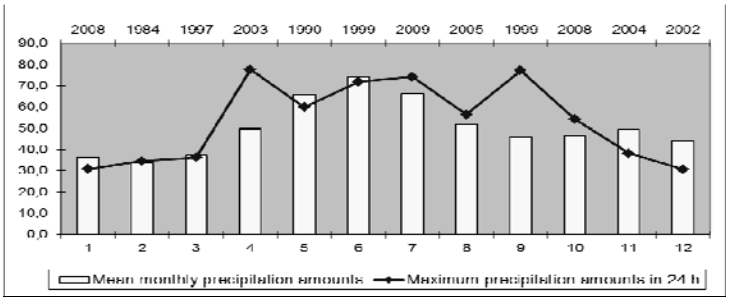

Fig. 4 Maximum precipitation amounts in 24 h (1970-2009)

Drought and dryness phenomena affect the perimeter of the fringe especially in the second part of summer; under certain circumstances, drought starts even in spring. We noticed an increase of the frequency and intensity of these phenomena, mainly in the decade 1991-2000 (the two driest years in the last 50 years: 1992 – 293.5 mm and 2000 – 339.0 mm), which was followed by a period marked by precipitation excess at annual level, but with drought period in July-August (2003, 2004, 2007).

Wind features. Wind characteristics are highly important if we refer to population’s health state within the fringe. The dispersion of pollutants depends on the location of the industrial units and wind main direction and speed. There predominate the winds from eastern and western sector, 21.4%, respectively 22.1% of the total number of cases. Atmospheric calm also holds a high rate – 24.6% (Fig. 5, Fig. 6). Mean annual speed is 3.7 m/s, while maximum speed can reach 28-29 m/s.

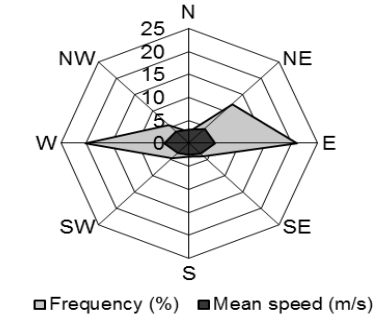

Fig. 5 Wind frequency and mean speed at Craiova (1970-2009)

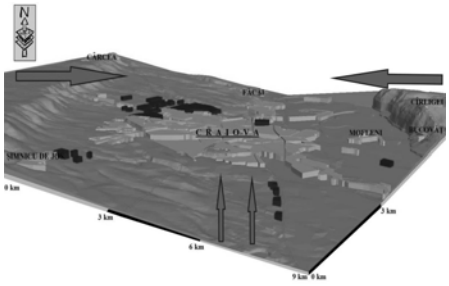

Fig. 6 The culoir effect for air masses circulation

3.2 Topoclimatic features

The features of the active surface represent the main factor that triggers territorial differences of the climatic parameters, generating a series of topoclimates within the area of Craiova rural-urban fringe. According to the preponderance of the influence factor, we distinguished between *natural topoclimates* (generated by the presence of forests, different crops or aquatic units, altitude, shape, inclination and exposition of slopes, etc.) and *anthropogenic topoclimates* [9] (mainly induced by the physical characteristics of the construction materials, height, density, and disposition of the buildings, by the characteristics of the sewerage system, distribution of green spaces, sources of artificial heating and air pollution, etc.) (Fig. 7).

In the category of natural topoclimates, we identified – valley topoclimate, forest topoclimate, lakes topoclimate, crops and meadows topoclimate. Even if the analysed surface is not very large, it is quite inhomogeneous. The Jiu river develop its entire terrace system on the left, the right slope being steep, high and without terraces. At the same time, most of the river alluvial plain develops on the left, as well. Thus, the altitude difference (> 100 m) between the upper terrace and the alluvial plain influences the values of the meteorological parameters.

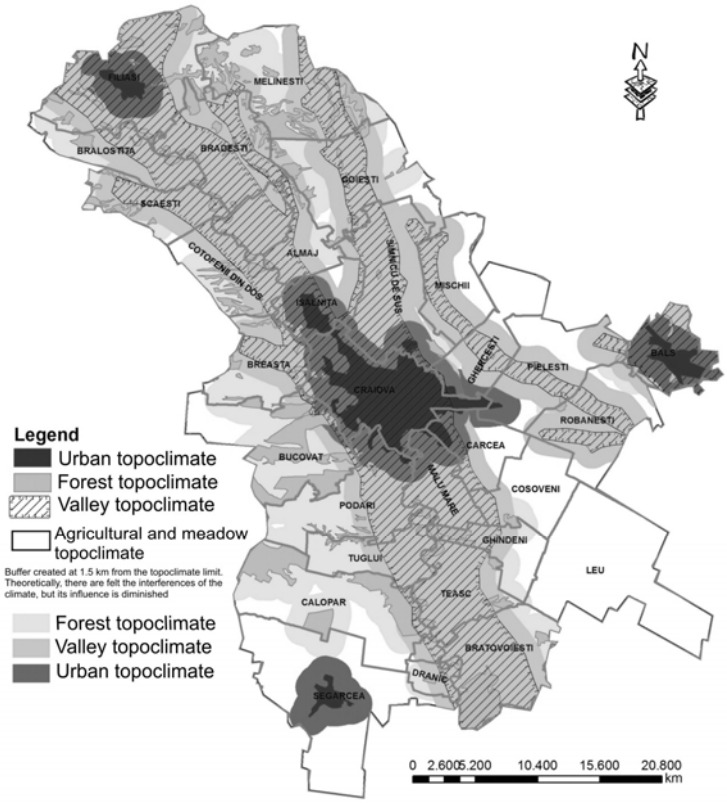

Fig. 7 Topoclimates within the perimeter of Craiova rural-urban fringe

The local measurements indicated a slow thermal inversion, especially in winter, between the alluvial plain (Balta) and the top of the terrace (TAROM) (Fig. 8), with differences of 2-3°C induced by the stagnation of cold dense air on the bottom of the valley. In summer, the temperatures registered in the low area are higher due to the sheltering effect that does not favour air intense circulation. Besides altitude, there are other factors that trigger differences of the climatic parameters. We refer to the soil type, as in the neighbourhood of the river, in the areas covered by sand air temperature is 3 to 4°C higher than in the areas with vegetation. The measurements indicated large differences, up to 6°C between forests and (in the north – Melineşti and west – Bucovăţ, Capolăr) and areas covered by meadow or crop vegetation that cover large surfaces towards the external limit of the fringe. The presence of aquatic units (Craioviţa Pool, Tanchiştilor Lake, Işalniţa Lake, the reservoirs located on the Preajba Valley) determines the development of a lake topoclimate, characterized by greater values of the relative humidity, smaller diurnal and annual thermal amplitudes. Their influence is reduce, as data indicated differences only on

small surfaces located in their immediate proximity, maximum 200-300 m around.

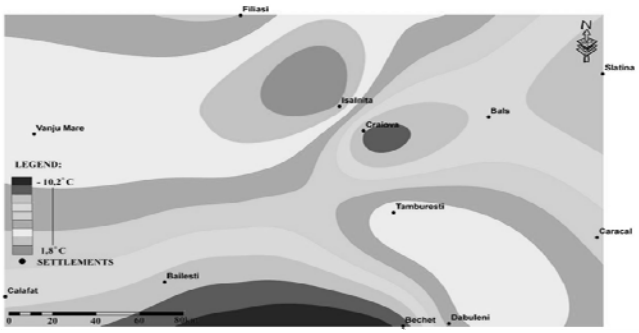

Fig. 8 Spatial distribution of the minimum temperatures in February 2003 within Craiova rural-urban fringe

In the category of anthropogenic topoclimates, we identified several types – the topoclimate of the residential areas with tall buildings (the urban area), the topoclimate of the residential areas with small buildings (corresponding to rural settlements), the topoclimate of industrial areas and the topoclimate of green areas (inner city). Generally, the topoclimate of the residential areas with tall buildings is determined by the characteristics of the construction materials – high caloric capacity, reduced caloric conductibility and albedo. This type is characteristic to the main urban pole and to the central parts of the secondary urban poles (smaller towns). Consequently, temperature displays higher values, with greater differences in winter (4-5°C). In Craiova for example, in the central area, which does not have a high rate of green spaces and presents an intense traffic, there appears the effect of heat island (Fig. 9). Humidity and evaporation are lower compared to the open field. The atmospheric calm registers a higher frequency, but there are also situations when wind speed increased due to the couloir effect exerted by tall buildings placed on both sides of large roads. Visibility is also modified, mainly due to the greater amounts of noxae resulted from a more intense traffic.

The topoclimate of the residential areas with small buildings characterizes the built perimeters of rural settlements. Due to a greater homogeneity of the active surface, the differences of temperature, air humidity, wind frequency and intensity compared to the open field are smaller than in the previous case.

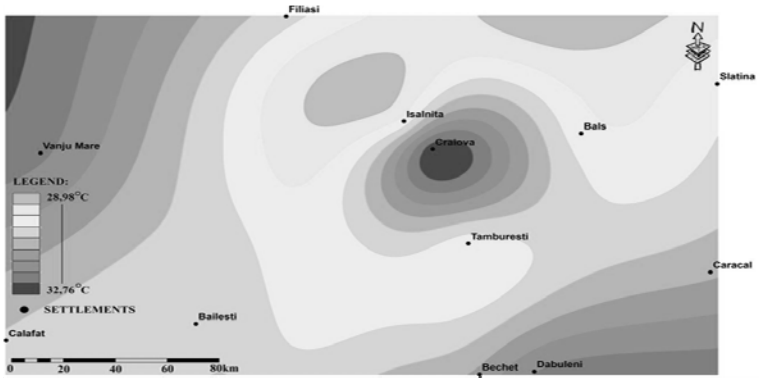

Fig. 9 Spatial distribution of maximum temperatures in July 2007 within Craiova rural-urban fringe

The topoclimate of green areas covers larger surfaces in Craiova (Nicolae Romanescu Park, Balta Craioviţei, Tineretului Park, The Botanical Garden), compared to the other urban settlements. We noticed lower diurnal temperatures and amplitudes by comparison with the residential area (instrumental measurements revealed 2-4°C lower values, especially in summer). Air humidity registers significant increase due to the intensification of evapotranspiration, while wind speed diminishes.

With regard to the topoclimate of the industrial areas, we monitored the areas located in the immediate proximity of the city (the North Industrial Platform – Işalniţa Power Plant and Chemical Combine, Bear Factory, ElPreco, CET Craiova II; the East Industrial Platform – Ford Car Factory, Electroputere, etc.). Besides the thermal differences, the respective areas are mainly characterized by a higher rate of pollutants. The role of solid substances dispersed in the atmosphere should not be ignored as they influence fog and low clouds formation. We noticed the situations characterized by turbulence when ash wastes located near CET Işalniţa and CET Craiova (II) are affected by vortexes that rise huge amounts of impurities, reduce visibility and contribute to the increase of the number of days with fog.

5. CONCLUSIONS

The analysis of the main climatic parameters in the area of Craiova fringe emphasized that climate is generally favourable for the development of social-economic activities. On the background of a temperate moderate continental climate, there occur certain phenomena that affect activities – drought, dryness, extreme heat, fog, torrential rainfalls etc. Some of these phenomena have entirely natural causes, but, the impact of the others is enhanced by human activities. At the same time, settlements especially

modify the general features of the climate leading to the development of topoclimates. On the basis of the meteorological data (supplied by the stations located in the area and sampled by our research team in the last years), we identified several natural and anthropogenic topoclimates. The last category caught our attention as built perimeters continuously extend reducing the surfaces covered by forests and meadows. Thus, we consider this study just a preliminary stage of a wider research the purpose of which is to render the way climate can be modified locally and regionally by anthropogenic factor.

REFERENCES

1. Doherty, N., (1970), Rurality, Poverty and Health: Medical Problems in rural Areas, *Economic Research*, Washington
2. Spectrosky, A. C. (1955), *The Exurbanites*. Lippincott, Philadelphia
3. Fishman, R., (1990), *Megalopolis unbound*, Wilson Quarterly Winter
4. Garreau, J., (1991), *Edge City: Life on the New Frontier*. Doubleday. New York
5. Pryor, R.J. (1968): Defining the Rural-Urban Fringe. *Social Forces* 47: 202-215
6. Xu Feng, (2004*), Modelling the spatial patterns of urban fringe – Case study Hongshan (Wuhan), International Institute for Geo-Information Science and Earth Observation*, Enschede, Netherland
7. *** (1962), *Clima RPR,* I, IM, Bucureşti;
8. Vladuţ, A. (2007) The pluviometric and thermal regime within the Oltenia Plain*, Analele Universităţii din Craiova, Seria Geografie*, vol. X, Serie Nouă, pag. 21-28, Editura Universitaria, Craiova
9. Dumiter, A.F (2007) *Clima si topoclimatele orasului Oradea,* Ed. Universitatii din Oradea, Oradea

ENVIRONMENTAL IMPACTS OF TOURISM IN PIRIN NATIONAL PARK

Antoaneta Milikina
Department of Geography, Ecology and Environment Protection, Faculty of Mathematics and Natural Science, South- West University “Neofit Rilski”, 66 Ivan Mihailov Str., 2700 Blagoevgrad, Bulgaria, e- mail: tonika_77@abv.bg

Abstract: *Environmental impacts of tourism relate primarily to the effects, positive and negative, that tourism development has on the natural environment.*

With the development of a system of protected areas in Bulgaria are found many cases of destruction of their conservation status as a result of different economic activities or of fraudulent actions of individuals. This causes negative changes in the components of nature or total damage to the natural landscape.

In the report are presented the results of a survey conducted among employees of the park in order to obtain the necessary expert information.

Keywords: *national park, park region, environmental impact, arrangements*

In recent years started paying more attention to questions related to the impacts of tourism on the environment. Tourism should be a key driver of efforts to protect the environment, as in the absence of high-quality environment, tourists would prefer to visit alternative destinations.

Effects (positive and negative) that tourism development has on the natural environment is commonly referred to environmental impacts. [4]

With the development of a system of protected areas in Bulgaria are found many cases of destruction of their conservation status as a result of different economic activities or of fraudulent actions of individuals. This causes negative changes in the components of nature or total damage to the natural landscape. [2] Natural tourism resources have some stocks, which in most cases are limited. This limitation theoretically is determined by their threshold load above which resources are significantly altered in the direction towards less attractive or degrade. Overexploitation of resources always leads to their destruction. [5]

One of the problems associated with the development of tourism is that it does not guide only tourists on threatened areas. Along with them are accommodated and structures to which tourists are accustomed to their place of residence and the necessary accommodation base and infrastructure needed to meet their needs. [3]

Activities violating the status of protected areas may be conditionally divided into several groups:

Business

Often the various businesses represented distortion factor of the environment in protected areas (construction of roads, ski runs, building the equipment and unfolding villa construction undertaken in close proximity to the boundaries of protected areas; harvest; fisheries; grazing cattle; picking of herbs, wild berries and mushrooms and other)[2]

Pollution by waste

There is in all protected areas that are subject to tourist visits.

Pollution by waste leads to a number of negative changes in components of the environment and to violation of the aesthetics of the landscape on which it loses its attractiveness to tourists. [5]

Damage or destruction of facilities

To this group of activities refers- damage or destruction of lighting, fences, buildings, guard rails, bridges, fountains, tables, benches and bowers, indicative and illustrative plates, signs, information boards; displaced information arrows and other.

Damage or destruction of natural formations

The development of speleotourism prejudices the speleological heritage in karts region. In many caves are destroyed caves formations and are disturbed their occupants.

Excavations of treasure hunters

Much of the historical and archaeological sites located in protected areas and adjacent territories (settlements around them) are subject to mass tourist visits, which harms the environment around and within them. Natural and historical attractions are subject to abuse and deception regarding by visitors as collection of minerals, rocks and fossils; production of unique rock formation for souvenirs and other.

Exploratory activities

Although rare, disorders of the nature of the protected areas are caused by different types of studies- geological, geophysical and archaeological. [2]

Pollution of the three components- air, water and soil

The main causes of air pollution can be summarized as follows:

1. Traffic on the huge flow of vehicles during peak periods;
2. Pollution of air environment from the noise;
3. Air pollution during the tourist season from the separation of gas emissions and harmful huge amount of dust in the production of electricity from local sources;
4. Air pollution from the release of harmful gas emissions in local and central heating.

The main causes of water pollution can be summarized as follows:

1. Water pollution due to discharge of untreated wastewater;

2. Lack of environmental consciousness by tourists;

3. Increasing numbers of vessels.

The reasons for the negative impacts of tourism on soil and rock composition of the earth as a whole are as follows:

1. Soil compaction due to overload of tourists and non-compliance of walking trails lead to distortion of the mineral composition;

2. Large scale felling of forests caused erosion and increased the risk of avalanches;

3. Occurrence of fires.

Damage to the flora and fauna

Species diversity of organisms’ decreases with each passing day as a result of human activity and human ambitions to derive maximum dividends from tourism development without complying with the laws of nature. The most common causes of damage are:

1. The construction of tourist facilities and accommodation base leads to the disappearance of valuable vegetation and many small animals and insects;

2. The construction of roads, cableways and other engineering facilities of the infrastructure network lead to imbalances in the ecological balance in certain territories;

3. The poaching;

4. Disappearance of plant and animal species in areas of mass tourism. [3]

Other disorders

To this category may be referred:

1. Uncontrolled penetration and crowding of large masses of people in the recreational forest areas. The presence of even one person does not pass without a trace. In the mass tourist visiting the process of destruction outrun the recovery process. The loss of ecosystem’s sustainability is a result of modification of all its components. [1]

2. Uncontrolled entry and movement of motor vehicles in protected areas. The consequences of that are: air pollution by waste gases, pollution of rivers and lakes and increase in noise.

3. Willfully camping of tourists- use of facilities for the construction of camps in places where not permitted and thus unfair behavior of tourists cause direct harm to the living nature. [5]

4. Fires caused by indiscriminately burning of fires. Burning in the forest fire, except that it carries a risk of fire, ravaged piece of land, which was located about 5-7 years. [1]

One of the methods used to study the environmental impacts of tourism in Pirin National Park is the inquiry method.

In the report are presented the results of a survey conducted among employees of the park in order to obtain the necessary expert information.

The territory of Pirin National Park is divided into five park regions (PR). With the permission of the Director of the park were interviewed 10 employees, two of each park area.

Based on the specified responses from the questionnaire was formulated type of violations found within the area of respondent officer and measures taken to their elimination, the answers of employees in one park region matched.

Tab.

№	Type of violation	Park region	Taken measures
1	Trodden grass	„Vihren"- Bansko „Bayuvi dupki"- Razlog „Sinanica"- Kresna	Installing warning boards
2	Erosion	„Vihren"- Bansko „Kamenica"- Sandanski „Bezbog"- Dobrinishte	Strengthening
3	Waste scattered outside the regulated site	„Vihren"- Bansko „Bayuvi dupki"- Razlog „Sinanica"- Kresna „Bezbog"- Dobrinishte	Cleaning of park guards
4	Contaminated water areas with waste from tourists	„Bezbog"- Dobrinishte	1. Installing warning boards; 2. Cleaning of park guards;
5	Fires outside the regulated site	„Vihren"- Bansko „Bayuvi dupki"- Razlog „Sinanica"- Kresna „Kamenica"- Sandanski	1. Installing warning boards; 2. Composition of a protocol;
6	Tension tents of unauthorized places	„Vihren"- Bansko „Bayuvi dupki"- Razlog „Sinanica"- Kresna „Kamenica"- Sandanski	1. Control; 2. Composition of a protocol;
7	Damaged information boards	„Vihren"- Bansko „Bayuvi dupki"- Razlog	Replace with new
8	Damaged tables, benches and bowers	„Vihren"- Bansko „Bayuvi dupki"- Razlog „Sinanica"- Kresna	Repair
9	Illegal hunting	„Vihren"- Bansko „Sinanica"- Kresna	Composition of an act
10	Illegal fishing	„Sinanica"- Kresna	Composition of an act
11	Illegal logging	„Bayuvi dupki"- Razlog	Composition of an act
12	Illegal grazing	„Sinanica"- Kresna „Kamenica"- Sandanski	Composition of a protocol
13	Inappropriate ways of gathering herbs and mushrooms	„Bayuvi dupki"- Razlog „Bezbog"- Dobrinishte	Installing warning boards
14	Illegal business	„Bayuvi dupki"- Razlog	Composition of an act

On the territory of Pirin National Park are established 14 types of violations in park regions as follows:

„Vihren”- Bansko- 8 types of violations;

„Bayuvi dupki”- Razlog- 9 types of violations;

„Sinanica”- Kresna- 8 types of violations;

„Kamenica”- Sandanski- 4 types of violations;

„Bezbog”- Dobrinishte- 4 types of violations;

Highest number of violations are found in Bayuvi Dupki - Razlog (9), followed by Vihren - Bansko and Sinanitsa - Kresna (8) and at least number of violations are found in Kamenitza - Sandanski and Bezbog – Dobrinishte (4).

Most often are found 10 (from 14) types of violations- Trodden grass; Erosion; Waste scattered outside the regulated site; Fires outside the regulated site; Tension tents of unauthorized places; Damaged information boards; Damaged tables, benches and bowers; Illegal hunting; Illegal grazing; Inappropriate ways of gathering herbs and mushrooms.

Management and planning of environmental impacts is important for the sustainable development of destinations, because the tourism and the lives of local people depend heavily on the quality of the environment. This makes their studying very necessary. The question about the study of these effects is still standing "open" due to the complex and dynamic nature of the environmental impacts of tourism.

REFERENCES

[1] Marinov, M. (1980) *Reproduction and conservation of forest ecosystems*. Sofia;

[2] Stoilov, D. (1997) *Fundamentals of environmental engineering*. Blagoevgrad;

[3] Vodenska, M. (2001) *Economic, social and environmental impacts of tourism*. Sofia;

[4] Vodenska, M. (2006) *Tourism and society*. Sofia;

[5] Zhechev, V., D. Stoilov (1999) *Tourist natural resources and ecotourism*. Blagoevgrad;

Weather station at SWU – statistical analysis and reports

Mavrevski R. [1] **and Stoilov A.** [2]

[1]*Department of Informatics; South-West University, Ivan Mihailov Str. 66, 2700 Blagoevgrad, Bulgaria;* [2]*Department of Physics; South-West University, Ivan Mihailov Str. 66, 2700 Blagoevgrad, Bulgaria*

Abstract*: A weather station is a facility, either on land, with instruments and equipment for observing atmospheric conditions to provide information for weather forecasts and to study the weather and climate. The measurements taken include temperature, barometric pressure, humidity, wind speed, wind direction and etc. In this study are present results from such facility installed at South-West University of Blagoevgrad, Bulgaria. Statistical analysis and reports were conducted for month and yearly.*

Keywords: *weather station, temperature, pressure, humidity, wind speed;*

1. INTRODUCTION

Unmanned weather stations play an essential role in the effort to analyze and predict the world's ever-changing weather patterns. The unmanned stations, based on sensors investigation, collect large amounts of weather data and then download the data in real time to a back-end host for analysis and long-term storage. The present wireless weather station is composed of a remote station and a base station. Monitoring weather conditions or environmental parameters is paramount for agriculture, sailing, flying and more.

2. METHODS

The base station La Crosse WS2350 measures the indoor environment of its surrounding area and receives weather data from the following three outdoor sensors:

1) Thermo-Hygro Sensor
2) Wind Sensor
3) Rain Sensor

The meteorological sensors transform the data measured onto electric current. The received data is continuously updated to bring you the latest weather information on the base station’s LCD (receiver). The thermo-hygro sensor is the main data communication unit since both the wind and rain sensors are connected to the thermo-hygro sensor for operating power and rely on it to communicate to the base station. Weather data sent from the thermo-hygro sensor can be done by wireless 433MHz transmission (up to 100 meters in open space) or by cable connection.

The thermo-hygro sensor measures the outdoor temperature and relative humidity. It also collects the readings from the rain and wind sensors before transmitting the data to the base station by wireless 433MHz or by the 10 meter cable included in this set.

The wind sensor measures wind speed and wind direction and sends the data to thermo-hygro sensor which in turn transmits the data to the base station. Operating power is taken from the thermo-hygro sensor using a 10 meter cable connection.

The rain sensor measures the rainfall and sends the data to thermo-hygro sensor which in turn transmits the data to the base station. Operating power is taken from the thermo-hygro sensor by a 10 meter cable connection. Using 433MHz wireless transmission of weather data from the sensor to the base station will provide users greater freedom as to where units can be positioned without the need to be restricted by cable.

2.1. Technical specification

The technical specification of weather station was present in Tab.1.

Tab. 1: Technical specification of weather station La Crosse WS2350

Parameter	Unit	Range	Precision	Accuracy
Barometric Pressure	hPa; mmHg	300 hPa ÷ 1099 hPa	-	-
Indoor Temperature	°F ; °C	–9.9 °C ÷ +59.9 °C	0.1 °C	-
Indoor Humidity	% RH	1 % ÷ 99 %	1 %	+/- 3 %
Outdoor Temperature	°F ; °C	–29.9 °C ÷ +69.9 °C	0.1 °C	-
Outdoor Humidity	% RH	1 % ÷ 99 %	1 %	+/- 3 %
Wind Speed	km/h; m/s; mph	1 m/s ÷ 49.9 m/s	-	-
Rain Gauge	mm; inch	0 mm ÷ 999.9 mm	0.5 mm	-

2.2. Weather station - installation and operation

Weather station is located in the courtyard of South-West University (Fig.1). Sensors are located 2 meters above the grass. Thermo-Hygro Sensor is located in the Stevenson screen. Receiver module is located 40 meters line of sight from the transmitter in a specialized laboratory. Coordinates of measurement unit are 42^0 01" N and 23^0 02" E. This weather station consists of a base station and three sensors and software for use to upload all weather data from the base station to the Internet. The base station measures the indoor and receives the outdoor weather information from 3 outdoor sensors (thermo-hygro, wind and rain sensors).

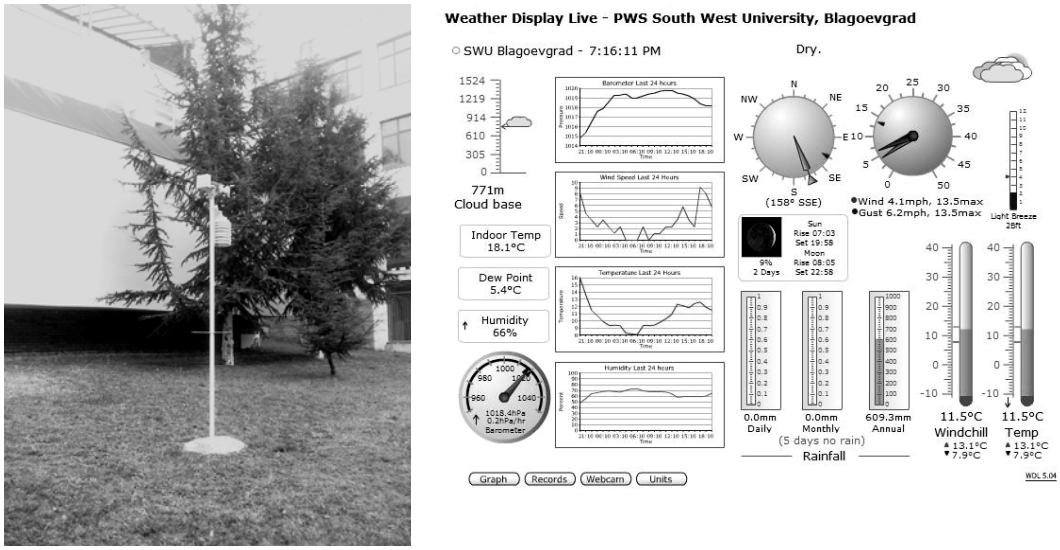

Fig.1. Weather station view and software

3. RESULTS AND DISCUSSIONS

3.1. Reports

Weather station was full-time operated in 2009. The sample rate of measured data was 1 min. This provided possibility to summarize the data obtained and presented in table (Tab.2) and graphics (Fig.2) on annual report.

Tab. 2: Metrological data for each month of 2009, Blagoevgrad, Bulgaria

Month	Temperature, C	Pressure, kPa	Wind speed, m/s	Monthly rain, litre	Dew point	Heat index
JAN	4.88	961.69	0.93	67.30	2.10	4.94
FEB	2.81	964.03	1.78	12.20	-2.16	2.85
MAR	6.71	964.58	1.81	48.20	0.49	5.63
APR	13.37	967.61	1.12	82.20	4.66	13.93
MAY	18.17	968.98	1.43	17.50	8.09	23.80
JUN	22.84	965.54	2.82	59.40	8.74	23.12
JUL	23.89	966.74	3.75	18.50	14.03	24.94
AUG	24.85	968.53	3.64	32.90	14.43	25.55
SEP	20.68	969.88	3.06	17.40	11.86	21.68
OCT	12.97	967.67	3.44	48.20	8.13	13.55
NOV	7.78	969.12	2.16	32.90	4.02	7.78
DEC	5.65	962.95	2.95	84.40	3.06	3.50

The measured data were averaged for individual months (temperature, pressure, wind speed, dew point and heat index), for the monthly rainfall data are presented cumulatively.

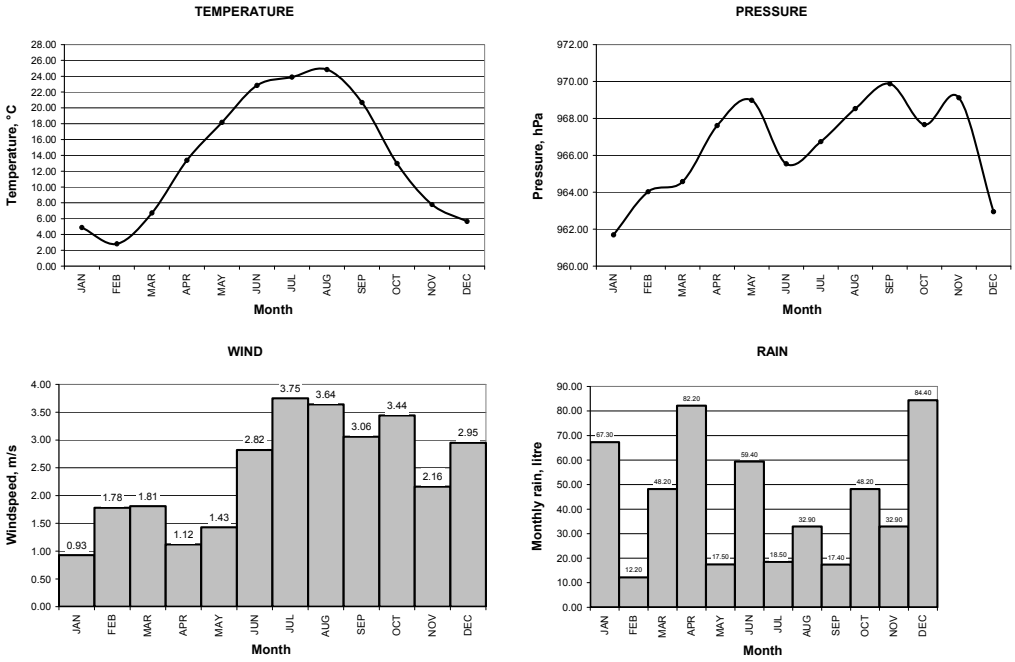

Fig.2. Graphical yearly report for 2009 – temperature, pressure, wind speed and monthly rain

Relative humidity is the amount of water vapor held in suspension in a air-water mixture. The relative part of humidity refers the percentage of water vapor in the air-water suspension versus the amount of total amount of water vapor the air-water mixture at a given temperature.

Dewpoint is the temperature in which air must be cooled at a constant barometric pressure for water vapor to condense in to water.

Heat index is the "human-percieved" temperature. This measurement is rather subjective and can be the subject of speculation.

Barometric Pressure (sometimes called Atmospheric Pressure), is the measurement of pressure exerted by the atmosphere.

3.2. Discussions

Apart from the main meteorological parameters that were measured also was calculated average dew point and heat index (Fig.3.).

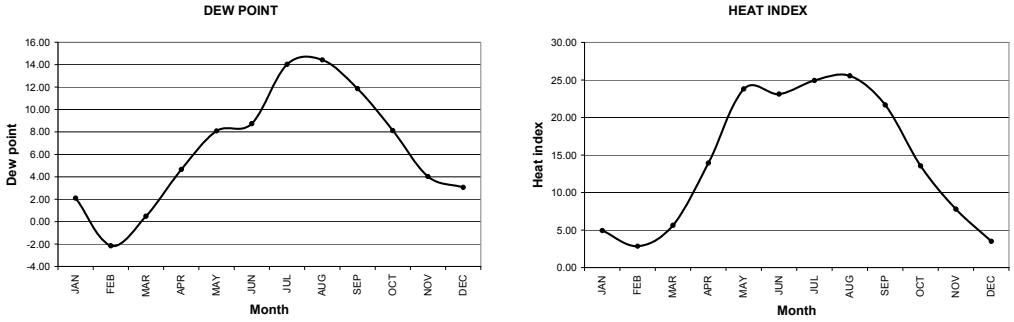

Fig.3. Dew point and heat index graph

4. CONCLUSIONS

The weather station can be used in a large area: weather forecasting, commercial and private farms, agricultural engineers, agronomy researchers. The system use vanguard techniques like: wireless transmitting, Power Line Comunications, Field Point modules. The station is based around state-of-the-art instrumentation that features proven reliability, even in harsh environments.

5. REFERENCES

[1] Allen, R. G., Brockway, C. E., and Wright, J. L. 1983. Weather station siting and consumptive use estimates. J. Water Resour. Ping, and Mgmt. Div., ASCE 109 (2): 134-146.

[2] Fuchs, M., and C. B. Tanner, 1965: Radiation shields for air temperature thermometers. J. Appl. Meteor., 4, 544–547.
[3] Nachtigal, C. L., 1990: Instrumentation and Control: Fundamentals and Applications. Wiley-Interscience, 890 pp.
[4] Tanner, B. D., 1990: Automated weather stations. Remote Sens. Rev., 5, 73–98.
[5] Hubbard, K. G., and X. Lin, 2002: Realtime data filtering models for air temperature measurements. Geophys. Res. Lett., 29, 1425,doi:10.1029/2001GL013191.

Research on Safety of Buildings for Human Evacuation

Veselina Stoyanova, Petya Tsvetkova, Lyuben Elenkov
South-West University "Neofit Rilski", Blagoevgrad, Bulgaria

***Abstract*:** *Increasing safety and security of crowded buildings is a main requirement for designers and builders. Irrespective of the requirements normative documents provide for, infringements are frequently allowed, especially after sites being put into exploitation. They are usually related to furnishing of evacuation routes, offices and rooms faced with improper facing materials and rooms used in contradiction with their functions.*

***Key words**: human evacuation, evacuation routes, ignitable material, safety, experimental researches*

1. INTRODUCTION

Modern housing and facility construction makes use of more and more diverse and new polymeric and ignitable materials widely used for facings, coverings, heat and sound insulations, parts of constructive elements, equipments and furniture. Some of them are capable of liberating quantities of smoke and heat for a short period of time when burning. Combining this with a mistake or flaws in designed and exploited buildings gives extremely dangerous situations in case of fire occurrence. Statistics of many countries on fire and fire damages indicate smoke liberated during combustion to be the reason for 64-73% of human deaths. This makes it necessary for experts to concentrate their efforts on searching and developing new volumetric planning and special technical solutions consistent with the function of buildings and their constructive and architectural requirements. [1,2]

Each second matters for leaving the room and evacuation routes outside building's volume. Not letting planned exits leading outside the building close is of significant importance.

Fire hazard in buildings obliges control bodies in charge for fires and environment protection from harmful contaminations interfere actively for elimination of infringements allowed.

Task Formulation. Purpose of research

Abiding building and occupant safety rules is of significant essence. There are many examples to prove the importance of evacuation from crowded buildings. Even in buildings with greatest safety and security level (the European Parliament in Brussels) are held evacuation trainings. Thus, in 2011, for an instance, a Bulgarian governmental delegation paid a planned visit to the European Parliament in Brussels. Due to the ongoing planned evacuation of parliament occupants at that time, the visit was delayed until the training had been finished.

The purpose of this report is to make a research on a crowded building (Educational Campus No. 2 of the South-West University) and the condition of evacuation routes in particular.

Experimental researches

Evacuation routes’ walls are covered with ignitable materials – panelwork - that has been observed not clinging closely to walls, which is unacceptable. There are mirrors hanged along the evacuation route that might confuse evacuating people. (Fig. 1 and Fig. 2)

Fig. 1

Fig. 2

In order to establish the level of fire hazard of materials in the building of EC No. 2 – velter and panelwork, several experiments have been held to establish their flammability and duration of burning in a complicated hazardous situation.

Experiments have been made with experimental stand. For carrying out the experiment the following materials have been selected and approved– velter and wooden panelwork, Teracol adhesive, fire source – torch, and bucket-pump. Each material – velter and panelwork, has been tested twice

– in the first case on the stand and in the second case – glued on the wall with the adhesive. Materials are ignited with one and the same fire source.

a) b) c)

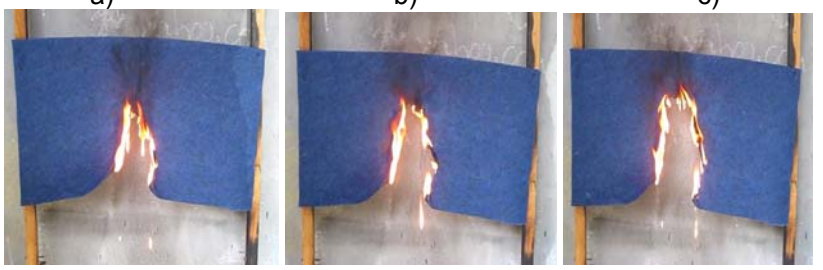

d) e) f)

Fig. 3: Experiment with velter on stand

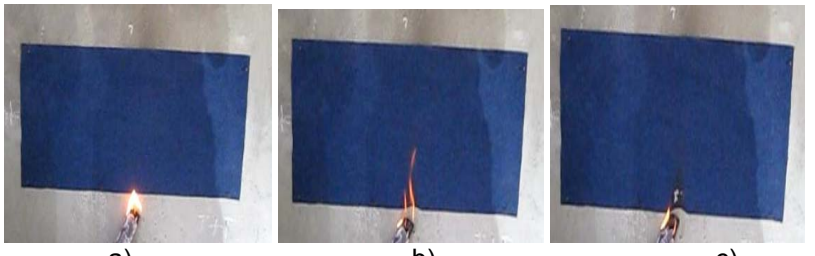

a) b) c)

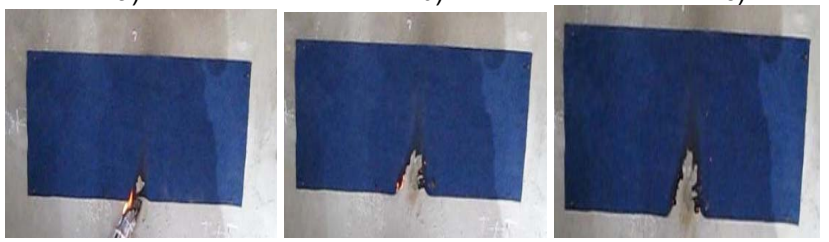

d) e) f)

Fig. 4: Experiment with ignited on the wall velter with Teracol

From the experiment on the stand it has become clear that at the ignition of the velter combustion products start liberating strong parallel smoking (Fig. 3) in different periods of time (5 seconds). It is obvious from the figure that after taking away the fire source, material burns independently and strong suffocant smell liberates.

In the case with closely glued on the wall velter (fig 4), the longest exposure on the fire source leads to material’s surface scorch and almost insignificant liberation of combustion products. Taking away the fire source makes fire cease.

A complicated situation of smoking, restricted vision and hard breathing might occur in buildings with veltered walls in cases it is nor closely glued on the wall.

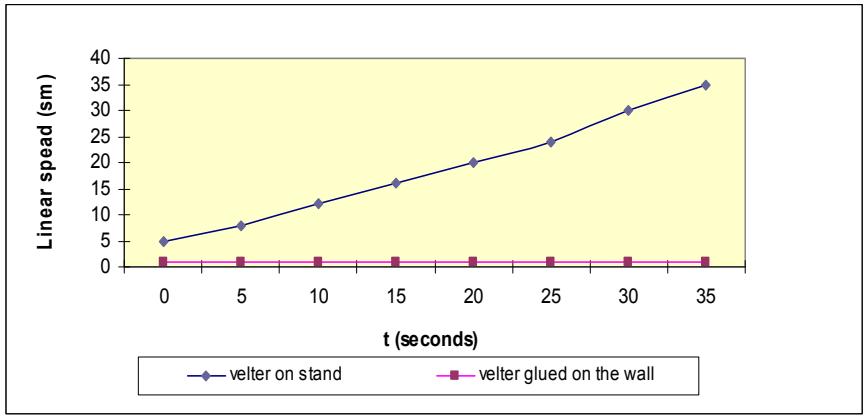

Fig. 5: Comparison of linear burning speed of velter on a stand and velter closely glued on the wall

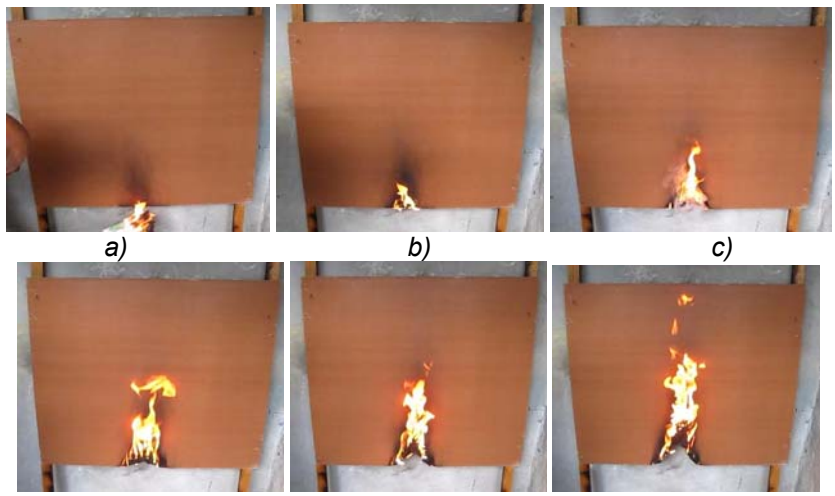

Fig. 6: Experiment with wooden panelwork on a stand

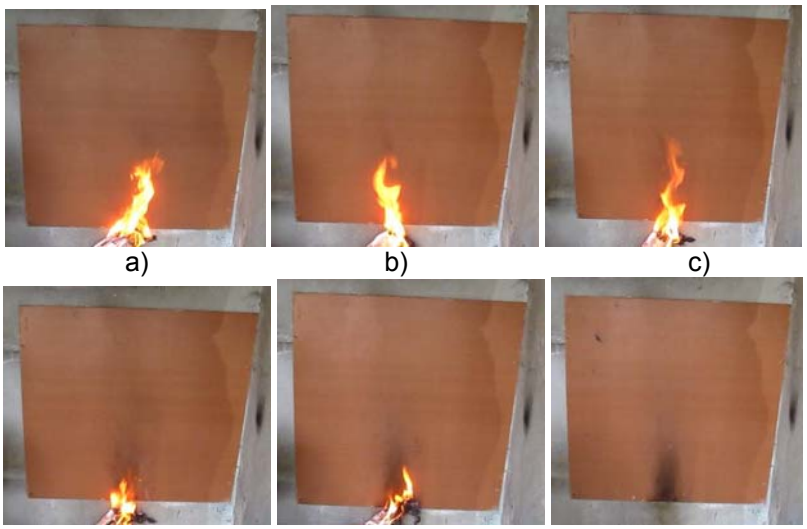

Fig. 7: Experiment with wooden panelwork glued on the wall

From the experiment with wooden panelwork on a stand (fig 6) has been established that during the ignition combustion products with intensive smoking start being liberated. One can conclude that after taking away fire source, panelwork continues burning independently with liberation of strong asphyxiating smell.

In the case of the experiment with closely glued on the wall wooden panelwork (fig 7), longer exposure on fire source leads to surface scorch and almost insignificant liberation of combustion products. Combustion ceases when fire source has been taken away.

The conclusion has been drawn that in cases when wooden panelwork is not clinging closely to the wall it burns independently, which provokes occurrence of a complicated situation related to smoking, restricted vision and difficulties in breathing, while in cases when it is clinging closely to the wall, combustion is difficult to develop.

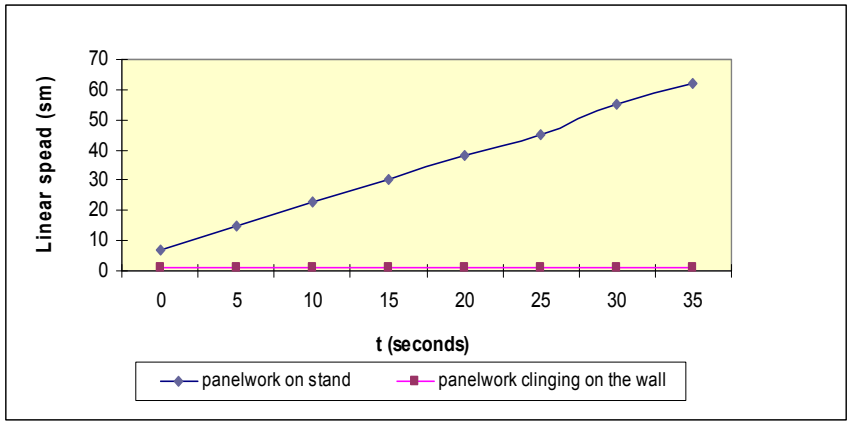

Fig. 8: Comparison of linear burning speed of panelwork on a stand and panelwork closely clinging to the wall

2. CONCLUSIONS

- Evacuation routes and rooms are covered with ignitable and synthetic materials hiding the risk of smoking when ignited.
- Experiments carried out confirm that in cases of non-closely clinging materials to the wall unpleasant asphyxiating smell, strong OC smoking, harmful emissions of carbon dioxide, hydrocyanogen, peroxide of nitrogen, etc. occur.
- According to normative requirements, no ignitable materials are to be used for evacuation route panelling and no mirror are to be hanged on them.

3. REFERENCES

[1] Dimitrov, St. (1995) *Human evacuation at room and building fires*. Sofia; Bulgariq

[2] Elenkov, L. (2005) Evacuation of working environment damages using sucker nozzles, SWU “Neofit Rilski” Blagoevgrad, Collection of Reports 8.11.2006, 521-526.

Research on Flammability of Broken and Compact Ignitable Materials

Veselina Stoyanova, Asen Nachov, Lyuben Elenkov
South-West University "Neofit Rilski", Blagoevgrad, Bulgaria

Abstract: *Dynamic burning processes of broken (disperse) ignitable materials and solid ones follow a particular pattern. Knowing them allows defining an algorithm for localization of hazardous processes.*

Key words*: broken ignitable materials, compact ignitable materials, experimental researches*

1. INTRODUCTION

Ignitable materials in wooded ecosystems burn volumetrically on the surface when in hazardous environment. It is a well-known fact, for an instance, that forest fires develop and spread in volume unlike all other fires [1]. Forest ignitable material is every particle of organic matter that can ignite and burn: boughs, fir-cones, leaves, pieces of bark, stems, trunks, stumps, lichens, mosses, etc [2]. Boughs, leaf masses, coniferous leaves, fir-cones, they are all representatives of broken stationary-like dispersed ignitable materials, for which they burn in volume. Compact large ignitable materials (fallen dry trees, boughs) burn longer on the surface.

Task Formulation. Purpose of Research

Forest fires start under specific circumstances when grasses dry up in March, April, July, August and September. Forest fires ignite from dried grasses, which facilitate conveyance of fire on bushes and trees (Fig. 1).

Fire can spread either from bushes themselves or forest vegetation. This might be due to damages of the technical and linear infrastructure (transmission lines, gas-mains, etc.) or fires in summer-houses areas, holiday houses, huts and camping-sites in the forest. [3]

Fig.1: Connection between grasses, bushes and trees

The purpose of this report is to research the ascending convective flow of a local stationary fire. In order to achieve this purpose we have carried out a number of experiments with different in their nature and thickness ignitable materials – varying from broken to compact ignitable materials.

Output ignitable materials are hay, straw and coarse compact 10-cm thick ignitable material. A metal grill has been used for the research to pile ignitable materials on. A metal pipe has been fixed in the middle of the frame and lined in 20-cm spaces functioning as a reference point for flame’s height.

1.2 Experiment with straw and hay

An experiment with straw and hay has been carried out. Both types of ignitable materials have been divided into two in advance to achieve greater precision of research. Ignitable materials have been piled on a grill to the height of 40 cm. Regimes have been consecutively shot with a digital camera (Fig. 2 and 3)

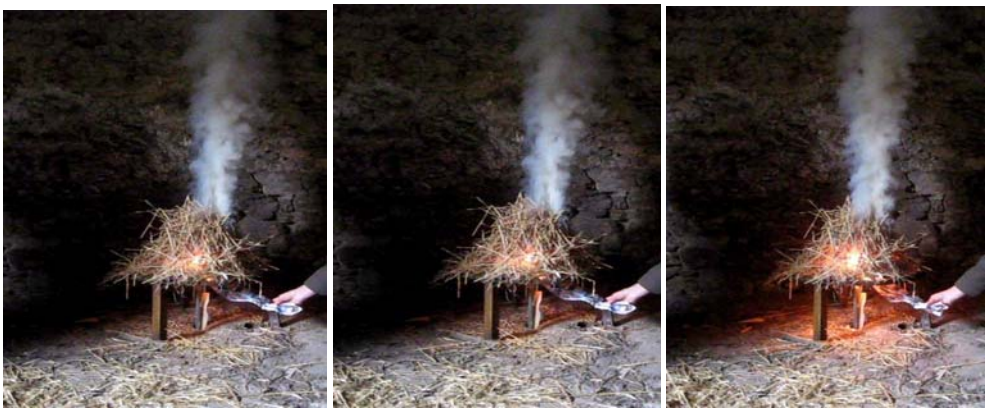

a) b) c)

d) e) f)

Fig. 2: Experiment with straw

a) b) c)

d) e) f)

Fig. 3: Experiment with hay

a) b)

c) d)

e) f)

Fig. 4 Experiment - Solid material

Analysis of the abovementioned regimes gave a clear view of the differences in burning of different ignitable materials. On this basis we are capable of comparing burning time and flame height. This comparison has been illustrated in Fig. 5 and 6.

From the analysis of outdoor burning of compact ignitable material we have ascertained a number of objective laws. Unlike burning of light materials, the process here continues many times longer. Flame is not very high, but rather stable.

Straw burns faster for several reasons. It is a light ignitable material with tube-like structure. Unlike the so called heavy materials, light ones need less heat to ignite. They burn in volume and flames. Straw's tube-like

structure facilitates faster burning by supplying sufficient quantities of oxygen to support burning.

Hay is considered light ignitable material as well. Unlike straw however, it has leaf-like structure. This forms greater convective flows and rises temperature of fire. Being finer particles, grasses burn in volleys, which is clearly seen in the hay experiment with fireballs ejected up in height (Fig. 3 d), f)).

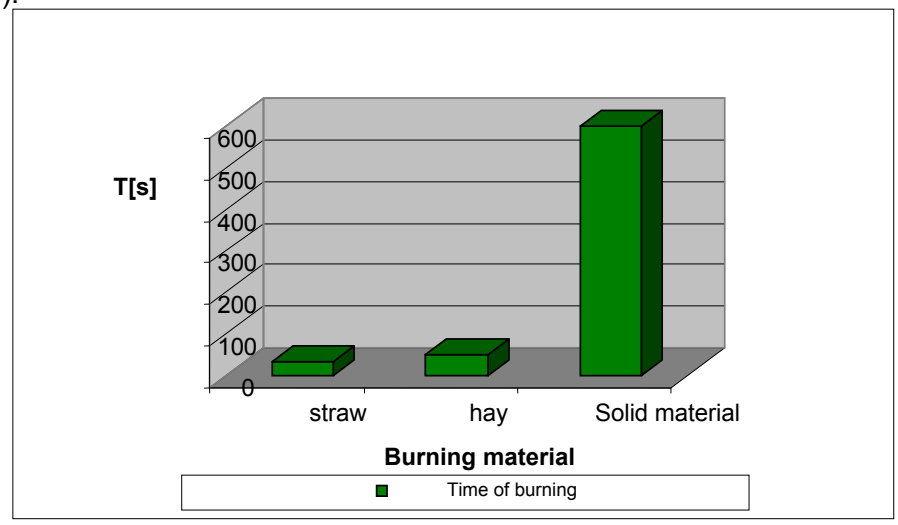

Fig. 5: Comparison of burning time of material

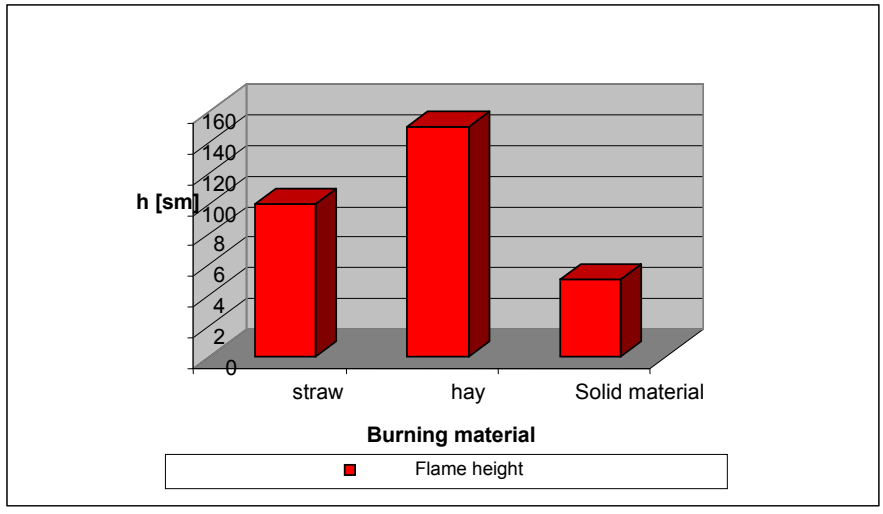

Fig. 6” Comparison of flame heights of different materials

Graphics show straw pile burns fastest and convective flows during hay burning are the highest.

2. CONCLUSIONS

Dispersed forest ignitable materials burn intensively and in volleys unlike compact wooden material, which is slower to ignite, burns on the surface, however its flames, although of low height, are more stable and more extended in time. Compact material is possible to burn without flames.

3. REFERENCES

[1]. Elenkov, L., (2011) Dynamics of forest fires, *Vulkan 4*

[2]. Panov, P. (2007), Extinguishing and prevention of forest fires manual, Sofia, Bulgaria

[3]. Stoyanova, V., (2011), “Forest fires in inversion environment”, *Academy of the Ministry of Interior, Collection of reports,* 140-146

Temperature conditions of the soils in the Blagoevgradska Bistritsa River basin (Rila mountain)

Stoyanov K., Stoilov A., Pulev A., Sakelarieva L. and Mavrevski R.
SWU “N.Rilski”, Blagoevgrad, Bulgaria

***Abstract**: The changes in the temperature conditions of the soils in the valley of the Blagoevgradska Bistritsa River have been observed. The DALLAS Instruments thermosensors with accuracy 0.125ºC have been used to record the soil temperature at three sites, located at 490 m, 920 m and 1480 m above the sea level for 6 months. Daily temperature variations at a depth of 60 cm have not been found out. Seasonal temperature variations have been observed. The second and the third Law of Fourier have been confirmed.*

***Keywords:** soil temperature, thermosensor, the Blagoevgradska Bistritsa River*

INTRODUCTION

The temperature of the soil is a quantitative measurement of its thermal condition. Solar radiation, absorbed by the soil surface, is transformed into heat. Part of it is used to warm up the ground air and to evaporate the water from the upper soil layer. The other part of the heat goes into the deeper soil layers. The warming up and the cooling down of the soil depends on the phase transitions of water and its physical features and characteristics - thermal capacity and thermal conductivity. The thermal capacity of the soil is smaller than that of the water and that is why when the heat flow is the same, the wet soil warms up and cools down far more slowly than the dry soil.

The temperature regime of the soil is determined by the impact of several basic climate-forming factors, which also influence the air temperature - latitude, atmospheric circulation and the type of surface. The microclimatic factors also play an important role - the form of the relief, the exposure, the physical features of the soil, like type, colour, structure and others. The temperature changes in depth follow the Laws of Fourier.

The experimental data about the distribution of the temperature in the deep soil layers are particularly valuable for determining the life cycles of the animals, which inhabit those layers.

METHODS AND RESULTS

The soil temperature was studied at three different altitudes - 490 m, 920 m and 1480 m above the sea level for the period 22.07.2010 – 22.01.2011. The sites are located in the valley of the Blagoevgradska Bistritsa River (Rila mountain) (Fig.1). The DALLAS Instruments DS1921G Thermochron iButton thermosensors with accuracy 0.125ºC have been used.

The DS1921G Thermochron iButton is a rugged, self-sufficient system that measures temperature and records the result in a protected memory section. The recording is done at a user-defined rate, both as a direct storage of temperature values as well as in the form of a histogram. Up to 2048 temperature values taken at equidistant intervals ranging from 1 to 255 minutes can be stored. Data is transferred serially via the 1-Wire protocol, which requires only a single data lead and a ground return. Every DS1921G thermosensor is factory-lasered with a guaranteed unique electrically readable 64-bit registration number that allows for absolute traceability. The durable stainless steel package is highly resistant to environmental hazards such as dirt, moisture, and shock.

The location of the thermosensors is specifically chosen, so that they can display comparative characteristics.

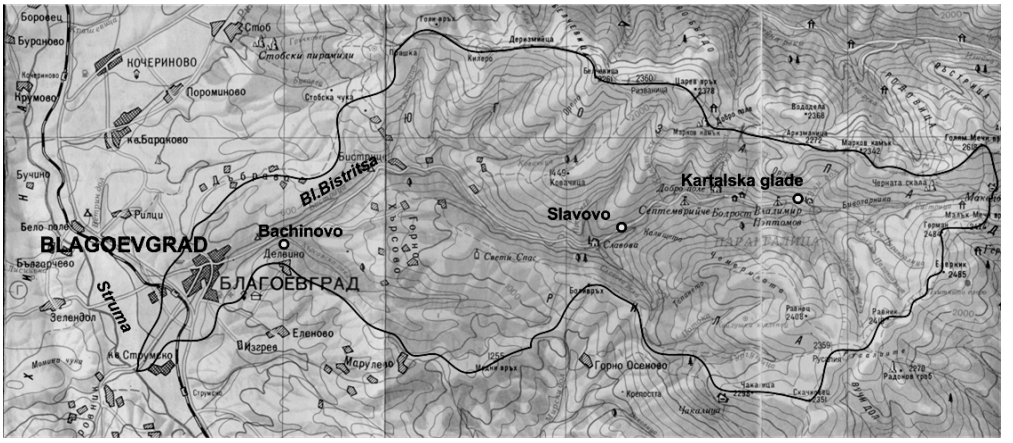

Fig. 1: Scheme of the position of the Blagoevgradska Bistritsa River basin

The first group of thermosensors are located in the yard of the South-West University "Neofit Rilski" Center "Bachinovo", in the low part of the left

valley slope of the Blagoevgradska Bistritsa River, close to the mouth of the Harsovska River at 490 m above the sea level. The area is with north-northwest exposure. The slope has a convex profile, with its biggest inclination of about 30º, and it gets smaller as the height increases. It rises to the elevation of 743,7 m - Orlovski chukar peak, as a left valley slope of the Blagoevgradska Bistritsa River. After that it gets larger in a southeast direction and outlines the left valley slope of the Harsovska River (Fig. 1).

The rocks in this region are part of the pre-Cambrian mantle of the Rila-Rhodope batolite. They are part of the gneiss-migmatite complex from the so-called Maleshevska group - biotite and muscovite gneisses and migmatites, which are the building blocks of the west slopes of Rila mountain [1]. The rocks are highly weathered and cracked on the surface, as a result of intensive tectonic transformation and the impact of the exogenous processes. In the valley of the Blagoevgradska Bistritsa River they form landfalls on the steep sections and on the ditches of the roads.

The soils in the region of Bachinovo are maroon forest soils. They are found on the already mentioned pre-Cambrian metamorphic rocks. They are moderate eroded with comparatively opulent vegetation [2]. You can find natural broad-leaved low-stemmed forests there. The slope above the University Center is afforested with black pine trees, which are 40 years old.

The coordinates of the area are: 42º02'00.8"N; 23º07'50,6"E, altitude - 490 m.

Data about the soil profile have been collected at a depth of 5, 20, 40 and 60 m (Fig. 2).

Site 2 - Slavovo is located at about 1 km before the mouth of the Slavova River, on the right valley-like bank, at 920 m above the sea level. The soil temperature values have been recorded at a depth of 60 m.

The valley of the Blagoevgradska Bistritsa River in this region has southwest direction and steep, raised and high slopes. The inclination at the bottom of the slopes reaches 45º. That to a great extent decreases the duration of sunshine and the flow of solar radiation, especially during the cold half-year.

The region is built up of amphibolites - the so-called Chetirska amphibolite suite of the Troskovska group, which is part of the pre-Cambrian mantle of the Rila-Rhodope batolite [1]. Because of the significant slope inclinations the rocks undergo intensive colluvial processes - stonefalls, landfalls and screes. This is particularly typical for the right valley slope, whose east exposure determines its poor forestation.

Site 2 - Slavovo is located at the lower borderline of distribution of the brown forest soils. Right into the river valley, as well as on its left valley slope, you can find dark brown forest soils. They have fairly strong humus-accumulative layer, 30 cm thick, dark colour, and light clayey-sandy composition. Under it there is a yellowish-brown soil layer, fresh and

compact, with a very few pieces of rock. Some of the pieces are 15 cm large. The soils are not eroded [2]. The region is well-forested with beech and birch trees.

The coordinates of the area are: 42º01'56.7"N; 23º16'40.3"E, altitude - 920 m.

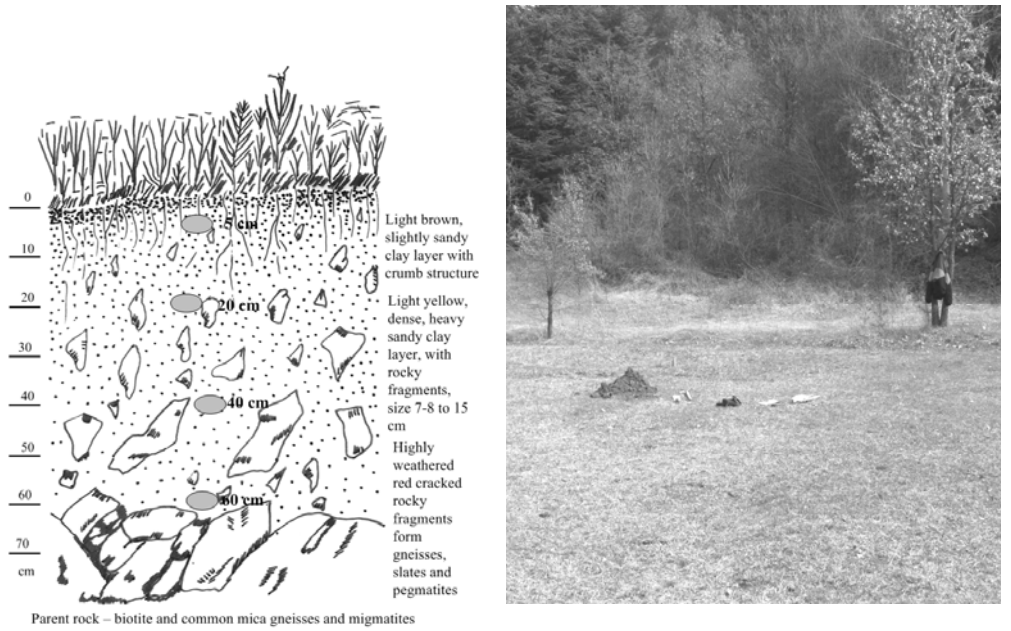

Fig. 2. Soil profile and view from site 1 – Bachinovo

Site 3 is located in the area of Kartalska glade, situated at the upper stream of the Blagoevgradska Bistritsa River, on the right river bank, at 1480 m above the sea level. The valley gets wider at this area and has a slightly elevated pattern, a small inclination and a south-southwest exposure. It is filled with colluvial, deluvial-proluvial and alluvial deposits, which have been brought by the steep valley banks and the movement of the river. Some of the deposits have a fluvio-glacial origin. The valley slopes around the glade are steep and have a raised cross section, which is a typical feature for the whole valley. This is particularly characteristic for the left slope, which is significantly longer and higher, but as it gets higher, its inclination gets smaller. The right valley slope has a big inclination (40-45º) up to 2100 m, it is clear of trees and is subjected to intensive erosion.

The rock base consists of Upper-Paleozoic average-granular biotite granites, which are part of the Rila-Rhodope batolite [1], the building blocks of vast parts of East, Southwest and Middle Rila mountain. A large part of the valley base is covered by deposited coarse boulders, coarse sand, gravel, sands and clay interlayers, which are the result of alluvial-proluvial

and fluvio-glacial processes. The base of the slopes is subjected to colluvial processes and it consists of pieces of rough rock mass.

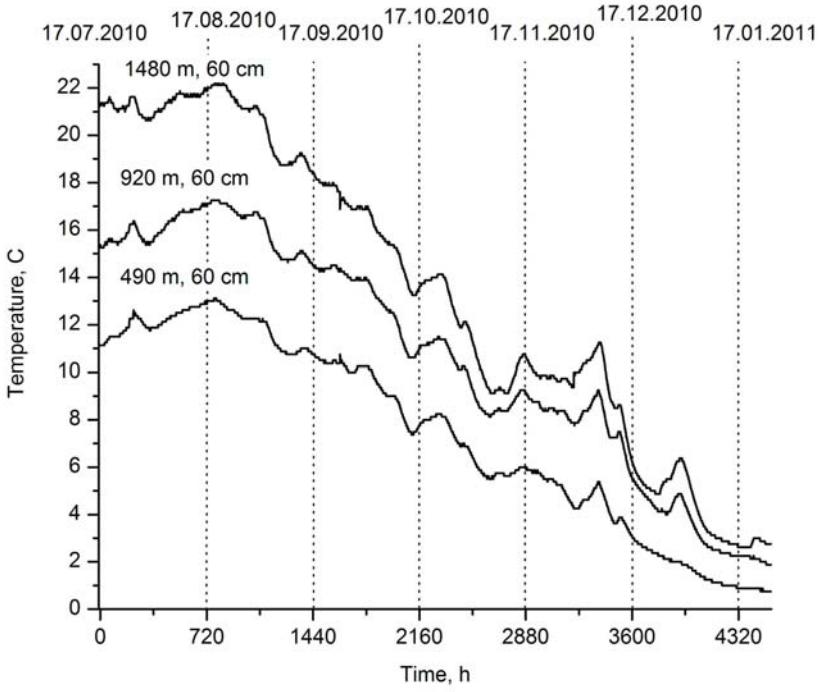

Fig.3 Changes in temperature at different altitudes

Kartalska glade is covered by brown forest secondary grassed, clayey-sandy soils [2]. They consist of a layer, rich in humus, which is up to 60-70 cm deep. You can find mainly cereal plants there and a fewer leguminous and others plants.

The coordinates of the area are: 42º02'33.7'N; 23º21'55.9'E, altitude - 1480 m.

The results of the temperature distribution at a depth of 60 cm at different altitudes for the entire period of study (Fig. 3) display a distinct dependence of the temperature at this depth from the seasonal temperature variations. There are no indications of daily temperature variations at this depth. The results also prove the decrease of the temperature with a 5-degree gradient at 500 m above the sea level in the summer-autumn period and with a 3-degree gradient at 500 m above the sea in the winter.

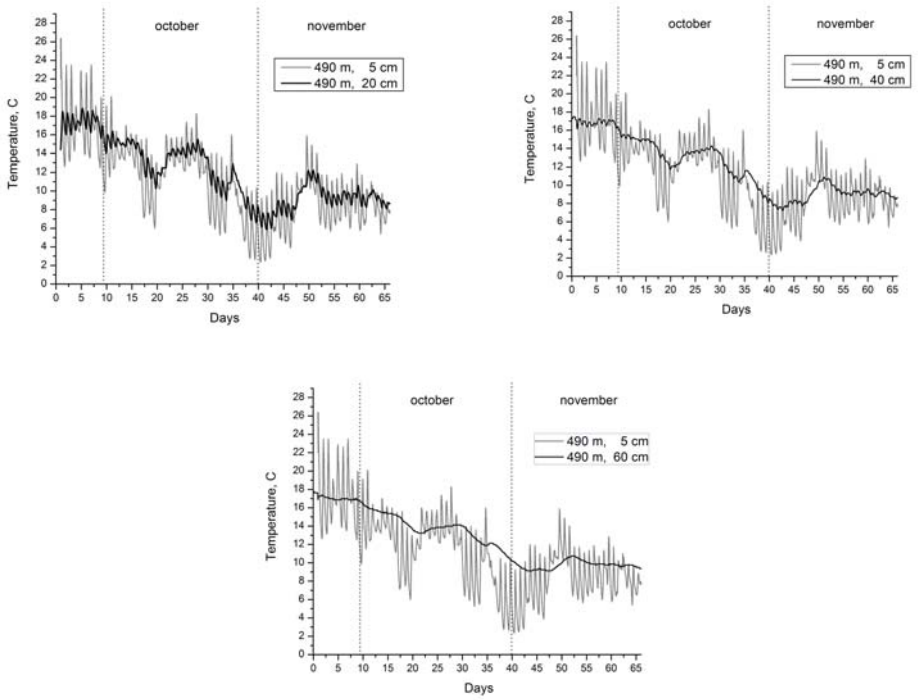

Fig. 4. Comparative graphs of the changes in temperature at a depth of 5 cm, 20 cm, 40 cm and 60 cm, the site of Bachinovo

CONCLUSIONS

As a result of the conducted experiments and the processing of the collected data, the following conclusions have been made:

- there is no indication of daily temperature variations at a depth of 60 cm;
- seasonal temperature variations have been recorded;
- the third Law of Fourier has been confirmed, with a delay of 6 hours at every 20 cm in depth;
- the second Law of Fourier has been confirmed.

REFERENCES

[1] Marinova, R., Zagorchev, I. (1991). *Geological map of Bulgaria, M 1:100000, sheet Blagoevgrad*, Geology and Geophisics (in Bulg.).

[2] Nikolov, B., Minkovska, R. (1984). *Mapping of soils in the Blagoevgradska Bistritsa River Basin for the purposes of the general scientific landscape map*, Forestry science, 2, 15-20 (in Bulg.).

Behavior of bears in the Park for re-adaptation of “dancing” bears (the town of Belitsa, Rila Mountain)

Lidia Sakelarieva, Kristina Yordanova
South-West University, Faculty of Mathematics and Natural Sciences, Department of Geography, Ecology and Environmental Protection, 2700 Blagoevgrad, Bulgaria

***Abstract**: Behavior is a set of actions that ensure the normal functioning of life processes and are important for the survival of individuals and species in nature. Any behavior is a result of the complex effect of heredity, environmental conditions, experience, anatomical and physiological characteristics of species. A lot of observations of bears in different parks and zoos have been done but still there are features of bear behavior that are not researched and cannot be explained.*

The survey was conducted in October 2009 in the Park for re-adaptation of “dancing” bears in the town of Belitsa region (Rila Mountain). Four behavioral elements - movement (foraging and feeding), time spent in rest (sleep), time spent in the pool and stereotyped behavior of two bears, a male and a female were observed before hibernation. The time spent at rest was the best presented behavioral element of the two bears. Their sluggishness was most likely due to the imminent beginning of winter.

***Kewords**: bear, behavior, park for “dancing” bears, the town of Ballista*

1. INTRODUCTION

Even in ancient times the animal behavior was of interest to people. The observations over certain actions of animals found an application in the everyday life of ancient people – they helped them in hunting and later on -

in the animal domesticating and training. In recent years the scientists' attention has been drawn to more extensive research of the animal behavior. The results from these studies do not only have scientific value, but are widely used in various men's practical activities. Thus a new and interesting science of biological bases and patterns of animal behavior called ethology arose [1, 2].

The largest predator in Bulgaria - the brown bear (*Ursus arctos* Linnaeus, 1758) has an individual behavior typical of the animals that live alone or in pairs. This species lives in Rila and Pirin mountains, in the Rhodopes, Stara Planina and even in Vitosha. People with their activity, such as the construction of roads and fences and deforestation, have been causing significant damages destroying their habitats and even kill them [3, 4].

2. MATERIAL AND METHODS

The Park for re-adaptation of "dancing" bears is located on the wooded slopes of the South part of Rila Mountain, in the area Andrianov Chark, about 12 km from the town of Belitsa, Blagoevgrad municipality, and 180 km from Sofia. It covers an area of 12 hectares from 1200 to 1345 m above sea level.

The park was built up with the help of world-renowned experts who has been studying the behavior and habits of brown bears. The park area offers to its residents dense forests and hills for walking and seclusion, meadows and specially differentiated sunny rest places, different in size and form pools for bathing and dens for sleeping. So the bears are provided with a natural and protected area for quiet life close to the normal for their species [6, 7, 8]. The survey was conducted for 4 days - from 24 to 27 October 2009. Four behavioral elements - movement (foraging and feeding), time spent in rest (sleep), time spent in the pool and stereotyped behavior of two bears, a male and a female - Gosho and Mariana, were studied before hibernation. Gosho bear was born in 1988 and was brought to the park in 2001. Mariana bear was born in 1987 and has been living in the park since 2000. The two bears were observed every day from 8.30 a.m. to 6.00 p.m. and their activities were recorded in tables in every 10 minutes.

The bears Gosho and Mariana live together in Sector 7 of the park, in completely natural environment, except for the concrete pool and two concrete tunnels with a diameter of 1 meter (Fig. 1). Sector 7 was separated in 2000 (along with Sectors 5 and 6). No other bears live in Sector 7 because Gosho bear does not stand to live with other bears, except Mariana.

Fig. 1. Gosho and Mariana bears in Sector 7 of the park.

3. RESULTS AND DISCUSSION

As a result of a study of the bears Mariana and Gosho behavioral elements of 8 behavioral systems were determined [5]:

1. behavior of comfort;
2. research behavior;
3. unusual behavior;
4. rest;
5.agressive behavior;
6. foraging;
7. fear;
8. others.

In the present study greater attention has been drawn to 4 basic behavioral elements: movement (foraging and feeding), rest (including sleep), time spent in the pool and stereotyped behavior. The four behaviors occurred in different parts of the sector where the two bears live. Therefore four zones can be identified: an area for foraging and feeding, a resting area, a swimming area, and a zone of manifesting stereotypic behavior.

1) Behavior of Gosho bear.

For the entire period of observation of the behavior of Gosho bear (Fig. 2) two behavioral elements prevailed - the rest and foraging. The two other behaviors - the expression of stereotype and the time spent in the pool were not well presented. Gosho bear spent most of the time in the resting area which probably was due to the imminent beginning of winter.

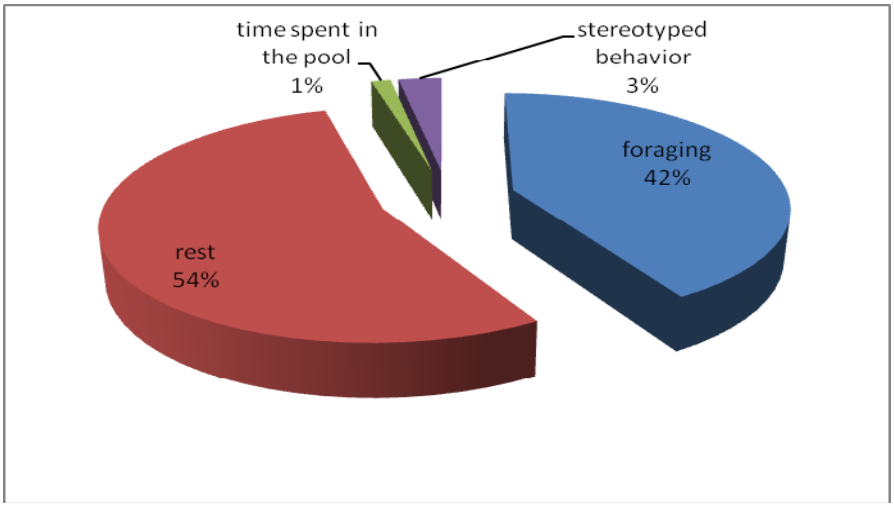

Fig. 2. Ratio (%) of the 4 key behaviors of Gosho bear for the period of observation.

The comparison of the behaviors of Gosho bear during the four days (Fig. 3) shows that foraging and rest are inversely related to each other, when more time was spent on rest, less time was spent on searching for food and vice versa. A similar conclusion can be drawn about the relationship between the expression of stereotyped behavior and the time spent in the pool, they also relate to one another inversely.

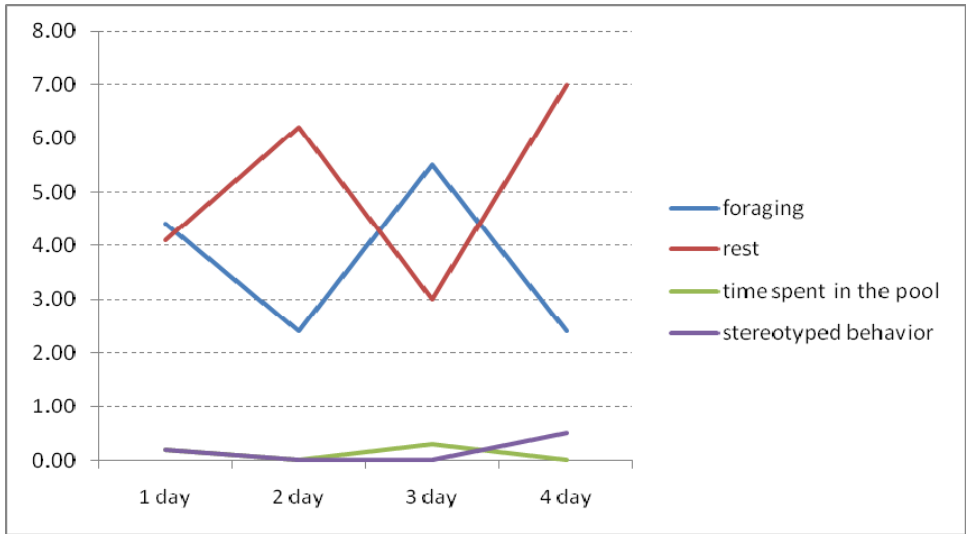

Fig. 3. Dynamics of the behaviors of Gosho bear for the period of observation.

2) Behavior of Mariana bear.

Throughout the four day period (Fig. 4), Mariana bear spent most of the time at rest, followed by searching for food and the expression of stereotyped behavior. The time spent in the pool was less than 1% of behavior, manifested during the period of observation.

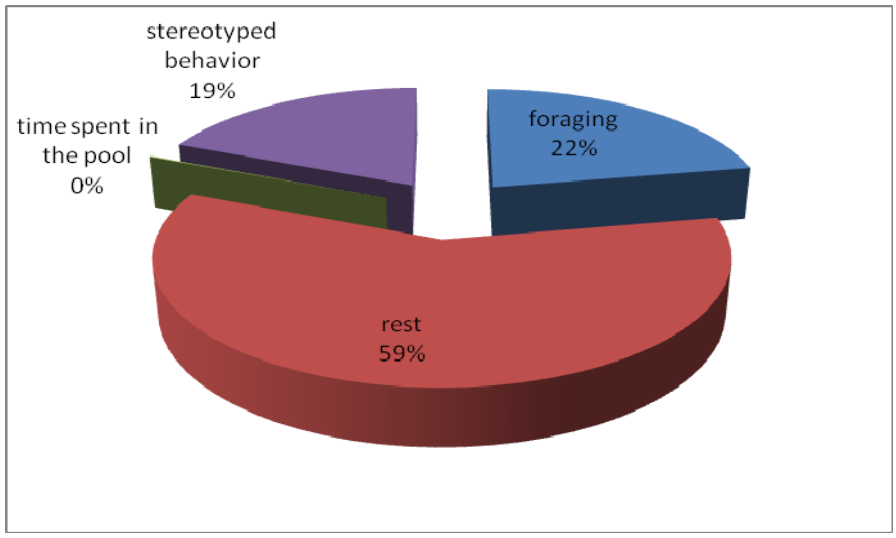

Fig. 4. Ratio (%) of the 4 key behaviors of Mariana bear for the entire period of observation.

When comparing the dynamics of the four behaviors (Fig. 5) of the female bear it is found that foraging and rest are in inverse relationship - when the time spent on rest increases, the time spent on searching for food and feeding decreases and vice versa. On the other hand, the foraging and the stereotyped behavior are in direct relationship - when the time spent on searching for food and feeding increases, the expression of stereotype also increases and vice versa. Mariana bear stayed in the pool for some time only during the first day, after that there was no manifestation of such behavior.

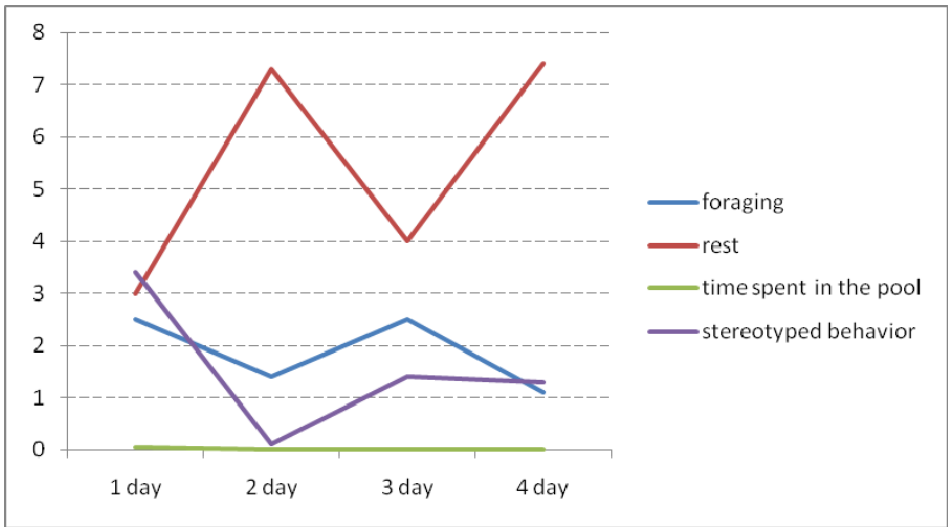

Fig. 5. Dynamics of the behaviors of Mariana bear for the period of observation.

3) Comparison between the behaviors of bears Mariana and Gosho.

For the entire four-day period of observation (Fig. 6), the time spent at rest prevailed in the behavior of the two bears, followed by the time for foraging and feeding, the expression of stereotypic behavior and the stay in the pool. Both bears are quite sluggish during the period, which most likely related to the impending onset of winter. Mariana bear demonstrated much more stereotyped behavior, which is probably connected with her life before she was brought to the park, when she was forced by starvation and pain to perform different artistic tricks.

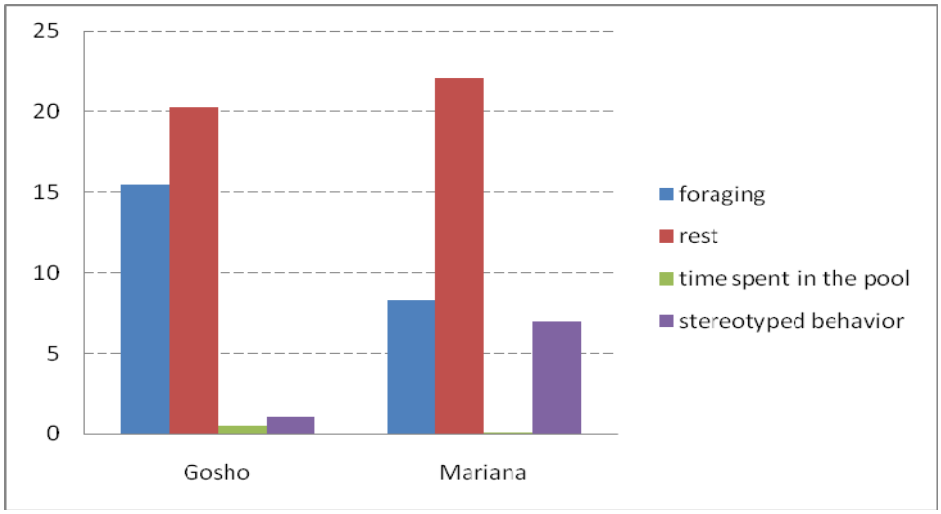

Fig. 6. Behavioral reactions of Gosho and Mariana bears.

4. CONCLUSIONS

The following conclusions can be drawn, based on the monitoring of bears Mariana and Gosho:

1. For the entire period of observation the time spent at rest was the best presented behavioral element of the two bears, followed by the time spent for foraging and feeding. Sluggishness of the bears was most likely due to the imminent beginning of winter.

2. An inverse relationship between two behavioral elements – resting and movement (foraging and feeding) was observed. When the activity increases the time spent in sleep decreases and vice versa.

3. Reducing the duration of stereotyped behavior is associated primarily with increased time for foraging and vice versa.

4. The comparison of the behavioral reactions of the two bears manifests some differences which could be explained by the fact that bears are quite individualistic. The male bear was considerably more active than the female, which in turn demonstrated more often stereotyped behavior.

5. REFERENCES

[1]. Convention on the conservation of European wildlife and natural habitats (Bern Convention). 82/72/EEC, 1981.

[2]. Boev, Z., 2010. Illustrated Encyclopedia of Animals Fiut Publishing.

[3]. Bozhkov, D., 1989. Predators and predation in the animal world, published by Science and Art, Sofia, 78-170.

[4]. Nikolov, G., 2009, Kartogravski pattern of distribution of brown bear, Thesis, South-west University "N. Rilski".
[5]. Geffen. K, 2005. HAS Den Bosch.
[6]. Website: http://park.belitsa.com/
[7]. Website: http://bg.wikipedia.org/wiki/% D0% 9C% D0% B5% D1% 87% D0% BA% D0%
[8]. Website: http://pirin.bg/pirin.bg/html/fauna/mecka.html

Nature and peculiarities of the stream order configuration in the Struma river basin

Assoc.prof. eng. **Michail As. Michailov**, PhD
South-West University „Neofit Rilski“ - Blagoevgrad, Bulgaria

Abstract: *The nature and the peculiarities of the stream order configuration in the Struma[*] river basin are being investigated. To assess their meaning, it is necessary to use a more complex approach – for example, as the River Continuum Concept (RCC). The results of different part of Struma* river are more correct and applicable for river basins management and environmental researches.*

Keywords: *water and river basins management, stream order configuration, River Continuum Concept (RCC), environmental requirements.*

INTRODUCTION

The river basin management is one of the main obligations, evolving from the “*Directive 2000/60/EC* establishing a framework for Community action in the field of water policy” - known as the Water Framework Directive (WFD). But the formal implementation of its requirements is not adequate prerequisite for successful management of the processes in the river basins. First of all, it is needed to be sure in our motivation (not with administrative sound only), second – to use scientifically based approaches and third – to discover, to explain, to assess and to manage not just the main factors, but and the regional or the local characteristics.

[*] - on the territory of Republic Bulgaria.

DATA AND METHODS

There are many investigations and a lot of publications have been done about the river basins structure and management, for the state of the river ecosystems and the possibilities for the keeping “natural” or “undisturbed” environmental conditions about them, etc. The main factors and characteristics are well studied.

To explain the processes in the river basins usually is used the River Continuum Concept (RCC) (*Vannote et al.,1980*). This is well known, scientific-based, “keystone” approach in stream ecology for description “the entire river system as a continuously integrating series of physical gradients and associated biotic adjustments as the river flows from headwater to mouth” or for fulfilment of the idea and strategic formulation “that every point along a river basins, from birth (headwater streams) to maturity (river mouth), reflects unique characteristics” with specific meaning for the different processes, widely popularized by many WEB pages – (www.dnr.state.mn.us/watershed_tool/rcc.html), (www.oxbowriver.com/), (www.rivercontinuum.org/), (www.cotf.edu/), etc.

The uniqueness does not mean any strangeness, including the stream order configuration (*Allan, J. D. 1995*) at the different part of the river length. As classic examples it is necessary to note:

- *stream ordering* is a process of assigning a number to each section of the river and it is useful as a base for RCC when comparisons between different rivers or along the reaches of any river are made. The river communities are grouped according to stream order procedure and channel size into headwaters (1 – 3 order), medium-sized (4 – 6 order) streams/rivers and large (7 – 12 order) rivers;

- a headwater streams (1 – 3 order) have had steep gradient with riffles, rapids and falls i.e. there are specific conditions for the processes. Energy sources are originating, first of all, outside of the streams in the terrestrial environment in the form of leaves and woody material which are transported into the water course;

- in headwater streams (1 – 3 order) have dominated coarse particulate organic matter (CPOM) and the shredder communities have played a major role in breaking down this coarse plant material;

- in the middle reaches (4 – 6 order) some stream/river parameters (width or depth) increases and others (gradient, velocity or shading) decreases. There are fewer riffles and more pools. The production/respiration ratio becomes larger and amounts to P:R>1. The percentage of shredders communities is less than that of the headwaters, so collectors and grazers make up a majority of the structure in water body. More significant becomes the role of the fine particulate organic matter (FPOM);

- there are too specific conditions in the large, lower reaches (7 – 12 order) of the rivers. Usually these are slow-flowing and deeper water bodies, where large amounts of suspended FPOM from the excess production of the middle reaches are contained, the water depth and the turbidity in the water column have limited primary production (the production/respiration ratio is again P:R <1, like the headwaters). Shredders and grazers are absent. As a result, collector-gatherers and filter-feeders communities are dominated downstream.

It is clear, the RCC is a well done structure for complex analysis and river basin investigations. But the standard differentiation, including headwater streams, middle reaches and lower reaches is rather rough construction for river basins presentation, than a useful management approach for different parts of the river length. As example, it is urgent to note an impressive conclusion about Struma* river basin "which is the only river in Bulgaria, we cannot talk about the upper, middle and lower reaches in its literal sense, because the average altitude of the watershed of the middle reaches is higher than that of the above. The average altitude of the river basin at Pernik is 1018 meters, at HMS "Razhdavitsa" - 884 m, at HMS "Nevestino" - 856 m, at HMS "Boboshevo"- 974 m, at HMS "Krupnik" - 973 m and 898 m at the country border" *(IWP) - BAS. 2000)*. Explanations like this have shown that the benefit of many investigations and projects is not effective enough, because of the methodological imperfections.

It should be noted that RCC has a lot more potential than to explain some features of the ongoing processes in rivers.

A little part of this idea is developed and some results for Struma* river basin are presented below.

RESULTS AND DISCUSSIONS

The core of the RCC implementation is consisted in perfect motivation for adequate performance of the unique physical, chemical and biotic characteristics at any point or at any reaches of the river length, presenting all factors – energy, nutrients, conditions, etc. or, in other words, describing different processes in the river basins.

As example for Struma* river basin it is established that there are more than common explanation of the peculiarities for this kind of river basins.

The diversity of geology, relief forms, specific climatic conditions, soils and vegetation are the natural basis for the formation of runoff and the main factors to clarify the differences in the regime of the tributaries of the Struma river in the different parts of the river basin. There are two types of reaches:

- one – from the river origin to Zemen town – with the increasing range of the stream order (up to the sixth and fifth - on its tributaries) and

- other – after Treklianska river (before HMS “Razhdavitsa”) to the country border - where the order remains the same and the increase the area of the catchment and the increase in runoff due to the tributaries - III, IV and V stream order (Fig. 1).

At the same time, as it was mentioned earlier – *Michailov M. (2005),(2009),* between village Razhdavitsa (HMS “Razhdavitsa”) and HMS “Marino pole” (Bulgarian-Greece boundary) the river reach is 164 km long and the Struma river basin increased by 8073 km^2. There are 36 tributaries, who is drained this area, whit three of them (Dragovishtitsa river, Lebnitsa and Strumeshnitsa rivers) that have their origins in Republic of Serbia and FROMacedonia. Transboundary tributaries have a significant share in the basin of Struma* (about 38% of catchment area for this reach).

Between HMS “Razhdavitsa” and Boboshevo town (HMS “Boboshevo”), length 52 km, the catchment area of the Struma river increased by 2150 km^2, of which 40% are Dragovishtitsa river, about 45% are right tributaries of Osogovo mountain and about 15 % of the left tributaries of Konyavska mountain.

In reach between Boboshevo town and village Krupnik (HMS “Krupnik”), length of 50 km, the increasing is 2457 km^2, of which about 70% for the left tributaries from the Rila mountain and about 30% - for the right tributaries from Vlahina mountain (here are considered border rivers for this region - Sushichka and Gradevska rivers respectively).

For reach from village Krupnik to HMS “Marino pole”, with a length of 62 km, the Struma river catchment area is growing with new 3466 km^2, of which about 28% for the left tributaries from the Pirin mountain, about 55% of Strumeshnitsa river and about 17% - for the other right tributaries from the Maleshevska and Ograzhden mountains.

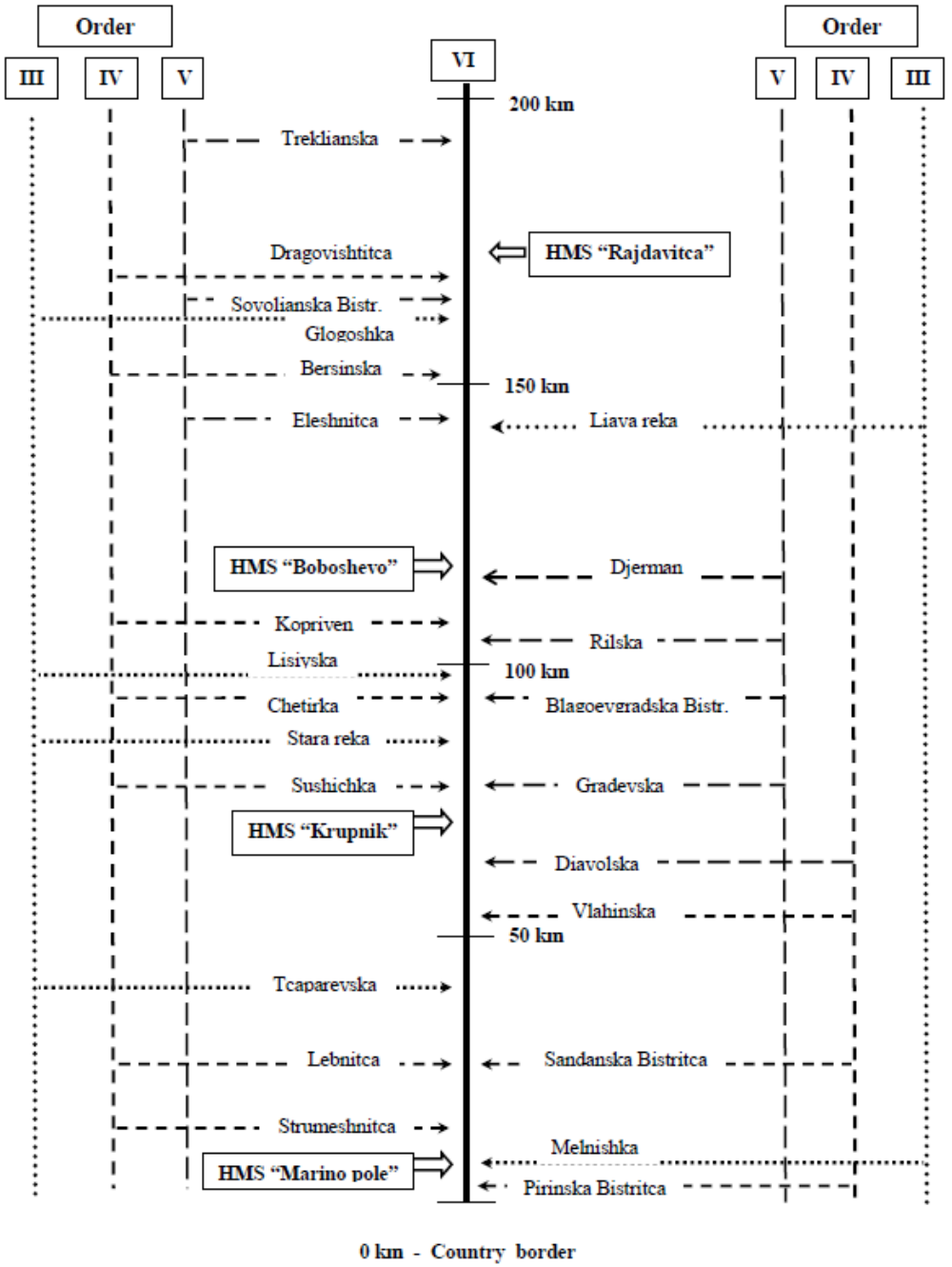

Fig. 1. Stream order configuration for basic part of the Struma* river basin

Conditionally, the average growth of area for Struma river basin in the first of these reaches is 41 km^2/km, in the second division – 49 km^2/km respectively, and in the third division - 56 km2/km. Due to the significant role of transboundary inflows from Dragovishtitsa and Strumeshnitsa rivers, respectively at the beginning of the first division and at the end of the third section, the indicator for the rest of their length is about 28 km^2/km.

The share of river Strumeshnitsa to outflow in the Struma ranged from 5 to 15%, average 10%. Much higher are values for some months. For example, for the months from November to March can reach 20-40%, and in dry years in its impact on the state of main river may be higher during the summer months of July and August.

To express the role of the additional impact and the relationships at different reaches along the Struma* river is used an indicator of the river flow increasing (IRFI):

$$K_{growth} = \frac{Q_{end} - Q_{beg}}{Q_{beg}}$$

where:

Q_{end} - river flow at the end of reach,

Q_{beg} - river flow at the beginning of reach.

The resulting values K_{growth} for several sections along the Struma River in the period 1937 -1995, are given in Fig.2. It should be noted that in each area an increase in the runoff against the previous section, the trend is maintained for an extended period of time.

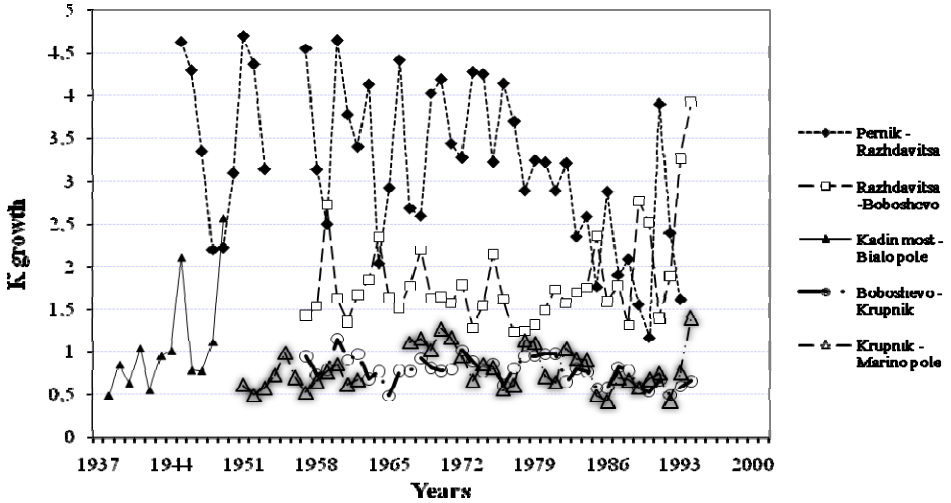

Fig. 2. Growth of the flow for different reaches of the Struma* river basin

Even in the period after the construction of “Pchelina” dam (after 1975) and more pronounced anthropogenic influence, in the reach Pernik - Razhdavitsa downstream to the mouth, the role of local factors (tributaries, etc.) remains very important.

This is an additional argument for a very important role of tributaries along Struma* river, especially after Boboshevo town. In these reaches the conditions for the formation of quantitative and qualitative parameters of the flow are practically determined primarily by local factors and to a lesser degree they are result of "adventitious" effects of the above areas.

Those results can be useful not only as ascertainment, but more as a challenge for a more precise discussion on the methods and tools for water management. Based on several contemporary approaches (the River Continuum Concept (RCC), hierarchical framework for stream habitat classification (structure of processes and habitats), stream order configuration, etc.) it should be redesigned a number of positions in promoting different legal standards and requirements, especially given for the conditions in Struma* river basin.

This is a little known point of view, but no less important event for assessment of the administrative approaches for the river basin and water management. In this context it is well to recall a few basic points about RCC and the other of mentioned methodical tools. There are not unimportant factors and conditions, because the processes in rivers are interrelated. In many cases they have had local or regional significance for the catchment area and therefore do not fall to the attention of researchers.

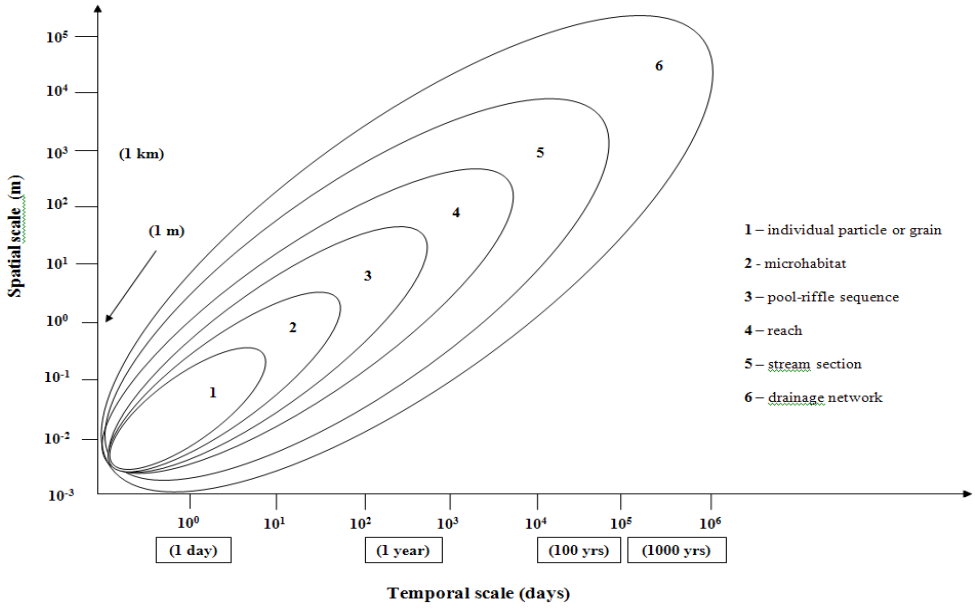

Fig. 3. Hierarchical framework for stream habitat classification (source: *Frissell, C. A. et al.,1986*)

Here is the place to mention the mandatory requirement that hierarchical links between various factors and conditions must be taken into account as a whole system (or subsystems - such as river basin, river section, reaches, habitat, etc.) (Fig. 3), rather than as a sequence of its separately presentation for one or other part of river length or time of happening (*Frissell, C. A. et al.,1986*).

Such an approach in studying of water courses is applied now, but in terms of management processes, there are opportunities for improvement in future. For example, requirements for water quality should not be bound only by administrative procedure for their approval (as it is formulated by *Water Act* [2]). Too often there are allowed and inexplicable requirements and errors.

As example, according to order № RD – 272/03.05.2001 (MEW [3]) it is regulated two type of reaches for Struma* river:

- after village Bosnek to Blagoevgradska Bistritca River - II category, and

- after Blagoevgradska Bistritca mouth to the country border - III category.

The requirements for each of these categories are defined after Ordinance № 7 (*OJ No.96/1986*) for indicators and standards for determining the quality of surface water – as permissible levels of

contamination of river flow at minimum monthly average level (a year with probability 95%) after discharging waste water in water bodies.

In the desire to solve the problems of river basins, too often we rely on the administrative activities, which are confirmed by the examples above. Usually the administration starts from the position of the inevitable contamination of the water.

Without any explanations or references to research results on the natural essence of the ongoing processes in the Struma River in an administrative way are perceived norms after Blagoevgrad, which instead of being helpful can lead to unwanted effects on the river state.

Here is pertinent to note that the requirements for minimum flow in the river are important for the regulation of responsibilities in the discharge of waste water into the rivers. The reference only to those norms in other cases it may cause misunderstandings, because failure to take account of additional factors and conditions with a much more prominent role in the processes in river (temperature, oxygen or sediment regime, entry of nutrients from the catchment area, river flow parameters – velocity, depth, width, etc.). As example for the Struma* river basin, there is a good relation between the mean velocity and the flow (at the main hydrometric stations – HMS) (Fig. 4). It is usable information about the main, driving parameters and the predominantly natural character of the processes in the river basin for a long period (1960-2005 years).

It is evident that the variety of local factors, stream order configuration and impacts in the Struma* River Basin is quite large. Knowing them is a good basis for clarifying the mechanism of the processes in the formation of flow of the Struma river, including and in connection with registered improvements in water quality in recent years (Fig. 5). Therefore, the effect of pollution of the Struma* river, because of the discharge of untreated waste water, should not be used as arguments to the state or as a prerequisite for the regulation of environmental requirements.

The results, shown and discussed here, are quite significant, especially as regards the activities of water basins management - categorization, maximum allowable concentrations, conditions for socio-economic activities at regional or local level for different reaches of the Struma* river length, etc.

May be, it is time to explain our position – there is not any meaning of the administrative activities and norms if we are unfamiliar with the tools, discussed here – the stream order configuration, the River Continuum Concept (RCC), the hierarchical framework for stream habitat classification, etc. An indicative example in this connection is shown at Fig. 5.

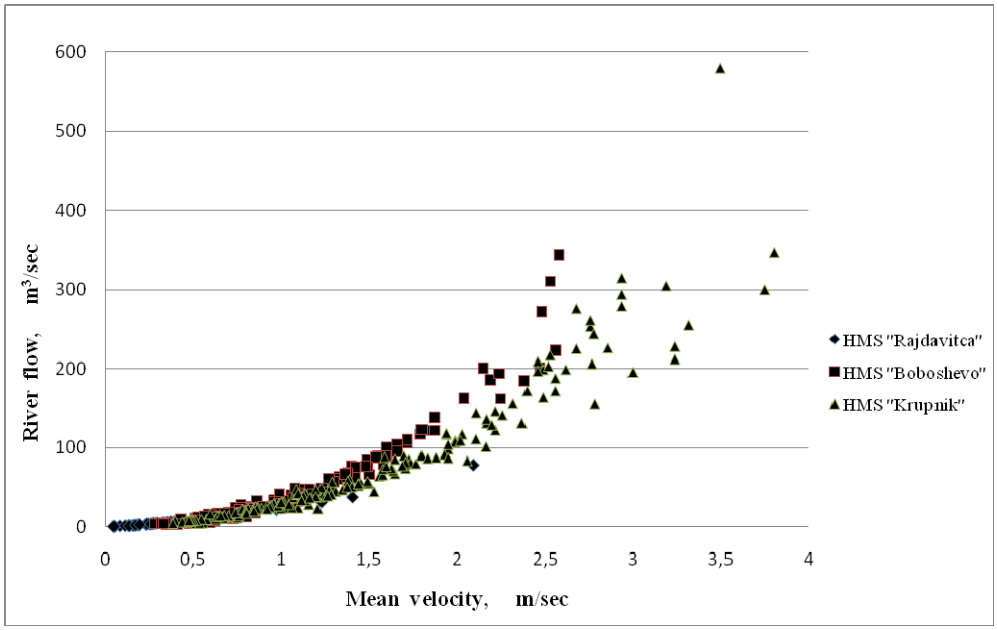

Fig. 4. Relation between the mean velocity and the flow for Struma* river basin
(at the main hydrometric stations – HMS, for 1960-2005 years)

It is clear, the administrative limitations for BOD_5 as water quality parameter:

- is well done legal procedure, but
- for Struma* river basin, at different monitoring stations from 1976 till 2005 year, as management tool it is not usable enough. The natural capacity of the Struma* river basin is very powerful and in a state to reduce the impacts, even from period between 1975 – 1990 year, when the economics activities has been more rough, because of the less treatment plants and discharging of polluted waste water in the river. It is one more reason for correction of our position toward the Struma* river basin management in the recent years.

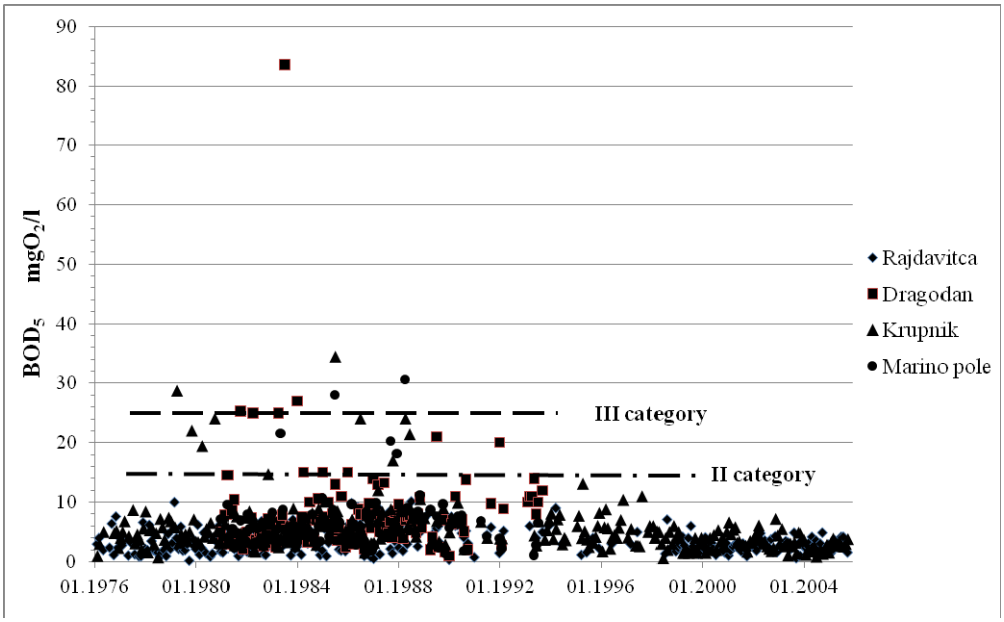

Fig. 5. Dynamic of BOD_5 as water quality parameter for Struma* river at different monitoring stations from 1976 till 2005 year

Inherently the results, shown here, are a little step at the area of the water investigations, but provoke a lot of questions toward the principle and tools for river basin management, especially for Struma* river basin.

CONCLUSION

The analysis of the stream order configuration is not yet used enough as a tool for assessment and management the processes in the river basins. In many cases this kind of information find place in the introductions or in the common part of the articles, publications, investigations, etc., usually as explanation without any analysis or comment.

The implementation of contemporary approaches (the River Continuum Concept (RCC), hierarchical framework for stream habitat classification (structure of processes and habitats), stream order configuration, etc.) for a river basin management has required more complex and fundamental knowledge for the nature and peculiarities of the processes in Struma* river basin.

There is necessity to take in view:

- first - the state of the stream (or river reach) in any place and in any time depends on the all factors and characteristics in the above-lying parts of the river basin, and
- second - affects the state of below-lying parts of watercourses.

The peculiarities of the Struma* river basin (for example stream order configuration) have had a driving function for regional and local level of management, because of which are needed for more serious attention.

References

1. Генерални схеми за използване на водите в районите за басейново управление. Том V. Западнобеломорски район. Генерална схема за използване на водите на поречието на река Струма. Институт по водни проблеми – БАН. 2000. (General schemes for water use in the basin areas. Tom V. General scheme for water use along the Struma river basin. Institute of Water Problems (IWP) - BAS. 2000).
2. Закон за водите. (Water Act – OJ No.67/1999, Corrected, OJ No.81/2000, …, OJ No.34/2001,…, OJ No.108/2001,…, OJ No.69/2003,…, OJ No.77/2005, …, OJ No.65/2006, ... OJ No.103/2009. Sofia.
3. МОСВ - Заповед № РД – 272 от 03.05.2001г. за категоризация на повърхностните води във водните обекти или в части от тях. (MEW - Order № RD – 272/03.05.2001 for categorization of surface water into water bodies or parts of them).
4. М.Ас.Михайлов (2005) - Особености при формирането на оттока на река Струма*. III конгрес на географите в Македония. Зборник. Македонско географско друштво. Скопие. (M.As.Michailov - Features in the formation of flow of the river Struma *. III Congress of Geography in Macedonia. Macedonian geographical society. Skopje).
5. Allan, J. D. (1995) - *Stream Ecology*, Kluwer Academic Publishers. Dordrecht. The Netherlands.
6. Directive 2000/60/EC establishing a framework for Community action in the field of water policy. OJ No. L 327.
7. Frissell, C. A., Liss, W. J., Warren, C. E. and Hurley, M. D. (1986) - A hierarchical framework for stream habitat classification: viewing streams in a watershed context. *Environmental Management* Vol.10, No.2, pp. 199-214.
8. Michailov M. As. (2009) - Water quality, physico-chemical and ecological status of the Struma river. „Mathematics and natural sciences“. Proceedings. SWU „Neofit Rilsky“, Blagoevgrad.

9. Vannote, R. L., Minshall, G. W., Cummins, K. W., Sedell, J.R., Cushing, C. E., (1980) The River Continuum concept. *Can. J. Fish. Aquat. Sci.* 37: pp.130–137.
10. www.cotf.edu/
11. www.dnr.state.mn.us/watershed_tool/rcc.html)
12. www.oxbowriver.com/
13. www.rivercontinuum.org/ - River Continuum Concept. P.O. Box 13, Willow Creek, MT 59760, 406-282-0050. Lab: 502 East Main, Manhattan, MT 59741

Testudines and Sauria (Reptilia) in the Territory of the Blagoevgrad Municipality

Alexander Pulev, Lidia Sakelarieva
South-West University, Faculty of Mathematics and Natural Sciences, Department of Geography, Ecology and Environmental Protection, 66 Ivan Mihailov Str., 2700 Blagoevgrad, Bulgaria

***Abstract**: The present observations of the herpetofauna in the territory of the Blagoevgrad municipality have been carried out since 1988 in order to summarize the available data about the amphibians and reptiles in this region. The results about the turtles and lizards are presented and discussed in this report. Three Testudines and eight Sauria species have been recorded - four of them - for the first time. Six species are widely distributed in large numbers in the studied area. Localities with accurate geographical coordinates, habitats, and some aspects of the ecology of certain species are reported for the first time.*

***Keywords**: Testudines, Sauria, distribution, ecology, Blagoevgrad municipality, Bulgaria*

1. INTRODUCTION

Some data about the Testudines and Sauria species, distributed in southwest Bulgaria, are found in the works of Buresch and Zonkow [1] and Duhalov [2], as well as in the collection of the Regional Historical Museum in the city of Blagoevgrad (RHM - Blagoebgrad).

The present survey of the herpetofauna in the territory of the Blagoevgrad municipality has been carried out since 1988 in order to update the available data about the taxonomy, distribution and ecology of the amphibian and reptile species in this region. The information about the species composition and distribution of the amphibians was summarized in the publication of Pulev and Sakelarieva [3].The results about the turtles and lizards (Reptilia) are presented and discussed in this report.

2. MATERIAL AND METHODS

The Blagoevgrad municipality is located in the South-West Bulgaria [3]. The observations of turtles and lizards have been made during day field trips. Some localities have been told by other

specialists. Only the localities with accurate geographical coordinates are put on maps.

3. RESULTS AND DISCUSSION

Three Testudines species (2 tortoises and 1 terrapin) out of 4 for the whole country have been found in the territory of the Blagoevgrad municipality:

***Eurotestudo hermanni* (Gmelin, 1789)**

Localities: Near the city of Blagoevgrad [1]; one specimen, the city of Blagoevgrad, Loven dom park, 08.1981, RHM - Blagoevgrad, Sl. Veselinski collect.; two specimens, the city of Blagoevgrad, Balarbashi area, 20.08.1974, 25.08.1974, RHM - Blagoevgrad, E. Andreeva collect.; one specimen, in the vicinity of the city of Blagoevgrad, 28.08.1975, RHM - Blagoevgrad, E. Andreeva collect.; one juvenile specimen, the village of Pokrovnik, 10.05.1984, RHM - Blagoevgrad, Sl. Veselinski collect.; one shell, the Marulevska River, left tributary of the Harsovska River, south-west of the village of Gorno Harsovo, in mixed forest (N42°00′44″ E23°10′08″, alt. *ca* 641 m), 30.08.1998; one crushed juvenile specimen, on the road to the village of Gorno Harsovo, two kilometers after the road fork (N42°01′47″ E23°08′30″, alt. *ca* 510 m), 05.10.1996; one specimen, on the road near the mouth of the Harsovska River (N42°02′02″ E23°08′02″, alt. *ca* 472 m), 16.07.2010; one specimen, the same locality, 08.2010, G. Manolev observ.; one juvenile specimen, South-West University Center Bachinovo, in mixed forest, (N42°02′00″ E23°07′51″, alt. *ca* 490 m), 22.04.2011; one specimen, north-east part of the city of Blagoevgrad (N42°01′42″ E23°06′26″, alt. *ca* 429 m), Hr. Peshev observ.; several specimens, the city of Blagoevgrad Drinking water treatment plant (N42°02′14″ E23°06′35″, alt. *ca* 563 m), Hr. Peshev observ.; several specimens, in sparse pine forest between the city of Blagoevgrad and the Drinking water treatment plant (N42°01′54″ E23°06′25″, alt. *ca* 523 m), Hr. Peshev observ.; one specimen, the city of Blagoevgrad, Loven dom park (N42°01′12″ E23°06′26″, alt. *ca* 484 m), 04.07.1998; several specimens, between the Strumsko residential area (the city of Blagoevgrad) and the village of Izgrev, in oak forest (N41°59′33″ E23°06′06″, alt. *ca* 428 m), summer of 1988; nine specimens, the Kaimenska chuka height, south of Blagoevgrad, in sparse pine forest (N41°58′35″ E23°05′35″, alt. *ca* 373 m), 16.07.1988; one shell, east of the village of Dolno Tserovo, in a gully (N41°56′42″ E23°06′40″, alt. *ca* 442 m), 22.07.1997; one specimen, the north-west part of the village of Dolno Tserovo, on the road (N41°56′47″ E23°05′52″, alt. *ca* 316 m), 28.07.2009; one specimen, north-west of the village of Belo pole, near the railway (N42°02′21″ E23°02′14″, alt. *ca* 348 m), 11.05.1997; two specimens, south of the village of Riltsi, in black locust (*Robinia pseudoacacia*) forest, close to

the road (E79) (N42°01′45″ E23°03′33″, alt. *ca* 369 m); one crushed specimen, the city of Blagoevgrad, at the exit to the city of Sofia (N42°00′55″ E23°04′21″, alt. *ca* 353 m), 07.03.1999; one specimen, the village of Debochitsa, Domozettsi neighbourhood, in an open grassy place (N41°51′34″ E22°57′41″, alt. *ca* 1120 m), L. Domozetski observ.; three specimens, two of which in copulation, in sparse broad-leaved forest south of the village of Selishte (N41°59′01″ E23°00′07″, alt. *ca* 599 m), 25.04.2002, R. Ivanova observ.; one shell, by the dam of the Stoikovtsi reservoir, in an open grassland (N41°58′50″ E22°58′47″, alt. *ca* 599 m), 23.04.2002; one specimen, the village of Obel, the neighbourhood of Plyangovtsi, in oak forest (N41°57′37″ E22°53′21″, alt. *ca* 971 m), G. Manolev observ.; two specimens (male and female together), in dense mixed forest, north-west of the village of Klisura (N42°00′34″ E22°53′44″, alt. *ca* 830 m), 12.00h,17.04.2003 (Fig. 1).

Remarks: The Hermann`s tortoise is a widely distributed species in comparatively high numbers in the territory of the Blagoevgrad municipality. It inhabits most often various types of forests and shrubby areas, but it is found also in open lands, close to settlements, in parks, vineyards, by the roads, between agricultural lands.

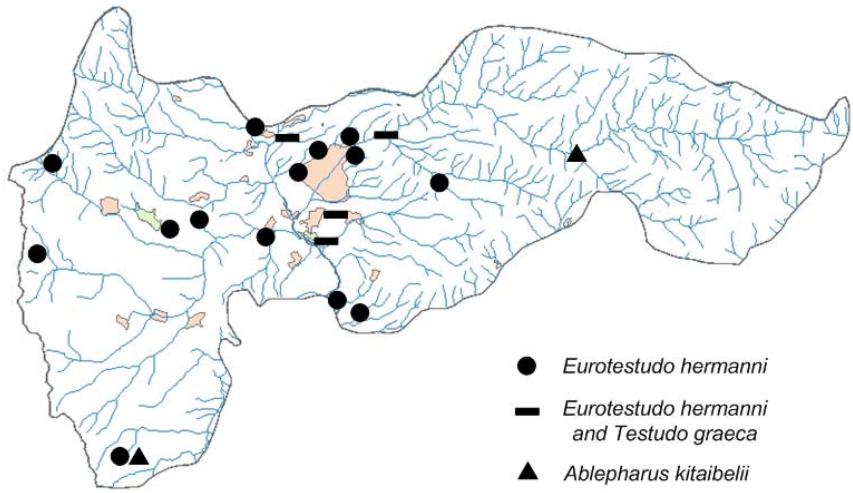

Fig. 1: Distribution of *Eurotestudo hermanni, Testudo graeca* and *Ablepharus kitaibelii* in the territory of the Blagoevgrad municipality

***Testudo graeca* Linnaeus, 1758**

Localities: two specimens, in the vicinity of the city of Blagoevgrad, 28.07.1974, 07.08.1974, RHM - Blagoevgrad, E. Andreeva collect.; one specimen, near the mouth of the Mishovets River, in broad-leaved forest (N42°02′14″ E23°08′25″, alt. *ca* 483 m), 03.05.1996; one specimen, between the Strumsko residential area (the city of Blagoevgrad) and the village of Izgrev, in oak forest (N41°59′33″ E23°06′06″, alt. *ca* 428 m), summer of 1988; three specimens, the Kaimenska chuka height, south of Blagoevgrad, in sparse pine forest (N41°58′35″ E23°05′35″, alt. *ca* 373 m), 16.07.1988; one specimen, south of the village of Riltsi, in black locust forest, close to the road (E79) (N42°01′45″ E23°03′33″, alt. *ca* 369 m) (Fig. 1).

Remarks: The spur-thighed tortoise is a species with limited distribution in low numbers in the territory of the Blagoevgrad municipality. It has always been found together with the Hermann`s tortoise. The relation between the number of the localities and between the number of specimens of the two species is 5:1 in favour of Hermann`s tortoise. The species has not been reported for the region before.

***Emys orbicularis* (Linnaeus, 1758)**

Localities: one specimen, the breeding-ponds along the Struma River near the Strumsko residential area (the city of Blagoevgrad), 18.05.1989, RHM - Blagoevgrad, K. Iliev collect.; several specimens, in a temporary marsh, north-east of the village of Riltsi (N42°02′51″ E23°04′55″, alt. *ca* 428 m), L. Domozetski observ.; several specimens, the left bank of the Struma River opposite the village of Zelen dol, in a small marsh (N42°00′50″ E23°03′05″, alt. *ca* 325 m), Il. Gotskov observ.; one specimen, the left bank of the Blagoevgradska Bistritsa River, by the road (E79) in a temporary marsh (N42°00′07″ E23°05′08″, alt. *ca* 347 m), summer of 1988; one specimen, the floods of the Struma River near the bridge to the village of Pokrovnik (N41°59′23″ E23°04′06″, alt. *ca* 321 m), L. Domozetski observ.; a lot of specimens, south-west of the city of Blagoevgrad, in a canal close to the breeding-ponds along the Struma River (N41°58′50″ E23°05′09″, alt. *ca* 316 m), Hr. Peshev observ.; several specimens, in a reservoir on the right bank of the Struma River opposite the breeding-ponds (N41°58′35″ E23°04′38″, alt. *ca* 315 m), Hr. Peshev observ.; one specimen, the Stoikovtsi reservoir, caught by a fisherman (N41°59′10″ E22°57′32″, alt. *ca* 607 m), G. Manolev observ.; several specimens, the village of Obel, in a marsh by the road (N41°58′06″ E22°55′31″, alt. *ca* 955 m), G. Manolev, M. Zlatkova observ (Fig. 2).

Remarks: In the territory of the Blagoevgrad municipality the European pond terrapin has been found mainly in and close to big bodies of water. It inhabits stagnant and slow flowing waters overgrown with high riverside vegetation. It has been found in high numbers only in the breeding-ponds near the Strumsko residential area. One of the specimens observed in a

canal close to the breeding-ponds was feeding on dead fish (carp). The locality of the village of Obel is one of the highest in Bulgaria. The species has not been reported for the region before.

Eight Sauria species (a skink, a slow worm and 6 lizards) out of 13 for the whole country have been found in the territory of the Blagoevgrad municipality:

***Ablepharus kitaibelii* Bibron & Bory, 1833**

Localities: one specimen, the left bank of the Blagoevgradska Bistritsa River, Slavovo area, in a high grassland among broad-leaved forests (N42°01′49″ E23°16′07″, alt. *ca* 878 m), 16.06.2010; one specimen, the village of Debochitsa, Domozettsi neighbourhood, in open grassland (N41°51′34″ E22°57′41″, alt. *ca* 1120 m), 09.1999, L. Domozetski observ (Fig. 1).

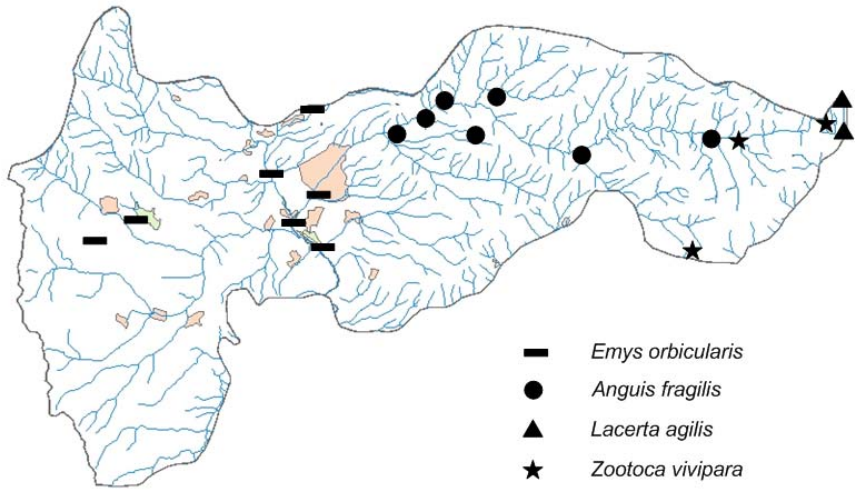

Fig. 2: Distribution of *Emys orbicularis, Anguis fragilis, Lacerta agilis* and *Zootoca vivipara* in the territory of the Blagoevgrad municipality

Remarks: The snake-eyed Skink is extremely rare in the endmost parts of the southwest Bulgaria. It is possible to find some more localities of the species in the region if we have in mind its sporadic distribution in the other parts of the country. The species is reported for the first time for the region.

***Anguis fragilis* Linnaeus, 1758**

Localities: one juvenile specimen, after the Kartalska glade in coniferous forest (N42°02′29″ E23°22′13″, alt. *ca* 1507 m), 30.08.2009, K. Tyufekchiev observ.; one specimen, the Kartalska glade (N42°02′30″ E23°22′01″, alt. *ca* 1480 m), G. Manolev observ.; one specimen, the Blagoevgradska Bistritsa River, near the influx of the Slavova River (N42°01′52″ E23°16′25″, alt. *ca* 905 m), G. Manolev observ.; one specimen, the Slavova River, 1 км before its mouth, in dense mixed forest (N42°01′25″ E23°16′39″, alt. *ca* 993 m); one specimen, the village of Bistritsa, Trenchovtsi neighbourhood, in the grass of a glade among broad-leaved forests (N42°03′29″ E23°12′49″, alt. *ca* 889 m), 19.06.2009; three crushed specimens, between the mouth of the Mishovets River and the village of Bistritsa, 17.05.2009, G. Manolev observ.; one crushed specimen, on the road west of the village of Bistritsa (N42°03′14″ E23°10′23″, alt. *ca* 559 m), 18.06.1998; one crushed specimen, the village of Bistritsa, Tepavitsa neighbourhood (N42°02′43″ E23°09′28″, alt. *ca* 522 m), 19.06.2006; several different age specimens, near the mouth of the Mishovets River (N42°02′12″ E23°08′21″, alt. *ca* 473 m; N42°02′07″ E23°08′24″, alt. *ca* 496 m), 03.05.1996; one specimen, the same locality by the road (N42°02′11″ E23°08′23″, alt. *ca* 482 m), 16.05.2000; one specimen, on the road from Burovtsi neighbourhood (the village of Gorno Harsovo) to Shopovtsi neighbourhood (the village of Bistritsa), 15.05.2009 (Fig. 2).

Remarks: The slow worm is widely distributed in the Blagoevgradska Bistritsa River Basin. It inhabits mainly broad-leaved and mixed forests but is also found in grasslands in high numbers. All specimens observed belong to *Anguis fragilis fragilis*. The species has not been reported for the region before.

***Lacerta agilis* Linnaeus, 1758**

Localities: Rila Mountain, near the city of Blagoevgrad; south of the peak Golyam Mechi vrah [1]; Macedonia hut [2] (Fig. 2).

Remarks: We have not found a sand lizard in the territory of the Blagoevgrad municipality. The locality reported - “Rila mountain, near the city of Blagoevgrad” [1], refered most likely to the higher parts of Rila Mountain. It is possible to find the species also in the western part of the region (in the higher parts of Vlahina Mountain).

***Lacerta viridis* Laurenti, 1768**

Localities: Rila Mountain, east of the city of Blagoevgrad; on the road along the Blagoevgradska Bistritsa River to Parangalitsa reserve [1]; three specimens, Bachinovo place, 18.08.1974, RHM - Blagoevgrad, G. Dimitrov collect.; two specimens, Strumsko residential area, 18.06.1974, RHM - Blagoevgrad, G. Dimitrov collect.; four specimens, in the vicinity of the city of Blagoevgrad, 09.07.1974, 28.07.1974, RHM - Blagoevgrad, E. Andreeva, G. Dimitrov collect; one specimen, the city of Blagoevgrad, 12.06.1986,

RHM - Blagoevgrad, K. Iliev collect.; three specimens, the village of Pokrovnik, 25.03.1983, 15.06.1986, RHM - Blagoevgrad, K. Iliev collect.

Remarks: The eastern green lizard is a common widely distributed species in the territory of the Blagoevgrad municipality. It inhabits mostly the outskirts of forests and dense bushes, but it can also be found on grassy lands, in sparse forests, on rocky spots, in settlements etc. Early in spring it becomes active later than the common wall, the Erhard`s wall and the Balkan wall lizards. The earliest time when we observed it was on 14.03.1998 (three male specimens) close to the mouth of the Mishovets River (N42°02′12″ E23°08′21″, alt. *ca* 473 m), and on 14.03.2002 (two male specimens), in the village of Buchino, Karakachanska neighbourhood (N42°03′07″ E22°59′03″, alt. *ca* 627 m).

***Podarcis erhardii* (Bedriaga, 1882)**

Localities: the southern sides of Rila Mountain, the region of the city of Blagoevgrad [1].

Remarks: Buresch and Tsonkow [1] gave one more locality in the region: „on the road along the Blagoevgradska Bistritsa River to Parangalitsa reserve, 1200 м above the sea level”. Most likely the indication of this locality was a technical mistake since at that altitude, in the valley of the Blagoevgradska Bistritsa River, only the common wall lizard is found. The highest place at which we observed the Erhard`s wall lizard was west of the village of Bistritsa, by the road (N42°03′00″ E23°10′03″, alt. *ca* 539 m) on 03.05.1996.

The Erhard`s wall lizard is a common species distributed in high numbers on rocky spots at lower altitudes in the territory of the Blagoevgrad municipality. In the transitional zones it is found together with the common wall lizard. The earliest time when we observed the Erhard`s wall lizard was on 06.02.2004, on the rocks in Loven dom park in sunny weather (about 15° C), the city of Blagoevgrad (N42°01′11″ E23°06′19″, alt. *ca* 441 m). Several specimens were observed west of Malinkovtsi neighbourhood, the village of Leshko (N41°56′36″ E22°55′47″, alt. *ca* 886 m), on 20.06.2002, which is one of the highest localities in Bulgaria. The specimens observed south-east of the village of Drenkovo, on the stone walls of an ancient construction, (N42°00′13″ E22°57′55″, alt. *ca* 574 m) were feeding also on fruits (cherries).

***Podarcis muralis* (Laurenti, 1768)**

Localities: on the road along the Blagoevgradska Bistritsa River to Parangalitsa reserve [1]; one specimen, close to the village of Pokrovnik, 20.04.1978, RHM - Blagoevgrad, E. Andreeva collect.

Remarks: The common wall lizard is widely distributed in high numbers in the region. It is found at high altitudes (higher then the area of distribution of the Erhard`s wall lizard) and in isolated places in the city of Blagoevgrad.

It is a typical petrophilic species but we have observed it also in the outskirts of forests and in open grasslands.

***Podarcis tauricus* (Pallas, 1814)**

Localities: the region of the city of Blagoevgrad [1].

Remarks: The Balkan wall lizard has been found at many places and in high numbers in the western part of the territory of Blagoevgrad municipality (Vlahina Mountain), and sparsely and in low numbers in its central and eastern parts. Often it inhabits one and the same areas together with the Erhard`s wall lizard and rarely with the common wall lizard. The open short grasslands on sand soils are its typical localities. Sometimes it inhabits sand or rocky lands, outskirts of forests, agricultural lands, and enters small settlements. We observed copulation on 13.03.2001, 11.00 am., south-east of the village of Drenkovo (N42°00′28″ E22°56′55″, alt. *ca* 642 m), and on 15.03.2002, 1.00 pm., the village of Buchino (Karakachanska neighbourhood) (N42°02′56″ E22°59′05″, alt. *ca* 613 m). Two specimens were observed west of Malinkovtsi neighbourhood (the village of Leshko) (N41°56′36″ E22°55′47″, alt. *ca* 886 m), on 20.06.2002, which is one of the highest localities reported for the species in Bulgaria. Several specimens were found at another high locality (Ovnarska Chuka peak) on a limestone terrain (N41°57′18″ E22°57′54″, alt. *ca* 761 m), on 21.03.2002.

***Zootoca vivipara* (Jacquin, 1787)**

Localities: south of the peak Golyam Mechi vrah [1]; several specimens, north-west of Macedonia hut, summer of 2002, Kr. Andonov observ.; one specimen, by the road from Kartalska glade to Macedonia hut, in wet grassland (N42°02′32″ E23°23′10″, alt. *ca* 1647 m), 13.06.2010, L. Domozetski observ.; one specimen, between the peaks Chakalitsa and Skachkovets, in short grassland, 09.05.2003, Kr. Andonov observ.

Remarks: The viviparous lizard has been found only in the highest eastern parts of the territory of the Blagoevgrad municipality (in Rila Mountain). The finding of the species in other parts of the region is not expected.

4. CONCLUSIONS

- Three Testudines and eight Sauria species have been recorded for the territory of the Blagoevgrad municipality although it represents only 0.56% of the territory of the country. Both the tortoises, one of the two terrapins and 62% of the lizard species found in Bulgaria are distributed in the region. The species diversity is quite high because of the diverse relief, the considerable difference in altitude, comparatively dense river system, favourable climatic conditions, various habitats and unpolluted environment.

- The localities reported supplement to a great extent the known distribution of Testudines and Sauria species in the studied area. Most of the localities are given with their accurate geographical coordinates.
- Four species – *Testudo graeca*, *Emys orbicularis*, *Ablepharus kitaibelii* and *Anguis fragilis* have been recorded for the first time for the territory of the Blagoevgrad municipality.
- Six species – *Eurotestudo hermanni, Anguis fragilis, Lacerta viridis, Podarcis erhardii, P. muralis* and *P. tauricus* are widely distributed in large numbers within the studied area.

5. REFERENCES

[1] Buresch, I., Zonkow J. (1933) Untersuchungen über die Verbreitung der Reptilien und Amphibien in Bulgarien und auf der Balkanhalbinsel. 1. Schildkrötten (Testudinata) und Eidechsen (Sauria). *Mitt. Königl. naturw.* Inst. Sofia, 6: 150-207. (In Bulgarian, German summary).

[2] Duhalov, D. 1999. Study on the distribution and the colour variations of the sand lizard (*Lacerta agilis* L.) in Bulgaria. Graduation paper, Sofia University “St Kliment Ohridski”, Faculty of Biology, 28 p.

[3] Pulev, Al., L. Sakelarieva. 2009. Observations of Amphibians (Amphibia) within the Territory of the Blagoevgrad Municipality. In: Mathematics and Natural Sciences, Proceedings of the International scientific conference 3–7.06.2009, SWU “Neofit Rilsky”, Blagoevgrad Vol. 2 (329-334).

Serpentes (Reptilia) in the Territory of the Blagoevgrad Municipality

Alexander Pulev, Lidia Sakelarieva
South-West University, Faculty of Mathematics and Natural Sciences, Department of Geography, Ecology and Environmental Protection, 66 Ivan Mihailov Str., 2700 Blagoevgrad, Bulgaria

***Abstract**: The available information about the taxonomy and distribution of snakes (Serpentes) in the territory of the Blagoevgrad municipality has been updated and summarized. Eight species, out of 18 for the whole country, have been recorded – three of them for the first time for Vlahina Mountain (its Bulgarian part). Four species are widely distributed in large numbers in the region. Localities with accurate geographical coordinates, habitats, and some aspects of the ecology of certain species are reported for the first time.*

***Keywords**: Serpentes, distribution, Blagoevgrad municipality, Bulgaria*

1. INTRODUCTION

Data about the snakes, distributed in southwest Bulgaria, are found in the works of Buresch and Zonkow [1, 2], as well as in the collection of the Regional Historical Museum in the city of Blagoevgrad (RHM - Blagoebgrad).

The present observation of the herpetofauna in the territory of the Blagoevgrad municipality has been carried out since 1988. The information about the species composition and distribution of the amphibians, turtles and lizards was summarized by Pulev and Sakelarieva [3, 4]. The results about the snakes (Reptilia) are presented and discussed in this report.

2. MATERIAL AND METHODS

The Blagoevgrad municipality is located in the south-west Bulgaria [3]. The snakes have been observed during day field trips. Some localities have been told by other specialists. Only the localities with accurate geographical coordinates are put on maps.

3. RESULTS AND DISCUSSION

Eight Serpentes species out of 18 for the whole country have been found in the territory of the Blagoevgrad municipality:

***Dolichophis caspius* (Gmelin, 1779)**

Localities: in the vicinity of the city of Blagoevgrad [2]; one specimen, the city of Blagoevgrad, 10.05.1983, RHM - Blagoevgrad, St. Ugrinova collect.; one specimen, in the vicinity of the city of Blagoevgrad, 10.05.1994, RHM - Blagoevgrad, G. Dimitrov collect.; one specimen, the city of Blagoevgrad, Strumsko residential area, 15.04.1975, RHM - Blagoevgrad, E. Andreeva collect.; one specimen, the village of Belo pole, 10.08.1985, RHM - Blagoevgrad, K. Iliev collect.; one specimen, at the mouth of the Mishovets River, in broad-leaved forest (N42°02′14″ E23°08′25″, alt. *ca* 483 m); one crushed specimen, at the road fork to the village of Gorno Harsovo (N42°02′06″ E23°08′02″, alt. *ca* 462 m); one crushed specimen, west of the village of Gorno Harsovo (N42°01′00″ E23°10′07″, alt. *ca* 619 m), 06.07.2003; one specimen, the right bank of the Blagoevgradska Bistritsa River at the mouth of the Sheitanski Andak River, on a small tree (N42°01′55″ E23°07′04″, alt. *ca* 435 m), summer of 2007; one dead specimen, same locality (N42°01′52″ E23°07′04″, alt. *ca* 424 m), spring 2010, Hr. Peshev observ.; one specimen, the Zoo of the city of Blagoevgrad, in the cage of rodents (N42°00′51″ E23°06′08″, alt. *ca* 425 m); two juvenile specimens (one of them dead), by the road from the city of Blagoevgrad to the village of Delvino (N42°01′23″ E23°07′23″, alt. *ca* 653 m), 28.08.2006, L. Domozetski observ.; one crushed specimen, the city of Blagoevgrad, Orlova chuka residential area, on the road to the village of Delvino (N42°00′42″ E23°06′30″, alt. *ca* 493 m), 01.06.2004; one dead specimen, the city of Blagoevgrad, the industrial area (N42°00′17″ E23°05′14″, alt. *ca* 351 m); one dead specimen, east of Strumsko residential area, by an irrigation canal (N41°59′20″ E23°05′50″, alt. *ca* 414 m), G. Manolev observ.; one specimen, the Kaimenska chuka height, south of Blagoevgrad, in sparse pine forest (N41°58′40″ E23°05′27″, alt. *ca* 348 m); one crushed specimen, south of the Kaimenska chuka height, on the road fork to the village of Izgrev (N41°58′28″ E23°05′38″, alt. *ca* 333 m), L. Domozetski observ.; one crushed specimen, south of Blagoevgrad, on the road before the road fork to the village of Tserovo (N41°58′23″ E23°05′41″, alt. *ca* 326 m), 14.07.2009; one crushed specimen, south of Blagoevgrad, on the road after the road fork to the village of Tserovo (N41°58′08″ E23°06′05″, alt. *ca* 426 m), G. Manolev observ.; one crushed specimen, south of Blagoevgrad, on the road to the village of Dolno Tserovo after the road fork to the village of Tserovo (N41°57′48″ E23°06′06″, alt. *ca* 319 m), G. Manolev observ.; one specimen, north of the village of Dolno Tserovo, on

the road (N41°57′02″ E23°06′08″, alt. *ca* 335 m); one crushed specimen, same locality, G. Manolev observ.; two shed snake skins, north of the village of Dolno Tserovo, by the road (N41°56′56″ E23°05′54″, alt. *ca* 325 m), 22.07.1997; one crushed specimen, east of the village of Riltsi (N42°02′42″ E23°04′58″, alt. *ca* 452 m), 04.05.2008; one crushed specimen, between the villages of Belo pole and Riltsi, on the road (E79) (N42°02′15″ E23°03′04″, alt. *ca* 390 m), 29.06.1996; one specimen, between the village of Pokrovnik and the Struma River, in agricultural land (N41°59′13″ E23°03′41″, alt. *ca* 326 m), G. Manolev observ.; one juvenile specimen, the village of Obel, Zlatkovtsi neighbourhood, M. Zlatkova observ (Fig. 1).

Remarks: The large whip snake has been one of the most frequently found species in the territory of the Blagoevgrad municipality. We suppose it has wider distribution in the region. The species inhabits open areas – agricultural and uncultivated lands, sparse forests, bushes, but also enters the settlements. It is reported for the first time for Vlahina Mountain (its Bulgarian part).

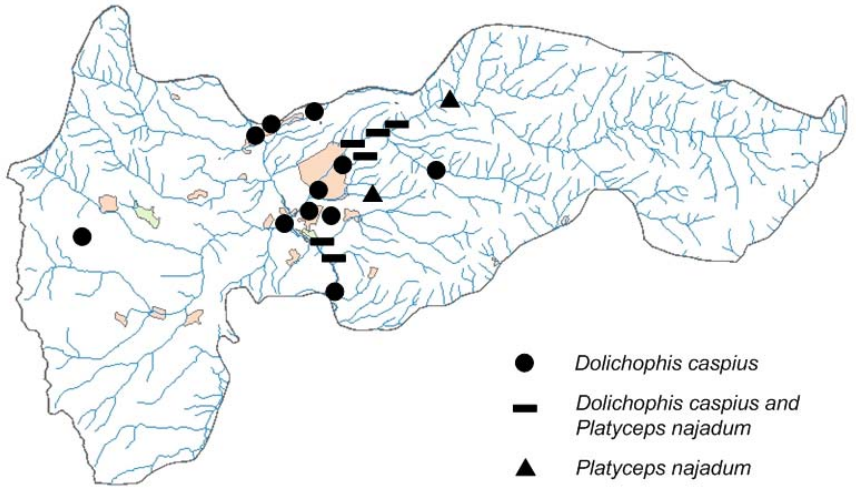

Fig. 1: Distribution of *Dolichophis caspius* and *Platyceps najadum* in the territory of the Blagoevgrad municipality

***Platyceps najadum* (Eichwald, 1831)**

Localities: in the vicinity of the city of Blagoevgrad; the village of Bistritsa [2]; four different age specimens, the village of Elenovo,

06.07.1982, 14.04.1983, 20.04.1983, RHM - Blagoevgrad, Vl. Aleksov collect.; one specimen, the right bank of the Blagoevgradska Bistritsa River, upwards the mouth of the Mishovets River (N42°02′18″ E23°08′30″, alt. *ca* 482 m), G. Manolev observ.; one specimen, Bachinovo area, on the road (N42°01′57″ E23°07′31″, alt. *ca* 448 m), 14.06.2003, G. Manolev observ.; one juvenile specimen, the right bank of the Blagoevgradska Bistritsa River, at the mouth of the Sheitanski Andak River, in pine forest (N42°01′56″ E23°07′10″, alt. *ca* 441 m), 03.09.2010, L. Domozetski observ.; one dead juvenile specimen, the north-east outskirts of Blagoevgrad (N42°01′45″ E23°06′44″, alt. *ca* 421 m), 19.05.2008; one specimen, by the road between the city of Blagoevgrad and the village of Delvino (N42°01′23″ E23°07′23″, alt. *ca* 653 m), 31.08.2004, L. Domozetski observ.; one juvenile specimen, the same locality, 04.09.2006, L. Domozetski observ.; one specimen, the Kaimenska chuka height, south of Blagoevgrad (N41°58′36″ E23°05′40″, alt. *ca* 375 m), G. Manolev observ.; two crushed specimen, south of Blagoevgrad, on the road after the road fork to the village of Tserovo (N41°58′25″ E23°06′16″, alt. *ca* 371 m), 26.05.2009, G. Manolev observ.; one crushed specimen, the same locality, 16.06.2009, G. Manolev observ (Fig. 1).

Remarks: The Dahl`s whip snake has been comparatively frequently found in the territory of the Blagoevgrad municipality. Very often it inhabits the same areas as the large whip snake. We presume the species has wider distribution in the western parts of the region. The new localities reported supplement to a great extent its known distribution in the Struma River basin. The locality “by the road between the city of Blagoevgrad and the village of Delvino” is one of the highest in Bulgaria (653 m).

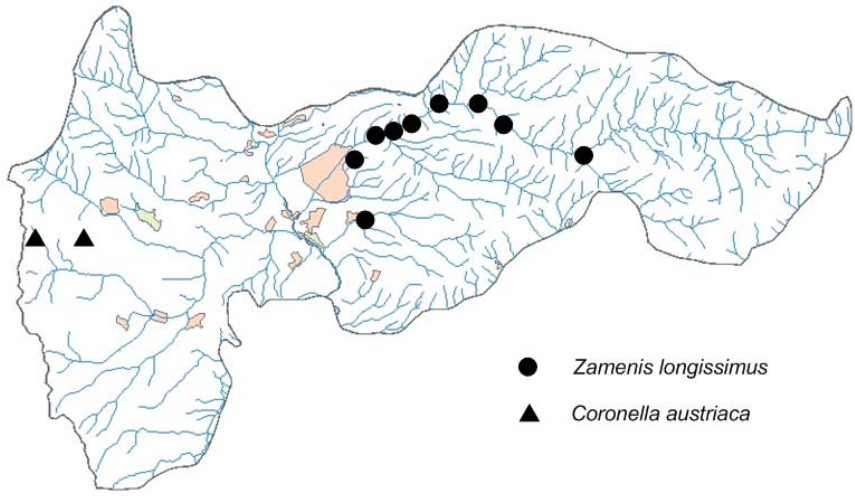

Fig. 2: Distribution of *Zamenis longissimus* and *Coronella austriaca* in the territory of the Blagoevgrad municipality

***Zamenis longissimus* (Laurenti, 1768)**

Localities: near the Blagoevgradska Bistritsa River, on the road to Parangalitsa reserve [2]; one specimen, the city of Blagoevgrad, 20.08.1991, RHM - Blagoevgrad, Kr. Samardjiev collect.; one crushed specimen, the Blagoevgradska Bistritsa River, up from the Slavova River, in mixed forest (N42°01′51″ E23°16′22″, alt. *ca* 898 m), 22.09.2010; one specimen, the Slavova River, 1 km up from its mouth, in dense mixed forest (N42°01′25″ E23°16′39″, alt. *ca* 993 m), 18.07.1998; one dead specimen, by the road in Brakadantsi neighbourhood (the village of Bistritsa) (N42°02′42″ E23°12′54″, alt. *ca* 700 m), 18.07.1998; one specimen, the village of Bistritsa, Kovachitsa neighbourhood, in the evening, in dark (N42°03′10″ E23°11′51″, alt. *ca* 619 m), 14.07.2009, G. Manolev observ.; one specimen, west of the village of Bistritsa (N42°03′12″ E23°10′18″, alt. *ca* 559 m), 17.05.2009, G. Manolev observ.; one crushed specimen, on the road between Bachinovo area and the village of Bistritsa, in mixed forest (N42°02′26″ E23°08′59″, alt. *ca* 503 m), 20.05.2003; two crushed specimens, at the mouth of the Mishovets River (N42°02′08″ E23°08′19″, alt. *ca* 483 m), 17.05.2009, G. Manolev observ.; one crushed specimen, on the road fork to the village of Gorno Harsovo (N42°02′06″ E23°08′02″, alt. *ca* 462 m), 18.06.1998; one juvenile specimen, the right bank of the Blagoevgradska Bistritsa River, Bachinovo area (N42°02′07″ E23°07′35″,

alt. *ca* 453 m), 15.05.1990; one dead specimen, the city of Blagoevgrad, Loven dom park (N42°01′10″ E23°06′17″, alt. *ca* 436 m), 16.05.2000; one specimen, the village of Izgrev, in the yard of a house (N41°59′25″ E23°07′02″, alt. *ca* 407 m), 08.06.2010 (Fig. 2).

Remarks: The aesculapian snake is one of the most frequently found snakes in the forests along the Blagoevgradska Bistritsa River. It inhabits broad-leaved and mixed forests, parks, but also enters the settlements. Probably it has wider distribution in higher parts of Vlahina Mountain.

***Coronella austriaca* Laurenti, 1768**

Localities: Parangalitsa reserve, 1900 m above sea level [2]; one juvenile specimen, the village of Obel, Zlatkovtsi neighbourhood, M. Zlatkova observ.; one dead juvenile specimen, the village of Obel, after the road fork to Plyangovtsi neighbourhood (N41°58′35″ E22°53′02″, alt. *ca* 1115 m), G. Manolev observ (Fig. 2).

Remarks: We presume that the smooth snake has wider distribution in the region. The species is reported for the first time for Vlahina Mountain (its Bulgarian part).

***Natrix natrix* Linnaeus, 1758**

Localities: in the vicinity of the city of Blagoevgrad [2].

Remarks: The grass snake is widely distributed in the water objects in the territory of the Blagoevgrad municipality. It has been more frequently found than the dice snake. All specimens observed belong to *Natrix natrix natrix*.

***Natrix tessellata* (Laurenti, 1768)**

Localities: in the vicinity of the city of Blagoevgrad [2].

Remarks: The dice snake, as more thermophilic species, has been found only in the water objects located at lower altitude. We observed three specimens on the stone wall of the Blagoevgradska Bistritsa River in the city of Blagoevgrad on 07.04.1998 (N42°00′39″ E23°05′32″, alt. *ca* 362 m). They climbed very well the crevices of the almost vertical wall.

***Vipera ammodytes* (Linnaeus, 1758)**

Localities: in the vicinity of the city of Blagoevgrad (*Vipera ammodytes meridionalis*) [2]; one specimen, at the mouth of the MIshovets River, in dense broad-leaved forest (N42°02′14″ E23°08′25″, alt. *ca* 483 m); one dead specimen with features of *Vipera ammodytes meridionalis*, the Harsovska River, by the road, 2 km east of the village of Gorno Harsovo (N42°00′51″ E23°11′37″, alt. *ca* 774 m), 03.08.1998; two crushed specimens, on the road between the road fork to the village of Gorno Harsovo and the village, in an area zoned for summer-houses (N42°01′20″ E23°09′21″, alt. *ca* 552 m), 05.10.1996; one specimen, near the mouth of the Harsovska River (N42°02′03″ E23°08′00″, alt. *ca* 471 m), 18.05.1990; two specimens, the right bank of the Blagoevgradska Bistritsa River, Bachinovo area, in mixed forest (N42°02′08″ E23°07′39″, alt. *ca* 450 m),

17.05.1990, 18.05.1990; one dead specimen, the right bank of the Blagoevgradska Bistritsa River, at the mouth of the Sheitanski Andak River (N42°01′55″ E23°07′04″, alt. *ca* 435 m), 17.05.1990; one specimen, the same locality, summer of 2007; one dead specimen, the north-east outskirts of the city of Blagoevgrad (N42°01′45″ E23°06′44″, alt. *ca* 421 m), 18.05.1990; one specimen, the north-east part of the city of Blagoevgrad, in the yard of a house (N42°01′42″ E23°06′26″, alt. *ca* 429 m), Hr. Peshev observ.; one specimen, by the road between the city of Blagoevgrad and the village of Delvino (N42°01′23″ E23°07′23″, alt. *ca* 653 m), L. Domozetski observ.; one crushed specimen, south of Blagoevgrad, on the road after the road fork to the village of Tserovo (N41°58′25″ E23°06′16″, alt. *ca* 371 m), 16.06.2009, G. Manolev observ.; one juvenile specimen, north-east of the village of Dolno Tserovo, in sparse pine forest (N41°56′55″ E23°06′21″, alt. *ca* 408 m); one specimen, in dense mixed forest, north-west of the village of Klisura (N42°00′34″ E22°53′44″, alt. *ca* 830 m), 17.04.2003; one specimen, the village of Obel, south of Barkovtsi neighbourhood (N41°58′15″ E22°54′00″, alt. *ca* 1029 m), G. Manolev observ.; one specimen, the same locality, in pine forest (N41°58′18″ E22°54′03″, alt. *ca* 1019 m), G. Manolev observ.; several specimens, the village of Obel, Zlatkovtsi neighbourhood, M. Zlatkova observ. (Fig. 3).

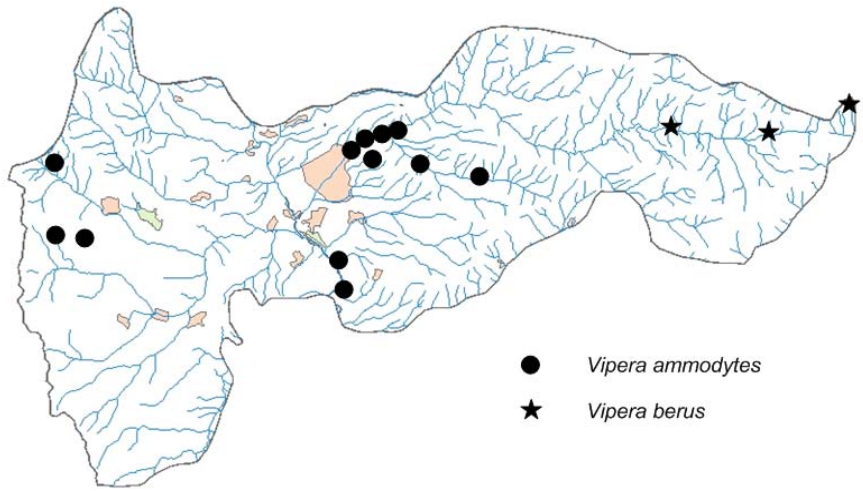

Fig. 3: Distribution of *Vipera ammodytes* and *Vipera berus* in the territory of the Blagoevgrad municipality

Remarks: The nose-horned viper is widely distributed in the sunny areas of the territory of the Blagoevgrad municipality. It also enters the outskirts of the settlements. All specimens were observed during the day, standing still at dappled shade or basking in the sun. We presume much wider distribution of the species in the west parts of the region. The species is reported for the first time for Vlahina Mountain (its Bulgarian part).

***Vipera berus* (Linnaeus, 1758)**

Localities: Golyam Mechi vrah peak, 2650 m above sea level [1]; one specimen, Bodrost resort, 12.07.1983, RHM - Blagoevgrad, Vl. Aleksov collect.; one specimen, by the road between Kartalska glade and Macedonia hut, in sparse coniferous forest (N42°02′40″ E23°24′07″, alt. *ca* 1832 m), 28.07.2006, L. Domozetski observ (Fig. 3).

Remarks: The adder has limited distribution only in the highest eastern parts of the territory of the Blagoevgrad municipality, in Rila Mountain. We suppose the finding of other localities in this region.

4. CONCLUSIONS

- Eight species or 44% of the Serpentes species distributed in Bulgaria inhabit the territory of the Blagoevgrad municipality. In spite of the small area the species diversity is rather high because of the diverse natural conditions. An increase in species composition as a result of future observations has not been expected.
- The localities reported supplement to a great extent the known distribution of the snake species in the studied area. Most of the localities are given with their accurate geographical coordinates.
- Three snake species - *Dolichophis caspius*, *Coronella austriaca* and *Vipera ammodytes* have been recorded for the first time for Vlahina Mountain (its Bulgarian part).
- Four snake species - *Dolichophis caspius*, *Zamenis longissimus*, *Natrix natrix* and *Vipera ammodytes* are widely distributed in large numbers in the studied area.

5. REFERENCES

[1] Buresch, I., Zonkow J. (1932) Die Verbreitung der Giftschlangen (Viperidae) in Bulgarien und auf der Balkanhalbinsel. *Trav. Soc. Bulg. Sc. Natur*., 15-16: 189-206. (In Bulgarian).

[2] Buresch, I., Zonkow J. (1934) Untersuchungen über die Verbreitung der Reptilien und Amphibien in Bulgarien und auf der Balkanhalbinsel. 2. Schlangen (Serpentes). *Mitt. Königl. naturw*. Inst. Sofia, 7: 106-188. (In Bulgarian, German summary).

[3] Pulev, Al., L. Sakelarieva. 2009. Observations of Amphibians (Amphibia) within the Territory of the Blagoevgrad Municipality. In: Mathematics and Natural Sciences, Proceedings of the International scientific conference 3–7.06.2009, SWU “Neofit Rilsky”, Blagoevgrad Vol. 2 (329-334).

[4] Pulev, Al., L. Sakelarieva. 2011. Testudines and Sauria (Reptilia) in the Territory of the Blagoevgrad Municipality In: Mathematics and Natural Sciences, Proceedings of the International scientific conference 8–11.06.2011, SWU “Neofit Rilsky”, Blagoevgrad (in print).

Hydrological regime in Bulgaria according to the monthly maxima and minima of runoff

Nelly Hristova
Sofia University "St. Kliment Ohridsku", Sofia, Bulgaria

***Abstract**: This work offers a classification of river regime according to so-called discriminating periods, defined by the first, the second and the third highest and lowest monthly river flow. It uses data for the runoff for 218 catchments. The results show three types regime of river flow, each of which corresponds to the predominant genetic sources of flow.*

***Keywords:** hydrological regime, monthly flow, monthly maximum and minimum river flow.*

1. INTRODUCTION

Typification of river flow regime is important issue in theoretical hydrology, because it is based for defining of hydrological regions and for creating of models for hydrological processes. The methodology for flow regime classification uses two different approaches – genetic and statistical. This work is built on method for the hydrological regime classification developed for the Nordic countries by Gottschalk *et al*. (1979), because it is new approach for analyzing of water regime in Bulgaria. There are some purposeful typification of river flow regime in Bulgaria – by Lvovich (1966), Zjapkov *et al*. (1989) and Hristova (2004). They use different method and results are different. Lvovich (1966) uses three indicators (seasonal distribution of river runoff, genetic sources of flow formation and annual fluctuation of river runoff) and defines three hydrological areas (moderate continental, Mediterranean and alpine) with nine types hydrological regime. The similar is results by Hristova (2004), who uses duration and timing of periods with high waters and low waters and who separates three types river flow regime - moderate continental, continental-Mediterranean and alpine. Zjapkov *et al*. (1989) isolate two class river regime – continental and Mediterranean, like the results by Marinov (1968) and Stoychev (1982).

This work concentrates on classification of river regime by new point of view and analyses geographical aspects of isolated types hydrological regimes.

2. METHODS AND DATA

The classification of hydrological regime is done by assessment of the occurrence of the discriminating periods, defining by the by the first, the second and the third highest and lowest monthly river flow noted with MAX1, MAX2, MAX3, MIN1, MIN2, MIN3 (Figure1). This methodology, which is based on the time of occurrence of high and low flows, is offered by Gottschalk *et al*. (1979). It is used for defining of nine types river flow regime in Europe (Arnel, *et al*. 1993).

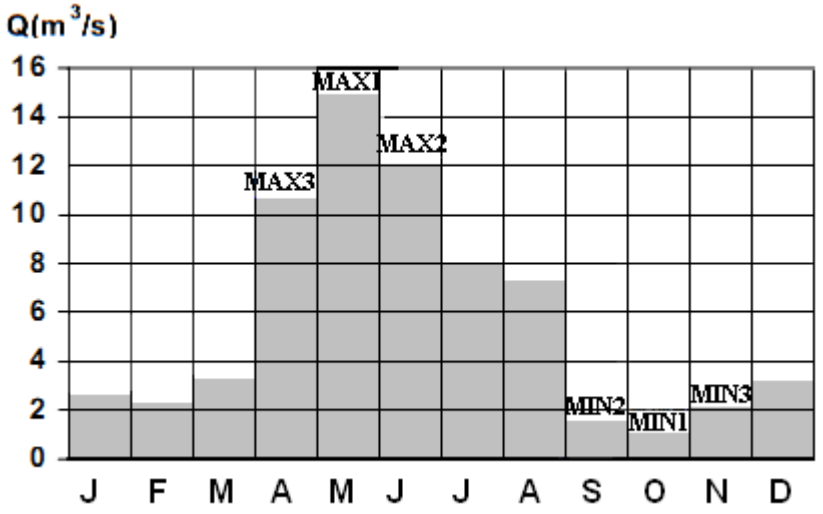

Fig. 1: Discriminating periods

Krasovskaja *et al*. (1992) offer the next areas, which is isolated on this method: for high waters – H1, if the three months belong to spring or early summer (May - July), H2, when the second highest or third highest monthly runoff takes place in autumn (October, November), H3 - highest monthly runoff takes place in autumn or early winter (November-December); for low waters – L1, when the two months with the lowest runoff both belong to winter or early spring (February - March), L2 - when the two months with the lowest runoff do not belong to the same time in the year (February and July), L3, when dominate summer low flow.

Data for this work are monthly runoff for 229 catchments. The observer period is different, but not below 30 years.

3. RESULTS

The first maximum appears during March - June in 198 watersheds – 86.5 % of all and during January - February in 31 catchments (Table 1). This distribution shows two groups river basins – with highest runoff in spring hydrological season (March - June) and with highest runoff in winter hydrological season (November - February) in Bulgaria. The first group river basins cover the most part of territory of the country and forms type river regime H1. There are seven subtypes according the second and the third monthly maximum of river flow. Three of these subtypes (monthly maximum during II - III, III - V and IV - VI) include the most river basins. The rest sub-types (monthly maximum III – II - V, V – IV - II, V - VI - VII and VI - V - VII) includes individual catchments.

Tab. 1: Months with highest and lowest water

First monthly maximum/minimum	Months	Number	%
First monthly maximum	January	3	1.0
	February	28	12.0
	March	50	22.0
	April	55	24.0
	May	89	39.0
	June	4	2.0
First monthly minimum	January	2	1.0
	February	15	6.0
	July	1	1.0
	August	85	37.0
	September	94	41.0
	October	29	12.0
	November	2	1.0
	December	1	1.0

The second group covers East Rhodopes, Burgas plain, the lower Tundja and Marista, small part of northeast Bulgaria (Suha River, Batova River and Luda Kamchia River) and forms type river regime H2. This type is divided into three subtypes: II - I - III (for the most river basins in this group), II - III - IV (for the some rivers in southeast part of Black sea catchment), II - XII – I (for the rivers in East Rhodopes).

The first monthly minimum appears during July – October in 189 river basins and during November – February – in 20 catchments (Table 1). There are two types hydrological regime according to this indicator. First type is classified as L1 and includes the river basin with lowest monthly flow during summer-autumn hydrological season. This group includes a lot of sub-types according to second and third monthly minimum of runoff. The

most typical subtype river basins have second and third monthly minimum in August, September or October. The second type, named L2, includes all river basins with lowest monthly runoff in the winter. It covers alpine catchments.

Three main regimes have been obtained on the prepositional method – H1L1 – spring highest monthly runoff and summer - autumn lowest runoff, H1L2 – spring highest monthly runoff and winter lowest runoff, and H2L1 – winter highest monthly runoff and summer - autumn lowest runoff (Figure 2a). The first type is typical for North Bulgaria and hill and mountain catchments in South Bulgaria (Figure 3).

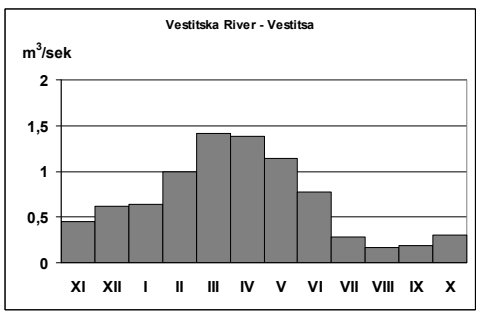

a) H1L1

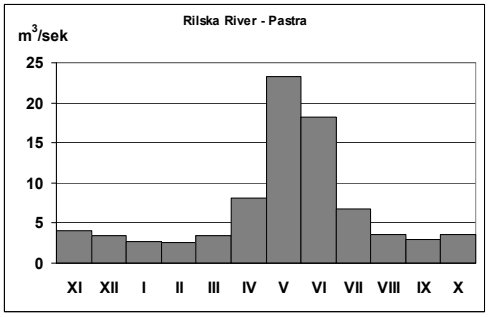

b) H1L1

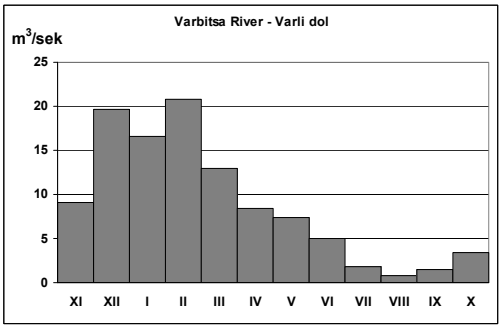

c) H2L1

Fig. 2: Types hydrological regime according to monthly maximum and monthly minimum runoff

The second type includes alpine catchments in Rila Mountain (upper stream of Iskar, Maritsa and, Mesta), Pirin Mountain (Demjanitsa River), West Rhodopes (Chairska River), West and Central Balkan Mountains (Figure 2b).

The third type shows in southeast watersheds and north part of the Black sea seaside (Figure 2c). There are some sub-types for every type. These sub-types are subject to further study.

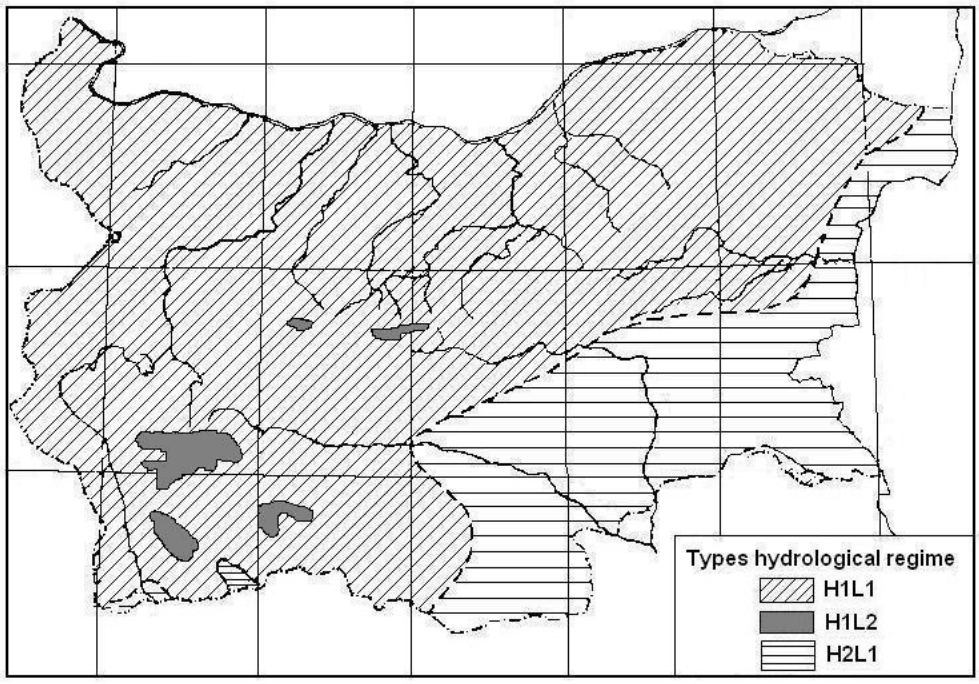

Fig. 3: Geographical distribution of the types hydrological regime

4. CONCLUSIONS

Typification of hydrological regime in Bulgaria trough monthly maximum and monthly runoff gives three types river flow regime. These types cover areas which correspond with regions of dominant genetic source of flow formation. First type (H1L1) includes area, where more then 50 % of overland flow are precipitations. The second type (H1L2) is typical for river basins, where predominate snowmelt. Third type (H2L1) covers watersheds with dominant rainfall runoff. The classification complements researches on the types of hydrological regime in the country and gives base for hydrological regionalization.

5. REFERENCES

[1] Arnell, N.W, Krasovskaia, I., Gottschalk L. (1993) River flow regime in Europe. In: *Flow Regimes from International Experimental and Network Data* (FRIEND), vol.1, Hydrological studies, Wallingford, Oxford sire, UK, 111-121.

[2] Hristova, N. (2004) Typification of river flow in Bulgaria. **Annuaire de l'Université de Sofia *"St. Kliment Ohridski",*** *Faculté de Geologe et Geographie*, 129-153.
[3] Krasovskaia, I., Gottschalk L. (1992) Stability of River Flow Regime. Nordic Hydrology, 23, 137-154.
[4] Lvovich, M. (1966) Tipove rechen regim. In: *Geografia na Bulgaria*, 1, Sofia, 360-367.
[5] Marinov, I, Panajotov, T. (1968) Hidrolozko rajonirane na Bulgaria. *Izvestia na Instituta po hidrologia I meteorologia*, 14, 5-55.
[6] Stoichev, K. (1982) rezim na rechnite vodi. In: *Geografia na Bulgaria*, 1, Sofia, 312-317.
[7] Zjapkov, L, Jordanova, M. (1989) Vatreshnogodishno razpredelenie na rechnite void. In: *Prirodnojat I ikonomicheski potentsial na planinite v Bulgaria*, Sofia, 211-216.

Table of contents

MATHEMATICS

INFORMATICS AND COMPUTER TECHNOLOGY

METHODOLOGY IN EDUCATION

CHEMISTRY

PHYSICS

RENEWABLE ENERGY TECHNOLOGIES

GEOGRAPHY AND ECOLOGY